DYSFUNCTION AND REPAIR OF NEURAL CIRCUITS FOR MOTOR CONTROL

EDITED BY: John Martin, George Mentis and Andrew Paul Tosolini
PUBLISHED IN: Frontiers in Molecular Neuroscience

frontiers Research Topics

frontiers

ISSN 1664-8714
ISBN 978-2-88966-705-5
DOI 10.3389/978-2-88966-705-5

About Frontiers

Frontiers is more than just an open-access publisher of scholarly articles: it is a pioneering approach to the world of academia, radically improving the way scholarly research is managed. The grand vision of Frontiers is a world where all people have an equal opportunity to seek, share and generate knowledge. Frontiers provides immediate and permanent online open access to all its publications, but this alone is not enough to realize our grand goals.

Frontiers Journal Series

The Frontiers Journal Series is a multi-tier and interdisciplinary set of open-access, online journals, promising a paradigm shift from the current review, selection and dissemination processes in academic publishing. All Frontiers journals are driven by researchers for researchers; therefore, they constitute a service to the scholarly community. At the same time, the Frontiers Journal Series operates on a revolutionary invention, the tiered publishing system, initially addressing specific communities of scholars, and gradually climbing up to broader public understanding, thus serving the interests of the lay society, too.

Dedication to Quality

Each Frontiers article is a landmark of the highest quality, thanks to genuinely collaborative interactions between authors and review editors, who include some of the world's best academicians. Research must be certified by peers before entering a stream of knowledge that may eventually reach the public - and shape society; therefore, Frontiers only applies the most rigorous and unbiased reviews.
Frontiers revolutionizes research publishing by freely delivering the most outstanding research, evaluated with no bias from both the academic and social point of view. By applying the most advanced information technologies, Frontiers is catapulting scholarly publishing into a new generation.

What are Frontiers Research Topics?

Frontiers Research Topics are very popular trademarks of the Frontiers Journals Series: they are collections of at least ten articles, all centered on a particular subject. With their unique mix of varied contributions from Original Research to Review Articles, Frontiers Research Topics unify the most influential researchers, the latest key findings and historical advances in a hot research area! Find out more on how to host your own Frontiers Research Topic or contribute to one as an author by contacting the Frontiers Editorial Office: frontiersin.org/about/contact

DYSFUNCTION AND REPAIR OF NEURAL CIRCUITS FOR MOTOR CONTROL

Topic Editors:
John Martin, City College of New York (CUNY), United States
George Mentis, Columbia University, United States
Andrew Paul Tosolini, University College London, United Kingdom

Citation: Martin, J., Mentis, G., Tosolini, A. P., eds. (2021). Dysfunction and Repair of Neural Circuits for Motor Control. Lausanne: Frontiers Media SA.
doi: 10.3389/978-2-88966-705-5

Table of Contents

frontiers in Molecular Neuroscience

EDITORIAL
published: 22 March 2021
doi: 10.3389/fnmol.2021.669824

Editorial: Dysfunction and Repair of Neural Circuits for Motor Control

Andrew Paul Tosolini[1]*, *George Z. Mentis*[2]*† and *John H. Martin*[3]*†

[1] Department of Neuromuscular Diseases, UCL Queen Square Institute of Neurology, University College London, London, United Kingdom, [2] Department of Pathology & Cell Biology and Neurology, Center for Motor Neuron Biology and Disease, Columbia University, New York, NY, United States, [3] Department of Molecular, Cellular and Biomedical Sciences, Center for Discovery and Innovation, City University of New York School of Medicine, New York, NY, United States

Keywords: motor neurons, sensory neurons, regeneration, spinal cord injury, ALS, SMA, inflammation, glia

Editorial on the Research Topic

Dysfunction and Repair of Neural Circuits for Motor Control

The dissolution of normal behavior in pathological conditions, after trauma, or in neurodegenerative diseases is often attributed to the selective dysfunction and degeneration of particular classes of vulnerable neurons. However, vulnerable neurons are embedded in neuronal circuits that often play major roles in the progression of the pathophysiological state, by cell-autonomous and non-cell autonomous mechanisms. For example, voluntary motor behavioral impairments occur after brain or spinal cord injury because descending projection neurons are vulnerable to axonal damage and are unable to regenerate anew. This limitation reflects both a loss of intrinsic axon regenerative capacity in mature neurons and extrinsic regulation by non-neuronal cells. Similarly, motor neurons deprived of supraspinal inputs or in neurodegeneration (e.g., ALS, SMA) undergo an array of well-described molecular events (Schwab and Bartholdi, 1996; Brown and Al-Chalabi, 2017; Groen et al., 2018) that also include morphological remodeling (Bose et al., 2005; Dukkipati et al., 2018). If therefore, repair or restoration of normal function is sought after, a clear understanding is required for the molecular, cellular, and neuronal circuit mechanisms involved. Over the last decade, several significant advances in our understanding of the development and operational principles of neural circuits demonstrate the complexity of the central nervous system under normal conditions and the diverse mechanisms that lead to dysfunction.

Everyday actions in essential complex behaviors such as walking, feeding, and breathing, require the specific integration of neural circuits that flawlessly operate with precision, co-ordination, and synchrony (Arber, 2012). As summarized in **Figure 1**, for voluntary movement to occur, the motor cortical areas must initiate communication with the spinal cord circuitry, which in turn convey these commands *via* spinal motor neurons to the skeletal muscles. Equally important, sensory information from the periphery is essential for the proper activation and function of neural circuits involved in motor control. Intrinsic to these processes are the influences of spinal excitatory and inhibitory interneurons.

However, after injury or in disease states, these neural circuits may be affected in subtle ways but over time may result in a multitude of effects causing dysfunction; not only in vulnerable neurons but also by disrupting the signaling and connectivity of integrated neural circuits. As neural circuits are disrupted through trauma [spinal cord injury (SCI), peripheral nerve injury, stroke] or in neurodegenerative diseases [amyotrophic lateral sclerosis (ALS), spinal muscular atrophy (SMA)], determining the timing and primacy of the earliest pathological events are critical questions to be addressed if normal function is to be restored. Uncovering therefore the initiating pathogenic events are critical steps in proposing potential therapeutic avenues.

OPEN ACCESS

Edited by:
Peter Claus,
Hannover Medical School, Germany

Reviewed by:
Lars Klimaschewski,
Innsbruck Medical University, Austria

***Correspondence:**
Andrew Paul Tosolini
a.tosolini@ucl.ac.uk
George Z. Mentis
gzmentis@columbia.edu
John H. Martin
jmartin@med.cuny.edu

† These authors have contributed equally to this work

Received: *19 February 2021*
Accepted: *26 February 2021*
Published: *22 March 2021*

Citation:
Tosolini AP, Mentis GZ and Martin JH (2021) Editorial: Dysfunction and Repair of Neural Circuits for Motor Control. Front. Mol. Neurosci. 14:669824. doi: 10.3389/fnmol.2021.669824

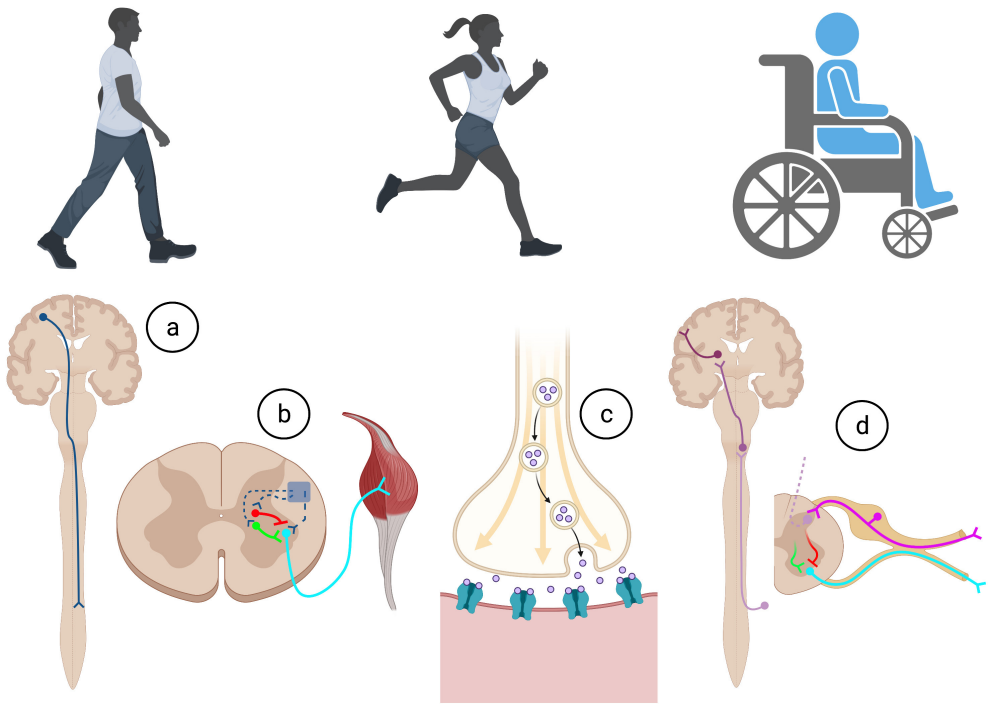

FIGURE 1 | Execution of all movements in health and after trauma require a complex series of co-ordination of cellular and molecular actions involved within the **(A)** descending motor system, **(B)** intrinsic spinal cord circuitry, **(C)** neuromuscular junction, and **(D)** afferent feedback through the ascending sensory system. Created with BioRender.com.

However, a paramount challenge for the field is to harmonize and integrate effectively the increasing number of studies that separately focus on molecular events in single cells (e.g., transcriptomics, proteomics) or on cellular phenotypes in neurons and glia (e.g., neuronal dysfunction, neurodegeneration, synaptic plasticity, astrocytic, or microglia proliferation) (Stuart and Satija, 2019). To this end, an exciting challenge is to decipher adaptive from maladaptive molecular and cellular changes within individual neurons and their supporting cells and the influence they exert on motor circuits after neural trauma (Ilieva et al., 2009; Eroglu and Barres, 2010; Huntley, 2012). We launched this Research Topic to provide a platform to encourage discussion on recent advances in knowledge and/or therapeutic tools to investigate motor circuitry following certain pathological conditions.

The topic on *Dysfunction and Repair of Neural Circuits for Motor Control* is devoted to neuronal circuits involving cortical, spinal, and peripheral neurons in healthy and pathological conditions. The articles in this collection—comprising five original studies, three extensive-reviews and two mini-reviews—explore how certain circuits regulate and integrate their actions, how they are altered in disease or after trauma, and efforts to repair circuits to restore normal function. Discussions span human and animal models of impaired motor circuits and a focus that includes much of the neuraxis: the motor cortex, hindbrain, spinal cord, somatic sensory neurons, and peripheral nerves.

The five original studies traverse the neuroanatomical spectrum, spanning hindbrain neurons, upper motor neurons, and sensory neurons to glial-peripheral nerve interactions, with particular focus on regeneration, inflammation, and excitability in ALS animal models (**Table 1**). Huang et al. study the modulation of miR-133b to promote axon regeneration of Mauthner-cells in zebrafish hindbrain. Ballou et al. characterize the inflammatory and glial response to cortical transplants after injury. Chen et al. reveal the involvement of Schwann cells in peripheral nerve regeneration. Zeng et al. describe inflammation cascades in DRG sensory neurons. Jara et al. describe circuitry changes in the motor cortex of pre-symptomatic ALS mice.

The five reviews discuss signaling cascades involving motor neurons, sensory neurons, spinal motor circuits, and electrical stimulation relevant for ALS, SMA, SCI, and regeneration (**Table 2**). Sobrido-Cameán and Barreiro-Iglesias consider apoptotic signaling cascades after SCI. Shorrock et al. discuss sensory-motor molecular mechanisms in SMA. Eisdorfer et al. contemplate how epidural electrical stimulation can enhance motility after SCI. Alvarez et al. examine the influence of spinal cord circuitry in regeneration of peripheral nerves. Falgairolle and O'Donovan deliberate on the influence of motor circuits on motor neuron vulnerability in ALS and SMA.

TABLE 1 | Highlights from the original research published within this Research Topic.

Paper	Purpose	Highlights	Model and neuron location
Huang et al.	To examine the role of miR-133b in Mauthner-cell regeneration in zebrafish	• Overexpression of miR-133b inhibited axon regeneration, whereas down-regulation of miR-133b, promoted axon outgrowth • miR-133b regulates axon regeneration by directly targeting *tppp3*, a novel regeneration-associated gene which belongs to Tubulin polymerization-promoting protein family • miR-133b overexpression attenuated mitochondrial motility in M-cells *in vivo,* correlating with enhanced axon regenerative properties	Wild-type, Zebrafish, Hindbrain
Ballout et al.	• To determine the extent to which post-traumatic inflammation following cortical lesion could influence the survival of grafted neurons, • To understand the development of their projections to target brain regions whilst understanding how transplanted cells can modulate host inflammation	• Embryonic motor cortical tissue grafted 1 week after adult motor cortex lesion resulted in an increasing numbers of astrocytes, microglia, oligodendrocytes and hematopoietic cells, compared to implanted grafts at the time of lesion • One week after cortical lesion resulted in more recruitment and activation of inflammatory brain resident mediators and peripheral infiltrating cells compared to day 0 • Graft implantation one week after cortical lesion resulted in (i) increased recruitment of A2 astrocytes in the host transplant and adjacent cortex, (ii) increased oligodendrocytes only within the transplant, and (iii) decreased M1 microglia only within the transplant	Wild-type Mouse, Motor cortex
Chen et al.	• To understand the behavior of Schwann cells migrating into a nerve gap following a transection injury • To reveal their interactions with regenerating axons within the nerve bridge	• After peripheral transection, axonal outgrowth first begins from the proximal stump, followed by Schwann cells migration from proximal and distal nerve stumps • Schwann cells overtake the axonal outgrowth, forming Schwann cell cords within the nerve bridge and most regenerating axons attach to the migrating Schwann cells and follow their trajectory across the nerve gap • Schwann cells play a crucial role in controlling the directionality and speed of axon regeneration across the nerve gap	Wild-type Mouse, Peripheral Nerve
Zeng et al.	Uncover the effects of SIRT1 on IL-33/ST2 signaling and initiation of the inflammatory cascade by TNF-α and IL-1β modulation	• After spared nerve injury, IL-33 and its receptor ST2 were upregulated in sensory neurons in dorsal root ganglia • Intrathecal injections of IL-33 or ST2 antibodies alleviated mechanical allodynia whilst downregulating the expression of TNF-α and IL-1β induced by injury • Reductions of SIRT1 activates IL-33/ST2 signaling and subsequently triggers the TNF-α and IL1β inflammatory cascades that contribute to the mechanical allodynia induced by spared nerve injury	Wild-type Rats, Dorsal Root Ganglia Sensory Neurons
Jara et al.	Determine the mechanisms that contribute to upper motor neuron vulnerability in hSOD1^{G93A} mice	• Pre-symptomatic hSOD1^{G93A} mice display altered inhibitory, but not excitatory, circuitry specific to the L2/3 pyramidal neurons in the motor cortex • Exon microarray analysis provides some molecular evidence of altered inhibitory transmission in hSOD1^{G93A} upper motor neurons • GABA and potassium receptor subunits are differentially expressed in diseased corticospinal motor neurons in hSOD1^{G93A} mice	hSOD1^{G93A} Mouse, Motor cortex

TABLE 2 | Highlights from the mini- and full- reviews published within this Research Topic.

Paper	Highlights	Paper type	Disease/Dysfunction model
Sobrido-Cameán and Barreiro-Iglesias	• Reviews the literature on caspase-8 mediated cell death after spinal cord injury in a variety of animal models • Discusses caspase-8 activated signaling pathways following spinal cord injury • Proposes novel areas to advance the knowledge on the role of caspase-8 and Fas in cell death after spinal cord injury	Mini-Review	Spinal Cord Injury (SCI)
Shorrock et al.	• Highlights that defects in sensory components of the sensory-motor system contribute to motor neuron dysfunction early in SMA • Emphasizes that cell types other than motor neurons play an important role in SMA pathogenesis • Reiterates that therapeutic interventions must rescue the wide array of defects that are observed in SMA	Mini-Review	Spinal Muscular Atrophy (SMA)
Eisdorfer et al.	• Describes the utility of epidural electrical stimulation (EES) in enhancing motility in SCI patients • Identifies several sensorimotor plasticity mechanisms that are considered to be evoked by EES through the activation of peripheral afferents • Evaluates emerging genetic modification tools that modulate afferent fibers to uncovering molecular and circuit mechanisms of EES-induced recovery from SCI	Review	Spinal Cord Injury (SCI)
Alvarez et al.	• Provides a comprehensive conceptual framework to understand how different types of nerve injuries that result in motor neuron axotomy induce distinct regenerative programs that drastically differ in motoneuron preservation, and speed and efficiency of regeneration • Proposes that synaptic plasticity of axotomized motor neurons should be divided into two distinct processes: (1) a reversible, rapid, cell-autonomous, microglia-independent shedding of synapses; and (2) a slower, microglial dependent mechanism that permanently alters spinal cord circuitry • Considers the significance of differential removal of excitatory and inhibitory synapses on synaptic plasticity of axotomized motor neurons	Review	Peripheral Nerve Injury
Falgairolle and O'Donovan	• Discusses abnormalities in the spinal cord circuitry in both ALS and SMA • Describes the sensitivity of the different motor neuron subtypes in both motor neuron diseases • Deliberates on if the selective vulnerability or resistance of different motor neuron types in ALS/SMA can be attributed to their intraspinal connectivity	Review	Amyotrophic lateral sclerosis (ALS) and spinal muscular atrophy (SMA)

Overall, this *Research Topic* describes anatomical, electrophysiological, cellular, and molecular interactions between neural networks and how advancing technologies enable clearer characterizations of dysfunctional neural circuitry.

AUTHOR CONTRIBUTIONS

All authors listed have made a substantial, direct and intellectual contribution to the work, and approved it for publication.

FUNDING

AT holds a postdoctoral position supported by a Wellcome Trust Senior Investigator Award [107116/Z/15/Z] to Giampietro Schiavo (Institute of Neurology, University College London). GZM has been supported by the NINDS, NIH (R01-NS078375), The NIH Blueprint for Neuroscience Research, NIAAA and NINDS (R01-AA027079), the Department of Defense (GR.10235006), The SMA Foundation and Project-ALS. JHM was supported by NIH (R01NS064004), NYS Dept of Health Spinal Cord Injury Research Board (C31291GG), Paralyzed Veterans Association (3160), and The Craig H Neilsen Foundation (547040).

REFERENCES

Arber, S. (2012). Motor circuits in action: specification, connectivity, and function. *Neuron.* 74, 975–989. doi: 10.1016/j.neuron.2012.05.011

Bose, P., Parmer, R., Reier, P. J., and Thompson, F. J. (2005). Morphological changes of the soleus motoneuron pool in chronic midthoracic contused rats. *Exp. Neurol.* 191, 13–23. doi: 10.1016/j.expneurol.2004.08.028

Brown, R. H., and Al-Chalabi, A. (2017). Amyotrophic lateral sclerosis. *N. Engl. J. Med.* 377, 162–172. doi: 10.1056/NEJMra1603471

Dukkipati, S. S., Garrett, T. L., and Elbasiouny, S. M. (2018). The vulnerability of spinal motoneurons and soma size plasticity in a mouse model of amyotrophic lateral sclerosis. *J. Physiol.* 596, 1723–1745. doi: 10.1113/JP275498

Eroglu, C., and Barres, B. A. (2010). Regulation of synaptic connectivity by glia. *Nature* 468, 223–231. doi: 10.1038/nature09612

Groen, E. J. N., Talbot, K., and Gillingwater, T. H. (2018). Advances in therapy for spinal muscular atrophy: promises and challenges. *Nat. Rev. Neurol.* 14, 214–224. doi: 10.1038/nrneurol.2018.4

Huntley, G. W. (2012). Synaptic circuit remodelling by matrix metalloproteinases in health and disease. *Nat. Rev. Neurosci.* 13, 743–757. doi: 10.1038/nrn3320

Ilieva, H., Polymenidou, M., and Cleveland, D. W. (2009). Non-cell autonomous toxicity in neurodegenerative disorders: ALS and beyond. *J. Cell Biol.* 187, 761–772. doi: 10.1083/jcb.200908164

Schwab, M. E., and Bartholdi, D. (1996). Degeneration and regeneration of axons in the lesioned spinal cord. *Physiol. Rev.* 76, 319–370. doi: 10.1152/physrev.1996.76.2.319

Stuart, T., and Satija, R. (2019). Integrative single-cell analysis. *Nat. Rev. Genetics* 20, 257–272. doi: 10.1038/s41576-019-0093-7

Conflict of Interest: The authors declare that the research was conducted in the absence of any commercial or financial relationships that could be construed as a potential conflict of interest.

frontiers in Molecular Neuroscience

ORIGINAL RESEARCH
published: 21 November 2017
doi: 10.3389/fnmol.2017.00375

MicroRNA-133b Negatively Regulates Zebrafish Single Mauthner-Cell Axon Regeneration through Targeting *tppp3 in Vivo*

Rongchen Huang[1†], *Min Chen*[1†], *Leiqing Yang*[1], *Mahendra Wagle*[2], *Su Guo*[2] *and Bing Hu*[1*]

[1] *Chinese Academy of Sciences Key Laboratory of Brain Function and Disease, School of Life Sciences, University of Science and Technology of China, Hefei, China,* [2] *Programs in Human Genetics and Biological Sciences, Department of Bioengineering and Therapeutic Sciences, University of California, San Francisco, San Francisco, CA, United States*

Axon regeneration, fundamental to nerve repair, and functional recovery, relies on rapid changes in gene expression attributable to microRNA (miRNA) regulation. MiR-133b has been proved to play an important role in different organ regeneration in zebrafish, but its role in regulating axon regeneration *in vivo* is still controversial. Here, combining single-cell electroporation with a vector-based miRNA-expression system, we have modulated the expression of miR-133b in Mauthner-cells (M-cells) at the single-cell level in zebrafish. Through *in vivo* imaging, we show that overexpression of miR-133b inhibits axon regeneration, whereas down-regulation of miR-133b, promotes axon outgrowth. We further show that miR-133b regulates axon regeneration by directly targeting a novel regeneration-associated gene, *tppp3*, which belongs to Tubulin polymerization-promoting protein family. Gain or loss-of-function of *tppp3* experiments indicated that *tppp3* was a novel gene that could promote axon regeneration. In addition, we observed a reduction of mitochondrial motility, which have been identified to have a positive correlation with axon regeneration, in miR-133b overexpressed M-cells. Taken together, our work provides a novel way to study the role of miRNAs in individual cell and establishes a critical cell autonomous role of miR-133b in zebrafish M-cell axon regeneration. We propose that up-regulation of the newly founded regeneration-associated gene *tppp3* may enhance axonal regeneration.

Keywords: axon regeneration, miR-133b, single-cell level, single-cell electroporation, *tppp3, in vivo* imaging

OPEN ACCESS

Edited by:
John Martin,
City College of New York (CUNY), United States

Reviewed by:
Antón Barreiro-Iglesias, Universidade de Santiago de Compostela, Spain
Xiao-Feng Zhao, University of Michigan, United States

***Correspondence:**
Bing Hu
bhu@ustc.edu.cn

[†] *These authors have contributed equally to this work.*

Received: *28 August 2017*
Accepted: *27 October 2017*
Published: *21 November 2017*

Citation:
Huang R, Chen M, Yang L, Wagle M, Guo S and Hu B (2017) MicroRNA-133b Negatively Regulates Zebrafish Single Mauthner-Cell Axon Regeneration through Targeting tppp3 in Vivo. Front. Mol. Neurosci. 10:375. doi: 10.3389/fnmol.2017.00375

INTRODUCTION

Axonal regeneration, critical for the maintenance of the nervous system, requires the coordinated expression of many regeneration-associated genes in the soma (Wu et al., 2012). Growing evidence indicates that microRNAs (miRNAs) play a crucial role during this process (Kloosterman and Plasterk, 2006; Strickland et al., 2011; Wu and Murashov, 2013; Li S. et al., 2016; Tedeschi and Bradke, 2017). MiRNAs are small, non-coding RNAs that function as negative regulators of gene expression, through imperfect base-pairing with the 3′-untranslated region (UTR) of target mRNAs thereby promoting mRNA degradation or inhibiting protein translation (Hong et al., 2014). Their ability to simultaneously regulate the expression of several genes suggests that miRNAs are crucial coordinators of complex gene expression programs.

Zebrafish exhibit high regenerative capacity in many tissues and organs, including heart muscles, spinal cord, sensory hair cells, appendages, and blood vessels (Stoick-Cooper et al., 2007). Moreover, many miRNAs have been implicated in these regenerative processes. For example, miR-101a regulates adult zebrafish heart regeneration (Beauchemin et al., 2015), and miR-10 regulates angiogenesis by affecting the behavior of endothelial cells (Hassel et al., 2012). MiR-133b, the miRNA of interest in this study, has been widely reported to participate in many regulatory processes. For example, miR-133b is considered as a tumor repressor in various human cancers, such as colorectal cancer (Hu et al., 2010; Akçakaya et al., 2011; Xiang and Li, 2014), gastric cancer (Wen et al., 2013), and gastrointestinal stromal tumor (Yamamoto et al., 2013). It also plays an important role in enhancing differentiation among different cell types, including muscle cells (Koutsoulidou et al., 2011) and neurons (Heyer et al., 2012). However, miR-133b exhibits different effects on different tissue regeneration. It has been shown to be a negative regulator in fin regeneration by targeting mps1 (Yin et al., 2008), while promoting spinal cord functional recovery after injury by targeting RhoA (Yu et al., 2011; Theis et al., 2017). Although, it also has been reported to promote neurite outgrowth at cellular level (Lu et al., 2015), its role, if any, in single-cell axon regeneration is not known.

In vivo imaging of single-axon regeneration in intact vertebrate is a powerful approach to gain mechanistic insights into this process (Kerschensteiner et al., 2005; Canty et al., 2013; Lorenzana et al., 2015; Xu et al., 2017). Although, previous studies have established miRNAs as crucial regulators in regenerative processes, little is known regarding their role in a single neuron during regeneration. Since nerve injury often associates with damages of both the nerve and neighboring tissues, it has been difficult to unveil autonomous vs. non-autonomous factors that influence axon regeneration *in vivo* (Rieger and Sagasti, 2011).

Using two-photo axotomy, a technology that can precisely injure a single axon (O'Brien et al., 2009; Canty et al., 2013; Xu et al., 2017), we have demonstrated that Mauthner-cells, a hindbrain neuronal type with large soma and long axons projecting toward the spinal cord, have the capacity to regenerate (Xu et al., 2017). In this study, we examined the role of miR-133b in M-cell regeneration. By single-cell electroporation and a vector-based expression system, we successfully altered the expression of miR-133b specifically in the M-cell. With a combination of gain-of-function and loss-of-function experiments, we demonstrated that miR-133b inhibits the regenerative process in M-cells. We further uncovered a novel regeneration-associated gene, *tppp3*, as a direct target of miR-133b in this process. Collectively, our findings identify a cell intrinsic mechanism involving miR-133b and its direct target *tppp3* in regulating axon regeneration *in vivo*.

MATERIALS AND METHODS

Animal Care

Zebrafish (*Danio rerio*) WT/AB line was used in this study. Zebrafish embryos were maintained in embryo medium on a 14/10 light/dark cycle at 28.5°C. In case of the formation of pigment, 0.2 mM N-phenylthiourea (PTU, sigma) was added to the embryo medium at 24 h post fertilization (hpf). All animal manipulations were preformed strictly following the guidelines and regulations presented by the University of Science and Technology of China (USTC) Animal Resources Center and University Animal Care and Use Committee. The protocol was approved by the Committee on the Ethics of Animal Experiments of the USTC (Permit Number: USTCACUC1103013).

Plasmids Construction

To overexpress miRNAs, a construct containing pri-miR-133b/pri-miR-23a/pri-miR-21 was made by amplifying a genomic region containing the miR-133b/miR-23a/miR-21 precursor. The resulting PCR fragments were then inserted into the linearized pUAS-mCherry digested by NotI, locating at the 3′-UTR of mCherry.

To knock down miR-133b, we used the miRNA "sponge" assay, which presents an efficient and permanent miRNA loss-of-function by imperfectly binding to a miRNA of interest (Cohen, 2009). The plasmid pUAS-mcherry-8 × miR-133b sponge was designed by ourselves and then constructed by Sangon (Shanghai, China).

To generate overexpression of TPPP3 construct, full-length *tppp3* was initially amplified from complementary DNA (cDNA) of the WT/AB zebrafish strain. The PCR fragment was inserted into a plasmid backbone containing UAS. Plasmid UAS-tppp3 was co-delivered with both pUAS-mCherry and pCMV-Gal4-VP16 while electroporation.

ShRNA design was performed using the siRNA design tool under the following website: http://www.genscript.com/design_center.html (Dong et al., 2013). We selected the top five shRNAs (shRNA1-shRNA5) for further experiment. ShRNA expression vector was constructed in the following way: The modified mir30e backbone (Dong et al., 2013) was firstly synthesized with PacI-NheI sites for cloning target shRNA oligos. This modified mir30e precursor was cloned into pmini-Tol2-UAS-tdTOM vector downstream of tdTOM ORF to generate pmT2-UAS-tdTOM-mir30e-ShRNA (SG1180-A). We then cloned the fragment containing miR-shRNA structures (guide sequence, loop sequence, target sequence, and the flanking sequences) into pUAS-mCherry plasmid, locating in mCherry 3′-UTR. Target shRNA structures were synthesized by Sangon (Shanghai, China) and then cloned into PacI-NheI site.

Microinjection and Quantitative Real-Time PCR

One-cell stage zebrafish embryos were injected with a solution consisting of 30 ng/μl CMV-Gal4-VP16 plasmid and 30 ng/μl pUAS-mCherry/pUAS-mCherry-mircoRNA/pUAS-mCherry-miR-shRNA. To detect miRNAs level, 3 days post fertilization (dpf) zebrafish larvae with relatively high mosaic red fluorescence were selected for total RNAs isolation by miRNA Isolation Kit (Tiangen), according to the manufacturer's protocols. Each sample was reverse-transcribed into cDNA by miRNA First-Strand cDNA Synthesis Kit (Tiangen) and was subjected to qRT-PCR analysis with qPCR Detection Kit (Tiangen). To detect mRNAs levels, 10 hpf zebrafish embryos

expressing red fluorescence were selected to isolate total RNAs with the same kit mentioned above. Each sample was reverse-transcribed into cDNA with HiScriptII Q RT SuperMix (Vazyme) and was subjected to qRT-PCR analysis with AceQ qPCR SYBR Master Mix (Vazyme). Each experiment was carried out with three biological and experimental replicate. Results were shown as mean fold changes ±s.e.m. qRT–PCR primers were shown in Table S1.

Single-Cell Electroporation

Before electroporation, 4 dpf zebrafish larvae were embedded in 1% low-melting agarose gel on an electroporation chamber. Using a micropipette (WPI, USA) pulled by a micropipette puller (P-97, Sutter, USA) to electroporate plasmids into the M-cell soma by pushing the tip against it with a series of pulses at 14–16 V. CMV-Gal4-VP16 plasmid was co-delivered into the unilateral M-cell of zebrafish larva with pUAS-mCherry-microRNAs (plasmids used to overexpress specific miRNA)/pUAS-mCherry-microRNA sponge (plasmid used to inhibit specific miRNA)/pUAS-mCherry-miR-shRNA (plasmid used to inhibit *tppp3*). Each plasmid concentration is 120 ng/μl. Zebrafish electroporated with pCMV-Gal4-VP16 and pUAS-mCherry were treated as control. For the experiment to overexpress TPPP3, pUAS-tppp3 was delivered into cell soma with both pCMV-Gal4-VP16 and pUAS-mCherry. After electroporation, larvae were returned back to embryo medium containing PTU. Then we selected morphologically healthy zebrafish expressing red fluorescence in M-cells for later experiment.

Two-Photon Axotomy

Before axotomy, 6 dpf zebrafish larvae expressing red fluorescence in unilateral M-cells were anesthetized in MS222 (Sigma, USA) and fixed in 1% low-melting agarose. A Zeiss microscope (LSM710, Germany) was used to ablate the M-cell axons over cloacal pores. We normally set the 800 nm two-photon laser at an intensity of 12–15% to damage axon over ∼1.5 s (Xu et al., 2017).

In Vivo Imaging and Data Analysis

Before imaging, embryos were anesthetized by MS222 and then embedded in 1% low melting point agarose in embryo medium containing MS222. All images and time-lapse movies were taken from lateral views of the spinal cord, anterior to the left, and dorsal toward the top.

To observe M-cells regrowth after ablation at 6 dpf, anesthetized zebrafish were imaged at 1–2 days post-axotomy (dpa) using Olympus FV1000 confocal microscope (Olympus, Tokyo, Japan) equipped with a 40x, 0.8 N.A. water-immersion objective at 2-μm intervals. All images well spliced using with Photoshop CS4 (Adobe, USA). We defined the starting point of regrowth as the ablated site of axons just above cloacal pores, and the axonal terminal of regeneration was stipulated as the end point of regrowth axons. In this article, regeneration length refers to the maximum regenerated axon length of one branch, while total regeneration length refers to all the regenerated axon branches length combined. All regenerative length was calibrated to convert pixels into distance using FV10-ASW 4.2 viewer software.

For investigating mitochondrial transport in single M-cell *in vivo*, zebrafish larva electroplated with pUAS-mito-eGFP (plasmid used to label mitochondria) were imaged at 6 dpf using a confocal microscope with a 60x, 0.9 N.A. water-immersion objective. 2.5-min movies of the axonal area, locating within 200 nm proximal to the site above the cloacal pores, were taken with an imaging frequency about 1.5 s, and the imaging length of axons was ∼43 mm at the site of the axon. All images were processed with Fiji/ImageJ (National Institutes of Health, USA). The quantification of mitochondrial dynamics were measured as previously described (Misgeld et al., 2007; Plucinska et al., 2012; Takihara et al., 2015; Xu et al., 2017). Mitochondrial motility was defined as the percentage of moving mitochondria, which were identified to move more than 2 μm, during the 2.5-min time-lase movies. The velocity of a moving mitochondrion referred to the total moving distance of a mitochondrion divided by its observed moving time.

EGFP Sensor Assay

In vitro transcription of EGFP-tppp3 3′-UTR, EGFP-tppp3 mut-3′-UTR and mCherry mRNAs were performed with mMESSAGE mMACHINE T7 Ultra Kit (Invitrogen) and these synthesized mRNAs were purified with MEGAclearTM Kit (Invitrogen). Zebrafish embryos at one-cell stage were injected with a combing solution of sensor mRNA and mCherry mRNA. When applicable, 10 μM miR-133b duplex was added as an experimental group, while 10 μM non-sense duplex was added as a control. EGFP fluorescence was quantified at 24–28 h post-fertilization (hpf) using software Fiji-imageJ.

Statistical Analysis

The distribution of data points was expressed as mean ± standard error of the mean (S.E.M.), or as relative proportion of 100% as mentioned in the appropriate legends. Depending on the number of the groups and independent factors, student's *t*-tests, one-way analyses of variance (ANOVA) and non-parametric tests were used as indicated in the figures. Results were classed as significant as follows: $^{*}P < 0.05$, $^{**}P < 0.01$, and $^{***}P < 0.001$.

RESULTS

Overexpression of miR-133b in Single M-Cell Inhibits Axon Regeneration

We have identified in our previous study that M-cells have strong regenerative capacity (Xu et al., 2017). More than 90% of two-photo ablated M-cells could regenerate a certain length in our experiments. To explore the role of miR-133b in M-cell axon regeneration, we performed cell type-specific overexpression. A vector-based miRNA expression was used to achieve enduring expression of the miRNA during our experimental time window. We constructed a vector containing dre-pri-miR-133b sequence (miRBase Accession: MI0001994) in the 3′-UTR of mCherry, which conveniently marked the cells that expressed the miR-133b (**Figure 1A**). The plasmid UAS-mCherry-miR-133b was co-injected with pCMV-Gal4-VP16 into one-cell zebrafish embryos.

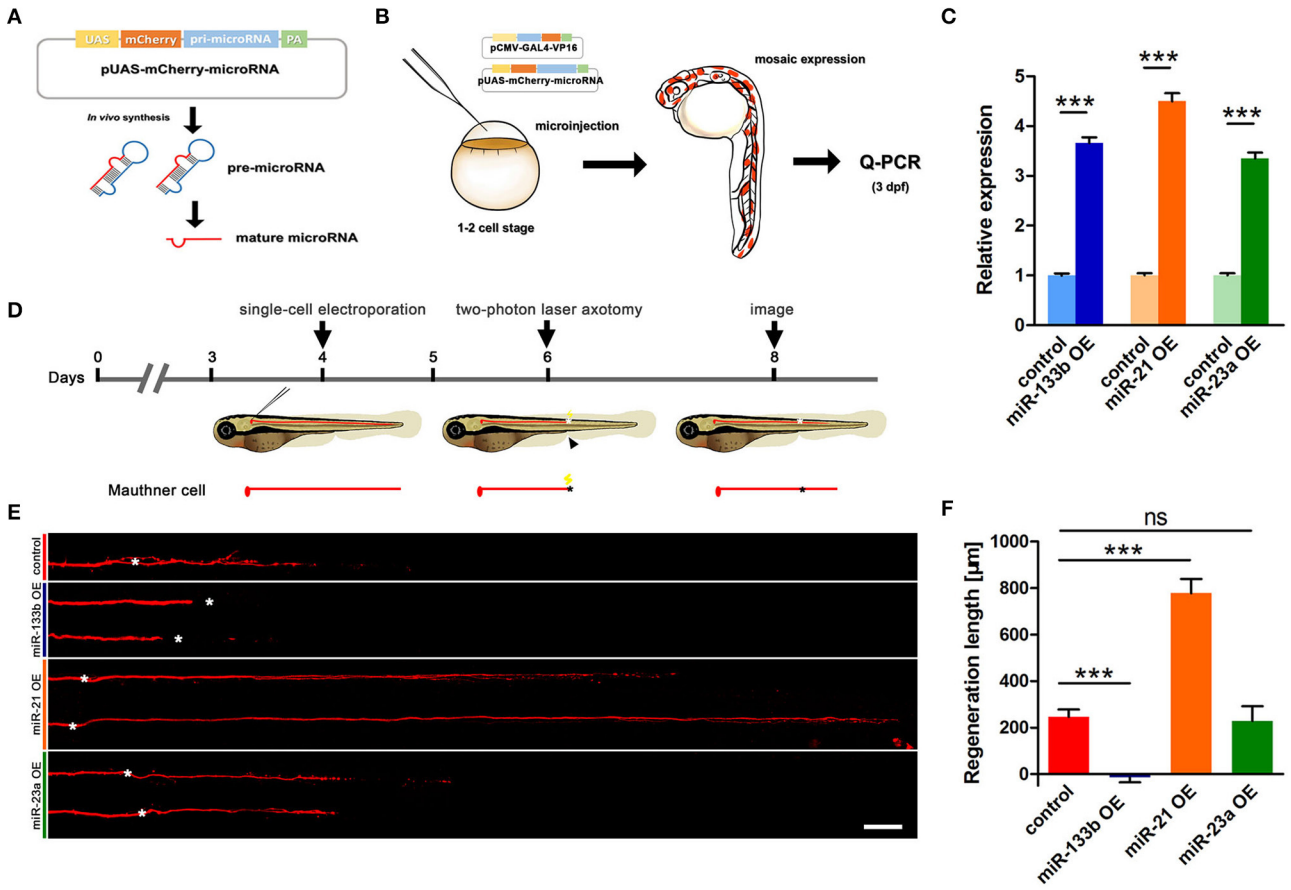

FIGURE 1 | Vector-based overexpression of miR-133b by single-cell electroporation inhibits M-cell regeneration. **(A)** Construction of the vector-based microRNA expression system. Plasmids express only mCherry served as control vector. **(B)** Validation of the vector-based expression system. Choose the larvae at 3 dpf with relatively high mosaic expression to detect the expression of microRNA. **(C)** Quantitative RT-PCR analysis exhibited an increase of different miRNA levels by vector-based expression *in vivo*. The control vector-injected embryos served as controls. **(D)** Design for microRNA-expression vector electroporation studies. Axons of Mauthner-cell labored with red fluorescent was ablated at 6 dpf right above the cloacal pores (black arrow), and confocal image at 8 dpf (2 dpa). Black asterisk: ablation point. **(E)** Confocal imaging of M-cells expressing different miRNAs at 2 dpa. White asterisk: ablation point. Scale bar: 50 μm. **(F)** Regeneration length at 2 dpa. One-way ANOVA, $P < 0.0001$: Student's two-tailed *t*-test, control vs. miR-133b OE, $P < 0.0001$; control vs. miR-21 OE, $P < 0.0001$; control vs. miR-23a OE, $P = 0.8312$. $^{*}P < 0.05$, $^{***}P < 0.001$. Error bars represent S.E.M.

As a control, embryos were injected with pUAS-mCherry and pCMV-Gal4-VP16. We then selected zebrafish larvae with relatively high mosaic red fluorescence at 3 dpf to isolate the total RNA (**Figure 1B**). Our qRT-PCR data showed that miR-133b in experimental group (EG) was more than three times of that in control, indicating that our constructed plasmid UAS-mCherry-miR-133b could successfully drive overexpression of miR-133b (**Figure 1C**).

Next, we used this vector system to overexpress miR-133b in individual M-cells at 4 dpf via single-cell electroporation. We selected the zebrafish with red fluorescence in unilateral M-cell at 6 dpf for two-photon laser axotomy and visualized axon regeneration at 2 dpa (**Figure 1D**). Our imaging data showed that most M-cells in control could regenerate a certain length, while M-cell overexpressing miR-133b could hardly regenerate [control: 243.7 ± 32.9 μm, $n = 33$ fish vs. miR-133b overexpression (OE): −14.8 ± 20.7 μm, $n = 16$ fish] (**Figures 1E,F**). To further verify the specific role of miR-133b in regulating axon regeneration, we overexpressed another two miRNAs, miR-23a and miR-21, with the same assay as mentioned above. Together with qRT-PCR results confirming that miR-23a and miR-21 were indeed overexpressed in zebrafish via vector-based miRNA expression assay (**Figure 1C**), we found out that miR-23a, a miRNA that has not been reported to be associated with axon regeneration, had no obvious effect on M-cell axon regeneration; while miR-21, which has been shown to promote regeneration in different organs (Strickland et al., 2011; Han et al., 2014; Hoppe et al., 2015), remarkably promoted M-cell axon regeneration (control: 243.7 ± 32.9 μm, $n = 33$ fish vs. miR-23a OE: 229.0 ± 62.4 μm, $n = 10$ fish vs. miR-21 OE: 778.4 ± 60.8 μm, $n = 12$ fish; **Figures 1E,F**).

Since researches on dre-miRNAs often explore their roles in different processes using miRNA duplex, to further verify miR-133b's role on axon regeneration, we also expressed the miR-133b duplex in M-cell by single-cell electroporation. M-cells expressing only rhodamine-dextran (3,000 molecular

weight, Invitrogen) (named None) seemed to have similar outgrowths to those expressing non-sense duplex (named Negative Control), while both explicated a slight increase, even though without significant discrepancy, compared to M-cells in experimental group (expressing miR-133b duplex), not matter at 1 dpa or 2 dpa (1 dpa: None: 142.3 ± 19.0 μm, $n = 26$ fish; Negative control: 140.0 ± 15.8 μm, $n = 24$ fish; miR-133b duplex: 102.7 ± 17.6 μm, $n = 23$ fish; 2 dpa: None: 464.8 ± 40.5 μm, $n = 20$ fish; Negative control: 396.7 ± 32.5 μm, $n = 22$ fish; miR-133b duplex: 373.4 ± 33.9 μm, $n = 23$ fish; **Figure S1**). This result was consistent with the results obtained by vector-based system, indicating that miR-133b has negatively effects on M-cell axon regeneration. Together, these results indicate that the reduction of M-cell regenerative capability by miR-133b is specific and cell intrinsic.

Impairment of miR-133b Function in M-Cell Promotes Axon Outgrowth

To determine whether loss of miR-133b in single M-cells could also regulate its axon regeneration, we needed an assay that could achieve long-term miRNA loss-of-function. MiRNA sponges have been shown to efficiently bind to endogenous miRNAs and block their silencing activity with bulged miRNA binding sites (Ebert et al., 2007; Cohen, 2009; Otaegi et al., 2011). Moreover, the bulged sites can protect against cleavage and degradation of sponge RNA by the Ago2 component of the RISC (Ebert et al., 2007; Ebert and Sharp, 2010), which can satisfy our experimental requirement.

We constructed a plasmid containing 8 bulged target sites complementary to miR-133b in 3′-UTR of mCherry reporter gene driven by the UAS promoter (**Figure 2A**). To testify the ability of this plasmid in blocking miR-133b activity in zebrafish, we examined the expression of a known miR-133b target gene, *mps1* (Yin et al., 2008), in 10 hpf zebrafish embryos injected with a combination of pUAS-mCherry-8 × miR-133b sponge and pCMV-GAL4-VP16 at one-cell stage. The *mps1* mRNA level increased in zebrafish larvae expressing the miR-133b sponge, suggesting that it could reduce miR-133b activity in zebrafish (**Figure 2B**).

Next, we examined the consequence of knocking down miR-133b activity in axon regeneration. Remarkably, most axons regenerated with supernumerary branches (**Figure 2C**). The longest regeneration length of a single axon had no significant difference between control and experimental group (control: 253.7 ± 34.9 μm, $n = 30$ fish vs. miR-133b sponges: 296.7 ± 40.5 μm, $n = 20$ fish; **Figure 2D**). However, the total regeneration length, all branches combined, was significantly different (control: 486.7 ± 78.8 μm, $n = 30$ fish vs. miR-133b sponges: 835.2 ± 131.4 μm, $n = 20$ fish; **Figure 2E**). The experimental group had significantly more axonal branches than the control (control: 2.13 ± 0.28, $n = 30$ fish vs. miR-133b sponges: 4.50 ± 0.83 μm, $n = 20$ fish; **Figure 2F**). Collectively, these results demonstrate that blocking the function of miR-133b promotes M-cell axon outgrowth, which is a phenotype that is complementary to overexpressing miR-133b in M-cells.

Tppp3 Is an *in Vivo* Target of miR-133b

Typically, one miRNA can suppress the expression of many genes by interacting with the 3′-UTR or the coding regions of the targets mRNAs (Lewis et al., 2005; Duursma et al., 2008; Forman et al., 2008). We searched several databases, including TargetScan Fish, miRBase and microcosm Targets, and identified potential targets containing complementary regions to miR-133b seed sequences in their 3′-UTR. We focused on one gene, *tppp3*, which has a single binding site for miR-133b at its 3′-UTR. In addition, *tppp3* corresponds perfectly to nucleotides 2–7 of the mature miR-133b in zebrafish (**Figure 3A**). TPPP3 is a member of tubulin polymerization promoting protein family. Previous studies identified TPPP3 as a potent inducer of tubulin polymerization (Vincze et al., 2006) and human TPPP3 binds and stabilizes microtubules (MTs; Oláh et al., 2017). Since regulation of axonal microtubule (MT) dynamics influence axon regeneration (Sengottuvel and Fischer, 2011; Bradke et al., 2012; Hur et al., 2012), and pharmacological stabilization of MTs by paclitaxel or related molecules promotes axon regeneration *in vitro* and *in vivo* (Hellal et al., 2011; Sengottuvel et al., 2011; Ruschel et al., 2015), we hypothesized that miR-133b might regulate axon regeneration through directly modulating *tppp3* mRNA *in vivo*.

We firstly detected the mRNA level of *tppp3* in miR-133b overexpressed or miR-133b sponge expression zebrafish embryos. Our qRT-PCR results showed that the mRNA level of *tppp3* in 10 hpf zebrafish embryos overexpressing miR-133b was lower than that in control (**Figure 3B**), while *tppp3* mRNA level was increased in embryos expressing miR-133b sponge compared with that in control (**Figure 3C**). We then used zebrafish embryo sensor assays (Giraldez et al., 2005). Two mRNAs were synthesized, one encoding enhanced green fluorescent protein (EGFP) with 3′- UTR of *tppp3* and the other composed of mCherry fluorescent protein with a poly(A) alone. These mRNAs were co-injected into one-cell zebrafish embryos, in the presence of miR-133b RNA duplex or non-sense duplex (GenePharma). Injections of these two mRNAs along with a non-sense RNA duplex (negative control) resulted in both high EGFP expression and mCherry expression. However, when a synthesized duplex of miR-133b was co-injected, EGFP signals were dampened by almost 50% with no detective changes in mCherry signals (negative control: 100.0 ± 7.0%, $n = 10$ fish vs. miR-133b duplex: 43.5 ± 3.7%, $n = 10$ fish; **Figures 3D,E**). When the seed sequence in the 3′-UTR of *tppp3* was mutated, we found no difference in EFGP signals between non-sense RNA duplex and miR-133b RNA duplex (negative control: 100.0 ± 11.9%, $n = 10$ fish vs. miR-133b duplex: 117.1 ± 12.0%, $n = 10$ fish; **Figures 3F,G**).

In conclusion, our results indicate that *tppp3* is a downstream gene of miR-133b *in vivo*.

TPPP3 Is Critical to Enhance Axonal Outgrowth

Given the effects of miR-133b on *tppp3* expression and the role of miR-133b in neurite outgrowth, we next planned to investigate the effects of gain or loss-of-function of *tppp3* on

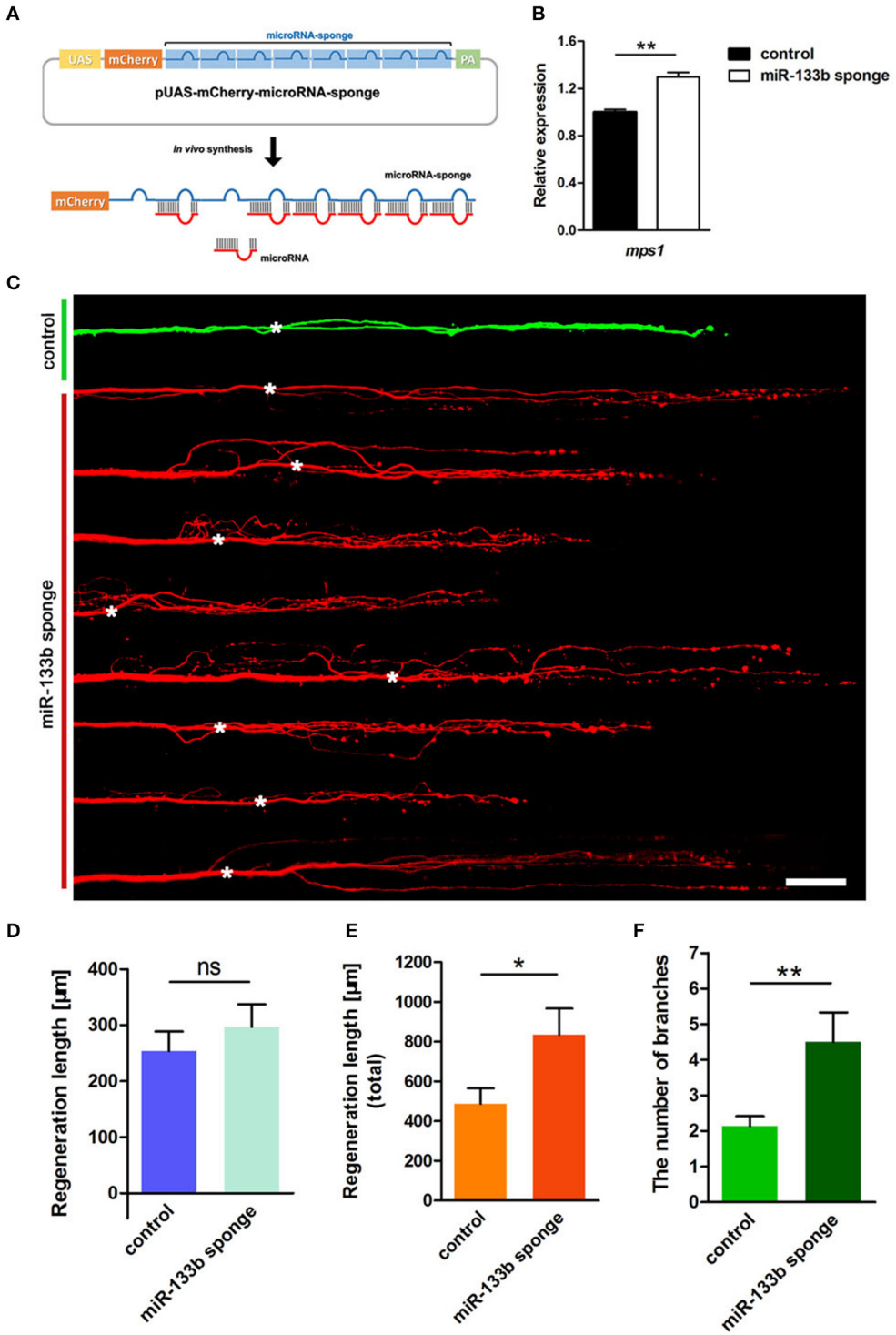

FIGURE 2 | Knockdown of miR-133b by expressing miR-133b sponge facilitates M-cell regeneration. **(A)** Design of miRNA sponges. The construction of miRNA sponges was manipulated by inserting multiple microRNA binding sites in the 3′-UTR of the mcherry reporter gene. Plasmids express only mCherry served as control vector. **(B)** Quantitative RT-PCR analysis exhibited an increase in *mps1* mRNA expression in 10 hpf zebrafish embryos by miR-133b sponge expression *in vivo*. **(C)** Confocal imaging of M-cell at 2 dpa. White asterisk: ablation point. Scale bar: 50μm. **(D)** Regeneration length at 2 dpa. Student's two-tailed *t*-test, $P = 0.4300$. **(E)** Total regeneration length at 2 dpa. Student's two-tailed *t*-test, $P = 0.0194$. **(F)** The number of branches at 2 dpa. Non-parametric tests, $P = 0.0047$. $^{*}P < 0.05$, $^{**}P < 0.001$. Error bars represent S.E.M.

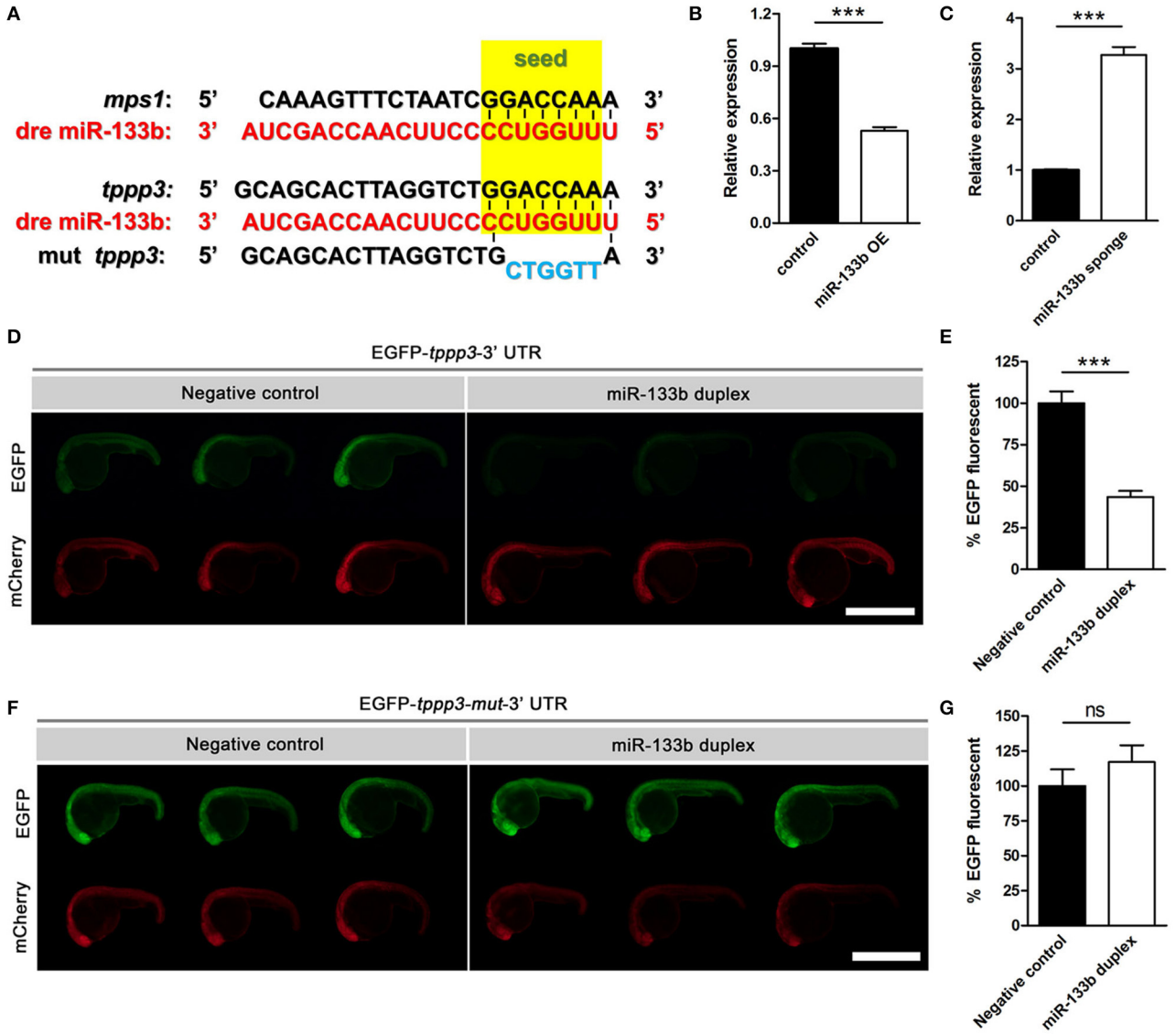

FIGURE 3 | Sequence alignment and the EGFP sensor assay show that miR-133b targets *tppp3*. **(A)** Sequence alignment of zebrafish miR-133b, *tppp3* 3′UTR and its mutation version (within the 2–7 nt mutated) was shown, with the seed sequences highlighted in yellow box and the mutational nucleotides in blue. *mps1* 3′UTR was shown as a control. **(B)** Quantitative RT-PCR analysis exhibited a decrease in *tppp3* mRNA expression in 10 hpf zebrafish embryos by the vector-based miR-133b overexpression *in vivo*. **(C)** Quantitative RT-PCR analysis exhibited an increase in *tppp3* mRNA expression in 10 hpf zebrafish embryos by miR-133b sponge expression *in vivo*. **(D)** EGFP-*tppp3* 3′UTR shown strong fluorescent signals when co-injected with non-sense duplex (as negative control), but failed to give fluorescent signals when co-injected with miR-133b duplex. mCherry mRNA was injected as a control. **(E)** The EGFP-*tppp3* 3′UTR fluorescence was expressed as a percentage of fluorescent signal observed from the negative control. Student's two-tailed *t*-test, $P < 0.0001$. $n = 10$ for each group. **(F)** Both groups shown strong fluorescent signals whenever the EGFP-*tppp3* mut-3′UTR coinjected with the miR-133b duplex or non-sense duplex. **(G)** The EGFP-*tppp3* mut-3′UTR fluorescence was expressed as a percentage of fluorescent signal observed from the negative control. Student's two-tailed *t*-test, $P = 0.3219$. $n = 10$ for each group. ***$P <$ 0.001. Error bars represent S.E.M.

regenerative axon growth. We firstly overexpressed *tppp3* by electroplating into M-cell at 4 dpf a plasmid containing the zebrafish *tppp3* cDNA. As a control, pUAS-mcherry and pCMV-GAL4 was delivered. Consistent with the effects of miR-133b sponge on axonal regeneration (**Figure 4A**), overexpression of *tppp3* in M-cell significantly increased the total regeneration length (Regenerative length: control: 255.6 ± 37.2 μm, $n = 27$ fish vs. TPPP3 OE: 382.9 ± 66.6 μm, $n = 15$ fish; total regeneration length: control: 476.2 ± 83.2 μm, $n = 27$ fish vs. TPPP3 OE: 855.2 ± 177.4 μm, $n = 15$ fish; **Figures 4B,C**), although there is no significant difference in branching number (control: 2.11 ± 0.29, $n = 27$ fish vs. TPPP3 OE: 3.60 ± 0.73, $n = 15$ fish; **Figure 4D**).

To test whether knockdown of *tppp3* might cause regenerative defects similar to miR-133b overexpression, we used designed

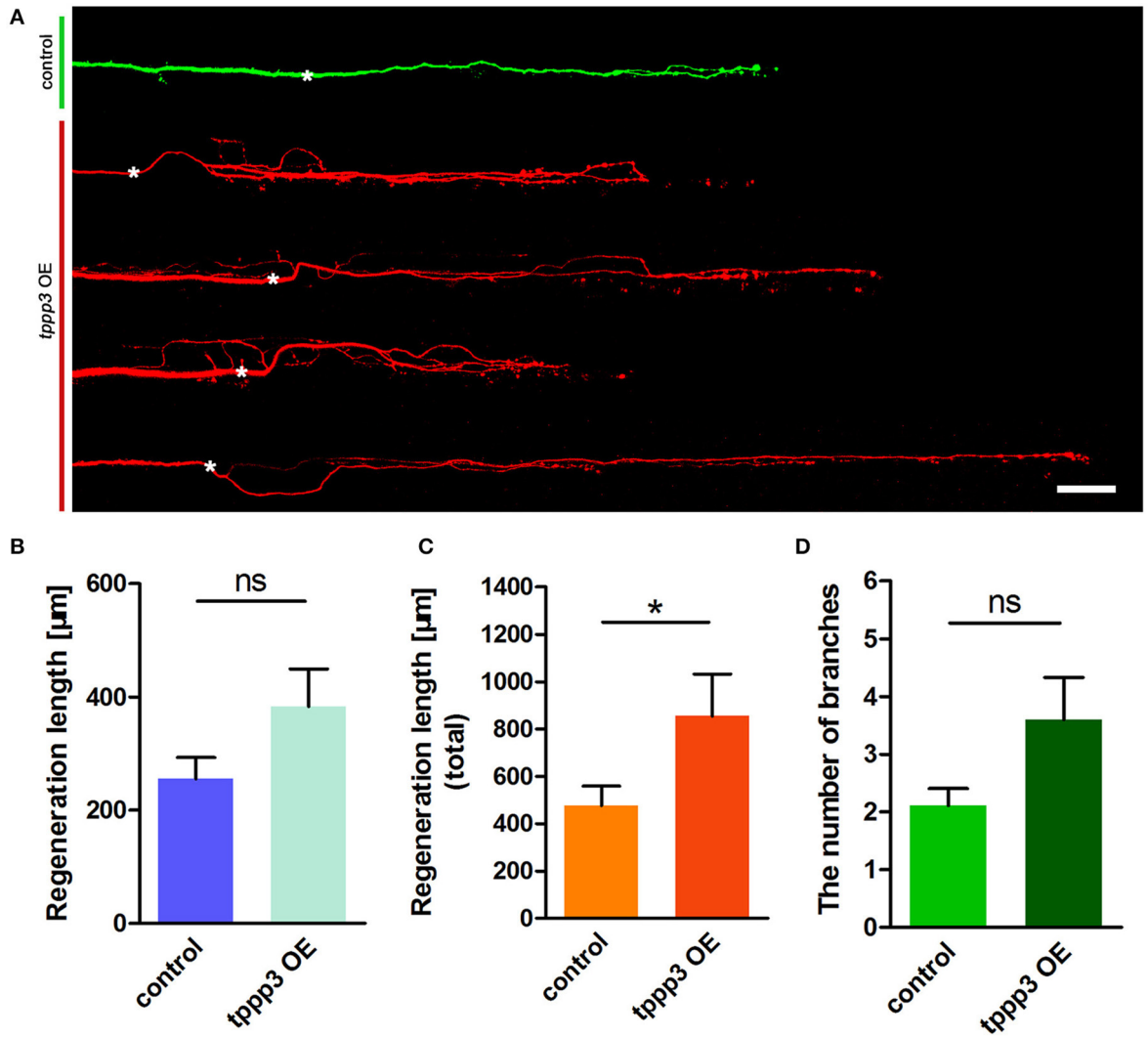

FIGURE 4 | Overexpression of *tppp3* by single-cell electroporation promotes M-cell regeneration. **(A)** Confocal imaging of M-cell at 2 dpa. White asterisk: ablation point. Scale bar: 50 μm. **(B)** Regeneration length at 2 dpa. Student's two-tailed *t*-test, $P = 0.0775$. **(C)** Total regeneration length at 2 dpa. Student's two-tailed *t*-test, $P = 0.0338$. **(D)** The number of branches at 2 dpa. Non-parametric tests, $P = 0.0516$. $^*P < 0.05$. Error bars represent S.E.M.

shRNAs to silence *tppp3* based on the miR-ShRNAs system. MiR-shRNAs have now been widely used in mammals and zebrafish (De Rienzo et al., 2012; Dong et al., 2013; Shinya et al., 2013), *in vitro* and *in vivo* (Giraldez et al., 2005; Zuber et al., 2011), due to its higher efficiency than simple hairpin designs. We designed shRNAs employing the primary miR-30 backbone. Based on the Web-based shRNA design tool (https://www.genscript.com), five shRNAs (shRNA1-shRNA5) targeting the *tppp3* gene were selected (**Figure S2**). mCherry was used as a fluorescent reporter to mark the zebrafish embryos that expressed the miR-shRNA (**Figure 5A**). To valid the function of these shRNAs, we injected the miR-shRNA expressing plasmids combing with pCMV-GAL4 into one-cell stage embryos and isolated mRNA of these embryos exhibiting red fluorescence at 10 hpf to examine the *tppp3* mRNA level. We found that, among these five shRNAs, shRNA-5 exhibited the significant reduction of *tppp3* mRNA level (**Figure 5B**). We then investigated the effects of shRNA-5 on axonal regeneration by delivering it into M-cells via single-cell electroporation at 4 dpf. To avoid the effects of other miR-shRNA structures (guide sequence, loop sequence, and the flanking sequences) on the capability of regeneration, cells expressing shRNA-1, which had little effects on reducing *tppp3* mRNA (**Figure 5B**), were used as an additional control. Both imaging and quantitative results indicated that shRNA-5 diminished the regenerative length of damaged axons, while shRNA-1did not (control: 278.2 ± 33.1 μm, $n = 26$ fish vs. miR-shRNA-1: 314.2 ± 42.7 μm, $n = 8$ fish vs. miR-shRNA-5: 97.6 ± 47.7 μm, $n = 20$ fish; **Figures 5C,D**).

Taken together, these results indicate that *tppp3* is critical to promote axon outgrowth.

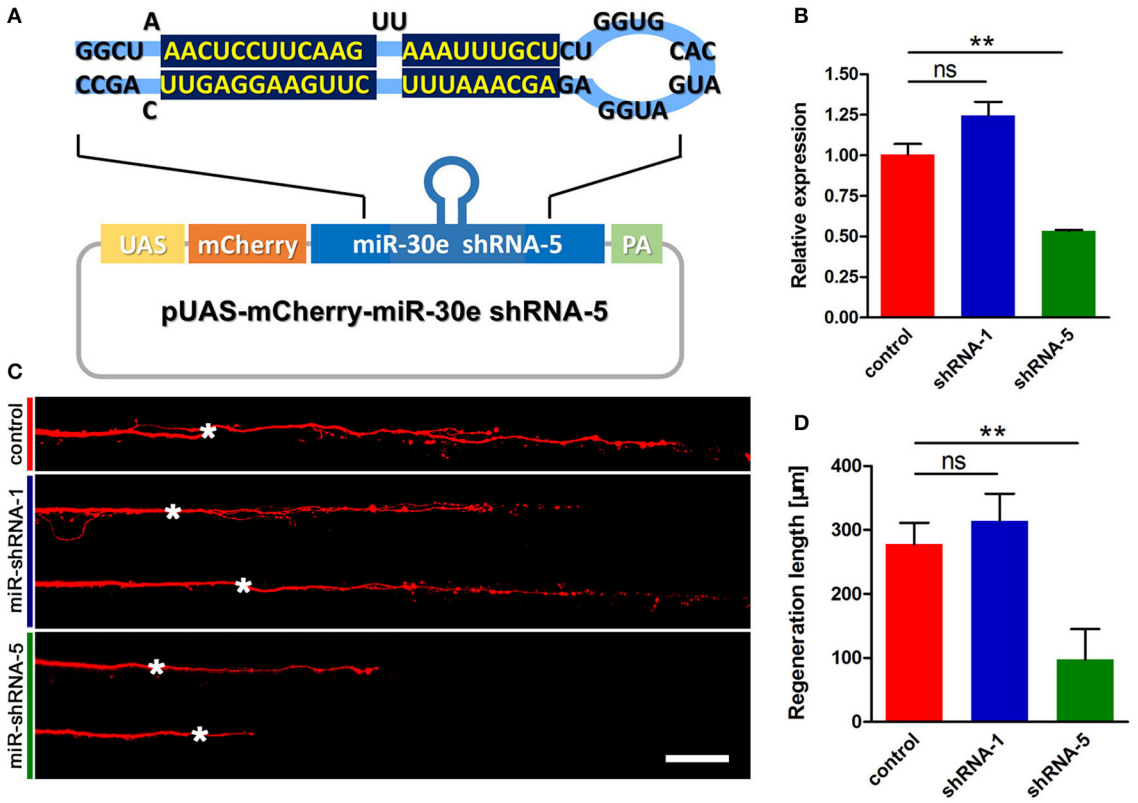

FIGURE 5 | miR-shRNA based gene silence of *tppp3* diminishes regenerative length of M-cell **(A)** Diagram of miR-shRNA system. Sequence of ShRNA-5 was presented here, with the guide strand (bottom) highlighted in dark blue. **(B)** Quantitative RT-PCR analysis exhibited a deduction of *tppp3* mRNA in shRNA-5 expressing embryos. **(C)** Confocal imaging of M-cell at 2 dpa. White asterisk: ablation point. Scale bar: 50 μm. **(D)** Regeneration length at 2 dpa. Student's two-tailed *t*-test, control vs. shRNA-1, $P = 0.5807$; control vs. shRNA-5, $P = 0.0025$. $^{**}P < 0.01$. Error bars represent S.E.M.

Mir-133b Attenuates Mitochondrial Motility in M-Cell

Mitochondria plays a critical role in axon regeneration, a highly energy-demanding process. Our previous study has indicated that mitochondrial trafficking is associated with axon regenerative capacity, suggesting that axons having more motile mitochondria regenerate better than those having less ones (Xu et al., 2017). Moreover, another research group finds out that mature injured axons in mice can regenerate by enhancing mitochondrial motility via genetic manipulation, which helps remove damage mitochondria and recruit new ones to meet the energy demands at injury sites during regenerative process (Zhou et al., 2016).

To examine whether miR-133b overexpression had any effects on mitochondrial dynamics, we co-transfected pUAS-mito-EGFP and pUAS-mcherry-miR-133b driven by the expression of pCMV-GAL4 via single-cell electroporation at 4 dpf and visualized the movement of mitochondria at 6 dpf via *in vivo* time-lapse confocal imaging, through which stable vs. mobile mitochondria could be discerned (**Figure 6A**, **Video S1**). By counting and analyzing mitochondria in M-cells, we identified that the percentage of motile mitochondria was much lower in miR-133b overexpressing conditions than in control (**Figure 6B**, **Video S2**), and this reduction was more significant in retrograde than in anterograde directions (Total: control: 20.31 ± 2.34%, $n = 11$ fishes vs. miR-133b OE: 10.70 ± 2.14%, $n = 13$ fishes; antero: control: 13.21 ± 1.89%, $n = 11$ fishes vs. miR-133b OE: 7.91 ± 1.92%, $n = 13$ fishes; retro: control: 7.10 ± 1.11%, $n = 11$ fishes vs. miR-133b OE: 2.79 ± 0.77%, $n = 13$ fishes; **Figure 6C**). Moreover, mitochondrial velocity in the miR-133b overexpression group was slower in both transport directions compared with that in control, though in retrogradely moving mitochondria it did not reach significance (Total: control: 0.501 ± 0.018 μm/s, $n = 54$ mitos from 11 fishes vs. miR-133b OE: 0.404 ± 0.015 μm/s, $n = 55$ mitos from 13 fishes; antero: control: 0.488 ± 0.015 μm/s, $n = 39$ mitos from 11 fishes vs. miR-133b OE: 0.396 ± 0.017 μm/s, $n = 41$ mitos from 13 fishes; retro: control: 0.535 ± 0.052 μm/s, $n = 15$ mitos from 11 fishes vs. miR-133b OE: 0.4294± 0.034 μm/s, $n = 14$ mitos from 13 fishes; **Figure 6D**). Together, our results suggest that miR-133b is an important cell intrinsic regulator of mitochondrial dynamics during M-cell axon regeneration.

DISCUSSION

Through modulating miRNA in single neuron and *in vivo* imaging, we have made several new findings in this study. First,

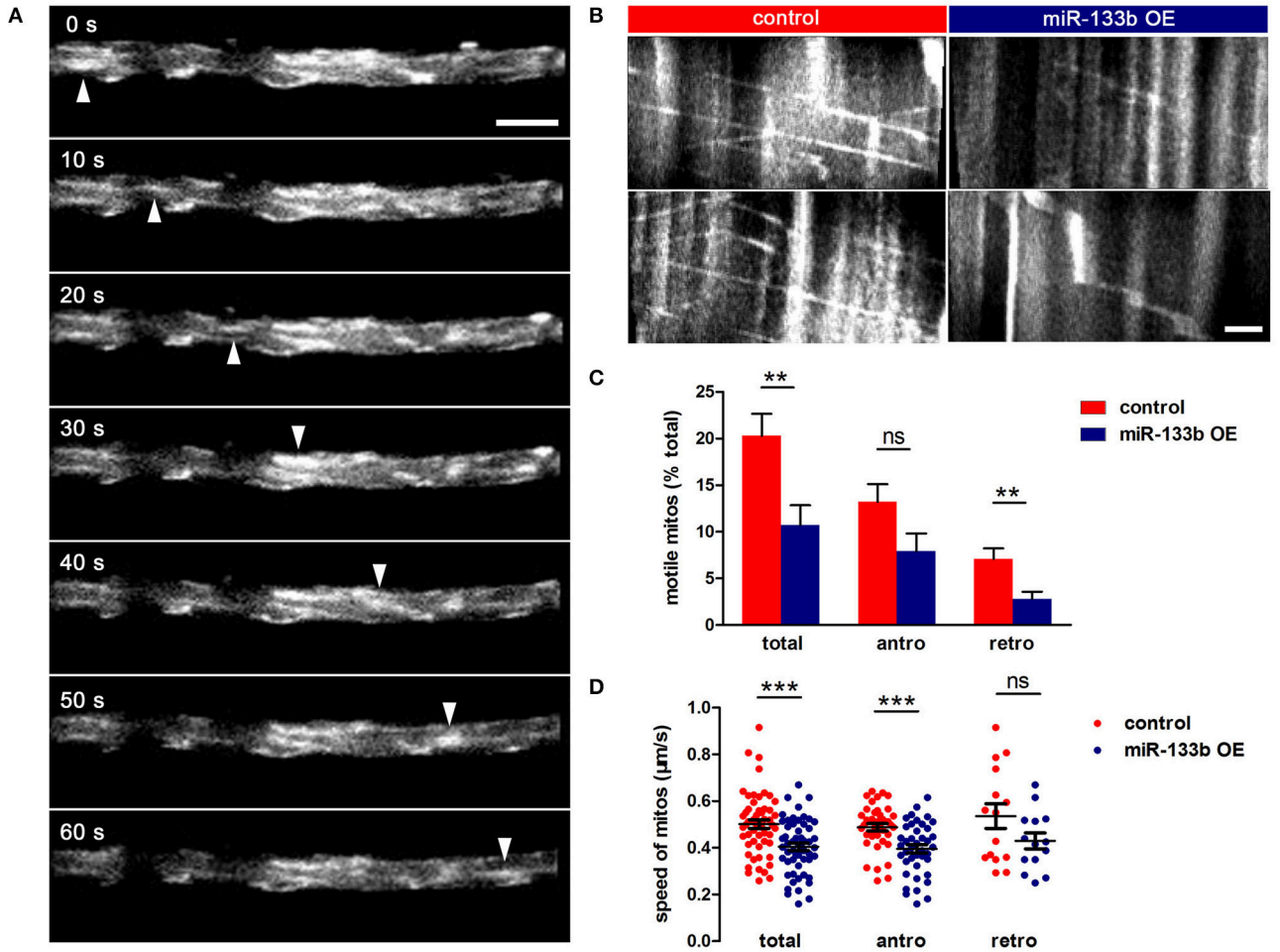

FIGURE 6 | miR-133b attenuates mitochondrial transport in M-cell. **(A)** *In vivo* time-lapse sequences showing a moving mitochondrion (white arrowhead). Scale bar: 5 μm. **(B)** Kymographs depict mitochondrial movement in control (left) and miR-133b OE group (right) at 6 dpf. Scale bar: 5μm. **(C)** Comparison of mitochondrial motility in control and miR-133b OE group, including total, anterograde and retrograde. Student's two-tailed *t*-test, total: control vs. miR-133b OE, $P = 0.0063$; antero: control vs. miR-133b OE, $P = 0.0640$; retro: control vs. miR-133b OE, $P = 0.0038$. **(D)** Comparison of mitochondrial moving speed in control and miR-133b OE group, including total, anterograde, and retrograde. Student's two-tailed *t*-test, total: control vs. miR-133b OE, $P = 0.0001$; antero: control vs. miR-133b OE, $P = 0002$; retro: control vs. miR-133b OE, $P = 0.1081$, $^{**}P < 0.01$, $^{***}P < 0.001$. Error bars represent S.E.M.

using Mauthner cells as the model, we demonstrate, through both loss and gain-of-function experiments, a critical cell-intrinsic role of miR-133b in inhibiting axon regeneration. Second, we uncover a previously unknown molecular target of miR-133b, *tppp3*, and show that it is a critical cell-intrinsic factor in promoting axon outgrowth. Finally, we reveal that miR-133b negatively regulates mitochondrial dynamics, which further supports the negative effects of miR-133b on axon regeneration.

Maunther cells, a pair of myelinated neurons with large soma and a long axon extending from hindbrain to tail in zebrafish, have been proved to have regenerative capacity in our previous study (Xu et al., 2017). Distinct from conventional miRNA over-expression system in zebrafish with the RNA duplex, our study used a vector-based system that enabled long-term expression of miRNAs. With another two miRNAs (miR-23a and miR-21) having different effects on axon regeneration, we reported that overexpression of miR-133b specifically reduced the regenerative length in M-cell (**Figure 7**). To further verify the validity of our vector-based system, we also delivered the miR-133b duplex into M-cell via single-cell electroporation. MiR-133b duplex delivered group exhibits a reduction tendency in axon regeneration length, although without a significant change, which might be due to the application of low dose of RNA duplex during single-cell electroporation compared with that in microinjection. What's more, we found that this tendency seems shrunk at 2 dpa, which might be due to a degradation of miR-133b duplex. Combining with the results of axon outgrowth in miR-133b sponge group, we identified the negative role of miR-133b during M-cell regenerative process.

We have further identified *tppp3* as the target of miR-133b in regulating axonal regeneration in zebrafish M-cell (**Figure 7**). The direct interaction between miR-133b and *tppp3* mRNA was

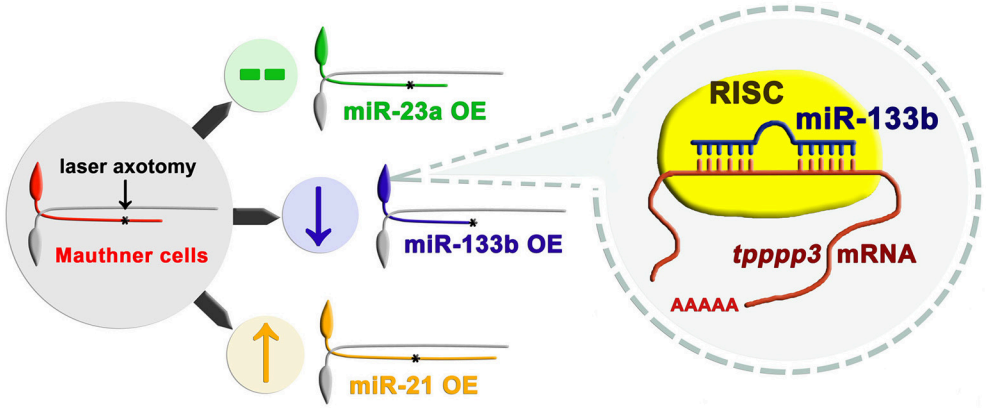

FIGURE 7 | Working model of how miR-133b involved in regulating axonal regeneration of M-cell. Different miRNAs play different roles on axonal regeneration. MiR-133b modulates M-cell regenerative capacity via diminishing *tppp3* mRNA level, a novel gene that regulates axon outgrowth. Black asterisk: ablation point.

confirmed by EGFP sensor assay. *Tppp3* expression was down-regulated by miR-133b at the mRNA level. Although we did not detect the change at protein level of *tppp3* because of the limitation of antibody performing in zebrafish, it did not cast much doubts on the credibility that *tppp3* is a downstream gene of miR-133b *in vivo*. At the same time, our data do not exclude possibility that there is another gene that is regulated by miR-133b in this process too.

Tppp3 was originally discovered as a member of the tubulin polymerization-promoting family that induces tubulin polymerization and has been extensively studied recently (Vincze et al., 2006; Staverosky et al., 2009; Juneja, 2013; Orosz, 2015). Researches has identified its critical role on promoting proliferation and preventing apoptosis *in vitro* (Zhou et al., 2010; Li Y. et al., 2016). Moreover, there is a study confirms its expression in motor neuron and suggests it may play a role in regulating sensory neuron regeneration in zebrafish (Aoki et al., 2014). Although, there has been no direct evidence demonstrating that *tppp3* can promote regeneration, a mount of studies confirms that microtubule stability, which has been identified to be one role of *tppp3* in human, is crucial to improve regenerative capability. Thus, concerning with the highly evolutional conservation of *tppp3* between human and zebrafish (Orosz, 2012; Oláh et al., 2017), which indicates that there may be a functional similarity between them, we speculate *tppp3* may involve in promoting axon regeneration in zebrafish M-cells. In our study, *tppp3* gain or loss-of-function produced a regulation on axon outgrowth mimicking the effect of miR-133b loss or gain-of-function. Thus, *tppp3* can be defined as a new regulator of axon regeneration, at least in zebrafish M-cells.

To figure out whether miR-133b has an effects on mitochondrial motility or not, we performed an experiment to visualizing mitochondrial motility in miR-133b overexpression group, as mitochondrial dynamics has shown to have a positive correlation with regenerative capability (Zhou et al., 2016; Xu et al., 2017). Consistent with our axonal regeneration data, motile mitochondria rate and mitochondrial velocity were both decreased accompanying worsening regenerative capability upon miR-133b overexpressing. While the mechanism on this finding needs to be further explored, this result that miR-133b reduces mitochondrial dynamics, at least, further reinforces our conclusion that miR-133b diminishes regenerative capacity in M-cells.

The role of dre-miR-133b in regeneration appears context-dependent in different organs (Yin et al., 2008, 2012; Yu et al., 2011; Xin et al., 2013). Similar to the adverse function of miR-133b during M-cell regeneration process, it inhibits fin regeneration in adult zebrafish by targeting Mps1 (Yin et al., 2008) and negatively regulates zebrafish heart regeneration via restricting injury-induced cardiomyocyte proliferation (Yin et al., 2012). Also, miR-133b can enhance axon regeneration and promote functional recovery after SCI in zebrafish and mice by targeting RhoA (Yu et al., 2011; Theis et al., 2017). As for the divergence between our results and the results showing miR-133b can promote regeneration after SCI by targeting RhoA, one plausible explanation might be related to the different modes of injury. We regulated the expression of miR-133b at single-cell level and severed axons by two-photon laser axotomy, which only damaged axon at a minuscule area, separating the intracellular and intercellular factors influencing axon regeneration *in vivo* and reflecting the intrinsic role of miR-133b during axon regeneration process. For SCI, a complete transection of the spinal cord was carried out, which inevitably damaged a large number of neurons and extracellular milieu. Since miR-133b has been proved to reduce the activated microglias/microphoges at injury site (Theis et al., 2017), it is possible that miR-133b enables the neurons a higher regenerative capacity after SCI by, to some degree, playing a significant role in diminishing the inhibitory extracellular milieu. In addition, it has been proved that miR-133b enhance neurite outgrowth in cultured neurons (Lu et al., 2015; Theis et al., 2017). Cultured neurons are, however, developing cells, which normally stemmed from embryos or newborn animals, and axon growth occurs from the cell body rather than from the tip of a damaged axon. As axons only contain a subset of molecules that are found in the cell body, outgrowth from the soma may have different underlying biology

to that of regeneration from the end of a cut axon (Bradke et al., 2012). Moreover, we cannot totally deny that miR-133b might play a role in differentiation in cultured neurons and miR-133b has been reported to promote differentiation process via ERK 1/2 pathway (Sanchez-Simon et al., 2010; Feng et al., 2013). Thus, as we focus on miR-133b's role during regeneration process of M-cells in our experiments, which has been mature during our experimental time window, we believe our conclusion of miR-133b inhibiting M-cell axon regeneration does not conflict with the conclusions mentioned above.

A large number of studies have demonstrated the critical role of miRNAs in regeneration process, however, many reports explore the function of miRNA in cell populations, masking the important information connecting single cell fate and miRNA function in it (Verdú et al., 2000). Studying miRNA role in one single cell is important because it allows deep understanding of the correlations between the miRNAs and cell function (Meacham and Morrison, 2013; Wills et al., 2013). In order to have a comprehensive understanding of miRNA function, we built a model to identify the miRNA function in zebrafish Mauthner cell regeneration by single-cell electroporation, presenting a new method to understand intrinsic miRNA function in regenerative process, without concerning with effects from intercellular context. Through combining effectively with other gene interference technology and subcellular organization mitochondria labeled by single-cell electroporation, we provided a new tool to explore functions of different genes in single cell *in vivo*.

In summary, our study identifies miR-133b as cell-intrinsic inhibitor of axon regeneration, which performs its function, at least partly, via regulating *tppp3* (**Figure 7**). These results, together with our single cell analysis approach, not only contribute significantly to the fundamental understanding of miRNA regulation in regeneration, but also have implications in developing therapeutic strategies for nerve injury.

AUTHOR CONTRIBUTIONS

Designed the experiments: RH, MC, and BH. Performed the experiments: RH, MC, and LY. Contributed critical reagents: MW and SG. Analyzed the data: RH and MC. Wrote the manuscript: RH. Revised the manuscript: BH and SG.

FUNDING

This research was supported by National Natural Science Foundation of China (grant no. 31571068, grant no. 31771183) and in part by GSK R&D China, and US National Institute of Health NIH NS095734 and DA035680 (MW and SG).

ACKNOWLEDGMENTS

We are grateful to Prof. Xiangting Wang (University of Science and Technology of China, China) to provide instructive suggestions for this research. We also appreciate for Wu Yin to offer us miR-133b duplex.

SUPPLEMENTARY MATERIAL

The Supplementary Material for this article can be found online at: https://www.frontiersin.org/articles/10.3389/fnmol.2017.00375/full#supplementary-material

Figure S1 | miR-133b duplex inhibits M-cell regeneration **(A)** Confocal imaging of M-cell at 1 dpa (top) and 2 dpa (bottom). White asterisk: ablation point. Scale bar: 50 μm. **(B)** Regeneration length at 1 and 2 dpa. One days post-axotomy: One-way ANOVA, $P = 0.2195$. Two days post-axotomy: One-way ANOVA, $P = 0.1847$.

Figure S2 | The design of miR-shRNAs targeting *tppp3*. **(A)** The sequences of five shRNAs targeting *tppp3*. The guide strands (bottom) are highlighted in dark blue. **(B)** The location of shRNA target sites in the *tppp3* mRNA.

Video S1 | *In vivo* imaging of mitochondrial movement in control Axonal mitochondrial motility along M-cell axon labeled with mito-EGFP and mCherry. 2.5-min time-lapse images were acquired with a 60 × lens and recorded for a total of 100 frames at 1.5-s intervals.

Video S2 | *In vivo* imaging of mitochondrial movement in miR-133b overexpressed group Axonal mitochondrial motility along M-cell axon overexpressing miR-133b. M-cell was labeled with mito-EGFP and mCherry-miR-133b. 2.5-min time-lapse images were acquired with a 60 × lens and recorded for a total of 100 frames at 1.5-s intervals.

REFERENCES

Akçakaya, P., Ekelund, S., Kolosenko, I., Caramuta, S., Ozata, D. M., Xie, H., et al. (2011). miR-185 and miR-133b deregulation is associated with overall survival and metastasis in colorectal cancer. *Int. J. Oncol.* 39, 311–318. doi: 10.3892/ijo.2011.1043

Aoki, M., Segawa, H., Naito, M., and Okamoto, H. (2014). Identification of possible downstream genes required for the extension of peripheral axons in primary sensory neurons. *Biochem. Biophys. Res. Commun.* 445, 357–362. doi: 10.1016/j.bbrc.2014.01.193

Beauchemin, M., Smith, A., and Yin, V. P. (2015). Dynamic microRNA-101a and Fosab expression controls zebrafish heart regeneration. *Development* 142, 4026–4037. doi: 10.1242/dev.126649

Bradke, F., Fawcett, J. W., and Spira, M. E. (2012). Assembly of a new growth cone after axotomy: the precursor to axon regeneration. *Nat. Rev. Neurosci.* 13, 183–193. doi: 10.1038/nrn3176

Canty, A. J., Huang, L., Jackson, J. S., Little, G. E., Knott, G., Maco, B., et al. (2013). *In-vivo* single neuron axotomy triggers axon regeneration to restore synaptic density in specific cortical circuits. *Nat. Commun.* 4:2038. doi: 10.1038/ncomms3038

Cohen, S. M. (2009). Use of microRNA sponges to explore tissue-specific microRNA functions *in vivo*. *Nat. Methods* 6, 873–874. doi: 10.1038/nmeth1209-873

De Rienzo, G., Gutzman, J. H., and Sive, H. (2012). Efficient shRNA-mediated inhibition of gene expression in zebrafish. *Zebrafish* 9, 97–107. doi: 10.1089/zeb.2012.0770

Dong, Z., Peng, J., and Guo, S. (2013). Stable gene silencing in zebrafish with spatiotemporally targetable RNA interference. *Genetics* 193, 1065–1071. doi: 10.1534/genetics.112.147892

Duursma, A. M., Kedde, M., Schrier, M., le Sage, C., and Agami, R. (2008). miR-148 targets human DNMT3b protein coding region. *RNA* 14, 872–877. doi: 10.1261/rna.972008

Ebert, M. S., Neilson, J. R., and Sharp, P. A. (2007). MicroRNA sponges: competitive inhibitors of small RNAs in mammalian cells. *Nat. Methods* 4, 721–726. doi: 10.1038/nmeth1079

Ebert, M. S., and Sharp, P. A. (2010). MicroRNA sponges: progress and possibilities. *RNA* 16, 2043–2050. doi: 10.1261/rna.2414110

Feng, Y., Niu, L. L., Wei, W., Zhang, W. Y., Li, X. Y., Cao, J. H., et al. (2013). A feedback circuit between miR-133 and the ERK1/2 pathway involving an exquisite mechanism for regulating myoblast proliferation and differentiation. *Cell Death Dis.* 4:e934. doi: 10.1038/cddis.2013.462

Forman, J. J., Legesse-Miller, A., and Coller, H. A. (2008). A search for conserved sequences in coding regions reveals that the let-7 microRNA targets Dicer within its coding sequence. *Proc. Natl. Acad. Sci. U.S.A.* 105, 14879–14884. doi: 10.1073/pnas.0803230105

Giraldez, A. J., Cinalli, R. M., Glasner, M. E., Enright, A. J., Thomson, J. M., Baskerville, S., et al. (2005). MicroRNAs regulate brain morphogenesis in zebrafish. *Science* 308, 833–838. doi: 10.1126/science.1109020

Han, Z., Chen, F., Ge, X., Tan, J., Lei, P., and Zhang, J. (2014). miR-21 alleviated apoptosis of cortical neurons through promoting PTEN-Akt signaling pathway *in vitro* after experimental traumatic brain injury. *Brain Res.* 1582, 12–20. doi: 10.1016/j.brainres.2014.07.045

Hassel, D., Cheng, P., White, M. P., Ivey, K. N., Kroll, J., Augustin, H. G., et al. (2012). MicroRNA-10 regulates the angiogenic behavior of zebrafish and human endothelial cells by promoting vascular endothelial growth factor signaling. *Circ. Res.* 111, 1421–1433. doi: 10.1161/CIRCRESAHA.112.279711

Hellal, F., Hurtado, A., Ruschel, J., Flynn, K. C., Laskowski, C. J., Umlauf, M., et al. (2011). Microtubule stabilization reduces scarring and causes axon regeneration after spinal cord injury. *Science* 331, 928–931. doi: 10.1126/science.1201148

Heyer, M. P., Pani, A. K., Smeyne, R. J., Kenny, P. J., and Feng, G. (2012). Normal midbrain dopaminergic neuron development and function in miR-133b mutant mice. *J. Neurosci.* 32, 10887–10894. doi: 10.1523/JNEUROSCI.1732-12.2012

Hong, P., Jiang, M., and Li, H. (2014). Functional requirement of dicer1 and miR-17-5p in reactive astrocyte proliferation after spinal cord injury in the mouse. *Glia* 62, 2044–2060. doi: 10.1002/glia.22725

Hoppe, B., Pietsch, S., Franke, M., Engel, S., Groth, M., Platzer, M., et al. (2015). MiR-21 is required for efficient kidney regeneration in fish. *BMC Dev. Biol.* 15:43. doi: 10.1186/s12861-015-0089-2

Hu, G., Chen, D., Li, X., Yang, K., Wang, H., and Wu, W. (2010). miR-133b regulates the MET proto-oncogene and inhibits the growth of colorectal cancer cells *in vitro* and *in vivo*. *Cancer Biol. Ther.* 10, 190–197. doi: 10.4161/cbt.10.2.12186

Hur, E. M., Saijilafu, and Zhou, F. Q. (2012). Growing the growth cone: remodeling the cytoskeleton to promote axon regeneration. *Trends Neurosci.* 35, 164–174. doi: 10.1016/j.tins.2011.11.002

Juneja, S. C. (2013). Cellular distribution and gene expression profile during flexor tendon graft repair: a novel tissue engineering approach*. *J. Tissue Eng.* 4:2041731413492741. doi: 10.1177/2041731413492741

Kerschensteiner, M., Schwab, M. E., Lichtman, J. W., and Misgeld, T. (2005). *In vivo* imaging of axonal degeneration and regeneration in the injured spinal cord. *Nat. Med.* 11, 572–577. doi: 10.1038/nm1229

Kloosterman, W. P., and Plasterk, R. H. A. (2006). The diverse functions of MicroRNAs in animal development and disease. *Dev. Cell* 11, 441–450. doi: 10.1016/j.devcel.2006.09.009

Koutsoulidou, A., Mastroyiannopoulos, N. P., Furling, D., Uney, J. B., and Phylactou, L. A. (2011). Expression of miR-1, miR-133a, miR-133b and miR-206 increases during development of human skeletal muscle. *BMC Dev. Biol.* 11:34. doi: 10.1186/1471-213X-11-34

Lewis, B. P., Burge, C. B., and Bartel, D. P. (2005). Conserved seed pairing, often flanked by adenosines, indicates that thousands of human genes are microRNA targets. *Cell* 120, 15–20. doi: 10.1016/j.cell.2004.12.035

Li, S., Zhang, R., Yuan, Y., Yi, S., Chen, Q., Gong, L., et al. (2016). MiR-340 regulates fibrinolysis and axon regrowth following sciatic nerve injury. *Mol. Neurobiol.* 54, 4379–4389. doi: 10.1007/s12035-016-9965-4

Li, Y., Xu, Y., Ye, K., Wu, N., Li, J., Liu, N., et al. (2016). Knockdown of tubulin polymerization promoting protein family member 3 suppresses proliferation and induces apoptosis in non-small-cell lung cancer. *J. Cancer* 7, 1189–1196. doi: 10.7150/jca.14790

Lorenzana, A. O., Lee, J. K., Mui, M., Chang, A., and Zheng, B. (2015). A surviving intact branch stabilizes remaining axon architecture after injury as revealed by *in vivo* imaging in the mouse spinal cord. *Neuron* 86, 947–954. doi: 10.1016/j.neuron.2015.03.061

Lu, X. C., Zheng, J. Y., Tang, L. J., Huang, B. S., Li, K., Tao, Y., et al. (2015). MiR-133b Promotes neurite outgrowth by targeting RhoA expression. *Cell. Physiol. Biochem.* 35, 246–258. doi: 10.1159/000369692

Meacham, C. E., and Morrison, S. J. (2013). Tumour heterogeneity and cancer cell plasticity. *Nature* 501, 328–337. doi: 10.1038/nature12624

Misgeld, T., Kerschensteiner, M., Bareyre, F. M., Burgess, R. W., and Lichtman, J. W. (2007). Imaging axonal transport of mitochondria *in vivo*. *Nat. Methods* 4, 559–561. doi: 10.1038/nmeth1055

O'Brien, G. S., Rieger, S., Martin, S. M., Cavanaugh, A. M., Portera-Cailliau, C., and Sagasti, A. (2009). Two-photon axotomy and time-lapse confocal imaging in live zebrafish embryos. *J. Vis. Exp.* e1129. doi: 10.3791/1129

Oláh, J., Szenasi, T., Szabo, A., Kovacs, K., Low, P., Stifanic, M., et al. (2017). Tubulin binding and polymerization promoting properties of tubulin polymerization promoting proteins are evolutionarily conserved. *Biochemistry* 56, 1017–1024. doi: 10.1021/acs.biochem.6b00902

Orosz, F. (2012). A fish-specific member of the TPPP protein family? *J. Mol. Evol.* 75, 55–72. doi: 10.1007/s00239-012-9521-4

Orosz, F. (2015). On the tubulin polymerization promoting proteins of zebrafish. *Biochem. Biophys. Res. Commun.* 457, 267–272. doi: 10.1016/j.bbrc.2014.12.099

Otaegi, G., Pollock, A., Hong, J., and Sun, T. (2011). MicroRNA miR-9 modifies motor neuron columns by a tuning regulation of FoxP1 levels in developing spinal cords. *J. Neurosci.* 31, 809–818. doi: 10.1523/JNEUROSCI.4330-10.2011

Plucinska, G., Paquet, D., Hruscha, A., Godinho, L., Haass, C., Schmid, B., et al. (2012). *In vivo* imaging of disease-related mitochondrial dynamics in a vertebrate model system. *J. Neurosci.* 32, 16203–16212. doi: 10.1523/JNEUROSCI.1327-12.2012

Rieger, S., and Sagasti, A. (2011). Hydrogen peroxide promotes injury-induced peripheral sensory axon regeneration in the zebrafish skin. *PLoS Biol.* 9:e1000621. doi: 10.1371/journal.pbio.1000621

Ruschel, J., Hellal, F., Flynn, K. C., Dupraz, S., Elliott, D. A., Tedeschi, A., et al. (2015). Axonal regeneration. Systemic administration of epothilone B promotes axon regeneration after spinal cord injury. *Science* 348, 347–352. doi: 10.1126/science.aaa2958

Sanchez-Simon, F. M., Zhang, X. X., Loh, H. H., Law, P. Y., and Rodriguez, R. E. (2010). Morphine regulates dopaminergic neuron differentiation via miR-133b. *Mol. Pharmacol.* 78, 935–942. doi: 10.1124/mol.110.066837

Sengottuvel, V., and Fischer, D. (2011). Facilitating axon regeneration in the injured CNS by microtubules stabilization. *Commun. Integr. Biol.* 4, 391–393. doi: 10.4161/cib.15552

Sengottuvel, V., Leibinger, M., Pfreimer, M., Andreadaki, A., and Fischer, D. (2011). Taxol facilitates axon regeneration in the mature CNS. *J. Neurosci.* 31, 2688–2699. doi: 10.1523/JNEUROSCI.4885-10.2011

Shinya, M., Kobayashi, K., Masuda, A., Tokumoto, M., Ozaki, Y., Saito, K., et al. (2013). Properties of gene knockdown system by vector-based siRNA in zebrafish. *Dev. Growth Differ.* 55, 755–765. doi: 10.1111/dgd.12091

Staverosky, J. A., Pryce, B. A., Watson, S. S., and Schweitzer, R. (2009). Tubulin polymerization-promoting protein family member 3, Tppp3, is a specific marker of the differentiating tendon sheath and synovial joints. *Dev. Dyn.* 238, 685–692. doi: 10.1002/dvdy.21865

Stoick-Cooper, C. L., Moon, R. T., and Weidinger, G. (2007). Advances in signaling in vertebrate regeneration as a prelude to regenerative medicine. *Genes Dev.* 21, 1292–1315. doi: 10.1101/gad.1540507

Strickland, I. T., Richards, L., Holmes, F. E., Wynick, D., Uney, J. B., and Wong, L. F. (2011). Axotomy-induced miR-21 promotes axon growth in adult dorsal root ganglion neurons. *PLoS ONE* 6:e23423. doi: 10.1371/journal.pone.0023423

Takihara, Y., Inatani, M., Eto, K., Inoue, T., Kreymerman, A., Miyake, S., et al. (2015). *In vivo* imaging of axonal transport of mitochondria in the diseased and aged mammalian CNS. *Proc. Natl. Acad. Sci. U.S.A.* 112, 10515–10520. doi: 10.1073/pnas.1509879112

Tedeschi, A., and Bradke, F. (2017). Spatial and temporal arrangement of neuronal intrinsic and extrinsic mechanisms controlling axon regeneration. *Curr. Opin. Neurobiol.* 42, 118–127. doi: 10.1016/j.conb.2016.12.005

Theis, T., Yoo, M., Park, C. S., Chen, J., Kügler, S., Gibbs, K. M., et al. (2017). Lentiviral delivery of miR-133b improves functional recovery after spinal cord injury in mice. *Mol. Neurobiol.* 54, 4659–4671. doi: 10.1007/s12035-016-0007-z

Verdú, E., Ceballos, D., Vilches, J. J., and Navarro, X. (2000). Influence of aging on peripheral nerve function and regeneration. *J. Peripher. Nerv. Syst.* 5, 191–208. doi: 10.1046/j.1529-8027.2000.00026.x

Vincze, O., Tökési N, N., Oláh, J., Hlavanda, E., Zotter, A., Horváth, I., et al. (2006). Tubulin polymerization promoting proteins (TPPPs): members of a new family with distinct structures and functions. *Biochemistry* 45, 13818–13826. doi: 10.1021/bi061305e

Wen, D., Li, S., Ji, F., Cao, H., Jiang, W., Zhu, J., et al. (2013). miR-133b acts as a tumor suppressor and negatively regulates FGFR1 in gastric cancer. *Tumour Biol.* 34, 793–803. doi: 10.1007/s13277-012-0609-7

Wills, Q. F., Livak, K. J., Tipping, A. J., Enver, T., Goldson, A. J., Sexton, D. W., et al. (2013). Single-cell gene expression analysis reveals genetic associations masked in whole-tissue experiments. *Nat. Biotechnol.* 31, 748–752. doi: 10.1038/nbt.2642

Wu, D., and Murashov, A. K. (2013). MicroRNA-431 regulates axon regeneration in mature sensory neurons by targeting the Wnt antagonist Kremen1. *Front. Mol. Neurosci.* 6:35. doi: 10.3389/fnmol.2013.00035

Wu, D., Raafat, A., Pak, E., Clemens, S., and Murashov, A. K. (2012). Dicer-microRNA pathway is critical for peripheral nerve regeneration and functional recovery *in vivo* and regenerative axonogenesis *in vitro*. *Exp. Neurol.* 233, 555–565. doi: 10.1016/j.expneurol.2011.11.041

Xiang, K. M., and Li, X. R. (2014). MiR-133b acts as a tumor suppressor and negatively regulates TBPL1 in colorectal cancer cells. *Asian Pac. J. Cancer Prev.* 15, 3767–3772. doi: 10.7314/APJCP.2014.15.8.3767

Xin, H., Li, Y., Liu, Z., Wang, X., Shang, X., Cui, Y., et al. (2013). MiR-133b promotes neural plasticity and functional recovery after treatment of stroke with multipotent mesenchymal stromal cells in rats via transfer of exosome-enriched extracellular particles. *Stem Cells* 31, 2737–2746. doi: 10.1002/stem.1409

Xu, Y., Chen, M., Hu, B., Huang, R., and Hu, B. (2017). *In vivo* Imaging of mitochondrial transport in single-axon regeneration of zebrafish mauthner cells. *Front. Cell. Neurosci.* 11:4. doi: 10.3389/fncel.2017.00004

Yamamoto, H., Kohashi, K., Fujita, A., and Oda, Y. (2013). Fascin-1 overexpression and miR-133b downregulation in the progression of gastrointestinal stromal tumor. *Mod. Pathol.* 26, 563–571. doi: 10.1038/modpathol.2012.198

Yin, V. P., Lepilina, A., Smith, A., and Poss, K. D. (2012). Regulation of zebrafish heart regeneration by miR-133. *Dev. Biol.* 365, 319–327. doi: 10.1016/j.ydbio.2012.02.018

Yin, V. P., Thomson, J. M., Thummel, R., Hyde, D. R., Hammond, S. M., and Poss, K. D. (2008). Fgf-dependent depletion of microRNA-133 promotes appendage regeneration in zebrafish. *Genes Dev.* 22, 728–733. doi: 10.1101/gad.1641808

Yu, Y. M., Gibbs, K. M., Davila, J., Campbell, N., Sung, S., Todorova, T. I., et al. (2011). MicroRNA miR-133b is essential for functional recovery after spinal cord injury in adult zebrafish. *Eur. J. Neurosci.* 33, 1587–1597. doi: 10.1111/j.1460-9568.2011.07643.x

Zhou, B., Yu, P., Lin, M. Y., Sun, T., Chen, Y., and Sheng, Z. H. (2016). Facilitation of axon regeneration by enhancing mitochondrial transport and rescuing energy deficits. *J. Cell Biol.* 214, 103–119. doi: 10.1083/jcb.201605101

Zhou, W., Wang, X., Li, L., Feng, X., Yang, Z., Zhang, W., et al. (2010). Depletion of tubulin polymerization promoting protein family member 3 suppresses HeLa cell proliferation. *Mol. Cell. Biochem.* 333, 91–98. doi: 10.1007/s11010-009-0208-0

Zuber, J., McJunkin, K., Fellmann, C., Dow, L. E., Taylor, M. J., Hannon, G. J., et al. (2011). Toolkit for evaluating genes required for proliferation and survival using tetracycline-regulated RNAi. *Nat. Biotechnol.* 29, 79–83. doi: 10.1038/nbt.1720

Conflict of Interest Statement: The authors declare that the research was conducted in the absence of any commercial or financial relationships that could be construed as a potential conflict of interest.

frontiers in Molecular Neuroscience

MINI REVIEW
published: 03 April 2018
doi: 10.3389/fnmol.2018.00101

Role of Caspase-8 and Fas in Cell Death After Spinal Cord Injury

*Daniel Sobrido-Cameán and Antón Barreiro-Iglesias**

Department of Functional Biology, CIBUS, Faculty of Biology, Universidade de Santiago de Compostela, Santiago de Compostela, Spain

Spinal cord injury (SCI) causes the death of neurons and glial cells due to the initial mechanical forces (i.e., primary injury) and through a cascade of secondary molecular events (e.g., inflammation or excitotoxicity) that exacerbate cell death. The loss of neurons and glial cells that are not replaced after the injury is one of the main causes of disability after SCI. Evidence accumulated in last decades has shown that the activation of apoptotic mechanisms is one of the factors causing the death of intrinsic spinal cord (SC) cells following SCI. Although this is not as clear for brain descending neurons, some studies have also shown that apoptosis can be activated in the brain following SCI. There are two main apoptotic pathways, the extrinsic and the intrinsic pathways. Activation of caspase-8 is an important step in the initiation of the extrinsic pathway. Studies in rodents have shown that caspase-8 is activated in SC glial cells and neurons and that the Fas receptor plays a key role in its activation following a traumatic SCI. Recent work in the lamprey model of SCI has also shown the retrograde activation of caspase-8 in brain descending neurons following SCI. Here, we review our current knowledge on the role of caspase-8 and the Fas pathway in cell death following SCI. We also provide a perspective for future work on this process, like the importance of studying the possible contribution of Fas/caspase-8 signaling in the degeneration of brain neurons after SCI in mammals.

Keywords: first apoptosis signal receptor, apoptosis antigen 1, cluster of differentiation 95, tumor necrosis factor receptor superfamily member 6, caspase-8, Fas ligand, neuron, oligodendrocyte

OPEN ACCESS

Edited by:
Andrew Paul Tosolini, University College London, United Kingdom

Reviewed by:
Lee J. Martin, Johns Hopkins University, United States
Michael G. Fehlings, Toronto Western Hospital, Canada

****Correspondence:***
Antón Barreiro-Iglesias
anton.barreiro@usc.es

Received: *01 February 2018*
Accepted: *15 March 2018*
Published: *03 April 2018*

Citation:
Sobrido-Cameán D and Barreiro-Iglesias A (2018) Role of Caspase-8 and Fas in Cell Death After Spinal Cord Injury. Front. Mol. Neurosci. 11:101. doi: 10.3389/fnmol.2018.00101

INTRODUCTION

Spinal cord injury (SCI) can cause permanent disability due to the dysfunction of motor, autonomic and sensory systems. There are also high economical costs associated with the care of SCI patients. In the USA, the lifetime cost of a SCI patient is between 1.1 and 4.6 million US dollars (National Spinal Cord Injury Statistical Center, 2016). So, it is of crucial importance to develop new and effective treatments for SCI patients. Nowadays, only a few treatments have been translated to the clinic: a treatment with methylprednisolone (which is still controversial), hypertensive therapy and early decompressive surgery (for a recent review see Ulndreaj et al., 2017). These treatments aim to stop further degeneration after SCI, but they only lead to limited improvements. One of the main causes of permanent deficits after SCI is due to the loss of cells (oligodendrocytes and neurons) that are not effectively replaced after the injury. Regeneration strategies are difficult to implement due to the complexity of the central nervous system; therefore, the development of neuroprotective therapies is one of the most promising strategies for clinical translation.

SCI has been divided in two stages, the primary and secondary injuries. The primary injury is caused by the mechanical forces of the traumatic event. Following the primary injury, a molecular cascade of secondary events is initiated, which expands the damage even to tissue that was not directly affected by the primary injury. Secondary injury events star within seconds of the occurrence of the primary injury and delay and progress over time. Inflammatory cells enter the injury site due to the disruption of the blood-spinal cord (SC) barrier and trigger the release of cytokines and reactive oxygen species (reviewed by Ahuja et al., 2017). Excitatory amino acids like glutamate are also massively released (Fernández-López et al., 2014, 2016) leading to elevated intracellular calcium levels. These processes cause the loss of cells by necrotic and apoptotic mechanisms. The final outcome of a SCI will depend on the extent of secondary damage; therefore, understanding the molecular pathways that lead to its progression will benefit the development of neuroprotective therapies for SCI patients.

Apoptosis is a process that occurs during development or aging and as a homeostatic mechanism to maintain cell populations in different tissues, but it is also activated after tissue damage. Cell death during secondary injury after SCI is caused in part by the activation of apoptotic mechanisms (Crowe et al., 1997; Shuman et al., 1997; Emery et al., 1998). There are two main apoptotic pathways: the extrinsic or death receptor pathway and the intrinsic or mitochondrial pathway. The extrinsic pathway involves the activation of death receptors, which leads to the activation of initiator caspases like caspase-8 or caspase-10. Several studies have shown the activation of caspase-8 in intrinsic SC cells following SCI in rodents (Casha et al., 2001, 2005; Keane et al., 2001; Takagi et al., 2003; Cantarella et al., 2010; Chen et al., 2011). More recently, work in lampreys has also shown that caspase-8 is retrogradely activated in identifiable descending brain neurons after SCI (Barreiro-Iglesias and Shifman, 2012, 2015; Barreiro-Iglesias et al., 2017). Here, we review our current knowledge on the role of caspase-8 in cell death after SCI. Since the activation of Fas receptors (also known as CD95 or APO-1) plays an important role in this process, we also focused our review on the role of this signaling pathway in caspase-8 activation following SCI. Finally, we propose new lines of work to advance our knowledge on the role of caspase-8 and Fas in cell death after SCI.

ACTIVATION OF THE FAS/CASPASE-8 APOPTOTIC PATHWAY IN THE SPINAL CORD

Procaspase-8 is an initiator caspase that can process itself after ligation with the Fas-tumor necrosis factor family of death receptors (Kischkel et al., 1995). After biding of the Fas-ligand [FasL (or CD95L)], the Fas receptor (a 45 kDa membrane receptor) forms a death-inducing signaling complex (DISC) with the adaptor protein FADD (a member of the death domain superfamily) and procaspase-8. Then, activated caspase-8 can initiate downstream cleavage of caspase-3, among other targets, by direct or mitochondrial-dependent mechanisms (see **Figure 1A**). Some studies have also shown that caspase-8 activation after SCI can be mediated through other members of the TNF receptor superfamily (Cantarella et al., 2010; Chen et al., 2011), but we have focused our review on the role of FasL/Fas in caspase-8 activation after SCI.

One of the first reports showing that the Fas/caspase-8 pathway is activated after SC damage came from a study using a model of ischemic SCI (Matsushita et al., 2000). In this study, the authors developed a model of SC ischemia in mice by clamping the left subclavian artery. After ischemia, the number of Fas-positive neurons and the intensity of Fas-immunoreactivity increased. Also, ischemia induced the formation of a complex between Fas and procaspase-8 in the SC suggesting that ischemia induces the formation of DISC. Ischemia also induced and increase in procaspase-8 expression and caspase-8 cleavage/activation. Specifically, activated caspase-8 was detected in neurons (Matsushita et al., 2000). These authors did not establish how the ischemic damage leads to the formation of DISC and caspase-8 activation in neurons. But, interestingly, after cerebral ischemia there is an upregulation of Fas and the FasL (Martin-Villalba et al., 1999), suggesting that FasL release after SC ischemia could induce the formation of DISC and caspase-8 activation in neurons. This work has important implications for traumatic SCI, because the disruption of blood-vessels after SCI can also cause secondary ischemic damage.

The first reports demonstrating caspase-8 activation in intrinsic SC cells following a traumatic SCI came in 2001 from two studies by Casha et al. (2001) and Keane et al. (2001). The study by Keane et al. (2001) showed that a contusion injury at T9-T10 in rats leads to the appearance of caspase-8 immunoreactivity 6 h after the injury in neurons of the gray matter and in cells of the white matter (possibly oligodendrocytes). Immunoblots showed that this immunoreactivity correspond to the expression of the cleaved subunit of caspase-8 (Keane et al., 2001). In the same year, Casha et al. (2001) reported the first results showing the possible involvement of Fas receptors in cell death following a cervical SCI (the most common level of human SCI). These authors showed that, in rats, a clip compression C7-T1 SCI caused cell death in the SC. Apoptotic cells were mainly oligodendrocytes located along degenerating axons. Double immunohistochemistry with Fas and TUNEL revealed the presence of Fas-positive dying glia after the injury (Casha et al., 2001). Expression of FasL was observed in astrocytes and microglia. Interestingly, the appearance of Fas expression after the injury in dying glia correlated with increased levels of activated caspase-8 as revealed by western blots. Moreover, levels of FLIP-L (caspase-8 inhibitor; **Figure 1**) decreased after SCI at time points in which caspase-8 activation was observed (Casha et al., 2001). Similar results were later reported in mice after a T9-T10 contusion injury (Takagi et al., 2003). These authors showed that caspase-8 enzyme activity increased in the SC of mice after SCI (Takagi et al., 2003).

These earlier results suggested that activation of Fas after SCI could lead to activation of caspase-8 and cell death.

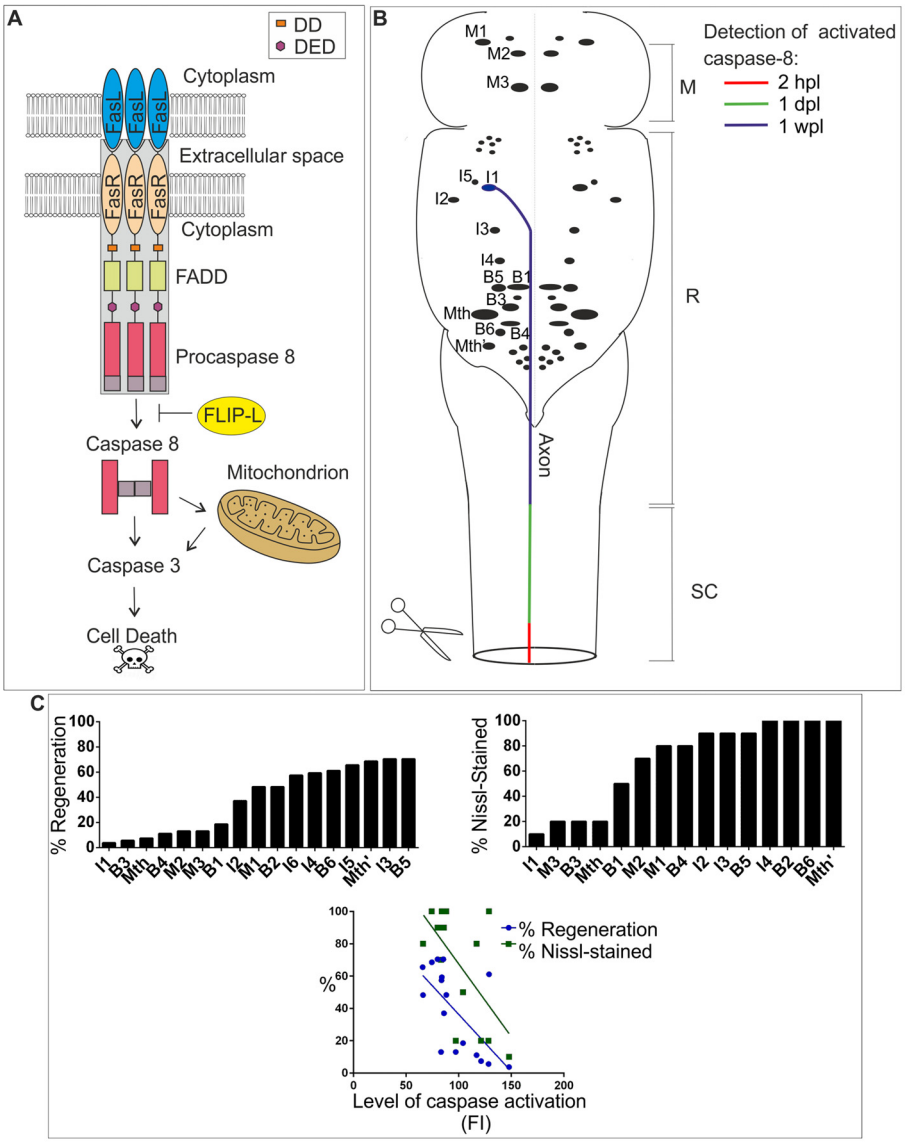

FIGURE 1 | (A) FasL/Fas/caspase-8 signaling pathway. Binding of FasL (expressed in neurons, glial cells or immune system cells) to Fas (expressed in neurons or glial cells) induces oligomerization of the receptor, which causes the activation of the internal domain of Fas triggering FADD binding. The adaptor protein FADD binds to Fas via homophilic DD interactions. FADD recruits procaspase-8, which binds to FADD through the DED, causing the formation of death-inducing signaling complex (DISC; gray box). The formation of DISC is followed by cleavage of procaspase-8 into large and small subunits. Two large and two small subunits associate with each other to form an active caspase-8 heterodimer. The resulting mature caspase-8 is released to the cytosol and initiates downstream apoptosis directly by activating caspase-3 or indirectly through the mitochondrial pathway. FLIP-L can inhibit the activation of procaspase-8. **(B)** Schematic drawing of a dorsal view of the sea lamprey brainstem showing the location of identifiable descending neurons (for most neurons only the soma is represented). The I1 neuron is used as an example to show the progressive detection of activated caspase-8 after a complete spinal cord injury (SCI; from Barreiro-Iglesias and Shifman, 2015). Activated caspase-8 is detected first in the injured axon at the site of injury (within 2 h post-lesion, hpl), then in the axon at rostral SC levels (within 1 day post-lesion, dpl) and finally in the soma of descending neurons (1 week post-lesion, wpl). This timing of caspase-8 activation has been color-coded in the I1 neuron/axon. Rostral is to the top and the SCI site to the bottom. Abbreviations: M, Mesencephalon; R, Rhombencephalon; SC, Spinal cord. **(C)** The top graphs show the regenerative and survival abilities of identifiable descending neurons of lampreys. The regenerative ability is expressed as the percentage of times a given neuron regenerates its axon 5 mm below the site of injury 10 weeks after a complete SCI (from Jacobs et al., 1997). The survival ability is expressed as the percentage of times that a given neuron shows Nissl staining 1 year after a complete SCI (from Shifman et al., 2008). The bottom graph shows a significant correlation between the level of activated caspases (fluorescence intensity, FI) 2 wpl (from Barreiro-Iglesias et al., 2017) and the regenerative (from Jacobs et al., 1997) and survival abilities (from Shifman et al., 2008) of identifiable descending neurons. *P*-values of Pearson correlation are 0.0044 (Barreiro-Iglesias et al., 2017) and 0.0122, respectively.

However, the first true experimental demonstration showing that the activation of Fas leads to apoptosis following SCI came in 2004 with the studies by Demjen et al. (2004) and Yoshino et al. (2004). Demjen et al. (2004) showed that an acute treatment with neutralizing antibodies against FasL (CD95L) reduced neuronal apoptosis (TUNEL), promoted regeneration

of corticospinal tract fibers and improved functional recovery in mice with a dorsal transection of the SC (two-thirds of the cord were transected) at T8-T9. Yoshino et al. (2004) also showed that locomotor recovery, after a contusion SCI, was improved in Fas-deficient mutant mice and that this correlated with reduced tissue damage and apoptosis. In Fas-deficient mice, fewer TUNEL positive cells undergoing apoptosis were observed (mainly neurons, although also oligodendrocytes and astrocytes). This correlated with the presence of Fas-expressing neurons after the injury in control mice and the presence of FasL-positive cells both in Fas-deficient and control mice (Yoshino et al., 2004). These functional studies confirmed that biding of the FasL to Fas receptors causes cell death after SCI and that inhibition of this signaling pathway could be a valuable therapeutic target for SCI patients.

Similar results were then obtained by Casha et al. (2005) using a model of T5-T6 clip compression SCI in mice. These authors detected post-traumatic apoptosis (activated caspase-8 and TUNEL) in neurons and oligodendrocytes. Apoptosis was reduced in $Fas^{Lpr/Lpr}$ mutant mice. However, in contrast to the results of Yoshino et al. (2004), the reduction in apoptosis was mainly observed in oligodendrocytes. Fas deficiency led to improved locomotor recovery after SCI, which was associated to increased axonal sparing and a significant improvement in white matter myelin (Casha et al., 2005). Whether Fas leads to caspase-8 activation and apoptotic death mainly in neurons or oligodendrocytes might depend on the type of injury (contusion/transection vs. clip compression, which causes a more severe ischemia).

Subsequent work has confirmed that neutralization of Fas signaling is beneficial for recovery after SCI (Ackery et al., 2006; Robins-Steele et al., 2012). Authors of these studies developed a treatment with soluble Fas receptors to improve recovery after SCI in rats. An immediate treatment with a soluble Fas receptor after a clip compression injury at C7-T1 in rats reduced the number of TUNEL positive cells 5 days post-injury and the expression of activated caspase-3 7 days post-injury (Ackery et al., 2006). This correlated with enhanced survival of neurons and oligodendrocytes, increased axonal integrity and improved behavioral recovery (Ackery et al., 2006). Results from this work were then confirmed by Robins-Steele et al. (2012). These authors showed that a delayed treatment (which is more clinically relevant) with a soluble Fas receptor 8–24 h after a clip compression injury at C7-T1 in rats enhances oligodendrocyte and neuronal survival, reduces cavity size and improves behavioral recovery (Robins-Steele et al., 2012).

A recent study has also shown that the transgenic overexpression of p45 (another member of the death domain superfamily) increases neuronal survival, decreases retraction of corticospinal tract fibers and improves functional recovery after a transection SCI at T9 in mice (Sung et al., 2013). p45 is able to form a complex with FADD attenuating FasL-induced caspase-8 activation and cell death caused by SCI (Sung et al., 2013).

The studies in rodent models have important implications for human SCI, because the Fas pathway is also activated in primates, including humans, after SCI (Jia et al., 2011; Yu and Fehlings, 2011). In rhesus monkeys, a T11 SC hemisection induced an increase in Fas and FasL immunoreactivity in the ventral horn at time points in which the number of apoptotic TUNEL positive cells also increased (Jia et al., 2011). A large number of Fas and FasL immunoreactive neurons and glial cells also accumulated at the injury epicenter in SCs from acutely injured human patients, while these were rarely observed in control or chronically injured SCs (Yu and Fehlings, 2011). This correlated with the appearance of TUNEL and active caspase positive cells in the SC of acutely injured patients. Moreover, double immunolabeling revealed the presence of Fas or FasL and caspase-3 positive cells and of Fas or FasL expressing macrophages/neutrophils (Yu and Fehlings, 2011). These studies highlight the importance of understanding apoptotic processes to develop effective therapies for patients with SCI. As shown in this section, neutralization of FasL/Fas signaling (antibodies or soluble receptors) leads to improvements in behavioral recovery after SCI in rodent models (Demjen et al., 2004; Ackery et al., 2006; Robins-Steele et al., 2012; **Table 1**). In addition, several potential treatments that have been effective in animal models reduced FasL/Fas signaling and/or caspase-8 activation (**Table 1**), indicating that this can be a key target when developing neuroprotective therapies for SCI patients. This includes therapies that have been translated to the clinic or that are in clinical trials for SCI patients (**Table 1**).

ACTIVATION OF CASPASE-8 IN THE BRAIN

As shown in the previous section, most studies focused on the role of caspase-8 and Fas in apoptosis of intrinsic SC cells. But, some of these studies also showed that the manipulation of FasL/Fas signaling leads to a significant increase in the regeneration/preservation of descending axons (Demjen et al., 2004; Casha et al., 2005; Ackery et al., 2006; Sung et al., 2013). These results suggest that inhibition of Fas signaling could be beneficial to preserve brain descending neurons and innervation after SCI. However, even with this evidence, no study in mammalian models has yet looked at the expression of Fas receptors or activated caspase-8 in descending neurons of the brain after SCI. We should take into account that there is still controversy on the topic of cell death in the brain following SCI. Several studies have shown the death of brain neurons after SCI in mammals, including humans (Holmes and May, 1909; Feringa and Vahlsing, 1985; Fry et al., 2003; Hains et al., 2003; Wu et al., 2003; Lee et al., 2004; Klapka et al., 2005). However, two recent studies in rats did not find any evidence of the death of corticospinal neurons after SCI (Nielson et al., 2010, 2011). The study by Nielson et al. (2011) suggested that corticospinal neurons suffer atrophy after SCI but do not die. The death/atrophy of descending neurons appears to involve and apoptotic mechanism as revealed by the appearance of TUNEL staining (although TUNEL can also label necrotic cells in some instances) and activated caspase-3 immunoreactivity in descending neurons of the brain (Hains et al., 2003; Wu et al., 2003; Lee et al., 2004).

TABLE 1 | Table showing treatments (genetic or pharmacological) used by different authors as potential therapies for SCI and that have been shown to reduce FasL/Fas signaling and/or caspase-8 activation in animal models.

Reference	SCI type	Species	Treatment	Molecular effect	Functional effect
Demjen et al. (2004)	Transection at T8/9	Mice	FasL-neutralizing antibody	Inhibits FasL signaling	↑ BBB score
Yoshino et al. (2004)	Contusion	MRL/Mp mice	FAS*lpr/lpr* mutant mice	Fas deficiency	↑ BBB score
Casha et al. (2005)	Compression at T5/6	C57BL/6 background matched mice	FAS*lpr/lpr* mutant mice	Fas deficiency	↑ BBB score
Ackery et al. (2006)	Compression at C7-T1	Wistar rats	Soluble Fas receptor	Inhibits Fas signaling	↑ BBB score
Genovese et al. (2007a)	Compression at T6/7	CD1 mice	Dexamethasone + Etanercept	↓ FasL	↑ BBB score
Genovese et al. (2007b)	Compression at T6/7	Mice	Melatonin + Dexamethasone	↓ FasL	↑ BBB score
Dasari et al. (2008)	Contusion at T10	Lewis rats	Umbilical Cord Blood Stem Cell	↓ FasL ↓ Fas ↓FADD	↑ BBB score
Genovese et al. (2008a)	Compression at T6/7	CD1 mice	15d-PGJ2	↓ FasL	↑ BBB score
Genovese et al. (2008b)	Compression at T5/8	CD1 mice	PD98059	↓ FasL	↑ BBB score
Genovese et al. (2008c)	Compression at T5/8	TNF-α WT mice	TNF-R1 knockout mice	↓ FasL	↑ BBB score
Genovese et al. (2008d)	Compression at T5/8	CD1 mice	Montelukast	↓ FasL	↑ BBB score
Genovese et al. (2008d)	Compression at T5/8	CD1 mice	Zileuton	↓ FasL	↑ BBB score
Genovese et al. (2009)	Compression at T5/8	CD1 mice	Ethyl pyruvate	↓ FasL	↑ BBB score
Cantarella et al. (2010)	Compression at T5/8	CD1 mice	TRAIL-neutralizing antibody	↓ FasL ↓ Caspase-8	↑ BBB score
Esposito et al. (2010)	Compression at T5/T8	CD1 mice	Olprinone	↓ FasL	↑ BMS score
Paterniti et al. (2010a)	Compression at T5/T8	CD1 mice	GW0742	↓ FasL	↑ BBB score
Paterniti et al. (2010b)	Compression at T5/T8	CD1 mice	T0901317	↓ FasL	↑ BBB score
Di Paola et al. (2011)	Compression at T6/7	CD1 mice	Carnosine	↓ FasL	↑ BMS score
Marsh and Flemming (2011)	Compression at T4	Wistar rats	Reparixin	↓ Fas	↑ BBB score
Paterniti et al. (2011)	Compression at T5/8	CD1 mice	SCH58261	↓ FasL	↑ BMS score
Impellizzeri et al. (2012a)	Compression at T5/8	CD1 mice	Ole aglycone	↓ FasL	↑ BMS score
Impellizzeri et al. (2012b)	Compression at T5/8	CD1 mice	Fasudil	↓ FasL	↑ BMS score
Ning et al. (2012)	Spinal cord ischemia	Sprague-Dawley rats	Methylprednisolone	↓ FasL ↓ Fas	↑ BBB score
Ning et al. (2012)	Spinal cord ischemia	Sprague-Dawley rats	Panax notoginsenoside	↓ FasL ↓ Fas	↑ BBB score
Ok et al. (2012)	Contusion at T9	Sprague–Dawley rats	Epidural hypothermia	↓ Caspase-8	↑ BBB score
Ok et al. (2012)	Contusion at T9	Sprague–Dawley rats	Systemic hypothermia	↓ Caspase-8	↑ BBB score
Robins-Steele et al. (2012)	Compression at C7-T1	Wistar rats	Soluble Fas receptor	Inhibits Fas signaling	↑ BBB score
Chengke et al. (2013)	Contusion at T10	Sprague-Dawley rats	Infliximab	↓ FADD	↑ BBB score
Chengke et al. (2013)	Contusion at T10	Sprague-Dawley rats	Methylprednisolone	↓ FADD	↑ BBB score
Chengke et al. (2013)	Contusion at T10	Sprague-Dawley rats	Infliximab + Methylprednisolone	↓ FADD	↑ BBB score
Sung et al. (2013)	Transection at T9	Mice	Thy1-p45 transgenic mice	↓ Fas-FADD-Caspase-8 signaling	↑ BMS score
Paterniti et al. (2014)	Compression at T6/7	CD1 mice	Docosahexaenoic acid	↓ FasL	↑ BMS score
Liu et al. (2015)	Contusion at T8	Sprague–Dawley rats	Carvedilol	↓ FasL ↓ Fas	↑ BBB score
Seo et al. (2015)	Contusion at T9	Sprague–Dawley rats	Methylprednisolone	↓ Caspase-8	↑ BBB score
Seo et al. (2015)	Contusion at T9	Sprague–Dawley rats	Therapeutic hypothermia	↓ Caspase-8	↑ BBB score
Huang et al. (2016)	Contusion at T10	Sprague-Dawley rats	Tetramethylpyrazine	↓ FasL	↑ BBB score
He et al. (2016)	Spinal cord ischemia	Wistar rats	miRNA-21	↓ FasL	↓ MDI score

In the "Molecular effect" column the arrows indicate a decreased expression of the corresponding molecule/s. The type of injury and the behavioral tests used to reveal behavioral improvements are also indicated in the table. Treatments that have been translated to the clinic or that are in clinical trials are highlighted in gray. Abbreviations: BBB, Basso, Beattie, Bresnahan score; BMS, Basso mouse scale score; MDI, motor deficit index score.

In contrast to mammals, lampreys show an amazing capacity for functional recovery following SCI. The regeneration of descending neurons is a key event in the recovery of swimming after SCI in lampreys (see Shifman et al., 2007; Rodicio and Barreiro-Iglesias, 2012). Regenerated descending axons of lampreys are able to establish new synapses with their target

neurons below the site of injury and the recovery of function depends, among other events, on the re-establishment of these connections (see Shifman et al., 2007). However, even in lampreys not all descending neurons are able to regenerate their axon after a complete SCI. The lamprey brainstem contains several individually identifiable descending neurons (**Figure 1B**) that vary greatly in their regenerative abilities after SCI (**Figure 1C**; Davis and McClellan, 1994; Jacobs et al., 1997; Barreiro-Iglesias et al., 2014). Some of these neurons are classified as "good regenerators" (i.e., they regenerate their axon more than 55% of the times) and others are considered "bad regenerators" (i.e., they regenerate their axon less than 30% of the times; **Figure 1C**; Jacobs et al., 1997). In recent years, mounting evidence has confirmed that descending neurons of lampreys known to be "bad regenerators" suffer a process of delayed death and are also "poor survivors" after a complete SCI (**Figure 1C**; Shifman et al., 2008; Barreiro-Iglesias and Shifman, 2012, 2015; Busch and Morgan, 2012; Hu et al., 2013, 2017; Zhang et al., 2014; Barreiro-Iglesias, 2015; Fogerson et al., 2016; Barreiro-Iglesias et al., 2017). The occurrence of cell death in a subset of identifiable descending neurons after SCI in lampreys was confirmed based on the disappearance of Nissl staining (**Figure 1C**), the loss of neurofilament expression, the absence of labeling when using retrograde tracers (Shifman et al., 2008), and the early staining of these neurons with Fluoro-Jade C (Busch and Morgan, 2012; Barreiro-Iglesias et al., 2017), which is a marker for degenerating neurons. In addition, the appearance of TUNEL staining (Shifman et al., 2008; Hu et al., 2013) and activated caspases (**Figure 1C**; Barreiro-Iglesias and Shifman, 2012, 2015; Hu et al., 2013; Barreiro-Iglesias et al., 2017) in the soma of axotomized descending neurons suggests that their death after SCI is apoptotic. The detection of activated caspase-8 in the first 2 weeks after the injury (**Figure 1B**; Barreiro-Iglesias and Shifman, 2012; Barreiro-Iglesias et al., 2017) and the lack of cytochrome-c release from mitochondria (Barreiro-Iglesias et al., 2017) indicates that the extrinsic apoptotic pathway is activated in descending neurons of lampreys after SCI. Caspase-8 activation in the soma of descending neurons of lampreys is preceded by the activation of caspases in the axotomized axons at the lesion site within the first hours after the injury (**Figure 1A**; Barreiro-Iglesias and Shifman, 2015; Barreiro-Iglesias et al., 2017). Caspase activation is progressively detected in descending axons at higher spinal levels and finally in the soma of descending neurons after SCI (**Figure 1A**; Barreiro-Iglesias and Shifman, 2015; Barreiro-Iglesias et al., 2017), which indicates that the degenerative process is initiated in the damaged axon in the SC. Taxol, which improves recovery from SCI in mammalian models (Hellal et al., 2011), prevented the appearance of activated caspase-8 in the soma of descending neurons (Barreiro-Iglesias et al., 2017) of lampreys. This indicates that death signals (or caspase-8 itself) are retrogradely transported by microtubules to the soma of descending neurons after SCI in lampreys.

The work in lampreys suggests that activated caspase-8 could also play a role in the death of descending neurons of mammals after SCI. Interestingly, in olfactory neurons of mice, appearance of activated caspase-8 in the cell body after olfactory bulbectomy depends on microtubule-based retrograde transport of activated caspase-8 by its association with dynactin $p150^{Glued}$ (Carson et al., 2005), which might reveal conserved mechanisms with descending neurons of lampreys. In addition, the preservation of axonal projections in the SC after experimental inhibition of Fas signaling indicates that Fas receptors could play a role in the activation of caspase-8 in descending neurons after SCI.

CONCLUSION

Several reports have confirmed that the activation of caspase-8 and the extrinsic apoptotic pathway is one of the mechanisms causing cell death after SCI and that the FasL/Fas signaling pathway plays a key role in this process. Surprisingly, no study has yet attempted to directly inhibit caspase-8 after SCI. This experimental approach could be of interest, especially because caspase-8 activation is not only caused by Fas receptor activation, which could lead to further improvements in recovery from SCI. Also, another aim for future work, and based on the lamprey results, should be to investigate the possible activation of caspase-8 in descending neurons of mammals after SCI and the implication of Fas signaling and microtubule retrograde transport in this process. Finally, translation of all this knowledge to pre-clinical studies or even clinical trials is of obvious and crucial importance.

AUTHOR CONTRIBUTIONS

AB-I wrote the manuscript with help from DS-C. DS-C prepared the figure and the table. All the work was supervised by AB-I.

FUNDING

This work was supported by a grant from the Spanish Ministry of Economy and Competitiveness and the European Regional Development Fund 2007–2013 (BFU2014-56300-P). AB-I was supported by a grant from the Xunta de Galicia (2016-PG008) and a grant from the crowdfunding platform *Precipita* (FECYT; Spanish Ministry of Economy and Competitiveness; grant number 2017-CP081).

ACKNOWLEDGMENTS

The authors would like to acknowledge the following individual donors of the crowdfunding campaign in *Precipita*: Emilio Río, Guillermo Vivar, Pablo Pérez, Jorge Férnandez, Ignacio Valiño, Pago de los Centenarios, Eva Candal, María del Pilar Balsa, Jorge Faraldo, Isabel Rodríguez-Moldes, José Manuel López, Juan José Pita, María E. Cameán, Jesús Torres, José Pumares, Verónica Rodríguez, Sara López, Tania Villares Balsa, Rocío Lizcano, José García, Ana M. Cereijo, María Pardo, Nerea Santamaría, Carolina Hernández, Jesús López and María Maneiro.

REFERENCES

Ackery, A., Robins, S., and Fehlings, M. G. (2006). Inhibition of Fas-mediated apoptosis through administration of soluble Fas receptor improves functional outcome and reduces posttraumatic axonal degeneration after acute spinal cord injury. *J. Neurotrauma* 23, 604–616. doi: 10.1089/neu.2006.23.604

Ahuja, C. S., Wilson, J. R., Nori, S., Kotter, M. R., Druschel, C., Curt, A., et al. (2017). Traumatic spinal cord injury. *Nat. Rev. Dis. Primers* 3:17018. doi: 10.1038/nrdp.2017.18

Barreiro-Iglesias, A. (2015). "Bad regenerators" die after spinal cord injury: insights from lampreys. *Neural Regen. Res.* 10, 25–27. doi: 10.4103/1673-5374.150642

Barreiro-Iglesias, A., and Shifman, M. I. (2012). Use of fluorochrome-labeled inhibitors of caspases to detect neuronal apoptosis in the whole-mounted lamprey brain after spinal cord injury. *Enzyme Res.* 2012:835731. doi: 10.1155/2012/835731

Barreiro-Iglesias, A., and Shifman, M. I. (2015). Detection of activated caspase-8 in injured spinal axons by using fluorochrome-labeled inhibitors of caspases (FLICA FLICA). *Methods Mol. Biol.* 1254, 329–339. doi: 10.1007/978-1-4939-2152-2_23

Barreiro-Iglesias, A., Sobrido-Cameán, D., and Shifman, M. I. (2017). Retrograde activation of the extrinsic apoptotic pathway in spinal-projecting neurons after a complete spinal cord injury in lampreys. *Biomed Res. Int.* 2017:5953674. doi: 10.1155/2017/5953674

Barreiro-Iglesias, A., Zhang, G., Selzer, M. E., and Shifman, M. I. (2014). Complete spinal cord injury and brain dissection protocol for subsequent wholemount in situ hybridization in larval sea lamprey. *J. Vis. Exp.* 14:e51494. doi: 10.3791/51494

Busch, D. J., and Morgan, J. R. (2012). Synuclein accumulation is associated with cell-specific neuronal death after spinal cord injury. *J. Comp. Neurol.* 520, 1751–1771. doi: 10.1002/cne.23011

Cantarella, G., Di Benedetto, G., Scollo, M., Paterniti, I., Cuzzocrea, S., Bosco, P., et al. (2010). Neutralization of tumor necrosis factor-related apoptosis-inducing ligand reduces spinal cord injury damage in mice. *Neuropsychopharmacology* 35, 1302–1314. doi: 10.1038/npp.2009.234

Carson, C., Saleh, M., Fung, F. W., Nicholson, D. W., and Roskams, A. J. (2005). Axonal dynactin p150Glued transports caspase-8 to drive retrograde olfactory receptor neuron apoptosis. *J. Neurosci.* 25, 6092–6104. doi: 10.1523/JNEUROSCI.0707-05.2005

Casha, S., Yu, W. R., and Fehlings, M. G. (2001). Oligodendroglial apoptosis occurs along degenerating axons and is associated with FAS and p75 expression following spinal cord injury in the rat. *Neuroscience* 103, 203–218. doi: 10.1016/s0306-4522(00)00538-8

Casha, S., Yu, W. R., and Fehlings, M. G. (2005). FAS deficiency reduces apoptosis, spares axons and improves function after spinal cord injury. *Exp. Neurol.* 196, 390–400. doi: 10.1016/j.expneurol.2005.08.020

Chen, K. B., Uchida, K., Nakajima, H., Yayama, T., Hirai, T., Watanabe, S., et al. (2011). Tumor necrosis factor-α antagonist reduces apoptosis of neurons and oligodendroglia in rat spinal cord injury. *Spine* 36, 1350–1358. doi: 10.1097/BRS.0b013e3181f014ec

Chengke, L., Weiwei, L., Xiyang, W., Ping, W., Xiaoyang, P., Zhengquan, X., et al. (2013). Effect of infliximab combined with methylprednisolone on expressions of NF-κB, TRADD, and FADD in rat acute spinal cord injury. *Spine* 38, 861–869. doi: 10.1097/BRS.0b013e318294892c

Crowe, M. J., Bresnahan, J. C., Shuman, S. L., Masters, J. N., and Crowe, M. S. (1997). Apoptosis and delayed degeneration after spinal cord injury in rats and monkeys. *Nat. Med.* 3, 73–76. doi: 10.1038/nm0197-73

Dasari, V. R., Spomar, D. G., Li, L., Gujrati, M., Rao, J. S., and Dinh, D. H. (2008). Umbilical cord blood stem cell mediated downregulation of fas improves functional recovery of rats after spinal cord injury. *Neurochem. Res.* 33, 134–149. doi: 10.1007/s11064-007-9426-6

Davis, G. R. Jr., and McClellan, A. D. (1994). Extent and time course of restoration of descending brainstem projections in spinal cord-transected lamprey. *J. Comp. Neurol.* 344, 65–82. doi: 10.1002/cne.903440106

Demjen, D., Klussmann, S., Kleber, S., Zuliani, C., Stieltjes, B., Metzger, C., et al. (2004). Neutralization of CD95 ligand promotes regeneration and functional recovery after spinal cord injury. *Nat. Med.* 10, 389–395. doi: 10.1038/nm1007

Di Paola, R., Impellizzeri, D., Salinaro, A. T., Mazzon, E., Bellia, F., Cavallaro, M., et al. (2011). Administration of carnosine in the treatment of acute spinal cord injury. *Biochem. Pharmacol.* 82, 1478–1489. doi: 10.1016/j.bcp.2011.07.074

Emery, E., Aldana, P., Bunge, M. B., Puckett, W., Srinivasan, A., Keane, R. W., et al. (1998). Apoptosis after traumatic human spinal cord injury. *J. Neurosurg.* 89, 911–920. doi: 10.3171/jns.1998.89.6.0911

Esposito, E., Mazzon, E., Paterniti, I., Impellizzeri, D., Bramanti, P., and Cuzzocrea, S. (2010). Olprinone attenuates the acute inflammatory response and apoptosis after spinal cord trauma in mice. *PLoS One* 5:e12170. doi: 10.1371/journal.pone.0012170

Feringa, E. R., and Vahlsing, H. L. (1985). Labeled corticospinal neurons one year after spinal cord transection. *Neurosci. Lett.* 58, 283–286. doi: 10.1016/0304-3940(85)90067-9

Fernández-López, B., Barreiro-Iglesias, A., and Rodicio, M. C. (2016). Anatomical recovery of the spinal glutamatergic system following a complete spinal cord injury in lampreys. *Sci. Rep.* 6:37786. doi: 10.1038/srep37786

Fernández-López, B., Valle-Maroto, S. M., Barreiro-Iglesias, A., and Rodicio, M. C. (2014). Neuronal release and successful astrocyte uptake of aminoacidergic neurotransmitters after spinal cord injury in lampreys. *Glia* 62, 1254–1269. doi: 10.1002/glia.22678

Fogerson, S. M., van Brummen, A. J., Busch, D. J., Allen, S. R., Roychaudhuri, R., Banks, S. M., et al. (2016). Reducing synuclein accumulation improves neuronal survival after spinal cord injury. *Exp. Neurol.* 278, 105–115. doi: 10.1016/j.expneurol.2016.02.004

Fry, E. J., Stolp, H. B., Lane, M. A., Dziegielewska, K. M., and Saunders, N. R. (2003). Regeneration of supraspinal axons after complete transection of the thoracic spinal cord in neonatal opossums (*Monodelphis domestica*). *J. Comp. Neurol.* 466, 422–444. doi: 10.1002/cne.10904

Genovese, T., Esposito, E., Mazzon, E., Di Paola, R., Meli, R., Caminiti, R., et al. (2009). Beneficial effects of ethyl pyruvate in a mouse model of spinal cord injury. *Shock* 32, 217–227. doi: 10.1097/SHK.0b013e31818d4073

Genovese, T., Esposito, E., Mazzon, E., Di Paola, R., Muia, C., Meli, R., et al. (2008a). Effect of cyclopentanone prostaglandin 15-deoxy-Δ12, 14PGJ2 on early functional recovery from experimental spinal cord injury. *Shock* 30, 142–152. doi: 10.1097/SHK.0b013e31815dd381

Genovese, T., Esposito, E., Mazzon, E., Muià, C., Di Paola, R., Meli, R., et al. (2008b). Evidence for the role of mitogen-activated protein kinase signaling pathways in the development of spinal cord injury. *J. Pharmacol. Exp. Ther.* 325, 100–114. doi: 10.1124/jpet.107.131060

Genovese, T., Mazzon, E., Crisafulli, C., Di Paola, R., Muià, C., Esposito, E., et al. (2008c). TNF-α blockage in a mouse model of SCI: evidence for improved outcome. *Shock* 29, 32–41. doi: 10.1097/shk.0b013e318059053a

Genovese, T., Rossi, A., Mazzon, E., Di Paola, R., Muià, C., Caminiti, R., et al. (2008d). Effects of zileuton and montelukast in mouse experimental spinal cord injury. *Br. J. Pharmacol.* 153, 568–582. doi: 10.1038/sj.bjp.0707577

Genovese, T., Mazzon, E., Crisafulli, C., Esposito, E., Di Paola, R., Muià, C., et al. (2007a). Combination of dexamethasone and etanercept reduces secondary damage in experimental spinal cord trauma. *Neuroscience* 150, 168–181. doi: 10.1016/j.neuroscience.2007.06.059

Genovese, T., Mazzon, E., Crisafulli, C., Esposito, E., Di Paola, R., Muià, C., et al. (2007b). Effects of combination of melatonin and dexamethasone on secondary injury in an experimental mice model of spinal cord trauma. *J. Pineal Res.* 43, 140–153. doi: 10.1111/j.1600-079x.2007.00454.x

Hains, B. C., Black, J. A., and Waxman, S. G. (2003). Primary cortical motor neurons undergo apoptosis after axotomizing spinal cord injury. *J. Comp. Neurol.* 462, 328–341. doi: 10.1002/cne.10733

He, F., Ren, Y., Shi, E., Liu, K., Yan, L., and Jiang, X. (2016). Overexpression of microRNA-21 protects spinal cords against transient ischemia. *J. Thorac. Cardiovasc. Surg.* 152, 1602–1608. doi: 10.1016/j.jtcvs.2016.07.065

Hellal, F., Hurtado, A., Ruschel, J., Flynn, K. C., Laskowski, C. J., Umlauf, M., et al. (2011). Microtubule stabilization reduces scarring and causes

axon regeneration after spinal cord injury. *Science* 331, 928–931. doi: 10.1126/science.1201148

Holmes, G., and May, W. P. (1909). On the exact origin of the pyramidal tracts in man and other mammals. *Proc. R. Soc. Med.* 2, 92–100. doi: 10.1093/brain/32.1.1

Hu, J., Zhang, G., Rodemer, W., Jin, L. Q., Shifman, M., and Selzer, M. E. (2017). The role of RhoA in retrograde neuronal death and axon regeneration after spinal cord injury. *Neurobiol. Dis.* 98, 25–35. doi: 10.1016/j.nbd.2016.11.006

Hu, J., Zhang, G., and Selzer, M. E. (2013). Activated caspase detection in living tissue combined with subsequent retrograde labeling, immunohistochemistry or in situ hybridization in whole-mounted lamprey brains. *J. Neurosci. Methods* 220, 92–98. doi: 10.1016/j.jneumeth.2013.08.016

Huang, J. H., Cao, Y., Zeng, L., Wang, G., Cao, M., Lu, H. B., et al. (2016). Tetramethylpyrazine enhances functional recovery after contusion spinal cord injury by modulation of MicroRNA-21, FasL, PDCD4 and PTEN expression. *Brain Res.* 1648, 35–45. doi: 10.1016/j.brainres.2016.07.023

Impellizzeri, D., Esposito, E., Mazzon, E., Paterniti, I., Di Paola, R., Bramanti, P., et al. (2012a). The effects of a polyphenol present in olive oil, oleuropein aglycone, in an experimental model of spinal cord injury in mice. *Biochem. Pharmacol.* 83, 1413–1426. doi: 10.1016/j.bcp.2012.02.001

Impellizzeri, D., Mazzon, E., Paterniti, I., Esposito, E., and Cuzzocrea, S. (2012b). Effect of fasudil, a selective inhibitor of Rho kinase activity, in the secondary injury associated with the experimental model of spinal cord trauma. *J. Pharmacol. Exp. Ther.* 343, 21–33. doi: 10.1124/jpet.111.191239

Jacobs, A. J., Swain, G. P., Snedeker, J. A., Pijak, D. S., Gladstone, L. J., and Selzer, M. E. (1997). Recovery of neurofilament expression selectively in regenerating reticulospinal neurons. *J. Neurosci.* 17, 5206–5220.

Jia, L., Yu, Z., Hui, L., Yu-Guang, G., Xin-Fu, Z., Chao, Y., et al. (2011). Fas and FasL expression in the spinal cord following cord hemisection in the monkey. *Neurochem. Res.* 36, 419–425. doi: 10.1007/s11064-010-0357-2

Keane, R. W., Kraydieh, S., Lotocki, G., Bethea, J. R., Krajewski, S., Reed, J. C., et al. (2001). Apoptotic and anti-apoptotic mechanisms following spinal cord injury. *J. Neuropathol. Exp. Neurol.* 60, 422–429. doi: 10.1093/jnen/60.5.422

Kischkel, F. C., Hellbardt, S., Behrmann, I., Germer, M., Pawlita, M., Krammer, P. H., et al. (1995). Cytotoxicity-dependent APO-1 (Fas/CD95)-associated proteins form a death-inducing signaling complex (DISC) with the receptor. *EMBO J.* 14, 5579–5588.

Klapka, N., Hermanns, S., Straten, G., Masanneck, C., Duis, S., Hamers, F. P., et al. (2005). Suppression of fibrous scarring in spinal cord injuryof rat promotes long-distance regeneration of corticospinal tract axons, rescue of primary motoneurons in somatosensory cortex and significant functional recovery. *Eur. J. Neurosci.* 22, 3047–3058. doi: 10.1111/j.1460-9568.2005.04495.x

Lee, B. H., Lee, K. H., Kim, U. J., Sohn, J. H., Choi, S. S., Yi, I. G., et al. (2004). Injury in the spinal cord may produce cell death in the brain. *Brain Res.* 1020, 37–44. doi: 10.1016/j.brainres.2004.05.113

Liu, D., Huang, Y., Li, B., Jia, C., Liang, F., and Fu, Q. (2015). Carvedilol promotes neurological function, reduces bone loss and attenuates cell damage after acute spinal cord injury in rats. *Clin. Exp. Pharmacol. Physiol.* 42, 202–212. doi: 10.1111/1440-1681.12345

Marsh, D. R., and Flemming, J. M. P. (2011). Inhibition of CXCR1 and CXCR2 chemokine receptors attenuates acute inflammation, preserves gray matter and diminishes autonomic dysreflexia after spinal cord injury. *Spinal Cord* 49, 337–344. doi: 10.1038/sc.2010.127

Martin-Villalba, A., Herr, I., Jeremias, I., Hahne, M., Brandt, R., Vogel, J., et al. (1999). CD95 ligand (Fas-L/APO-1L) and tumor necrosis factor-related apoptosis-inducing ligand mediate ischemia-induced apoptosis in neurons. *J. Neurosci.* 19, 3809–3817.

Matsushita, K., Wu, Y., Qiu, J., Lang-Lazdunski, L., Hirt, L., Waeber, C., et al. (2000). Fas receptor and neuronal cell death after spinal cord ischemia. *J. Neurosci.* 20, 6879–6887.

National Spinal Cord Injury Statistical Center. (2016). *Facts and Figures at a Glance.* Birmingham, AL: University of Alabama at Birmingham.

Nielson, J. L., Sears-Kraxberger, I., Strong, M. K., Wong, J. K., Willenberg, R., and Steward, O. (2010). Unexpected survival of neurons of origin of the pyramidal tract after spinal cord injury. *J. Neurosci.* 30, 11516–11528. doi: 10.1523/JNEUROSCI.1433-10.2010

Nielson, J. L., Strong, M. K., and Steward, O. (2011). A reassessment of whether cortical motor neurons die following spinal cord injury. *J. Comp. Neurol.* 519, 2852–2869. doi: 10.1002/cne.22661

Ning, N., Dang, X., Bai, C., Zhang, C., and Wang, K. (2012). Panax notoginsenoside produces neuroprotective effects in rat model of acute spinal cord ischemia-reperfusion injury. *J. Ethnopharmacol.* 139, 504–512. doi: 10.1016/j.jep.2011.11.040

Ok, J. H., Kim, Y. H., and Ha, K. Y. (2012). Neuroprotective effects of hypothermia after spinal cord injury in rats: comparative study between epidural hypothermia and systemic hypothermia. *Spine* 37, 1551–1559. doi: 10.1097/BRS.0b013e31826ff7f1

Paterniti, I., Esposito, E., Mazzon, E., Galuppo, M., Di Paola, R., Bramanti, P., et al. (2010a). Evidence for the role of peroxisome proliferator-activated receptor-β/δ in the development of spinal cord injury. *J. Pharmacol. Exp. Ther.* 333, 465–477. doi: 10.1124/jpet.110.165605

Paterniti, I., Genovese, T., Mazzon, E., Crisafulli, C., Di Paola, R., Galuppo, M., et al. (2010b). Liver X receptor agonist treatment regulates inflammatory response after spinal cord trauma. *J. Neurochem.* 112, 611–624. doi: 10.1111/j.1471-4159.2009.06471.x

Paterniti, I., Impellizzeri, D., Di Paola, R., Esposito, E., Gladman, S., Yip, P., et al. (2014). Docosahexaenoic acid attenuates the early inflammatory response following spinal cord injury in mice: *in-vivo* and *in-vitro* studies. *J. Neuroinflammation* 11:6. doi: 10.1186/1742-2094-11-6

Paterniti, I., Melani, A., Cipriani, S., Corti, F., Mello, T., Mazzon, E., et al. (2011). Selective adenosine A_{2A} receptor agonists and antagonists protect against spinal cord injury through peripheral and central effects. *J. Neuroinflammation* 8:31. doi: 10.1186/1742-2094-8-31

Robins-Steele, S., Nguyen, D. H., and Fehlings, M. G. (2012). The delayed post-injury administration of soluble fas receptor attenuates post-traumatic neural degeneration and enhances functional recovery after traumatic cervical spinal cord injury. *J. Neurotrauma* 29, 1586–1599. doi: 10.1089/neu.2011.2005

Rodicio, M. C., and Barreiro-Iglesias, A. (2012). Lampreys as an animal model in regeneration studies after spinal cord injury. *Rev. Neurol.* 55, 157–166.

Seo, J. Y., Kim, Y. H., Kim, J. W., Kim, S. I., and Ha, K. Y. (2015). Effects of therapeutic hypothermia on apoptosis and autophagy after spinal cord injury in rats. *Spine* 40, 883–890. doi: 10.1097/BRS.0000000000000845

Shifman, M. I., Jin, L. Q., and Selzer, M. E. (2007). "Regeneration in the lamprey spinal cord," in *Model Organisms in Spinal Cord Regeneration* (Vol. 1), eds C. G. Becker and T. Becker (Weinheim: Wiley-VCH), 229–262.

Shifman, M. I., Zhang, G., and Selzer, M. E. (2008). Delayed death of identified reticulospinal neurons after spinal cord injury in lampreys. *J. Comp. Neurol.* 510, 269–282. doi: 10.1002/cne.21789

Shuman, S. L., Bresnahan, J. C., and Beattie, M. S. (1997). Apoptosis of microglia and oligodendrocytes after spinal cord contusion in rats. *J. Neurosci. Res.* 50, 798–808. doi: 10.1002/(sici)1097-4547(19971201)50:5<798::aid-jnr16>3.3.co;2-#

Sung, T. C., Chen, Z., Thuret, S., Vilar, M., Gage, F. H., Riek, R., et al. (2013). P45 forms a complex with FADD and promotes neuronal cell survival following spinal cord injury. *PLoS One* 8:e69286. doi: 10.1371/journal.pone.0069286

Takagi, T., Takayasu, M., Mizuno, M., Yoshimoto, M., and Yoshida, J. (2003). Caspase activation in neuronal and glial apoptosis following spinal cord injury in mice. *Neurol. Med. Chir.* 43, 20–30. doi: 10.2176/nmc.43.20

Ulndreaj, A., Badner, A., and Fehlings, M. G. (2017). Promising neuroprotective strategies for traumatic spinal cord injury with a focus on the differential effects among anatomical levels of injury. *Research* 6:1907. doi: 10.12688/f1000research.11633.1

Wu, K. L., Chan, S. H., Chao, Y. M., and Chan, J. Y. (2003). Expression of pro-inflammatory cytokine and caspase genes promotes neuronal apoptosis in pontine reticular formation after spinal cord transection. *Neurobiol. Dis.* 14, 19–31. doi: 10.1016/s0969-9961(03)00078-0

Yoshino, O., Matsuno, H., Nakamura, H., Yudoh, K., Abe, Y., Sawai, T., et al. (2004). The role of Fas-mediated apoptosis after traumatic spinal cord injury. *Spine* 29, 1394–1404. doi: 10.1097/01.brs.0000129894.34550.48

Yu, W. R., and Fehlings, M. G. (2011). Fas/FasL-mediated apoptosis and inflammation are key features of acute human spinal cord injury: implications for translational, clinical application. *Acta Neuropathol.* 122, 747–761. doi: 10.1007/s00401-011-0882-3

Zhang, G., Hu, J., Li, S., Huang, L., and Selzer, M. E. (2014). Selective expression of CSPG receptors PTPσ and LAR in poorly regenerating reticulospinal neurons of lamprey. *J. Comp. Neurol.* 522, 2209–2222. doi: 10.1002/cne.23529

Conflict of Interest Statement: The authors declare that the research was conducted in the absence of any commercial or financial relationships that could be construed as a potential conflict of interest.

frontiers in Molecular Neuroscience

MINI REVIEW
published: 04 March 2019
doi: 10.3389/fnmol.2019.00059

Molecular Mechanisms Underlying Sensory-Motor Circuit Dysfunction in SMA

Hannah K. Shorrock[1,2†], Thomas H. Gillingwater[1,2] and Ewout J. N. Groen[1,2]*

[1] Edinburgh Medical School: Biomedical Sciences, The University of Edinburgh, Edinburgh, United Kingdom, [2] Euan MacDonald Centre for Motor Neurone Disease Research, The University of Edinburgh, Edinburgh, United Kingdom

Activation of skeletal muscle in response to acetylcholine release from the neuromuscular junction triggered by motor neuron firing forms the basis of all mammalian locomotion. Intricate feedback and control mechanisms, both from within the central nervous system and from sensory organs in the periphery, provide essential inputs that regulate and finetune motor neuron activity. Interestingly, in motor neuron diseases, such as spinal muscular atrophy (SMA), pathological studies in patients have identified alterations in multiple parts of the sensory-motor system. This has stimulated significant research efforts across a range of different animal models of SMA in order to understand these defects and their contribution to disease pathogenesis. Several recent studies have demonstrated that defects in sensory components of the sensory-motor system contribute to dysfunction of motor neurons early in the pathogenic process. In this review, we provide an overview of these findings, with a specific focus on studies that have provided mechanistic insights into the molecular processes that underlie dysfunction of the sensory-motor system in SMA. These findings highlight the role that cell types other than motor neurons play in SMA pathogenesis, and reinforce the need for therapeutic interventions that target and rescue the wide array of defects that occur in SMA.

Keywords: spinal muscular atrophy, SMN, sensory-motor circuit, proprioception, motor neuron, neurodegenaration

OPEN ACCESS

Edited by:
Andrew Paul Tosolini, University College London, United Kingdom

Reviewed by:
Chien-Ping Ko, University of Southern California, United States
George Mentis, Columbia University, United States

***Correspondence:**
Ewout J. N. Groen
e.groen@ed.ac.uk

†*Present address:*
Hannah K. Shorrock, Center for NeuroGenetics, Department of Molecular Genetics and Microbiology, College of Medicine, University of Florida, Gainesville, FL, United States

Received: *14 December 2018*
Accepted: *15 February 2019*
Published: *04 March 2019*

Citation:
Shorrock HK, Gillingwater TH and Groen EJN (2019) Molecular Mechanisms Underlying Sensory-Motor Circuit Dysfunction in SMA. Front. Mol. Neurosci. 12:59. doi: 10.3389/fnmol.2019.00059

INTRODUCTION

Lower motor neurons, whose cell bodies are resident in the ventral gray horn of spinal cord, represent the "final common pathway" (Sherrington, 1906) through which neuronal activity has to pass in order to generate the contraction of skeletal muscle required for movement. Whilst a large proportion of the synaptic inputs controlling lower motor neuron function arise from descending pathways, including upper motor neurons, pioneering work begun by Sir John Eccles and colleagues in the 1950s has revealed the additional influence of synaptic inputs arising from proprioceptive sensory neurons (including group Ia afferents), whose cell bodies are located in the dorsal root ganglia (DRG) (Eccles et al., 1957; Brown, 1981; Mears and Frank, 1997). These sensory inputs have been shown to form monosynaptic connections with lower motor neurons (**Figure 1**), whereby they can regulate motor neuron firing patterns as part of the monosynaptic spinal stretch reflex arc as well as in other locomotor behaviors (Rossignol et al., 2006).

Recent work has begun to uncover the complex molecular pathways regulating the formation and maintenance of such sensory-motor connectivity in the spinal cord, highlighting key roles for pathways incorporating Sema3e–Plxnd1 signaling (Pecho-Vrieseling et al., 2009) and the RNaseIII protein Dicer (Imai et al., 2016). Moreover, several studies have highlighted how disruption of sensory-motor connectivity can result from perturbations in genes and proteins underlying a diverse range of neurodegenerative conditions, including; amyotrophic lateral sclerosis (ALS) (Jiang et al., 2009), post-polio muscular atrophy (PPMA) (Soliven and Maselli, 1992), and spinal muscular atrophy (SMA) (see below). In this review we provide an overview of the contributions that sensory-motor connectivity defects make to the pathogenesis of SMA, incorporating new insights into underlying molecular pathways that suggest the existence of common mechanisms across diverse neuromuscular conditions.

SENSORY-MOTOR DEFECTS IN SPINAL MUSCULAR ATROPHY (SMA)

SMA is a hereditary form of motor neuron disease, characterized by degeneration and death of lower (alpha) motor neurons in the ventral horn of spinal cord (Lunn and Wang, 2008; Groen et al., 2018b). This leads to progressive proximal muscle weakness, atrophy and, in severe cases, paralysis and death. SMA is caused by homozygous deletion of, or other deleterious variants in, the *SMN1* gene, leading to a significant reduction in the expression of full-length survival motor neuron protein (SMN). SMN is a ubiquitously expressed protein that has been implicated in numerous cellular processes, including snRNP biogenesis, cytoskeletal dynamics, protein homeostasis, and mitochondrial function and is required for cellular survival. A detailed discussion of the cellular roles of SMN can be found in a number of recent review papers [for example (Hosseinibarkooie et al., 2017; Singh et al., 2017; Chaytow et al., 2018)].

In line with the ubiquitous expression of SMN, SMA is not solely a disease of the lower motor neuron. For example, it is now known that multiple different organ systems and cell types are affected in SMA (Nash et al., 2016), including defects in the heart, vasculature and skeletal muscles (Hamilton and Gillingwater, 2013; Shababi et al., 2014). Alongside these systemic pathologies, defects in sensory neurons have been reported in SMA patients, including abnormal sensory conduction (Duman et al., 2013; Yonekawa et al., 2013) or complete absence of sensory nerve action potentials (Yuan and Jiang, 2015; Reid et al., 2016), along with axonal degeneration and loss of myelinated fibers within sensory nerves (Korinthenberg et al., 1997; Omran et al., 1998; Rudnik-Schoneborn et al., 2003). Depending on the type of SMA, varying structural abnormalities in muscle spindles have been described, although some of these findings are contradictory and would require further investigation (Marshall and Duchen, 1975; Bobele et al., 1996; Kararizou et al., 2006). Several studies conducted on presumed SMA cases (patients diagnosed with SMA before genetic testing was available for the disease) also identified degeneration of sensory nerves, glial bundles within dorsal roots, ballooned neurons and chromatolysis within the DRG (Marshall and Duchen, 1975; Carpenter et al., 1978; Shishikura et al., 1983; Murayama et al., 1991). Importantly, reduced synaptophysin expression has been observed adjacent to anterior horn neuron cell bodies in SMA patients, indicating a reduction in the number of or disconnection of afferent nerve fibers, including sensory synapses (Ikemoto et al., 1996). Not only do these studies demonstrate defects within the sensory neurons themselves but they also demonstrate the possibility of alterations and lack of connectivity at both extremities of the sensory neuron.

Sensory-Motor Defects in Mouse Models of SMA

The SMA research field has benefited greatly from the availability of a number of animal models that mimic key pathological features of SMA, such as motor neuron death, degeneration of the neuromuscular junction and organ pathology (Hamilton and Gillingwater, 2013; Edens et al., 2015). Indeed, model systems of SMA also recapitulate core defects of the sensory nervous system seen in SMA patients. For example, sensory neurons cultured from a severe mouse model of SMA show defects in neurite outgrowth and growth cone morphology, along with a reduction of beta-actin protein and mRNA in growth cones (Jablonka et al., 2006) – a phenotype that is similar to that observed in SMN deficient motor neurons (Rossoll et al., 2003). In mouse models of SMA, sensory neurons are smaller, consistent with an appearance of overall reduced size of DRGs (Shorrock et al., 2018b). Moreover, the ratio of different subtypes of sensory neurons in SMA DRG is altered (see Section "Molecular Mechanisms Associated With Sensory Neuron Dysfunction in SMA and Related Conditions") (Shorrock et al., 2018b). It has also been shown that there is a reduction in myelinated dorsal root axons in SMA mice compared to controls (Ling et al., 2010) and a reduction of sensory fibers passing into the ventral horn in SMA mice (Mentis et al., 2011).

Importantly, in line with what has been observed in SMA patients, these structural defects occurring in sensory neurons have also been associated with defects at the level of synapses formed by sensory neurons in SMA mice (Fletcher and Mentis, 2016). The total number of synapses onto motor neurons in the lumbar region of the spinal cord is significantly reduced in mouse models of SMA (Ling et al., 2010). The largest contribution to this overall reduction of sensory synapses comes from a reduction in the number of vGlut1-positive synapses which primarily originate from proprioceptive neurons. This central feature of sensory-motor pathology has now been observed across multiple different SMA mouse models, including the commonly used *Taiwanese* and *delta7* models, suggesting that it is a conserved feature of the disease (Ling et al., 2010; Mentis et al., 2011; Shorrock et al., 2018b). Within the lumbar region of spinal cord, the reduction in proprioceptive synapses onto motor neurons is most severe at the level of L1 motor neurons and medial L5 motor neurons (Mentis et al., 2011). Interestingly, this reduction is observed presymptomatically, (Mentis et al., 2011; Fletcher et al., 2017) and is associated with significant functional deficits (Fletcher et al., 2017). Thus, sensory-motor connectivity defects reported in SMA mice consistently affect DRGs and

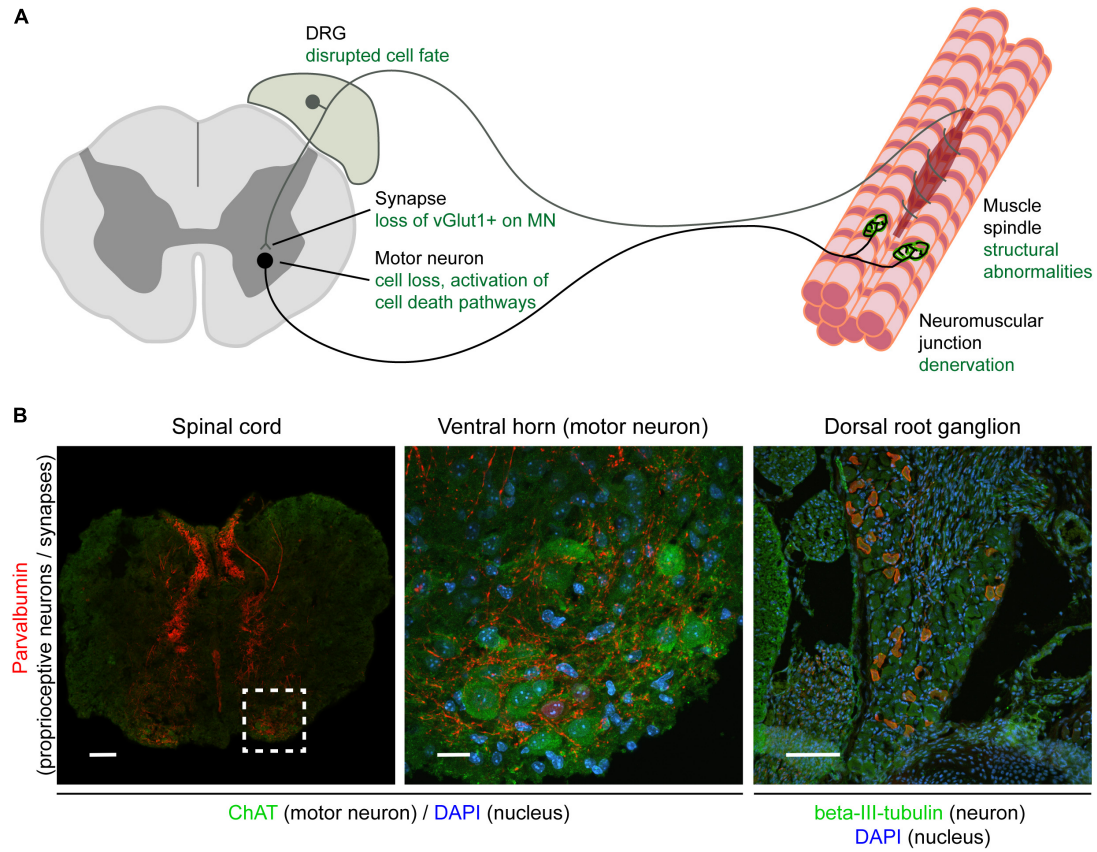

FIGURE 1 | Overview of the sensory-motor system and pathologies observed in SMA. Schematic **(A)** and immunohistochemical **(B)** representation of the sensory-motor system, focusing on structures, cell types, and subcellular compartments that have been implicated in SMA pathogenesis. In **(A)**, the text in green indicates the primary pathological changes occurring in specific cell types or in specific subcellular compartments. In **(B)**, immunofluorescence was used to label parvalbumin-expressing cells and projections (proprioceptive neurons; red), neuronal cell bodies (ChAT for motor neurons, beta-III-tubulin for DRG cell bodies; green), and nuclei (DAPI; blue). Note that only a subgroup of DRG cell bodies express parvalbumin and that other markers such as NF200^{+} (mechano- and proprioceptive) and peripherin^{+} (nociceptive) can also be used to identify other types of sensory neurons. Scale bars: 100 μm (spinal cord and DRG); 20 μm (motor neuron). DRG, dorsal root ganglion; ChAT, acetylcholine transferase; DAPI, 4,6-diamidino-2-phenylindole; vGlut1, vesicular glutamate transporter 1; NF200, neurofilament heavy polypeptide (200 kDa).

motor neurons related to the body regions primarily affected in SMA patients, suggesting that defects occurring in SMA animal models are comparable to sensory-motor pathology observed in patients (**Figure 1**).

SMN Expression Is Required Throughout the Sensory-Motor System

Whilst motor neuron death is central to the pathogenesis of SMA, in mouse models motor neuron death is preceded by dysfunction of motor neuron and neuromuscular transmission characterized by hyperexcitability, increased input resistance, and decreased synaptic efficacy (Ling et al., 2010; Mentis et al., 2011; Fletcher et al., 2017). These functional defects, in combination with pathological findings that show sensory neuron and synapse loss in SMA patients and mouse models, indicate a complex interplay between the various components of the sensory-motor system eventually leading to motor neuron defects and death.

As loss of SMN expression is central to SMA pathogenesis, recent research has aimed to determine the requirements for SMN expression in the sensory-motor system. In wild-type mice, SMN is expressed throughout all components of the sensory-motor system, including DRGs (Shorrock et al., 2018b), muscle, brain and spinal cord (Lee et al., 2012; Groen et al., 2018a), as well as peripheral nerves (Hunter et al., 2016). In *Drosophila* models of SMA, pan-neuronal restoration of SMN rescues locomotion and motor rhythm phenotypes (Imlach et al., 2012). In mouse models of SMA, pan-neuronal SMN restoration completely rescues motor neuron numbers and the number of vGlut1^{+} synapses onto motor neurons (Lee et al., 2012). To explore this phenomenon further, several research groups have investigated the requirements of SMN expression by restoring SMN in specific cell types of the sensory-motor system, using a range of genetic tools and animal lines (Gogliotti et al., 2012; Imlach et al., 2012; Martinez et al., 2012; Hao le et al., 2015; Simon et al., 2016; Fletcher et al., 2017). However, it remains difficult to generate a consensus from these studies, meaning that the

exact cell-type and temporal requirements for SMN expression in the sensory-motor system remain to be fully determined (**Table 1**). Overall, however, these studies indicate that motor neuron *death* may be primarily due to cell-autonomous effects while the underlying cause of motor neuron *dysfunction* has a larger contribution from defects in proprioceptive neurons which provide a substantial non-cell autonomous component of motor neuron pathology. These findings highlight important issues when considering temporal and tissue specific requirements of SMN-targeted therapies for SMA as restoring SMN expression specifically in proprioceptive and motor neurons at the same time led to the biggest improvement in SMA-associated pathology compared to restoring SMN expression in either motor or proprioceptive neurons alone (Fletcher et al., 2017).

The importance of non-cell autonomous effects on motor neurons is further illustrated by several studies that have investigated the effect of defects intrinsic to specific types of sensory neurons on motor neuron function, in otherwise healthy animals. For example, blocking neurotransmission specifically in proprioceptive neurons in wild-type mice can cause severe motor defects, shortened lifespan and motor neuron dysfunction (Fletcher et al., 2017). Similarly, inhibiting cholinergic neuron activity in *Drosophila* causes reduced locomotion, increased spontaneous rhythmic motor activity and increased EPSPs at the neuromuscular junction by reducing excitatory cholinergic input to motor neurons (Imlach et al., 2012). Likewise, pharmacological inhibition of excitatory neurotransmission in an embryonic stem cell model of

TABLE 1 | Overview of studies investigating SMN expression requirements in various components of the sensory-motor system.

Model system	Neuron subtype	Driver(s)	Effect of neuron subtype specific SMN restoration on sensory-motor phenotypes	Reference
Mouse (severe)	Motor neuron	Hb9-Cre	Full rescue of vGlut1$^+$ puncta per 100 μm perimeter of motor neuron soma Complete rescue of cervical, thoracic and lumbar medial motor column motor neuron number	Gogliotti et al., 2012
Zebrafish (maternal zygotic *smn* mutant)	Motor neuron	mnx1/hb9 Cre	Partial rescue of dorsal root ganglion neuron number Rescue of DRG neuron axon length Complete rescue of motor axon branches total length	Hao le et al., 2015
Mouse (delta 7)	Motor neuron	Chat-Cre	Partial rescue of vGlut1$^+$ synapses per motor neuron soma (L1) Partial rescue of L1 motor neuron number	Martinez et al., 2012
Mouse (delta 7)	Motor neuron	Chat-Cre	No rescue of vGlut1$^+$ synapses onto motor neurons (L2) No rescue of motor neuron firing frequency Partial rescue of L2 motor neuron number	Fletcher et al., 2017
	Proprioceptive neuron	Pv-Cre	Rescue of vGlut1$^+$ synapses per motor neuron soma and dendrites (L2) Correction of motor neuron firing frequency No rescue of L2 motor neuron number	
Drosophila (*smn−/−*)	Motor neuron	OK371-Gal4; OK6-Gal4	No improvement of defective locomotion velocity, NMJ ePSPs or motor rhythm	Imlach et al., 2012
	Cholinergic neuron (including proprioceptive neurons)	Cha-Gal4	Complete rescue of defective locomotion velocity, NMJ ePSPs, and motor rhythm	
Embryonic stem cell-derived motor circuit	Motor neuron	*Smn* RNAi *Smn* RNAi*	Reduced motor neuron survival No reduction of vGlut2 excitatory synapses onto motor neurons No change in motor neuron hyperexcitability	Simon et al., 2016
	Excitatory interneuron	*Smn* RNAi#	Loss of vGlut2 excitatory synapses onto motor neurons Induced motor neuron hyperexcitability	

ChAT, choline acetyltransferase; Cha, choline acetyltransferase; Pv, Parvalbumin alpha; Hb9/mnx1, Motor neuron and pancreas homeobox protein 1; Smn, survival motor neuron protein; RNAi, RNA interference; L1/2, lumbar segment 1/2; DRG, dorsal root ganglia; NMJ, neuromuscular junction; ePSPs, excitatory postsynaptic potentials. **co-cultured with wild-type excitatory interneurons;* #*co-cultured with wild-type motor neurons.*

the motor circuit induced motor neuron hyperexcitability but not motor neuron death (Simon et al., 2016). Finally, mutations in the mechanosensitive ion channel responsible for mechanosensation of light touch and proprioception, *PIEZO2*, cause a neuromuscular disease characterized by muscle atrophy, aberrant muscle development and function, mild sensory involvement, delayed motor milestones, and scoliosis (Chesler et al., 2016; Delle Vedove et al., 2016). Together these studies indicate that defects within sensory neurons themselves can lead to both motor neuron and muscle dysfunction in the absence of defects intrinsic to motor neurons.

In summary, the above work illustrates that SMA mouse models reliably reflect pathological changes in the sensory-motor system of SMA patients. Moreover, it also illustrates the importance of homeostasis of the sensory-motor system: correct functioning of each of its parts is required for it to function correctly as a whole. Mechanistically, these studies have largely focused on motor neuron pathology and SMN requirements. Further molecular studies will be required to better understand the cellular pathways that are involved in regulating these pathological changes. In the next section of this review, we will focus on studies that have aimed to address this issue, also drawing on molecular insights obtained by studying other diseases of the sensory-motor system.

MOLECULAR MECHANISMS UNDERLYING SENSORY-MOTOR CONNECTIVITY DEFECTS IN SMA

The presence of sensory-motor connectivity defects in SMA (as illustrated by the loss of proprioceptive vGlut1$^+$ synapses), alterations in sensory neuron development, and the requirement for SMN expression in different neuronal subpopulations have all been clearly established (**Figure 1**). In SMA, SMN depletion is at the basis of each of these pathological changes. However, the molecular mechanisms that modulate these changes downstream of SMN depletion are still unclear. It is by further studying the changes downstream of SMN depletion that we will be able to better understand why certain cell types are more sensitive to SMN depletion than others, why defects in certain cellular pathways affect certain cell types more than others, and, ultimately, how SMN depletion leads to SMA, including disruption of sensory-motor connectivity.

Molecular Mechanisms Linked to Motor Neuron Death and Pathology in SMA

As illustrated by the cell-type specific SMN requirements discussed above, pathways leading to motor neuron death appear to be largely cell autonomous. A better understanding of the molecular mechanisms associated with motor neuron death was gained from studies that compared gene expression profiles of vulnerable and resistant pools of motor neurons. These studies identified differences in basal bioenergetics profiles between vulnerable and resistant motor neuron pools (Boyd et al., 2017), as well as differences in activation of the cell death-regulating protein p53 and differential regulation of its downstream targets (Murray et al., 2015; Simon et al., 2017). Mechanistically, it has been shown that the alternative splicing of *Mdm2* and *Mdm4* downstream of and concurrently with disrupted snRNP biogenesis acts synergistically to induce p53 accumulation in SMA (Van Alstyne et al., 2018). However, despite rescuing the reduction of MN numbers seen in SMA mice, neither the inhibition of p53 signaling nor virus-mediated overexpression of full-length *Mdm2* and *Mdm4* is able to rescue vGlut1$^+$-synapse loss (Simon et al., 2017; Van Alstyne et al., 2018).

Other factors have also been linked to motor circuit function in SMA, including stasimon (Lotti et al., 2012). Decreasing stasimon expression in zebrafish phenocopied motor axon branching defects seen in *smn* morpholino zebrafish, which in turn could be rescued by overexpressing stasimon. Similarly, in a *Drosophila* model of SMA, expressing stasimon in cholinergic (proprioceptive) neurons, but not motor neurons, rescued neurotransmitter release at the NMJ and muscle size defects (Lotti et al., 2012). All of these studies indicate that, while motor neuron death itself can be rescued by targeting the pathways that directly lead to motor neuron death (such as p53 activation, and Mdm2 and Mdm4 missplicing), this does not rescue motor neuron dysfunction or other motor neuron-associated phenotypes in models of SMA (Lotti et al., 2012; Van Alstyne et al., 2018). Other molecular factors such as agrin and plastin3 that are linked to and important for NMJ organization and AMPA receptor functioning have also been implicated in SMA (Zhang et al., 2013; Hosseinibarkooie et al., 2016; Kim et al., 2017). These factors could be important for the reduced synaptic transmission seen in SMA. Moreover, complement C1q, an important factor in postsynaptic pruning, is upregulated in SMA motor neurons (Zhang et al., 2013); a event which, along with an increased association of microglia with SMA motor neurons (Ling et al., 2010), might contribute to the impaired sensory-motor connectivity observed in SMA.

In summary, the above studies have provided important insights into the molecular mechanisms that underlie motor neuron death in SMA. However, in line with previous pathological and SMN expression studies (see Section "SMN Expression Is Required Throughout the Sensory-Motor System"), these studies also illustrate the importance of non cell-autonomous processes in sensory-motor dysfunction in SMA.

Molecular Mechanisms Associated With Sensory Neuron Dysfunction in SMA and Related Conditions

The number of studies investigating the molecular mechanisms that underlie sensory neuron dysfunction in SMA is limited. Therefore, adapting biological findings generated from studies of other, related neuromuscular diseases that are characterized by sensory neuron dysfunction has been of benefit to the SMA research field. For example, Charcot-Marie-Tooth (CMT) disease is a hereditary motor and sensory neuropathy that, depending on its genetic cause, has a variable clinical presentation. CMT type 2D, caused by mutations in the tRNA synthetase *GARS* (glycine tRNA-ligase or GlyRS), has a predominant motor phenotype,

although sensory defects are also present (Motley et al., 2010). In CMT2D, sensory defects have been shown to be linked to a disruption in sensory neuron fate, downstream of increased expression of mutant GARS (Sleigh et al., 2017). Specifically, when determining sensory neuron subtypes in DRGs from two CMT2D mouse models, fewer large cell body NF200-positive (neurofilament heavy) cell bodies were present in favor of an increased number of peripherin-positive, smaller neurons (Sleigh et al., 2017). Taking this observation into the SMA context provides a possible explanation for the loss of sensory synapses onto lower motor neurons that occurs in the SMA spinal cord, as a shift in sensory neuron cell fate would also lead to changes at the level of their synaptic contacts. Indeed, when investigating sensory neuron development in the *Taiwanese* mouse model of SMA, it was shown that a similar change in sensory neuron fate occurs when SMN expression levels are reduced: a decrease in the number of NF200-positive mechano- and proprioceptive sensory neurons is accompanied by an increase in the number of peripherin-positive nociceptive sensory neurons (Shorrock et al., 2018b). Correspondingly, protein levels of GARS were also found to be changed in the spinal cord of SMA mice, as well as in DRGs, in a way that is comparable to changes in GARS observed in mouse models of CMT2D.

The upregulation of GARS in SMA was shown to be regulated by the E1 ubiquitin-activating enzyme, UBA1. UBA1 expression has previously been shown to be significantly decreased in SMA from very early in the pathogenic process and is therapeutically targetable (Wishart et al., 2014; Powis et al., 2016). When investigating protein changes that occur downstream of UBA1, GARS expression was found to depend on UBA1 expression (Shorrock et al., 2018b). In line with this, GARS-dependent pathological features of SMA, including altered sensory neuron fate and loss of proprioceptive synapses in the spinal cord, were rescued when UBA1 levels were elevated using a gene therapy approach (Shorrock et al., 2018b). These findings provide an interesting pathological link between SMA and CMT2D, but also indicate possible molecular pathways that may underlie sensory-motor pathology in SMA and provide starting points for further research. For example, possible mechanistic links related to disruption of GARS-mediated pathways have been shown to involve dysfunctional Nrp1 / VEGF and Trk signaling (He et al., 2015; Sleigh et al., 2017). Mutant GARS can aberrantly bind these proteins and this aberrant binding is thought to disrupt their function. However, to what extent these pathways are relevant for sensory defects associated with SMA remains to be determined.

In addition to defects in Trk and Nrp1/VEGF signaling, mutations in GARS are known to lead to increased levels of alpha-tubulin acetylation (d'Ydewalle et al., 2011). Alpha-tubulin acetylation depends on HDAC activity (Zhang et al., 2003), and, interestingly, both a broad spectrum HDAC inhibitor (trichostatin A) as well as a specific HDAC6 inhibitor (tubastatin A) reversed increases in alpha-tubulin acetylation in a range of cellular and animal models of CMT2D (d'Ydewalle et al., 2011; Benoy et al., 2018; Mo et al., 2018). Intriguingly, the broad spectrum HDAC inhibitor trichostatin A was previously found to rescue vGlut1^{+}-synapse loss on spinal motor neurons in the *delta7* model of SMA (Mentis et al., 2011). To what extent this process is also related to alpha-tubulin acetylation or is due to other effects of HDAC inhibition in SMA remains to be determined. However, this provides an intriguing possible link between HDAC inhibition, GARS function, DRG pathology and sensory synapse loss.

In summary, these findings illustrate how molecular pathways that were previously identified in other disorders, such as CMT2D, can assist discovery of novel mechanisms and therapeutic targets that underlie sensory-motor connectivity defects in SMA.

CONCLUDING REMARKS

Motor neurons rely on a range of synaptic inputs, both from within the central nervous system and from sensory neurons projecting from the periphery, to regulate and finetune their activity. In SMA, multiple components of this sensory-motor system have been shown to be disrupted, contributing to motor neuron dysfunction and death. Several molecular pathways have now been identified that regulate sensory neuron dysfunction and these pathways form interesting novel targets for further study and potential therapy development.

The SMA research field is currently at a defining moment. The first disease-modifying therapy for SMA was recently approved, while other therapies are currently in advanced stages of clinical development (Shorrock et al., 2018a). However, the fact that current therapies are targeted to the nervous system specifically and do not benefit all patients equally, illustrates that fundamental SMA research is still needed, perhaps more than ever (Groen et al., 2018b). Furthering our understanding of the molecular mechanisms that underlie pathological changes occurring in specific cell types, such as sensory neurons, will aid the discovery of novel therapeutic strategies. Moreover, this process may be sped up by scrutinizing the existing knowledge from other, related disorders, as is illustrated by the recent identification of shared molecular mechanisms between SMA and CMT2D. Combining advances in these areas of research will be necessary to be able to eventually provide therapies that will benefit and support all SMA patients equally and efficiently.

AUTHOR CONTRIBUTIONS

HS and EG performed the literature search and generated the table and figure. HS, TG, and EG prepared and wrote the manuscript.

FUNDING

The authors gratefully acknowledge funding from the Wellcome Trust (to EG and TG, grant 106098/Z/14/Z), the Euan MacDonald Centre for MND Research (to HS and TG), SMA Europe (to TG and EG), MND Scotland (to TG), and the UK SMA Research Consortium (by the SMA Trust, to TG). Open access publication fees are covered by the Charity Open Access Fund, administered through the University of Edinburgh.

REFERENCES

Benoy, V., Van Helleputte, L., Prior, R., d'Ydewalle, C., Haeck, W., Geens, N., et al. (2018). HDAC6 is a therapeutic target in mutant GARS-induced Charcot-Marie-Tooth disease. *Brain* 141, 673–687. doi: 10.1093/brain/awx375

Bobele, G. B., Feeback, D. L., Leech, R. W., and Brumback, R. A. (1996). Hypertrophic intrafusal muscle fibers in infantile spinal muscular atrophy. *J. Child. Neurol.* 11, 246–248. doi: 10.1177/088307389601100318

Boyd, P. J., Tu, W. Y., Shorrock, H. K., Groen, E. J. N., Carter, R. N., Powis, R. A., et al. (2017). Bioenergetic status modulates motor neuron vulnerability and pathogenesis in a zebrafish model of spinal muscular atrophy. *PLoS Genet.* 13:e1006744. doi: 10.1371/journal.pgen.1006744

Brown, A. G. (1981). *Organization in the Spinal Cord : The Anatomy and Physiology of Identified Neurones*. New York, NY: Springer-Verlag. doi: 10.1007/978-1-4471-1305-8

Carpenter, S., Karpati, G., Rothman, S., Watters, G., and Andermann, F. (1978). Pathological involvement of primary sensory neurons in Werdnig-Hoffmann disease. *Acta Neuropathol.* 42, 91–97. doi: 10.1007/BF00690973

Chaytow, H., Huang, Y. T., Gillingwater, T. H., and Faller, K. M. E. (2018). The role of survival motor neuron protein (SMN) in protein homeostasis. *Cell Mol. Life Sci.* 75, 3877–3894. doi: 10.1007/s00018-018-2849-1

Chesler, A. T., Szczot, M., Bharucha-Goebel, D., Ceko, M., Donkervoort, S., Laubacher, C., et al. (2016). The Role of PIEZO2 in Human Mechanosensation. *N. Engl. J. Med.* 375, 1355–1364. doi: 10.1056/NEJMoa1602812

Delle Vedove, A., Storbeck, M., Heller, R., Holker, I., Hebbar, M., Shukla, A., et al. (2016). Biallelic loss of proprioception-related PIEZO2 causes muscular atrophy with perinatal respiratory distress, arthrogryposis, and scoliosis. *Am. J. Hum. Genet.* 99, 1206–1216. doi: 10.1016/j.ajhg.2016.09.019

Duman, O., Uysal, H., Skjei, K. L., Kizilay, F., Karauzum, S., and Haspolat, S. (2013). Sensorimotor polyneuropathy in patients with SMA type-1: electroneuromyographic findings. *Muscle Nerve* 48, 117–121. doi: 10.1002/mus.23722

d'Ydewalle, C., Krishnan, J., Chiheb, D. M., Van Damme, P., Irobi, J., Kozikowski, A. P., et al. (2011). HDAC6 inhibitors reverse axonal loss in a mouse model of mutant HSPB1-induced charcot-marie-tooth disease. *Nat. Med.* 17, 968–974. doi: 10.1038/nm.2396

Eccles, J. C., Eccles, R. M., and Lundberg, A. (1957). The convergence of monosynaptic excitatory afferents on to many different species of alpha motoneurones. *J. Physiol.* 137, 22–50. doi: 10.1113/jphysiol.1957.sp005794

Edens, B. M., Ajroud-Driss, S., Ma, L., and Ma, Y. C. (2015). Molecular mechanisms and animal models of spinal muscular atrophy. *Biochim. Biophys. Acta* 1852, 685–692. doi: 10.1016/j.bbadis.2014.07.024

Fletcher, E. V., and Mentis, G. Z. (2016). "Motor circuit dysfunction in spinal muscular atrophy," in *Spinal Muscular Atrophy*, eds C. J. Sumner, S. Paushkin, and C. P. Ko (London: Elsevier), 153–165.

Fletcher, E. V., Simon, C. M., Pagiazitis, J. G., Chalif, J. I., Vukojicic, A., Drobac, E., et al. (2017). Reduced sensory synaptic excitation impairs motor neuron function via Kv2.1 in spinal muscular atrophy. *Nat. Neurosci.* 20, 905–916. doi: 10.1038/nn.4561

Gogliotti, R. G., Quinlan, K. A., Barlow, C. B., Heier, C. R., Heckman, C. J., and Didonato, C. J. (2012). Motor neuron rescue in spinal muscular atrophy mice demonstrates that sensory-motor defects are a consequence, not a cause, of motor neuron dysfunction. *J. Neurosci.* 32, 3818–3829. doi: 10.1523/JNEUROSCI.5775-11.2012

Groen, E. J. N., Perenthaler, E., Courtney, N. L., Jordan, C. Y., Shorrock, H. K., van der Hoorn, D., et al. (2018a). Temporal and tissue-specific variability of SMN protein levels in mouse models of spinal muscular atrophy. *Hum. Mol. Genet.* 27, 2851–2862. doi: 10.1093/hmg/ddy195

Groen, E. J. N., Talbot, K., and Gillingwater, T. H. (2018b). Advances in therapy for spinal muscular atrophy: promises and challenges. *Nat. Rev. Neurol.* 14, 214–224. doi: 10.1038/nrneurol.2018.4

Hamilton, G., and Gillingwater, T. H. (2013). Spinal muscular atrophy: going beyond the motor neuron. *Trends Mol. Med.* 19, 40–50. doi: 10.1016/j.molmed.2012.11.002

Hao le, T., Duy, P. Q., Jontes, J. D., and Beattie, C. E. (2015). Motoneuron development influences dorsal root ganglia survival and Schwann cell development in a vertebrate model of spinal muscular atrophy. *Hum. Mol. Genet.* 24, 346–360. doi: 10.1093/hmg/ddu447

He, W., Bai, G., Zhou, H., Wei, N., White, N. M., Lauer, J., et al. (2015). CMT2D neuropathy is linked to the neomorphic binding activity of glycyl-tRNA synthetase. *Nature* 526, 710–714. doi: 10.1038/nature15510

Hosseinibarkooie, S., Peters, M., Torres-Benito, L., Rastetter, R. H., Hupperich, K., Hoffmann, A., et al. (2016). The power of human protective modifiers: PLS3 and CORO1C unravel impaired endocytosis in spinal muscular atrophy and rescue sma phenotype. *Am. J. Hum. Genet.* 99, 647–665. doi: 10.1016/j.ajhg.2016.07.014

Hosseinibarkooie, S., Schneider, S., and Wirth, B. (2017). Advances in understanding the role of disease-associated proteins in spinal muscular atrophy. *Expert Rev. Proteomics* 14, 581–592. doi: 10.1080/14789450.2017.1345631

Hunter, G., Powis, R. A., Jones, R. A., Groen, E. J., Shorrock, H. K., Lane, F. M., et al. (2016). Restoration of SMN in Schwann cells reverses myelination defects and improves neuromuscular function in spinal muscular atrophy. *Hum. Mol. Genet.* 25, 2853–2861. doi: 10.1093/hmg/ddw141

Ikemoto, A., Hirano, A., Matsumoto, S., Akiguchi, I., and Kimura, J. (1996). Synaptophysin expression in the anterior horn of werdnig-hoffmann disease. *J. Neurol. Sci.* 136, 94–100. doi: 10.1016/0022-510X(95)00297-F

Imai, F., Chen, X., Weirauch, M. T., and Yoshida, Y. (2016). Requirement for dicer in maintenance of monosynaptic sensory-motor circuits in the spinal cord. *Cell Rep.* 17, 2163–2172. doi: 10.1016/j.celrep.2016.10.083

Imlach, W. L., Beck, E. S., Choi, B. J., Lotti, F., Pellizzoni, L., and McCabe, B. D. (2012). SMN is required for sensory-motor circuit function in *Drosophila*. *Cell* 151, 427–439. doi: 10.1016/j.cell.2012.09.011

Jablonka, S., Karle, K., Sandner, B., Andreassi, C., von Au, K., and Sendtner, M. (2006). Distinct and overlapping alterations in motor and sensory neurons in a mouse model of spinal muscular atrophy. *Hum. Mol. Genet.* 15, 511–518. doi: 10.1093/hmg/ddi467

Jiang, M., Schuster, J. E., Fu, R., Siddique, T., and Heckman, C. J. (2009). Progressive changes in synaptic inputs to motoneurons in adult sacral spinal cord of a mouse model of amyotrophic lateral sclerosis. *J. Neurosci.* 29, 15031–15038. doi: 10.1523/JNEUROSCI.0574-09.2009

Kararizou, E., Manta, P., Kalfakis, N., Gkiatas, K., and Vassilopoulos, D. (2006). Morphological and morphometrical study of human muscle spindles in Werdnig-Hoffmann disease (infantile spinal muscular atrophy type I). *Acta Histochem.* 108, 265–269. doi: 10.1016/j.acthis.2006.03.020

Kim, J. K., Caine, C., Awano, T., Herbst, R., and Monani, U. R. (2017). Motor neuronal repletion of the NMJ organizer, agrin, modulates the severity of the spinal muscular atrophy disease phenotype in model mice. *Hum. Mol. Genet.* 26, 2377–2385. doi: 10.1093/hmg/ddx124

Korinthenberg, R., Sauer, M., Ketelsen, U. P., Hanemann, C. O., Stoll, G., Graf, M., et al. (1997). Congenital axonal neuropathy caused by deletions in the spinal muscular atrophy region. *Ann. Neurol.* 42, 364–368. doi: 10.1002/ana.410420314

Lee, A. J., Awano, T., Park, G. H., and Monani, U. R. (2012). Limited phenotypic effects of selectively augmenting the SMN protein in the neurons of a mouse model of severe spinal muscular atrophy. *PLoS One* 7:e46353. doi: 10.1371/journal.pone.0046353

Ling, K. K., Lin, M. Y., Zingg, B., Feng, Z., and Ko, C. P. (2010). Synaptic defects in the spinal and neuromuscular circuitry in a mouse model of spinal muscular atrophy. *PLoS One* 5:e15457. doi: 10.1371/journal.pone.0015457

Lotti, F., Imlach, W. L., Saieva, L., Beck, E. S., Hao le, T., Li, D. K., et al. (2012). An SMN-dependent U12 splicing event essential for motor circuit function. *Cell* 151, 440–454. doi: 10.1016/j.cell.2012.09.012

Lunn, M. R., and Wang, C. H. (2008). Spinal muscular atrophy. *Lancet* 371, 2120–2133. doi: 10.1016/S0140-6736(08)60921-6

Marshall, A., and Duchen, L. W. (1975). Sensory system involvement in infantile spinal muscular atrophy. *J. Neurol. Sci.* 26, 349–359. doi: 10.1016/0022-510X(75)90207-5

Martinez, T. L., Kong, L., Wang, X., Osborne, M. A., Crowder, M. E., Van Meerbeke, J. P., et al. (2012). Survival motor neuron protein in motor neurons determines synaptic integrity in spinal muscular atrophy. *J. Neurosci.* 32, 8703–8715. doi: 10.1523/JNEUROSCI.0204-12.2012

Mears, S. C., and Frank, E. (1997). Formation of specific monosynaptic connections between muscle spindle afferents and motoneurons in the mouse. *J. Neurosci.* 17, 3128–3135. doi: 10.1523/JNEUROSCI.17-09-03128.1997

Mentis, G. Z., Blivis, D., Liu, W., Drobac, E., Crowder, M. E., Kong, L., et al. (2011). Early functional impairment of sensory-motor connectivity in a mouse model of spinal muscular atrophy. *Neuron* 69, 453–467. doi: 10.1016/j.neuron.2010.12.032

Mo, Z., Zhao, X., Liu, H., Hu, Q., Chen, X. Q., Pham, J., et al. (2018). Aberrant GlyRS-HDAC6 interaction linked to axonal transport deficits in Charcot-Marie-Tooth neuropathy. *Nat. Commun.* 9:1007. doi: 10.1038/s41467-018-03461-z

Motley, W. W., Talbot, K., and Fischbeck, K. H. (2010). GARS axonopathy: not every neuron's cup of tRNA. *Trends Neurosci.* 33, 59–66. doi: 10.1016/j.tins.2009.11.001

Murayama, S., Bouldin, T. W., and Suzuki, K. (1991). Immunocytochemical and ultrastructural studies of werdnig-hoffmann disease. *Acta Neuropathol.* 81, 408–417. doi: 10.1007/BF00293462

Murray, L. M., Beauvais, A., Gibeault, S., Courtney, N. L., and Kothary, R. (2015). Transcriptional profiling of differentially vulnerable motor neurons at pre-symptomatic stage in the Smn (2b/-) mouse model of spinal muscular atrophy. *Acta Neuropathol. Commun.* 3:55. doi: 10.1186/s40478-015-0231-1

Nash, L. A., Burns, J. K., Chardon, J. W., Kothary, R., and Parks, R. J. (2016). Spinal muscular atrophy: more than a disease of motor neurons? *Curr. Mol. Med.* 16, 779–792. doi: 10.2174/1566524016666161128113338

Omran, H., Ketelsen, U. P., Heinen, F., Sauer, M., Rudnik-Schoneborn, S., Wirth, B., et al. (1998). Axonal neuropathy and predominance of type II myofibers in infantile spinal muscular atrophy. *J. Child. Neurol.* 13, 327–331. doi: 10.1177/088307389801300704

Pecho-Vrieseling, E., Sigrist, M., Yoshida, Y., Jessell, T. M., and Arber, S. (2009). Specificity of sensory-motor connections encoded by Sema3e-Plxnd1 recognition. *Nature* 459, 842–846. doi: 10.1038/nature08000

Powis, R. A., Karyka, E., Boyd, P., Come, J., Jones, R. A., Zheng, Y., et al. (2016). Systemic restoration of UBA1 ameliorates disease in spinal muscular atrophy. *JCI Insight* 1:e87908. doi: 10.1172/jci.insight.87908

Reid, D., Zinger, Y., and Raheja, D. (2016). Sensory neuronopathy in spinal muscular atrophy: a case presentation. *J. Clin. Neuromuscul. Dis.* 18, 44–46. doi: 10.1097/CND.0000000000000124

Rossignol, S., Dubuc, R., and Gossard, J. P. (2006). Dynamic sensorimotor interactions in locomotion. *Physiol. Rev.* 86, 89–154. doi: 10.1152/physrev.00028.2005

Rossoll, W., Jablonka, S., Andreassi, C., Kroning, A. K., Karle, K., Monani, U. R., et al. (2003). Smn, the spinal muscular atrophy-determining gene product, modulates axon growth and localization of beta-actin mRNA in growth cones of motoneurons. *J. Cell Biol.* 163, 801–812. doi: 10.1083/jcb.200304128

Rudnik-Schoneborn, S., Goebel, H. H., Schlote, W., Molaian, S., Omran, H., Ketelsen, U., et al. (2003). Classical infantile spinal muscular atrophy with SMN deficiency causes sensory neuronopathy. *Neurology* 60, 983–987. doi: 10.1212/01.WNL.0000052788.39340.45

Shababi, M., Lorson, C. L., and Rudnik-Schoneborn, S. S. (2014). Spinal muscular atrophy: a motor neuron disorder or a multi-organ disease? *J. Anat.* 224, 15–28. doi: 10.1111/joa.12083

Sherrington, C. S. (1906). *The Integrative Action of the Nervous System*. New York, NY: C. Scribner's sons.

Shishikura, K., Hara, M., Sasaki, Y., and Misugi, K. (1983). A neuropathologic study of Werdnig-Hoffmann disease with special reference to the thalamus and posterior roots. *Acta Neuropathol.* 60, 99–106. doi: 10.1007/BF00685353

Shorrock, H. K., Gillingwater, T. H., and Groen, E. J. N. (2018a). Overview of current drugs and molecules in development for spinal muscular atrophy therapy. *Drugs* 78, 293–305. doi: 10.1007/s40265-018-0868-8

Shorrock, H. K., van der Hoorn, D., Boyd, P. J., Llavero Hurtado, M., Lamont, D. J., Wirth, B., et al. (2018b). UBA1/GARS-dependent pathways drive sensory-motor connectivity defects in spinal muscular atrophy. *Brain* 141, 2878–2894. doi: 10.1093/brain/awy237

Simon, C. M., Dai, Y., Van Alstyne, M., Koutsioumpa, C., Pagiazitis, J. G., Chalif, J. I., et al. (2017). Converging mechanisms of p53 activation drive motor neuron degeneration in spinal muscular atrophy. *Cell Rep.* 21, 3767–3780. doi: 10.1016/j.celrep.2017.12.003

Simon, C. M., Janas, A. M., Lotti, F., Tapia, J. C., Pellizzoni, L., and Mentis, G. Z. (2016). A stem cell model of the motor circuit uncouples motor neuron death from hyperexcitability induced by SMN deficiency. *Cell Rep.* 16, 1416–1430. doi: 10.1016/j.celrep.2016.06.087

Singh, R. N., Howell, M. D., Ottesen, E. W., and Singh, N. N. (2017). Diverse role of survival motor neuron protein. *Biochim. Biophys. Acta Gene. Regul. Mech.* 1860, 299–315. doi: 10.1016/j.bbagrm.2016.12.008

Sleigh, J. N., Dawes, J. M., West, S. J., Wei, N., Spaulding, E. L., Gomez-Martin, A., et al. (2017). Trk receptor signaling and sensory neuron fate are perturbed in human neuropathy caused by Gars mutations. *Proc. Natl. Acad. Sci. U.S.A.* 114, E3324–E3333. doi: 10.1073/pnas.1614557114

Soliven, B., and Maselli, R. A. (1992). Single motor unit H-reflex in motor neuron disorders. *Muscle Nerve* 15, 656–660. doi: 10.1002/mus.880150604

Van Alstyne, M., Simon, C. M., Sardi, S. P., Shihabuddin, L. S., Mentis, G. Z., and Pellizzoni, L. (2018). Dysregulation of Mdm2 and Mdm4 alternative splicing underlies motor neuron death in spinal muscular atrophy. *Genes Dev.* 32, 1045–1059. doi: 10.1101/gad.316059.118

Wishart, T. M., Mutsaers, C. A., Riessland, M., Reimer, M. M., Hunter, G., Hannam, M. L., et al. (2014). Dysregulation of ubiquitin homeostasis and beta-catenin signaling promote spinal muscular atrophy. *J. Clin. Invest.* 124, 1821–1834. doi: 10.1172/JCI71318

Yonekawa, T., Komaki, H., Saito, Y., Sugai, K., and Sasaki, M. (2013). Peripheral nerve abnormalities in pediatric patients with spinal muscular atrophy. *Brain Dev.* 35, 165–171. doi: 10.1016/j.braindev.2012.03.009

Yuan, P., and Jiang, L. (2015). Clinical characteristics of three subtypes of spinal muscular atrophy in children. *Brain Dev.* 37, 537–541. doi: 10.1016/j.braindev.2014.08.007

Zhang, Y., Li, N., Caron, C., Matthias, G., Hess, D., Khochbin, S., et al. (2003). HDAC-6 interacts with and deacetylates tubulin and microtubules in vivo. *EMBO J.* 22, 1168–1179. doi: 10.1093/emboj/cdg115

Zhang, Z., Pinto, A. M., Wan, L., Wang, W., Berg, M. G., Oliva, I., et al. (2013). Dysregulation of synaptogenesis genes antecedes motor neuron pathology in spinal muscular atrophy. *Proc. Natl. Acad. Sci. U.S.A.* 110, 19348–19353. doi: 10.1073/pnas.1319280110

Conflict of Interest Statement: The authors declare that the research was conducted in the absence of any commercial or financial relationships that could be construed as a potential conflict of interest.

frontiers in Molecular Neuroscience

ORIGINAL RESEARCH
published: 25 June 2019
doi: 10.3389/fnmol.2019.00160

Characterization of Inflammation in Delayed Cortical Transplantation

Nissrine Ballout[1,2], *Tristan Rochelle*[1], *Sebastien Brot*[1], *Marie-Laure Bonnet*[1,3], *Maureen Francheteau*[1], *Laetitia Prestoz*[1], *Kazem Zibara*[2] *and Afsaneh Gaillard*[1]*

[1]*Laboratoire de Neurosciences Expérimentales et Cliniques, Université de Poitiers, INSERM U1084, Poitiers, France,* [2]*Laboratory of Stem Cells, PRASE, DSST, Department of Biology, Faculty of Sciences-I, Lebanese University, Beirut, Lebanon,* [3]*CHU Poitiers, Poitiers, France*

We previously reported that embryonic motor cortical neurons transplanted 1-week after lesion in the adult mouse motor cortex significantly enhances graft vascularization, survival, and proliferation of grafted cells, the density of projections developed by grafted neurons and improves functional repair and recovery. The purpose of the present study is to understand the extent to which post-traumatic inflammation following cortical lesion could influence the survival of grafted neurons and the development of their projections to target brain regions and conversely how transplanted cells can modulate host inflammation. For this, embryonic motor cortical tissue was grafted either immediately or with a 1-week delay into the lesioned motor cortex of adult mice. Immunohistochemistry (IHC) analysis was performed to determine the density and cell morphology of resident and peripheral infiltrating immune cells. Then, *in situ* hybridization (ISH) was performed to analyze the distribution and temporal mRNA expression pattern of pro-inflammatory or anti-inflammatory cytokines following cortical lesion. In parallel, we analyzed the protein expression of both M1- and M2-associated markers to study the M1/M2 balance switch. We have shown that 1-week after the lesion, the number of astrocytes, microglia, oligodendrocytes, and CD45+ cells were significantly increased along with characteristics of M2 microglia phenotype. Interestingly, the majority of microglia co-expressed transforming growth factor-β1 (TGF-β1), an anti-inflammatory cytokine, supporting the hypothesis that microglial activation is also neuroprotective. Our results suggest that the modulation of post-traumatic inflammation 1-week after cortical lesion might be implicated in the improvement of graft vascularization, survival, and density of projections developed by grafted neurons.

Keywords: motor cortex, cortical lesion, embryonic transplantation, neuroinflammation, delay

OPEN ACCESS

Edited by:
John Martin,
City College of New York (CUNY), United States

Reviewed by:
Orion Furmanski,
Uniformed Services University of the Health Sciences, United States
Athena Soulika,
University of California, Davis, United States

***Correspondence:**
Afsaneh Gaillard
afsaneh.gaillard@univ-poitiers.fr

Received: *22 October 2018*
Accepted: *07 June 2019*
Published: *25 June 2019*

Citation:
Ballout N, Rochelle T, Brot S, Bonnet M-L, Francheteau M, Prestoz L, Zibara K and Gaillard A (2019) Characterization of Inflammation in Delayed Cortical Transplantation. Front. Mol. Neurosci. 12:160. doi: 10.3389/fnmol.2019.00160

Abbreviations: BDNF, brain-derived neurotrophic factor; CNS, central nervous system; DAPI, 4′,6-diamidino-2-phenylindole; GDNF, Glial cell-line derived neurotrophic factor; GFAP, Glial fibrillary acidic protein; GFP, green fluorescent protein; IHC, immunohistochemistry; IL, interleukin; ISH, *in situ* hybridization; LIF, leukemia inhibitory factor; LPS, Lipopolysaccharide; NGF, nerve growth factor; PBS, phosphate-buffered saline; PCR, polymerase chain reaction; TGF-β1, transforming growth factor-β1; TNFα, tumor necrosis factor α.

INTRODUCTION

Loss of cortical neurons is a common characteristic of numerous neuropathological conditions. The inhibitory nature of the adult mammalian central nervous system (CNS) prevents spontaneous axonal regeneration following injury (Davies et al., 1997, 1999), which could be overcome by transplantation of embryonic neurons. We have previously reported that embryonic motor cortical neurons grafted immediately after a cortical lesion of the adult mouse motor cortex allowed reestablishment of the damaged motor pathways. Indeed, the transplanted neurons developed projections towards all cortical and subcortical targets of the motor cortex, including distant targets such as the spinal cord (Gaillard et al., 2007; Ballout et al., 2016). While these results were encouraging for CNS repair, a serious limitation in a clinical setting is the time delay of transplantation after injury as neurons derived from embryonic or induced pluripotent stem cells may not be immediately available in terms of harvesting, cell processing, and transplantation (Cox et al., 2017; Wang et al., 2017). We have recently shown that a 1-week delay between the cortical lesion and transplantation can significantly enhance graft vascularization, cell proliferation, survival, and density of projections developed by grafted neurons, leading to a beneficial impact on functional repair and recovery (Péron et al., 2017). However, mechanisms responsible for this improvement attributed to delay are not well-defined. It could be hypothesized that potential benefits may be due to the release of trophic factors secreted by cells surrounding the lesion (Nieto-Sampedro et al., 1983), the secretion of pro-angiogenic factors (Sköld et al., 2005; Dray et al., 2009), or a decrease in toxin (Gonzalez and Sharp, 1987) and inflammation levels, characterized by activated microglia and astrocytes (Zhang et al., 2010; Burda et al., 2016).

The response of astrocytes to injury proceeds through several stages and depends on the extent of trauma. Within 24 h after injury, there is a rapid activation of astrocytes whose main function is to create a physical barrier between damaged and healthy tissue (Raivich et al., 1999). Activation of astrocytes may have antagonistic effects depending on the context in which they occur, i.e., the degree, type and time point after injury (Farina et al., 2007). For example, the production of neurotrophic factors by astrocytes and reduction in the spread of toxic substances released from dead cells promote neuronal survival (Faulkner et al., 2004; Myer et al., 2006; Rolls et al., 2009; Sofroniew and Vinters, 2010). Conversely, glial scar formation impairs adult CNS regeneration (Itoh et al., 2007; Wanner et al., 2008; Rolls et al., 2009). In parallel, released pro-inflammatory cytokines, such as tumor necrosis factor α (TNFα), inhibit neurite growth and kill oligodendrocytes (Neumann et al., 2002).

Phagocytic immune cells found around the lesion site are mainly composed of two types: specialized CNS-resident microglia and infiltrating macrophages. Microglia are active contributors to neuronal damage in neurodegenerative diseases (Block et al., 2007), whose response in acute injury reaches its maximum at 5–7 days after injury (Davalos et al., 2005; Ladeby et al., 2005), before gradually disappearing. As for macrophages, they infiltrate into the brain as early as 12 h post-injury and recruit more neutrophils by releasing pro-inflammatory cytokines and up-regulating adhesion molecules in endothelial cells (Huang et al., 2006; Gelderblom et al., 2009). After activation, microglial cells and macrophages proliferate and migrate to the site of injury where they can have two phenotypes (Gordon, 2003; Mantovani et al., 2004). Depending on the stimuli in their local microenvironment, they can be polarized to have distinct effector functions (Colton, 2009; Xiong et al., 2016). Studies have shown that the presence of lipopolysaccharides (LPS) and TNFα promote M1 phenotype (Kumar et al., 2013). The latter produces high levels of pro-inflammatory cytokines such as interleukin 1 and 6 (IL-1 and IL-6), leukemia inhibitory factor (LIF; Chao et al., 1995) and oxidative metabolites that are essential for host defense and phagocytic activity, but that can also cause damage to healthy cells and tissues (Lynch, 2009). In contrast, activated microglia/macrophages, in the presence of anti-inflammatory cytokines such as IL-4 and IL-10, promote M2 phenotype (Chhor et al., 2013) and reduce M1 cytokines and other pro-inflammatory mediators (Gordon, 2003; Mantovani et al., 2004). It is thought that M2 microglia/macrophages promote repair processes such as angiogenesis by secreting anti-inflammatory cytokines such as transforming growth factor-β1 (TGF-β1; Kiefer et al., 1996). Moreover, they may enhance neuronal survival by removing cell debris (Rapalino et al., 1998) and releasing protective neurotrophic factors such as nerve growth factor (NGF), brain-derived neurotrophic factor (BDNF) or glial cell-line derived neurotrophic factor (GDNF; Neumann et al., 2006; Schwartz et al., 2006; Madinier et al., 2009). Furthermore, they can also stimulate axonal regeneration and enhance the turnover and maturation of oligodendrocyte lineage cells (Schonberg et al., 2007; Gensel et al., 2008).

Several clinical studies showed that transplantation of stem cells is feasible, safe and therapeutically promising. For instance, autologous bone marrow mononuclear cells (BM-MNCs) have been injected intravenously within 36–48 h of injury to treat traumatic brain injury (TBI) patients (Cox et al., 2017). Post-treatment follow-up showed a trend for higher preservation of the white matter volume and a reduction in pro-inflammatory cytokines. Another clinical study investigated the feasibility and safety of intravenous or intrathecal injections of neural stem cells from BM-MNCs at 20–60 days after severe TBI (Wang et al., 2017). For 6 months, no major complications were observed, the neurological score of seven patients over 10 was improved and serum levels of neurotrophic factors were higher following transplantation.

Currently, no pharmacological treatment has received FDA approval for patients with TBI (Diaz-Arrastia et al., 2014). One of the reasons for the absence of treatment is that most preclinical studies measure drugs directly or soon after TBI (Diaz-Arrastia et al., 2014). This experimental protocol does not take into consideration the treatment gap observed in clinical cases after brain trauma (Tanielian and Jaycox, 2008; Demakis and Rimland, 2010). Some drugs limit considerably the extent of secondary injury, they are effective by targeting one mechanism

of secondary injury. The progress of secondary injury induces the loss of drug targets which reduces rapidly their efficacy and their therapeutic effect of targeting one mechanism of secondary injury. Thus, drugs delivered at longer intervals after injury may have multiple targets which can still reduce secondary injury. As for stem cells, the therapeutic window remains unclear, whereas stem cells can be used for neuroprotective strategy, for cell replacement strategy or both.

Taken together, the impact of inflammatory responses on neuronal survival seems to depend on a balance between pro- and anti-inflammatory mechanisms induced by different mediators (Bernardino et al., 2005; Vezzani et al., 2008). Inflammatory changes occurring in the post-lesioned environment and their effects on axonal regeneration in adult CNS have been extensively investigated. However, few studies examined the deleterious or beneficial consequences of these changes on axonal growth of transplanted embryonic neurons in the injured adult brain. Therefore, in the present study, we aimed at characterizing the impact of a 1-week delay between the motor cortical lesion and transplantation on post-traumatic inflammation. For this, we have characterized the density, morphology, and phenotype of resident and peripheral infiltrating immune cells, the distribution and temporal mRNA expression pattern of pro- and anti-inflammatory cytokines and the temporal kinetics of microglia/macrophage polarization.

MATERIALS AND METHODS

Animals

All animal experimentation and housing were carried out in accordance with the guidelines of the French Agriculture and Forestry Ministry (decree 87849) and the European Communities Council Directive (2010/63/EU). The procedures referenced under the file number APAFIS#4928–20 16041 117503028 v3, were approved by ethics committee N°84 COMETHEA Poitou-Charentes. All experiments were conducted in compliance with current Good Clinical Practice standards and in accordance with relevant guidelines and regulations and the principles set forth under the Declaration of Helsinki (1989). All efforts were made to reduce the number of animals used and their suffering. A total of 82 C57BL/6 mice were used in this study: 16 mice were used as controls (without a lesion), 66 mice were lesioned, among which 42 mice were used as "lesioned group" (without transplantation) 12 mice were transplanted without delay (immediately after lesion) and 12 mice were transplanted with 1-week delay (**Figure 1**).

Lesion and Transplantation Procedures

Adult (4–6 months old) C57BL/6 mice (n = 66, Janvier Labs, Le Genest-Saint-Isl, France) were lesioned. Briefly, animals were anesthetized with a mixture of xylazine/ketamine (intra-peritoneal, ip., 10 and 100 mg/kg, respectively) and the motor cortex was aspirated from 0.5 to 2.5 mm rostral to the Bregma and from 0.5 to 2.5 mm lateral to the midline, with the corpus callosum left intact. Among these mice, 42 were used in the "lesioned group" and 24 were transplanted as described previously (Gaillard et al., 1998, 2007). The transplanted mice were selected randomly. Motor cortical tissue was obtained from embryonic day 14 transgenic mice overexpressing the enhanced green fluorescent protein (EGFP) under the control of a chicken β-actin promotor [C57BL/6-TgN(beta-act-EGFP)] Osb strain (Okabe et al., 1997). Motor cortical tissue was deposited into the host lesion cavity either immediately, without delay (n = 12), or with a delay of 1-week (n = 12) after the lesion. Care was taken to maintain the original dorso-ventral and anteroposterior orientations of the cortical fragments during the transplantation procedure. We did not perform immunosuppression during transplantation since it has been demonstrated in several previous studies including ours (Gaillard et al., 2007, 2009; Thompson et al., 2009; Klein et al., 2013; Wang et al., 2016; Péron et al., 2017), that immunosuppression is not necessary for grafted fetal mouse cells to survive in a mouse brain as performed in the present study. No animal was excluded after histological analysis.

Tissue Processing and Immunohistochemistry (IHC)

At different time points (**Figure 1**), mice were injected with a lethal dose of xylazine/ketamine and perfused transcardiacally with 100 ml of saline (0.9%), followed by 200 ml of ice-cold paraformaldehyde (PFA, 4%) in 0.1 M phosphate buffer (PB, pH 7.4). Brains were removed, post-fixed in 4% PFA overnight at 4°C, and cryoprotected in 30% (w/v) sucrose, 0.1 M sodium phosphate buffer (pH 7.4). Brains were cut in six series on a freezing microtome (Microm HM450, Thermo Scientific) in 40 μm-thick coronal sections and stored in a cryoprotective solution (20% glucose, 40% ethylene glycol, 0.025% sodium azide, 0.05M phosphate buffer pH 7.4). For immunohistochemistry (IHC), free-floating sections were incubated in a blocking solution [3% bovine serum, 0.3% Triton X-100 in phosphate-buffered saline (PBS) 0.1 M pH 7.4] for 90 min at room temperature (RT). Primary antibodies, diluted in blocking solution, were applied overnight at 4°C. Appropriate secondary antibodies were diluted in blocking solution and applied for 1 h at RT. The following antibodies were used to label activated microglia and hematopoietic cells, astrocytes, oligodendrocytes and neurons, respectively: rabbit anti-Iba1 (1:500, Wako) and rat anti-CD45 (1:500, Abcam), chicken anti-Glial fibrillary acidic protein (GFAP; 1:1,000, Abcam), rabbit anti-olig2 (1:500, Millipore) and mouse anti-NeuN (1:500, Millipore). Rabbit anti-CD86 (1:200, Abcam) and goat anti-Arg1 (1:250, Santa Cruz) were used for M1 and M2 phenotype respectively. Rat anti-C3 (1:200, Abcam) and rabbit anti-CD109 (1:200, Abcam) were used for A1 and A2 phenotype respectively. Chicken anti-green fluorescent protein (GFP; 1:1,000, Abcam) or Rabbit anti-GFP (1:1,000, Invitrogen) were used to label transplanted cells whereas nuclei were labeled with DAPI (1:2,000, Sigma). The sections were covered with DePeX (VWR) mounting medium.

In situ Hybridization (ISH)

For *in situ* hybridization (ISH), brains were collected, cryoprotected in 30% (w/v) sucrose and quickly frozen in

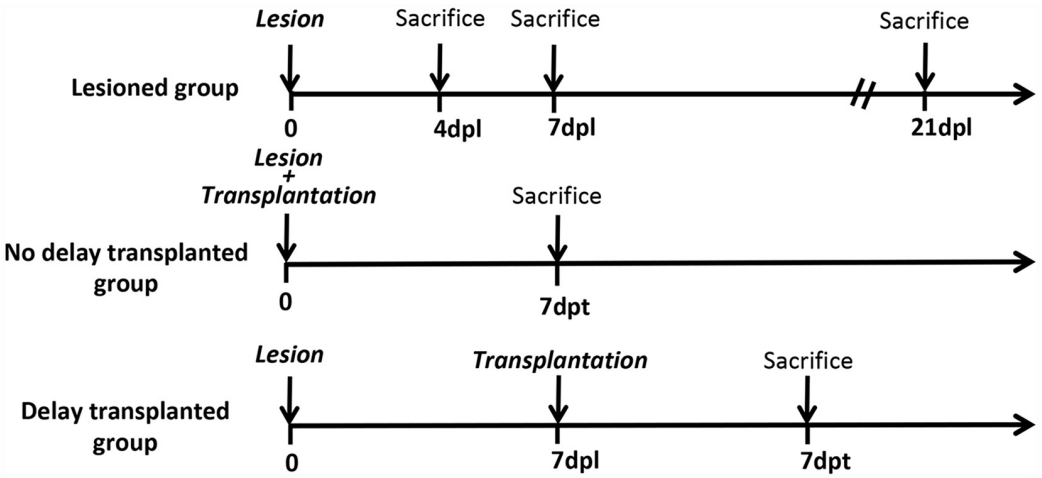

FIGURE 1 | Timeline of the study. Timeline of the study representing the different groups and the different time points of mice sacrifices. Dpl, days post-lesion; dpt, days post-transplantation.

isopentane (2-methylbutane, VWR) cooled at −45°C. Brains were then cut in 6 series on a cryostat (HM550, Microm) in 16 μm-thick coronal sections, mounted on super-frost slides (Superfrost Plus, VWR) and stored at −80°C.

ISH was performed in order to characterize the spatiotemporal expression of pro-inflammatory cytokines IL-1α, IL-1β, IL-6, TNFα, and LIF and anti-inflammatory cytokines: TGFβ1, IL-4, and IL-10, at day 0, 4 and 7 days after cortical lesion. Specific digoxygenin-labeled cRNA probes were prepared from cDNA fragments (450 bp to 800 bp) of these murine cytokines. cDNAs were amplified by polymerase chain reaction (PCR) using specific primers from cDNA banks obtained from different sources (brain, liver, spleen, skin, adipose tissue and LPS-treated bone marrow-derived macrophages). cDNA fragments were then cloned into pGEM®-T Easy vectors (Promega, Charbonnières-les-Bains, France) and verified by sequencing. Complementary (antisense) and non-complementary (sense) RNA probes were produced using T7 or SP6 RNA polymerase (Riboprobes® System-T7, Promega Corporation, Madison, WI, USA). Before exposing to the probes, sections were digested by proteinase K (5 μg/ml) for 10 min at 37°C followed by an acetylation step in triethanolamine buffer (100 mM triethanolamine, 0.25% acetic anhydride) to reduce non-specific binding. Hybridization was carried out overnight at 65°C in a humidified chamber using probes at a final concentration of 500 ng/ml diluted in hybridization buffer containing 50% formamide, 1× Denhardt's solution, 10% dextran sulfate, 1 mg/ml yeast tRNA in salt solution (200 mM NaCl, 10 mM Tris-HCl pH 7.5, 10 mM phosphate buffer pH 7.4, 5 mM EDTA pH 8). The following day, sections were washed at RT in 1X sodium saline citrate (SSC), 50% formamide, 0.1% Tween 20 at 65°C, and in MABT buffer (0.15 M NaCl, 0.1 M Maleic acid, 0.2 M NaOH, 0.1% Tween 20, pH 7.5). After blocking in 10% B10 reagent (Roche Diagnostics, Mannheim, Germany) and 10% sheep serum, sections were incubated overnight at RT with an alkaline phosphatase-labeled anti-digoxigenin antibody (Roche Diagnostics, Mannheim, Germany) diluted 1:2,000 in blocking buffer. Sections were finally washed with NTMT buffer (0.1 M NaCl, 0.1 M Tris–HCl pH 9.5, 0.05 M $MgCl_2$, 0.1 M Tween 20, pH 9.5) before being incubated in detection buffer containing 0.045% nitroblue tetrazolium, 0.35% 5-bromo-4-chloro-3-idolyl phosphate (Roche Diagnostics, Mannheim, Germany) and 0.1% levamisole (Sigma) in NTMT buffer. Slides were then dried and mounted with DePeX (BDH Laboratories, Poole, UK). Results with antisense probes were compared with sense probes and were confirmed by testing six animals for each group.

The anti-Iba1 antibody was used to define whether macrophage/microglia could be the source of IL-1β and TGF-β1. Briefly, after ISH, sections were incubated in blocking solution (3% bovine serum, 0.3% Triton X-100 in PBS 0.1 M pH 7.4) for 90 min at RT. Anti-Iba1 primary antibody (1:500, Wako) diluted in blocking solution was applied overnight at 4°C. Sections were then incubated with biotinylated goat anti-rabbit antibody (1:200, Vector, Burlingame, CA, USA) for 1 h 30 min at RT. After washing, sections were treated with 0.3% hydrogen peroxide (Sigma, Seelze, Germany) to quench endogenous peroxidases and were reacted with avidin-biotin peroxidase complex (Vectastain® ABC Kit, Vector, Burlingame, CA, USA) for 1 h at RT. The sections were subsequently incubated in 0.1 M PB containing 0.33 mg/ml 3,3′-diaminobenzidine tetrahydrochloride (Sigma, St Louis, MO, USA) and 0.0006% hydrogen peroxide. Mounted sections were dried and covered with DePeX (VWR).

Western Blot Analysis

At different time points after the lesion (**Figure 1**), mice were injected with a lethal dose of xylazine/ketamine and perfused transcardiacally with 100 ml of saline (0.9%), then brains were removed and kept on ice. The control (intact animal) and lesioned cortex were collected and sonicated using protein lysis buffer (RIPA 50 mM Tris pH 8.0, 150 mM

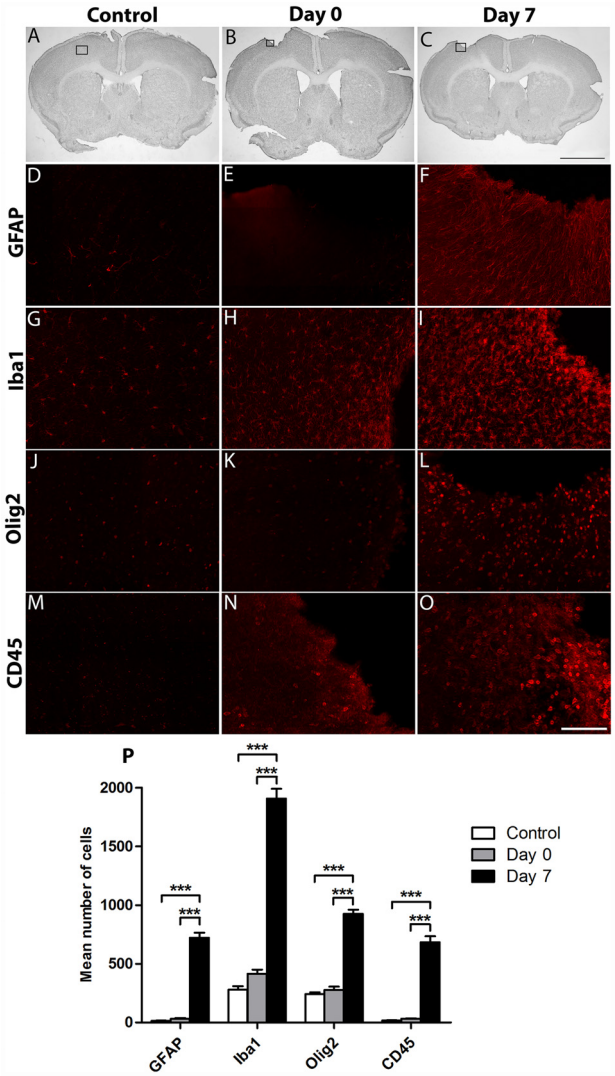

FIGURE 2 | Characterization of the environment surrounding cortical lesion. The effect of cortical lesion on the number of resident immune cells and peripheral infiltrating cells in the injured cortex was evaluated in three groups of mice: control without lesion, Day 0 of lesion or Day 7 after lesion. Black squares show area of interest in Control **(A)**, Day 0 **(B)** or Day 7 **(C)** groups. Immunostaining using antibodies against Glial fibrillary acidic protein (GFAP; **D–F**), Iba1 **(G–I)**, Olig2 **(J–L)** or CD45 **(M–O)** allowed the detection of astrocytes, microglia, oligodendrocytes or hematopoietic cells in control, day 0, and day 7 after cortical lesion; respectively. **(P)** Histogram showing the quantification of the number of Iba1+, GFAP+, Olig2+ or CD45+ cells in different groups. The *p*-value was determined using two-way analysis of variance (ANOVA) followed by Bonferroni test. Values for $^{***}p < 0.0001$ were considered significant. Results are expressed as mean ± SEM. Results are representatives of $n = 6$ animals per group. Scale bar: **(A,B)** 2 mm **(D–O)** 80 μm.

NaCl, 1% NP-40, 0.1% SDS, 0.5% sodium deoxycholate with protease cocktail inhibitor). The brain homogenates were then incubated for 2 h at 4°C, centrifuged at 13,000 rpm for 5 min at 4°C, and the supernatants were then collected and stored at −80°C. After protein extraction, equal amounts of proteins were loaded either onto 7.5% or 10% resolving gel for electrophoresis then transferred onto a nitrocellulose membrane (Bio-Rad, Munich, Germany). Membranes were blocked with 5% milk powder in PBS 0.1 M, 0.1% Tween 20 and incubated overnight at 4°C with primary antibodies. The following antibodies were used: rabbit anti-CD86 (M1 phenotype, 1/1,000, Abcam), goat anti-CD206 (M2 phenotype, 1/500, R&D systems, Minneapolis, MN, USA), goat anti-Arg1 (M2 phenotype, 1/250, Santa Cruz, CA, USA), and mouse anti-α tubulin (Loading control, 1/2,000, Sigma). After washing three times using 0.1 M PBS, 0.1% Tween 20, the membrane was incubated with horseradish peroxidase (HRP)-conjugated anti-rabbit, anti-goat or anti-mouse immunoglobulin G (1/50,000, Jackson ImmunoResearch, West Grove, PA, USA) for 1 h at RT. The membranes were washed three times and then revealed by Luminata Forte Western HRP substrate (Millipore, MA, USA). Pictures were taken using the PXi imaging system (Syngene, Cambridge, UK) and band intensity was quantified using ImageJ software (Bethesda, MD, USA).

Data Acquisition and Quantification

For each mouse, images of injury area were acquired with a Zeiss Axio Imager. M2 Apotome microscope at x20 magnification, at the rostral, middle and caudal part of the lesion or the graft. On mosaic acquisition, three images corresponding to the areas of interest were used for all quantifications using ZEN software (Zeiss). For control mice, equivalent sections were selected at the same anteroposterior coordinates as the lesioned sections. Areas of interest were further analyzed and photographed with a confocal laser-scanning microscope FV1000 (Olympus, Rungis, France). The counts were expressed per mm^2.

Statistical Analysis

Statistical analyses were performed using a two-tailed student's *t*-test, two-way analysis of variance (ANOVA) followed by a Bonferroni correction or Kruskal-Wallis test followed by Dunn's multiple comparisons test. Data are expressed as mean ± SEM. Differences were considered statistically significant when $p < 0.05$, $p < 0.001$, $p < 0.0001$ (*, **, ***; respectively).

RESULTS

Cortical Lesion Increases Brain Resident Immune and Peripheral Infiltrating Cells

To examine the effects of cortical lesion on the number of resident immune cells and peripheral infiltrating cells, IHC was used to identify GFAP+ astrocytes, Iba1+ microglial cells/macrophages, Olig2+ oligodendrocytes, and CD45+ hematopoietic cells (**Figures 2A–C**). As expected, the basal number of GFAP+ (13 ± 2; **Figures 2D,P**); Iba1+ (279 ± 29; **Figures 2G,P**); Olig2+ (240 ± 17; **Figures 2J,P**) and CD45+ (17 ± 2; **Figures 2M,P**) cells was low in the cortex of control group. At the day of lesion (day 0), no significant change of the number of cells was observed, in comparison to controls (GFAP: 31 ± 6; Iba1: 415 ± 34; Olig2: 277 ± 28; CD45: 32 ± 3; **Figures 2E,H,K,N,P**). However, at day 7 after the lesion, the number of astrocytes (721 ± 43), microglia (1,907 ± 82),

oligodendrocytes (925 ± 36) and hematopoietic cells (683 ± 51) was significantly increased, in comparison to control and day 0 groups (***, $p < 0.0001$; **Figures 2F,I,L,O,P**). In addition, astrocytes and microglia showed morphological changes; indeed, astrocytes became hypertrophic whereas microglia presented an ameboid morphology (**Figures 2F,I**). Thus, a delay of 1-week after cortical lesion results in the recruitment and activation of inflammatory brain resident mediators and peripheral infiltrating cells.

Differential Expression Kinetics of IL-1β and TGF-β1 Following Cortical Lesion

To evaluate the level of neuroinflammation following cortical lesion, using ISH, we investigated the spatiotemporal mRNA expression profile of pro- and anti-inflammatory cytokines, Interleukin-1 β (IL-1β) and TGF-β1; respectively. Both cytokines exhibited a differential expression at the lesion site, whereas they were neither present in the contralateral side nor in the cortex adjacent to the lesion site (data not shown).

Expression of IL-1β and TGF-β1 was not detected in the cortex of control animals with no lesion or in the cortex at day 0 of the lesion (**Figures 3A–D,I**). However, a strong expression of IL-1β was observed 4 days after lesion, within the cortex around the lesion cavity (**Figures 3E,I**), which disappeared at 1-week after the lesion (**Figures 3G,I**). On the other hand, TGF-β1 expression was strongly concentrated in the vicinity of the cortical lesion and to a lesser extent in the corpus callosum adjacent to the lesion site, 4 days after injury (**Figures 3F,I**). However, expression of TGF-β1 decreased significantly, but was still present, at 1-week after the lesion (**Figures 3H,I**).

Furthermore, the microglial/macrophagic phenotype (Iba1+) of the cells expressing IL-1β and TGF-β1 was analyzed 4 days after the lesion, using IHC in combination with ISH. Results showed that only TGF-β1+ cells expressed Iba1 marker (**Figures 3J,K**). On the other hand, IL-1α, IL-4, IL-6, IL-10, TNFα and LIF transcripts were not detected at day 0, day 4 or day 7 time points (data not shown).

Temporal Kinetics of Microglia/Macrophage Polarization After Cortical Lesion

In order to further clarify whether the activated microglia/macrophages observed after cortical lesion were neurotoxic or neuroprotective, temporal changes in the phenotypes of M1- or M2- associated proteins (CD86 vs. CD206 and Arg1, respectively) were investigated in the motor cortex of control, day 0, day 7, and day 21 lesioned groups (**Figure 4A**). Quantitative analysis showed that the expression of M1 marker CD86 slightly increased at day 0 and day 7, while a significant increase was observed at day 21 after injury. In contrast, the expression of M2 marker Arg1 peaked at 1-week after the lesion and returned to pre-injury levels at day 21 (**Figure 4B**) whereas M2 marker CD206 showed no significant difference between the 4 groups. Our results demonstrated that an M1 microglia phenotype is dominant in the vicinity of the lesion. However, an M1-to-

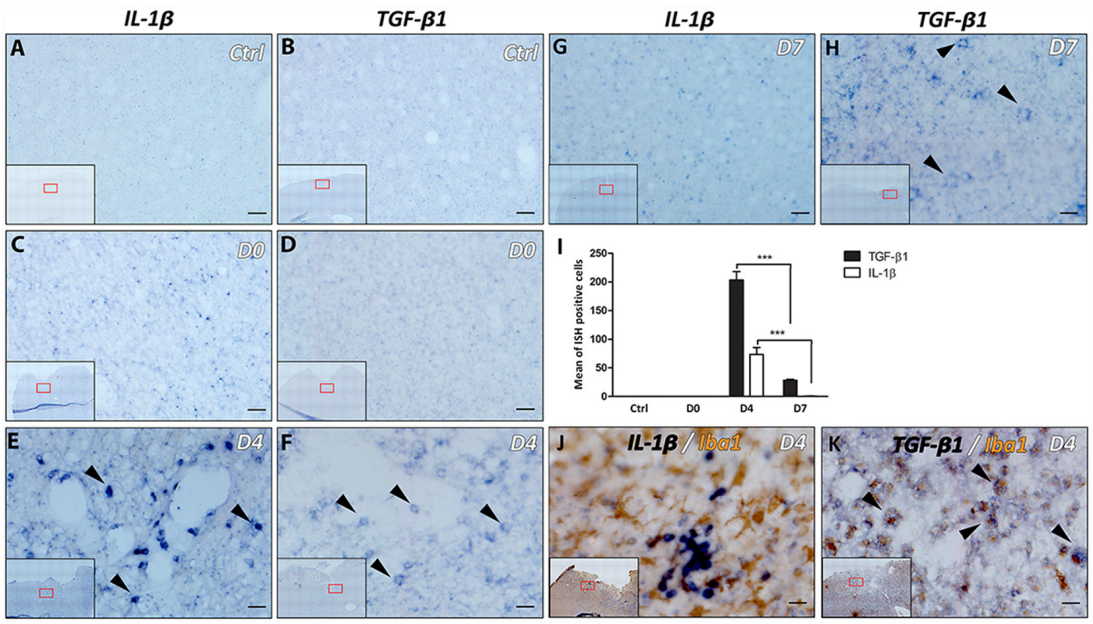

FIGURE 3 | Differential expression of IL-1β and transforming growth factor-β1 (TGF-β1) following lesion of the motor cortex. The presence of IL-1β and TGF-β1 mRNAs was tested in the cortex without lesion (Ctrl; **A,B**) at the day of lesion (D0; **C,D**), 4 days (D4; **E,F**) and 7 days (D7; **G,H**) after the lesion (in blue, black arrowheads). Quantification analysis of the mean number of IL-1β and TGF-β1-expressing cells, in Ctrl, D0, D4 and D7 groups **(I)**. Co-labeling of IL-1β **(J)** or TGF-β1 **(K)** transcripts (in blue) with Iba1 macrophage/microglia marker (in brown) 4 days after lesion (black arrowheads). Red squares in inserts show area of interest. Data are presented as group mean ± SEM and asterisk indicates statistically significant differences (Student's *T*-test, ***$p < 0.0001$). Scale bar: 20 μm.

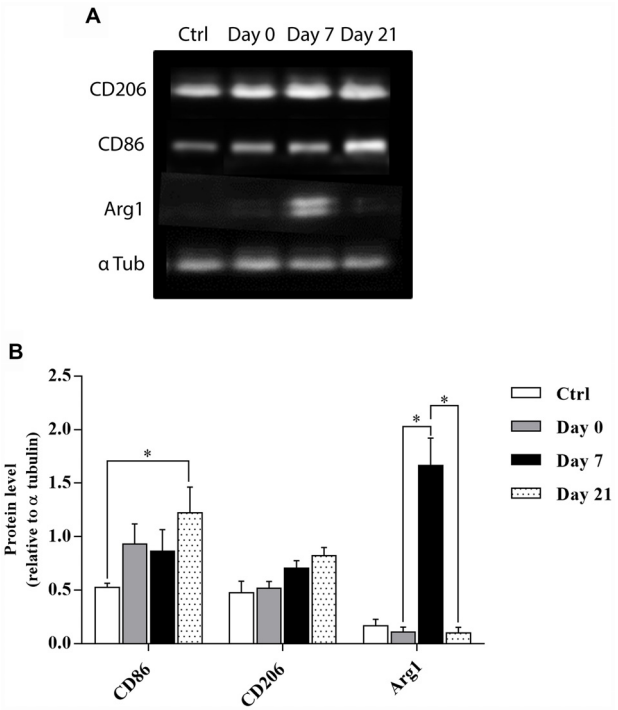

FIGURE 4 | Temporal kinetics of microglia/macrophage polarization after cortical lesion. Western blot analysis for CD86, CD206, and Arg1 protein expression from the cell lysate of control and lesioned motor cortex sacrificed at different time points: day 0, day 7 and day 21 **(A)**. Quantification analysis of CD86, CD206, and Arg1 expression by normalizing to α tubulin level in ctrl, day 0, day 7, and day 21 groups **(B)**. The *p*-value was determined using Kruskal-Wallis test followed by Dunn's multiple comparisons test. Values for $*p < 0.05$ were considered significant. Results are expressed as mean ± SEM. Results are representatives of $n = 4$ animals per group.

M2 switch was observed at 1-week after the lesion followed by a replacement of the transient M2 response by an M1 response at day 21 post-lesion.

Cortical Transplantation Modified Brain Resident Immune and Peripheral Infiltrating Cells

The effects of a 1-week delay or no delay, between lesion and transplantation on inflammatory responses were examined at 4- or 7-days post-transplantation, in the graft and the cortical surrounding areas. Four days after transplantation, the number of brain resident immune cells (Iba1+, GFAP+, Olig2+) and peripheral infiltrating cells (CD45+) were not significantly different between the two groups of transplanted animals, with or without delay, whether in the host cortex adjacent to the transplant (Iba1+, No delay: 665 ± 116; Delay: 652 ± 65; GFAP+, No delay: 477 ± 56; Delay: 661 ± 128; Olig2+, No delay: 513 ± 41; Delay: 543 ± 61; CD45+, No delay: 365 ± 27; Delay: 491 ± 20) or within the transplant (Iba1+, No delay: 24 ± 2; Delay: 53 ± 9; GFAP+, No delay: 17 ± 4; Delay: 71 ± 8; Olig2, No delay: 13 ± 2; Delay: 22 ± 5; CD45+, No delay: 30 ± 3; Delay: 24 ± 2; **Figure 5A**).

Seven days after transplantation, the number of microglial (Iba1+) and hematopoietic (CD45+) cells were not significantly different between the two groups of transplanted animals, with or without delay, whether in the host cortex adjacent to the transplant (Iba1+, No delay: 1,329 ± 57; Delay: 1349 ± 47; **Figures 6I–P**, **5B**; CD45+, No delay: 666 ± 38; Delay: 596 ± 30; **Figures 7I–P**, **5B**) or within the transplant (Iba1+, No delay: 196 ± 15; Delay: 191 ± 11; **Figures 6I–P**, **5B**), (CD45+, No delay: 191 ± 15; Delay: 149 ± 11; **Figures 7I–P**, **5B**). However, a significant increase in the number of astrocytes (GFAP+ cells) was observed in the host cortex in the group of animals transplanted with a delay of 1-week, compared to the no delay group (GFAP+, No delay: 632 ± 75; Delay: 1,047 ± 61; **Figures 6A–H**, **5B**). Similarly, a significant increase in astrocytes was also detected in the transplant in the delay group (No delay: 68 ± 16; Delay: 610 ± 109; **Figures 6A–H**, **5B**). On the other hand, while numerous oligodendrocytes (Olig2+ cells) were detected in the host cortex, no significant difference was found between the two groups (Olig2+, No delay: 740 ± 50; Delay: 729 ± 58; **Figures 7A–H**, **5B**). However, a significant increase was observed in the transplant for the group with a delay of 1-week, in comparison to that with no delay (Olig2, No delay: 209 ± 20; Delay: 1,163 ± 84; **Figures 7A–H**, **5B**). In addition, astrocytes and microglia showed morphological changes. Indeed, astrocytes presented different morphologies depending on their distance from the transplant. In fact, astrocytes were more elongated and showed "palisading" morphology in the vicinity of the transplant. Furthermore, hypertrophic astrocytes were orientated towards the injury site, whereas GFAP+ astrocytes were present but showed no signs of hypertrophy at the border of the unaffected corpus callosum. Palisading astrocytes were more observed in the host cortex in the no delay group in comparison to the delay group (**Figures 6A,E**). However, microglia were more ameboid/less ramified in the no delay group compared to the delay group (**Figures 6I,M**). Our results showed that a 1-week delay between lesion and transplantation enhanced the number of astrocytes in the host adjacent cortex as well as in the transplant, whereas oligodendrocytes increased only within the transplant.

Astrocytes and Microglia/Macrophage Polarization After Cortical Transplantation

In order to examine the pro-inflammatory vs. anti-inflammatory profile of microglia/macrophage and astrocytes, IHC was used to identify astrocytes and microglia/macrophage subpopulation in the graft and the cortical surrounding areas at 7-days post-transplantation. While numerous A1 astrocytes (C3+ cells) were detected in the host cortex and transplant, no significant difference was found between the two groups (Host cortex, No delay: 87 ± 4.96%; Delay: 89.93 ± 2.15%; Transplant, No delay: 81.72 ± 3%; Delay: 84.2 ± 0.43%; **Figures 8A–F,M**). In contrast, a significant increase in the percentage of A2 astrocytes (CD109+ cells) was observed in the host cortex for the group with a 1-week delay, in comparison to that with no delay (No delay: 5.43 ± 1.4%; Delay: 16.8 ± 4.9%; **Figures 8G–M**). Regarding microglia/macrophage polarization, we performed double labeling of Iba1 with

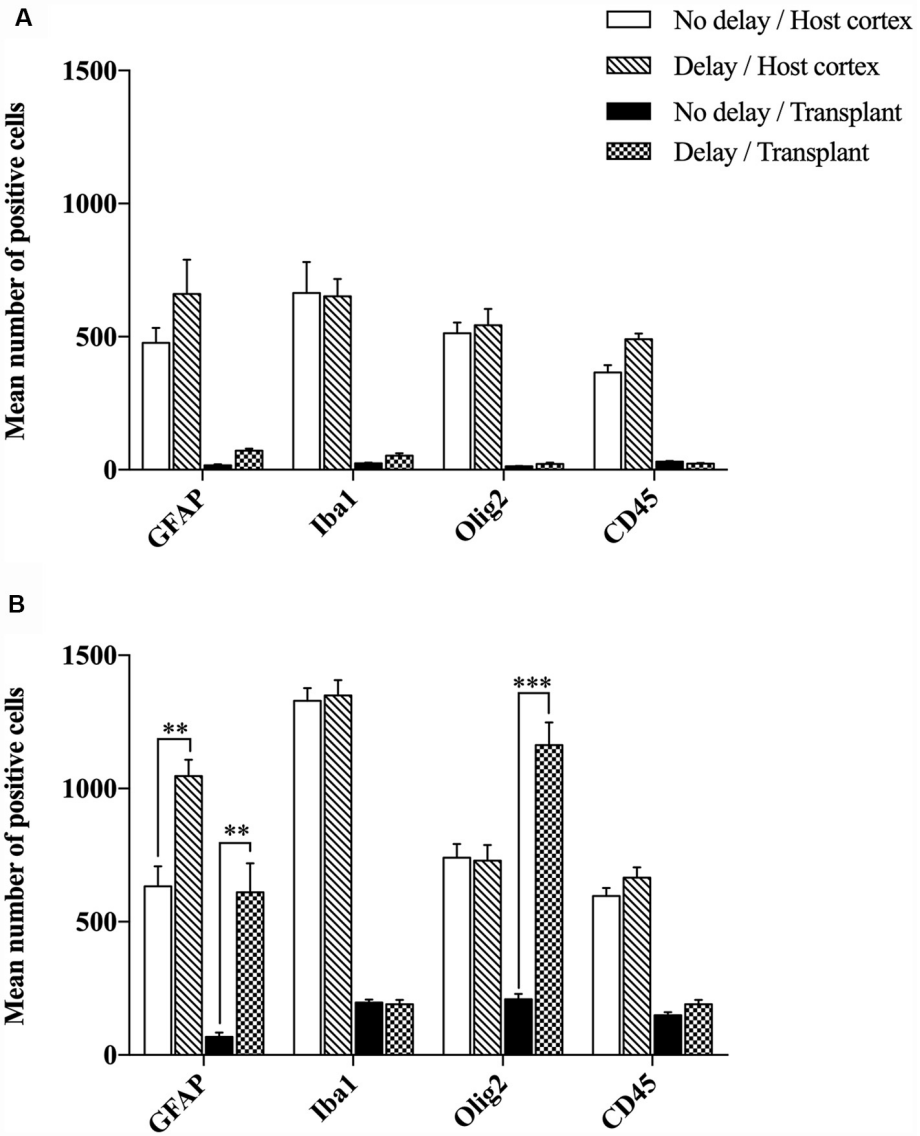

FIGURE 5 | Histogram showing quantifications of GFAP+, Iba1+, Olig2+ or CD45+ cells at 4 days **(A)** and 7 days **(B)** after cortical transplantation. Results are expressed as mean ± SEM. Results are representatives of $n = 6$ animals per group. The p-value was determined using Student's T-test. Values for $^{***}p < 0.0001$ and $^{**}p < 0.001$ were considered significant.

arginase-1 (Arg1, M2 phenotype) and showed that the percentage of Iba1+/Arg1+ cells was not significantly different between the two groups of transplanted animals, with or without delay, whether in the host cortex adjacent to the transplant (No delay: 2.50 ± 0.17%; Delay: 12.27 ± 3.53%; **Figures 9A,C,D,F,M**) or within the transplant (No delay: 28.08 ± 1.66%; Delay: 25.08 ± 4.15%; **Figures 9A,B,D,E,M**). In addition, we performed double labeling of Iba1 with M1 phenotype marker, CD86, and showed no significant difference in the percentage of Iba+/CD86+ cells in the host cortex adjacent to the transplant in the two groups of transplanted animals (No delay: 5.19 ± 0.46%; Delay: 4.52 ± 1.65%; **Figures 9G,I,J,L,M**). Substantially, more Iba1+ cells expressed the M1 marker CD86 in the transplant of animals transplanted without a delay, compared to the delay group (No delay: 24.21 ± 5.95%; Delay: 5.47 ± 1.85%; **Figures 9G,H,J,K,M**). Our results showed that a 1-week delay between lesion and transplantation increased the percentage of A2 astrocytes in the host adjacent cortex, whereas M1 microglia decreased only within the transplant.

DISCUSSION

We have recently shown that a time delay of 1-week between a lesion in the adult mouse motor cortex and homotopic cortical transplantation of embryonic cells significantly enhance

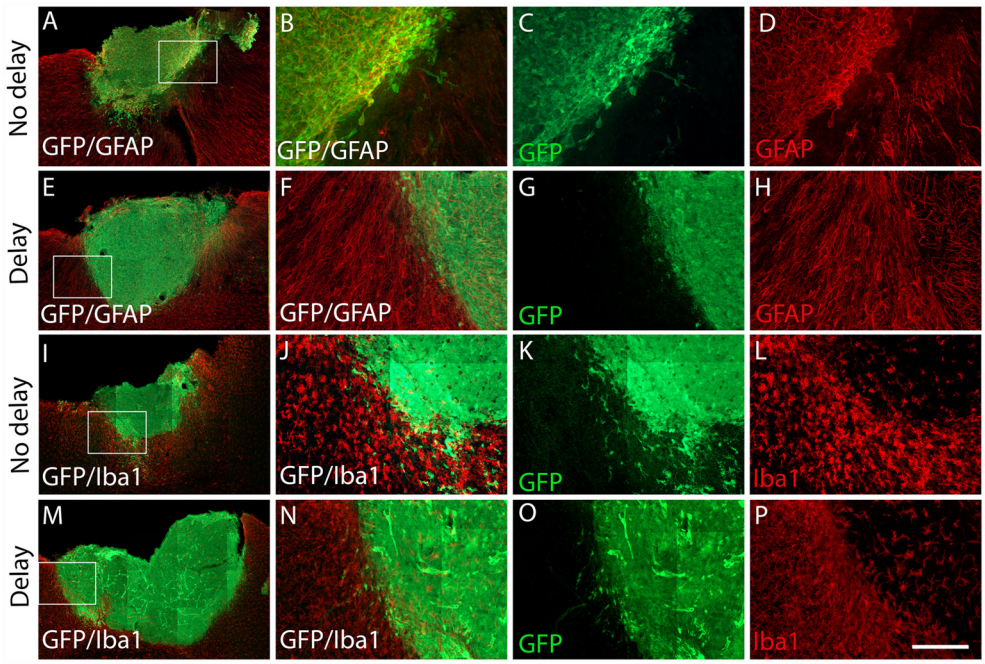

FIGURE 6 | Expression of astrocytes and microglia at 7 days after cortical transplantation. Low magnification photomicrographs of coronal sections illustrating the immunolabeled immune cells (red) in the GFP+ transplants (green) at day 7 after transplantation **(A,E,I,M)**. Astrocytes **(A,E)** and microglia **(I,M)** after transplantation with no delay **(A,I)** or with delay of 1-week **(E,M)** after the cortical lesion. High magnification images from regions of interest showing immunolabeled astrocytes **(B–D,F–H)**, microglia **(J–L,N–P)**, in the GFP+ transplants (in green) after transplantation with no delay **(B–D,J–L)** or with delay **(F–H,N–P)** of 1-week after the cortical lesion. Scale bars: **(A,E,I,M)** 480 μm, **(B–D,F–H,J–L,N–P)** 80 μm.

vascularization, proliferation, and survival of grafted cells as well as density projections developed by grafted neurons. Moreover, we have also shown that this delay has beneficial impacts on functional repair and recovery (Péron et al., 2017). The mechanisms leading to these positive outcomes have not been yet defined. It has been postulated that potential benefits of introducing a delay between the lesion and transplantation may result from the release of trophic factors secreted by cells surrounding the lesion (Nieto-Sampedro et al., 1983), the secretion of pro-angiogenic factors (Sköld et al., 2005; Dray et al., 2009), the decrease of toxin levels (Gonzalez and Sharp, 1987) or the modulation of inflammation levels (Zhang et al., 2010; Burda et al., 2016). Thus, the present study was designed to determine the effect of a 1-week delay on post-traumatic inflammation.

Here, we showed morphological changes in astrocytes and microglia, but also an increase in the number of astrocytes, microglia, oligodendrocytes and CD45+ cells 7 days after the lesion, in comparison to lesion at day 0. In accordance with our results, many studies have shown that microglia responds rapidly to CNS injuries, becoming hypertrophic and reaching its maximum level within the first week after cortical lesion before gradually disappearing (Davalos et al., 2005; Ladeby et al., 2005; Turtzo et al., 2014). In addition, the blood-brain barrier is damaged after the lesion allowing circulating macrophage cells to infiltrate into the site of injury (Shlosberg et al., 2010). In parallel, it has been shown that within 24 h after injury astrocytes proliferate, increase their expression of GFAP, and become hypertrophic (Raivich et al., 1999; Burda et al., 2016) as demonstrated in this study. Following a cortical stab injury, GFAP+ cells were absent at day 2 and 4 post-lesion in the area close to the lesion whereas large numbers of hypertrophic astrocytes were revealed at day 7, demonstrating that most of the increase in GFAP+ cells near the lesion is not due to cell division but is caused by process extension or migration (Hampton et al., 2004). Furthermore, a strong astrogliosis was identified from 7 days until 2 months after injury, where astrocytes contributed to the formation of the glial scar (Villapol et al., 2014).

While activated microglial and macrophage cells express pro- and anti-inflammatory cytokines, we found that the expression of pro-inflammatory cytokine IL-1β starts 1 day after the lesion (data not shown), increased at day 4 and became undetectable at 1-week. In addition, anti-inflammatory cytokine TGF-β1 was strongly expressed at 4 days after the lesion, which decreased significantly at 7 days, but was still detectable. Interestingly, 19% of TGF-β1+ cells co-expressed Iba1, which supports the previous hypothesis that microglial/macrophages activation is also neuroprotective (Lai and Todd, 2006). Based on our previous work showing that a delay of 1-week between cortical lesion and transplantation leads to a transient but significant increase in graft vascularization (Péron et al., 2017) along with the knowledge that TGF-β1 is pro-angiogenic

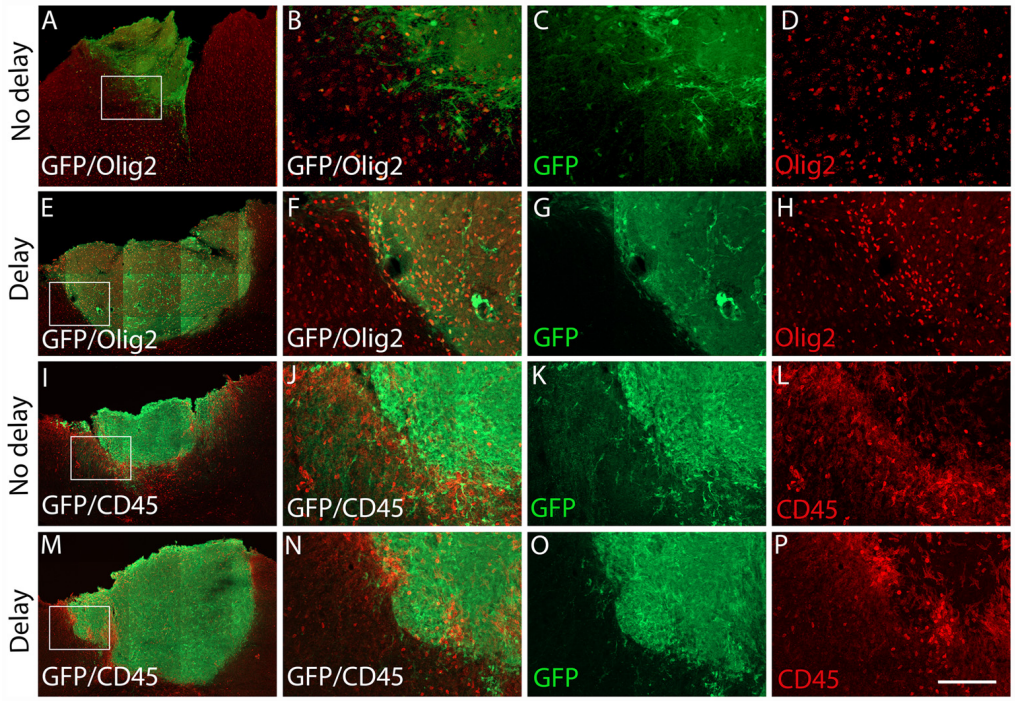

FIGURE 7 | Expression of oligodendrocytes and hematopoietic cells after cortical transplantation. Low magnification photomicrographs of coronal sections illustrating the immunolabeled immune cells (red) in the GFP+ transplants (green) at day 7 after transplantation **(A,E,I,M)**. Oligodendrocytes **(A,E)** and hematopoietic cells **(I,M)** after transplantation with no delay **(A,I)** or with delay of 1-week **(E,M)** after the cortical lesion. High magnification images from regions of interest showing immunolabeled oligodendrocytes **(B–D,F–H)** and hematopoietic cells **(J–L,N–P)** in the GFP+ transplants (in green) after transplantation with no delay **(B–D,J–L)** or with delay of 1-week **(F–H,N–P)** after the cortical lesion. Scale bars: **(A,E,I,M)** 480 μm, **(B–D,F–H,J–L,N–P)** 80 μm.

in vivo and induces angiogenesis (Roberts et al., 1986; Madri et al., 1988; Yang and Moses, 1990; Evrard et al., 2012), we suggest that the increase in graft vascularization observed in the delay group could be in part due to the increased expression of TGF-β1.

Multiple reports on microglia in the injured CNS provide strong support for dual microglial roles, both beneficial and deleterious, as well as differential microglial activation into M1 (pro-inflammatory) or M2 (anti-inflammatory) phenotypes (Kigerl et al., 2009; Perry et al., 2010). In other words, microglia can either promote delayed cell damage by generating pro-inflammatory cytokines and oxidative stress or participate in regenerative processes by clearing debris *via* phagocytosis and release of trophic factors (Hu et al., 2015). In order to further clarify the role of activated microglia/macrophages observed after cortical lesion, M1 and M2 phenotypes were discriminated through further analyses. M1 phenotype was found to dominate the cortical lesion site immediately after the lesion (at day 0) while an M1-to-M2 switch was observed at 1-week after lesion, demonstrated by the expression of Arg1. However, the transient M2 response was replaced by a chronic M1 response (M2-to-M1 switch) at 21 days after lesion. Similar switches have already been reported in models of spinal cord injury (SCI) where an M2 macrophage response was observed depleting within 3–7 days after SCI and which returned to baseline at 14 days (Kigerl et al., 2009; David and Kroner, 2011). In addition, an alternatively activated subset of M2 microglia/macrophage occupied the site of lesion at day 5 after and phased out within 7 days followed by a shift to M1 phenotype (Wang et al., 2013) until 28 days post-injury (Jin et al., 2012). Interestingly, studies of microglia and macrophages after demyelinating lesion revealed an M1-to-M2 switch at the initiation of remyelination, identifying the regenerative capacity of M2 cells in the CNS (Miron et al., 2013).

It is likely that M1 and M2 exist in a state of dynamic equilibrium within the acute lesion microenvironment in the brain. Neuroinflammation is initially a protective response, however, excess inflammatory responses are detrimental, and they may inhibit neuronal regeneration (Russo and McGavern, 2016). Previous studies suggested that expression of M1 microglia/macrophages impair axonal regrowth (David and Kroner, 2011) in contrast to the expression of M2 microglial factors that promote CNS repair while limiting secondary inflammation in the context of neuronal injury (Kigerl et al., 2009). Therefore, M1/M2 switching may help therapeutic effectiveness in traumatic injuries, ischemic damages, and neurodegenerative diseases (Le et al., 2016; Orihuela et al., 2016). It is thus conceivable that the M1-to-M2 shift observed in our model at 1-week post-lesion, in comparison to day 0 and day 21, could enhance clearance of necrotic debris without causing toxicity while also promoting

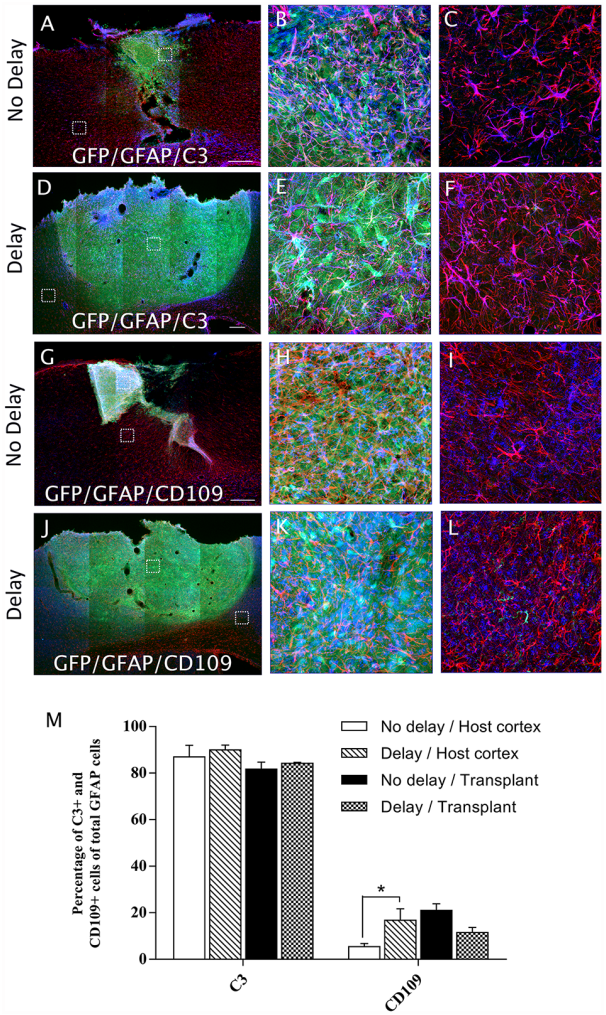

FIGURE 8 | Astrocytes polarization after cortical transplantation. Low magnification photomicrographs of coronal sections illustrating the astrocytes (red) and their phenotype (blue) in the GFP+ transplants (green) at day 7 after transplantation **(A,D,G,J)**. A1 astrocytes (GFAP+/C3+; **A,D**) and A2 astrocytes (GFAP+/CD109+; **G,J**) after transplantation with no delay **(A,G)** or with 1-week delay **(D,J)** after the cortical lesion. High magnification images from regions of interest showing GFAP+/C3 cells **(B,C,E,F)**, GFAP+/CD109 cells **(H,I,K,L)**, in the GFP+ transplants (in green) after transplantation with no delay **(B,C,H,I)** or with delay **(E,F,K,L)** of 1-week after the cortical lesion. Scale bars: **(A,D,G,J)** 480 μm. Histogram showing quantifications of the percentage of C3+ or CD109+ cells of total GFAP+ cells. **(M)** Results are expressed as mean ± SEM. The *p*-value was determined using Kruskal-Wallis test and Dunn's multiple comparison *post hoc* test, $^*p < 0.05$.

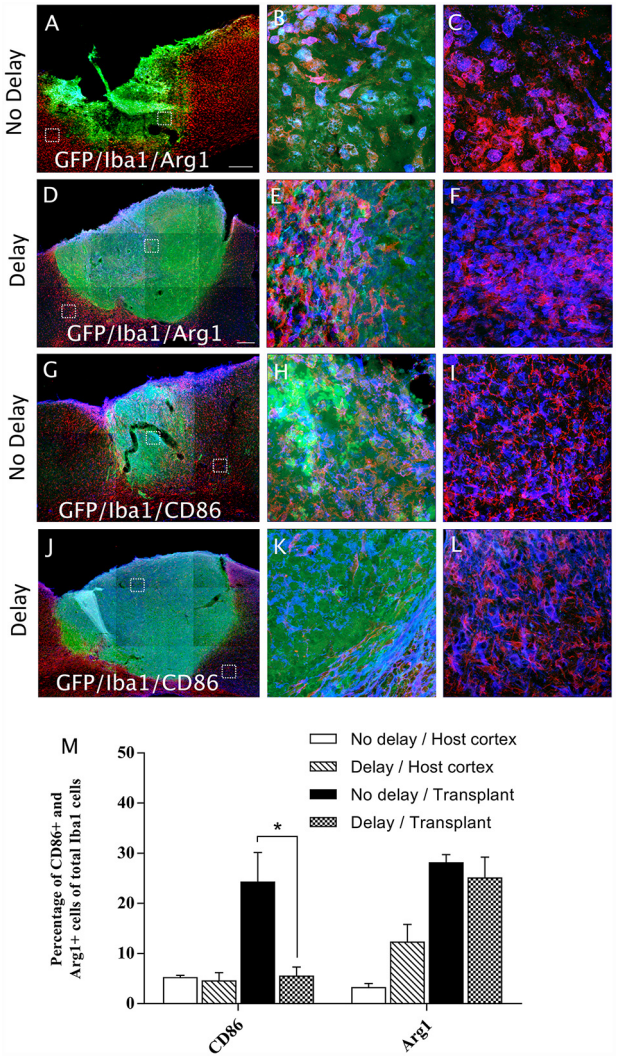

FIGURE 9 | Microglia/macrophage polarization after cortical transplantation. Low magnification photomicrographs of coronal sections illustrating the microglia cells (red) and their phenotype (blue) in the GFP+ transplants (green) at day 7 after transplantation **(A,D,G,J)**. M2 microglia phenotype (Iba1+/Arg1+; **A,D)** and M1 microglia phenotype, (Iba1+/CD86+; **G,J**) after transplantation with no delay **(A,G)** or with delay of 1-week **(D,J)** after the cortical lesion. High magnification images from regions of interest showing Iba1+/Arg1+ cells **(B,C,E,F)**, Iba1+/CD86+ cells **(H,I,K,L)**, in the GFP+ transplants (in green) after transplantation with no delay **(B,C,H,I)** or with delay **(E,F,K,L)** of 1-week after the cortical lesion. Scale bars: **(A,D,G,J)** 480 μm. Histogram showing quantifications of the percentage of Arg1+ or CD86+ cells of total Iba1+ cells. **(M)** Results are expressed as mean ± SEM. The *p*-value was determined using Kruskal-Wallis test and Dunn's multiple comparison *post hoc* test, $^*p < 0.05$.

the outgrowth of grafted neurons. Therefore, the polarized M2 microglia/macrophages response observed nearby the lesion at 1-week post-injury, but not immediately after the lesion (day 0), may represent an endogenous effort to restrict brain damage and might be implicated in the ameliorations that we observed previously when transplanting with time delay (Péron et al., 2017).

The influence of transplanted cells was then studied on the modulation of inflammatory response in the host after transplantation, with or without a delay of 1 week. Seven days post-transplantation, we observed an increase in the number of astrocytes in the host cortex adjacent to the transplant and in the transplant. In addition, despite a high percentage of A1 astrocyte phenotype in the cortex and the transplant in grafted animals with or without delay, no significant differences were observed between groups. In

contrast, a significant increase in the percentage of A2 astrocyte phenotype was observed in the host cortex of the delay group in comparison to no delay group. It has been shown that host astrocytes re-expressed developmental factors to direct axonal growth of the transplant (Gaillard and Jaber, 2007). In addition, astrocytes presented an early phenotype that can partially cause the active migration of transplanted neurons and neuronal precursors (Leavitt et al., 1999). Previous studies have suggested that the main function of reactive astrocytes is to create a physical barrier between damaged and healthy cells (Silver and Miller, 2004), repair the blood-brain barrier (Faulkner et al., 2004), and reduce the excess of glutamate (Zou et al., 2010). Astrocytes can also secrete different growth factors such as BDNF (Schwartz et al., 1994) and VEGF (Rosenstein and Krum, 2004). Astrocytes, as a result of their close relationships with neurons, microglia, and blood vessels have long been hypothesized to be involved in cerebrovascular regulation (Sochocka et al., 2013). In line with our study, it has been demonstrated that astrocytes, starting at 7 days after injury, establish a link with large vessels at the border of the lesion site (Villapol et al., 2014). In summary, we suggest that the expression of trophic factors by astrocytes after transplantation creates a more favorable environment for the development of the transplant. On the other hand, the 1-week delay did not show any effect on the expression of microglia and hematopoietic cells in the transplanted groups. Conversely, the number of microglia decreased after transplantation, which suggests that microglia would act mainly to remove cell debris and promote tissue integration 1-week after the lesion. Among microglia, we have observed a higher percentage of Iba1+ cells expressing proinflammatory M1 marker CD86 in the transplant of the no delay group in comparison to the delay group. These observations suggest that, in no delay transplantation group, host environment induced M1 polarization of microglia within the graft which could be deleterious for the grafted neurons. Indeed, M1 activation in the brain can induce neurotoxicity due to the release of pro-inflammatory factors and neurotoxic mediators (Gao et al., 2003; Qin et al., 2004).

In a previous study, we grafted embryonic motor cortical neurons into the adult mouse motor cortex immediately after the lesion and reported that 30% of the axons derived grafted neurons were myelinated (Gaillard et al., 2007). Interestingly, in the present study, the number of oligodendrocytes was higher in the transplant grafted with a delay compared to no delay, suggesting a more favorable myelination of transplanted neuronal axons with delay.

CONCLUSION

The introduction of a delay of 1-week between the cortical lesion and transplantation of embryonic neurons is beneficial at the neuroanatomical level and functional recovery. Our data on a delay of 1-week resulted into: (1) an increase of inflammation levels; (2) presence of anti-inflammatory cytokine TGF-β1 and absence of pro-inflammatory cytokine IL-1β; and (3) domination of M2 phenotype response. We have also shown an increased expression of GFAP+ cells after transplantation with delay. These results suggested that neuroinflammation observed 1-week after cortical lesion might be promoting debris clearance, graft vascularization, myelination of transplanted neurons axons, and development of projections by grafted neurons. Thus, the environment surrounding cortical lesion could be favorable to the development of transplanted neurons. A detailed analysis of toxins, trophic, and pro-angiogenic factors and the time course of their release is necessary to determine their implication in the benefits shown when transplanted with a 1-week delay. It is also important to identify the molecular and cellular cues that drive microglia and macrophages toward an M2 phenotype after cortical lesion. By doing so, the inflammatory response could be shifted away from the harmful M1 phenotype and complementary therapeutic targets could be revealed.

Currently, various sources of cells are investigated for cell-based therapies. Fetal tissue transplants represent a promising strategy in cell-based regenerative medicine; however, their use is ethically restricted which limit the development of such an approach (Lindvall et al., 2004). To overcome this limitation, cortical neurons derived from embryonic stem cells (ESCs) or induced pluripotent stem cells (iPSCs) represent a promising alternative cell source for cell therapy (Tornero et al., 2013; Dunkerson et al., 2014). Indeed, several studies reported that mouse (Gaspard et al., 2008; Michelsen et al., 2015) and human (Espuny-Camacho et al., 2013, 2018) ESCs can be differentiated into cortical neurons. Cortical neurons derived stem cells grafted into the cortex of newborn (Gaspard et al., 2008; Espuny-Camacho et al., 2013) or adult mice (Michelsen et al., 2015; Espuny-Camacho et al., 2018) send long-distance projections to appropriate cortical and subcortical targets. Extensive investigations are necessary to secure motor cortical identity/fate of the neurons derived from pluripotent stem cells for successful transplantation.

ETHICS STATEMENT

All animal experimentation and housing were carried out in accordance with the guidelines of the French Agriculture and Forestry Ministry (decree 87849) and the European Communities Council Directive (2010/63/EU). All experiments were conducted in compliance with current Good Clinical Practice standards and in accordance with relevant guidelines and regulations and the principles set forth under the Declaration of Helsinki (1989). All efforts were made to reduce the number of animals used and their suffering.

AUTHOR CONTRIBUTIONS

AG conceived the idea and supervised the whole project. NB performed the majority of the experiments with the help of SB, LP, TR, M-LB and MF. NB analyzed the data. AG, NB, KZ, SB and LP interpreted the data and wrote the article.

FUNDING

This work was funded by grants from the Institut pour la Recherche sur la Moelle èpinière et l'Encèphale, the financial participation of the European Union's FEDER funds and the region of Nouvelle Aquitaine, the INSERM, Poitiers University.

ACKNOWLEDGMENTS

This work has benefited from the facilities and expertise of PREBIOS animal facility and Image'UP platforms (University of Poitiers). We thank M. Okabe for the GFP mice, Drs Serge Rivest and Steve Lacroix for the gift of IL1b, TNFa, IL-6, LIF plasmids.

REFERENCES

Ballout, N., Frappé, I., Péron, S., Jaber, M., Zibara, K., and Gaillard, A. (2016). Development and maturation of embryonic cortical neurons grafted into the damaged adult motor cortex. *Front. Neural Circuits* 10:55. doi: 10.3389/fncir.2016.00055

Bernardino, L., Xapelli, S., Silva, A. P., Jakobsen, B., Poulsen, F. R., Oliveira, C. R., et al. (2005). Modulator effects of interleukin-1β and tumor necrosis factor-α on AMPA-induced excitotoxicity in mouse organotypic hippocampal slice cultures. *J. Neurosci.* 25, 6734–6744. doi: 10.1523/JNEUROSCI.1510-05.2005

Block, M. L., Zecca, L., and Hong, J.-S. (2007). Microglia-mediated neurotoxicity: uncovering the molecular mechanisms. *Nat. Rev. Neurosci.* 8:57. doi: 10.1038/nrn2038

Burda, J. E., Bernstein, A. M., and Sofroniew, M. V. (2016). Astrocyte roles in traumatic brain injury. *Exp. Neurol.* 275, 305–315. doi: 10.1016/j.expneurol.2015.03.020

Chao, C. C., Hu, S., and Peterson, P. K. (1995). Glia, cytokines, and neurotoxicity. *Crit. Rev. Neurobiol.* 9, 189–205.

Chhor, V., Le Charpentier, T., Lebon, S., Oré, M.-V., Celador, I. L., Josserand, J., et al. (2013). Characterization of phenotype markers and neuronotoxic potential of polarised primary microglia *in vitro*. *Brain Behav. Immun.* 32, 70–85. doi: 10.1016/j.bbi.2013.02.005

Colton, C. A. (2009). Heterogeneity of microglial activation in the innate immune response in the brain. *J. Neuroimmune Pharmacol.* 4, 399–418. doi: 10.1007/s11481-009-9164-4

Cox, J. C. S., Hetz, R. A., Liao, G. P., Aertker, B. M., Ewing-Cobbs, L., Juranek, J., et al. (2017). Treatment of severe adult traumatic brain injury using bone marrow mononuclear cells. *Stem Cells* 35, 1065–1079. doi: 10.1002/stem.2538

Davalos, D., Grutzendler, J., Yang, G., Kim, J. V., Zuo, Y., Jung, S., et al. (2005). ATP mediates rapid microglial response to local brain injury *in vivo*. *Nat. Neurosci.* 8, 752–758. doi: 10.1038/nn1472

David, S., and Kroner, A. (2011). Repertoire of microglial and macrophage responses after spinal cord injury. *Nat. Rev. Neurosci.* 12, 388–399. doi: 10.1038/nrn3053

Davies, S. J. A., Fitch, M. T., Memberg, S. P., Hall, A. K., Raisman, G., and Silver, J. (1997). Regeneration of adult axons in white matter tracts of the central nervous system. *Nature* 390, 680–683. doi: 10.1038/37776

Demakis, G. J., and Rimland, C. A. (2010). Untreated mild traumatic brain injury in a young adult population. *Arch. Clin. Neuropsychol.* 25, 191–196. doi: 10.1093/arclin/acq004

Davies, S. J. A., Goucher, D. R., Doller, C., and Silver, J. (1999). Robust regeneration of adult sensory axons in degenerating white matter of the adult rat spinal cord. *J. Neurosci.* 19, 5810–5822. doi: 10.1523/JNEUROSCI.19-14-05810.1999

Diaz-Arrastia, R., Kochanek, P. M., Bergold, P., Kenney, K., Marx, C. E., and Grimes, C. J. (2014). Pharmacotherapy of traumatic brain injury: state of the science and the road forward: report of the Department of Defense Neurotrauma Pharmacology Workgroup. *J. Neurotrauma* 31, 135–158. doi: 10.1089/neu.2013.3019

Dray, C., Rougon, G., and Debarbieux, F. (2009). Quantitative analysis by *in vivo* imaging of the dynamics of vascular and axonal networks in injured mouse spinal cord. *Proc. Natl. Acad. Sci. U S A* 106, 9459–9464. doi: 10.1073/pnas.0900222106

Dunkerson, J., Moritz, K. E., Young, J., Pionk, T., Fink, K., Rossignol, J., et al. (2014). Combining enriched environment and induced pluripotent stem cell therapy results in improved cognitive and motor function following traumatic brain injury. *Restor. Neurol. Neurosci.* 32, 675–687. doi: 10.3233/RNN-140408

Espuny-Camacho, I., Michelsen, K. A., Gall, D., Linaro, D., Hasche, A., Bonnefont, J., et al. (2013). Pyramidal neurons derived from human pluripotent stem cells integrate efficiently into mouse brain circuits *in vivo*. *Neuron* 7, 440–456. doi: 10.1016/j.neuron.2012.12.011

Espuny-Camacho, I., Michelsen, K. A., Linaro, D., Bilheu, A., Acosta-Verdugo, S., Herpoel, A., et al. (2018). Human pluripotent stem-cell-derived cortical neurons integrate functionally into the lesioned adult murine visual cortex in an area-specific way. *Cell Rep.* 23, 2732–2743. doi: 10.1016/j.celrep.2018.04.094

Evrard, S. M., d'Audigier, C., Mauge, L., IsraËL-Biet, D., Guerin, C. L., Bieche, I., et al. (2012). The profibrotic cytokine transforming growth factor-β1 increases endothelial progenitor cell angiogenic properties. *J. Thromb. Haemost.* 10, 670–679. doi: 10.1111/j.1538-7836.2012.04644.x

Farina, C., Aloisi, F., and Meinl, E. (2007). Astrocytes are active players in cerebral innate immunity. *Trends Immunol.* 28, 138–145. doi: 10.1016/j.it.2007.01.005

Faulkner, J. R., Herrmann, J. E., Woo, M. J., Tansey, K. E., Doan, N. B., and Sofroniew, M. V. (2004). Reactive astrocytes protect tissue and preserve function after spinal cord injury. *J. Neurosci.* 24, 2143–2155. doi: 10.1523/JNEUROSCI.3547-03.2004

Gaillard, A., and Jaber, M. (2007). Is the outgrowth of transplant-derived axons guided by host astrocytes and myelin loss? *Cell Adh. Migr.* 1, 161–164. doi: 10.4161/cam.1.4.5274

Gaillard, A., Decressac, M., Frappé, I., Fernagut, P. O., Prestoz, L., Besnard, S., et al. (2009). Anatomical and functional reconstruction of the nigrostriatal pathway by intranigral transplants. *Neurobiol. Dis.* 35, 477–488. doi: 10.1016/j.nbd.2009.07.003

Gaillard, A., Gaillard, F., and Roger, M. (1998). Neocortical grafting to newborn and adult rats: developmental, anatomical and functional aspects. *Adv. Anat. Embryol. Cell Biol.* 148, 1–86. doi: 10.1007/978-3-642-72179-3_1

Gaillard, A., Prestoz, L., Dumartin, B., Cantereau, A., Morel, F., Roger, M., et al. (2007). Reestablishment of damaged adult motor pathways by grafted embryonic cortical neurons. *Nat. Neurosci.* 10, 1294–1299. doi: 10.1038/nn1970

Gao, H. M., Liu, B., and Hong, J. S. (2003). Critical role for microglial NADPH oxidase in rotenone-induced degeneration of dopaminergic neurons. *J. Neurosci.* 23, 6181–6187. doi: 10.1523/JNEUROSCI.23-15-06181.2003

Gaspard, N., Bouschet, T., Hourez, R., Dimidschstein, J., Naeije, G., van den Ameele, J., et al. (2008). An intrinsic mechanism of corticogenesis from embryonic stem cells. *Nature* 455, 351–357. doi: 10.1038/nature07287

Gelderblom, M., Leypoldt, F., Steinbach, K., Behrens, D., Choe, C.-U., Siler, D. A., et al. (2009). Temporal and spatial dynamics of cerebral immune cell accumulation in stroke. *Stroke* 40, 1849–1857. doi: 10.1161/strokeaha.108.534503

Gensel, J. C., Almad, A. A., Alexander, J. K., Schonberg, D. L., and Tripathi, R. B. (2008). Does chronic remyelination occur for all spared axons after spinal cord injury in mouse? *J. Neurosci.* 28, 8385–8386. doi: 10.1523/JNEUROSCI.2533-08.2008

Gonzalez, M., and Sharp, F. (1987). Fetal frontal cortex transplanted to injured motor/sensory cortex of adult rats. I. NADPH-diaphorase neurons. *J. Neurosci.* 7, 2991–3001. doi: 10.1523/JNEUROSCI.07-10-02991.1987

Gordon, S. (2003). Alternative activation of macrophages. *Nat. Rev. Immunol.* 3, 23–35. doi: 10.1038/nri978

Hampton, D. W., Rhodes, K. E., Zhao, C., Franklin, R. J. M., and Fawcett, J. W. (2004). The responses of oligodendrocyte precursor cells, astrocytes and microglia to a cortical stab injury, in the brain. *Neuroscience* 127, 813–820. doi: 10.1016/j.neuroscience.2004.05.028

Hu, X., Leak, R. K., Shi, Y., Suenaga, J., Gao, Y., Zheng, P., et al. (2015). Microglial and macrophage polarization—new prospects for brain repair. *Nat. Rev. Neurol.* 11, 56–64. doi: 10.1038/nrneurol.2014.207

Huang, J., Upadhyay, U. M., and Tamargo, R. J. (2006). Inflammation in stroke and focal cerebral ischemia. *Surg. Neurol.* 66, 232–245. doi: 10.1016/j.surneu.2005.12.028

Itoh, T., Satou, T., Nishida, S., Hashimoto, S., and Ito, H. (2007). Immature and mature neurons coexist among glial scars after rat traumatic brain injury. *Neurol. Res.* 29, 734–742. doi: 10.1179/016164107x208086

Jin, X., Ishii, H., Bai, Z., Itokazu, T., and Yamashita, T. (2012). Temporal changes in cell marker expression and cellular infiltration in a controlled cortical impact model in adult male C57BL/6 mice. *PLoS One* 7:e41892. doi: 10.1371/journal.pone.0041892

Kiefer, R., Funa, K., Schweitzer, T., Jung, S., Bourde, O., Toyka, K. V., et al. (1996). Transforming growth factor-β 1 in experimental autoimmune neuritis. Cellular localization and time course. *Am. J. Pathol.* 148, 211–223.

Kigerl, K. A., Gensel, J. C., Ankeny, D. P., Alexander, J. K., Donnelly, D. J., and Popovich, P. G. (2009). Identification of two distinct macrophage subsets with divergent effects causing either neurotoxicity or regeneration in the injured mouse spinal cord. *J. Neurosci.* 29, 13435–13444. doi: 10.1523/JNEUROSCI.3257-09.2009

Klein, A., Lane, E. L., and Dunnett, S. B. (2013). Brain repair in a unilateral rat model of Huntington's disease: new insights into impairment and restoration of forelimb movement patterns. *Cell Transplant.* 22, 1735–1751. doi: 10.3727/096368912x657918

Kumar, A., Stoica, B. A., Sabirzhanov, B., Burns, M. P., Faden, A. I., and Loane, D. J. (2013). Traumatic brain injury in aged animals increases lesion size and chronically alters microglial/macrophage classical and alternative activation states. *Neurobiol. Aging* 34, 1397–1411. doi: 10.1016/j.neurobiolaging.2012.11.013

Ladeby, R., Wirenfeldt, M., Garcia-Ovejero, D., Fenger, C., Dissing-Olesen, L., Dalmau, I., et al. (2005). Microglial cell population dynamics in the injured adult central nervous system. *Brain Res. Rev.* 48, 196–206. doi: 10.1016/j.brainresrev.2004.12.009

Lai, A. Y., and Todd, K. G. (2006). Microglia in cerebral ischemia: molecular actions and interactions. *Can. J. Physiol. Pharmacol.* 84, 49–59. doi: 10.1139/Y05-143

Le, W., Wu, J., and Tang, Y. (2016). Protective microglia and their regulation in Parkinson's disease. *Front. Mol. Neurosci.* 9:89. doi: 10.3389/fnmol.2016.00089

Leavitt, B. R., Hernit-Grant, C. S., and Macklis, J. D. (1999). Mature astrocytes transform into transitional radial glia within adult mouse neocortex that supports directed migration of transplanted immature neurons. *Exp. Neurol.* 157, 43–57. doi: 10.1006/exnr.1999.6982

Lindvall, O., Kokaia, Z., and Martinez-Serrano, A. (2004). Stem cell therapy for human neurodegenerative disorders-how to make it work. *Nat. Med.* 10, S42–S50. doi: 10.1038/nm1064

Lynch, M. A. (2009). The multifaceted profile of activated microglia. *Mol. Neurobiol.* 40, 139–156. doi: 10.1007/s12035-009-8077-9

Madinier, A., Bertrand, N., Mossiat, C., Prigent-Tessier, A., Beley, A., Marie, C., et al. (2009). Microglial involvement in neuroplastic changes following focal brain ischemia in Rats. *PLoS One* 4:e8101. doi: 10.1371/journal.pone.0008101

Madri, J., Pratt, B., and Tucker, A. (1988). Phenotypic modulation of endothelial cells by transforming growth factor-β depends upon the composition and organization of the extracellular matrix. *J. Cell Biol.* 106, 1375–1384. doi: 10.1083/jcb.106.4.1375

Mantovani, A., Sica, A., Sozzani, S., Allavena, P., Vecchi, A., and Locati, M. (2004). The chemokine system in diverse forms of macrophage activation and polarization. *Trends Immunol.* 25, 677–686. doi: 10.1016/j.it.2004.09.015

Michelsen, K. A., Acosta-Verdugo, S., Benoit-Marand, M., Espuny-Camacho, I., Gaspard, N., Saha, B., et al. (2015). Area-specific reestablishment of damaged circuits in the adult cerebral cortex by cortical neurons derived from mouse embryonic stem cells. *Neuron* 85, 982–997. doi: 10.1016/j.neuron.2015.02.001

Miron, V. E., Boyd, A., Zhao, J.-W., Yuen, T. J., Ruckh, J. M., Shadrach, J. L., et al. (2013). M2 microglia/macrophages drive oligodendrocyte differentiation during CNS remyelination. *Nat. Neurosci.* 16, 1211–1218. doi: 10.1038/nn.3469

Myer, D. J., Gurkoff, G. G., Lee, S. M., Hovda, D. A., and Sofroniew, M. V. (2006). Essential protective roles of reactive astrocytes in traumatic brain injury. *Brain* 129, 2761–2772. doi: 10.1093/brain/awl165

Neumann, H., Schweigreiter, R., Yamashita, T., Rosenkranz, K., Wekerle, H., and Barde, Y.-A. (2002). Tumor necrosis factor inhibits neurite outgrowth and branching of hippocampal neurons by a rho-dependent mechanism. *J. Neurosci.* 22, 854–862. doi: 10.1523/JNEUROSCI.22-03-00854.2002

Neumann, J., Gunzer, M., Gutzeit, H. O., Ullrich, O., Reymann, K. G., and Dinkel, K. (2006). Microglia provide neuroprotection after ischemia. *FASEB J.* 20, 714–716. doi: 10.1096/fj.05-4882fje

Nieto-Sampedro, M., Manthrope, M., Barbin, G., Varon, S., and Cotman, C. (1983). Injury-induced neuronotrophic activity in adult rat brain: correlation with survival of delayed implants in the wound cavity. *J. Neurosci.* 3, 2219–2229. doi: 10.1523/JNEUROSCI.03-11-02219.1983

Okabe, M., Ikawa, M., Kominami, K., Nakanishi, T., and Nishimune, Y. (1997). 'Green mice' as a source of ubiquitous green cells. *FEBS Lett.* 407, 313–319. doi: 10.1016/s0014-5793(97)00313-x

Orihuela, R., McPherson, C. A., and Harry, G. J. (2016). Microglial M1/M2 polarization and metabolic states. *Br. J. Pharmacol.* 173, 649–665. doi: 10.1111/bph.13139

Péron, S., Droguerre, M., Debarbieux, F., Ballout, N., Benoit-Marand, M., Francheteau, M., et al. (2017). A delay between motor cortex lesions and neuronal transplantation enhances graft integration and improves repair and recovery. *J. Neurosci.* 37, 1820–1834. doi: 10.1523/JNEUROSCI.2936-16.2017

Perry, V. H., Nicoll, J. A. R., and Holmes, C. (2010). Microglia in neurodegenerative disease. *Nat. Rev. Neurol.* 6, 193–201. doi: 10.1038/nrneurol.2010.17

Qin, L., Liu, Y., Wang, T., Wei, S. J., Block, M. L., Wilson, B., et al. (2004). NADPH oxidase mediates lipopolysaccharide-induced neurotoxicity and proinflammatory gene expression in activated microglia. *J. Biol. Chem.* 279, 1415–1421. doi: 10.1074/jbc.m307657200

Raivich, G., Bohatschek, M., Kloss, C. U. A., Werner, A., Jones, L. L., and Kreutzberg, G. W. (1999). Neuroglial activation repertoire in the injured brain: graded response, molecular mechanisms and cues to physiological function. *Brain Res. Rev.* 30, 77–105. doi: 10.1016/s0165-0173(99)00007-7

Rapalino, O., Lazarov-Spiegler, O., Agranov, E., Velan, G. J., Yoles, E., Fraidakis, M., et al. (1998). Implantation of stimulated homologous macrophages results in partial recovery of paraplegic rats. *Nat. Med.* 4, 814–821. doi: 10.1038/nm0798-814

Roberts, A. B., Sporn, M. B., Assoian, R. K., Smith, J. M., Roche, N. S., Wakefield, L. M., et al. (1986). Transforming growth factor type β: rapid induction of fibrosis and angiogenesis *in vivo* and stimulation of collagen formation *in vitro*. *Proc. Natl. Acad. Sci. U S A* 83, 4167–4171. doi: 10.1073/pnas.83.12.4167

Rolls, A., Shechter, R., and Schwartz, M. (2009). The bright side of the glial scar in CNS repair. *Nat. Rev. Neurosci.* 10, 235–241. doi: 10.1038/nrn2591

Rosenstein, J. M., and Krum, J. M. (2004). New roles for VEGF in nervous tissue—beyond blood vessels. *Exp. Neurol.* 187, 246–253. doi: 10.1016/j.expneurol.2004.01.022

Russo, M. V., and McGavern, D. B. (2016). Inflammatory neuroprotection following traumatic brain injury. *Science* 353, 783–785. doi: 10.1126/science.aaf6260

Schonberg, D. L., Popovich, P. G., and McTigue, D. M. (2007). Oligodendrocyte generation is differentially influenced by toll-like receptor (TLR) 2 and TLR4-mediated intraspinal macrophage activation. *J. Neuropathol. Exp. Neurol.* 66, 1124–1135. doi: 10.1097/nen.0b013e31815c2530

Schwartz, J. P., Nishiyama, N., Wilson, D., and Taniwaki, T. (1994). Receptor-mediated regulation of neuropeptide gene expression in astrocytes. *Glia* 11, 185–190. doi: 10.1002/glia.440110212

Schwartz, M., Butovsky, O., Brück, W., and Hanisch, U.-K. (2006). Microglial phenotype: is the commitment reversible? *Trends Neurosci.* 29, 68–74. doi: 10.1016/j.tins.2005.12.005

Shlosberg, D., Benifla, M., Kaufer, D., and Friedman, A. (2010). Blood-brain barrier breakdown as a therapeutic target in traumatic brain injury. *Nat. Rev. Neurol.* 6, 393–403. doi: 10.1038/nrneurol.2010.74

Silver, J., and Miller, J. H. (2004). Regeneration beyond the glial scar. *Nat. Rev. Neurosci.* 5, 146–156. doi: 10.1038/nrn1326

Sköld, M. K., von Gertten, C., Sandbergnordqvist, A.-C., Mathiesen, T., and Holmin, S. (2005). VEGF and VEGF receptor expression after experimental brain contusion in rat. *J. Neurotrauma* 22, 353–367. doi: 10.1089/neu.2005.22.353

Sochocka, M., Koutsouraki, E., Gasiorowski, K., and Leszek, J. (2013). Vascular oxidative stress and mitochondrial failure in the pathobiology of Alzheimer's disease: a new approach to therapy. *CNS Neurol. Disord. Drug Targets* 12, 870–881. doi: 10.2174/18715273113129990072

Sofroniew, M. V., and Vinters, H. V. (2010). Astrocytes: biology and pathology. *Acta Neuropathol.* 119, 7–35. doi: 10.1007/s00401-009-0619-8

Tanielian, T., and Jaycox, L. H. (Eds). (2008). *Invisible Wounds of War: Psychological and Cognitive Injuries, Their Consequences, and Services to Assist Recovery*. Santa Monica, CA: RAND Corporation.

Thompson, L. H., Grealish, S., Kirik, D., and Björklund, A. (2009). Reconstruction of the nigrostriatal dopamine pathway in the adult mouse brain. *Eur. J. Neurosci.* 30, 625–638. doi: 10.1111/j.1460-9568.2009.06878.x

Tornero, D., Wattananit, S., Grønning Madsen, M., Koch, P., Wood, J., Tatarishvili, J., et al. (2013). Human induced pluripotent stem cell-derived cortical neurons integrate in stroke-injured cortex and improve functional recovery. *Brain* 136, 3561–3577. doi: 10.1093/brain/awt278

Turtzo, L. C., Lescher, J., Janes, L., Dean, D. D., Budde, M. D., and Frank, J. A. (2014). Macrophagic and microglial responses after focal traumatic brain injury in the female rat. *J. Neuroinflammation* 11:82. doi: 10.1186/1742-2094-11-82

Vezzani, A., Balosso, S., and Ravizza, T. (2008). The role of cytokines in the pathophysiology of epilepsy. *Brain Behav. Immun.* 22, 797–803. doi: 10.1016/j.bbi.2008.03.009

Villapol, S., Byrnes, K. R., and Symes, A. J. (2014). Temporal dynamics of cerebral blood flow, cortical damage, apoptosis, astrocyte-vasculature interaction and astrogliosis in the pericontusional region after traumatic brain injury. *Front. Neurol.* 5:82. doi: 10.3389/fneur.2014.00082

Wang, Z., Luo, Y., Chen, L., and Liang, W. (2017). Safety of neural stem cell transplantation in patients with severe traumatic brain injury. *Exp. Ther. Med.* 13, 3613–3618. doi: 10.3892/etm.2017.4423

Wang, C., Tao, S., Fang, Y., Guo, J., Zhu, L., and Zhang, S. (2016). Infiltrating cells from host brain restore the microglial population in grafted cortical tissue. *Sci. Rep.* 6:33080. doi: 10.1038/srep33080

Wang, G., Zhang, J., Hu, X., Zhang, L., Mao, L., Jiang, X., et al. (2013). Microglia/macrophage polarization dynamics in white matter after traumatic brain injury. *J. Cereb. Blood Flow Metab.* 33, 1864–1874. doi: 10.1038/jcbfm.2013.146

Wanner, I. B., Deik, A., Torres, M., Rosendahl, A., Neary, J. T., Lemmon, V. P., et al. (2008). A new *in vitro* model of the glial scar inhibits axon growth. *Glia* 56, 1691–1709. doi: 10.1002/glia.20721

Xiong, X.-Y., Liu, L., and Yang, Q.-W. (2016). Functions and mechanisms of microglia/macrophages in neuroinflammation and neurogenesis after stroke. *Prog. Neurobiol.* 142, 23–44. doi: 10.1016/j.pneurobio.2016.05.001

Yang, E., and Moses, H. (1990). Transforming growth factor β 1-induced changes in cell migration, proliferation and angiogenesis in the chicken chorioallantoic membrane. *J. Cell Biol.* 111, 731–741. doi: 10.1083/jcb.111.2.731

Zhang, Q., Raoof, M., Chen, Y., Sumi, Y., Sursal, T., Junger, W., et al. (2010). Circulating mitochondrial DAMPs cause inflammatory responses to injury. *Nature* 464, 104–107. doi: 10.1038/nature08780

Zou, J., Wang, Y.-X., Dou, F.-F., Lü, H.-Z., Ma, Z.-W., Lu, P.-H., et al. (2010). Glutamine synthetase downregulation reduces astrocyte protection against glutamate excitotoxicity to neurons. *Neurochem. Int.* 56, 577–584. doi: 10.1016/j.neuint.2009.12.021

Conflict of Interest Statement: The authors declare that the research was conducted in the absence of any commercial or financial relationships that could be construed as a potential conflict of interest.

frontiers in Molecular Neuroscience

ORIGINAL RESEARCH
published: 10 December 2019
doi: 10.3389/fnmol.2019.00308

Analysis of Schwann Cell Migration and Axon Regeneration Following Nerve Injury in the Sciatic Nerve Bridge

Bing Chen[1]*, *Quan Chen*[1], *David B. Parkinson*[2] and *Xin-peng Dun*[2]

[1]Department of Neurology, The Affiliated Huai'an No.1 People's Hospital of Nanjing Medical University, Huai'an, China,
[2]Faculty of Health: Medicine, Dentistry and Human Sciences, Plymouth University, Plymouth, United Kingdom

While it is proposed that interaction between Schwann cells and axons is key for successful nerve regeneration, the behavior of Schwann cells migrating into a nerve gap following a transection injury and how migrating Schwann cells interact with regenerating axons within the nerve bridge has not been studied in detail. In this study, we combine the use of our whole-mount sciatic nerve staining with the use of a proteolipid protein-green fluorescent protein (PLP-GFP) mouse model to mark Schwann cells and have examined the behavior of migrating Schwann cells and regenerating axons in the sciatic nerve gap following a nerve transection injury. We show here that Schwann cell migration from both nerve stumps starts later than the regrowth of axons from the proximal nerve stump. The first migrating Schwann cells are only observed 4 days following mouse sciatic nerve transection injury. Schwann cells migrating from the proximal nerve stump overtake regenerating axons on day 5 and form Schwann cell cords within the nerve bridge by 7 days post-transection injury. Regenerating axons begin to attach to migrating Schwann cells on day 6 and then follow their trajectory navigating across the nerve gap. We also observe that Schwann cell cords in the nerve bridge are not wide enough to guide all the regenerating axons across the nerve bridge, resulting in regenerating axons growing along the outside of both proximal and distal nerve stumps. From this analysis, we demonstrate that Schwann cells play a crucial role in controlling the directionality and speed of axon regeneration across the nerve gap. We also demonstrate that the use of the PLP-GFP mouse model labeling Schwann cells together with the whole sciatic nerve axon staining technique is a useful research model to study the process of peripheral nerve regeneration.

Keywords: peripheral nerve, injury, nerve bridge, Schwann cell, migration, axon regeneration

OPEN ACCESS

Edited by:
John Martin,
City College of New York (CUNY), United States

Reviewed by:
Paul David Morton,
Virginia Tech, United States
Rosario Arévalo,
University of Salamanca, Spain

***Correspondence:**
Bing Chen
chenbing2007@163.com

Received: *23 September 2019*
Accepted: *29 November 2019*
Published: *10 December 2019*

Citation:
Chen B, Chen Q, Parkinson DB and Dun X (2019) Analysis of Schwann Cell Migration and Axon Regeneration Following Nerve Injury in the Sciatic Nerve Bridge. Front. Mol. Neurosci. 12:308. doi: 10.3389/fnmol.2019.00308

INTRODUCTION

Peripheral nerve injuries are common in both civil and military environments and are primarily transection injuries (Deumens et al., 2010; Ray and Mackinnon, 2010; Daly et al., 2012). Transection injuries can occur during motor vehicle accidents, sports activities, surgery or other forms of penetrating trauma. Damage to the peripheral nervous system typically leads

to the development of neuropathic pain and life-long loss of motor and sensory function. The effective treatment of peripheral nerve transection injuries is a clinically significant and challenging area and further research is required in order to improve the outcome of peripheral nerve repair (Moore et al., 2009; Daly et al., 2012).

Accumulating evidence indicates that following injury, regenerating axons are unable to cross a peripheral nerve gap without Schwann cell guidance at their migrating growth front (Torigoe et al., 1996; Parrinello et al., 2010; Webber et al., 2011; Rosenberg et al., 2014; Cattin et al., 2015; Dun and Parkinson, 2015). Using an anti-mitotic agent (mitomycin C) to prevent Schwann cell division, Hall (1986) showed that inhibition of Schwann cell proliferation and migration after mouse sciatic nerve transection injury significantly impeded axon regeneration. In the zebrafish motor axon transection injury model, regenerating axons lost their direction and traveled along ectopic trajectories in the nerve bridge when Schwann cells were genetically ablated (Rosenberg et al., 2014). Additionally, in elegant experiments using a vascular endothelial growth factor (VEGF) bound bead to misdirect both blood vessel regeneration and Schwann cell migration in the rat sciatic nerve gap, regenerating axons followed the path of ectopic migrating Schwann cells and left the nerve bridge (Cattin et al., 2015). These findings showed that Schwann cells play a pivotal role in controlling the directionality of regenerating axons in the peripheral nerve gap. Thus, understanding how Schwann cells direct axon regeneration in a nerve gap, and the relative chronology of Schwann cell migration and axonal growth, is vital in order to develop new therapeutic strategies for boosting peripheral nerve repair. To date, how migrating Schwann cells interact with regenerating axons in the peripheral nerve bridge during regeneration has not been fully studied, largely due to the inability to visualize Schwann cell-axon interaction *in vivo*, and this is the purpose of this current study.

Recently, we developed a whole-mount staining method to study the pattern of axon regeneration in the nerve gap following mouse sciatic nerve transection injury (Dun and Parkinson, 2015). The use of this technique has allowed us to precisely map patterns of axon regeneration within the nerve bridge. In this study, we apply the whole-mount staining technique on nerve bridge tissue in the proteolipid protein-green fluorescent protein (PLP-GFP) mouse strain (Mallon et al., 2002), which expresses GFP in Schwann cells of the peripheral nerves driven by the mouse myelin PLP gene promoter. We examined *in vivo* axon regeneration, Schwann cell migration and Schwann cell-axon interactions in the mouse sciatic nerve bridge. Combining our whole-mount staining method with the PLP-GFP mouse model, we demonstrate that Schwann cells play a crucial role in guiding axon regeneration across a nerve gap after peripheral nerve transection. We also demonstrate that the use of the PLP-GFP mouse model labeling Schwann cells together with the whole sciatic nerve axon staining technique could provide a useful research model to study the process of peripheral nerve regeneration.

MATERIALS AND METHODS

Animal Husbandry and Peripheral Nerve Surgery

The PLP-GFP mouse transgenic strain was used in this study (Mallon et al., 2002). Originally made to label oligodendrocytes in the central nervous system driven GFP expression by the mouse myelin PLP gene promoter, the PLP-GFP mice also express cytoplasmic GFP in both myelinating and non-myelinating Schwann cells of the peripheral nerves (Mallon et al., 2002; Carr et al., 2017; Stierli et al., 2018; Dun et al., 2019). All work involving animals was performed according to Home Office regulation under the UK Animals (Scientific Procedures) Act 1986. Ethical approval for all experiments was granted by Plymouth University Animal Welfare and Ethical Review Board. For sciatic nerve surgery, equal numbers of 2-month-old male and female mice were anesthetized with isoflurane, the right sciatic nerve was exposed and transected at approximately 0.5 cm proximal to the sciatic nerve trifurcation site and no re-anastomosis of the severed nerve was performed. This approach allowed analysis of axon pathfinding and Schwann cell migration within the nerve bridge that forms between the retracted proximal and distal nerve stumps. Following nerve transection surgery, the overlying muscle was sutured and the skin was closed with an Autoclip applier. All animals undergoing surgery were given appropriate post-operative analgesia and monitored daily. At the indicated time points post-surgery for each experiment described, animals were euthanased humanely by CO_2 in accordance with UK Home Office regulations.

Whole-Mount Staining

At the described time points following surgery, nerves were dissected out together with surrounding muscle to ensure the nerve bridge structure remained fully intact. Nerves together with surrounding muscles were fixed in 4% paraformaldehyde for 5 h at 4°C. Following fixation and PBS wash, surrounding muscle tissue was carefully removed in PBS using a dissecting microscope. Nerves were then washed in PTX (1% Triton X-100; Sigma, T9284) in PBS three times for 10 min each wash and then incubated with blocking solution [10% fetal bovine serum (FBS) in PTX] overnight at 4°C. The following day, nerves were transferred into primary antibodies in PTX containing 10% FBS and incubated for 72 h at 4°C with gentle rocking. The primary antibody used for the experiments is an anti-neurofilament heavy chain chicken polyclonal (1:100, Abcam, ab4680, immunogen, cow full-length intermediate filaments). After the incubation, nerves were washed three times with PTX for 15 min each wash, followed by washing in PTX for 6 h at room temperature, with a change of PTX every hour. Alexa Fluor 568 dye conjugated anti-chicken secondary antibody (1:500, Invitrogen, Carlsbad, CA, USA) was diluted in PTX containing 10% FBS, and incubated with the nerve preparation for 48 h at 4°C with gentle rocking. Nerves were then washed in PTX three times for 15 min each, followed by washing in PTX for 6 h at room temperature, changing the PTX each hour, and then washed overnight without changing PTX, at 4°C. Due to the nature of long time antibody

incubation of this whole nerve staining method, buffers were filtered through 0.45 μm filters to maintain sterile conditions. Nerves were cleared sequentially with 25%, 50%, 75% (v/v) glycerol (Sigma, G6279) in PBS between 12–24 h for each glycerol concentration. Following clearing, nerves were mounted in CitiFluor (Agar Scientific, R1320) for confocal microscopy and image acquisition.

Imaging

Images were obtained with a Zeiss LSM510 confocal microscope. Several Z-series were captured, covering the entire field of interest. The individual series were then flattened into a single image for each location and combined into one image using Adobe Photoshop software (Adobe Systems, San Jose, CA, USA).

Data Quantification and Statistical Analysis

The bridge length, the distance of leading Schwann cells from the nerve ends, the area of migrating Schwann cells in the nerve bridge and the speed of axonal growth were measured using Image-J following image acquisition. The bridge length was measured as the distance between the two nerve ends (indicated by two dashed lines in all Figures). The distance of leading Schwann cells on day 4, day 5 and day 6 was measured as the distance from the nerve ends to the leading migrating Schwann cells. To calculate the average speed of axonal growth on day 6 and day 7, the distance of leading axons from the proximal nerve end was measured on day 5 and day 7. The average speed of axonal growth (μm/day) was calculated using the distance difference between day 7 and day 5 divided by 2 (day 6 and day 7). Statistical analysis was carried out using the student's *t*-test. Data were presented as Mean ± SEM in the article, $n = 4$ for each timepoint.

RESULTS

Axon Regeneration Is Ahead of Schwann Cell Migration in the Proximal Nerve Stump

Sciatic nerve transection is the most frequently used research model for studying peripheral nerve regeneration in rodents (Dun and Parkinson, 2018). Previous studies have confirmed that Schwann cells of the peripheral nerves express high levels of GFP in the PLP-GFP mouse model, which allows us to accurately visualize Schwann cell behavior and migration following sciatic nerve transection (Mallon et al., 2002; Cattin et al., 2015; Carr et al., 2017; Stierli et al., 2018; Dun et al., 2019). In our experiments, sciatic nerve transection generated a nerve bridge gap of 1.62 ± 0.29 mm, allowing us to observe the axon extension from the proximal nerve stump together with Schwann cell migration from both proximal and distal nerve stumps.

In agreement with previous findings using the S100 marker to identify migrating Schwann cells (Parrinello et al., 2010; Cattin et al., 2015), we also observed that GFP positive Schwann cells start to migrate into the nerve bridge from both proximal and distal nerve ends at 4 days post-transection in our whole-mount PLP-GFP sciatic nerve preparations (**Figure 1A**). In both the proximal and the distal nerve stumps on day 4, a few Schwann cells have migrated past the transection site (indicated by dashed lines in **Figures 1A,I**) and into the nerve bridge. While Schwann cells are migrating at this timepoint, whole-mount nerve neurofilament staining showed that regenerating axons in the proximal end are clearly proceeding in front of migrating Schwann cells on day 4 (**Figures 1B,C**). At this early timepoint, there are no Schwann cells associated with the front wave of regenerating axons (**Figures 1C,K**). On day 4 in the proximal nerve stump, Schwann cells appear to use regenerating axons as a substrate to migrate toward the nerve bridge (indicated by white arrows in **Figure 1K**). On day 4 in the distal nerve stump, about 40% of the leading Schwann cells have two or three leading processes (**Figure 1F**), indicating that they are pioneer cells and are seemingly responsible for detecting environmental signals and searching for a substrate upon which to migrate (**Figure 1H**). In contrast, leading Schwann cells from the proximal nerve do not have several processes at 4 days, perhaps because they are using regenerating axons as a substrate to migrate (**Figure 1G**). On day 4, distances of the leading migrating Schwann cells were 275.42 ± 10.1 μm from the proximal stump and 189.79 ± 11.96 μm from the distal nerve stump (**Figure 1D**). The area of Schwann cells migrating into the nerve bridge from the proximal stump is bigger than 0.2 mm^2 but the area of Schwann cells migrating into the nerve bridge from the distal nerve stump is smaller than 0.1 mm^2 (**Figure 1E**). The distance and area difference between the proximal and the distal nerve stump indicate that Schwann cells from the proximal nerve stump migrate faster than those from the distal nerve stump on day 4, potentially due to the fact that Schwann cells in the proximal nerve stump are using axons as a substrate upon which to migrate at this time.

Previously using whole-mount staining in C57BL/6 mice, we showed that 5 or 6 regenerating axons formed axon bundles resulting in seemingly large diameter axons observed at this stage of regeneration, a ball shape is often formed at the tips of these axon bundles (Dun and Parkinson, 2015). In the PLP-GFP mice, we also observed the ball shape at the tips of regenerating axons (**Figure 1J**). Occasionally, three to five single axons could be observed extending further into the nerve bridge but were not facing towards the distal nerve stump (**Figures 1J,K**, indicated by yellow arrows). These observations indicate that axon regeneration occurs significantly earlier than Schwann cell migration but axons appear to lack directionality at this early stage of regeneration.

From day 5, robust Schwann cell migration into the nerve bridge was seen from both nerve stumps (**Figures 2A–C**). On day 5, distances of the furthest leading Schwann cells from the cut sites are 379.08 ± 16.73 μm from the proximal nerve stump and 272.97 ± 14.68 μm from the distal nerve stump (**Figure 2D**). The area of Schwann cells migrating into the nerve bridge was more than 0.3 mm^2 from the proximal stump and lesser than 0.2 mm^2 from the distal nerve stump (**Figure 2E**). Similarly as for the migration rates for day 4, the difference in the migration distances and area between the proximal stump and the distal nerve stump may result from Schwann cells in the proximal nerve stump using axons as a substrate to migrate upon. On day 5 post-injury, migrating Schwann cells in the

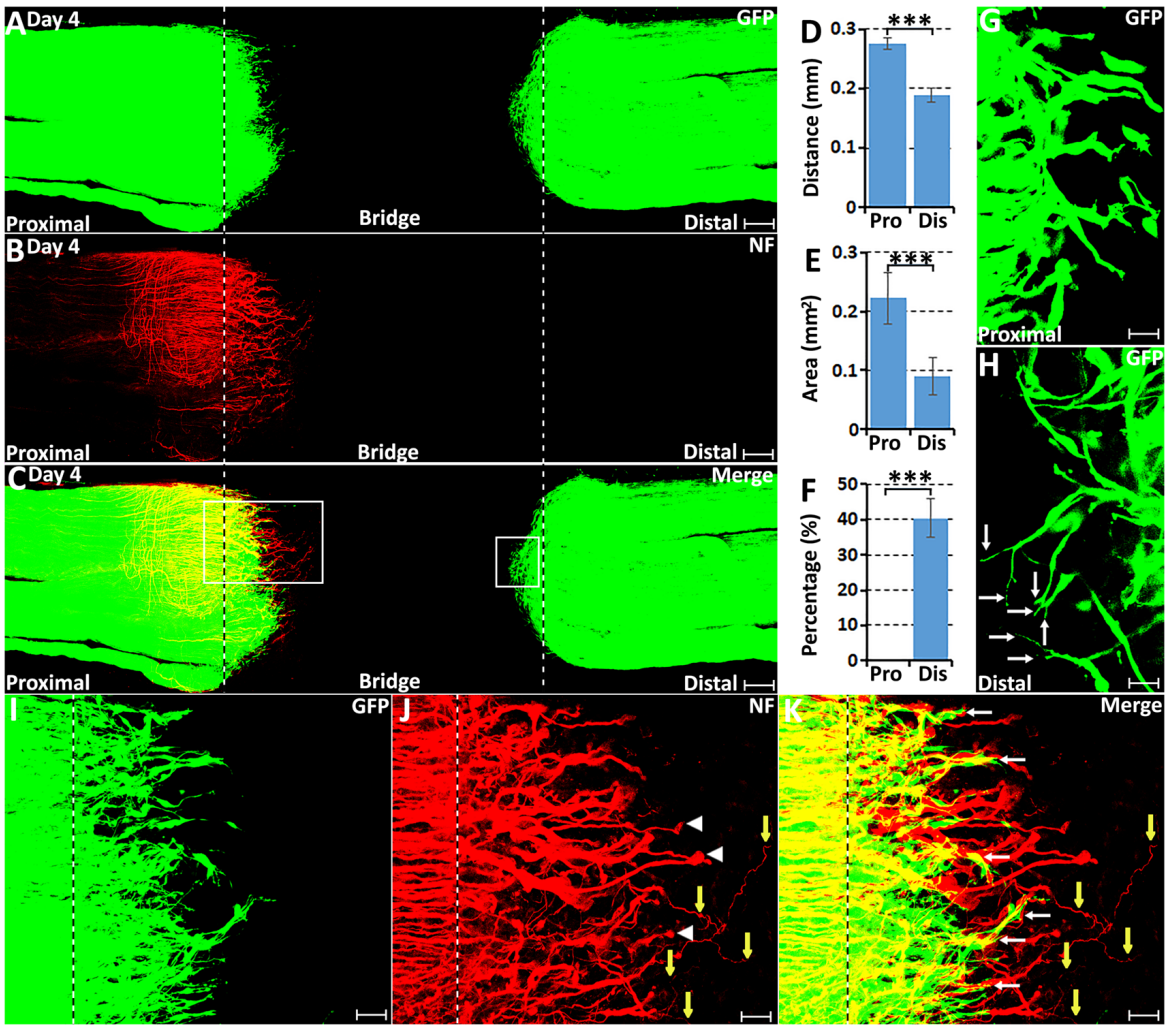

FIGURE 1 | Axon regeneration and Schwann cell migration in the sciatic nerve bridge at 4 days post-injury. **(A–C)** Whole nerve preparation at 4 days post-injury shows regenerating axons and migrating Schwann cells in the nerve bridge of proteolipid protein-green fluorescent protein (PLP-GFP) mice. **(D)** Distances of the leading migrating Schwann cells from the proximal (Pro) stump and the distal (Dis) nerve ends. **(E)** The area of migrating Schwann cells in the proximal (Pro) part and the distal (Dis) part of the nerve bridge. **(F)** Percentage of leading Schwann cells having two or three leading processes. **(G)** On day 4, leading Schwann cells migrating from the proximal stump appear to have a single migrating process, whereas **(H)** about 40% leading Schwann cells migrating from the distal nerve stump show two or three leading processes (indicated by arrows). **(I–K)** Higher magnification images from the box area of proximal nerve stump in **(C)** showing regenerating axons proceeding in front of migrating Schwann cells in the proximal nerve stump at 4 days post-injury. Regenerating axons form axon bundles and appear to have ball shapes at their tips (indicated by white arrow heads in **J**). White arrows in **(K)** indicate Schwann cells apparently migrating along the regrowing axons. Yellow arrows in **(J,K)** show several single regenerating axons growing in a random direction within the nerve bridge. The sites of transection for both the proximal and distal nerve stumps are indicated by dashed lines in each image. ***$P < 0.001$. Scale bars in **(A–C)** 150 μm. Scale bars in **(G,H)** 25 μm. Scale bars in **(I–K)** 50 μm.

proximal nerve end still could be observed using regenerating axons as a substrate upon which to migrate (**Figures 3A–C**), however, a few migrating Schwann cells begin to proceed in front of the regenerating axons on day 5 (**Figures 3D–F**). Interestingly, about 20% leading Schwann cells in the proximal nerve stump start to show two or more processes once they migrate past the front of regenerating axons (**Figures 2F**, **3G**), indicating that they have now apparently become pioneer cells and are starting to search for a new substrate to migrate upon. On day 5 in the distal nerve stump, more than 80% leading Schwann cells show two or three leading processes (**Figures 2F**, **3H**). From our analysis, before day 5 it appears that Schwann cells are following axons from the proximal nerve stump; following day 5, Schwann cells overtake regenerating axons and proceed in front of the regrowing axon front.

Migrating Schwann Cells, Leaders to Direct Regenerating Axons Across the Nerve Gap

At 6 days following transection, more migrating Schwann cells were observed within the nerve bridge (**Figure 4A**), but an

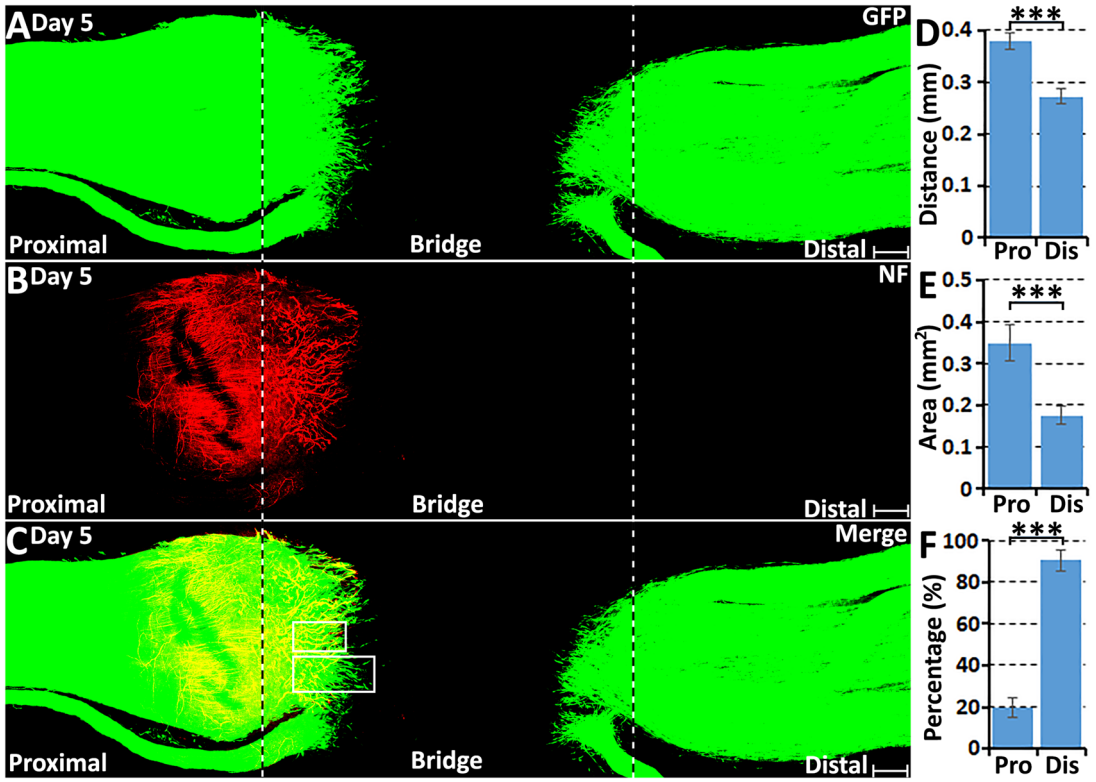

FIGURE 2 | Axon regeneration and Schwann cell migration in the sciatic nerve bridge on day 5 post-injury. **(A–C)** Whole nerve preparation on day 5 shows regenerating axons and migrating Schwann cells in the nerve bridge of PLP-GFP mice. The cut ends of both proximal and distal nerves are indicated by dashed lines. **(D)** Distances of the leading migrating Schwann cells from the proximal (Pro) stump and the distal (Dis) nerve ends. **(E)** The area of migrating Schwann cells in the proximal (Pro) part and the distal (Dis) part of the nerve bridge. **(F)** Percentage of leading Schwann cells having two or three leading processes. ***$P < 0.001$. Scale bars in **(A–C)** 150 μm.

area free of Schwann cells was still present in the middle of the nerve bridge between migrating cells from both nerve stumps (**Figures 4A–C**). Distances of the leading migrating Schwann cells were 474.67 ± 13.56 μm from the proximal stump and 473.67 ± 14.78 μm from the distal nerve stump (**Figure 4D**). This measurement showed that the distance of the leading migrating Schwann cells in the proximal nerve stump is similar to the distance of the leading migrating Schwann cells from the distal nerve stump on day 6. As indicated by generating several leading processes of leading migrating Schwann cells in the proximal nerve stump once they localize in front of regenerating axons from day 5 onwards, the searching for a new substrate to migrate upon may potentially slow down the migration of Schwann cells in the proximal nerve stump between day 5 and day 6. The area of Schwann cells in the nerve bridge from proximal nerve stump on day 6 nearly reaches to 0.6 mm^2 but the area of Schwann cells from the distal nerve stump is only 0.3 mm^2 due to regenerating axons provide a much wider substrate for Schwann cell migration on day 4 and day 5 (**Figure 4E**).

On day 6 post-injury, more than 70% pioneer migrating Schwann cells from the proximal stump and more than 80% pioneer migrating Schwann cells from the distal nerve stump show two or three leading processes (**Figures 4F**, **5G,H**). Following the pioneer cells, Schwann cells attach to each other and form a chain to migrate towards the middle of the nerve bridge (**Figures 5G,H**). Thus, *in vivo* Schwann cell migration after peripheral nerve transection injury appears to represent classic cell chain migration behavior with the leading cells guiding the followers and forming a chain of migrating cells. Interestingly on day 6, regenerating axons start to change their morphology when there are many migrating Schwann cells in front of regenerating axons (**Figures 5A–F**). Axon bundles lose their typical ball shape at their tips and single axons start to emerge from axon bundles (**Figures 5B,E**). Single regenerating axons can be seen to apparently follow the Schwann cell chains and elongate toward the distal nerve stump (**Figures 5D–F**). This indicates that the rapid single axon growth is seemingly induced by the presence of migrating Schwann cells ahead of the axon front.

On day 7 post-transection, migrating Schwann cells from both the proximal stump and the distal nerve stump have mixed in the middle of the nerve bridge and Schwann cell cords have formed to direct axons regenerating towards the distal nerve stump (**Figures 6A–C**). Schwann cells within

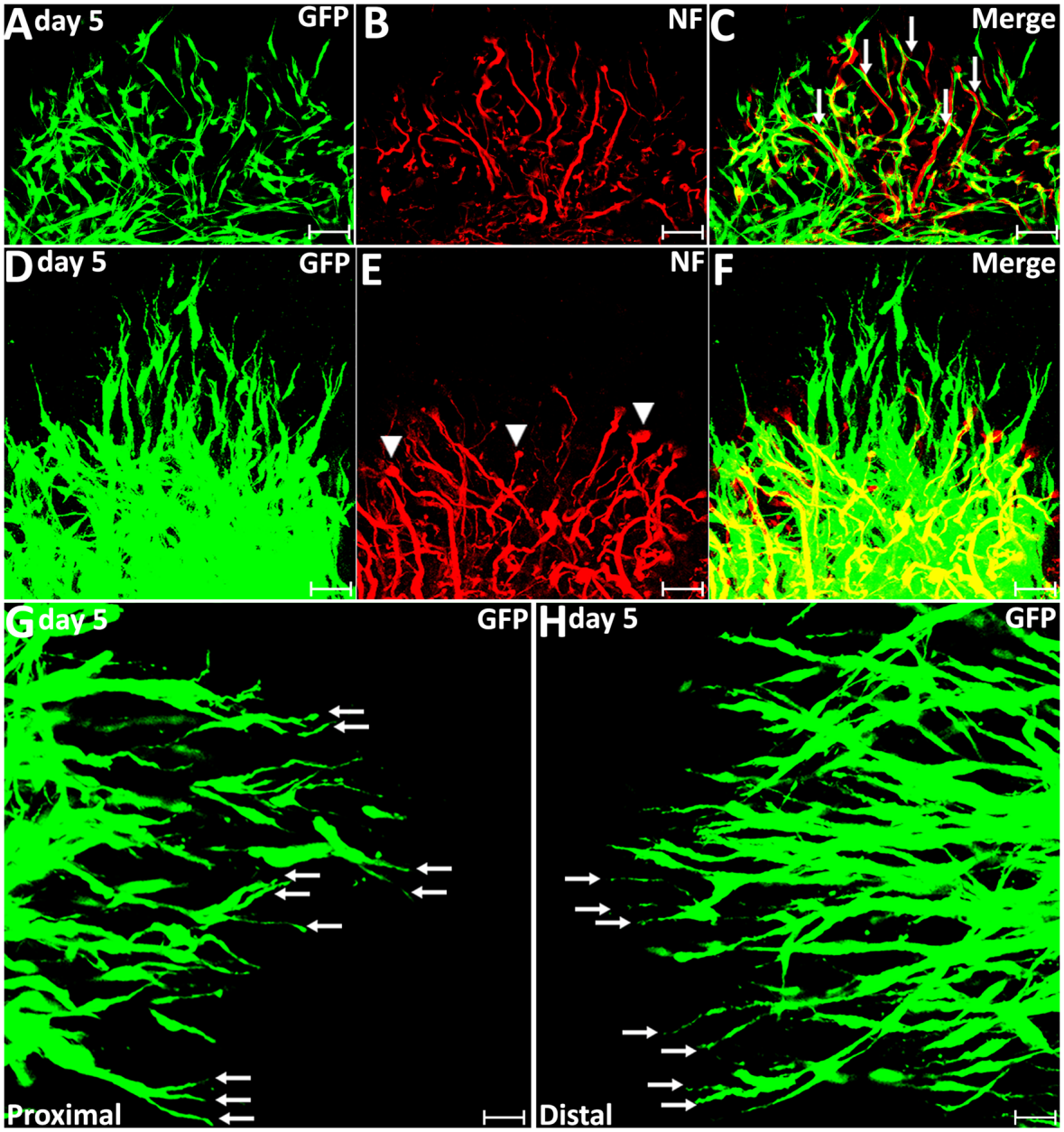

FIGURE 3 | Axon regeneration and Schwann cell migration in the sciatic nerve bridge on day 5 post-injury. **(A–C)** On day 5 in the proximal nerve stump, Schwann cells appear to use regenerating axons as a substrate to migrate upon, indicated by white arrows in **(C)**. **(D–F)** A few migrating Schwann cells start to proceed ahead of the regenerating axon front from day 5 post-injury in the proximal nerve stump. Arrow heads in **(E)** show the ball shape at the tips of regenerating axons. **(G,H)** On day 5, leading Schwann cells from both proximal and distal nerve stumps show two or three leading processes (indicated by arrows). Chain Schwann cell migration is easily visible from the distal nerve stump on day 5. Scale bars in **(A–F)** 40 μm. Scale bars in **(G–H)** 25 μm.

the cords can be seen to attach to each other and form longitudinal chains connecting the proximal and distal nerve stumps (**Figures 6D–F**). Single regenerating axons inside the Schwann cell cords could be observed attaching to the Schwann cell cords and elongating towards the distal nerve stump (**Figures 6D–F**). At 7 days post-injury, about 78% of Schwann cell cords are associated with a single regenerating axon in the proximal part of the nerve bridge (**Figures 6D–F**, **7H**). On day 7, we observed that a subset of axons inside the Schwann cell cords (indicated by white arrows in **Figure 6B**) have regenerated much more rapidly than axons (indicated by yellow arrows in **Figure 6B**), which lack Schwann cell guidance at their front (**Figure 6C**). As a measure of how the association between Schwann cells with regenerating axons accelerates axonal regeneration, we have measured the average speed of axons growing inside the Schwann cell cord on day 6

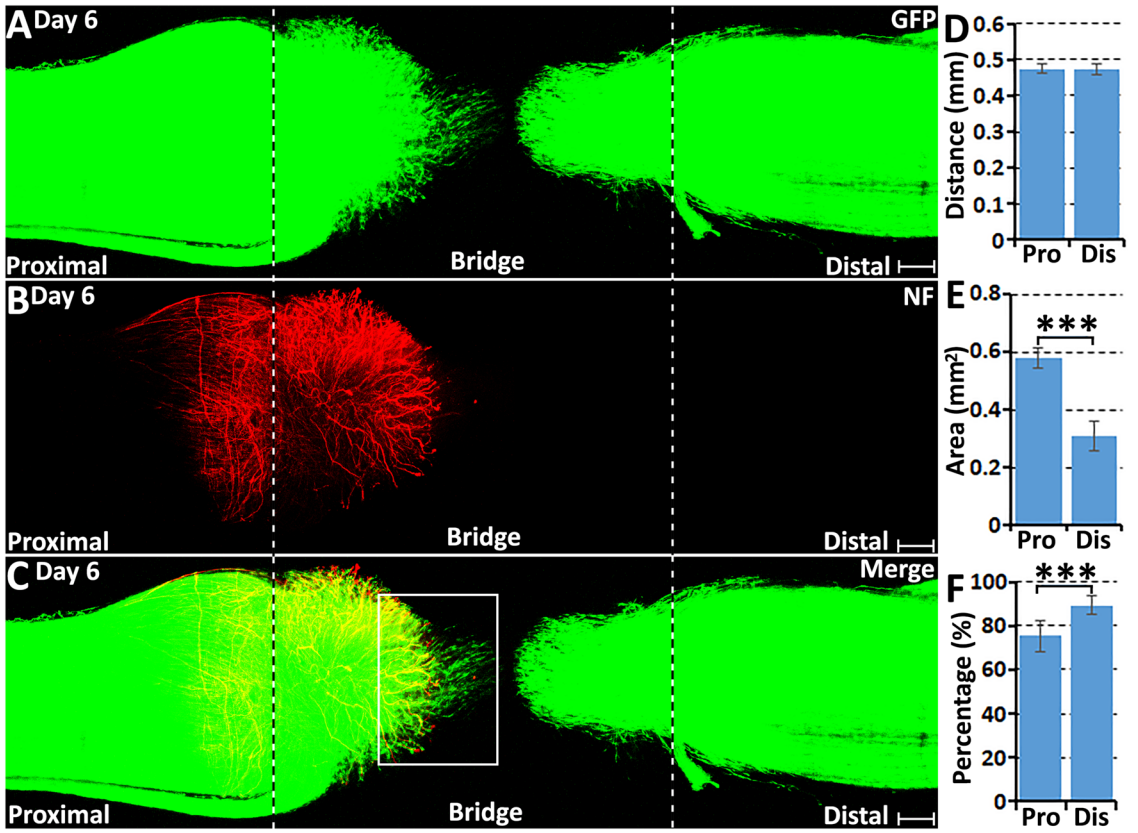

FIGURE 4 | Axon regeneration and Schwann cell migration in the sciatic nerve bridge at 6 days post-injury. **(A–C)** Whole nerve preparation on day 6 shows regenerating axons and migrating Schwann cells in the nerve bridge of PLP-GFP mice. The cut ends of both proximal and distal nerves are indicated by dashed lines. **(D)** Distances of the leading migrating Schwann cells from the proximal (Pro) stump and the distal (Dis) nerve ends. **(E)** The area of migrating Schwann cells in the proximal (Pro) part and the distal (Dis) part of the nerve bridge. **(F)** Percentage of leading Schwann cells having two or three leading processes. ***$P < 0.001$. Scale bars in **(A–C)** 150 μm.

and day 7 as 433.1 ± 32.1 μm/day; this is in contrast, the speed of non-Schwann cell-associated axons, which is only 85.7 ± 9.2 μm/day.

On day 9 and day 14 post-injury, more Schwann cells and regenerating axons could be observed in the nerve bridge (**Figures 7**, **8**). On day 9 and day 14, Schwann cell cords in the nerve bridge are still clearly visible and all Schwann cell cords have regenerating axons associated with them (**Figures 7D–F,H**). On day 9 and day 14, it appears that each Schwann cell cord in the nerve bridge has several regenerating axons associated with it (**Figures 7D–F**).

Regenerating Axons Lose Their Directionality in the Nerve Bridge Owing to the Lack of Schwann Cell Guidance

On day 7 post-injury, Schwann cell cords have formed to guide the regenerating axons across the nerve bridge (**Figure 6A**). However, the Schwann cell cords formed in the nerve bridge are always not wide enough to guide all the regenerating axons across the nerve gap from the proximal nerve stump (**Figure 6C**). In the PLP-GFP mice on day 7, the diameter of Schwann cell cords in the nerve bridge could be easily observed by the GFP signal. Measuring the GFP signal showed that the diameter of the proximal nerve ends is about 1.01 ± 0.067 mm but the diameter of Schwann cell cords in the nerve bridge is only 0.41 ± 0.077 mm which is less than half of the diameter of the proximal nerve stump end (**Figure 7G**). The small diameter of Schwann cell cords in the nerve bridge resulted in more than half of regenerating axons apparently lacking guidance by Schwann cells (**Figures 6A–C**). On day 7, regenerating axons can be clearly classified into two populations in the nerve bridge due to the diameter of Schwann cell cords in the nerve bridge not being wide enough to guide all the regenerating axons across the nerve gap (**Figure 6B**). One population of axons growing inside the Schwann cell cords (indicated by white arrows in **Figure 6B**) will eventually cross the nerve gap and reach the distal nerve stump. The other population of axons (indicated by yellow arrows in **Figure 6B**), which are located outside of the Schwann cell cords are unable to grow further because they lack migrating Schwann cells at their front for guidance (**Figures 6C,G–I**). Indicated by their large diameter and the ball shape at the tip of the axons (**Figures 6G–I**), this population of axons are still

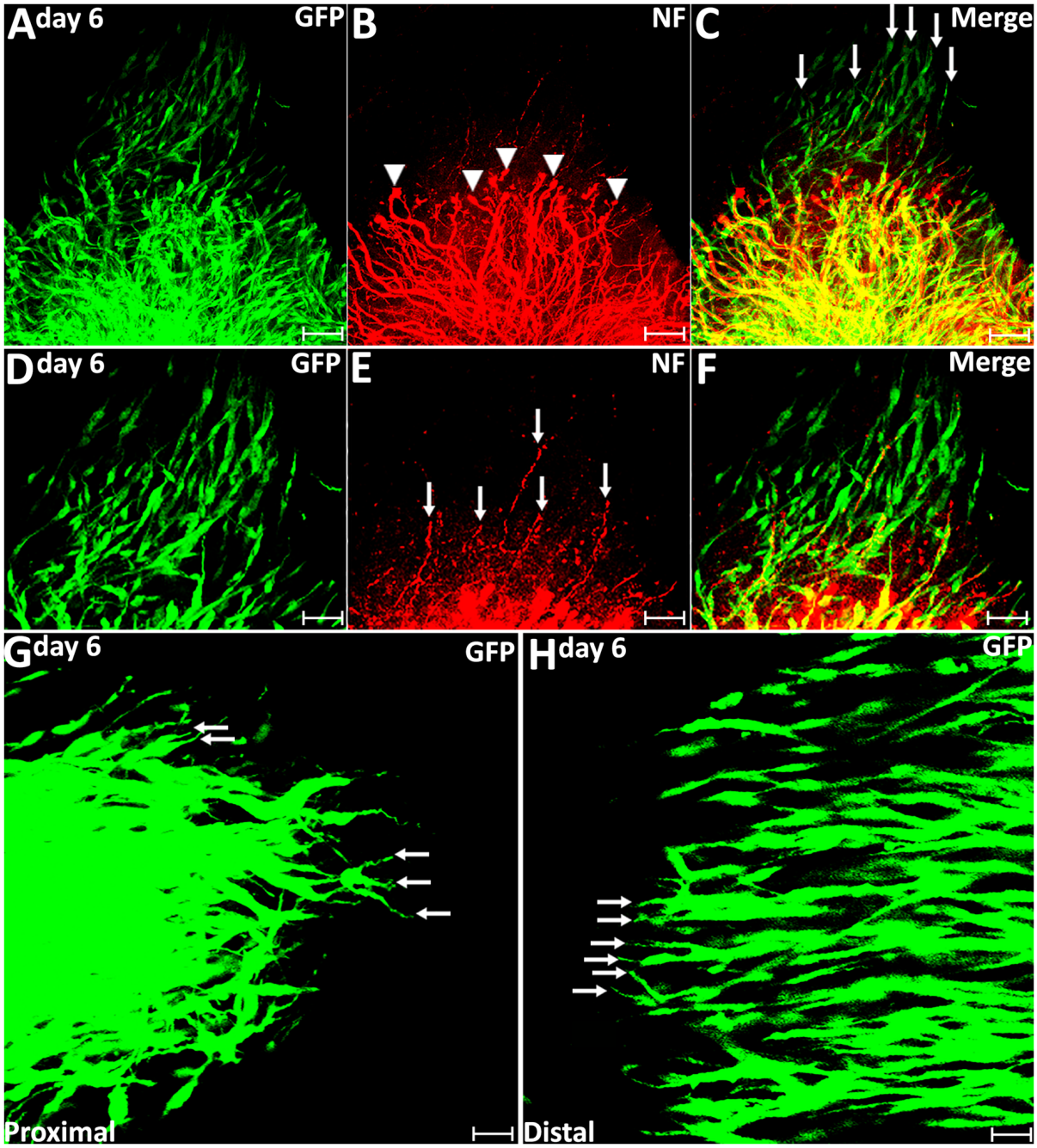

FIGURE 5 | Axon regeneration and Schwann cell migration in the sciatic nerve bridge at 6 days post-injury. **(A–C)** More migrating Schwann cells localize in front of regenerating axon front on day 6 in the proximal nerve stump. Arrow heads in **(B)** indicate the ball shape at the tips of axon bundles. Arrows in **(C)** indicate migrating Schwann cells localized in front of regenerating axons. **(D–F)** Single regenerating axons follow Schwann cell chains on day 6 post-injury in the proximal nerve end. Arrows in **(E)** indicate single axons following the migrating Schwann cell chains. **(G,H)** On day 6, leading Schwann cells from both proximal and distal nerve stumps still show two or three leading processes (indicated by arrows) with chain Schwann cell migration visible in both the proximal stump and the distal nerve stump. Scale bars in **(A–C)** 75 μm. Scale bars in **(D–H)** 50 μm. Scale bars in **(G–H)** 25 μm.

in a state of random extension due to the lack of Schwann cell guidance. On day 7, they have formed at various angles relative to the nerve bridge, some axons near the epineurium can be seen that have turned their direction and have started to grow towards the proximal nerve stump (**Figure 6B**). With staining at the later timepoint of 9 days post-injury, we found that this population of axons have turned and grown along the outside of the proximal nerve trunk (indicated by white arrows in proximal

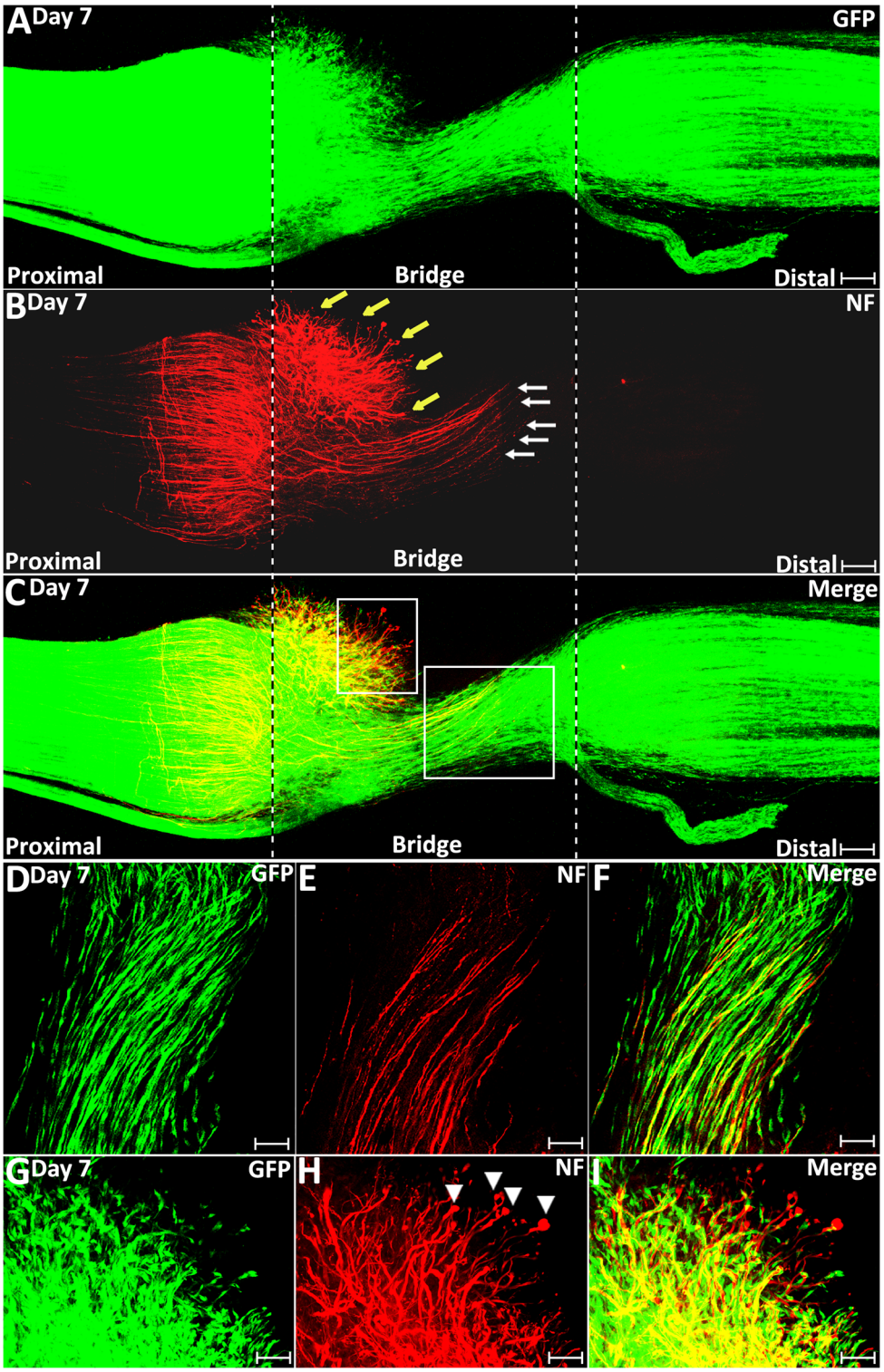

FIGURE 6 | Schwann cell cord formation and axon-Schwann cell interaction in the nerve bridge on day 7 post-injury. **(A–C)** Whole nerve preparation on day 7 post-transection shows regenerating axons and Schwann cell cords in the nerve bridge of PLP-GFP mice. Two populations of regenerating axons (yellow vs. white arrows in **B**) are distinguishable in the nerve bridge at this timepoint. The cut ends of both proximal and distal nerves are indicated by dashed lines. **(D–F)** A population of regenerating axons (indicated by white arrows in **B** and the area of the larger box in C) follow Schwann cell cords and cross the nerve bridge. **(G–I)** A population of regenerating axons (indicated by yellow arrows in **B** and the area of the small box in C) lack Schwann cell guidance in front on day 7 in the nerve bridge. Scale bars in **(A–C)** 150 μm. Scale bars in **(D–F)** 50 μm. Scale bars in **(G–I)** 30 μm.

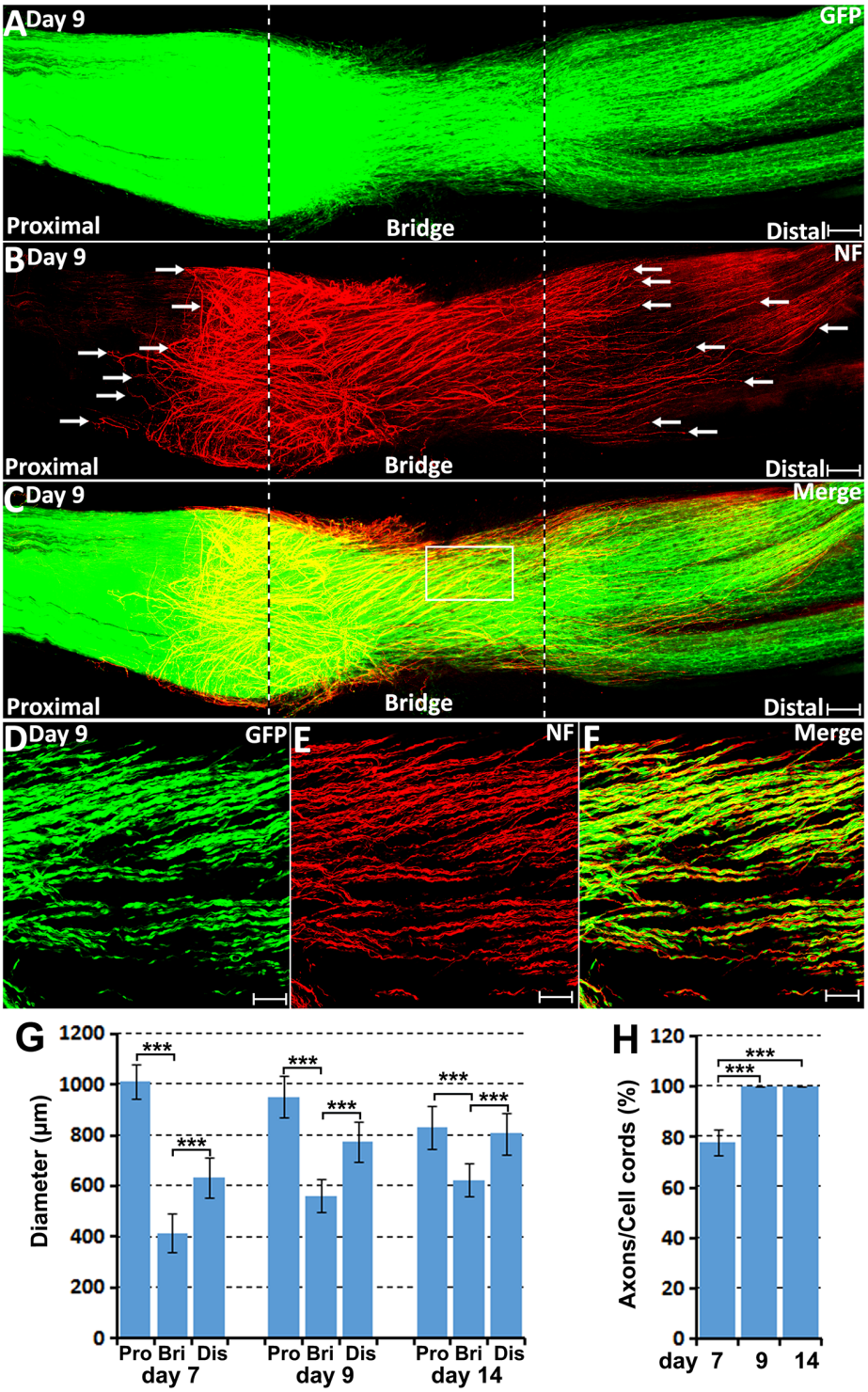

FIGURE 7 | Axon-Schwann cell interactions in the nerve bridge on day 9 in the PLP-GFP mouse. **(A–C)** Whole nerve preparation on 9 days post-injury shows axon-Schwann cell interactions in the nerve bridge. Misdirected axons in the proximal nerve stump were observed growing back along the surface of proximal nerve stump (indicated in the proximal nerve stump by arrows in **B**). Misdirected axons in the distal nerve stump start also to grow along the surface of the distal nerve stump (indicated in the distal nerve stump by arrows in **B**). The cut ends of both proximal and distal nerves are indicated by dash lines. **(D–F)** Several regenerating axons associate with each Schwann cell cord in the nerve bridge on day 9 post-injury. **(G)** The diameter of the proximal nerve end, the diameter of Schwann cell cords in the nerve bridge and the diameter of the distal nerve end on day 7, 9 and 14. **(H)** The percentage of Schwann cell cords associated with regenerating axons in the nerve bridge on day 7, 9 and 14. ***$P < 0.001$. Scale bars in **(A–C)** 150 μm. Scale bars in **(D–F)** 100 μm.

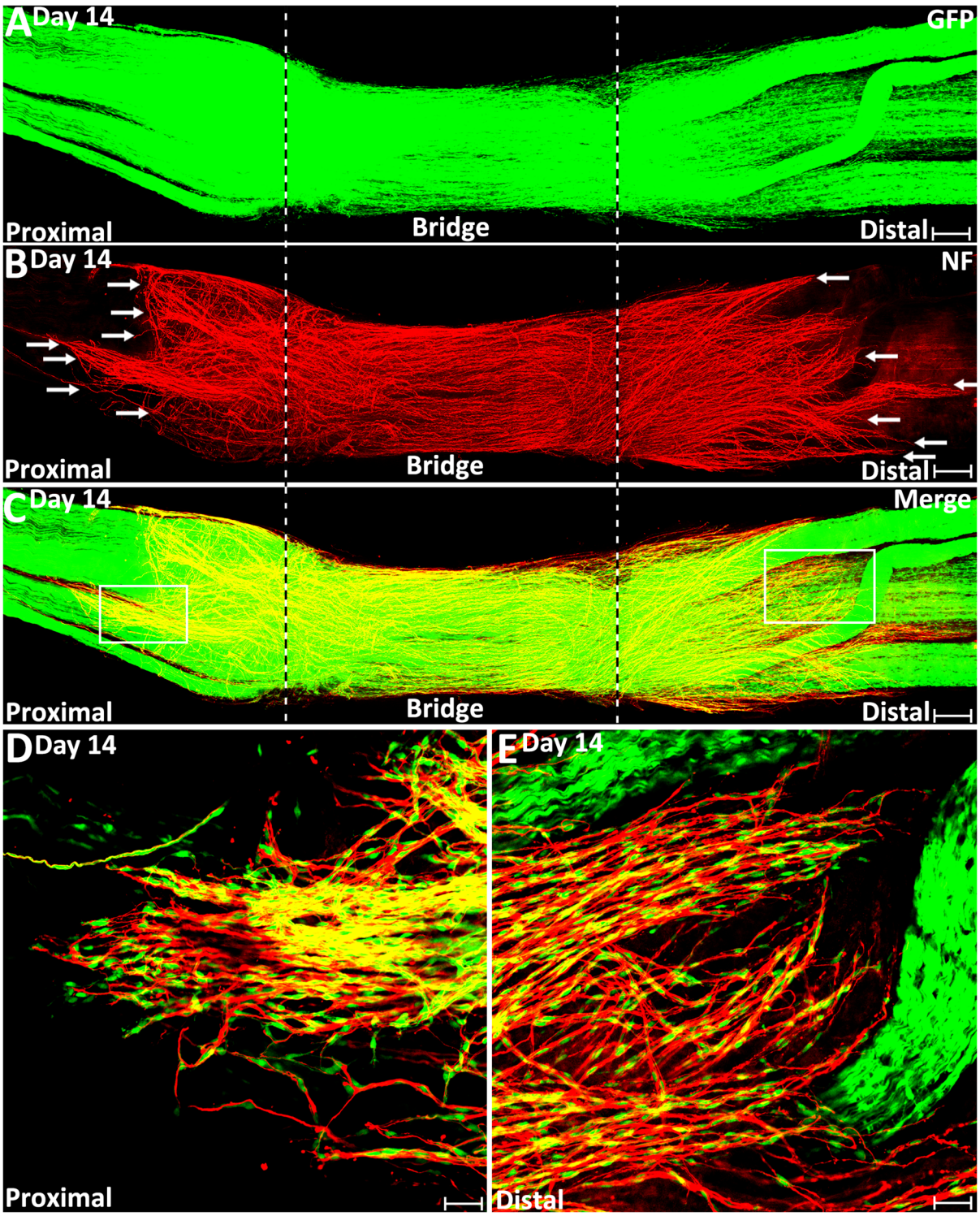

FIGURE 8 | Misdirected axons around the nerve bridge on day 14 post-injury in the PLP-GFP mice. **(A–C)** Whole nerve preparation on day 14 post-injury shows regenerating axons and Schwann cells around the nerve bridge. There are more misdirected axons on the surface of both proximal and distal nerve stumps on day 14 than on day 9 (indicated by arrows). The cut ends of both proximal and distal nerve are indicated by dashed lines. **(D)** Higher magnification image from the box area of proximal nerve stump in **(C)** shows misdirected axons growing along the surface of the proximal nerve stump. **(E)** Higher magnification image from the box area of distal nerve stump in **(C)** shows misdirected axons growing along the surface of the distal nerve stump. Scale bars in **(A–C)** 150 μm. Scale bars in **(D,E)** 50 μm.

nerve stump in **Figure 7B**). On day 14, we observed that more axons were growing along the outside of the proximal nerve trunk (**Figures 8B,D**). Thus, due to the lack of Schwann cell guidance in the front, a large population of regenerating axons from the proximal nerve stump have lost their directionality and failed to cross the injury site. This clearly showed that regenerating axons in the nerve bridge require Schwann cell guidance in order to cross the newly generated nerve bridge.

Previously, we also showed by whole-mount staining that there were regenerating axons extending along the outside the distal nerve stump on day 10, day 14 and day 90 post-transection (Dun and Parkinson, 2015). In this current study, we first observed regenerating axons growing along the outside the distal nerve in the PLP-GFP mice at 9 days post-injury (indicated by white arrows in distal nerve stump in **Figure 7B**), and this population of mis-directed axons is much easier to observe on day 14 (**Figures 8B,E**). Thus, some axons have followed the Schwann cell cords and crossed the nerve bridge, but they fail to enter into the distal nerve stump. Instead, they now misdirect their growth along the outside of distal nerve stump.

We further studied how migrating Schwann cells interact with misdirected regenerating axons on the surface of both the proximal and the distal nerve stumps on day 14. We always observed that the front of mis-directed axons are naked and there are no Schwann cells associated with them (**Figures 8D,E**). Further back on these mis-directed axons, Schwann cells could be observed associating with the axon bundles and these Schwann cells are often held by several axons (**Figures 8D,E**). In our previous study, these two populations of mis-directed axons extending along the outside of the nerve stumps were still observed on day 90 on the surface of both proximal and distal nerve stumps (Dun and Parkinson, 2015), suggesting that the neurons of mis-directed regenerating axons have still survived at this late timepoint, despite having not correctly re-innervated their targets.

In clinical peripheral nerve repair, a nerve graft or conduit repair is required for the treatment of nerve gaps equal to or greater than 5 mm in length (Deumens et al., 2010; Ray and Mackinnon, 2010; Daly et al., 2012). Schwann cell cords are unable to form and regenerating axons from proximal nerve are unable to cross a 5 mm nerve gap and enter into the distal nerve stump without a nerve graft or conduit repair. Finally, we generated 5 mm length sciatic nerve gaps by removing a piece of nerve to study how migrating Schwann cells interact with regenerating axons in a 5 mm sciatic nerve gap in the PLP-GFP mice on day 14. We found the Schwann cell cords were never formed across a 5 mm mouse sciatic nerve gap (**Figure 9A**). In the proximal nerve stump, even on day 14, regenerating axons are still seen extending in front of Schwann cells migrating from the proximal stump. Several regenerating axons form bundles and hold Schwann cells and a ball shape is often seen at the tips of regenerating axons. Regenerating axons appear more scattered and form a fan shape due to the lack of their directionality (**Figures 9B–D**). In the distal nerve end, Schwann cells still form chains and migrate out from the distal nerve end, but the majority of them are not facing towards the proximal nerve ends (**Figure 9A**). These observations further suggest that the lack of Schwann cell guidance is the primary reason resulting in axon mis-targeting in the nerve bridge.

DISCUSSION

Schwann cells are the peripheral nerve glia and the injury-induced Schwann cell plasticity is essential for the success of peripheral nerve regeneration and tissue repair (Lopez-Verrilli et al., 2013; Jessen and Mirsky, 2016; Carr and Johnston, 2017). Current evidences suggest that peripheral nerve-associated Schwann cells possess the capacity to promote repair in multiple tissue including peripheral nerve gap bridging, skin wound healing and digit tip regeneration (Johnston et al., 2016; Carr and Johnston, 2017; Parfejevs et al., 2018). In this study, we showed that the PLP-GFP mouse is an excellent mouse model to visualize *in vivo* Schwann cell migration after peripheral nerve transection injury. Several other genetic approaches have been used to label Schwann cells with fluorescent proteins in the mouse such as S100-GFP (Zuo et al., 2004), S100-BFP, S100-RFP (Hirrlinger et al., 2005) and Sox10-Venus (Hirrlinger et al., 2005). Among all of them, the PLP-GFP and S100-GFP mice are the best characterized mouse models to reveal *in vivo* Schwann cell migration during peripheral nerve regeneration (Hayashi et al., 2007; Tomita et al., 2009; Whitlock et al., 2010; Cattin et al., 2015; Stierli et al., 2018; Zigmond and Echevarria, 2019).

The basic behavior of *in vivo* axon regeneration and Schwann cell migration after peripheral nerve transection injury has been studied by Torigoe et al. (1996) using the film model. In the film model, the transected mouse proximal peroneal nerve was sandwiched between two thin plastic fluorine resin films. A very thin layer of regenerating tissue could be formed between two films. Therefore, tissue sectioning was not needed for subsequent analysis in this model. Using this method, Torigoe et al. (1996) analyzed axon regeneration on the film in the early phase of regeneration up to 6 days. However, a nerve bridge is unable to form in the film model, therefore the film model cannot mimic the full *in vivo* nerve bridge microenvironment for axon regeneration and Schwann cell migration. In our study, combining our whole-mount staining method with the use of the PLP-GFP mouse model, we are able to study the basic behavior and the time course of *in vivo* axon regeneration, Schwann cell migration and Schwann cell-axon interaction in the nerve bridge. We were able to provide much clearer images covering the whole field of the injury site of a transected mouse sciatic nerve at different time points and to analyze the regeneration events in the mouse sciatic nerve bridge. Using this methodology, we not only demonstrated that Schwann cells play a crucial role in guiding axon regeneration across the nerve gap, but also revealed that the lack of Schwann cell guidance in the nerve gap is the apparent reason for axons misdirection during regeneration.

Since Ramón y Cajal's initial observations, there have been intensive debates about whether axons regenerate randomly in the nerve gap without the guidance of Schwann cells or they are actually guided by Schwann cells (Lobato, 2008). Questions

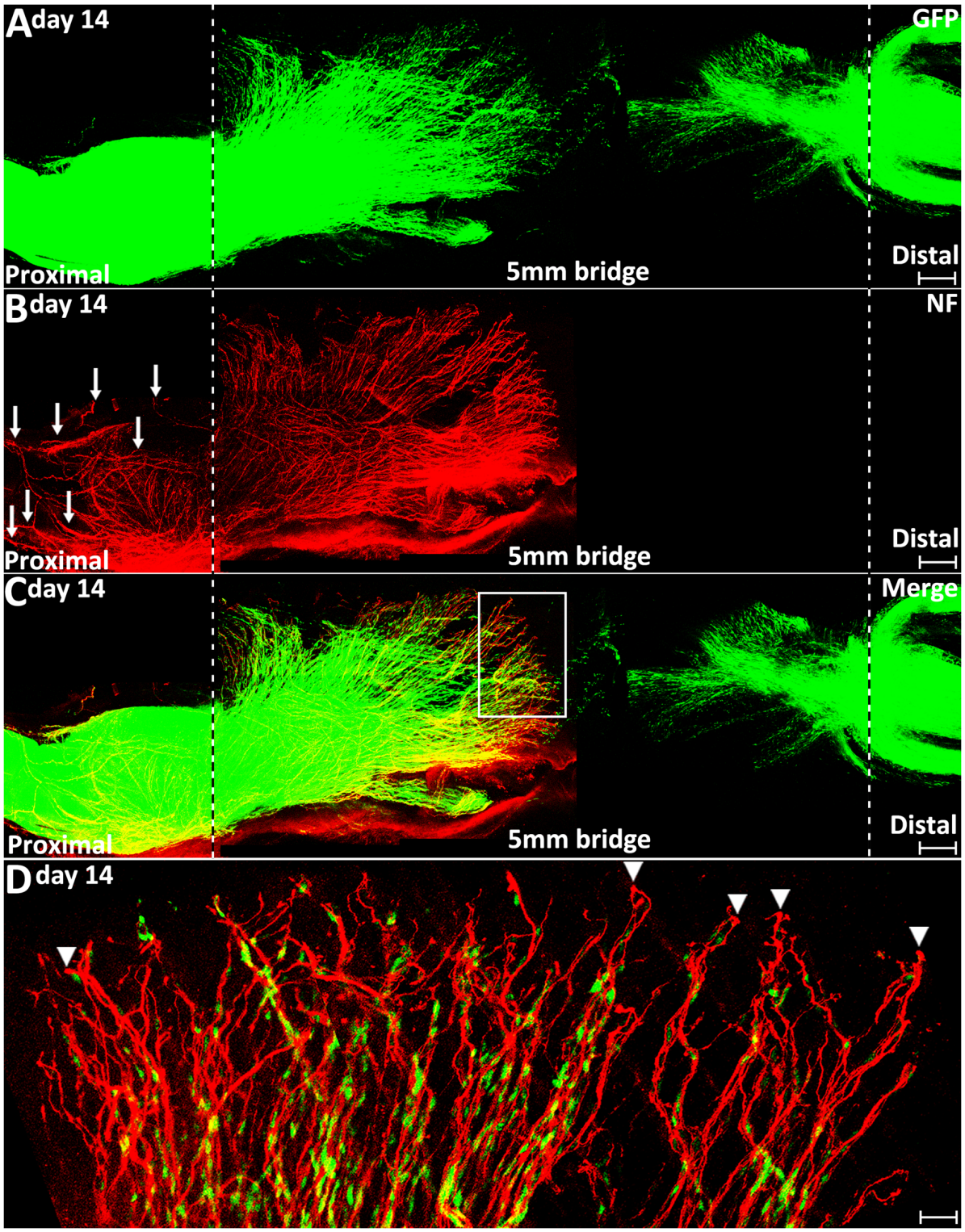

FIGURE 9 | Axon regeneration and Schwann cell migration in a 5 mm sciatic nerve gap on day 14 post-injury. **(A–C)**. Whole nerve preparation at 14 days post-injury shows regenerating axons and migrating Schwann cells in a 5 mm sciatic nerve gap of PLP-GFP mice. The cut ends of both proximal and distal nerve are indicated by dashed lines. Arrows in **(B)** indicate regenerating axons growing along the outside of the proximal nerve stump. **(D)** Higher magnification image from the box area in **(C)** shows regenerating axons proceeding in front of migrating Schwann cells in the proximal nerve end on day 14 post-injury. Arrowheads indicate the ball shape at the tips of regenerating axons. Scale bars in **(A–C)** 250 μm. Scale bar in **(D)** 30 μm.

have also been raised whether Schwann cells act as a leader or a follower during the period of axons navigation across the peripheral nerve gap (Keynes, 1987). Using the film model, Torigoe et al. (1996) analyzed Schwann cell migration on the film after S-100 antibody staining. In their study, Schwann cells start to appear on day 3 near the transected nerve stump and the number of Schwann cells gradually increased on day 4. At this stage, Schwann cells showed a preference for axonal surfaces as a migrating pathway over any other environmental structure (Torigoe et al., 1996). The expression of adhesion molecules on the axonal surface has been suggested as the primary reason that Schwann cells migrate along the regenerating axons (Torigoe et al., 1996). In this study, we also showed that regenerating axons proceed in front of the migrating Schwann cells on day 4 post-injury. There are no Schwann cells associated with the front of regenerating axons and these axons have been previously described by Cajal as "naked axons" (Lobato, 2008). Thus, Torigoe et al.'s (1996) observation together with our finding have provided evidence that axons regenerate randomly when there are no preceding Schwann cells.

In response to peripheral nerve injury, neurons rapidly activate a remarkable intrinsic program to regenerate (Chen et al., 2007; Rishal and Fainzilber, 2010; Jessen and Mirsky, 2016). In mouse, regenerating neurites sprout from the first node of Ranvier proximal to the site of nerve injury just 3 h after axotomy and they pass the tips of the proximal nerve 6 h after axotomy (Torigoe et al., 1996). Following a transection injury, Schwann cells near the injury site of the proximal nerve stump and all Schwann cells in the distal nerve stumps undergo a rapid process of dedifferentiation and proliferation (Jessen and Mirsky, 2016). These processes take 2–3 days to complete before they can migrate, this could be the primary reason that the start of Schwann cell migration is much later than the start of axon extension.

Torigoe et al. (1996) showed in the film model that migrating Schwann cells proceed in front of regenerating axons on day 5 following mouse peroneal nerve transection injury (Torigoe et al., 1996). In this study, we also observed that migrating Schwann cells in the proximal nerve stump start to proceed in front of regenerating axons on day 5. They use regenerating axons as a substrate to migrate before day 5 following mouse sciatic nerve transection injury. Thus, migratory Schwann cells in the proximal nerve stump initially follow the regenerating axons and migrate into the nerve bridge, they are followers of regenerating axons before day 5 of regeneration. From day 5 onwards, migrating Schwann cells locate in the front of regenerating axons and become leaders to direct axon regeneration across the nerve gap.

Migration of Schwann cells into the nerve gap after peripheral nerve transection injury is essential for successful peripheral nerve regeneration. They form Schwann cell cords in the nerve gap to guide axons from the proximal nerve stump into the distal nerve stump. Using the film model, Torigoe et al. (1996) revealed that the speed of axon extension has two phases, an initial slow phase (77 μm/day) when axons are naked followed by a faster phase (283 μm/day) when Schwann cell migrate into the front. The appearance of migrating Schwann cells to the regenerating edge coincides with the onset of the second phase of axon growth, therefore migrating Schwann cells appear to be responsible for the acceleration of axonal growth in the second phase (Torigoe et al., 1996). In our study, we demonstrated that random extension axons grow with both a low speed (85.7 μm/day) combined with a lack of directionality without Schwann cells at the front. Axons increase their speed to 433.1 μm/day when there are migrating Schwann cells acting as substrates for extension. In comparison to the film model, we observed a slightly faster speed of axon regeneration in both phases following injury than Torigoe et al.'s (1996) measurement; one explanation for this faster regeneration rate may be that the nerve bridge is correctly formed in our research model.

The morphology of migrating Schwann cells have been largely studied using *in vitro* culture conditions (Wang et al., 2012). In vitro, Schwann cells have a bipolar shape and often only have one migrating process in the front. Interestingly, we have observed *in vivo* that the pioneer cells often have two or three leading processes during migration, which indicates that these cells seem to be detecting environmental signals suitable for migration. Previous studies have suggested that fibrin deposits are the substrates for Schwann cell migration in the nerve bridge (Williams et al., 1983; Schröder et al., 1993). However, a recent report showed that Schwann cells use newly formed blood vessels as a substrate to migrate upon Cattin et al. (2015). In agreement with Torigoe et al.'s (1996) finding, our observation also showed that migrating Schwann cells in the proximal nerve stump use regenerating axons as a substrate to migrate upon before day 5. These observations showed that Schwann cells may use multiple sources of substrate for migration in the nerve bridge.

In our experiments, we did not remove the epineurium for the whole-mount staining in order to preserve the full pattern of regenerating axons around the nerve bridge area. The epineurium prevents antibody penetration. Therefore, the neurofilament antibody staining will only reveal regenerating axons inside the nerve bridge as well as regenerating axons growing on the outer surface of both nerve stumps (Dun and Parkinson, 2015). Our observations showed that there are two populations of mis-guided regenerating axons growing along the surface of both the proximal and the distal nerve stumps. One population of axons leave the proximal nerve, turn back and then grow back along the outside of the proximal nerve stump, presumably due to the lack of guidance by migrating Schwann cells. We showed by the GFP signal in the PLP-GFP mice that Schwann cells cords in the nerve bridge appear apparently not wide enough for all the regenerating axons that are required to cross the newly formed nerve bridge at this timepoint. Previously, Williams et al. (1983) also showed in a silicone tube nerve conduit apparatus that the nerve bridge has a conical shape and the diameter of the nerve bridge is always narrower than both the nerve ends. This conical bridge shape has also been reported in the studies of peripheral nerve gap repaired with modern biodegradable nerve guidance conduits (Belkas et al., 2004; Moore et al., 2009; Sun et al., 2010). Schwann cell cords are the key component in the nerve

bridge to guide axon regeneration. Thus, our observation in the PLP-GFP mice has identified the most important reason for the misdirection of regenerating axons in the nerve bridge, which is that the area of Schwann cell cords in the nerve bridge is not wide enough to guide all the regenerating axons from the proximal nerve stump across the nerve bridge. We believe that providing enough Schwann cells as a substrate to guide all the regenerating axons cross the nerve gap will be one of the important strategies to improve functional recovery after peripheral nerve injury.

DATA AVAILABILITY STATEMENT

All datasets generated for this study are included in the article.

ETHICS STATEMENT

The animal study was reviewed and approved by Plymouth University Animal Welfare and Ethical Review Board.

AUTHOR CONTRIBUTIONS

XD designed the research. BC, QC and XD performed experiments and analyzed the data. XD and DP wrote the article.

FUNDING

This research was supported by National Natural Science Foundation of China (81371353).

REFERENCES

Belkas, J. S., Shoichet, M. S., and Midha, R. (2004). Peripheral nerve regeneration through guidance tubes. *Neurol. Res.* 26, 151–160. doi: 10.1179/016164104225013798

Carr, M. J., and Johnston, A. P. (2017). Schwann cells as drivers of tissue repair and regeneration. *Curr. Opin. Neurobiol.* 47, 52–57. doi: 10.1016/j.conb.2017.09.003

Carr, L., Parkinson, D. B., and Dun, X. P. (2017). Expression patterns of Slit and Robo family members in adult mouse spinal cord and peripheral nervous system. *PLoS One* 12:e0172736. doi: 10.1371/journal.pone.0172736

Cattin, A. L., Burden, J. J., Van Emmenis, L., Mackenzie, F. E., Hoving, J. J., Garcia Calavia, N., et al. (2015). Macrophage-induced blood vessels guide schwann cell-mediated regeneration of peripheral nerves. *Cell* 162, 1127–1139. doi: 10.1016/j.cell.2015.07.021

Chen, Z. L., Yu, W. M., and Strickland, S. (2007). Peripheral regeneration. *Annu. Rev. Neurosci.* 30, 209–233. doi: 10.1146/annurev.neuro.30.051606.094337

Daly, W., Yao, L., Zeugolis, D., Windebank, A., and Pandit, A. (2012). A biomaterials approach to peripheral nerve regeneration: bridging the peripheral nerve gap and enhancing functional recovery. *J. R. Soc. Interface* 9, 202–221. doi: 10.1098/rsif.2011.0438

Deumens, R., Bozkurt, A., Meek, M. F., Marcus, M. A., Joosten, E. A., Weis, J., et al. (2010). Repairing injured peripheral nerves: bridging the gap. *Prog. Neurobiol.* 92, 245–276. doi: 10.1016/j.pneurobio.2010.10.002

Dun, X. P., Carr, L., Woodley, P. K., Barry, R. W., Drake, L. K., Mindos, T., et al. (2019). Macrophage-derived slit3 controls cell migration and axon pathfinding in the peripheral nerve bridge. *Cell Rep.* 26, 1458.e4–1472.e4. doi: 10.1016/j.celrep.2018.12.081

Dun, X. P., and Parkinson, D. B. (2015). Visualizing peripheral nerve regeneration by whole mount staining. *PLoS One* 10:e0119168. doi: 10.1371/journal.pone.0119168

Dun, X. P., and Parkinson, D. B. (2018). Transection and crush models of nerve injury to measure repair and remyelination in peripheral nerve. *Methods Mol. Biol.* 1791, 251–262. doi: 10.1007/978-1-4939-7862-5_20

Hall, S. M. (1986). The effect of inhibiting Schwann cell mitosis on the re-innervation of acellular autografts in the peripheral nervous system of the mouse. *Neuropathol. Appl. Neurobiol.* 12, 401–414. doi: 10.1111/j.1365-2990.1986.tb00151.x

Hayashi, A., Koob, J. W., Liu, D. Z., Tong, A. Y., Hunter, D. A., Parsadanian, A., et al. (2007). A double-transgenic mouse used to track migrating Schwann cells and regenerating axons following engraftment of injured nerves. *Exp. Neurol.* 207, 128–138. doi: 10.1016/j.expneurol.2007.06.004

Hirrlinger, P. G., Scheller, A., Braun, C., Quintela-Schneider, M., Fuss, B., Hirrlinger, J., et al. (2005). Expression of reef coral fluorescent proteins in the central nervous system of transgenic mice. *Mol. Cell. Neurosci.* 30, 291–303. doi: 10.1016/j.mcn.2005.08.011

Jessen, K. R., and Mirsky, R. (2016). The repair Schwann cell and its function in regenerating nerves. *J. Physiol.* 594, 3521–3531. doi: 10.1113/jp270874

Johnston, A. P., Yuzwa, S. A., Carr, M. J., Mahmud, N., Storer, M. A., Krause, M. P., et al. (2016). Dedifferentiated schwann cell precursors secreting paracrine factors are required for regeneration of the mammalian digit tip. *Cell Stem Cell* 19, 433–448. doi: 10.1016/j.stem.2016.06.002

Keynes, R. J. (1987). Schwann-cells during neural development and regeneration: leaders or followers. *Front. Psychol.* 10, 137–141. doi: 10.1016/0166-2236(87)90037-3

Lobato, R. D. (2008). Historical vignette of Cajal's work "Degeneration and regeneration of the nervous system" with a reflection of the author. *Neurocirugia* 19, 456–468. doi: 10.1016/s1130-1473(08)70215-x

Lopez-Verrilli, M. A., Picou, F., and Court, F. A. (2013). Schwann cell-derived exosomes enhance axonal regeneration in the peripheral nervous system. *Glia* 61, 1795–1806. doi: 10.1002/glia.22558

Mallon, B. S., Shick, H. E., Kidd, G. J., and Macklin, W. B. (2002). Proteolipid promoter activity distinguishes two populations of NG2-positive cells throughout neonatal cortical development. *J. Neurosci.* 22, 876–885. doi: 10.1523/JNEUROSCI.22-03-00876.2002

Moore, A. M., Kasukurthi, R., Magill, C. K., Farhadi, H. F., Borschel, G. H., and Mackinnon, S. E. (2009). Limitations of conduits in peripheral nerve repairs. *Hand* 4, 180–186. doi: 10.1007/s11552-008-9158-3

Parfejevs, V., Debbache, J., Shakhova, O., Schaefer, S. M., Glausch, M., Wegner, M., et al. (2018). Injury-activated glial cells promote wound healing of the adult skin in mice. *Nat. Commun.* 9:236. doi: 10.1038/s41467-017-01488-2

Parrinello, S., Napoli, I., Ribeiro, S., Wingfield Digby, P., Fedorova, M., Parkinson, D. B., et al. (2010). EphB signaling directs peripheral nerve regeneration through Sox2-dependent Schwann cell sorting. *Cell* 143, 145–155. doi: 10.1016/j.cell.2010.08.039

Ray, W. Z., and Mackinnon, S. E. (2010). Management of nerve gaps: autografts, allografts, nerve transfers, and end-to-side neurorrhaphy. *Exp. Neurol.* 223, 77–85. doi: 10.1016/j.expneurol.2009.03.031

Rishal, I., and Fainzilber, M. (2010). Retrograde signaling in axonal regeneration. *Exp. Neurol.* 223, 5–10. doi: 10.1016/j.expneurol.2009.08.010

Rosenberg, A. F., Isaacman-Beck, J., Franzini-Armstrong, C., and Granato, M. (2014). Schwann cells and deleted in colorectal carcinoma direct regenerating motor axons towards their original path. *J. Neurosci.* 34, 14668–14681. doi: 10.1523/JNEUROSCI.2007-14.2014

Schröder, J. M., May, R., and Weis, J. (1993). Perineurial cells are the first to traverse gaps of peripheral nerves in silicone tubes. *Clin. Neurol. Neurosurg.* 95, S78–S83. doi: 10.1016/0303-8467(93)90040-n

Stierli, S., Napoli, I., White, I. J., Cattin, A. L., Monteza Cabrejos, A., Garcia Calavia, N., et al. (2018). The regulation of the homeostasis and regeneration of peripheral nerve is distinct from the CNS and independent of a stem cell population. *Development* 145:dev170316. doi: 10.1242/dev.170316

Sun, M., Kingham, P. J., Reid, A. J., Armstrong, S. J., Terenghi, G., and Downes, S. (2010). *In vitro* and *in vivo* testing of novel ultrathin PCL and PCL/PLA blend

films as peripheral nerve conduit. *J. Biomed. Mater. Res. A* 93, 1470–1481. doi: 10.1002/jbm.a.32681

Tomita, K., Hata, Y., Kubo, T., Fujiwara, T., Yano, K., and Hosokawa, K. (2009). Effects of the *in vivo* predegenerated nerve graft on early Schwann cell migration: quantitative analysis using S100-GFP mice. *Neurosci. Lett.* 461, 36–40. doi: 10.1016/j.neulet.2009.05.075

Torigoe, K., Tanaka, H. F., Takahashi, A., Awaya, A., and Hashimoto, K. (1996). Basic behavior of migratory Schwann cells in peripheral nerve regeneration. *Exp. Neurol.* 137, 301–308. doi: 10.1006/exnr.1996.0030

Wang, Y., Teng, H. L., and Huang, Z. H. (2012). Intrinsic migratory properties of cultured Schwann cells based on single-cell migration assay. *PLoS One* 7:e51824. doi: 10.1371/journal.pone.0051824

Webber, C. A., Christie, K. J., Cheng, C., Martinez, J. A., Singh, B., Singh, V., et al. (2011). Schwann cells direct peripheral nerve regeneration through the Netrin-1 receptors, DCC and Unc5H2. *Glia* 59, 1503–1517. doi: 10.1002/glia.21194

Whitlock, E. L., Myckatyn, T. M., Tong, A. Y., Yee, A., Yan, Y., Magill, C. K., et al. (2010). Dynamic quantification of host Schwann cell migration into peripheral nerve allografts. *Exp. Neurol.* 225, 310–319. doi: 10.1016/j.expneurol.2010.07.001

Williams, L. R., Longo, F. M., Powell, H. C., Lundborg, G., and Varon, S. (1983). Spatial-temporal progress ofperipheral nerve regeneration within a silicone chamber: parameters for a bioassay. *J. Comp. Neurol.* 218, 460–470. doi: 10.1002/cne.902180409

Zigmond, R. E., and Echevarria, F. D. (2019). Macrophage biology in the peripheral nervous system after injury. *Prog. Neurobiol.* 173, 102–121. doi: 10.1016/j.pneurobio.2018.12.001

Zuo, Y., Lubischer, J. L., Kang, H., Tian, L., Mikesh, M., Marks, A., et al. (2004). Fluorescent proteins expressed in mouse transgenic lines mark subsets of glia, neurons, macrophages, and dendritic cells for vital examination. *J. Neurosci.* 24, 10999–11009. doi: 10.1523/JNEUROSCI.3934-04.2004

Conflict of Interest: The authors declare that the research was conducted in the absence of any commercial or financial relationships that could be construed as a potential conflict of interest.

frontiers in Molecular Neuroscience

ORIGINAL RESEARCH
published: 12 February 2020
doi: 10.3389/fnmol.2020.00017

Reduction of Silent Information Regulator 1 Activates Interleukin-33/ST2 Signaling and Contributes to Neuropathic Pain Induced by Spared Nerve Injury in Rats

Yanyan Zeng[1†], Yu Shi[1†], Hongrui Zhan[1,2], Wei Liu[1], Guiyuan Cai[1], Haili Zhong[1], Yaping Wang[1], Shangjie Chen[3], Shimin Huang[1] and Wen Wu[1]**

[1]Department of Rehabilitation, Zhujiang Hospital, Southern Medical University, Guangzhou, China, [2]Department of Rehabilitation, The Fifth Affiliated Hospital of Sun Yat-sen University, Zhuhai, China, [3]Department of Rehabilitation, Baoan Hospital, Southern Medical University, Shenzhen, China

OPEN ACCESS

Edited by:
John Martin, City College of New York (CUNY), United States

Reviewed by:
Vicente Barrios, Niño Jesús University Children's Hospital, Spain
Sun Kwang Kim, Kyung Hee University, South Korea

***Correspondence:**
Wen Wu
wuwen66@163.com
Shangjie Chen
csjme@163.com

[†]These authors have contributed equally to this work and share first authorship

Received: *24 September 2019*
Accepted: *20 January 2020*
Published: *12 February 2020*

Citation:
Zeng Y, Shi Y, Zhan H, Liu W, Cai G, Zhong H, Wang Y, Chen S, Huang S and Wu W (2020) Reduction of Silent Information Regulator 1 Activates Interleukin-33/ST2 Signaling and Contributes to Neuropathic Pain Induced by Spared Nerve Injury in Rats. Front. Mol. Neurosci. 13:17. doi: 10.3389/fnmol.2020.00017

Emerging studies have demonstrated that interleukin (IL)-33 and its receptor ST2 act as key factors in inflammatory diseases. Moreover, accumulating evidence has suggested that cytokines, including tumor necrosis factor (TNF)-α and IL-1β, trigger an inflammatory cascade. SIRT1 has been shown to suppress the expression of inflammatory cytokines. However, the effects of SIRT1 on IL-33/ST2 signaling and initiation of the inflammatory cascade *via* modulation of TNF-α and IL-1β by IL-33 remain unclear. In the present study, we found that the dorsal root ganglion (DRG) IL-33 and ST2 were upregulated in a rat model of spared nerve injury (SNI) and intrathecal injection of either IL-33 or ST2 antibodies alleviated mechanical allodynia and downregulated TNF-α and IL-1β induced by SNI. In addition, activation of SIRT1 decreased enhanced DRG IL-33/ST2 signaling in SNI rats. Artificial inactivation of SIRT1 *via* intrathecal injection of an SIRT1 antagonist could induce mechanical allodynia and upregulate IL-33 and ST2. These results demonstrated that reduction in SIRT1 could induce upregulation of DRG IL-33 and ST2 and contribute to mechanical allodynia induced by SNI in rats.

Keywords: neuropathic pain, IL-33, ST2, SIRT1, inflammation

INTRODUCTION

Chronic pain, often characterized by allodynia, hyperalgesia, and spontaneous pain affects approximately one-third of the world's population (Alford et al., 2008). In the United States, direct and indirect costs of chronic pain have been estimated to be approximately $100 billion annually, which is more than the combined costs of cancer, heart disease, and diabetes (Pizzo and Clark, 2012). It is well established that peripheral and central sensitizations are the basic mechanisms of chronic pain (Meacham et al., 2017). Inflammation has been extensively reported to be associated with peripheral and central sensitization (Ji et al., 2018).

However, the type of inflammatory cytokine that triggers the inflammation cascade remains controversial.

Interleukin (IL)-33 belongs to a member of the IL-1 family and exerts its effects *via* binding to its receptor ST2 (Xu et al., 2019). It has been demonstrated that IL-33 plays a vital role in many inflammatory conditions, including septic shock (Ding et al., 2019), atherosclerosis (Buckley et al., 2019) and rheumatoid arthritis (Pinto et al., 2019). Furthermore, other studies have suggested that IL-33 modulates cutaneous hyper-nociception in inflammatory pain in mice (Verri et al., 2008) and has been implicated in activating astrocytes in the spinal cord in mouse models of bone pain (Zhao et al., 2013). However, the role of IL-33 in the dorsal root ganglion (DRG) in neuropathic pain remains unclear.

The silent information regulator 1 (SIRT1) is an NAD^+-dependent deacetylase belonging to the SIRT family (Hattori and Ihara, 2016). Among SIRT family, SIRT1 has been validated to be most related in this family and function as deacetylating and regulating histones (Ling et al., 2018) as well as a wide range of non-histone substrates, such as NF-κB (Kauppinen et al., 2013), p53 (Nakamura et al., 2017), FOXO (Brunet et al., 2004), ERK (Han et al., 2017), peroxisome proliferator-activated receptor γ (PPARγ) and others (Kauppinen et al., 2013). With regulating this protein, SIRT1 plays a central role in regulating cellular processes, including apoptosis (Ling et al., 2017), cellular proliferation (Jablonska et al., 2016), and inflammation (Zhang et al., 2017). In the nervous system, SIRT1 suppress the neurodegenerative diseases such as Alzheimer's disease and Parkinson's disease *via* anti-apoptosis, anti-inflammation (Singh et al., 2017; Gomes et al., 2018). Recently, several studies have reported that the activation of SIRT1 in the spinal cord alleviates neuropathic pain induced by chronic constriction injury (CCI) surgery in rats and mice *via* inhibition of the inflammatory cascade (Shao et al., 2014; Lv et al., 2015). In addition, SIRT1 in the spinal cord epigenetically upregulates inflammasome NALP1 expression and contributes to the chronic pain induced by the chemotherapeutic drug bortezomib (Chen et al., 2018). However, whether SIRT1 modulates the inflammatory cytokine IL-33 remains unclear.

In the present study, we performed spared nerve injury (SNI) surgery in rats to establish a neuropathic pain model and hypothesized that downregulation of SIRT1 in the DRG induced by SNI enhances IL-33/ST2 signaling and triggers a downstream inflammatory cascade leading to mechanical allodynia.

MATERIALS AND METHODS

Animals

Male Sprague-Dawley rats, weighing 200–250 g, were obtained from the Institute of Experimental Animals of Southern Medical University (Guangzhou, China; Approval number: SCXK 2016-0041). The animals were housed in standard cages in a temperature-controlled (24 ± 1°C) colony room under a 12 h light/dark cycle regimen, with *ad libitum* access to food and water. The experimental protocols were approved by the Southern Medical University Animal Care and Use Committee and were performed in accordance with the National Institutes of Health Guide for the Care and Use of Laboratory Animals.

Surgery and Drug Administration

SNI model rats were developed in accordance with previously described procedures (Decosterd and Woolf, 2000). Briefly, after making an incision on the skin at the lateral surface of the thigh, a section was made directly through the biceps femoris muscle to expose the sciatic nerve and its three terminal branches, the sural, common peroneal, and tibial nerves. The SNI procedure involves axotomy and ligation of the tibial and common peroneal nerves but leaves the sural nerve intact. The common peroneal and tibial nerves were tightly ligated using 5.0 silk and transected distal to the ligation, removing approximately 4 mm of the distal nerve stump. Care was taken to avoid any damage to the nearby sural nerve. After surgery, all wounds were irrigated with sterile saline and closed in layers. In the sham group, an identical procedure was performed to expose the sciatic nerve and its three terminal branches, but without any nerve injury. For intrathecal delivery of the SIRT1 agonist SRT1720, the animals were implanted with catheters during the same surgery, as previously reported (Hirai et al., 2014). Briefly, a sterile catheter filled with saline was inserted through the lumbar (L) 5/6 intervertebral space, and the tip of the tube was positioned at the lumbosacral spinal level. Animals that exhibited hind limb paralysis or paresis after surgery were excluded. For animals without movement disorders, lidocaine (2%) was administered through the catheter to verify the intraspinal location. An immediate bilateral hind limb paralysis (within 15 s) lasting 20–30 min confirmed the correct catheterization. Animals without the aforementioned features were not used in the experiments that followed. The SIRT1 agonist SRT1720 and antagonist EX-527 were dissolved in DMSO and intrathecal administration at concentration of 15 mg/kg and 10 mg/kg respectively. IL-33 (rIL-33; 3626-ML) and ST2- neutralizing antibody (AF1004) were purchased from R&D Systems (Minneapolis, MN, USA). The rIL-33 and ST2 antibodies were diluted in sterile phosphate buffer solution (PBS).

Behavioral Test

Mechanical sensitivity was assessed using von Frey hairs and the up-down method, as previously described (Chaplan et al., 1994). Briefly, after acclimatization to the testing environment for 2 h per day on three consecutive days, the rats were placed in separate transparent testing chambers positioned on a wire mesh floor. After a 10-min adaptation period, each stimulus consisted of a 2–3 s application of von Frey hairs to the middle of the plantar surface of the hind paws and the lateral surface of ipsilateral hind paws for SNI rats, with a 5-min interval between consecutive tests. Quick withdrawal or licking of the paw in response to the stimulus was considered a positive response. The operator performing the behavioral tests was blinded to the study design.

Immunohistochemistry

The animals were deeply anesthetized using 50 mg/kg sodium pentobarbital (intraperitoneal) and perfused through the ascending aorta with saline, followed by 4% paraformaldehyde

in 0.1 M phosphate buffer (4°C, pH 7.4), as previously described. After perfusion, the L4, L5, and L6 DRGs were removed and post-fixed in the same fixative for 3 h, which was subsequently replaced with 30% sucrose (in 0.1 M PBS) overnight. Frozen tissues were sectioned in the longitudinal plane with a thickness of 16 mm using a microtome and processed for immunofluorescence staining. All sections were blocked with 3% donkey serum in 0.3% Triton X-100 for 1 h at room temperature and incubated over two nights at 4°C with primary antibodies. After incubation with primary antibodies, the tissue sections were washed three times in 0.01 M PBS and then incubated in Cy3-conjugated donkey anti-rabbit IgG (diluted 1:300; Jackson ImmunoResearch, West Grove, PA, USA) for 1 h at room temperature. For double immunofluorescence staining, tissue sections were incubated with a mixture of anti-SIRT1 [1:200, Cell Signaling Technologies (CST), Danvers, MA, USA] antibody with neurofilament-200 [NF-200 (a marker for myelinated A-fibers), 1:200; Chemicon/Thermo-Fisher Scientific, Waltham, MA, USA], IB4 [FITC-conjugated (a marker for nonpeptidergic C-type neurons), 20 mg/ml (Sigma)], anti-calcitonin gene-related peptide [CGRP (a marker of peptidergic C-type neurons), 1:500, Abcam, Cambridge, MA, USA], IL-33 (1:300, Abcam, Cambridge, MA, USA), ST2 (1:400, Abcam, Cambridge, MA, USA) over two nights at 4°C. Except for isolectin-B4 (IB4)-treated tissue sections, all of the aforementioned sections were treated with a mixture of FITC and Cy3-conjugated secondary antibodies for 1 h at room temperature. The sections were rinsed with 0.01 M PBS three times and mounted on gelatin-coated slides and air-dried. The stained sections were examined using a fluorescence microscope (Leica, Wetzlar, Germany) and images were captured using a charge-coupled device spot camera.

Western Blotting

Western blotting was performed according to the method described in a previous study (Hnasko and Hnasko, 2015). Briefly, L4–L6 DRG tissues of animals were removed and homogenized in 15 mmol/L Tris containing a cocktail of proteinase inhibitors after the animals were anesthetized with 50 mg/kg sodium pentobarbital (intraperitoneal). Next, the L4–L6 DRG lysates were prepared and separated using sodium dodecyl polyacrylamide gel electrophoresis and transferred to a polyvinylidene fluoride membrane. The membranes were then pre-incubated with blocking buffer for 1 h at room temperature. After incubating with diluted primary antibodies against SIRT1 (1:1,000, CST), IL-33 (1:1,000, Abcam), ST2

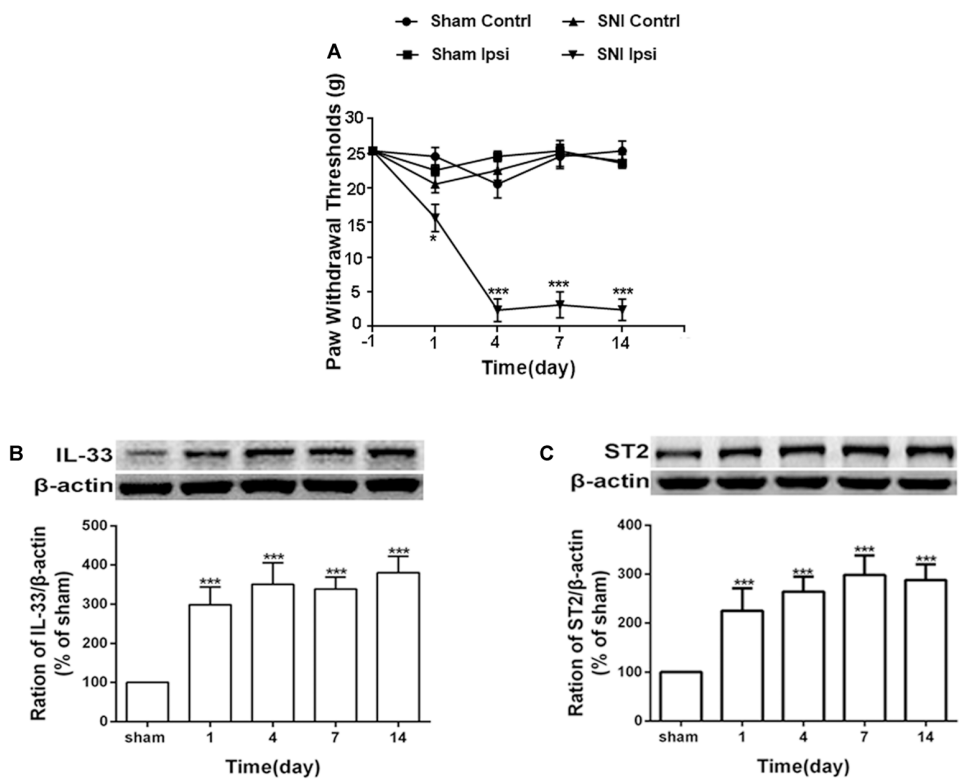

FIGURE 1 | Spared nerve injury (SNI) induced mechanical allodynia and enhanced expression of interleukin (IL)-33 and ST2 in dorsal root ganglion (DRG) of rats. **(A)** SNI induced mechanical allodynia in the ipsilateral but not contralateral hind paw ($n = 6$), but the sham operation did not induce changes in bilateral hind paw($n = 6$). **(B,C)** Compared with the sham rats, expression of IL-33 and its receptor ST2 increased in L4-L6 DRG since day 1 and persisted till day 14 after SNI ($n = 4$). $^{*}p < 0.05$, $^{***}p < 0.001$ compared with the sham group.

(1:1,000, Abcam), tumor necrosis factor (TNF)-α (1:1,000, Abcam), and/or β-actin (1:2,000, Abcam) overnight at 4°C, the membranes were incubated in horseradish peroxidase-conjugated secondary antibody for 1 h at room temperature. Finally, protein bands on the membranes were visualized using a commercially available enhanced chemiluminescence assay (Pierce, USA) according to the manufacturer's instructions. The bands were subsequently quantified using a computer-assisted imaging analysis system.

Statistical Analysis

All data are expressed as mean ± standard error of the mean (SEM). Statistical analysis was performed using SPSS version 20.0 (IBM Corporation, Armonk, NY, USA). For the behavior test, one- or two-way analysis of variance (ANOVA) with repeated measures, followed by a Tukey *post hoc* test, was performed. Western blot was analyzed using one-way ANOVA followed by the Turkey *post hoc* test. Differences with p 0.05 were considered statistically significant.

RESULTS

IL-33 and Its Receptor ST2 in DRG Were Induced and Upregulated by SNI in Rats

Consistent with the results of a previous study (Boccella et al., 2018), the mechanical withdrawal threshold was significantly reduced in SNI rats (**Figure 1A**). To further study the role of IL-

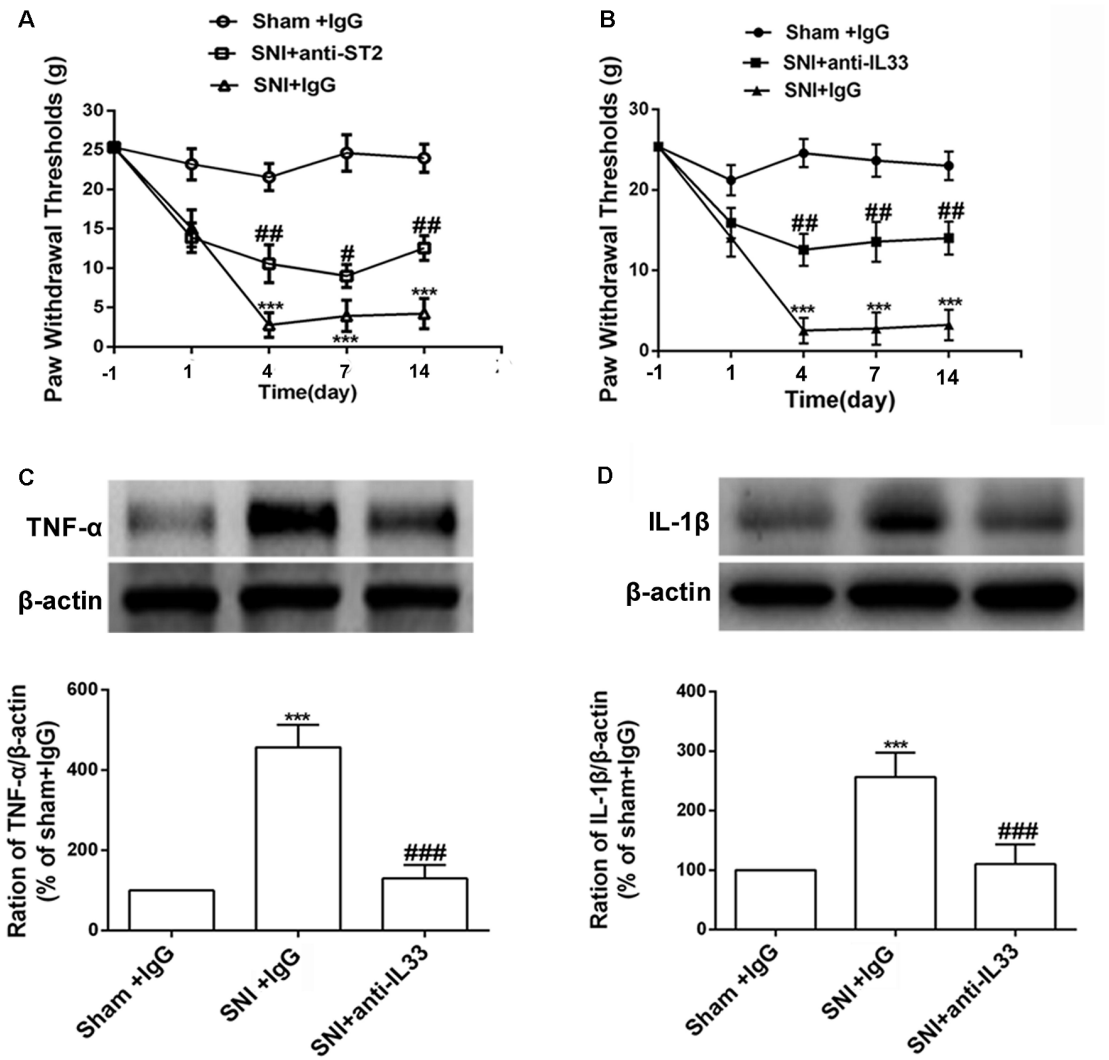

FIGURE 2 | Intrathecal injection both IL-33 and its receptor ST2 neutralization antibody ameliorated mechanical allodynia and reversed the increased expression of tumor necrosis factor (TNF)-α and IL-1β. **(A,B)** Intrathecal application of IL-33 or ST2 neutralization antibody alleviated SNI-induced mechanical allodynia but IgG treatment did not show effects on mechanical allodynia induced by SNI. The dose of IL-33 or ST2 neutralization antibody was 100 ng for consecutive 10 days and 250 ng for consecutive 10 days, respectively. The time point for intrathecal injection was 15 min before SNI surgery, n = 6/group. **(C,D)** Upregulation of TNF-α and IL-1β was blocked after intrathecal injection of IL-33 neutralization antibody on day 7 (n = 4/group). $^{***}p < 0.001$ compared with sham group, $^{\#}p < 0.05$, $^{\#\#}p < 0.01$, $^{\#\#\#}p < 0.001$ compared with SNI+IgG group.

33/ST2 signaling in neuropathic pain induced by SNI, western blot assay was performed to analyze protein expression of IL-33 and ST2. As shown in **Figures 1B,C**, IL-33, and ST2 in DRG (L4-L6) was markedly increased on day 1 following SNI surgery and lasted at least until day 14.

Enhanced IL-33 and ST2 Expression Contributed to Mechanical Allodynia Induced by SNI

We determined whether the increased expression of IL-33 and ST2 was involved in the development of mechanical allodynia in SNI rats. We investigated the behavior response after intrathecally injecting IL-33 and ST2 neutralizing antibodies. The results revealed that both IL-33 and ST2 neutralizing antibodies alleviated mechanical allodynia induced by SNI surgery for seven consecutive days (**Figures 2A,B**). Studies have reported that TNF-α and IL-1β activate the inflammatory cascade (Cavaillon et al., 2003; Iwawaki, 2017) and that IL-33 may also play an important role in it. To determine the role of IL-33 in the inflammation, we used the western blot assay to quantify the expression of TNF-α and IL-1β after intrathecal administration of IL-33 antibodies. The results revealed that both TNF-α and IL-1β levels were significantly decreased in the DRG (**Figure 2**).

Reduction of SIRT1 Is Involved in the Mechanical Allodynia Induced by SNI

SIRT1 plays an important role in synaptic plasticity and chronic pain. The levels of SIRT1 protein in the DRG started to decrease on day 1 following SNI surgery, which lasted until at least day 14 (**Figure 3B**). Meanwhile, behavior testing demonstrated that intrathecal administration of the SIRT1 agonist SRT1720 remarkably decreased the paw withdraw thresholds induced by SNI in rats (**Figure 3A**).

SIRT1 Is Expressed in DRG Neurons

It has been reported that SIRT1 is only expressed in neurons in the spinal cord; however, the distribution of SIRT1 in DRG remains unclear. To further verify the distribution of SIRT1 in the DRG of rats, double immunofluorescent staining was performed. As shown in **Figure 4**, SIRT1 was primarily expressed in NF200-positive cells (large-diameter neurons), IB4-positive cells, and CGRP-positive cells (small- and medium-diameter neurons).

Activation of SIRT1 Downregulated IL-33/ST2, TNF-α, and IL-1β

Several recent studies have presented evidence that SIRT1 mediates chronic pain through modulation of inflammation in the spinal cord. Thus, we determined whether SIRT1 regulated the DRG IL-33/ST2 signaling in rats with SNI-induced neuropathic pain. The double immunofluorescence staining showed that SIRT1 colocalized with IL-33 and ST2 (**Supplementary Figure S1**). As shown in **Figures 5A,B**, DRG IL-33 and its receptor ST2 were remarkably downregulated on day 7 following intrathecal injection of the SIRT1 agonist SRT1720. Similarly, the expression of the inflammatory cytokines TNF-α and IL-1β was reduced on day 7 after the injection of SRT1720 (**Figures 5C,D**). Furthermore, the enhanced acetylation of NF-κB was significantly alleviated by SRT1720 but have no effects on *p*-ERK (**Supplementary Figure S2**).

SIRT1 Antagonist EX527 Induced Mechanical Allodynia in Naïve Rats

To further define the effects of SIRT1 in DRG on pain behavior, the rats were intrathecally administered the SIRT1 antagonist EX-527 at a dose of 10 mg/kg for five consecutive days. A mechanical allodynia behavior test using von Frey filaments demonstrated that the paw withdrawal threshold was decreased in naïve rats from day 2 and lasted until day 8 after EX-527 treatment. However, the naïve rats that were administered saline

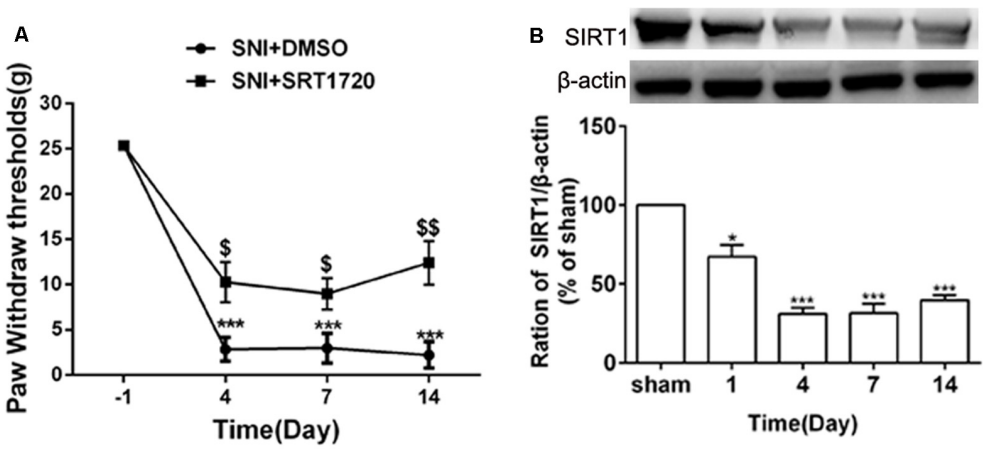

FIGURE 3 | SNI reduced expression of DRG SIRT1 and intrathecal administration of SIRT1 agonist alleviated SNI-induced mechanical allodynia. **(A)** Intrathecal injection of SIRT1 agonist (15 mg/kg) 15 min before SNI surgery for consecutive 10 days alleviated the mechanical allodynia. **(B)** The time courses of the changes in the expression of SIRT1 after SNI surgery. $^{*}p < 0.05$, $^{***}p < 0.001$ compared with sham group, $^{\$}p < 0.05$, $^{\$\$}p < 0.01$ compared with SNI+DMSO group.

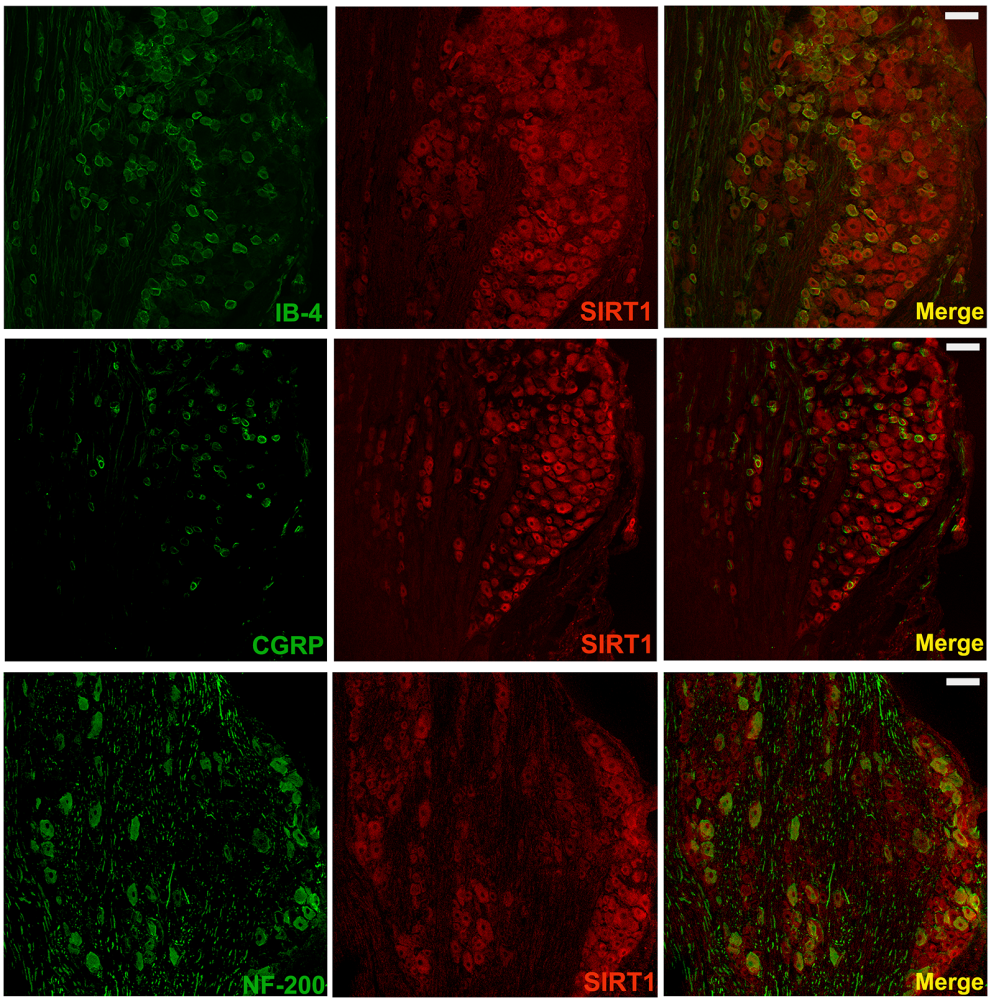

FIGURE 4 | SIRT1 in DRG mainly expressed in neurons of rats. Double immunofluorescence staining showed that SIRT1 expressed in peptidergic neurons (CGRP marked) and non-peptidergic (IB-4 and NF-200 marked) neurons in DRG. Scale bar 200 μm.

exhibited no significant mechanical allodynia compared with naïve rats. Therefore, the EX-527 treatment in naïve rats induced mechanical allodynia (**Figure 6**).

Inactivation of SIRT1 Can Enhance the Expression of IL-33 and ST2 in Naïve Rats

Having observed that the SIRT1 antagonist contributed to mechanical allodynia in naïve rats, we tested whether the inactivation of SIRT1 modulated the expression of IL-33 and ST2. The results of the western blot analysis demonstrated that both IL-33 and ST2 proteins were upregulated on day 5 after intrathecal administration of EX-527 compared with saline treatment in naïve rats (**Figures 7A,B**).

DISCUSSION

In the present study, we found that the expression of IL-33 and its receptor ST2 in DRG increased after SNI surgery. Intrathecal administration of both IL-33 and ST2 antibodies alleviated mechanical allodynia induced by SNI. Intrathecal injection of IL-33 antibody and rat recombinant IL-33 decreased the enhanced expression of TNF-α and IL-β in SNI rats and induced the expression of TNF-α and IL-β in naïve rats, respectively. In addition, SNI surgery reduced the expression of SIRT1 in DRG neurons, and intrathecal injection of the SIRT1 agonist SRT1720 ameliorated mechanical allodynia and reversed the upregulation of IL-33 induced by SNI. Collectively, our results revealed a new mechanism in which reduction of SIRT1 activates IL-33/ST2 signaling and subsequently triggers the TNF-α and IL-1β inflammatory cascade, thus contributing to the mechanical allodynia induced by SNI.

The Role of IL-33 in Triggering Inflammatory Cascade in Neuropathic Pain Following SNI

IL-33 is a cytokine in human endothelial cells that was discovered in 2003 (Baekkevold et al., 2003), it exerts its biological

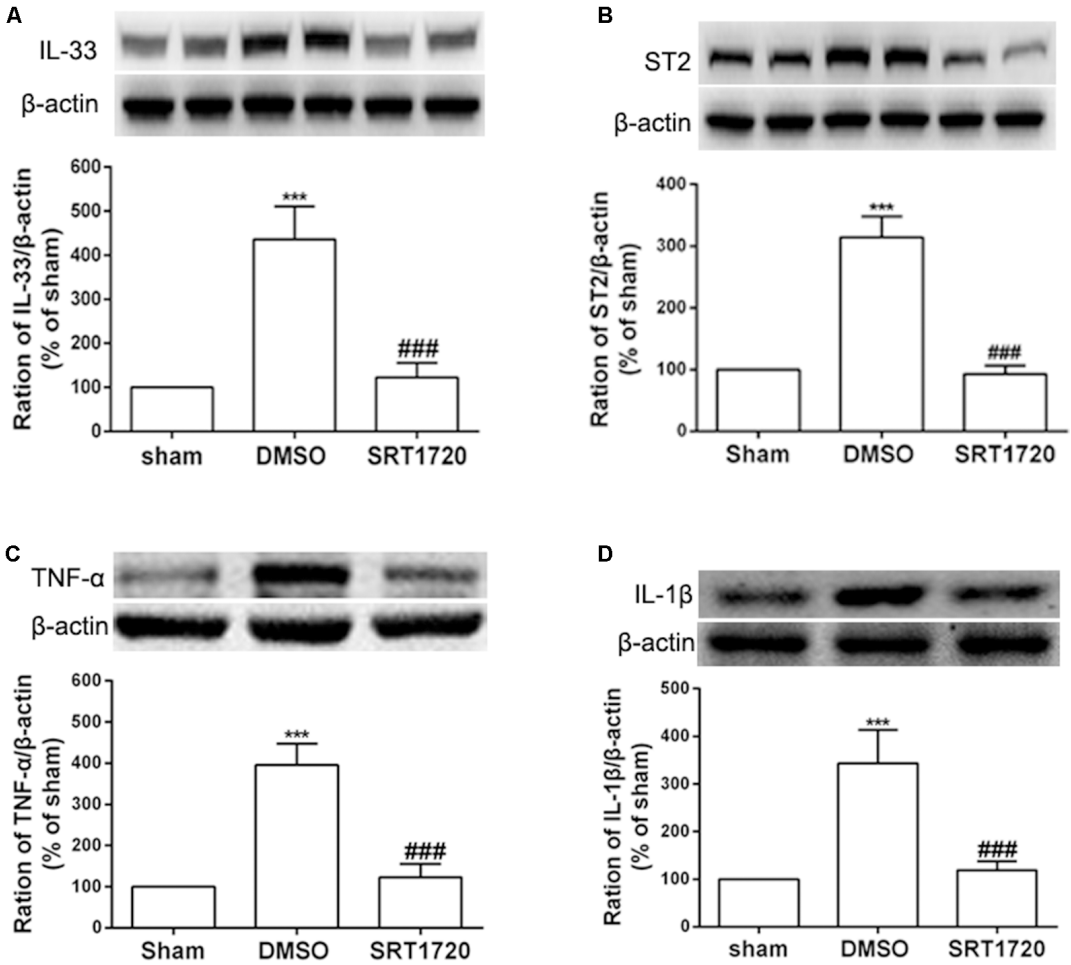

FIGURE 5 | The increased expression of IL-33, ST2, TNF-α, and IL-1β were retarded by intrathecal injection of SIRT1 agonist SRT1720. **(A,B)** Application of SRT1720(i.t.) reduced the expression of IL-33 and its receptor ST2 after SNI surgery on day 7. **(C,D)** Inflammatory cytokines TNF-α and IL-1β were significantly downregulated by delivery of SRT1720(i.t.) on day 7, $n = 4$/group, $^{***}p < 0.001$ compared with the sham group, $^{###}p < 0.001$ compared with SNI+DMSO group.

effects through the ST2/IL-1RAcP (IL-1 receptor accessory protein) receptor complex. Recent evidence has shown that IL-33 deficiency results in reduced innate papain-induced lung inflammation (Oboki et al., 2010). More recent studies have suggested that IL-33/ST2 contributes to the development of pain. For example, the expression of spinal IL-33 and ST2 was enhanced in mice with formalin-induced inflammatory pain (Zarpelon et al., 2013). Furthermore, activation of spinal IL-33 and ST2 has been reported to contribute to bone cancer pain (Zhao et al., 2013). In this study, we first found that the expression of DRG IL-33 and ST2 increased in a rat model of neuropathic pain induced by SNI. Intrathecal administration of IL-33 and ST2 antibodies alleviated mechanical allodynia. It has been firmly established that inflammatory cytokines are involved in the development and maintenance of neuropathic pain (Old et al., 2015; Ronchetti et al., 2017). Both TNF-α and IL-β have been reported to be cytokines that trigger the inflammatory cascade (Rider et al., 2011; Zelová and Hošek, 2013). In our study, we found that intrathecal administration of IL-33 and ST2 antibodies in SNI-treated rats could reduce the enhanced expression of TNF-α and IL-β. These results demonstrated that SNI could activate the IL-33/ST2 signaling pathway in DRG, subsequently trigger the inflammatory cascade, and contribute to the mechanism of allodynia.

SIRT1 in DRG Contributes to the Activation of IL-33/ST2 Signaling Following SNI

Accumulating evidence has demonstrated that SIRT1 modulates the expression of inflammatory cytokines *via* targeting nuclear factor (NF)-κB (Yeung et al., 2004; Kauppinen et al., 2013). A recent study revealed that SRT1720 ameliorated chronic pain induced by chronic CCI through the regulation of spinal cord inflammation (Lv et al., 2015). Similarly, we found that intrathecal injection of the SIRT1 agonist SRT1720 suppressed the upregulation of TNF-α and IL-1β in the DRG and alleviated mechanical allodynia in SNI-treated rats. We also observed that the reduction of SIRT1 in DRG neurons contributed to the activation of the IL-33/ST2 signaling pathway.

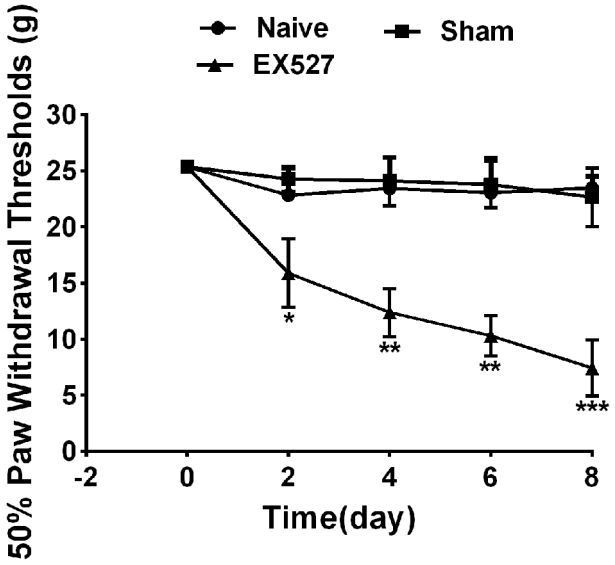

FIGURE 6 | Continuous intrathecal injection of SIRT1 agonist EX527 at a dose of 10 mg/kg for successive 5 days induced mechanical allodynia in naïve rats. n = 6/group, $^{*}p < 0.05$, $^{**}p < 0.01$,$^{***}p < 0.001$ compared with sham group.

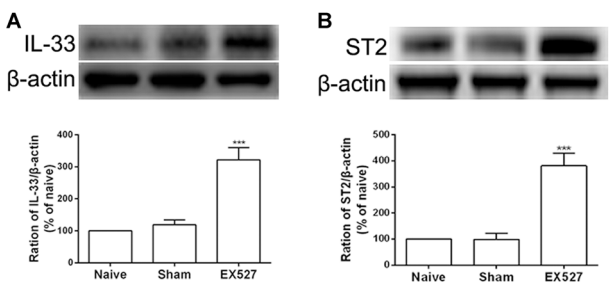

FIGURE 7 | Continuous intrathecal injection of SIRT1 antagonist EX-527 upregulated DRG IL-33 and ST2. **(A,B)** The expression of IL-33 and ST2 significantly upregulated on day 5 after continuous delivery EX-527 in naïve rats. n = 4/group, $^{***}p < 0.001$ compared with the sham group.

SIRT1 is an important deacetylase that directly deacetylates NF-κB (Deng et al., 2017). In addition, IL-33 can activate NF-κB through binding to ST2 (Numata et al., 2016). In our study, we observed that SRT1720 dramatically reduced the acetylation of NF-κB p65 induced by SNI. It is possible that the reduction of SIRT1 in the DRG increased acetylated NF-κB, upregulated IL-33, and triggered the inflammatory cascade, which may have played a vital role in the development of mechanical allodynia induced by SNI surgery.

Collectively, our results demonstrate that IL-33 in DRG and its receptor ST2 upregulated and modulated the expression of TNF-α and IL-1β in neuropathic pain induced by SNI. In addition, we observed that the reduction of DRG SIRT1 activated IL-33/ST2 signaling and contributed to mechanical allodynia in SNI rats. These results may suggest a new potential therapeutic target for neuropathic pain.

DATA AVAILABILITY STATEMENT

The raw data supporting the conclusions of this article will be made available by the authors, without undue reservation, to any qualified researcher.

ETHICS STATEMENT

The animal study was reviewed and approved by Southern medical university animal protection and use committee.

AUTHOR CONTRIBUTIONS

YZ conceived and designed the experiments. YZ, YS, HZha, WL, GC, HZho, YW, and SH performed the experiments. YZ and YS collected and analyzed the data and wrote the article. HZha and WL contributed the reagents, materials and analysis tools. WW and SC provided the financial support. The first communication author in this article is WW, and the second communication author is SC.

FUNDING

This work was supported by: (1) National Natural Science Foundation of China (NNSFC), China; Contract grant number: 81772430; (2) Clinical Research Foundation of Southern Medical University, China; Contract grant number: LC2016PY037; (3) Guangzhou Science and Technology Project, China; Contract grant number: 201607010288; and (4) Science and Technology Planning Project of Guangdong Province, China; Contract grant number: 2015A030401070; (5) China Postdoctoral Science Foundation, China; Contract grant number: 2019M662995.

ACKNOWLEDGMENTS

We would like to thank Hui Deng for excellent technical support of intrathecal injection, Huifang Shi for guiding animal injection, Wenchao Liu for the guidance of modeling and the extraction of nerve tissue, Luying Lai for guiding basic experiment related skills, Cuicui Liu for guiding the animal behavior test, Zhengnan Zhou and Xiaolan Wang for their suggestions on the experimental scheme, and Mengyu Yao for critical comments on a previous version of the manuscript.

SUPPLEMENTARY MATERIAL

The Supplementary Material for this article can be found online at: https://www.frontiersin.org/articles/10.3389/fnmol.2020.00017/full#supplementary-material.

FIGURE S1 | The colocalization of SIRT1/IL-33 and SIRT1/ST2. Double immunofluorescence staining showed that SIRT1 colocalized with IL-33 **(A–C)** and ST2 in DRG **(D–F)**. Scale bar 100 μm.

FIGURE S2 | SIRT1 agonist reduced the acetylation of NF-κB p65 but had no effects on p-ERK. **(A)** The enhanced acetylation of NF-κB p65 in DRG was significantly alleviated in SNI rats by intrathecal administration SIRT1 agonist SRT1720 (n = 4/group). **(B)** SIRT1 agonist SRT1720 showed no effects on the increased p-ERK in DRG of SNI rats (n = 4/group). $^{***}p < 0.001$ compared with the sham group, $^{\#\#}p < 0.01$ compared with the SNI+DMSO group.

REFERENCES

Alford, D. P., Liebschutz, J., Chen, I. A., Nicolaidis, C., Panda, M., Berg, K. M., et al. (2008). Update in pain medicine. *J. Gen. Intern. Med.* 23, 841–845. doi: 10.1007/s11606-008-0570-8

Baekkevold, E. S., Roussigne, M., Yamanaka, T., Johansen, F. E., Jahnsen, F. L., Amalric, F., et al. (2003). Molecular characterization of NF-HEV, a nuclear factor preferentially expressed in human high endothelial venules. *Am. J. Pathol.* 163, 69–79. doi: 10.1016/s0002-9440(10)63631-0

Boccella, S., Guida, F., Palazzo, E., Marabese, I., Novellis de, V., Maione, S., et al. (2018). Spared nerve injury as a long-lasting model of neuropathic pain. *Methods Mol. Biol.* 1727, 373–378. doi: 10.1007/978-1-4939-7571-6_28

Brunet, A., Sweeney, L. B., Sturgill, J. F., Chua, K. F., Greer, P. L., Lin, Y., et al. (2004). Stress-dependent regulation of FOXO transcription factors by the SIRT1 deacetylase. *Science* 303, 2011–2015. doi: 10.1126/science.1094637

Buckley, M. L., Williams, J. O., Chan, Y. H., Laubertova, L., Gallagher, H., Moss, J. W. E., et al. (2019). The interleukin-33-mediated inhibition of expression of two key genes implicated in atherosclerosis in human macrophages requires MAP kinase, phosphoinositide 3-kinase and nuclear factor-κB signaling pathways. *Sci. Rep.* 9:11317. doi: 10.1038/s41598-019-47620-8

Cavaillon, J. M., Adib-Conquy, M., Fitting, C., Adrie, C., and Payen, D. (2003). Cytokine cascade in sepsis. *Scand. J. Infect. Dis.* 35, 535–544. doi: 10.1080/00365540310015935

Chaplan, S. R., Bach, F. W., Pogrel, J. W., Chung, J. M., and Yaksh, T. L. (1994). Quantitative assessment of tactile allodynia in the rat paw. *J. Neurosci. Methods* 53, 55–63. doi: 10.1016/0165-0270(94)90144-9

Chen, K., Fan, J., Luo, Z. F., Yang, Y., Xin, W. J., and Liu, C. C. (2018). Reduction of SIRT1 epigenetically upregulates NALP1 expression and contributes to neuropathic pain induced by chemotherapeutic drug bortezomib. *J. Neuroinflammation* 15:292. doi: 10.1186/s12974-018-1327-x

Decosterd, I., and Woolf, C. J. (2000). Spared nerve injury: an animal model of persistent peripheral neuropathic pain. *Pain* 87, 149–158. doi: 10.1016/s0304-3959(00)00276-1

Deng, Z., Jin, J., Wang, Z., Wang, Y., Gao, Q., and Zhao, J. (2017). The metal nanoparticle-induced inflammatory response is regulated by SIRT1 through NF-κB deacetylation in aseptic loosening. *Int. J. Nanomedicine* 12, 3617–3636. doi: 10.2147/ijn.s124661

Ding, X., Jin, S., Shao, Z., Xu, L., Yu, Z., Tong, Y., et al. (2019). The IL-33-ST2 pathway contributes to ventilator-induced lung injury in septic mice in a tidal volume-dependent manner. *Shock* 52, e1–e11. doi: 10.1097/shk.0000000000001260

Gomes, B. A. Q., Silva, J. P. B., Romeiro, C. F. R., Dos Santos, S. M., Rodrigues, C. A., Goncalves, P. R., et al. (2018). Neuroprotective mechanisms of resveratrol in Alzheimer's disease: role of SIRT1. *Oxid. Med. Cell. Longev.* 2018:8152373. doi: 10.1155/2018/8152373

Han, Y., Luo, H., Wang, H., Cai, J., and Zhang, Y. (2017). SIRT1 induces resistance to apoptosis in human granulosa cells by activating the ERK pathway and inhibiting NF-κB signaling with anti-inflammatory functions. *Apoptosis* 22, 1260–1272. doi: 10.1007/s10495-017-1386-y

Hnasko, T. S., and Hnasko, R. M. (2015). The Western Blot. *Methods Mol. Biol.* 1318, 87–96. doi: 10.1007/978-1-4939-2742-5_9

Hattori, Y., and Ihara, M. (2016). [SIRT1]. *Nihon Rinsho* 74, 589–594.

Hirai, T., Enomoto, M., Kaburagi, H., Sotome, S., Yoshida-Tanaka, K., Ukegawa, M., et al. (2014). Intrathecal AAV serotype 9-mediated delivery of shRNA against TRPV1 attenuates thermal hyperalgesia in a mouse model of peripheral nerve injury. *Mol. Ther.* 22, 409–419. doi: 10.1038/mt.2013.247

Iwawaki, T. (2017). [From property of IL-1β to imaging of inflammation]. *Nihon Rinsho Meneki Gakkai Kaishi* 40, 329–336. doi: 10.2177/jsci.40.329

Jablonska, B., Gierdalski, M., Chew, L. J., Hawley, T., Catron, M., Lichauco, A., et al. (2016). Sirt1 regulates glial progenitor proliferation and regeneration in white matter after neonatal brain injury. *Nat. Commun.* 7:13866. doi: 10.1038/ncomms13866

Ji, R. R., Nackley, A., Huh, Y., Terrando, N., and Maixner, W. (2018). Neuroinflammation and central sensitization in chronic and widespread pain. *Anesthesiology* 129, 343–366. doi: 10.1097/ALN.0000000000002130

Kauppinen, A., Suuronen, T., Ojala, J., Kaarniranta, K., and Salminen, A. (2013). Antagonistic crosstalk between NF-κB and SIRT1 in the regulation of inflammation and metabolic disorders. *Cell. Signal.* 25, 1939–1948. doi: 10.1016/j.cellsig.2013.06.007

Ling, L., Gu, S., and Cheng, Y. (2017). Resveratrol inhibits adventitial fibroblast proliferation and induces cell apoptosis through the SIRT1 pathway. *Mol. Med. Rep.* 15, 567–572. doi: 10.3892/mmr.2016.6098

Ling, H., Peng, L., Wang, J., Rahhal, R., and Seto, E. (2018). Histone deacetylase SIRT1 targets Plk2 to regulate centriole duplication. *Cell Rep.* 25, 2851.e3–2865.e3. doi: 10.1016/j.celrep.2018.11.025

Lv, C., Hu, H. Y., Zhao, L., Zheng, H., Luo, X. Z., and Zhang, J. (2015). Intrathecal SRT1720, a SIRT1 agonist, exerts anti-hyperalgesic and anti-inflammatory effects on chronic constriction injury-induced neuropathic pain in rats. *Int. J. Clin. Exp. Med.* 8, 7152–7159.

Meacham, K., Shepherd, A., Mohapatra, D. P., and Haroutounian, S. (2017). Neuropathic pain: central vs. peripheral mechanisms. *Curr. Pain Headache Rep.* 21:28. doi: 10.1007/s11916-017-0629-5

Nakamura, K., Zhang, M., Kageyama, S., Ke, B., Fujii, T., Sosa, R. A., et al. (2017). Macrophage heme oxygenase-1-SIRT1–p53 axis regulates sterile inflammation in liver ischemia-reperfusion injury. *J. Hepatol.* 67, 1232–1242. doi: 10.1016/j.jhep.2017.08.010

Numata, T., Ito, T., Maeda, T., Egusa, C., and Tsuboi, R. (2016). IL-33 promotes ICAM-1 expression *via* NF-κB in murine mast cells. *Allergol. Int.* 65, 158–165. doi: 10.1016/j.alit.2015.10.004

Oboki, K., Ohno, T., Kajiwara, N., Arae, K., Morita, H., Ishii, A., et al. (2010). IL-33 is a crucial amplifier of innate rather than acquired immunity. *Proc. Natl. Acad. Sci. U S A* 107, 18581–18586. doi: 10.1073/pnas.1003059107

Old, E. A., Clark, A. K., and Malcangio, M. (2015). The role of glia in the spinal cord in neuropathic and inflammatory pain. *Handb. Exp. Pharmacol.* 227, 145–170. doi: 10.1007/978-3-662-46450-2_8

Pinto, M. R. C., Kakehasi, A. M., Souza, A. J., Tavares, W. C. Jr., Rocha, M. A., Trant, C., et al. (2019). Methotrexate use, not interleukin 33, is associated with lower carotid intima-media thickness in patients with rheumatoid arthritis. *Adv. Rheumatol.* 59:15. doi: 10.1186/s42358-019-0060-1

Pizzo, P. A., and Clark, N. M. (2012). Alleviating suffering 101—pain relief in the United States. *N. Engl. J. Med.* 366, 197–199. doi: 10.1056/nejmp1109084

Rider, P., Carmi, Y., Guttman, O., Braiman, A., Cohen, I., Voronov, E., et al. (2011). IL-1α and IL-1β recruit different myeloid cells and promote different stages of sterile inflammation. *J. Immunol.* 187, 4835–4843. doi: 10.4049/jimmunol.1102048

Ronchetti, S., Migliorati, G., and Delfino, D. V. (2017). Association of inflammatory mediators with pain perception. *Biomed. Pharmacother.* 96, 1445–1452. doi: 10.1016/j.biopha.2017.12.001

Shao, H., Xue, Q., Zhang, F., Luo, Y., Zhu, H., Zhang, X., et al. (2014). Spinal SIRT1 activation attenuates neuropathic pain in mice. *PLoS One* 9:e100938. doi: 10.1371/journal.pone.0100938

Singh, P., Hanson, P. S., and Morris, C. M. (2017). SIRT1 ameliorates oxidative stress induced neural cell death and is down-regulated in Parkinson's disease. *BMC Neurosci.* 18:46. doi: 10.1186/s12868-017-0364-1

Verri, W. A. Jr., Guerrero, A. T., Fukada, S. Y., Valerio, D. A., Cunha, T. M., Xu, D., et al. (2008). IL-33 mediates antigen-induced cutaneous and articular hypernociception in mice. *Proc. Natl. Acad. Sci. U S A* 105, 2723–2728. doi: 10.1073/pnas.0712116105

Xu, D., Barbour, M., Jiang, H. R., and Mu, R. (2019). Role of IL-33/ST2 signaling pathway in systemic sclerosis and other fibrotic diseases. *Clin. Exp. Rheumatol.* 119, 141–146.

Yeung, F., Hoberg, J. E., Ramsey, C. S., Keller, M. D., Jones, D. R., Frye, R. A., et al. (2004). Modulation of NF-κB-dependent transcription and cell survival by the SIRT1 deacetylase. *EMBO J.* 23, 2369–2380. doi: 10.1038/sj.emboj.7600244

Zarpelon, A. C., Cunha, T. M., Alves-Filho, J. C., Pinto, L. G., Ferreira, S. H., McInnes, I. B., et al. (2013). IL-33/ST2 signalling contributes to carrageenin-induced innate inflammation and inflammatory pain: role of cytokines, endothelin-1 and prostaglandin E2. *Br. J. Pharmacol.* 169, 90–101. doi: 10.1111/bph.12110

Zelová, H., and Hošek, J. (2013). TNF-α signalling and inflammation: interactions between old acquaintances. *Inflamm. Res.* 62, 641–651. doi: 10.1007/s00011-013-0633-0

Zhang, H., Shan, Y., Wu, Y., Xu, C., Yu, X., Zhao, J., et al. (2017). Berberine suppresses LPS-induced inflammation through modulating Sirt1/NF-κB signaling pathway in RAW264.7 cells. *Int. Immunopharmacol.* 52, 93–100. doi: 10.1016/j.intimp.2017.08.032

Zhao, J., Zhang, H., Liu, S. B., Han, P., Hu, S., Li, Q., et al. (2013). Spinal interleukin-33 and its receptor ST2 contribute to bone cancer-induced pain in mice. *Neuroscience* 253, 172–182. doi: 10.1016/j.neuroscience.2013.08.026

Conflict of Interest: The authors declare that the research was conducted in the absence of any commercial or financial relationships that could be construed as a potential conflict of interest.

frontiers in Molecular Neuroscience

REVIEW
published: 30 April 2020
doi: 10.3389/fnmol.2020.00068

Synaptic Plasticity on Motoneurons After Axotomy: A Necessary Change in Paradigm

Francisco J. Alvarez[1], Travis M. Rotterman[1,2], Erica T. Akhter[1†], Alicia R. Lane[1], Arthur W. English[3] and Timothy C. Cope[2]*

[1]*Department of Physiology, Emory University School of Medicine, Atlanta, GA, United States,* [2]*Department of Biomedical Engineering, School of Biological Sciences, Georgia Institute of Technology, Atlanta, GA, United States,* [3]*Department of Cellular Biology, Emory University School of Medicine, Atlanta, GA, United States*

Motoneurons axotomized by peripheral nerve injuries experience profound changes in their synaptic inputs that are associated with a neuroinflammatory response that includes local microglia and astrocytes. This reaction is conserved across different types of motoneurons, injuries, and species, but also displays many unique features in each particular case. These reactions have been amply studied, but there is still a lack of knowledge on their functional significance and mechanisms. In this review article, we compiled data from many different fields to generate a comprehensive conceptual framework to best interpret past data and spawn new hypotheses and research. We propose that synaptic plasticity around axotomized motoneurons should be divided into two distinct processes. First, a rapid cell-autonomous, microglia-independent shedding of synapses from motoneuron cell bodies and proximal dendrites that is reversible after muscle reinnervation. Second, a slower mechanism that is microglia-dependent and permanently alters spinal cord circuitry by fully eliminating from the ventral horn the axon collaterals of peripherally injured and regenerating sensory Ia afferent proprioceptors. This removes this input from cell bodies and throughout the dendritic tree of axotomized motoneurons as well as from many other spinal neurons, thus reconfiguring ventral horn motor circuitries to function after regeneration without direct sensory feedback from muscle. This process is modulated by injury severity, suggesting a correlation with poor regeneration specificity due to sensory and motor axons targeting errors in the periphery that likely render Ia afferent connectivity in the ventral horn nonadaptive. In contrast, reversible synaptic changes on the cell bodies occur only while motoneurons are regenerating. This cell-autonomous process displays unique features according to motoneuron type and modulation by local microglia and astrocytes and generally results in a transient reduction of fast synaptic activity that is probably replaced by embryonic-like slow GABA depolarizations, proposed to relate to regenerative mechanisms.

Keywords: motoneuron, axotomy, regeneration, synaptic plasticity, microglia, astrocytes, Ia afferent synapses, sensorimotor integration

OPEN ACCESS

Edited by:
George Mentis, Columbia University, United States

Reviewed by:
Patrick John Whelan, University of Calgary, Canada
Daniel Zytnicki, Université Paris Descartes, France
Pascal Branchereau, Université de Bordeaux, France

****Correspondence:***
Francisco J. Alvarez
francisco.j.alvarez@emory.edu

†Present address:
Erica T. Akhter, College of Arts and Sciences, Georgia State University, Atlanta, GA, United States

Received: *03 February 2020*
Accepted: *08 April 2020*
Published: *30 April 2020*

Citation:
Alvarez FJ, Rotterman TM, Akhter ET, Lane AR, English AW and Cope TC (2020) Synaptic Plasticity on Motoneurons After Axotomy: A Necessary Change in Paradigm. Front. Mol. Neurosci. 13:68. doi: 10.3389/fnmol.2020.00068

INTRODUCTION

Peripheral nerve injuries are widely used to study neuronal responses to physical damage and axotomy, as well as the induction of regeneration programs without confounding effects of direct injury to the surrounding CNS or complex neuropathology. Motor and sensory axons injured in peripheral nerves are disconnected from their targets but can regenerate through complex programs initiated in their cell bodies, located in the spinal cord and dorsal root ganglia respectively. However, despite regeneration many patients experience long-term motor dysfunction (reviewed in Lundborg, 2003; Brushart, 2011). Poor outcomes are often attributed to the slow pace of regeneration and incorrect targeting during regeneration (reviewed in Allodi et al., 2012; Gordon and English, 2016). Most developmental axon guidance cues are not present in the adult and regenerating axons can enter nerve fascicles directing them to the wrong muscles or even tissues. These errors scramble the original connectivity of motoneurons and proprioceptors causing functional deficiencies. On the other hand, the slow speed of axon growth frequently implies long-term muscle denervation inducing muscle fiber atrophy that can become irreversible with time. Moreover, the regeneration capacity of motoneurons decreases with time after injury (Fu and Gordon, 1995). Not surprisingly much work focused on advancing microsurgery techniques for nerve repair and on facilitating regeneration and accelerating axon growth with bioengineering solutions and pharmacological and rehabilitative manipulations (reviewed in Gordon and English, 2016; Gordon, 2016; Panagopoulos et al., 2017; Tajdaran et al., 2019). But in addition to regeneration mechanisms in the periphery, it is important to also consider changes in the CNS induced by nerve injuries (reviewed in Navarro et al., 2007). After axotomy, motoneurons undergo early and late changes in gene expression that switch them to a regenerative phenotype (reviewed in Gordon, 2016). These are paralleled by structural modifications in cell bodies and dendrites (chromatolytic reaction) as motoneurons shift cellular metabolism and protein synthesis towards producing materials for axon growth and regeneration (Lieberman, 1971; Gordon, 2016). One intriguing aspect of this response is the intense shedding of synapses, particularly those of glutamatergic origin, from motoneurons after axotomy and undergoing regeneration. The significance of this plasticity is yet unclear and is the focus of this review article.

Despite a wealth of studies on synaptic plasticity around axotomized motoneurons, a coherent comprehensive view of its significance and mechanisms is yet to be established. New evidence suggests the need to reconsider three significant ideas that have led to much experimentation and data interpretation in the past. First, the assumption that synaptic plasticity around axotomized motoneurons, usually referred to as "synaptic stripping," is a single phenomenon. There is now enough evidence suggesting that different synapses (excitatory or inhibitory, arising from injured peripheral sensory afferents or uninjured CNS neurons) undergo plastic changes that differ in mechanism, time-course, significance for regenerative processes, and functional implications after regeneration. Second, the assumption that synapse withdrawal is necessary for motoneurons entering an electrically silent state that favors regeneration. Current evidence, reviewed below, suggests this is not the case. Efficient manipulations to enhance regeneration include electrical stimulation and exercise, both based on increasing motoneuron activation (reviewed in Gordon and English, 2016). Third, synaptic changes on the cell body cannot be extrapolated to the whole input to the motoneuron. Synaptic inputs differ by whether they are lost from cell bodies only or also from dendrites.

We recently distinguished two types of synaptic plasticity after nerve injury (Alvarez et al., 2010, 2011; Rotterman et al., 2014, 2019). One type is the classically described transient loss of synapses that occurs specifically over the cell bodies of axotomized motoneurons affecting all types of synapses. These synaptic changes revert after motor axons reinnervate muscles and may be related to regeneration mechanisms. The second type induces a permanent change in spinal cord circuitry and affects the central synaptic arbors of axons (proprioceptive sensory or motor) injured peripherally. These synapses are lost not only over axotomized motoneurons but also on many other targets in the ventral horn and affect both cell bodies and dendritic arbors. The long-lasting loss of central synapses originating from proprioceptive and motor axons injured in the peripheral nerve likely reorganizes motor control spinal circuitries causing functional alterations after axons regenerate peripherally.

Additional confounds have been the diversity of models used to study this synaptic plasticity. Differences fall into three categories: the type of motoneuron (spinal, facial, hypoglossal, vagal. . .), nerve injury (different nerves, crush vs. cut, proximal vs. distal) and species (cats, rabbits, mice, rats, guinea pigs. . .). This diversity introduces high variance in reported results, but comparisons of similarities and differences also provide insights into mechanisms and significance. Importantly, different types of nerve injuries all result in axotomy of the motor axon and induce a regenerative program in the motoneuron; however, they drastically differ in motoneuron preservation and speed and efficiency of regeneration. The goal of this review is to organize this multiplicity of data to allow more precise interpretations of past results and more specific hypotheses moving forward.

THE HISTORY OF "SYNAPTIC STRIPPING" OVER MOTONEURONS AFTER NERVE INJURY: BACK TO THE ORIGINS

Removal of synapses from the cell body of motoneurons axotomized following nerve transections was first described in an electron microscopy (EM) analysis of the rat facial nucleus published in a landmark 1968 paper (Blinzinger and Kreutzberg, 1968). In this study, the cell bodies of axotomized motoneurons were reported to lose up to 80% of their synapses and become covered by microglia. No distinction was made among different types of synapses. In some electron micrographs, microglia processes were found interposed between the cell body surface and synaptic boutons, but with no evidence of synaptic bouton degeneration or

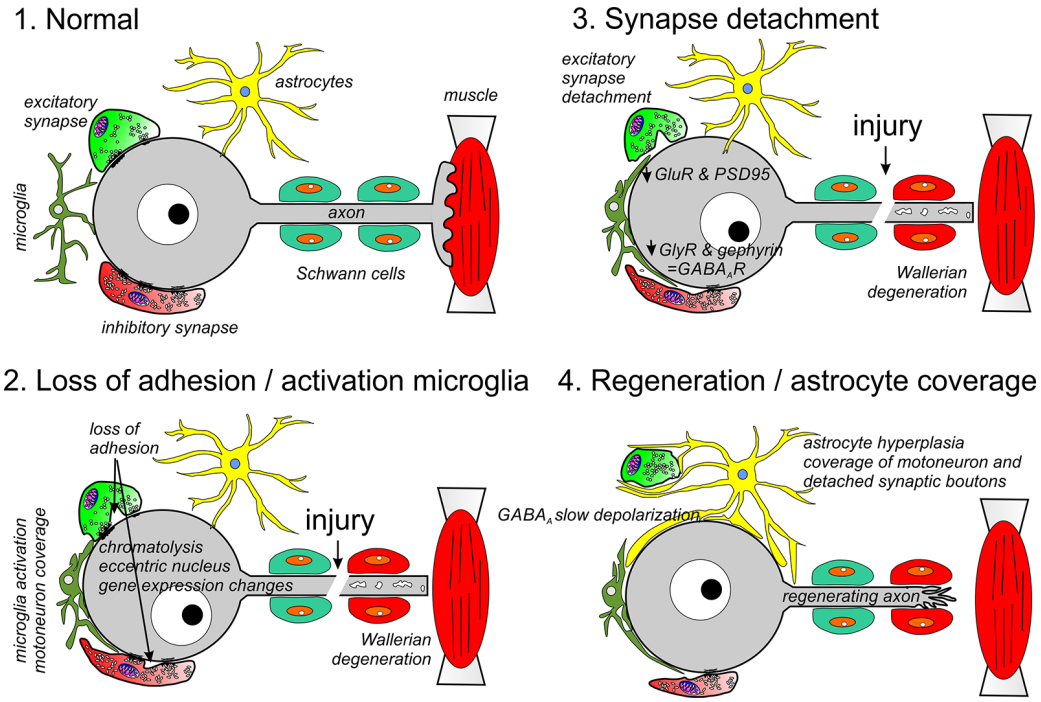

FIGURE 1 | Different phases of synaptic and glia plasticity around cell bodies of axotomized motoneurons. Axotomy induces chromatolysis and rapid changes in gene expression due to positive injury signals arriving at the cell body and negative signals due to lost trophic support from muscle. During an early phase (2), adhesion in non-junctional areas is reduced and activated microglia migrate towards the cell body replacing membrane regions previously covered by synaptic bouton. In the periphery, the cut distal segment undergoes Wallerian degeneration (2, 3) and Schwann cells modify phenotype to orchestrate the removal of axon debris and upregulate trophic factors and adhesion proteins to promote regeneration. This phase is followed by reduced motoneuron expression of synaptic genes, including GlyRs and GluRs, as well as, the synaptic organizers PSD95 and gephyrin (3). This results in full detachment of many excitatory synapses and some inhibitory synapses. Finally, the motoneuron is covered by astrocytic lamellae replacing microglia (4). All changes on the surface of the motoneurons revert after the motor axon successfully reinnervates muscle: astrocyte coverage disappears, inhibitory synapses enlarge and recuperate gephyrin and GlyRs, excitatory synapses are re-established and KCC2 expression recovers resulting in the return of normal excitatory and inhibitory synaptic activity on the cell body.

synapse phagocytosis (summarized in **Figure 1**). The EM images were interpreted as a "lifting" mechanism in which microglia displaced the synapses. Synapse detachment and replacement by microglia was confirmed shortly after in spinal motoneurons (Kerns and Hinsman, 1973), hypoglossal motoneurons (Hamberger et al., 1970; Sumner and Sutherland, 1973; Sumner, 1975a) and later on oculomotor motoneurons (Delgado-Garcia et al., 1988). It was found to be similar across species [mouse (Torvik and Skjorten, 1971); cat (Chen, 1978); rabbit (Hamberger et al., 1970)], including humans (Graeber et al., 1993). The term "synaptic stripping" was coined. Common among these studies was the finding that synapse losses were limited to cell bodies and proximal dendrites (Delgado-Garcia et al., 1988; Linda et al., 1992; Brännström and Kellerth, 1998) and that synapses are recovered after the motoneurons reinnervate muscle (Sumner and Sutherland, 1973; Cull, 1974; Chen, 1978; de la Cruz et al., 1994; Johnson et al., 1998; Brännström and Kellerth, 1999). Loss of presynaptic inputs was also found in invertebrate motoneurons innervating the locust leg (Horridge and Burrows, 1974), suggesting a conserved mechanism. The same phenomenon was described in some central neurons in which transection axotomies are experimentally feasible: spinocerebellar neurons (Chen et al., 1977), abducens internuclear interneurons (Pastor et al., 2000), and Mauthner cells (Wood and Faber, 1986).

Most studies interpreted EM images according to the hypothesis that microglia is responsible for "stripping" synapses, however, in none of these ultrastructural studies it was possible to determine whether microglia actively removed the synapses or just occupied space vacated by lost synapses. Discrepancies in the interpretation of the role of microglia can be found in some of the contemporary studies. In the rat hypoglossal nucleus, two phases of glia coverage were distinguished: a first phase reactive to axotomy and characterized by microglia coverage (up to 2 weeks post-axotomy) and a second phase during motoneuron regeneration in which the cell is covered by astrocytes (Sumner and Sutherland, 1973). Other analyses in the same model emphasized astrocytic coverage from the start, noting relatively few microglia (Reisert et al., 1984). The latter was consistent with EM observations in cat spinal motoneurons, in which the microglia reaction is weaker compared to rodents (Cova and Aldskogius, 1984, 1985, 1986) enabling parsing out synapse detachment vs. microglia coverage (Chen, 1978). Axotomized sympathetic postganglionic neurons are also subject to synapse detachment but in this case, there is no microglia in the ganglia and detached synaptic boutons can be recognized

at a distance from the cell body because, remarkably, the presynaptic active zone (PAZ) remains intact (Matthews and Nelson, 1975; Purves, 1975). Synaptic boutons detached from cat spinal motoneurons after sciatic nerve injuries disassemble their PAZs, but they are still recognizable in the vicinity of the motoneuron cell body frequently isolated by layers of astrocytic lamellae (Chen, 1978). Thus, alternative explanations for the loss of synapses included the involvement of astrocytes or cell-autonomous remodeling of postsynaptic membranes leading to synapse detachment (Sumner and Sutherland, 1973; Sumner, 1975a,b,c; Chen, 1978). The idea of cell-autonomous synaptic shedding lacked precise mechanistic explanations at the time, and the proposal that microglia (or astrocytes) physically remove synapses from the cell body prevailed and became the accepted hypothesis that continues to be cited in many past and present reviews (Kreutzberg, 1996; Moran and Graeber, 2004; Cullheim and Thams, 2007; Kettenmann et al., 2013; Spejo and Oliveira, 2015; Chen and Trapp, 2016).

MICROGLIA IS NOT THE UNIVERSAL "SYNAPTIC STRIPPER" OF ADULT AXOTOMIZED MOTONEURONS

Experiments to evaluate the microglia hypothesis were performed two decades after it was first proposed. The first test was a rather complex and indirect experiment that reduced microglia proliferation in the injured facial nucleus for a different goal: to reveal the microglia origins of brain macrophages (Graeber et al., 1989). In this study, the cytostatic agent adriamycin was injected in the facial nucleus, while at the same time the facial nerve received crush injuries combined with ricin application to induce motoneuron cell death and the appearance of brain macrophages. Adriamycin prevented microglia proliferation, the appearance of brain macrophages (therefore shown to derive from microglia in this model), and microglia migration to the surface of axotomized motoneurons. Qualitative EM observations of motoneurons treated with adriamycin revealed a normal complement of synapses after nerve crush. The authors concluded that synapse preservation in the absence of perineuronal microglia supported a role for microglia detaching synapses, but this conclusion was complicated by the effects of adriamycin on motoneuron metabolism and function (Bigotte and Olsson, 1983, 1984, 1987). Moreover, this observation was not supported in following experiments using quantitative approaches. One experiment blocked microglia proliferation and surface coverage of hypoglossal motoneurons by continuous infusion with mini-osmotic pumps of the anti-mitotic agent cytosine-arabinoside (ARA-C) and this resulted in no significant change in the number of synapses lost after axotomy (Svensson and Aldskogius, 1993). Another piece of evidence came from analysis of axotomized facial motoneurons in osteoporosis op/op mice that carry a spontaneous mutation disturbing expression of colony-stimulating factor 1 (CSF1; Kalla et al., 2001). These mice show decreased basal microglia numbers and after nerve injury, they display reduced microglia proliferation, lower expression of microglial activation markers and lack of coverage of the motoneuron surface (Raivich et al., 1994; Kalla et al., 2001). No differences in synaptic stripping were found between op/op mice and controls despite a blunted microglial response. Recent studies confirmed that CSF1 is upregulated in axotomized spinal motoneurons and is a necessary signal for microglia proliferation and migration towards the motoneuron surface (Akhter et al., 2019; Rotterman et al., 2019). Synaptic stripping proceeded normally in the absence of microglia interactions with the surfaces of axotomized motoneurons lacking *csf1*. In this experiment basal microglia numbers and nerve injury-induced activation of dorsal horn microglia were preserved, restricting the effects to microglia proliferation and activation in the ventral horn.

In conclusion, synaptic stripping was unaltered in several different experiments that prevented or modified microglia activation and their interaction with the cell bodies of hypoglossal, facial, or spinal motoneurons. Comparative analyses between species and mouse strains lead to similar conclusions. Transgenic mouse models with increased or decreased synaptic stripping over spinal motoneurons after sciatic injuries exhibited similar microglia reactions (Berg et al., 2013). Conversely, C57BL/6N mice display a higher microglia reaction around axotomized motoneurons compared to Wistar rats, despite lower synaptic stripping and functional loss (Yamada et al., 2008, 2011). The accumulated data confirmed long-held doubts about the microglia synaptic stripping hypothesis (reviewed in Aldskogius and Kozlova, 1998; Perry and O'Connor, 2010; Aldskogius, 2011) and suggest that the primary role of microglia around axotomized motoneurons is unlikely related to the induction of synapse stripping, although they probably exert modulatory roles as reviewed below.

ROLE OF ASTROCYTES IN SYNAPTIC REMODELING AROUND AXOTOMIZED MOTONEURONS

The EM observation of astrocytic processes covering the surface of motoneurons and enveloping synaptic boutons implicated them in synaptic stripping (summarized in **Figure 1**). Astrocytes around axotomized motoneurons do not proliferate but augment in size by increasing expression of glial fibrillary acid protein (GFAP) and vimentin (Sumner and Sutherland, 1973; Chen, 1978; Reisert et al., 1984; Graeber and Kreutzberg, 1986, 1988; Graeber et al., 1988; Tetzlaff et al., 1988; Gilmore et al., 1990; Svensson et al., 1994). Later, they extend sheet-like processes to cover the surface of axotomized motoneurons isolating their cell bodies from the rest of the neuropil and replacing microglia. Astrocytic lamellae also envelop detached synapses, but never engulf or degrade them. Synapse recovery following successful regeneration in the periphery coincides with the disappearance of astrocyte wrappings. If motoneurons are prevented from reinnervating muscle, the ensheathing of their cell bodies by astrocytes persists for long periods (Sumner, 1977a; Graeber and Kreutzberg, 1988; Laskawi and Wolff, 1996). Taking advantage of the astrocyte reaction around rat hypoglossal motoneurons being secondary and dependent on microglia activation, it

was shown that altering astrogliosis did not affect synaptic stripping (Svensson et al., 1993). Similarly, synaptic stripping on spinal motoneurons was not prevented in dual GFAP and vimentin knockouts with reduced astrogliosis (Berg et al., 2013). However, in these animals around 35% more synapses were found on axotomized spinal motoneurons. Astrocytic reactions vary with mouse strain: A/J mice show stronger reactions around axotomized motoneurons compared to C57BL/6J mice and this is correlated with fewer synapses after axotomy and impaired recovery (Emirandetti et al., 2006). Mutant mice with variations in astrocytosis levels after nerve injury showed co-related variations in the amount of synaptic loss (Victorio et al., 2010; Freria et al., 2012; Ribeiro et al., 2019). A more definitive study for proving causality used transection of the facial nerve and blocked the astrocytic reaction by astrocyte-specific deletion of *STAT3* (Tyzack et al., 2014). This resulted in reduced GFAP upregulation, fewer astrocytic lamellae extensions and decreased motoneuron cell body coverage. Surprisingly it also caused a larger and more permanent loss of synapses due to reduced production of thrombospondin 1 (TSP-1). TSP-1 is a well-known regulator of *de novo* synaptogenesis during normal development and after pathology (reviewed in Eroglu and Barres, 2010). The diversity of reported effects on synaptic coverage after altering the astrocytic reaction around axotomized motoneurons could be explained considering two sequential roles for astrocytes. First, during the regenerative phase (when the axon is growing in the peripheral nerve) enlarged astrocytes isolate pre and postsynaptic surfaces preventing synapse re-formation, and also providing trophic support (Tyzack et al., 2014; Jones et al., 2015). Second, after motor axons reinnervate muscle, astrocytes withdraw their processes exposing motoneuron surfaces that then become available for synaptogenesis actively promoted through TSP-1. Therefore, although astrocytes are most likely not directly involved in the initial phase of synapse stripping, their activity influences synapse recovery in the regenerating motoneuron.

MEMBRANE REMODELING IN AXOTOMIZED MOTONEURONS AND SYNAPTIC STRIPPING

The reviewed data suggest that neuron-glia interactions are not critical for the induction of synaptic stripping in axotomized motoneurons. EM support for the hypothesis of active postsynaptic membrane remodeling leading to synapse loss was suggested in early EM studies (see above) and later quantified over abducens motoneurons undergoing synaptic stripping induced by botulinum toxin (Pastor et al., 1997; Moreno-López et al., 1998). This model mimics synaptic changes occurring after the axotomy of motoneurons in the absence of injury and a microglia reaction (Sumner, 1977b). In this model, the first evidence of synapse detachment on the motoneuron cell body surface is the early separation of pre- and post-synaptic membranes in non-junctional areas. This is paralleled by a 3-fold increase in coated vesicles in the non-junctional postsynaptic membrane away from the postsynaptic density (PSD). Dissolution of inhibitory PSD gephyrin clusters and synaptic complexes occurs after much of the synaptic bouton has detached from the postsynaptic cell (Moreno-López et al., 1998). Finally, the motoneurons become covered by glial processes (Pastor et al., 1997; Moreno-López et al., 1998).

Overall, the EM observations suggest that synaptic stripping proceeds in three steps: (1) an increase in uptake of material from the membrane surface that correlates with reduced synaptic bouton adhesion throughout the non-junctional apposition; (2) dissolution of the PSD and PAZ and complete detachment of the synaptic bouton; and (3) coverage of pre and postsynaptic surfaces by glia (**Figure 1**). Work in the lab of Dr. Steffan Cullheim (Karolinska Institute) systematically cataloged in spinal motoneurons the expression of several synaptic adhesion (SynCAM 1–4, nectins 1 and 3, NCAM, N-cadherin, and Netrin-G2-ligand) and synaptic organizing molecules (PSD95, neuroligins 1–3) before and after sciatic nerve transection (Zelano et al., 2006, 2007, 2009a,b; Berg et al., 2010). This work generated a molecular picture that strikingly parallels the EM observations. A loss of synaptic adhesion in axotomized spinal motoneurons correlates with the early downregulation of mRNAs for SynCAM1, neuroligin-2 and -3 and Netrin-G2-ligand (Zelano et al., 2007; Berg et al., 2010). SynCAMs are involved, among other functions, in synaptic bouton adhesion through non-junctional sites (Kakunaga et al., 2005). Neuroligins, conversely, induce the formation of inhibitory and excitatory synaptic junctions and contribute to their functional and structural stability (Craig and Kang, 2007; Südhof, 2008). Netrin-G2-ligand interacts with PSD95 and regulates synapse number of specific subsets of excitatory synapses expressing netrin-G2 (Kim et al., 2006; Matsukawa et al., 2014). Synaptic adhesion is also modified by changes in the localization of adhesion proteins. N-cadherin mRNA expression was unaltered by axotomy, but the localization of the protein drastically changed from being clustered opposite to synaptic boutons on the cell bodies of intact motoneurons to be removed from this location after axotomy and shuttled to the regenerating axons (Zelano et al., 2006).

Proteins that organize PSD neurotransmitter receptor accumulations are downregulated with a slower time course compared to synaptic adhesion proteins. These include PSD95 at excitatory synapses (Che et al., 2000; Zelano et al., 2007) and gephyrin at inhibitory synapses (Moreno-López et al., 1998; Eleore et al., 2005b; Kim et al., 2018). The removal of these molecular organizers of excitatory and inhibitory synaptic PSDs is accompanied by changes in postsynaptic receptor expression that, as will be reviewed below, also occur with a time course slower than changes in synaptic adhesion. Altogether they induce dissolution of the PSD and synaptic complex after adhesion is reduced in non-junctional regions and thus fully detaching the synapse. These spaces are occupied by microglia first and astrocytes later (**Figure 1**).

Adhesion proteins of the nectin family have no basal expression in motoneurons but are quickly upregulated after axotomy (Zelano et al., 2006, 2009b). Upregulation of nectin-1 and -3 in Schwann cells and motoneurons, as well as nectin-like proteins 4 and 5 in motoneurons, could facilitate *cis* and

trans interactions in the peripheral nerve during motor axon regeneration. Nectins are also expressed by astrocytes and are necessary for astrocytic support of neurons (Miyata et al., 2016). It is thus tempting to speculate that nectins and nectin-like proteins concurrently facilitate adhesion of the cell bodies and axons of regenerating motoneurons with respectively, astrocytes and Schwann cells. These possibilities should be fully investigated in the future.

Changes in adhesion proteins revert following muscle reinnervation and in coincidence with synapse restoration on the motoneuron cell body (Zelano et al., 2009a; Berg et al., 2010). In summary, bi-directional replacement of synapses and glia coverage over the membrane of motoneurons correlates with changes in expression and localization of cell adhesion proteins, a process that is coupled to regenerative mechanisms in the peripheral nerve. Nonetheless, other mechanisms might be at play since mouse models with increased or decreased synaptic stripping (MHCI KOs and C3 KOs, respectively) did not show modifications in adhesion protein plasticity after axotomy (Berg et al., 2013). Alternatively, reduced synaptic adhesion could be interpreted as permissive, but not sufficient for complete synapse retraction. Determining whether these changes are necessary will require specific manipulations of adhesion protein expression in axotomized motoneurons during synaptic stripping. Future studies will also need to fit the idea of global changes in synaptic adhesion with the different susceptibilities of inhibitory and excitatory synapses to detachment (see below) and the maintenance of synapses throughout most of the dendrite.

A further mechanism inducing detachment of synaptic boutons from postsynaptic membranes involves nitric oxide (NO) disruption of the actin cytoskeleton in presynaptic boutons causing their retraction from axotomized motoneurons (reviewed in Moreno-López et al., 2011). Neuronal nitric oxide synthase (nNOS) is upregulated in cranial, but not spinal motoneurons, after a variety of peripheral nerve injuries (Yu, 1994, 1997; Sunico et al., 2005; Liu et al., 2006). nNOS upregulation was shown to be necessary for synaptic stripping in the hypoglossal nucleus: blocking nNOS with the generalized NOS antagonist L-NAME, the specific nNOS inhibitor 7-nitroindazole, or abrogating nNOS upregulation by overexpressing miR-shRNA for nNOS with lentiviral vectors all blocked synaptic stripping on hypoglossal motoneurons after nerve crush (Sunico et al., 2005; Montero et al., 2010). Synaptic preservation affected only excitatory synapses, since inhibitory synapses are not removed from adult hypoglossal motoneurons after axotomy (Sumner, 1975a; Sunico et al., 2005). nNOS expression was also found sufficient for inducing synaptic stripping. AAV transduction of intact hypoglossal motoneurons with nNOS caused a loss of excitatory synapses in the adult, and interestingly, induced additional loss of inhibitory synapses in neonates (Sunico et al., 2010), suggesting developmental changes in susceptibility to stripping. NO generated by axotomized motoneurons acts in a spatially restricted paracrine manner on overlying synaptic boutons by stimulating guanylyl cyclase (GC), production of cGMP and activation of cGMP-dependent protein kinase (PKG). Thus, treatment with a membrane-impermeable NO scavenger (preventing paracrine action) or inhibitors of GC or PKG, preserved excitatory synapses (Sunico et al., 2005). PKG targets were identified as Rho kinase (ROCK) and its substrate myosin light chain (MLC). Phosphorylated MLC correlated with excitatory synapse withdrawal, and two specific ROCK inhibitors prevented this synaptic loss (Sunico et al., 2010). One result of p-MLC is actomyosin contraction and reorganization of the peripheral F-acting cytoskeleton (Svitkina et al., 1997), a mechanism associated with neurite retraction (reviewed in Newey et al., 2005). It was then proposed that actomyosin activation could induce synaptic bouton deformation and withdrawal explaining EM images showing bouton curvatures and separations in non-junctional areas (Moreno-López et al., 2011). Both isoforms of ROCK (ROCKα and ROCKβ) localized preferentially to excitatory synapses, pointing to a property that might confer differential susceptibility to stripping.

These studies made a compelling case for the actions of NO on the stability of excitatory inputs on hypoglossal motoneurons, however, it is not universally applicable. Spinal motoneurons undergo synaptic stripping after crush and transection of peripheral nerves without the upregulation of nNOS (Zhang et al., 1993; Yu, 1994). Spinal motoneurons upregulate NO only after ventral root avulsion (Wu et al., 1994a,b), a type of injury that induces enhanced synaptic stripping, affecting especially excitatory synapses (Linda et al., 2000; Novikov et al., 2000; Oliveira et al., 2004) and also motoneuron death (Koliatsos et al., 1994). The NO/GC/PKG/ROCK pathway for synapse detachment might thus operate in spinal motoneurons after very proximal nerve injuries and have an additive effect, inducing larger stripping of excitatory synapses.

DIFFERENCES IN SYNAPSE REMOVAL AND MAINTENANCE ACCORDING TO THE TYPE OF SYNAPSE AND MOTONEURON

The proportion of excitatory and inhibitory synapses removed from the cell body of different types of motoneurons after axotomy is variable. Only excitatory synapses are removed on hypoglossal motoneurons (Sumner, 1975a), in contrast, inhibitory synapses are strongly stripped from abducens motoneurons (Delgado-Garcia et al., 1988). In the spinal cord, gamma motoneurons lose more synapses than alpha motoneurons after the same injury and the loss of inhibitory synapses over gamma motoneurons is two-fold higher compared to excitatory synapses (Johnson and Sears, 1989). The loss of inhibitory and excitatory synapses is similar over cat medial motor column (MMC) thoracic spinal cord alpha motoneurons (Johnson and Sears, 1989), while inhibitory synapses are preferentially preserved on the cat and rodent lumbar lateral motor column (LMC) motoneurons in which excitatory synapse losses increase with injury proximity (Linda et al., 1992, 2000; Brännström and Kellerth, 1998; Novikov et al., 2000; Oliveira et al., 2004; Alvarez et al., 2011).

Synapse recovery also differs between excitatory and inhibitory inputs. In a comparative study of glutamatergic excitatory (VGLUT2) and GABA/glycine inhibitory (VGAT/VIAAT) synapses over medial gastrocnemius (MG)

spinal motoneurons (a lumbar LMC pool) after tibial nerve transections in which regeneration was allowed (cut and repair) or not (cut and ligation), VGAT/VIAAT were lost to a lesser extent and recovered independently of muscle reinnervation (Alvarez et al., 2011). In contrast, VGLUT2 synapses were lost in larger numbers and recovered only after the motoneurons reinnervated muscles. This result suggests different requirements on peripheral factors for synapse detachment and recovery. The idea that synapse withdrawal after axotomy depends on trophic factors from peripheral targets has a long history. The earliest studies used silver methods to identify synaptic boutons around axotomized motoneurons and showed that blocking retrograde transport in peripheral nerves induced synapse withdrawal similar to axotomy, while functionally decoupling motoneurons from muscle (blocking impulse transmission in the nerve) did not (Cull, 1974). These findings were replicated on postganglionic sympathetic neurons whose axons were treated with colchicine (Purves, 1976). Target-dependence of motoneuron properties became a very active area of research with many comprehensive reviews on the topic (Mendell, 1984; Titmus and Faber, 1990; de la Cruz et al., 1996; Terenghi, 1999; Navarro et al., 2007; Benítez-Temiño et al., 2016). Here, we will focus on how these studies inform about differences in the removal and recovery of different synapses.

The two most thoroughly investigated neurotrophins concerning synaptic plasticity on axotomized motoneurons are Brain-Derived Neurotrophic Factor (BDNF) and Neurotrophin-3 (NT3). Continuous delivery of BDNF in the spinal subarachnoid space after ventral root avulsion did not prevent synaptic stripping evaluated with EM but facilitated synapse recovery in the absence of muscle reinnervation, especially inhibitory synapses (Novikov et al., 2000). NT3 applied to cut nerves preserved glutamatergic EPSPs on motoneurons from Ia afferent synapses (Mendell et al., 1999; more on this input later). NT3 and BDNF have now been proposed to mediate the effects of treadmill exercise on the preservation of synapses over axotomized spinal motoneurons (Krakowiak et al., 2015; Arbat-Plana et al., 2017).

A comprehensive direct comparison of the effects of different neurotrophins on preservation and recovery of specific synaptic inputs was carried out by the group of Dr. Angel Pastor (University of Seville) using as a model the axotomy of abducens motoneurons. This work draws on extensive knowledge about the synaptic inputs controlling tonic and phasic firing of abducens motoneurons in relation to eye position, eye velocity, and vestibular stimulation (reviewed in Benítez-Temiño et al., 2016). NT3 and BDNF were applied to the cut nerve at the time of injury (to test preservation) or after a 2-week delay allowing synaptic stripping (to test recovery). In all experiments, regeneration in the periphery was prevented, disallowing synapse recovery because of muscle reinnervation. NT3 and BDNF both preserved and recovered excitatory and inhibitory synapses in the absence of target reinnervation, but NT3 had preferential actions on phasic synaptic inputs modulating firing to eye velocity and BDNF on tonic inputs related to eye position (Davis-López de Carrizosa et al., 2009). Interestingly, excitatory vestibular inputs were recovered by BDNF and inhibitory vestibular inputs by NT3. In contrast to other motoneurons, abducens motoneurons are unique in that they also express TrkA (Morcuende et al., 2011). Nerve Growth Factor (NGF) activation of TrkA receptors (with $p75^{NTR}$ blocked) recovered all synapses and synaptic modulation from all inputs, although synaptic gains were abnormally enhanced (Davis-López de Carrizosa et al., 2010). Recently, this same group showed that Vascular Endothelial Growth Factor (VEGF) also recovers all inputs and synapses on abducens motoneurons and results in firing modulation in injured motoneurons that is indistinguishable from control (Calvo et al., 2018). Conversely, astrocytic coverage of axotomized abducens motoneurons was reduced by BDNF, NT3, NGF and VEGF. Similarly, microglia around spinal cord motoneurons is reduced by BDNF (Novikov et al., 2000; Rodrigues Hell et al., 2009). These studies suggest that: (1) trophic factors applied to the motoneuron cell body or cut axon increase synapse preservation/recovery while reducing glia coverage; (2) trophic actions on synapse preservation/recovery can be redundant; and (3) some trophic factors display preferences for specific inputs, suggesting differences on mechanisms that remove or recover specific synapses.

IMMUNE SYSTEM SIGNALING MECHANISMS, MICROGLIA AND SYNAPTIC PLASTICITY OF INHIBITORY SYNAPSES

Searches for immune system genes involved in motoneuron cell death after axotomy revealed the upregulation of MHC-I expression in spinal and facial motoneurons after nerve injuries and with the independence of cell death (Maehlen et al., 1989). In particular, β2-microglobulin, a component of the MHC-I complex required for surface expression and signaling, is dramatically increased after axotomy (Linda et al., 1998). Later, an unbiased screen for genes regulated by synaptic activity in visual pathways during the formation and maintenance of ocular dominance columns identified MHC-I as a critical gene involved in synaptic plasticity (Corriveau et al., 1998; Shatz, 2009). This finding prompted analysis of β2 KO mice after sciatic nerve injuries and, unexpectedly, a larger loss of specifically inhibitory synapses was observed (Oliveira et al., 2004). While this implied a protective role of MHC-I activity on inhibitory synapses, subsequent studies found that enhancing MHC-I upregulation by combining interferon treatment with axotomy, also resulted in excessive loss of inhibitory synapses (Zanon and Oliveira, 2006). Thus, inhibitory synapse protection by MHC-I may require finely balanced levels of MHC-I and the effects also depend on the cell types and locations involved.

Surprisingly, analyses of MHC-I protein localization in axotomized motoneurons found no increases in the cell body or dendrites, instead, newly produced MHC-I was trafficked to the regenerating axons (Thams et al., 2009). Within the spinal cord, MHC-I protein was mainly found in activated microglia surrounding axotomized motoneurons. Microglia also express MHC-I receptors (reviewed in Thams et al., 2008)

and intriguingly, β2 KOs showed an exaggerated microglial reaction the first few days after the injury that returned to normal levels within the first week (Cartarozzi et al., 2019). Microglia MHC-I is regulated by Toll-like receptor (TLR) activation. Global genetic deletion of TLR4 (KO) resulted in reductions of inhibitory synapse coverage of motoneurons cell body surfaces after axotomy while global deletion of TLR2 did the opposite; surface coverage by inhibitory synapses was larger in TLR2 KO axotomized motoneurons compared to wild-types. In both cases, there were reportedly no differences in bouton numbers being the changes in synaptic coverage explained by larger or smaller bouton sizes (Freria et al., 2012). These results need to be interpreted cautiously because inhibitory synapses also showed altered bouton sizes on uninjured motoneurons in these global KOs. Synapse bouton size is regulated during development and correlates with synaptic strength (Walmsley et al., 1998), thus size might influence synapse fates after injury in the adult. Nevertheless, a relationship between microglial activation and inhibitory synapse stability agrees with results suggesting that the rescue of inhibitory synapses on axotomized motoneurons by BDNF is paralleled by a decreased microglia reaction (Novikov et al., 2000; Rodrigues Hell et al., 2009). Similarly, studies in the cerebral cortex suggest that somatic wrapping of neurons by lipopolysaccharide (LPS)-activated microglia is neuroprotective through a mechanism that involves the removal of perisomatic GABA synapses and upregulation of anti-apoptotic genes (Chen et al., 2014). In contrast, inhibitory synapses are generally preserved over axotomized motoneurons and any neuroprotective role for microglia is at present controversial (reviewed in Aldskogius, 2011, but see Jones et al., 2015 and Tanaka et al., 2017). Regardless of the exact roles played by inhibitory synapses, MHC-I and TLRs have emerged as key modulators of inhibitory synapse plasticity after axotomy, potentially through microglia actions.

The last decade also highlighted the classical complement cascade through C1q and C3 as a canonical pathway for synapse opsonization and microglia-dependent removal of excitatory synapses during developmental pruning and in several pathologies (Stevens et al., 2007); reviewed in Stephan et al., 2012). C1q and C3 upregulation around hypoglossal, facial and spinal motoneurons are consistent findings after nerve injury (Svensson and Aldskogius, 1992; Svensson et al., 1995; Mattsson et al., 1998; Berg et al., 2012) although their cellular origins might differ. In all studies, C1q was found in microglia, but C3 was detected in microglia around injured brainstem motoneurons and astrocytes around injured spinal motoneurons. Synapse stripping on spinal motoneurons was altered in C3 KOs but not in C1q KOs, and the action was again biased towards inhibitory synapse preservation, while excitatory synapses (VGLUT2) were lost at normal levels (Berg et al., 2012). Thus, in contrast to complement-mediated microglia pruning of excitatory synapses in other brain regions during normal development or pathology, the removal of excitatory synapses from the cell body of adult axotomized motoneurons is independent of complement. This should not be too surprising since complement-mediated microglia removal of excitatory synapses occurs through engulfment and phagocytosis (reviewed in Stephan et al., 2012) and this is not the mechanism of synapse removal from motoneuron cell bodies after axotomy.

It should be emphasized that MHC-I and C3 effects occur over the subset of inhibitory synapses that undergo plasticity after axotomy. It is presently unknown if these correspond to specific types of inputs and how this relates to the diverse fates of inhibitory synapses on different types of axotomized motoneurons. Moreover, the known effects of C3 in peripheral nerves during regeneration (reviewed in Ramaglia et al., 2008) and of MHC-I on the neuromuscular junction (reviewed in Cullheim and Thams, 2010) cannot be dismissed when using global KOs. It is conceivable that actions in the periphery could influence the stability of inhibitory synapses centrally. In summary, mechanisms linking MHC-I, C3, and glia to inhibitory synapse plasticity deserve further study, but it is already established that these mechanisms differentiate between inhibitory and excitatory synapses on axotomized motoneurons.

FUNCTIONAL CORRELATES AND SIGNIFICANCE OF DIFFERENTIAL REMOVAL OF EXCITATORY AND INHIBITORY SYNAPSES

Differential removal of excitatory and inhibitory synapses predicts E/I imbalances that were hypothesized to promote motoneuron survival and/or the induction of a regenerative phenotype (Barron, 1989; Carlstedt and Cullheim, 2000; Navarro et al., 2007). The argument is that abolishing electrical activity focuses motoneuron resources on protein synthesis related to axon regeneration. Indeed, MHC-I and C3 KO mice with increased inhibitory synapse preservation correlate with faster axon regeneration and recovery of motor function (Oliveira et al., 2004; Berg et al., 2012); however, alternative interpretations due to possible effects in the periphery cannot be ruled out. MHC-I plays a critical role in neuromuscular junction development and stability (Thams et al., 2009; Cullheim and Thams, 2010), and many cellular elements of peripheral nerves regulate complement protein expression after injury (de Jonge et al., 2004). Complement inhibition has a variety of effects on peripheral regeneration, including acceleration of axon growth in certain situations (Ramaglia et al., 2008, 2009). Importantly, the role played by inhibitory synapses on regenerating motoneurons might be more complex than anticipated (see below). To better understand the outcomes of synapse stripping, it is important to consider first the functional changes associated with the loss of synapses in regenerating motoneurons.

The evidence for reduced excitatory synapse function on axotomized motoneurons is strong. Frequency and amplitude of spontaneous excitatory postsynaptic currents (sEPSCs) recorded in whole-cell mode *ex vivo* in brainstem slices initially increase at day 1 post-injury and then slowly decay below normal levels from 3 to 14 days postinjury in facial (Ikeda and Kato, 2005), vagal (Yamada et al., 2008), and hypoglossal rodent motoneurons (Yamada et al., 2011). The changes in frequency were large, while changes in amplitude were smaller and sometimes failed to reach significance. No changes were detected

in the size of quantal events (miniature (m)EPSCs recorded in tetrodotoxin). These results indicate a decrease in the number of presynaptic release sites or release probability without a large alteration in postsynaptic sensitivity to retained synapses. This matches the anatomical loss of synapses but is not consistent with the downregulation of postsynaptic AMPA, NMDA, and metabotropic glutamate receptors regularly reported in many different types of axotomized motoneurons (Piehl et al., 1995; Popratiloff et al., 1996; Alvarez et al., 1997, 2000; Kennis and Holstege, 1997; Tang and Sim, 1997; García Del Caño et al., 2000; Nagano et al., 2003; Eleore et al., 2005a). Reduced glutamate receptor expression is significant in rat motoneurons 7 days after axotomy coinciding with the dissolution of PSDs from excitatory synapses on the cell body. This downregulation is, however, subunit-specific, being intense for GluA2 and GluA3 but mild for GluA4, suggesting the appearance of calcium-permeable AMPA receptors in adult motoneurons (Alvarez et al., 2000; Eleore et al., 2005a). It is thus possible that while the synaptic current amplitude is not much changed in remaining synapses, their properties are significantly altered. Remarkably, AMPA receptor subunit expression returns to normal in facial, hypoglossal and spinal motoneurons 45–60 days post-axotomy even when muscle reinnervation does not occur (Kennis and Holstege, 1997; García Del Caño et al., 2000; Eleore et al., 2005a). Thus, recovery of normal AMPA receptor subunit expression is not necessarily correlated with synapse recovery, but might influence the function of retained synapses resistant to stripping. Interestingly, the time-course of AMPA subunit regulation parallels changes in regenerative capacity in rat spinal motoneurons (Fu and Gordon, 1995). This coincidence might reflect switches in the genetic program for regeneration or, perhaps more enthrallingly, a causal relationship between AMPA subunit expression and motor axon regeneration.

Changes in synaptic function recorded *ex vivo* in slices correlate with *in vivo* alterations in firing modulation of spinal and brainstem motoneurons by excitatory inputs after axotomy. Hypoglossal motoneurons show decreased firing modulation in response to excitatory inspiratory drive and hypercapnia (Sunico et al., 2005), while abducens motoneurons show decreased synaptic drive regulating firing according to eye velocity and position and vestibular input (Delgado-Garcia et al., 1988; Davis-López de Carrizosa et al., 2009, 2010). Analyses of excitatory inputs over axotomized spinal motoneurons overwhelmingly centered on analyses of the synapse between muscle-stretch sensitive Ia afferents and motoneurons in the anesthetized cat spinal cord. As will be reviewed later, the behavior of Ia-motoneuron synapses is a special case because, frequently, the presynaptic Ia sensory afferent is co-injured with the motor axon in the peripheral nerve. In situations in which the postsynaptic motoneuron is axotomized and the presynaptic Ia afferent axon left intact, the compound Ia monosynaptic EPSP showed an increase in amplitude during the first 3 days post-axotomy (Miyata and Yasuda, 1988; Seburn and Cope, 1998; Bichler et al., 2007) followed by a period in which rise time and amplitudes of the Ia EPSP gradually decreased (Eccles et al., 1958; Kuno and Llinas, 1970) and connectivity between Ia afferents and motoneurons significantly decreased (Mendell et al., 1976; see below).

In summary, there are complex changes in glutamatergic synaptic function during the first few days after axotomy that are followed by a consistent depression that correlates with the physical removal of synapses from the cell body and proximal dendrites. This should not be interpreted as a major anatomical loss of excitatory synapses, since >90% of the total input to motoneurons is distributed throughout dendrites (Rose and Neuber-Hess, 1991; Brännström, 1993; Starr and Wolpaw, 1994; Bae et al., 1999). To be sure, the dendritic arbor retracts and this occurs at the expense of distal and intermediate dendritic regions causing a 30% decrease in the available membrane at locations were excitatory synapses predominate (Sumner and Watson, 1971; Brännström et al., 1992; Brännström and Kellerth, 1998). Thus, while there is some loss of mid and distal dendritic synapses, most are retained and synaptic densities on dendrites do not change much (Delgado-Garcia et al., 1988; Brännström and Kellerth, 1998). After axotomy motoneurons also show increased excitability with decreased rheobase, increase input resistance and sometimes lower firing thresholds (reviewed in Mendell, 1984; Vanden Noven and Pinter, 1989; Titmus and Faber, 1990; González-Forero and Moreno-López, 2014). The lack of functional compensation by the synaptic drive on dendrites in these conditions is unexplained. Dendritic excitatory inputs could be affected by global changes in neurotransmitter receptor expression. Alternatively, dendritic synaptic integration mechanisms could be affected. It is well-accepted that propagation of EPSPs in the large dendritic arbors of motoneurons requires voltage-gated conductances to boost depolarizing currents and prevent their electrotonic decay before reaching the cell body (reviewed in Heckmann et al., 2005). Whether this mechanism is lost after nerve injury is unknown. Independent of mechanism, axotomy results in a period of reduced drive from glutamatergic synapses that coincides with the time the motoneuron regenerates or is attempting to regenerate its axon in the peripheral nerve. This functional depression reverts after motoneurons reinnervate muscle, in agreement with the hypothetical necessity of decreased excitatory activity on regenerating motoneurons. However, this does not mean that the motoneuron is electrically silent; GABA/glycine synapses can introduce a new source of excitatory drive, instead of further reducing it as has been assumed for decades.

The retention of inhibitory synapses on cell bodies of many types of motoneurons after axotomy, has been argued to promote inhibition. However, the function of GABA/glycine synapses depends not only on synaptic bouton numbers but also on the relative ratios of GABA and glycine release, the proportions of postsynaptic $GABA_A$ and glycine receptors, the subunit composition of $GABA_A$ receptors, the number of independent release sites and the driving forces through $GABA_A$ and glycine receptors set by the internal chloride concentration (reviewed in Alvarez, 2017). Retained inhibitory synapses undergo profound changes (summarized in **Figure 2**) that are reflected in large reductions in the frequency of spontaneous inhibitory postsynaptic currents (sIPSCs), as described over

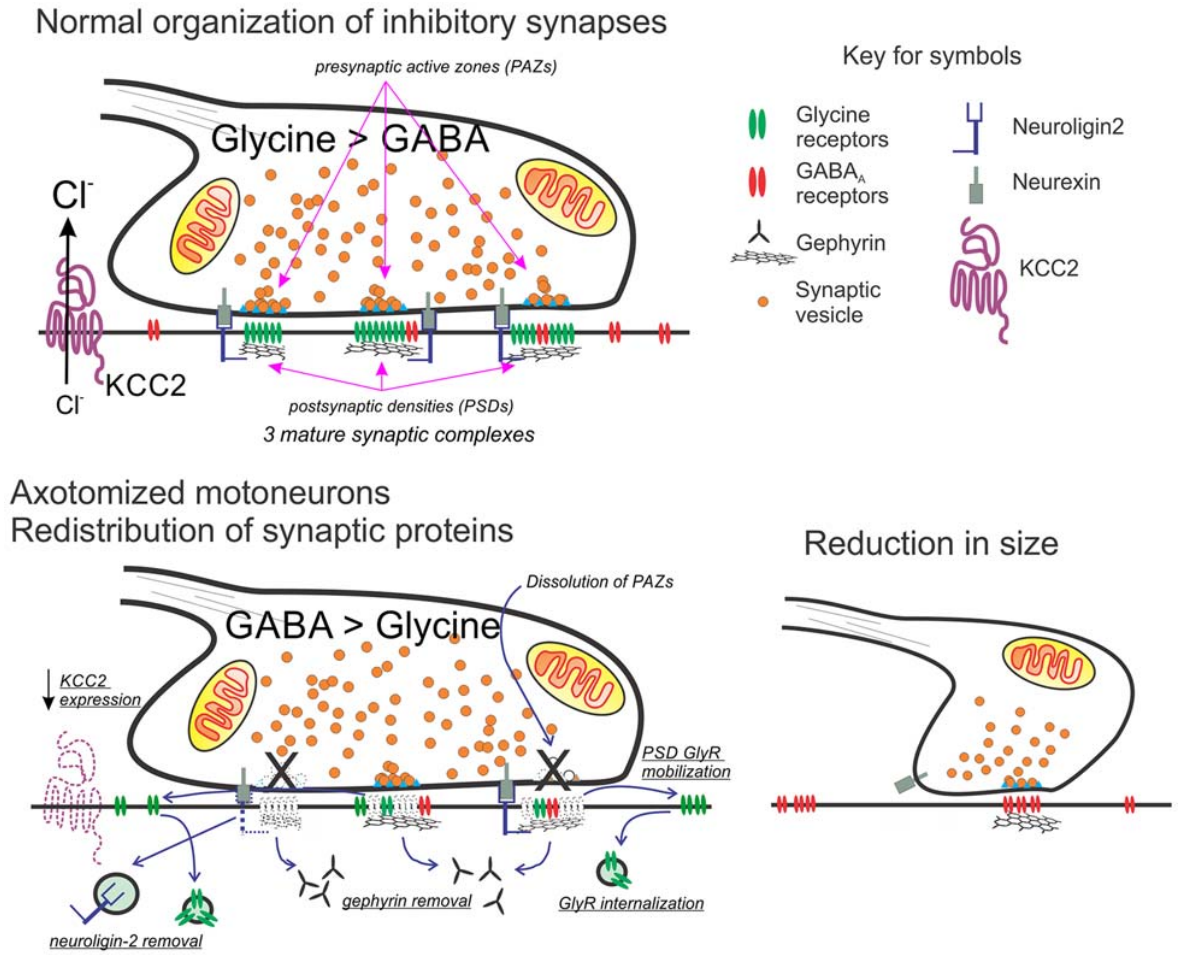

FIGURE 2 | Working model for the molecular and structural reorganization of inhibitory synapses on the cell surface of axotomized motoneurons. Top: normal organization of mixed GABA/glycine synapses on adult motoneurons. Glycine content is higher than GABA in mature synapses on the cell body of motoneurons. Each synaptic bouton forms multiple synaptic complexes (usually >6) and each has a postsynaptic density (PSD) formed by a gephyrin scaffold that co-clusters $GABA_A$ and glycine receptors, with glycine receptors at higher density in mature synapses. Neuroligin-2 interacts with gephyrin and binds presynaptic neurexin located adjacent to the release site or presynaptic active zone (PAZ). The direction of the ionic synaptic current is defined by the chloride concentration gradient maintained low intracellularly by the activity of KCC2. Bottom: after axotomy, neuroligin, gephyrin, and KCC2 are removed. Glycine receptors increase their mobility and internalization is unmatched by new membrane insertion since glycine receptor expression strongly decreases. In contrast, the expression of $GABA_A$ receptors with α2 and β2/3 subunits is maintained. In the presynaptic bouton, there is an increase in GABA synthesis. Bouton size is also reduced and contains fewer synaptic complexes and these now operate with a significant GABAergic component (see references in the text).

mouse and rat hypoglossal and vagal motoneurons recorded *ex vivo* in a whole-cell mode in slices after axotomy (Yamada et al., 2008, 2011). This functional reduction occurs even though no reduction in inhibitory synapse coverage was detected in these motoneurons in EM or immunocytochemical studies. The results agree with data *in vivo* showing lower amplitudes of IPSPs evoked in hypoglossal and trigeminal motoneurons in the anesthetized cat by stimulation of the lingual nerve or cortex (Takata, 1981; Takata and Nagahama, 1983, 1984, 1986), as well as a reduction in inhibition of spinal motoneurons after stimulation of the antagonistic muscle nerve (Kuno and Llinas, 1970). Curiously, recordings performed after axotomy in hypoglossal motoneurons found suppression of IPSPs in many motoneurons and their replacement by EPSPs (Takata and Nagahama, 1983). This was interpreted at the time as higher dysfunction in inhibitory compared to excitatory synapses, despite anatomical evidence to the contrary. Nowadays, these results can be re-interpreted considering the downregulation of the potassium chloride transporter 2 (KCC2) in axotomized motoneurons (vagal: Nabekura et al., 2002; facial: Toyoda et al., 2003; Kim et al., 2018; hypoglossal: Tatetsu et al., 2012). Similar KCC2 loss occurs throughout cell bodies and dendritic arbors of spinal motoneurons and restoration depends on signals reporting muscle innervation (Akhter et al., 2019). Thus, a potential role of KCC2 loss on motor axon regeneration was proposed. KCC2 removal causes a depolarization shift of +19 mV in E_{GABA} in facial motoneurons (Toyoda et al., 2003) and +13.4 mV

in vagal motoneurons (Nabekura et al., 2002), a difference that is probably explained by the lower basal expression of KCC2 in vagal motoneurons (Ueno et al., 2002). Analyses of facial motoneurons *ex vivo* (slices) demonstrated that this depolarization shift induces the reversal of GABA/glycine synaptic actions and appearance of low frequency spontaneous depolarizing GABA-mediated oscillations that activate NMDA and voltage-gated Ca^{2+} channels (Toyoda et al., 2003). The significance of these rhythmic GABA/NMDA/voltage-gated Ca^{2+} subthreshold calcium oscillations in adult motoneurons is currently unknown, but it is tempting to speculate that they might be part of the regeneration program. Similar rhythmic depolarizations are critical for many developmental processes including neurite growth (Ben-Ari, 2014) and are characteristic of early developing motoneurons (O'Donovan et al., 1998; Hanson et al., 2008; Czarnecki et al., 2014). Regenerating motoneurons might therefore not be electrically silent. On the contrary, they might replace high frequency glutamatergic excitatory synaptic depolarizations by low-frequency voltage oscillations that efficiently permeate calcium transients best adapted for promoting regeneration. The need for activity for optimal regeneration also agrees better with work that shows that electrical activity and exercise promote regeneration onset and axon growth speed (Gordon and English, 2016).

Axotomized motoneurons simultaneously show "inhibitory" synaptic bouton retention and lower frequency of spontaneous IPSCs, implying that release probability from retained synaptic boutons must be reduced. Individual "inhibitory" synapses on spinal and brainstem motoneuron cell bodies display multiple independent synaptic complexes, each one with an independent PAZ release site opposed by a gephyrin PSD cluster (Alvarez et al., 1997; González-Forero et al., 2004). Within this structural arrangement, a reduction in release probability likely occurs because of decreasing the number of release sites per bouton. Also, changes in $GABA_A$ and glycine receptor subunit expression have been reported in facial motoneurons after axotomy (Eleore et al., 2005b; Vassias et al., 2005). mRNAs for α1, β2 and γ2 $GABA_A$ subunits were decreased starting at day 3 post axotomy (although protein removal from the PSD lagged likely due to differences in mRNA and protein turnover). Changes in these subunits persisted through the last day of the study (60 days after injury) despite 80% re-innervation of muscle at this time point. In contrast, expression of $GABA_A$ α2, β1, and β3 subunits was unchanged. Glycine receptor α1 and β subunits were also downregulated, but this was reversed with muscle re-innervation 60 days after injury. These results suggest the disappearance of fast glycinergic currents (and the fast α1 GABA subunit) during regeneration in favor of slower GABAergic synaptic phenotypes. Also, after a transient initial decrease in presynaptic GABA synthetic machinery, these changes are overturned (Kikuchi et al., 2018) and even increased, resulting in larger than normal GABA presynaptic content (Vaughan, 1994). These changes have not been generalized to other motoneurons, but raise the possibility that injury may induce the reversal of the normal maturation of mixed GABA/glycine co-releasing synapses from early slow GABAergic mechanisms better tuned for developmental processes to later faster glycinergic mechanisms adapted to signal processing (Gao and Ziskind-Conhaim, 1995; Singer and Berger, 2000; Russier et al., 2002). Accordingly, the most apparent change of IPSPs on axotomized spinal motoneurons *in vivo* is an almost doubling of their duration (Kuno and Llinas, 1970).

Changes in inhibitory and excitatory synapses on the cell body of axotomized motoneurons might thus relate to the development of a regenerative phenotype requiring slow depolarizing GABAergic activity while simultaneously lowering fast glutamatergic and glycinergic activity and perhaps also blocking synaptic actions on dendrites from reaching the cell body. Microglia might exert modulatory actions on inhibitory synapse numbers as reviewed above, and additionally promote this functional switch. For example, LPS-activated microglia promotes a glycine to GABA conversion of synapses on spinal neurons by increasing glycine receptor membrane mobility and reducing its anchoring to the PSD, while maintaining $GABA_A$receptors. These changes are reflected in reduced glycinergic components in IPSCs with no change in the $GABA_A$ component (Cantaut-Belarif et al., 2017).

PROPRIOCEPTIVE INPUTS AXOTOMIZED IN THE PERIPHERAL NERVE UNDERGO SYNAPTIC PLASTICITY THAT IS PERMANENT AND DIFFER FROM SYNAPSE STRIPPING

One key input to spinal motoneurons arises from Ia proprioceptive afferents and, to a lesser extent, group II afferents, informing about muscle length and dynamics and respectively innervating primary and secondary endings of muscle spindles. In all species and spinal cord regions examined, Ia afferents project segmentally into medial lamina V/VI (or Clarke's Column in thoracic regions), lamina VII, and IX, where they make synapses on different kinds of interneurons and motoneurons (Brown and Fyffe, 1978; Burke et al., 1979; Ishizuka et al., 1979; Burke and Glenn, 1996; Nakayama et al., 1998; Vincent et al., 2017). In lamina IX, Ia afferents form dense synaptic arbors that make functional contacts with most motoneurons (>90%) in the homonymous motor pool (i.e., projecting to the same muscle; cat: Mendell and Henneman, 1968; rodent: Bullinger et al., 2011). They also make synapses with motoneurons innervating muscle synergists (similar motor action), though in this case the strength of the Ia EPSP and the connectivity index are both reduced (Scott and Mendell, 1976). The monosynaptic Ia-motoneuron connection forms the basis of the fast stretch-reflex and has been amply studied because its accessibility and because the reflex is easily tested and in the clinic is diagnostic of many neurological disorders characterized by hypo- or hyperreflexia.

Not surprisingly, Ia-motoneuron synapses were intensely investigated in the earliest electrophysiological studies of motoneurons after axotomy (Eccles et al., 1958, 1959; McIntyre et al., 1959; Kuno and Llinas, 1970; Mendell et al., 1974, 1976). The main observation was a reduction of the Ia EPSP

amplitude and a slowing of its rise time and time-to-peak accompanied by an increase in duration estimated by their half-widths. Similar changes were observed both in response to nerve volleys synchronously activating many Ia fibers and in response to input from single Ia fibers. The changes were consistently observed when Ia afferents were axotomized by the nerve injury, independent of whether the postsynaptic motoneuron was axotomized or not, or the distance between axotomy and the sensory afferent cell body (Eccles and McIntyre, 1953; Eccles et al., 1959; Gallego et al., 1979, 1980; Goldring et al., 1980). Specific axotomy of motoneurons (sparing presynaptic Ia afferents) resulted in more variable results. Changes in Ia EPSPs amplitude and time course were profound and rapid when the injury was proximal to the cell body, like after ventral root section (Eccles et al., 1958; Kuno and Llinas, 1970), but had a lesser and more protracted effect if the motor axon was transected at a distal location, typically close to the muscle (Eccles et al., 1959; Mendell et al., 1974, 1976; Gallego et al., 1979, 1980; Goldring et al., 1980). Changes in Ia EPSP properties were first interpreted according to the expected decay in electrical signals in passive dendrites predicted by Rall's cable-theory (Rall et al., 1967); decreased amplitudes along with slower rise times and increased half-widths of single Ia fiber EPSPs were explained as a change in the position of the synaptic input after axotomy from close to the cell body to more distal locations (Kuno and Llinas, 1970; Mendell et al., 1974). This was suggestive of the synapse stripping phenomenon. Changes in Ia EPSP properties preceded full disconnection of single Ia afferents from motoneurons (estimated by decreased percentages of motoneurons in the homonymous pool contacted by individual Ia fibers) suggesting that single Ia axons remove their proximal synapses before distal synapses and before total disconnection (Mendell et al., 1976). Similarities between Ia synapse plasticity and synaptic stripping was further supported by the recovery of Ia EPSP amplitudes after muscle re-innervation (Mendell and Scott, 1975; Gallego et al., 1980; Mendell et al., 1995).

Interpretation of the modifications of the Ia input as a case of synaptic stripping was proposed in the earliest study by Blinzinger and Kreutzberg (1968) in the facial nucleus and this view has continued unabated in reviews and commentaries to this day. However, there are important problems with this parallelism: (1) except trigeminal motoneurons (Yoshida et al., 1999), Ia afferent inputs do not exist on brainstem motoneurons, including facial motoneurons where this comparison was first made; (2) anatomically, only 1% of the synaptic coverage of motoneurons on the cell body corresponds to synapses of dorsal root origin (Conradi, 1969). Therefore, the fate of such a small proportion of synapses in EM studies was impossible to accurately predict without any means for identification; (3) the bulk of Ia synapses target dendrites (Burke et al., 1979; Brown and Fyffe, 1981; Redman and Walmsley, 1983a,b; Burke and Glenn, 1996), where they would be protected from synaptic stripping mechanisms as reviewed above; and (4) Ia EPSPs are similarly altered by damage of the presynaptic Ia afferent in the absence of motoneuron axotomy (Gallego et al., 1979).

Interpretation of changes in Ia EPSP amplitude and time course solely in terms of synapse location is more complex than initially predicted (Gustafsson and Pinter, 1984; Vanden Noven and Pinter, 1989). Moreover, direct comparisons of single Ia EPSPs with the dendritic locations of the synaptic boutons anatomically mapped on the reconstructed dendritic arbors revealed that the "unitary" Ia EPSP (from a single Ia bouton) amplitude and time course recorded at the soma is independent of dendritic location (Redman and Walmsley, 1983b). This was argued to occur because Ia synaptic conductances (postsynaptic sensitivities afforded by the number of glutamate receptor channels clustered in the PSD) were proposed to increase with distance from the cell body (Iansek and Redman, 1973; Jack et al., 1981). Another issue is that most early *in vivo* studies of Ia EPSP properties on axotomized motoneurons were done under anesthesia regimens that were later found to suppress synaptic integrative mechanisms of dendrites. These consist of voltage-gated persistent inward currents (PICs) that "boost" the amplitude of dendritic Ia synaptic currents close to four times, such that they effectively modulate firing at the initial segment (Lee and Heckman, 2000). PICs depend on neuromodulatory input arising from the brainstem which is suppressed by many forms of anesthesia (reviewed in Heckman et al., 2008). The status of Ia synapse PIC amplification after axotomy is unknown and its impact on EPSP amplitude and time course in axotomized and regenerating motoneurons needs further study.

A major problem was the lack of anatomical analyses of Ia synapses after nerve injuries. These did not occur until recently (Alvarez et al., 2010, 2011; Rotterman et al., 2014; Schultz et al., 2017) facilitated by the discovery of VGLUT1 as a marker of proprioceptive synapses in the ventral horn (Todd et al., 2003; Alvarez et al., 2004). VGLUT1 synapses in lamina IX and on motoneurons, are mostly Ia synapses, but a minority might also originate from type II afferents (Alvarez et al., 2011; Vincent et al., 2017). The synapses of Ib afferents innervating Golgi tendon organs and informing about muscle force are also VGLUT1 positive, but Ib afferents do not project to the ventral horn in cats or rodents (Brown and Fyffe, 1979; Vincent et al., 2017). Experiments in which both muscle afferents and motoneurons were simultaneously axotomized after tibial nerve injuries showed that the behavior of VGLUT1(Ia/II) synapses on motoneurons exhibited many differences with synaptic stripping and also with some of the conclusions derived from electrophysiological analyses of the Ia EPSP: VGLUT1(Ia/II) synapses are lost and reorganized throughout the whole dendritic arbor, not only the cell body, and the changes are not recoverable after the motoneuron reinnervates muscle (Alvarez et al., 2011; Rotterman et al., 2014). VGLUT1(Ia/II) synapses on rat motoneurons are normally distributed at high density in proximal and mid-distance dendrites (up to 400 μm from the cell body) with many forming tight clusters of closely grouped synapses. VGLUT1(Ia/II) synapses on distal dendrites occur at low density and in isolation from each other (Rotterman et al., 2014). Proximal VGLUT1(Ia/II) synapse clusters resemble earlier accounts of single Ia afferent axon terminal collaterals frequently establishing 2–5 closely spaced *en passant* or terminal

synaptic boutons on cat motoneuron dendrites (Brown and Fyffe, 1981; Redman and Walmsley, 1983a,b; Burke and Glenn, 1996). Parallel physiological analyses led to the conclusion that these synaptic groupings increase the strength of dendritic Ia EPSPs (Redman and Walmsley, 1983a,b). VGLUT1(Ia/II) synapse loss provokes the disappearance of synaptic clusters and the resulting synaptic organization is one of individual, isolated, VGLUT1(Ia/II) synapses occurring at low-density throughout the dendritic arbor (Rotterman et al., 2014). This predicts a non-recoverable weakening of Ia synapses and likely disconnection of individual Ia afferents from a large proportion of motoneurons.

Lack of recovery of VGLUT1(Ia/II) synapses after nerve transection and regeneration was in apparent contradiction to the general assumption that Ia EPSPs recover after muscle re-innervation. This conclusion was first derived from analyses of injuries in 5–8 days old kittens (Mendell and Scott, 1975). We now know that the first week after birth is a critical period for the developmental maturation of this input (Mentis et al., 2006; Siembab et al., 2010; Vukojicic et al., 2019) introducing significant interpretation confounds. When Ia EPSP recovery was studied in adult cats the results depend on the type of injury-inducing axotomy and the postsynaptic motoneuron tested. Ia EPSP amplitude recovery in homonymous and heteronymous connections was complete (and even above normal values) when axotomy was induced by crushing the nerve close to the muscle (Gallego et al., 1980). After nerve transection at the same location EPSP amplitudes from injured and regenerated Ia afferents onto heteronymous uninjured motoneurons recovered to around 50% of their original size (Mendell et al., 1995) while homonymous Ia EPSPs recovered much less in injury models affecting both Ia afferents and motoneurons (Eccles et al., 1959). These results agree with the good recovery of VGLUT1(Ia/II) synapses after nerve crush in rats (Schultz et al., 2017) compared to the lack of recovery when transecting the same nerve (Alvarez et al., 2011). Interestingly, recovered VGLUT1 (Ia/II) synapses following nerve crush displayed reduced presynaptic GABAergic P-boutons (Schultz et al., 2017), suggesting decreased presynaptic inhibition. In rats, the presence after regeneration of compound electrically-evoked Ia EPSPs and their normal amplitude modulation during high-frequency firing was confirmed in several studies (Haftel et al., 2005; Alvarez et al., 2011; Bullinger et al., 2011), but their exact level of recovery remained unknown because these studies were not designed to measure maximal amplitudes. Partial recovery of the compound Ia EPSP amplitude implies strengthening of remaining synapses but without physical recovery of lost synapses: single Ia afferents remain functionally disconnected from many motoneurons and VGLUT1 synapses remain depleted on motoneuron dendrites (Bullinger et al., 2011; Rotterman et al., 2014).

The loss of VGLUT1(Ia/II) synapses on motoneurons are the result of the removal of their axons from the ventral horn, not merely detachment of synapses from the membrane of axotomized motoneurons. Intra-axonal fills with neurobiotin of single afferents that regenerated and recovered muscle stretch responses typical of Ia afferents demonstrated that their central projections did not reach lamina IX. They also displayed fewer collaterals than normal in lamina VII, while their density appeared normal in lamina V and VI (Alvarez et al., 2011; Bullinger et al., 2011; Rotterman et al., 2014). Ia axon retraction towards the dorsal horn causes denervation of the motoneuron cell body and dendrites in lamina IX and VII and might prevent Ia synapse recovery after muscle re-innervation. An alternative explanation to axon retraction is that muscle spindles become reinnervated by Ib axons instead of the original Ia afferents. Ib afferents are capable of innervating vacated muscle spindles and in doing so, their responses to muscle stretch become indistinguishable from the original Ia afferents (Banks and Barker, 1989), however, Ib afferents do not project to the ventral horn. One electrophysiological study in the cat concluded that muscle spindles are reinnervated after axotomy by a random mix of Ia and Ib axons (Collins et al., 1986). In this study, Ia afferents were defined as muscle afferents with axons in the ventral horn and capable of generating field potentials in lamina IX, while Ib afferents were defined as lacking this projection and capacity. Using these criteria, 89% of afferents responding to muscle stretch were found to project to the ventral horn in normal cats, while this percentage decreased to 53% at 3 months, 50% at 6 months and 41% at 9 months after injury and repair of the cat MG nerve (Collins et al., 1986). The level of muscle re-innervation by motor axons in this model is moderate around 3 months and almost complete 9 months after injury (Foehring et al., 1986). Afferents without ventral horn projections were interpreted as Ib afferents, but many could be Ia afferents that retracted their ventral horn projections. This interpretation also fits better with the progressive loss of stretch-sensitive afferents with ventral projections, continuing even after muscle reinnervation. Regardless of the mechanism, the results suggest a dramatic drop in connectivity between Ia afferents and motoneurons in the homonymous motor pool. Similar to cats, single Ia afferents in the rat establish monosynaptic connections with >90% of motoneurons in the pool, but 6 months to 1 year after injury of the MG nerve and regeneration this percentage is only 17% (Bullinger et al., 2011). Partial transection of the MG nerve in the cat also showed a drop to 50–70% connectivity between intact Ia afferents coursing in the spared nerve region with axotomized MG motoneurons 60–77 days after injury (Mendell et al., 1974, 1976). Differences between these studies stem from the fact that Ia afferent disconnection might be more profound when both Ia afferents and motoneurons are axotomized. Also, the data in the cat study was gathered at an earlier time point and thus might not have progressed to the same level of disconnection as in the rat study.

In conclusion, nerve injury affects both Ia afferents and motoneurons, and we believe the diversity of reported functional changes in the Ia-motoneuron synapse fits reasonably well within a dual mechanism model (summarized in **Figure 3**). First, motoneuron axotomy causes Ia synapse stripping along with other excitatory synapses that are more intense when lesions are proximal to the cell body. Also, axotomy of the Ia afferent triggers a second mechanism that induces the removal of Ia axon collaterals from the ventral horn. This process has a slower time course and results in the loss of Ia synapses also from

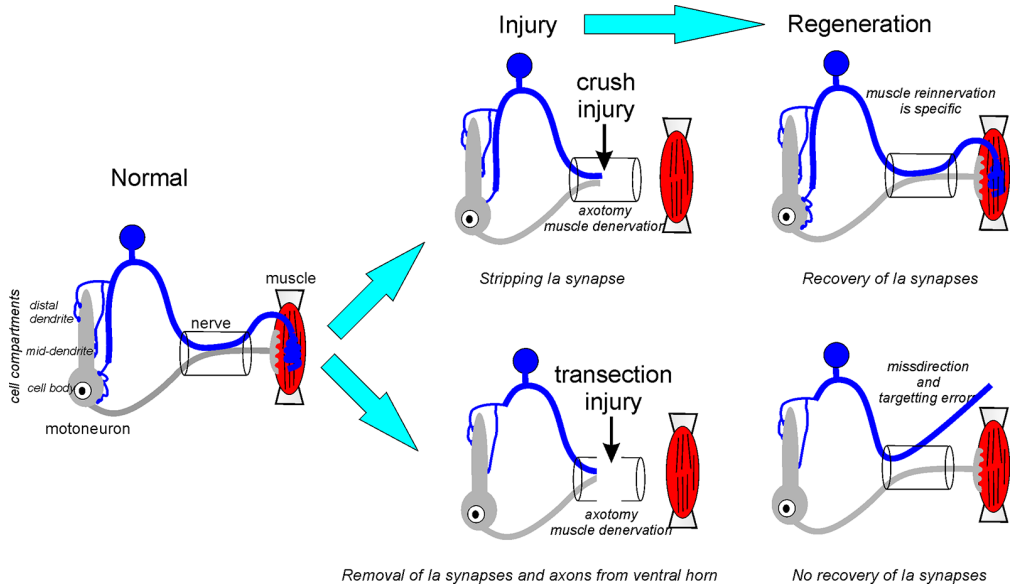

FIGURE 3 | Fate of the Ia afferents synapses after crush or transection neve injuries. After nerve crush, the continuity of endoneurial tubes is preserved and guides sensory and motor axons during regeneration to the original targets. Centrally, Ia afferent synapses undergo normal synaptic stripping after nerve crush and then recover in coincidence with axon regeneration and muscle reinnervation in the periphery. After nerve transection, continuity is lost and the sensory or motor axon (or both) can be routed to the wrong muscles. Also, Ia sensory axons targeting the correct muscle can be misguided to the wrong muscle sensory receptor and/or fail to reinnervate any muscle spindle. After nerve transection, Ia axon terminal collaterals are removed from the ventral horn causing massive and permanent denervation of motoneuron cell bodies and proximal and mid-distance dendrites where the majority of Ia synapses reside. These synapses are not recovered after muscle reinnervation resulting in an enduring loss of connectivity between Ia afferents and motoneurons.

dendrites, non-injured heteronymous motoneurons and likely other neurons in the ventral horn. This second mechanism is not reversible by muscle reinnervation and causes a permanent change in ventral horn circuitry. Ia axon die-back is dependent on the type of injury and does not occur after crush injuries. In this case, initial Ia synaptic stripping after motoneuron axotomy is reversible (**Figure 3**).

MECHANISMS OF Ia AXON REMOVAL FROM THE VENTRAL HORN AND MICROGLIA INVOLVEMENT

Genetic targeting of microglia activation after nerve injury demonstrated the necessity of specifically ventral horn microglia for permanent removal of VGLUT1(Ia/II) synapses from motoneuron cell bodies and dendrites (Rotterman et al., 2019). Abrogation of this microglia reaction rescues VGLUT1(Ia/II) synapses in regenerated motoneurons but does not prevent early transient stripping of these synapses along other excitatory synapses (labeled with VGLUT2) on the cell body. Thus, after transection nerve injuries, VGLUT1(Ia/II) synapses on the cell body of axotomized motoneurons undergo microglia-independent synapse stripping after which a different microglia-dependent mechanism induces the permanent loss of this input from dendrites.

Microglia actions are not a response to a degenerative mechanism intrinsic to the injured Ia afferent. Degeneration of central synapses and axons of trigeminal and spinal cutaneous sensory afferents axotomized by nerve injuries was detected in studies using silver-staining and/or EM to identify degenerating axons (Grant and Arvidsson, 1975; Knyihar and Csillik, 1976; Grant and Ygge, 1981; Aldskogius et al., 1985; Arvidsson et al., 1986). Some EM images even show possible microglia phagocytosis of these synapses (Arvidsson et al., 1986). The process was named "transganglionic anterograde degeneration." In some of these studies, the disintegration of central synapses was related to axotomy-induced degeneration or even cell death of certain types of sensory neurons in the dorsal root ganglion after nerve injuries. While some small afferent neurons are indeed susceptible to degeneration and cell death, the larger skin mechanoreceptors and muscle proprioceptors are not (Arvidsson et al., 1986; Tandrup et al., 2000). Accordingly, after sciatic nerve injury, most degenerating axons are concentrated in lamina III with little evidence of degeneration-associated axon argyrophilia in the projection areas of proprioceptors in the deep dorsal horn (laminae V and VI) or ventral horn (Arvidsson et al., 1986). Thus, the disappearance of ventrally directed Ia axons is unlikely to be due to degenerative processes in the axon, at least of the type associated with increased argyrophilia.

After peripheral nerve injury, microglia activation occurs in all spinal cord and brainstem areas receiving central projections from injured afferents; for sciatic nerve injuries, these include the dorsal horn, Clarke's column, and dorsal column nuclei (Eriksson et al., 1993). Some microglia activation might be associated with transganglionic degeneration of specific sensory afferents, but superficial laminae microglia activation in the

spinal cord is also related to CSF1 release from sensory afferents terminating in this region (Guan et al., 2016). Ventral horn microglia activation depends only on CSF1 released by injured motoneurons, while signals from injured proprioceptors might be minimal (Rotterman et al., 2019). The relation of dorsal and ventral horn microglia with the central projections of peripherally injured, non-degenerating large afferents, differs. Anatomical remodeling of the ventral projections of neurobiotin-filled Ia axons (Alvarez et al., 2011) is not paralleled by similar removal of dorsal horn projections of neurobiotin-filled cutaneous mechanoreceptors after nerve injury and regeneration (Koerber et al., 2006). This also agrees with the maintenance of dorsal horn projections from injured proprioceptors. Dorsal and ventral microglia may interact differently with central axons of sensory afferents injured in the peripheral nerve and emerging data suggest that many properties of microglia after nerve injury differ between dorsal and ventral horns (Akhter et al., 2019; Rotterman et al., 2019).

The mechanism by which activated ventral microglia recognizes the spinal projections of Ia afferents injured in the periphery is unknown. During normal development, microglia-dependent synaptic pruning of excess VGLUT1(Ia/II) synapses occurs at specific postnatal critical periods through C1q opsonization (Vukojicic et al., 2019). C1q targets ineffective or silent synapses, and an exaggeration of this mechanism was proposed to be responsible for the loss of Ia afferent inputs on motoneurons in a mouse model of spinal muscular atrophy (Mentis et al., 2011; Vukojicic et al., 2019). C1q removal did not alter synapse stripping after nerve injury in adult mice (Berg et al., 2012), but this study did not analyze VGLUT1(Ia/II) synaptic plasticity. This possibility thus needs to be tested, particularly because of the long silent period expected for Ia afferent synapses disconnected from their peripheral sensory organs. Nonetheless, chronic silencing of Ia afferents with tetrodotoxin applied to the peripheral nerve did not mimic the changes in Ia EPSPs found after injury (Gallego et al., 1979), and Ia axon removal after injury may differ in mechanism from developmental Ia synapse pruning.

In adults, a role was proposed for signaling between ventral microglia and the peripheral immune system through chemokine (C-C motif) ligand 2 (CCL2) activation of its receptor, CCR2 (Rotterman et al., 2019). In global CCR2 KOs, VGLUT1(Ia/II) synapses on dendrites were preserved while synapses on the cell body showed a trend towards preservation that did not reach significance. CCL2 upregulation in axotomized motoneurons was first shown in the facial nucleus (Flugel et al., 2001). CCL2 is also upregulated by sensory afferents in the dorsal root ganglion (Niemi et al., 2013, 2016) and by reactive Schwann cells (Carroll and Frohnert, 1998; Toews et al., 1998; Taskinen and Röyttä, 2000; Subang and Richardson, 2001). At these peripheral locations, CCL2 recruits CCR2-expressing immune cells. Interference with this mechanism affects sensory afferent axon growth in the regenerating nerve and the removal of debris from cut distal axon segments during Wallerian degeneration (reviewed by Zigmond and Echevarria, 2019). CCR2 activation inside the CNS is related to the recruitment of blood-derived immune cells after a variety of injuries or pathologies (Ransohoff, 2009). In the spinal cord, CCL2 exerts a variety of actions, including promoting nociceptive responses in the dorsal horn after nerve injury (Van Steenwinckel et al., 2011), removing damaged myelinated axons after spinal cord injury (Ma et al., 2002; McPhail et al., 2004; Evans et al., 2014) and promoting the breakdown of the blood spinal cord barrier (Echeverry et al., 2011). Infiltration of CCR2 positive immune cells was specifically observed in the ventral horn and only after nerve injuries causing maximal loss of VGLUT1(Ia/II) synapses (Rotterman et al., 2019). Their significance during the removal of ventral Ia axons remains to be fully explored.

FUNCTIONAL CONSEQUENCES OF THE REMOVAL OF Ia AFFERENT INPUT FOR MOTOR CONTROL OF BEHAVIORS

The most direct consequence of reduced Ia input on motoneurons is the loss of stretch reflexes. This was first analyzed in a study prompted by the large number of nerve injuries after World War II (Barker and Young, 1947). The goal was to identify differences amongst nerve injuries that could predict better or worse motor function recovery after regeneration. The authors tested the knee stretch reflex in rabbits after nerve crush or transection by measuring the strength of the kick following a tap on the patellar tendon. They found that the stretch reflex recovers (and overshoots) after nerve crush, but never recovers after transection, while muscle force similarly recovers after both injuries. This fits well with data on the Ia-motoneuron synapse reviewed above, but surprisingly the study was largely ignored. The lack of stretch reflexes after recovery from nerve transections was re-discovered in cats years later using electrophysiological methods (Cope and Clark, 1993; Cope et al., 1994) and was also confirmed in rodents (Haftel et al., 2005). The better recovery and even overshoot of stretch reflexes after nerve crush was also replicated in cat experiments (Cope and Clark, 1993; Prather et al., 2011) and agrees with the preservation of VGLUT1(Ia/II) synapses in rats following nerve crush (Schultz et al., 2017).

In contrast, the partial recovery of electrically-evoked Ia EPSPs following nerve transections does not match well with the lack of stretch reflexes after regeneration. The response of motoneurons to naturally evoked stretch synaptic potentials (SSPs) was found to correlate better with reflex function than Ia EPSP responses elicited by electrical stimulation. Thus, while all regenerated motoneurons display Ia EPSPs evoked by electrical afferent volleys in the nerve, many lack SSPs or these are strongly reduced (Haftel et al., 2005; Bullinger et al., 2011). This occurs despite normal stretch afferent responses recorded in dorsal roots entering the spinal cord. In contrast, after nerve crush, SSPs recovered to 75% of their normal size (Prather et al., 2011). One possible explanation is that after nerve transection injuries many Ia afferents fail to reinnervate muscle spindles and although they are recruited in electrically-evoked Ia EPSPs they cannot contribute to stretch-evoked responses. A working model was proposed suggesting a combination of peripheral deficits in spindle innervation and central deficits in

Ia synapses and/or their integration in dendrites to fully explain the phenomenon (Alvarez et al., 2010; Bullinger et al., 2011; Vincent et al., 2015).

The stretch reflex is just an easily testable motor behavior of the efficacy of Ia inputs modulating spinal motor output. Its absence, however, implies that ventral horn motor circuitries operate without Ia feedback about muscle lengths and dynamics after regeneration from nerve transections, thus affecting many critical spinal control mechanisms. Accordingly, motor tasks involving high forces and/or rapid and large muscle lengthening (steep slopes) show deficits (Abelew et al., 2000; Maas et al., 2007; Sabatier et al., 2011b; Lyle et al., 2017; Chang et al., 2018). Moreover, the lack of effective Ia inputs in the ventral horn might also affect circuitries like reciprocal inhibition and explain the presence of reciprocal excitation between antagonistic muscles and higher co-contraction and joint stiffness during motor function following regeneration from nerve transections (Sabatier et al., 2011a; Horstman et al., 2019; see Figure 10 in Horstman et al., 2019 for putative circuit mechanisms). Why would this occur after nerve transection but not after nerve crush? Nerve crush preserves continuity in the guiding endoneurial tubes that direct regenerating axons towards the original targets and therefore are characterized by more rapid and specific regeneration compared to the slow and rather poor regeneration specificity after nerve transection (Brushart and Mesulam, 1980; Bodine-Fowler et al., 1997; Valero-Cabré et al., 2004). Peripheral targeting errors must necessarily scramble motor pool organization in the spinal cord and the specific patterns of Ia connections with homonymous and heteronymous motoneurons while avoiding antagonists. This could render Ia connectivity in the ventral horn dysfunctional. Perhaps, evolutionary forces directed the appearance of mechanisms that recognize signals in the periphery correlated with injury severity such that synaptic reorganizations of Ia afferent connections induced by central microglia-neuroinflammation are scaled to the different levels of ambiguity in regeneration specificity in the periphery after different types of nerve injuries.

CONCLUSIONS

The reviewed data fits with a model considering two types of synaptic plasticity after nerve injury. One is a cell-autonomous mechanism that sheds synapses from the cell body (synaptic stripping) and affects GABA/glycine and glutamatergic synapses to different levels in different motoneurons according to modulatory influences from neighboring glial, local neurotrophic factors and the intrinsic susceptibility of different inputs to detachment. A second mechanism is microglia-dependent and induces the retraction from the ventral horn of axon collaterals and synapses originating from axons injured in the peripheral nerve. The degree of axon removal is governed by the type and location of the nerve injury and after removal, there is no recovery of these connections. This mechanism affects the ventral horn collaterals of muscle proprioceptors injured in the periphery, and probably also the intraspinal collaterals of motor axons (Havton and Kellerth, 1990). Thus, after nerve regeneration, the spinal cord ventral horn operates without feedback about muscle length (proprioceptive synapses) or motor output (recurrent motor axon collaterals) causing long-lasting changes in motor function. The extent to which the loss of these inputs represents an undesirable outcome affecting motor function recovery or an adaptive mechanism that optimizes central connections to the vagaries of jumbled connectivity in the periphery after regeneration is unknown and currently under investigation.

AUTHOR CONTRIBUTIONS

FA wrote the manuscript and designed the figures. TR compiled literature regarding synaptic stripping, microglia and provided the primary data on Ia afferent and motor axon plasticity. EA compiled the literature on KCC2 and inhibitory synaptic function after axotomy and provided some of the data on synaptic stripping. AL provided some of the primary data on synaptic stripping after preventing microglia reactions. TR, EA, and AL revised the manuscript. TC and AE were involved in the genesis of some ideas in this review.

FUNDING

This work was funded by National Institutes of Health (NIH) grants R56NS099092 to FA and R21NS114839 to FA and AE, Ruth L. Kirschstein National Research Service Awards F31NS095528 and F32NS112556 to TR and a National Science Foundation Graduate Fellowship DGE-1444932 to EA.

ACKNOWLEDGMENTS

We also thank Drs. Angel M. Pastor and Rosa de la Cruz (Department of Physiology, University of Seville) for comments on an earlier version of this manuscript. We wish to dedicate this review to Professor Staffan Cullheim from the Karolinska Institute for his remarkable contributions to the field without which the progress reviewed here will have not been possible.

REFERENCES

Abelew, T. A., Miller, M. D., Cope, T. C., and Nichols, T. R. (2000). Local loss of proprioception results in disruption of interjoint coordination during locomotion in the cat. *J. Neurophysiol.* 84, 2709–2714. doi: 10.1152/jn.2000.84.5.2709

Akhter, E. T., Griffith, R. W., English, A. W., and Alvarez, F. J. (2019). Removal of the potassium chloride co-transporter from the somatodendritic membrane of axotomized motoneurons is independent of BDNF/TrkB signaling but is controlled by neuromuscular innervation. *eNeuro* 6:ENEURO.0172-19.2019. doi: 10.1523/eneuro.0172-19.2019

Aldskogius, H. (2011). Mechanisms and consequences of microglial responses to peripheral axotomy. *Front. Biosci.* 3, 857–868. doi: 10.2741/192

Aldskogius, H., Arvidsson, J., and Grant, G. (1985). The reaction of primary sensory neurons to peripheral nerve injury with particular emphasis

on transganglionic changes. *Brain Res.* 357, 27–46. doi: 10.1016/0165-0173(85)90006-2

Aldskogius, H., and Kozlova, E. N. (1998). Central neuron-glial and glial-glial interactions following axon injury. *Prog. Neurobiol.* 55, 1–26. doi: 10.1016/s0301-0082(97)00093-2

Allodi, I., Udina, E., and Navarro, X. (2012). Specificity of peripheral nerve regeneration: interactions at the axon level. *Prog. Neurobiol.* 98, 16–37. doi: 10.1016/j.pneurobio.2012.05.005

Alvarez, F. J. (2017). Gephyrin and the regulation of synaptic strength and dynamics at glycinergic inhibitory synapses. *Brain Res. Bull.* 129, 50–65. doi: 10.1016/j.brainresbull.2016.09.003

Alvarez, F. J., Bullinger, K. L., Titus, H. E., Nardelli, P., and Cope, T. C. (2010). Permanent reorganization of Ia afferent synapses on motoneurons after peripheral nerve injuries. *Ann. N Y Acad. Sci.* 1198, 231–241. doi: 10.1111/j.1749-6632.2010.05459.x

Alvarez, F. J., Dewey, D. E., Carr, P. A., Cope, T. C., and Fyffe, R. E. (1997). Downregulation of metabotropic glutamate receptor 1a in motoneurons after axotomy. *Neuroreport* 8, 1711–1716. doi: 10.1097/00001756-199705060-00029

Alvarez, F. J., Fyffe, R. E., Dewey, D. E., Haftel, V. K., and Cope, T. C. (2000). Factors regulating AMPA-type glutamate receptor subunit changes induced by sciatic nerve injury in rats. *J. Comp. Neurol.* 426, 229–242. doi: 10.1002/1096-9861(20001016)426:2<229::aid-cne5>3.0.co;2-w

Alvarez, F. J., Titus-Mitchell, H. E., Bullinger, K. L., Kraszpulski, M., Nardelli, P., and Cope, T. C. (2011). Permanent central synaptic disconnection of proprioceptors after nerve injury and regeneration: I. Loss of VGLUT1/IA synapses on motoneurons. *J. Neurophysiol.* 106, 2450–2470. doi: 10.1152/jn.01095.2010

Alvarez, F. J., Villalba, R. M., Zerda, R., and Schneider, S. P. (2004). Vesicular glutamate transporters in the spinal cord, with special reference to sensory primary afferent synapses. *J. Comp. Neurol.* 472, 257–280. doi: 10.1002/cne.20012

Arbat-Plana, A., Cobianchi, S., Herrando-Grabulosa, M., Navarro, X., and Udina, E. (2017). Endogenous modulation of TrkB signaling by treadmill exercise after peripheral nerve injury. *Neuroscience* 340, 188–200. doi: 10.1016/j.neuroscience.2016.10.057

Arvidsson, J., Ygge, J., and Grant, G. (1986). Cell loss in lumbar dorsal root ganglia and transganglionic degeneration after sciatic nerve resection in the rat. *Brain Res.* 373, 15–21. doi: 10.1016/0006-8993(86)90310-0

Bae, Y. C., Nakamura, T., Ihn, H. J., Choi, M. H., Yoshida, A., Moritani, M., et al. (1999). Distribution pattern of inhibitory and excitatory synapses in the dendritic tree of single masseter α-motoneurons in the cat. *J. Comp. Neurol.* 414, 454–468. doi: 10.1002/(sici)1096-9861(19991129)414:4<454::aid-cne3>3.0.co;2-7

Banks, R. W., and Barker, D. (1989). Specificities of afferents reinnervating cat muscle spindles after nerve section. *J. Physiol.* 408, 345–372. doi: 10.1113/jphysiol.1989.sp017463

Barker, D., and Young, J. Z. (1947). Recovery of stretch reflexes after nerve injury. *Lancet* 1, 704–707. doi: 10.1016/s0140-6736(47)91454-2

Barron, K. D. (1989). "Neuronal responses to axotomy: consequences and possibilities for rescue from permanent atrophy or cell death," in *Neural Regeneration and Transplantation*, ed. F. J. Seil (New York, NY: Liss), 79–99.

Ben-Ari, Y. (2014). The GABA excitatory/inhibitory developmental sequence: a personal journey. *Neuroscience* 279, 187–219. doi: 10.1016/j.neuroscience.2014.08.001

Benítez-Temiño, B., Davis-López de Carrizosa, M. A., Morcuende, S., Matarredona, E. R., de la Cruz, R. R., and Pastor, A. M. (2016). Functional diversity of neurotrophin actions on the oculomotor system. *Int. J. Mol. Sci.* 17:E2016. doi: 10.3390/ijms17122016

Berg, A., Zelano, J., and Cullheim, S. (2010). Netrin G-2 ligand mRNA is downregulated in spinal motoneurons after sciatic nerve lesion. *Neuroreport* 21, 782–785. doi: 10.1097/wnr.0b013e32833cadd8

Berg, A., Zelano, J., Stephan, A., Thams, S., Barres, B. A., Pekny, M., et al. (2012). Reduced removal of synaptic terminals from axotomized spinal motoneurons in the absence of complement C3. *Exp. Neurol.* 237, 8–17. doi: 10.1016/j.expneurol.2012.06.008

Berg, A., Zelano, J., Thams, S., and Cullheim, S. (2013). The extent of synaptic stripping of motoneurons after axotomy is not correlated to activation of surrounding glia or downregulation of postsynaptic adhesion molecules. *Neural Dev.* 8:e59647. doi: 10.1371/journal.pone.0059647

Bichler, E. K., Nakanishi, S. T., Wang, Q. B., Pinter, M. J., Rich, M. M., and Cope, T. C. (2007). Enhanced transmission at a spinal synapse triggered *in vivo* by an injury signal independent of altered synaptic activity. *J. Neurosci.* 27, 12851–12859. doi: 10.1523/JNEUROSCI.1997-07.2007

Bigotte, L., and Olsson, Y. (1983). Cytotoxic effects of adriamycin on mouse hypoglossal neurons following retrograde axonal transport from the tongue. *Acta Neuropathol.* 61, 161–168. doi: 10.1007/bf00691980

Bigotte, L., and Olsson, Y. (1984). Cytotoxic effects of adriamycin on the central nervous system of the mouse—cytofluorescence and electron-microscopic observations after various modes of administration. *Acta Neurol. Scand. Suppl.* 100, 55–67.

Bigotte, L., and Olsson, Y. (1987). Degeneration of trigeminal ganglion neurons caused by retrograde axonal transport of doxorubicin. *Neurology* 37, 985–992. doi: 10.1212/wnl.37.6.985

Blinzinger, K., and Kreutzberg, G. (1968). Displacement of synaptic terminals from regenerating motoneurons by microglial cells. *Z. Zellforsch. Mikrosk. Anat.* 85, 145–157. doi: 10.1007/bf00325030

Bodine-Fowler, S. C., Meyer, R. S., Moskovitz, A., Abrams, R., and Botte, M. J. (1997). Inaccurate projection of rat soleus motoneurons: a comparison of nerve repair techniques. *Muscle Nerve* 20, 29–37. doi: 10.1002/(sici)1097-4598(199701)20:1<29::aid-mus4>3.0.co;2-j

Brännström, T. (1993). Quantitative synaptology of functionally different types of cat medial gastrocnemius α-motoneurons. *J. Comp. Neurol.* 330, 439–454. doi: 10.1002/cne.903300311

Brännström, T., Havton, L., and Kellerth, J. O. (1992). Changes in size and dendritic arborization patterns of adult cat spinal α-motoneurons following permanent axotomy. *J. Comp. Neurol.* 318, 439–451. doi: 10.1002/cne.903180408

Brännström, T., and Kellerth, J. O. (1998). Changes in synaptology of adult cat spinal α-motoneurons after axotomy. *Exp. Brain Res.* 118, 1–13. doi: 10.1007/s002210050249

Brännström, T., and Kellerth, J. O. (1999). Recovery of synapses in axotomized adult cat spinal motoneurons after reinnervation into muscle. *Exp. Brain Res.* 125, 19–27. doi: 10.1007/s002210050653

Brown, A. G., and Fyffe, R. E. (1978). The morphology of group Ia afferent fibre collaterals in the spinal cord of the cat. *J. Physiol.* 274, 111–127. doi: 10.1113/jphysiol.1978.sp012137

Brown, A. G., and Fyffe, R. E. (1979). The morphology of group Ib afferent fibre collaterals in the spinal cord of the cat. *J. Physiol.* 296, 215–226. doi: 10.1113/jphysiol.1979.sp013001

Brown, A. G., and Fyffe, R. E. (1981). Direct observations on the contacts made between Ia afferent fibres and α-motoneurones in the cat's lumbosacral spinal cord. *J. Physiol.* 313, 121–140. doi: 10.1113/jphysiol.1981.sp013654

Brushart, T. M. (2011). *Nerve Repair*. New York, NY: Oxford University Press.

Brushart, T. M., and Mesulam, M. M. (1980). Alteration in connections between muscle and anterior horn motoneurons after peripheral nerve repair. *Science* 208, 603–605. doi: 10.1126/science.7367884

Bullinger, K. L., Nardelli, P., Pinter, M. J., Alvarez, F. J., and Cope, T. C. (2011). Permanent central synaptic disconnection of proprioceptors after nerve injury and regeneration: II. Loss of functional connectivity with motoneurons. *J. Neurophysiol.* 106, 2471–2485. doi: 10.1152/jn.01097.2010

Burke, R. E., and Glenn, L. L. (1996). Horseradish peroxidase study of the spatial and electrotonic distribution of group Ia synapses on type-identified ankle extensor motoneurons in the cat. *J. Comp. Neurol.* 372, 465–485. doi: 10.1002/(sici)1096-9861(19960826)372:3<465::aid-cne9>3.0.co;2-0

Burke, R. E., Walmsley, B., and Hodgson, J. A. (1979). HRP anatomy of group Ia afferent contacts on α motoneurones. *Brain Res.* 160, 347–352. doi: 10.1016/0006-8993(79)90430-x

Calvo, P. M., de la Cruz, R. R., and Pastor, A. M. (2018). Synaptic loss and firing alterations in Axotomized Motoneurons are restored by vascular endothelial growth factor (VEGF) and VEGF-B. *Exp. Neurol.* 304, 67–81. doi: 10.1016/j.expneurol.2018.03.004

Cantaut-Belarif, Y., Antri, M., Pizzarelli, R., Colasse, S., Vaccari, I., Soares, S., et al. (2017). Microglia control the glycinergic but not the GABAergic synapses *via* prostaglandin E2 in the spinal cord. *J. Cell Biol.* 216, 2979–2989. doi: 10.1083/jcb.201607048

Carlstedt, T., and Cullheim, S. (2000). Spinal cord motoneuron maintenance, injury and repair. *Prog. Brain Res.* 127, 501–514. doi: 10.1016/s0079-6123(00)27025-8

Carroll, S. L., and Frohnert, P. W. (1998). Expression of *JE* (monocyte chemoattractant protein-1) is induced by sciatic axotomy in wild type rodents but not in C57BL/Wld^s mice. *J. Neuropathol. Exp. Neurol.* 57, 915–930. doi: 10.1097/00005072-199810000-00004

Cartarozzi, L. P., Perez, M., Kirchhoff, F., and Oliveira, A. L. R. (2019). Role of MHC-I expression on spinal motoneuron survival and glial reactions following ventral root crush in mice. *Cells* 8:E483. doi: 10.3390/cells8050483

Chang, Y. H., Housley, S. N., Hart, K. S., Nardelli, P., Nichols, R. T., Maas, H., et al. (2018). Progressive adaptation of whole-limb kinematics after peripheral nerve injury. *Biol. Open* 7:bio028852. doi: 10.1242/bio.028852

Che, Y. H., Tamatani, M., and Tohyama, M. (2000). Changes in mRNA for post-synaptic density-95 (PSD-95) and carboxy-terminal PDZ ligand of neuronal nitric oxide synthase following facial nerve transection. *Mol. Brain Res.* 76, 325–335. doi: 10.1016/s0169-328x(00)00013-9

Chen, D. H. (1978). Qualitative and quantitative study of synaptic displacement in chromatolyzed spinal motoneurons of the cat. *J. Comp. Neurol.* 177, 635–664. doi: 10.1002/cne.901770407

Chen, D. H., Chambers, W. W., and Liu, C. N. (1977). Synaptic displacement in intracentral neurons of Clarke's nucleus following axotomy in the cat. *Exp. Neurol.* 57, 1026–1041. doi: 10.1016/0014-4886(77)90125-x

Chen, Z., Jalabi, W., Hu, W., Park, H. J., Gale, J. T., Kidd, G. J., et al. (2014). Microglial displacement of inhibitory synapses provides neuroprotection in the adult brain. *Nat. Commun.* 5:4486. doi: 10.1038/ncomms5486

Chen, Z., and Trapp, B. D. (2016). Microglia and neuroprotection. *J. Neurochem.* 136, 10–17. doi: 10.1111/jnc.13062

Collins, W. F. III., Mendell, L. M., and Munson, J. B. (1986). On the specificity of sensory reinnervation of cat skeletal muscle. *J. Physiol.* 375, 587–609. doi: 10.1113/jphysiol.1986.sp016135

Conradi, S. (1969). Ultrastructure of dorsal root boutons on lumbosacral motoneurons of the adult cat, as revealed by dorsal root section. *Acta Physiol. Scand. Suppl.* 332, 85–115.

Cope, T. C., Bonasera, S. J., and Nichols, T. R. (1994). Reinnervated muscles fail to produce stretch reflexes. *J. Neurophysiol.* 71, 817–820. doi: 10.1152/jn.1994.71.2.817

Cope, T. C., and Clark, B. D. (1993). Motor-unit recruitment in self-reinnervated muscle. *J. Neurophysiol.* 70, 1787–1796. doi: 10.1152/jn.1993.70.5.1787

Corriveau, R. A., Huh, G. S., and Shatz, C. J. (1998). Regulation of class I MHC gene expression in the developing and mature CNS by neural activity. *Neuron* 21, 505–520. doi: 10.1016/s0896-6273(00)80562-0

Cova, J. L., and Aldskogius, H. (1984). Effect of nerve section on perineuronal glial cells in the CNS of rat and cat. *Anat. Embryol.* 169, 303–307. doi: 10.1007/bf00315635

Cova, J. L., and Aldskogius, H. (1985). A morphological study of glial cells in the hypoglossal nucleus of the cat during nerve regeneration. *J. Comp. Neurol.* 233, 421–428. doi: 10.1002/cne.902330402

Cova, J. L., and Aldskogius, H. (1986). Effect of axotomy on perineuronal glial cells in the hypoglossal and dorsal motor vagal nuclei of the cat. *Exp. Neurol.* 93, 662–667. doi: 10.1016/0014-4886(86)90187-1

Craig, A. M., and Kang, Y. (2007). Neurexin-neuroligin signaling in synapse development. *Curr. Opin. Neurobiol.* 17, 43–52. doi: 10.1016/j.conb.2007.01.011

Cull, R. E. (1974). Role of nerve-muscle contact in maintaining synaptic connections. *Exp. Brain Res.* 20, 307–310. doi: 10.1007/bf00238321

Cullheim, S., and Thams, S. (2007). The microglial networks of the brain and their role in neuronal network plasticity after lesion. *Brain Res. Rev.* 55, 89–96. doi: 10.1016/j.brainresrev.2007.03.012

Cullheim, S., and Thams, S. (2010). Classic major histocompatibility complex class I molecules: new actors at the neuromuscular junction. *Neuroscientist* 16, 600–607. doi: 10.1177/1073858410381534

Czarnecki, A., Le Corronc, H., Rigato, C., Le Bras, B., Couraud, F., Scain, A. L., et al. (2014). Acetylcholine controls GABA-, glutamate-, and glycine-dependent giant depolarizing potentials that govern spontaneous motoneuron activity at the onset of synaptogenesis in the mouse embryonic spinal cord. *J. Neurosci.* 34, 6389–6404. doi: 10.1523/JNEUROSCI.2664-13.2014

Davis-López de Carrizosa, M. A., Morado-Díaz, C. J., Morcuende, S., de la Cruz, R. R., and Pastor, A. M. (2010). Nerve growth factor regulates the firing patterns and synaptic composition of motoneurons. *J. Neurosci.* 30, 8308–8319. doi: 10.1523/JNEUROSCI.0719-10.2010

Davis-López de Carrizosa, M. A., Morado-Díaz, C. J., Tena, J. J., Benítez-Temiño, B., Pecero, M. L., Morcuende, S. R., et al. (2009). Complementary actions of BDNF and neurotrophin-3 on the firing patterns and synaptic composition of motoneurons. *J. Neurosci.* 29, 575–587. doi: 10.1523/JNEUROSCI.5312-08.2009

de Jonge, R. R., van Schaik, I. N., Vreijling, J. P., Troost, D., and Baas, F. (2004). Expression of complement components in the peripheral nervous system. *Hum. Mol. Genet.* 13, 295–302. doi: 10.1093/hmg/ddh029

de la Cruz, R. R., Pastor, A. M., and Delgado-García, J. M. (1994). Effects of target depletion on adult mammalian central neurons: morphological correlates. *Neuroscience* 58, 59–79. doi: 10.1016/0306-4522(94)90156-2

de la Cruz, R. R., Pastor, A. M., and Delgado-García, J. M. (1996). Influence of the postsynaptic target on the functional properties of neurons in the adult mammalian central nervous system. *Rev. Neurosci.* 7, 115–149. doi: 10.1515/revneuro.1996.7.2.115

Delgado-Garcia, J. M., Del Pozo, F., Spencer, R. F., and Baker, R. (1988). Behavior of neurons in the abducens nucleus of the alert cat—III. Axotomized motoneurons. *Neuroscience* 24, 143–160. doi: 10.1016/0306-4522(88)90319-3

Eccles, J. C., Krnjevic, K., and Miledi, R. (1959). Delayed effects of peripheral severance of afferent nerve fibres on the efficacy of their central synapses. *J. Physiol.* 145, 204–220. doi: 10.1113/jphysiol.1959.sp006136

Eccles, J. C., Libet, B., and Young, R. R. (1958). The behaviour of chromatolysed motoneurones studied by intracellular recording. *J. Physiol.* 143, 11–40. doi: 10.1113/jphysiol.1958.sp006041

Eccles, J. C., and McIntyre, I. A. (1953). The effects of disuse and of activity on mammalian spinal reflexes. *J. Physiol.* 121, 492–516. doi: 10.1113/jphysiol.1953.sp004961

Echeverry, S., Shi, X. Q., Rivest, S., and Zhang, J. (2011). Peripheral nerve injury alters blood-spinal cord barrier functional and molecular integrity through a selective inflammatory pathway. *J. Neurosci.* 31, 10819–10828. doi: 10.1523/jneurosci.1642-11.2011

Eleore, L., Vassias, I., Vidal, P. P., and de Waele, C. (2005a). Modulation of the glutamatergic receptors (AMPA and NMDA) and of glutamate vesicular transporter 2 in the rat facial nucleus after axotomy. *Neuroscience* 136, 147–160. doi: 10.1016/j.neuroscience.2005.06.026

Eleore, L., Vassias, I., Vidal, P. P., Triller, A., and de Waele, C. (2005b). Modulation of glycine receptor subunits and gephyrin expression in the rat facial nucleus after axotomy. *Eur. J. Neurosci.* 21, 669–678. doi: 10.1111/j.1460-9568.2005.03887.x

Emirandetti, A., Graciele Zanon, R., Sabha, M. Jr., and de Oliveira, A. L. (2006). Astrocyte reactivity influences the number of presynaptic terminals apposed to spinal motoneurons after axotomy. *Brain Res.* 1095, 35–42. doi: 10.1016/j.brainres.2006.04.021

Eriksson, N. P., Persson, J. K., Svensson, M., Arvidsson, J., Molander, C., and Aldskogius, H. (1993). A quantitative analysis of the microglial cell reaction in central primary sensory projection territories following peripheral nerve injury in the adult rat. *Exp. Brain Res.* 96, 19–27. doi: 10.1007/bf00230435

Eroglu, C., and Barres, B. A. (2010). Regulation of synaptic connectivity by glia. *Nature* 468, 223–231. doi: 10.1038/nature09612

Evans, T. A., Barkauskas, D. S., Myers, J. T., Hare, E. G., You, J. Q., Ransohoff, R. M., et al. (2014). High-resolution intravital imaging reveals that blood-derived macrophages but not resident microglia facilitate secondary axonal dieback in traumatic spinal cord injury. *Exp. Neurol.* 254, 109–120. doi: 10.1016/j.expneurol.2014.01.013

Flugel, A., Hager, G., Horvat, A., Spitzer, C., Singer, G. M., Graeber, M. B., et al. (2001). Neuronal MCP-1 expression in response to remote nerve injury. *J. Cereb. Blood Flow Metab.* 21, 69–76. doi: 10.1097/00004647-200101000-00009

Foehring, R. C., Sypert, G. W., and Munson, J. B. (1986). Properties of self-reinnervated motor units of medial gastrocnemius of cat: II. Axotomized

motoneurons and time course of recovery. *J. Neurophysiol.* 55, 947–965. doi: 10.1152/jn.1986.55.5.947

Freria, C. M., Velloso, L. A., and Oliveira, A. L. (2012). Opposing effects of Toll-like receptors 2 and 4 on synaptic stability in the spinal cord after peripheral nerve injury. *J. Neuroinflammation* 9:240. doi: 10.1186/1742-2094-9-240

Fu, S. Y., and Gordon, T. (1995). Contributing factors to poor functional recovery after delayed nerve repair: prolonged axotomy. *J. Neurosci.* 15, 3876–3885. doi: 10.1523/JNEUROSCI.15-05-03876.1995

Gallego, R., Kuno, M., Núñez, R., and Snider, W. D. (1979). Disuse enhances synaptic efficacy in spinal mononeurones. *J. Physiol.* 291, 191–205. doi: 10.1113/jphysiol.1979.sp012807

Gallego, R., Kuno, M., Núñez, R., and Snider, W. D. (1980). Enhancement of synaptic function in cat motoneurones during peripheral sensory regeneration. *J. Physiol.* 306, 205–218. doi: 10.1113/jphysiol.1980.sp013392

Gao, B. X., and Ziskind-Conhaim, L. (1995). Development of glycine- and GABA-gated currents in rat spinal motoneurons. *J. Neurophysiol.* 74, 113–121. doi: 10.1152/jn.1995.74.1.113

García Del Caño, G., Gerrikagoitia, I., Sarasa, M., Matute, C., and Martínez-Millán, L. (2000). Ionotropic glutamate receptor subunits are differentially regulated in the motoneuronal pools of the rat hypoglossal nucleus in response to axotomy. *J. Neurocytol.* 29, 509–523. doi: 10.1023/a:1007249829659

Gilmore, S. A., Sims, T. J., and Leiting, J. E. (1990). Astrocytic reactions in spinal gray matter following sciatic axotomy. *Glia* 3, 342–349. doi: 10.1002/glia.440030505

Goldring, J. M., Kuno, M., Núñez, R., and Snider, W. D. (1980). Reaction of synapses on motoneurones to section and restoration of peripheral sensory connexions in the cat. *J. Physiol.* 309, 185–198. doi: 10.1113/jphysiol.1980.sp013503

González-Forero, D., and Moreno-López, B. (2014). Retrograde response in axotomized motoneurons: nitric oxide as a key player in triggering reversion toward a dedifferentiated phenotype. *Neuroscience* 283C, 138–165. doi: 10.1016/j.neuroscience.2014.08.021

González-Forero, D., Pastor, A. M., Delgado-García, J. M., de la Cruz, R. R., and Alvarez, F. J. (2004). Synaptic structural modification following changes in activity induced by tetanus neurotoxin in cat abducens neurons. *J. Comp. Neurol.* 471, 201–218. doi: 10.1002/cne.20039

Gordon, T. (2016). Nerve regeneration: understanding biology and its influence on return of function after nerve transfers. *Hand. Clin.* 32, 103–117. doi: 10.1016/j.hcl.2015.12.001

Gordon, T., and English, A. W. (2016). Strategies to promote peripheral nerve regeneration: electrical stimulation and/or exercise. *Eur. J. Neurosci.* 43, 336–350. doi: 10.1111/ejn.13005

Graeber, M. B., Bise, K., and Mehraein, P. (1993). Synaptic stripping in the human facial nucleus. *Acta Neuropathol.* 86, 179–181. doi: 10.1007/bf00334886

Graeber, M. B., and Kreutzberg, G. W. (1986). Astrocytes increase in glial fibrillary acidic protein during retrograde changes of facial motor neurons. *J. Neurocytol.* 15, 363–373. doi: 10.1007/bf01611438

Graeber, M. B., and Kreutzberg, G. W. (1988). Delayed astrocyte reaction following facial nerve axotomy. *J. Neurocytol.* 17, 209–220. doi: 10.1007/bf01674208

Graeber, M. B., Streit, W. J., and Kreutzberg, G. W. (1989). Formation of microglia-derived brain macrophages is blocked by adriamycin. *Acta Neuropathol.* 78, 348–358. doi: 10.1007/bf00688171

Graeber, M. B., Tetzlaff, W., Streit, W. J., and Kreutzberg, G. W. (1988). Microglial cells but not astrocytes undergo mitosis following rat facial nerve axotomy. *Neurosci. Lett.* 85, 317–321. doi: 10.1016/0304-3940(88)90585-x

Grant, G., and Arvidsson, J. (1975). Transganglionic degeneration in trigeminal primary sensory neurons. *Brain Res.* 95, 265–279. doi: 10.1016/0006-8993(75)90106-7

Grant, G., and Ygge, J. (1981). Somatotopic organization of the thoracic spinal nerve in the dorsal horn demonstrated with transganglionic degeneration. *J. Comp. Neurol.* 202, 357–364. doi: 10.1002/cne.902020305

Guan, Z., Kuhn, J. A., Wang, X., Colquitt, B., Solorzano, C., Vaman, S., et al. (2016). Injured sensory neuron-derived CSF1 induces microglial proliferation and DAP12-dependent pain. *Nat. Neurosci.* 19, 94–101. doi: 10.1038/nn.4189

Gustafsson, B., and Pinter, M. J. (1984). Influence of post-synaptic properties on the time course of synaptic potentials in different types of cat lumbar α-motoneurons. *Neurosci. Lett.* 51, 67–72. doi: 10.1016/0304-3940(84)90264-7

Haftel, V. K., Bichler, E. K., Wang, Q. B., Prather, J. F., Pinter, M. J., and Cope, T. C. (2005). Central suppression of regenerated proprioceptive afferents. *J. Neurosci.* 25, 4733–4742. doi: 10.1523/JNEUROSCI.4895-04.2005

Hamberger, A., Hansson, H. A., and Sjöstrand, J. (1970). Surface structure of isolated neurons: detachment of nerve terminals during axon regeneration. *J. Cell Biol.* 47, 319–331. doi: 10.1083/jcb.47.2.319

Hanson, M. G., Milner, L. D., and Landmesser, L. T. (2008). Spontaneous rhythmic activity in early chick spinal cord influences distinct motor axon pathfinding decisions. *Brain Res Rev.* 57, 77–85. doi: 10.1016/j.brainresrev.2007.06.021

Havton, L., and Kellerth, J. O. (1990). Elimination of intramedullary axon collaterals of cat spinal α-motoneurons following peripheral nerve injury. *Exp. Brain Res.* 79, 65–74. doi: 10.1007/bf00228873

Heckmann, C. J., Gorassini, M. A., and Bennett, D. J. (2005). Persistent inward currents in motoneuron dendrites: implications for motor output. *Muscle Nerve* 31, 135–156. doi: 10.1002/mus.20261

Heckman, C. J., Hyngstrom, A. S., and Johnson, M. D. (2008). Active properties of motoneurone dendrites: diffuse descending neuromodulation, focused local inhibition. *J. Physiol.* 586, 1225–1231. doi: 10.1113/jphysiol.2007.145078

Horridge, G. A., and Burrows, M. (1974). Synapses upon motoneurons of locusts during retrograde degeneration. *Philos. Trans. R. Soc. Lond. B Biol. Sci.* 269, 95–108. doi: 10.1098/rstb.1974.0042

Horstman, G. M., Housley, S. N., and Cope, T. C. (2019). Dysregulation of mechanosensory circuits coordinating the actions of antagonist motor pools following peripheral nerve injury and muscle reinnervation. *Exp. Neurol.* 318, 124–134. doi: 10.1016/j.expneurol.2019.04.017

Iansek, R., and Redman, S. J. (1973). The amplitude, time course and charge of unitary excitatory post-synaptic potentials evoked in spinal motoneurone dendrites. *J. Physiol.* 234, 665–688. doi: 10.1113/jphysiol.1973.sp010366

Ikeda, R., and Kato, F. (2005). Early and transient increase in spontaneous synaptic inputs to the rat facial motoneurons after axotomy in isolated brainstem slices of rats. *Neuroscience* 134, 889–899. doi: 10.1016/j.neuroscience.2005.05.002

Ishizuka, N., Mannen, H., Hongo, T., and Sasaki, S. (1979). Trajectory of group Ia afferent fibers stained with horseradish peroxidase in the lumbosacral spinal cord of the cat: three dimensional reconstructions from serial sections. *J. Comp. Neurol.* 186, 189–211. doi: 10.1002/cne.901860206

Jack, J. J., Redman, S. J., and Wong, K. (1981). The components of synaptic potentials evoked in cat spinal motoneurones by impulses in single group Ia afferents. *J. Physiol.* 321, 65–96. doi: 10.1113/jphysiol.1981.sp013972

Johnson, I. P., Gowda, C. K., Sears, T. A., and Hunter, A. S. (1998). Differences in the synaptic complement of thoracic motoneurons of adult and ageing cats after permanent or reversible axotomy. *Synapse* 28, 176–184. doi: 10.1002/(sici)1098-2396(199802)28:2<176::aid-syn8>3.0.co;2-8

Johnson, I. P., and Sears, T. A. (1989). Organelle changes in cat thoracic α- and γ-motoneurons following axotomy. *Brain Res.* 489, 400–405. doi: 10.1016/0006-8993(89)90880-9

Jones, K. J., Lovett-Racke, A. E., Walker, C. L., and Sanders, V. M. (2015). CD4 + T cells and neuroprotection: relevance to motoneuron injury and disease. *J. Neuroimmune Pharmacol.* 10, 587–594. doi: 10.1007/s11481-015-9625-x

Kakunaga, S., Ikeda, W., Itoh, S., Deguchi-Tawarada, M., Ohtsuka, T., Mizoguchi, A., et al. (2005). Nectin-like molecule-1/TSLL1/SynCAM3: a neural tissue-specific immunoglobulin-like cell-cell adhesion molecule localizing at non-junctional contact sites of presynaptic nerve terminals, axons and glia cell processes. *J. Cell Sci.* 118, 1267–1277. doi: 10.1242/jcs.01656

Kalla, R., Liu, Z., Xu, S., Koppius, A., Imai, Y., Kloss, C. U., et al. (2001). Microglia and the early phase of immune surveillance in the axotomized facial motor nucleus: impaired microglial activation and lymphocyte recruitment but no effect on neuronal survival or axonal regeneration in macrophage-colony stimulating factor-deficient mice. *J. Comp. Neurol.* 436, 182–201. doi: 10.1002/cne.1060

Kennis, J. H., and Holstege, J. C. (1997). A differential and time-dependent decrease in AMPA-type glutamate receptor subunits in spinal motoneurons after sciatic nerve injury. *Exp. Neurol.* 147, 18–27. doi: 10.1006/exnr.1997.6576

Kerns, J. M., and Hinsman, E. J. (1973). Neuroglial response to sciatic neurectomy: II. Electron microscopy. *J. Comp. Neurol.* 151, 255–280. doi: 10.1002/cne.901510304

Kettenmann, H., Kirchhoff, F., and Verkhratsky, A. (2013). Microglia: new roles for the synaptic stripper. *Neuron* 77, 10–18. doi: 10.1016/j.neuron.2012.12.023

Kikuchi, R., Hamanoue, M., Koshimoto, M., Kohsaka, S., and Nakajima, K. (2018). Response of the GABAergic system to axotomy of the rat facial nerve. *Neurochem. Res.* 43, 324–339. doi: 10.1007/s11064-017-2427-1

Kim, S., Burette, A., Chung, H. S., Kwon, S. K., Woo, J., Lee, H. W., et al. (2006). NGL family PSD-95-interacting adhesion molecules regulate excitatory synapse formation. *Nat. Neurosci.* 9, 1294–1301. doi: 10.1038/nn1763

Kim, J., Kobayashi, S., Shimizu-Okabe, C., Okabe, A., Moon, C., Shin, T., et al. (2018). Changes in the expression and localization of signaling molecules in mouse facial motor neurons during regeneration of facial nerves. *J. Chem. Neuroanat.* 88, 13–21. doi: 10.1016/j.jchemneu.2017.11.002

Knyihar, E., and Csillik, B. (1976). Effect of peripheral anatomy on the fine structure and histochemistry of the Rolando substance: degenerative atrophy of central processes of pseudounipolar cells. *Exp. Brain Res.* 26, 73–87. doi: 10.1007/bf00235250

Koerber, H. R., Mirnics, K., and Lawson, J. J. (2006). Synaptic plasticity in the adult spinal dorsal horn: the appearance of new functional connections following peripheral nerve regeneration. *Exp. Neurol.* 200, 468–479. doi: 10.1016/j.expneurol.2006.03.003

Koliatsos, V. E., Price, W. L., Pardo, C. A., and Price, D. L. (1994). Ventral root avulsion: an experimental model of death of adult motor neurons. *J. Comp. Neurol.* 342, 35–44. doi: 10.1002/cne.903420105

Krakowiak, J., Liu, C., Papudesu, C., Ward, P. J., Wilhelm, J. C., and English, A. W. (2015). Neuronal BDNF signaling is necessary for the effects of treadmill exercise on synaptic stripping of axotomized motoneurons. *Neural Plast.* 2015:392591. doi: 10.1155/2015/392591

Kreutzberg, G. W. (1996). Principles of neuronal regeneration. *Acta Neurochir. Suppl.* 66, 103–106.

Kuno, M., and Llinas, R. (1970). Alterations of synaptic action in chromatolysed motoneurones of the cat. *J. Physiol.* 210, 823–838. doi: 10.1113/jphysiol.1970.sp009244

Laskawi, R., and Wolff, J. R. (1996). Changes in glial fibrillary acidic protein immunoreactivity in the rat facial nucleus following various types of nerve lesions. *Eur. Arch. Otorhinolaryngol.* 253, 475–480. doi: 10.1007/bf00179953

Lee, R. H., and Heckman, C. J. (2000). Adjustable amplification of synaptic input in the dendrites of spinal motoneurons *in vivo*. *J. Neurosci.* 20, 6734–6740. doi: 10.1523/JNEUROSCI.20-17-06734.2000

Lieberman, A. R. (1971). The axon reaction: a review of the principal features of perikaryal responses to axon injury. *Int. Rev. Neurobiol.* 14, 49–124. doi: 10.1016/s0074-7742(08)60183-x

Linda, H., Cullheim, S., and Risling, M. (1992). A light and electron microscopic study of intracellularly HRP-labeled lumbar motoneurons after intramedullary axotomy in the adult cat. *J. Comp. Neurol.* 318, 188–208. doi: 10.1002/cne.903180205

Linda, H., Hammarberg, H., Cullheim, S., Levinovitz, A., Khademi, M., and Olsson, T. (1998). Expression of MHC class I and β2-microglobulin in rat spinal motoneurons: regulatory influences by IFN-γ and axotomy. *Exp. Neurol.* 150, 282–295. doi: 10.1006/exnr.1997.6768

Linda, H., Shupliakov, O., Ornung, G., Ottersen, O. P., Storm-Mathisen, J., Risling, M., et al. (2000). Ultrastructural evidence for a preferential elimination of glutamate-immunoreactive synaptic terminals from spinal motoneurons after intramedullary axotomy. *J. Comp. Neurol.* 425, 10–23. doi: 10.1002/1096-9861(20000911)425:1< 10::aid-cne2>3.0.co;2-#

Liu, P. H., Yang, L. H., Wang, T. Y., Wang, Y. J., and Tseng, G. F. (2006). Proximity of lesioning determines response of facial motoneurons to peripheral axotomy. *J. Neurotrauma* 23, 1857–1873. doi: 10.1089/neu.2006.23.1857

Lundborg, G. (2003). Richard P. Bunge memorial lecture. Nerve injury and repair—a challenge to the plastic brain. *J. Peripher. Nerv. Syst.* 8, 209–226. doi: 10.1111/j.1085-9489.2003.03027.x

Lyle, M. A., Nichols, T. R., Kajtaz, E., and Maas, H. (2017). Musculotendon adaptations and preservation of spinal reflex pathways following agonist-to-antagonist tendon transfer. *Physiol. Rep.* 5:e13201. doi: 10.14814/phy2.13201

Ma, M., Wei, T., Boring, L., Charo, I. F., Ransohoff, R. M., and Jakeman, L. B. (2002). Monocyte recruitment and myelin removal are delayed following spinal cord injury in mice with CCR2 chemokine receptor deletion. *J. Neurosci. Res.* 68, 691–702. doi: 10.1002/jnr.10269

Maas, H., Prilutsky, B. I., Nichols, T. R., and Gregor, R. J. (2007). The effects of self-reinnervation of cat medial and lateral gastrocnemius muscles on hindlimb kinematics in slope walking. *Exp. Brain Res.* 181, 377–393. doi: 10.1007/s00221-007-0938-8

Maehlen, J., Nennesmo, I., Olsson, A. B., Olsson, T., Schroder, H. D., and Kristensson, K. (1989). Peripheral nerve injury causes transient expression of MHC class I antigens in rat motor neurons and skeletal muscles. *Brain Res.* 481, 368–372. doi: 10.1016/0006-8993(89)90816-0

Matsukawa, H., Akiyoshi-Nishimura, S., Zhang, Q., Luján, R., Yamaguchi, K., Goto, H., et al. (2014). Netrin-G/NGL complexes encode functional synaptic diversification. *J. Neurosci.* 34, 15779–15792. doi: 10.1523/JNEUROSCI.1141-14.2014

Matthews, M. R., and Nelson, V. H. (1975). Detachment of structurally intact nerve endings from chromatolytic neurones of rat superior cervical ganglion during the depression of synaptic transmission induced by post-ganglionic axotomy. *J. Physiol.* 245, 91–135. doi: 10.1113/jphysiol.1975.sp010837

Mattsson, P., Morgan, B. P., and Svensson, M. (1998). Complement activation and CD59 expression in the motor facial nucleus following intracranial transection of the facial nerve in the adult rat. *J. Neuroimmunol.* 91, 180–189. doi: 10.1016/s0165-5728(98)00178-7

McIntyre, A. K., Bradley, K., and Brock, L. G. (1959). Responses of motoneurons undergoing chromatolysis. *J. Gen. Physiol.* 42, 931–958. doi: 10.1085/jgp.42.5.931

McPhail, L. T., Stirling, D. P., Tetzlaff, W., Kwiecien, J. M., and Ramer, M. S. (2004). The contribution of activated phagocytes and myelin degeneration to axonal retraction/dieback following spinal cord injury. *Eur. J. Neurosci.* 20, 1984–1994. doi: 10.1111/j.1460-9568.2004.03662.x

Mendell, L. M. (1984). Modifiability of spinal synapses. *Physiol. Rev.* 64, 260–324. doi: 10.1152/physrev.1984.64.1.260

Mendell, L. M., and Henneman, E. (1968). Terminals of single Ia fibers: distribution within a pool of 300 homonymous motor neurons. *Science* 160, 96–98. doi: 10.1126/science.160.3823.96

Mendell, L. M., Johnson, R. D., and Munson, J. B. (1999). Neurotrophin modulation of the monosynaptic reflex after peripheral nerve transection. *J. Neurosci.* 19, 3162–3170. doi: 10.1523/JNEUROSCI.19-08-03162.1999

Mendell, L. M., Munson, J. B., and Scott, J. G. (1974). Connectivity changes of Ia afferents on axotomized motoneurons. *Brain Res.* 73, 338–342. doi: 10.1016/0006-8993(74)91054-3

Mendell, L. M., Munson, J. B., and Scott, J. G. (1976). Alterations of synapses on axotomized motoneurones. *J. Physiol.* 255, 67–79. doi: 10.1113/jphysiol.1976.sp011270

Mendell, L. M., Taylor, J. S., Johnson, R. D., and Munson, J. B. (1995). Rescue of motoneuron and muscle afferent function in cats by regeneration into skin. II. Ia-motoneuron synapse. *J. Neurophysiol.* 73, 662–673. doi: 10.1152/jn.1995.73.2.662

Mendell, L. M., and Scott, J. G. (1975). The effect of peripheral nerve cross-union on connections of single Ia fibers to motoneurons. *Exp. Brain Res.* 22, 221–234. doi: 10.1007/bf00234765

Mentis, G. Z., Blivis, D., Liu, W., Drobac, E., Crowder, M. E., Kong, L., et al. (2011). Early functional impairment of sensory-motor connectivity in a mouse model of spinal muscular atrophy. *Neuron* 69, 453–467. doi: 10.1016/j.neuron.2010.12.032

Mentis, G. Z., Siembab, V. C., Zerda, R., O'Donovan, M. J., and Alvarez, F. J. (2006). Primary afferent synapses on developing and adult Renshaw cells. *J. Neurosci.* 26, 13297–13310. doi: 10.1523/JNEUROSCI.2945-06.2006

Miyata, M., Mandai, K., Maruo, T., Sato, J., Shiotani, H., Kaito, A., et al. (2016). Localization of nectin-2delta at perivascular astrocytic endfoot processes and degeneration of astrocytes and neurons in nectin-2 knockout mouse brain. *Brain Res.* 1649, 90–101. doi: 10.1016/j.brainres.2016.08.023

Miyata, Y., and Yasuda, H. (1988). Enhancement of Ia synaptic transmission following muscle nerve section: dependence upon protein synthesis. *Neurosci. Res.* 5, 338–346. doi: 10.1016/0168-0102(88)90035-1

Montero, F., Sunico, C. R., Liu, B., Paton, J. F., Kasparov, S., and Moreno-López, B. (2010). Transgenic neuronal nitric oxide synthase expression induces axotomy-like changes in adult motoneurons. *J. Physiol.* 588, 3425–3443. doi: 10.1113/jphysiol.2010.195396

Moran, L. B., and Graeber, M. B. (2004). The facial nerve axotomy model. *Brain Res. Rev.* 44, 154–178. doi: 10.1016/j.brainresrev.2003.11.004

Morcuende, S., Matarredona, E. R., Benítez-Temiño, B., Muñoz-Hernández, R., Pastor, A. M., and De La Cruz, R. R. (2011). Differential regulation of the expression of neurotrophin receptors in rat extraocular motoneurons after lesion. *J. Comp. Neurol.* 519, 2335–2352. doi: 10.1002/cne.22630

Moreno-López, B., de la Cruz, R. R., Pastor, A. M., Delgado-García, J. M., and Alvarez, F. J. (1998). Effects of botulinum neurotoxin type A on the expression of gephyrin in cat abducens motoneurons. *J. Comp. Neurol.* 400, 1–17. doi: 10.1002/(sici)1096-9861(19981012)400:1<1::aid-cne1>3.0.co;2-d

Moreno-López, B., Sunico, C. R., and González-Forero, D. (2011). NO orchestrates the loss of synaptic boutons from adult "sick" motoneurons: modeling a molecular mechanism. *Mol. Neurobiol.* 43, 41–66. doi: 10.1007/s12035-010-8159-8

Nabekura, J., Ueno, T., Okabe, A., Furuta, A., Iwaki, T., Shimizu-Okabe, C., et al. (2002). Reduction of KCC2 expression and GABAA receptor-mediated excitation after *in vivo* axonal injury. *J. Neurosci.* 22, 4412–4417. doi: 10.1523/JNEUROSCI.22-11-04412.2002

Nagano, I., Murakami, T., Shiote, M., Abe, K., and Itoyama, Y. (2003). Ventral root avulsion leads to downregulation of GluR2 subunit in spinal motoneurons in adult rats. *Neuroscience* 117, 139–146. doi: 10.1016/s0306-4522(02)00816-3

Nakayama, K., Niwa, M., Sasaki, S. I., Ichikawa, T., and Hirai, N. (1998). Morphology of single primary spindle afferents of the intercostal muscles in the cat. *J. Comp. Neurol.* 398, 459–472. doi: 10.1002/(sici)1096-9861(19980907)398:4<459::aid-cne1>3.0.co;2-1

Navarro, X., Vivó, M., and Valero-Cabre, A. (2007). Neural plasticity after peripheral nerve injury and regeneration. *Prog. Neurobiol.* 82, 163–201. doi: 10.1016/j.pneurobio.2007.06.005

Newey, S. E., Velamoor, V., Govek, E. E., and Van Aelst, L. (2005). Rho GTPases, dendritic structure and mental retardation. *J. Neurobiol.* 64, 58–74. doi: 10.1002/neu.20153

Niemi, J. P., DeFrancesco-Lisowitz, A., Cregg, J. M., Howarth, M., and Zigmond, R. E. (2016). Overexpression of the monocyte chemokine CCL2 in dorsal root ganglion neurons causes a conditioning-like increase in neurite outgrowth and does so *via* a STAT3 dependent mechanism. *Exp. Neurol.* 275, 25–37. doi: 10.1016/j.expneurol.2015.09.018

Niemi, J. P., DeFrancesco-Lisowitz, A., Roldán-Hernández, L., Lindborg, J. A., Mandell, D., and Zigmond, R. E. (2013). A critical role for macrophages near axotomized neuronal cell bodies in stimulating nerve regeneration. *J. Neurosci.* 33, 16236–16248. doi: 10.1523/JNEUROSCI.3319-12.2013

Novikov, L. N., Novikova, L. N., Holmberg, P., and Kellerth, J. (2000). Exogenous brain-derived neurotrophic factor regulates the synaptic composition of axonally lesioned and normal adult rat motoneurons. *Neuroscience* 100, 171–181. doi: 10.1016/s0306-4522(00)00256-6

O'Donovan, M. J., Chub, N., and Wenner, P. (1998). Mechanisms of spontaneous activity in developing spinal networks. *J. Neurobiol.* 37, 131–145. doi: 10.1002/(sici)1097-4695(199810)37:1<131::aid-neu10>3.0.co;2-h

Oliveira, A. L., Thams, S., Lidman, O., Piehl, F., Hokfelt, T., Karre, K., et al. (2004). A role for MHC class I molecules in synaptic plasticity and regeneration of neurons after axotomy. *Proc. Natl. Acad. Sci. U S A* 101, 17843–17848. doi: 10.1073/pnas.0408154101

Panagopoulos, G. N., Megaloikonomos, P. D., and Mavrogenis, A. F. (2017). The present and future for peripheral nerve regeneration. *Orthopedics* 40, e141–e156. doi: 10.3928/01477447-20161019-01

Pastor, A. M., Delgado-Garcia, J. M., Martínez-Guijarro, F. J., López-García, C., and de la Cruz, R. R. (2000). Response of abducens internuclear neurons to axotomy in the adult cat. *J. Comp. Neurol.* 427, 370–390. doi: 10.1002/1096-9861(20001120)427:3<370::aid-cne5>3.0.co;2-m

Pastor, A. M., Moreno-López, B., De La Cruz, R. R., and Delgado-Garcia, J. M. (1997). Effects of botulinum neurotoxin type A on abducens motoneurons in the cat: ultrastructural and synaptic alterations. *Neuroscience* 81, 457–478. doi: 10.1016/s0306-4522(97)00200-5

Perry, V. H., and O'Connor, V. (2010). The role of microglia in synaptic stripping and synaptic degeneration: a revised perspective. *ASN Neuro* 2:e00047. doi: 10.1042/an20100024

Piehl, F., Tabar, G., and Cullheim, S. (1995). Expression of NMDA receptor mRNAs in rat motoneurons is down-regulated after axotomy. *Eur. J. Neurosci.* 7, 2101–2110. doi: 10.1111/j.1460-9568.1995.tb00632.x

Popratiloff, A., Weinberg, R. J., and Rustioni, A. (1996). AMPA receptor subunits underlying terminals of fine-caliber primary afferent fibers. *J. Neurosci.* 16, 3363–3372. doi: 10.1523/JNEUROSCI.16-10-03363.1996

Prather, J. F., Nardelli, P., Nakanishi, S. T., Ross, K. T., Nichols, T. R., Pinter, M. J., et al. (2011). Recovery of proprioceptive feedback from nerve crush. *J. Physiol.* 589, 4935–4947. doi: 10.1113/jphysiol.2011.210518

Purves, D. (1975). Functional and structural changes in mammalian sympathetic neurones following interruption of their axons. *J. Physiol.* 252, 429–463. doi: 10.1113/jphysiol.1975.sp011151

Purves, D. (1976). Functional and structural changes in mammalian sympathetic neurones following colchicine application to post-ganglionic nerves. *J. Physiol.* 259, 159–175. doi: 10.1113/jphysiol.1976.sp011459

Raivich, G., Moreno-Flores, M. T., Möller, J. C., and Kreutzberg, G. W. (1994). Inhibition of posttraumatic microglial proliferation in a genetic model of macrophage colony-stimulating factor deficiency in the mouse. *Eur. J. Neurosci.* 6, 1615–1618. doi: 10.1111/j.1460-9568.1994.tb00552.x

Rall, W., Burke, R. E., Smith, T. G., Nelson, P. G., and Frank, K. (1967). Dendritic location of synapses and possible mechanisms for the monosynaptic EPSP in motoneurons. *J. Neurophysiol.* 30, 1169–1193. doi: 10.1152/jn.1967.30.5.1169

Ramaglia, V., Daha, M. R., and Baas, F. (2008). The complement system in the peripheral nerve: friend or foe? *World J. Urol.* 45, 3865–3877. doi: 10.1016/j.molimm.2008.06.018

Ramaglia, V., Tannemaat, M. R., de Kok, M., Wolterman, R., Vigar, M. A., King, R. H., et al. (2009). Complement inhibition accelerates regeneration in a model of peripheral nerve injury. *Mol. Immunol.* 47, 302–309. doi: 10.1016/j.molimm.2009.09.019

Ransohoff, R. M. (2009). Chemokines and chemokine receptors: standing at the crossroads of immunobiology and neurobiology. *Immunity* 31, 711–721. doi: 10.1016/j.immuni.2009.09.010

Redman, S., and Walmsley, B. (1983a). Amplitude fluctuations in synaptic potentials evoked in cat spinal motoneurones at identified group Ia synapses. *J. Physiol.* 343, 135–145. doi: 10.1113/jphysiol.1983.sp014885

Redman, S., and Walmsley, B. (1983b). The time course of synaptic potentials evoked in cat spinal motoneurones at identified group Ia synapses. *J. Physiol.* 343, 117–133. doi: 10.1113/jphysiol.1983.sp014884

Reisert, I., Wildemann, G., Grab, D., and Pilgrim, C. (1984). The glial reaction in the course of axon regeneration: a stereological study of the rat hypoglossal nucleus. *J. Comp. Neurol.* 229, 121–128. doi: 10.1002/cne.902290109

Ribeiro, P., Castro, M. V., Perez, M., Cartarozzi, L. P., Spejo, A. B., Chiarotto, G. B., et al. (2019). Toll-like receptor 4 (TLR4) influences the glial reaction in the spinal cord and the neural response to injury following peripheral nerve crush. *Brain Res. Bull.* 155, 67–80. doi: 10.1016/j.brainresbull.2019.11.008

Rodrigues Hell, R. C., Silva Costa, M. M., Goes, A. M., and Oliveira, A. L. (2009). Local injection of BDNF producing mesenchymal stem cells increases neuronal survival and synaptic stability following ventral root avulsion. *Neurobiol. Dis.* 33, 290–300. doi: 10.1016/j.nbd.2008.10.017

Rose, P. K., and Neuber-Hess, M. (1991). Morphology and frequency of axon terminals on the somata, proximal dendrites and distal dendrites of dorsal neck motoneurons in the cat. *J. Comp. Neurol.* 307, 259–280. doi: 10.1002/cne.903070208

Rotterman, T. M., Akhter, E. T., Lane, A. R., MacPherson, K. P., Garcia, V. V., Tansey, M. G., et al. (2019). Spinal motor circuit synaptic plasticity after peripheral nerve injury depends on microglia activation and a CCR2 mechanism. *J. Neurosci.* 39, 3412–3433. doi: 10.1523/JNEUROSCI.2945-17.2019

Rotterman, T. M., Nardelli, P., Cope, T. C., and Alvarez, F. J. (2014). Normal distribution of VGLUT1 synapses on spinal motoneuron dendrites and their reorganization after nerve injury. *J. Neurosci.* 34, 3475–3492. doi: 10.1523/JNEUROSCI.4768-13.2014

Russier, M., Kopysova, I. L., Ankri, N., Ferrand, N., and Debanne, D. (2002). GABA and glycine co-release optimizes functional inhibition in rat brainstem motoneurons *in vitro*. *J. Physiol.* 541, 123–137. doi: 10.1113/jphysiol.2001.016063

Sabatier, M. J., To, B. N., Nicolini, J., and English, A. W. (2011a). Effect of axon misdirection on recovery of electromyographic activity and kinematics after peripheral nerve injury. *Cells Tissues Organs* 193, 298–309. doi: 10.1159/000323677

Sabatier, M. J., To, B. N., Nicolini, J., and English, A. W. (2011b). Effect of slope and sciatic nerve injury on ankle muscle recruitment and hindlimb kinematics during walking in the rat. *J. Exp. Biol.* 214, 1007–1016. doi: 10.1242/jeb.051508

Schultz, A. J., Rotterman, T. M., Dwarakanath, A., and Alvarez, F. J. (2017). VGLUT1 synapses and P-boutons on regenerating motoneurons after nerve crush. *J. Comp. Neurol.* 525, 2876–2889. doi: 10.1002/cne.24244

Scott, J. G., and Mendell, L. M. (1976). Individual EPSPs produced by single triceps surae Ia afferent fibers in homonymous and heteronymous motoneurons. *J. Neurophysiol.* 39, 679–692. doi: 10.1152/jn.1976.39.4.679

Seburn, K. L., and Cope, T. C. (1998). Short-term afferent axotomy increases both strength and depression at Ia-motoneuron synapses in rat. *J. Neurosci.* 18, 1142–1147. doi: 10.1523/JNEUROSCI.18-03-01142.1998

Shatz, C. J. (2009). MHC class I: an unexpected role in neuronal plasticity. *Neuron* 64, 40–45. doi: 10.1016/j.neuron.2009.09.044

Siembab, V. C., Smith, C. A., Zagoraiou, L., Berrocal, M. C., Mentis, G. Z., and Alvarez, F. J. (2010). Target selection of proprioceptive and motor axon synapses on neonatal V1-derived Ia inhibitory interneurons and Renshaw cells. *J. Comp. Neurol.* 518, 4675–4701. doi: 10.1002/cne.22441

Singer, J. H., and Berger, A. J. (2000). Development of inhibitory synaptic transmission to motoneurons. *Brain Res. Bull.* 53, 553–560. doi: 10.1016/s0361-9230(00)00389-0

Spejo, A. B., and Oliveira, A. L. (2015). Synaptic rearrangement following axonal injury: old and new players. *Neuropharmacology* 96, 113–123. doi: 10.1016/j.neuropharm.2014.11.002

Starr, K. A., and Wolpaw, J. R. (1994). Synaptic terminal coverage of primate triceps surae motoneurons. *J. Comp. Neurol.* 345, 345–358. doi: 10.1002/cne.903450303

Stephan, A. H., Barres, B. A., and Stevens, B. (2012). The complement system: an unexpected role in synaptic pruning during development and disease. *Annu. Rev. Neurosci.* 35, 369–389. doi: 10.1146/annurev-neuro-061010-113810

Stevens, B., Allen, N. J., Vazquez, L. E., Howell, G. R., Christopherson, K. S., Nouri, N., et al. (2007). The classical complement cascade mediates CNS synapse elimination. *Cell* 131, 1164–1178. doi: 10.1016/j.cell.2007.10.036

Subang, M. C., and Richardson, P. M. (2001). Influence of injury and cytokines on synthesis of monocyte chemoattractant protein-1 mRNA in peripheral nervous tissue. *Eur. J. Neurosci.* 13, 521–528. doi: 10.1046/j.1460-9568.2001.01425.x

Südhof, T. C. (2008). Neuroligins and neurexins link synaptic function to cognitive disease. *Nature* 455, 903–911. doi: 10.1038/nature07456

Sumner, B. E. (1975a). A quantitative analysis of boutons with different types of synapse in normal and injured hypoglossal nuclei. *Exp. Neurol.* 49, 406–417. doi: 10.1016/0014-4886(75)90097-7

Sumner, B. E. (1975b). A quantitative analysis of the response of presynaptic boutons to postsynaptic motor neuron axotomy. *Exp. Neurol.* 46, 605–615. doi: 10.1016/0014-4886(75)90129-6

Sumner, B. E. (1975c). A quantitative study of subsurface cisterns and their relationships in normal and axotomized hypoglossal neurones. *Exp. Brain Res.* 22, 175–183. doi: 10.1007/bf00237687

Sumner, B. E. (1977a). Responses in the hypoglossal nucleus to delayed regeneration of the transected hypoglossal nerve, a quantitative ultrastructural study. *Exp. Brain Res.* 29, 219–231. doi: 10.1007/bf00237043

Sumner, B. E. (1977b). Ultrastructural responses of the hypoglossal nucleus to the presence in the tongue of botulinum toxin, a quantitative study. *Exp. Brain Res.* 30, 313–321. doi: 10.1007/bf00237258

Sumner, B. E., and Sutherland, F. I. (1973). Quantitative electron microscopy on the injured hypoglossal nucleus in the rat. *J. Neurocytol.* 2, 315–328. doi: 10.1007/bf01104033

Sumner, B. E., and Watson, W. E. (1971). Retraction and expansion of the dendritic tree of motor neurones of adult rats induced *in vivo*. *Nature* 233, 273–275. doi: 10.1038/233273a0

Sunico, C. R., González-Forero, D., Dominguez, G., García-Verdugo, J. M., and Moreno-Lopez, B. (2010). Nitric oxide induces pathological synapse loss by a protein kinase G-, Rho kinase-dependent mechanism preceded by myosin light chain phosphorylation. *J. Neurosci.* 30, 973–984. doi: 10.1523/JNEUROSCI.3911-09.2010

Sunico, C. R., Portillo, F., González-Forero, D., and Moreno-López, B. (2005). Nitric-oxide-directed synaptic remodeling in the adult mammal CNS. *J. Neurosci.* 25, 1448–1458. doi: 10.1523/JNEUROSCI.4600-04.2005

Svensson, M., and Aldskogius, H. (1992). Evidence for activation of the complement cascade in the hypoglossal nucleus following peripheral nerve injury. *J. Neuroimmunol.* 40, 99–109. doi: 10.1016/0165-5728(92)90217-9

Svensson, M., and Aldskogius, H. (1993). Synaptic density of axotomized hypoglossal motorneurons following pharmacological blockade of the microglial cell proliferation. *Exp. Neurol.* 120, 123–131. doi: 10.1006/exnr.1993.1046

Svensson, M., Eriksson, N. P., and Aldskogius, H. (1993). Evidence for activation of astrocytes *via* reactive microglial cells following hypoglossal nerve transection. *J. Neurosci. Res.* 35, 373–381. doi: 10.1002/jnr.490350404

Svensson, M., Liu, L., Mattsson, P., Morgan, B. P., and Aldskogius, H. (1995). Evidence for activation of the terminal pathway of complement and upregulation of sulfated glycoprotein (SGP)-2 in the hypoglossal nucleus following peripheral nerve injury. *Mol. Chem. Neuropathol.* 24, 53–68. doi: 10.1007/bf03160112

Svensson, M., Mattsson, P., and Aldskogius, H. (1994). A bromodeoxyuridine labelling study of proliferating cells in the brainstem following hypoglossal nerve transection. *J. Anat.* 185, 537–542.

Svitkina, T. M., Verkhovsky, A. B., McQuade, K. M., and Borisy, G. G. (1997). Analysis of the actin-myosin II system in fish epidermal keratocytes: mechanism of cell body translocation. *J. Cell Biol.* 139, 397–415. doi: 10.1083/jcb.139.2.397

Tajdaran, K., Chan, K., Gordon, T., and Borschel, G. H. (2019). Matrices, scaffolds, and carriers for protein and molecule delivery in peripheral nerve regeneration. *Exp. Neurol.* 319:112817. doi: 10.1016/j.expneurol.2018.08.014

Takata, M. (1981). Lingually induced inhibitory postsynaptic potentials in hypoglossal motoneurons after axotomy. *Brain Res.* 224, 165–169. doi: 10.1016/0006-8993(81)91127-6

Takata, M., and Nagahama, T. (1983). Synaptic efficacy of inhibitory synapses in hypoglossal motoneurons after transection of the hypoglossal nerves. *Neuroscience* 10, 23–29. doi: 10.1016/0306-4522(83)90077-5

Takata, M., and Nagahama, T. (1984). Cortically induced postsynaptic potentials in hypoglossal motoneurons after axotomy. *Neuroscience* 13, 855–862. doi: 10.1016/0306-4522(84)90100-3

Takata, M., and Nagahama, T. (1986). Cortically and lingually induced postsynaptic potentials in trigeminal motoneurons after axotomy. *Exp. Brain Res.* 61, 272–279. doi: 10.1007/bf00239517

Tanaka, T., Murakami, K., Bando, Y., Nomura, T., Isonishi, A., Morita-Takemura, S., et al. (2017). Microglia support ATF3-positive neurons following hypoglossal nerve axotomy. *Neurochem. Int.* 108, 332–342. doi: 10.1016/j.neuint.2017.05.007

Tandrup, T., Woolf, C. J., and Coggeshall, R. E. (2000). Delayed loss of small dorsal root ganglion cells after transection of the rat sciatic nerve. *J. Comp. Neurol.* 422, 172–180. doi: 10.1002/(sici)1096-9861(20000626)422:2<172::aid-cne2>3.0.co;2-h

Tang, F. R., and Sim, M. K. (1997). Expression of glutamate receptor subunits 2/3 and 4 in the hypoglossal nucleus of the rat after neurectomy. *Exp. Brain Res.* 117, 453–456. doi: 10.1007/s002210050240

Taskinen, H. S., and Röyttä, M. (2000). Increased expression of chemokines (MCP-1, MIP-1α, RANTES) after peripheral nerve transection. *J. Peripher. Nerv. Syst.* 5, 75–81. doi: 10.1046/j.1529-8027.2000.00009.x

Tatetsu, M., Kim, J., Kina, S., Sunakawa, H., and Takayama, C. (2012). GABA/glycine signaling during degeneration and regeneration of mouse hypoglossal nerves. *Brain Res.* 1446, 22–33. doi: 10.1016/j.brainres.2012.01.048

Terenghi, G. (1999). Peripheral nerve regeneration and neurotrophic factors. *J. Anat.* 194, 1–14. doi: 10.1046/j.1469-7580.1999.19410001.x

Tetzlaff, W., Graeber, M. B., Bisby, M. A., and Kreutzberg, G. W. (1988). Increased glial fibrillary acidic protein synthesis in astrocytes during retrograde reaction of the rat facial nucleus. *Glia* 1, 90–95. doi: 10.1002/glia.440010110

Thams, S., Brodin, P., Plantman, S., Saxelin, R., Kärre, K., and Cullheim, S. (2009). Classical major histocompatibility complex class I molecules in motoneurons: new actors at the neuromuscular junction. *J. Neurosci.* 29, 13503–13515. doi: 10.1523/JNEUROSCI.0981-09.2009

Thams, S., Oliveira, A., and Cullheim, S. (2008). MHC class I expression and synaptic plasticity after nerve lesion. *Brain Res. Rev.* 57, 265–269. doi: 10.1016/j.brainresrev.2007.06.016

Titmus, M. J., and Faber, D. S. (1990). Axotomy-induced alterations in the electrophysiological characteristics of neurons. *Prog. Neurobiol.* 35, 1–51. doi: 10.1016/0301-0082(90)90039-j

Todd, A. J., Hughes, D. I., Polgar, E., Nagy, G. G., Mackie, M., Ottersen, O. P., et al. (2003). The expression of vesicular glutamate transporters VGLUT1 and VGLUT2 in neurochemically defined axonal populations in the rat spinal cord with emphasis on the dorsal horn. *Eur. J. Neurosci.* 17, 13–27. doi: 10.1046/j.1460-9568.2003.02406.x

Toews, A. D., Barrett, C., and Morell, P. (1998). Monocyte chemoattractant protein 1 is responsible for macrophage recruitment following injury to sciatic nerve. *J. Neurosci. Res.* 53, 260–267. doi: 10.1002/(sici)1097-4547(19980715)53:2<260::aid-jnr15>3.0.co;2-a

Torvik, A., and Skjorten, F. (1971). Electron microscopic observations on nerve cell regeneration and degeneration after axon lesions: II. Changes in the glial cells. *Acta Neuropathol.* 17, 265–282. doi: 10.1007/bf00685059

Toyoda, H., Ohno, K., Yamada, J., Ikeda, M., Okabe, A., Sato, K., et al. (2003). Induction of NMDA and $GABA_A$ receptor-mediated Ca^{2+} oscillations with KCC2 mRNA downregulation in injured facial motoneurons. *J. Neurophysiol.* 89, 1353–1362. doi: 10.1152/jn.00721.2002

Tyzack, G. E., Sitnikov, S., Barson, D., Adams-Carr, K. L., Lau, N. K., Kwok, J. C., et al. (2014). Astrocyte response to motor neuron injury promotes structural synaptic plasticity *via* STAT3-regulated TSP-1 expression. *Nat. Commun.* 5:4294. doi: 10.1038/ncomms5294

Ueno, T., Okabe, A., Akaike, N., Fukuda, A., and Nabekura, J. (2002). Diversity of neuron-specific K^+-Cl^- cotransporter expression and inhibitory postsynaptic potential depression in rat motoneurons. *J. Biol. Chem.* 277, 4945–4950. doi: 10.1074/jbc.m109439200

Valero-Cabré, A., Tsironis, K., Skouras, E., Navarro, X., and Neiss, W. F. (2004). Peripheral and spinal motor reorganization after nerve injury and repair. *J. Neurotrauma* 21, 95–108. doi: 10.1089/089771504772695986

Van Steenwinckel, J., Reaux-Le Goazigo, A., Pommier, B., Mauborgne, A., Dansereau, M. A., Kitabgi, P., et al. (2011). CCL2 released from neuronal synaptic vesicles in the spinal cord is a major mediator of local inflammation and pain after peripheral nerve injury. *J. Neurosci.* 31, 5865–5875. doi: 10.1523/JNEUROSCI.5986-10.2011

Vanden Noven, S., and Pinter, M. J. (1989). Effects of preventing reinnervation on axotomized spinal motoneurons in the cat: II. Changes in group Ia synaptic function. *J. Neurophysiol.* 62, 325–333. doi: 10.1152/jn.1989.62.2.325

Vassias, I., Lecolle, S., Vidal, P. P., and de Waele, C. (2005). Modulation of GABA receptor subunits in rat facial motoneurons after axotomy. *Mol. Brain Res.* 135, 260–275. doi: 10.1016/j.molbrainres.2004.12.010

Vaughan, D. W. (1994). Effects of peripheral axotomy on presynaptic axon terminals with GABA-like immunoreactivity. *Anat. Rec.* 238, 248–262. doi: 10.1002/ar.1092380211

Victorio, S. C., Havton, L. A., and Oliveira, A. L. (2010). Absence of IFNγ expression induces neuronal degeneration in the spinal cord of adult mice. *J. Neuroinflammation* 7:77. doi: 10.1186/1742-2094-7-77

Vincent, J. A., Gabriel, H. M., Deardorff, A. S., Nardelli, P., Fyffe, R. E. W., Burkholder, T., et al. (2017). Muscle proprioceptors in adult rat: mechanosensory signaling and synapse distribution in spinal cord. *J. Neurophysiol.* 118, 2687–2701. doi: 10.1152/jn.00497.2017

Vincent, J. A., Nardelli, P., Gabriel, H. M., Deardorff, A. S., and Cope, T. C. (2015). Complex impairment of IA muscle proprioceptors following traumatic or neurotoxic injury. *J. Anat.* 227, 221–230. doi: 10.1111/joa.12312

Vukojicic, A., Delestree, N., Fletcher, E. V., Pagiazitis, J. G., Sankaranarayanan, S., Yednock, T. A., et al. (2019). The classical complement pathway mediates microglia-dependent remodeling of spinal motor circuits during development and in SMA. *Cell Rep.* 29, 3087.e7–3100.e7. doi: 10.1016/j.celrep.2019.11.013

Walmsley, B., Alvarez, F. J., and Fyffe, R. E. (1998). Diversity of structure and function at mammalian central synapses. *Trends Neurosci.* 21, 81–88. doi: 10.1016/s0166-2236(97)01170-3

Wood, M. R., and Faber, D. S. (1986). Electrophysiological and morphological correlates of axotomy-induced deafferentation of the goldfish Mauthner cell. *J. Comp. Neurol.* 244, 413–429. doi: 10.1002/cne.902440402

Wu, W., Li, Y., and Schinco, F. P. (1994a). Expression of c-jun and neuronal nitric oxide synthase in rat spinal motoneurons following axonal injury. *Neurosci. Lett.* 179, 157–161. doi: 10.1016/0304-3940(94)90958-x

Wu, W., Liuzzi, F. J., Schinco, F. P., Depto, A. S., Li, Y., Mong, J. A., et al. (1994b). Neuronal nitric oxide synthase is induced in spinal neurons by traumatic injury. *Neuroscience* 61, 719–726. doi: 10.1016/0306-4522(94)90394-8

Yamada, J., Hayashi, Y., Jinno, S., Wu, Z., Inoue, K., Kohsaka, S., et al. (2008). Reduced synaptic activity precedes synaptic stripping in vagal motoneurons after axotomy. *Glia* 56, 1448–1462. doi: 10.1002/glia.20711

Yamada, J., Nakanishi, H., and Jinno, S. (2011). Differential involvement of perineuronal astrocytes and microglia in synaptic stripping after hypoglossal axotomy. *Neuroscience* 182, 1–10. doi: 10.1016/j.neuroscience.2011.03.030

Yoshida, A., Mukai, N., Moritani, M., Nagase, Y., Hirose, Y., Honma, S., et al. (1999). Physiologic and morphologic properties of motoneurons and spindle afferents innervating the temporal muscle in the cat. *J. Comp. Neurol.* 406, 29–50. doi: 10.1002/(sici)1096-9861(19990329)406:1<29::aid-cne3>3.0.co;2-0

Yu, W. H. (1994). Nitric oxide synthase in motor neurons after axotomy. *J. Histochem. Cytochem.* 42, 451–457. doi: 10.1177/42.4.7510317

Yu, W. H. (1997). Regulation of nitric oxide synthase expression in motoneurons following nerve injury. *Dev. Neurosci.* 19, 247–254. doi: 10.1159/000111213

Zanon, R. G., and Oliveira, A. L. (2006). MHC I upregulation influences astroglial reaction and synaptic plasticity in the spinal cord after sciatic nerve transection. *Exp. Neurol.* 200, 521–531. doi: 10.1016/j.expneurol.2006.03.004

Zelano, J., Berg, A., Thams, S., Hailer, N. P., and Cullheim, S. (2009a). SynCAM1 expression correlates with restoration of central synapses on spinal motoneurons after two different models of peripheral nerve injury. *J. Comp. Neurol.* 517, 670–682. doi: 10.1002/cne.22186

Zelano, J., Plantman, S., Hailer, N. P., and Cullheim, S. (2009b). Altered expression of nectin-like adhesion molecules in the peripheral nerve after sciatic nerve transection. *Neurosci. Lett.* 449, 28–33. doi: 10.1016/j.neulet.2008.10.061

Zelano, J., Wallquist, W., Hailer, N. P., and Cullheim, S. (2006). Expression of nectin-1, nectin-3, N-cadherin, and NCAM in spinal motoneurons after sciatic nerve transection. *Exp. Neurol.* 201, 461–469. doi: 10.1016/j.expneurol.2006.04.026

Zelano, J., Wallquist, W., Hailer, N. P., and Cullheim, S. (2007). Down-regulation of mRNAs for synaptic adhesion molecules neuroligin-2 and -3 and synCAM1 in spinal motoneurons after axotomy. *J. Comp. Neurol.* 503, 308–318. doi: 10.1002/cne.21382

Zhang, X., Verge, V., Wiesenfeld-Hallin, Z., Ju, G., Bredt, D., Synder, S. H., et al. (1993). Nitric oxide synthase-like immunoreactivity in lumbar dorsal root ganglia and spinal cord of rat and monkey and effect of peripheral axotomy. *J. Comp. Neurol.* 335, 563–575. doi: 10.1002/cne.903350408

Zigmond, R. E., and Echevarria, F. D. (2019). Macrophage biology in the peripheral nervous system after injury. *Prog. Neurobiol.* 173, 102–121. doi: 10.1016/j.pneurobio.2018.12.001

Conflict of Interest: The authors declare that the research was conducted in the absence of any commercial or financial relationships that could be construed as a potential conflict of interest.

frontiers in Molecular Neuroscience

ORIGINAL RESEARCH
published: 19 May 2020
doi: 10.3389/fnmol.2020.00073

The Electrophysiological Determinants of Corticospinal Motor Neuron Vulnerability in ALS

*Javier H. Jara[1], Patrick L. Sheets[2†], Maximiliano José Nigro[2], Mina Perić[3], Carolyn Brooks[1], Daniel B. Heller[1], Marco Martina[2], Pavle R. Andjus[3] and P. Hande Ozdinler[1]**

[1]Davee Department of Neurology and Clinical Neurological Sciences, Feinberg School of Medicine, Northwestern University, Chicago, IL, United States, [2]Department of Physiology, Feinberg School of Medicine, Northwestern University, Chicago, IL, United States, [3]Institute for Physiology and Biochemistry "Ivan Djaja", Faculty of Biology, University of Belgrade, Belgrade, Serbia

OPEN ACCESS

Edited by:
John Martin,
City College of New York (CUNY), United States

Reviewed by:
Gavin John Clowry,
Newcastle University, United Kingdom
Andrew Paul Tosolini,
University College London, United Kingdom
Marin Manuel,
Université Paris Descartes, France

***Correspondence:**
P. Hande Ozdinler
ozdinler@northwestern.edu

[†]**Present address:**
Patrick L. Sheets,
Department of Pharmacology and Toxicology, Indiana University School of Medicine, Indianapolis, IN, United States

Received: 26 November 2019
Accepted: 15 April 2020
Published: 19 May 2020

Citation:
Jara JH, Sheets PL, Nigro MJ, Perić M, Brooks C, Heller DB, Martina M, Andjus PR and Ozdinler PH (2020) The Electrophysiological Determinants of Corticospinal Motor Neuron Vulnerability in ALS. Front. Mol. Neurosci. 13:73. doi: 10.3389/fnmol.2020.00073

The brain is complex and heterogeneous. Even though numerous independent studies indicate cortical hyperexcitability as a potential contributor to amyotrophic lateral sclerosis (ALS) pathology, the mechanisms that are responsible for upper motor neuron (UMN) vulnerability remain elusive. To reveal the electrophysiological determinants of corticospinal motor neuron (CSMN, a.k.a UMN in mice) vulnerability, we investigated the motor cortex of hSOD1^{G93A} mice at P30 (postnatal day 30), a presymptomatic time point. Glutamate uncaging by laser scanning photostimulation (LSPS) revealed altered dynamics especially within the inhibitory circuitry and more specifically in L2/3 of the motor cortex, whereas the excitatory microcircuits were unchanged. Observed microcircuitry changes were specific to CSMN in the motor column. Electrophysiological evaluation of the intrinsic properties in response to the microcircuit changes, as well as the exon microarray expression profiles of CSMN isolated from hSOD1^{G93A} and healthy mice at P30, revealed the presence of a very dynamic set of events, ultimately directed to establish, maintain and retain the balance at this early stage. Also, the expression profile of key voltage-gated potassium and sodium channel subunits as well as of the inhibitory GABA receptor subunits and modulatory proteins began to suggest the challenges CSMN face at this early age. Since neurodegeneration is initiated when neurons can no longer maintain balance, the complex cellular events that occur at this critical time point help reveal how CSMN try to cope with the challenges of disease manifestation. This information is critically important for the proper modulation of UMNs and for developing effective treatment strategies.

Keywords: amyotrophic lateral sclerosis, corticospinal motor neurons, microcircuit, upper motor neurons, hereditary spastic paraplegia, primary lateral sclerosis, neuronal vulnerability

INTRODUCTION

Amyotrophic lateral sclerosis (ALS) is characterized by progressive degeneration of both upper motor neurons (UMNs) and spinal motoneurons (SMN; Brown and Robberecht, 2001; Bruijn et al., 2004). UMN has a unique ability to collect information from many different neuron types, including long-distance projection neurons, interneurons, and local circuitry

neurons so that they can convey the cerebral cortex's input to spinal cord targets (Lemon, 2008). The cortical component of the motor neuron circuitry is complex and understanding the intrinsic and extrinsic factors that contribute to UMN vulnerability is challenging. To emphasize their iimportant role in motor neuron circuitry and their projection from cortex to the spinal cord, we refer the UMN in mice the corticospinal motor neurons (CSMN). These neurons degenerate in both ALS patients (Genç et al., 2017) and in well characterized mouse models of the disease (Ozdinler et al., 2011; Joyce et al., 2015; Gautam et al., 2016, 2019; Fil et al., 2017).

Early cortical defects in ALS, especially in the form of high intracortical excitability, are well documented by various independent groups around the globe (Eisen et al., 1993; Prout and Eisen, 1994; Mills and Nithi, 1997; Ziemann et al., 1997; Vucic and Kiernan, 2006). Such defects are linked to spasticity and hyperreflexia, hallmarks of cortical pathology and ALS (Caramia et al., 2000; Vucic et al., 2008), and more recently cortical dysfunction and hyperexcitability were suggested to be used as an early detection marker for disease initiation (Geevasinga et al., 2016).

Since the overall activity of the neural circuitries is well maintained by the orchestrated events of both excitatory and inhibitory inputs, and that these events follow a dynamic profile over time, understanding what happens during distinct disease stages remains a challenge. Especially within the context of neuronal vulnerability, such dynamics need to be revealed with precision, so that appropriate modulations can be applied either to UMN directly or to the neurons/cells that modulate them. Therefore, understanding the extrinsic and intrinsic factors that contribute to UMN vulnerability is crucial.

Most of our understanding of ALS historically came from the hSOD1^{G93A} ALS mouse model (Gurney et al., 1994), as it had been the first mouse model generated for ALS with a phenotype and all pre-clinical testing had to include data obtained from this very mouse model, which also displayed progressive CSMN loss (Ozdinler et al., 2011). Even though CSMN numbers are not yet significantly reduced at P30, by P60 genes and canonical pathways related to apoptosis are observed in CSMN (Ozdinler Lab, unpublished results), their numbers become significantly lower than healthy controls as they fail to retain their health and integrity of their cytoarchitecture (Jara et al., 2012). We thus focused our attention on CSMN at P30, a critical early time in their neurodegeneration, and investigated both the extrinsic and the intrinsic contributors to their neuronal vulnerability.

To investigate the distinct contributions of extrinsic and intrinsic factors to CSMN vulnerability, we used a multifaceted approach. First, we investigated how CSMN functional connectivity is altered in cortical circuits using glutamate uncaging by laser scanning photostimulation (LSPS; Anderson et al., 2010). This approach allows the assessment of extrinsic contributors to CSMN function in both health and disease. To reveal intrinsic changes, we took two parallel approaches, one *via* electrophysiological recordings (Martina et al., 2007), and the other by performing exon microarray analysis to determine the changes in gene expression. Our results revealed how dynamic CSMN were at P30 and how they relentlessly tried to maintain their balance and electrophysiological properties by changing the expression of selected ion channel subunits that play a pivotal role for voltage-gated ion conductance. Even though an overall look may not reveal any significant change in intrinsic membrane properties at this critical age, CSMN were very active. Revealing the details of events, which at times may appear counteractive or opposing each other's impact, helped us understand the extent of problems UMNs are faced with and what solutions they developed to counteract them. Since neuronal vulnerability is initiated when a neuron fails to maintain its homeostasis, being able to see the components of the turmoil just before losing balance is pivotal. Defining these molecular determinants of early stages of neurodegeneration especially in CSMN is what we try to achieve in this study, because this information will help identify targets for future modulations so that effective and long-term treatment strategies can be developed.

MATERIALS AND METHODS

Animals

All procedures were approved by the Northwestern University Animal Care and Use Committee and conformed to the standards of the National Institutes of Health. Wild type (WT), hSOD1^{G93A} transgenic ALS mice (Gurney et al., 1994) in the C57BL/6 background were obtained from Jackson laboratories. Also, the UCHL1-eGFP mice (generated by the Ozdinler Lab and made available at Jackson Laboratory, stock#. 022476; Yasvoina et al., 2013), as well as hSOD1G93A-UeGFP mice (generated in the Ozdinler Lab), were used in this study. Genotypes of mice were determined by PCR, as reported previously (Yasvoina et al., 2013). All animal procedures were approved by the Northwestern University Animal Care and Use Committee and conformed to the standards of the National Institutes of Health.

Surgical Procedures

Surgeries were performed on mice that were deeply anesthetized with isoflurane, and placed into a stereotaxic platform. Micro-injections were performed using pulled-beveled glass micro-pipettes attached to a nanojector (Drummond Scientific, Broomall, PA, USA).

CSMN Retrograde Labeling

All surgeries were performed as previously described (Ozdinler et al., 2011). Briefly, a small laminectomy at the cervical spinal cord (C2-C3) level was performed to expose the spinal cord. CSMN were retrogradely labeled by injection of fluorescent microspheres (LumaFluor Inc., Naples, FL, USA; ∼207 nl) into the corticospinal tract (CST) that lies within the dorsal funiculus (df) at 0.3 mm depth. Surgeries were performed at P21 and mice were sacrificed at P30 (n = 3). Only neurons that are retrogradely labeled were used for electrophysiological recording. All retrogradely labeled neurons were in layer 5 of the motor cortex.

Callosal Projection Neuron (CPN) Labeling

All surgeries were performed as previously described (Ozdinler et al., 2011). Briefly, a small unilateral craniotomy of ∼3 mm^2

to target the motor cortex (coordinates = +0.5 mm anterior-posterior; 1.5 mm mediolateral) was performed into the left hemisphere using a micro drill (Fine Science Tools, Foster City, CA, USA). Callosal Projection Neurons (CPN) were retrogradely labeled by four injections of fluorescent microspheres (LumaFluor Inc., Naples, FL, USA; a total of ∼276 nl) within the craniotomy area. Surgeries were performed at P21 and mice were sacrificed at P30 ($n = 3$).

FACS Purification of CSMN

Retrogradely labeled projection neurons were purified from WT and hSOD1^{G93A} mice based on their green fluorescence and the forward and side scatter characteristics of large projection neurons. Since retrograde labeling marks the corticospinal projection neurons within the motor cortex, at P30 the motor cortex was microdissected using a fluorescence-equipped dissecting microscope (SMZ-1500; Nikon) in the presence of cold dissociation medium (20 mM glucose, 0.8 mM kynurenic acid, 0.05 mM D(-)-2-amino-5-phosphonovaleric acid (AP5), 50 U/ml penicillin, 0.05 mg/ml streptomycin, 0.9 M Na_2SO_4 and 0.014 M $MgCl_2$, pH = 7.35, and supplemented with B27) and enzymatically digested for 15–20 min (0.16 mg/liter L-cysteine HCl, 12 U/ml papain and 1U/ml DNAseI, pH = 7.35, prepared in dissociation medium) at 37°C. Enzymatic digestion was blocked by dissociation medium containing 10 mg/ml ovomucoid (Sigma) and 10 mg/ml bovine serum albumin (BSA), and cells were mechanically dissociated in trituration buffer (OPTIMEM, supplemented with 20 mM glucose, 0.4 mM kynurenic acid, 0.025 mM AP5, B27, and BSA). The supernatant was collected in trituration buffer for FACS purification using a FACSVantage SE Diva flow cytometer (Becton Dickinson). Retrograde labeling, dissociation and FACS purification yielded approximately 30,000 live CSMN per P30 mice. Each experiment was repeated at least 4–5 times and results were reproducible and comparable.

Exon Microarray Analysis

Total RNA was extracted from FACS-purified retrogradely labeled CSMN using TRIZOL reagent (Invitrogen Life Technologies, Grand Island, NY, USA) with DNase digestion to prevent DNA contamination. RNA was reprecipitated in ethanol, integrity, and quantity was assessed (Agilent 2100 Bioanalyzer; Agilent Technologies, Palo Alto, CA, USA). Only high-quality RNA (OD260/280 $\geq$ 1.8, RIN $>$ 7.0) were used. RNA isolated from two littermate pups with the same genotype was used, and total RNA was converted into biotinylated cRNA (Ambion Illumina RNA amplification kit; Ambion, Austin, TX, USA), it was quantified (ND-1000 Spectrophotometer; NanoDrop, Wilmington, DE, USA). Biotinylated cRNA (100 ng) was hybridized to Illumina MouseWG-6 v2 Expression BeadChips at 58°C overnight, according to the manufacturer's instructions (Illumina Inc., San Diego, CA, USA), and were scanned using the Illumina BeadArray Reader. Data was generated through the Illumina BeadStudio software (Illumina Inc., San Diego, CA, USA) and probe signal intensities were quantile normalized and log-transformed. The exon microarray analyses were performed three independent times and the averages of exon readings were color-coded to improve visualization and data analyses. These procedures were performed by the Genomics Core Facility of Northwestern University.

Preparation of Brain Slices

Coronal brain slices (300 μm) containing the motor cortex were prepared at postnatal day 29–30 as described (Anderson et al., 2010). Slices were cut in chilled choline-based solution (in mM: 110 choline chloride, 25 $NaHCO_3$, 25 D-glucose, 11.6 sodium ascorbate, 7 $MgSO_4$, 3.1 sodium pyruvate, 2.5 KCl, 1.25 NaH_2PO_4, and 0.5 $CaCl_2$), allowed to recover in 35°C ACSF (in mM: 127 NaCl, 25 $NaHCO_3$, 25 D-glucose, 2.5 KCl, 1 $MgCl_2$, 2 $CaCl_2$, and 1.25 NaH_2PO_4) for 30 min and maintained at 21–22°C thereafter.

Recordings

Circuit Mapping Using Laser Scanning Photostimulation (LSPS)

Local circuit maps of CSMN using LSPS were performed as described (Anderson et al., 2010). Briefly, slices were transferred to the recording chamber of an upright microscope (BX51, Olympus), and held in place with short pieces of flattened gold wire (0.813 mm diameter; Alfa Aesar). Fluorescently labeled CSMN with red microspheres were visualized in using epifluorescence optics and they were located in layer 5 (L5) of the motor cortex. Pipettes were fabricated from borosilicate capillaries with filaments (G150-F, Warner) using a horizontal puller (P-97, Sutter). A cesium-based intracellular solution was used for mapping excitatory and inhibitory inputs [composition, in mM: 128 mM $CsMeSO_3$, 10 HEPES, 1 EGTA, 4 $MgCl_2$, 4 ATP, and 0.4 GTP, 10 phosphocreatine, 3 ascorbate, and 0.05 Alexa-594 or 488 (Molecular Probes); pH 7.3]. The bath solution for photostimulation studies contained elevated concentrations of divalent cations (4 mM Ca^{2+} and 4 mM Mg^{2+}) and an NMDA receptor antagonist (5 μM CPP; Tocris), to dampen neuronal excitability. Gabazine and NBQX were not included in the bath solution for glu-LSPS mapping studies. Caged glutamate (0.2 mM) was added directly to the bath solution. Voltages were not corrected for liquid junction potential. Recordings were performed at 21°C and were monitored for series resistance (inclusion criterion: <35 MΩ; mean: 17.3 MΩ). Once a patch recording of a labeled neuron was established, an image of the slice (4× objective) was acquired before mapping for precise registration of the mapping grid. The mapping grid (16 × 16; 100 μm spacing) was rotated with the top row of the grid flush with the pia and the soma was centered horizontally in the grid. The grid locations were sampled (every 0.4 s) with a UV stimulus 1.0 msec in duration and 20 mW at the specimen plane. Excitation profiles (EPs) were mapped as described (Weiler et al., 2008; Wood and Shepherd, 2010).

Intrinsic Properties Recordings

Electrophysiology recordings were performed as previously described (Martina et al., 2007). Briefly, slices were transferred to the recording chamber of an upright microscope (BX51, Olympus), and held in place with short pieces of flattened gold wire (0.813 mm diameter; Alfa Aesar). Fluorescently labeled

CSMN neurons (GFP+ and red microsphere positive) were visualized using epifluorescence optics. Pipettes were fabricated from borosilicate capillaries with filaments (G150-F, Warner) using a horizontal puller (P-97, Sutter). The extracellular solution for these recordings was: (in mM: 125 NaCl, 1.25 KCl, 1.25 KH_2PO_4, 25 $NaHCO_3$, and 16 glucose), and recording of intrinsic properties was performed in presence of blockers of fast synaptic transmission 10 μM DNQX, 50 μM APV, and 50 μM picrotoxin). For analysis of intrinsic excitability, the input/output curves obtained from each neuron were fit individually and we then calculated the mean and SEM of the fit parameters (reported in the text). I/V curves were investigated using 1 s long depolarizing current injections, with 100 pA steps. AP properties were investigated with measuring the properties of the first AP generated using 10 ms current injections, in 10 pA steps.

Tissue Collection, Processing, and Immunocytochemistry

Mice were deeply anesthetized and perfused as previously described (Jara et al., 2012) The brain was dissected, post-fixed in 4% PFA overnight, stored in PBS with 0.01% sodium azide, and sectioned at 50 μm using Leica vibratome (Leica VT1000S, Leica Inc., Nussloch, Germany). Floating sections were processed for immunocytochemistry (Jara et al., 2017). In this study anti-GFP (1:500, Abcam, Cambridge, MA, USA), anti-GABARAPL1 (1:200, Proteintech, USA), anti-KCNV1 (1:200), anti-KCTD12 (1:200, Proteintech, USA), and anti-SCN3B (1:200, LSBio, USA) antibodies were used. All proper secondary antibodies were purchased from Abcam and used in 1:500 dilution. Immunocytochemistry was performed as previously reported (Jara et al., 2017). Expression of KCNV1, GABARAPL, KCTD12, and SCN3B was evaluated from three comparable sections of WT-UeGFP and $hSOD1^{G93A}$-UeGFP mice ($n = 3$) spanning the motor cortex at P30 (Jara et al., 2017). Immunoreaction with KCTD12 could not be optimized and thus results could not be included in the text.

Imaging and Data Collection

Nikon Eclipse TE2000-E (Nikon Inc., Melville, NY, USA), Leica TCS SP5 confocal microscope (Leica Inc., Bensheim, Germany), and Zeiss 880 confocal microscope (Carl Zeiss microscopy, Jena, Germany) were used to acquire low- and high-magnification images, respectively. Confocal microscopy imaging was performed at the Center for Advanced Microscopy/Nikon Imaging Center (CAM), at the Northwestern University Feinberg School of Medicine, Chicago. Plan Apo 40× Oil DIC H objective was used for image acquiring. All images were blindly taken with the same exposure and settings. The intensity of immunofluorescence was quantified using ImageJ software (NIH, USA). The soma of GFP+ CSMN in the motor cortex of both healthy and diseased mice were identified as regions of interest. The mean gray value depicting the level of immunofluorescent expression intensity for each protein investigated in this study were measured. At least 60 cells (from $n = 3$ mice) were examined for each protein of interest and each genotype.

Statistical Analyses

Analysis of electrophysiology data was performed using Ephus software (Suter et al., 2010). Data analysis was performed offline using Matlab routines (Mathworks, Inc., Natick, MA, USA). Statistical comparisons between groups were made using Student-tests (for normally distributed data) or rank-sum test (for non-normally distributed data), as indicated. Error bars in plots represent SEM. In all cases, statistically significant differences were taken at $p < 0.05$.

RESULTS

Intrinsic Subthreshold Characteristics and Photoexcitability of $hSOD1^{G93A}$ CSMN Are Comparable to Healthy Controls

CSMN were previously shown to display early signs of vulnerability in $hSOD1^{G93A}$ mice (Ozdinler et al., 2011). To investigate the potential impact of synaptic and intrinsic factors contributing to CSMN vulnerability, we performed both LSPS mapping and patch-clamp recordings on retrogradely labeled CSMN in both WT and $hSOD1^{G93A}$ mice (**Figure 1A**). Retrograde labeling surgeries are performed at P21 (post-natal day 21), and brain slices containing the motor cortex are prepared at P30, an early pre-symptomatic stage in the disease.

The local sources of excitatory and inhibitory synaptic inputs were mapped to these neurons using a photostimulation grid that was aligned to the pia of the motor cortex in coronal brain slice (**Figure 1B**). The 256 sites in the 16 × 16 square grids were visited at 1 Hz in a non-raster pattern that avoided the vicinity of recently stimulated sites, and excitatory responses were recorded in voltage-clamp mode at a holding potential of either −70 mV, close to the reversal potential for GABAergic responses, or 10 mV, close the reversal potential for glutamatergic responses, as previously reported (Weiler et al., 2008). Synaptic input maps were constructed by plotting the mean response amplitude in a 50 ms post-stimulus time window (**Figure 1C**). Responses contaminated by direct activation of the recorded neuron's dendrites were excluded and rendered as black pixels in input color maps (**Figure 1D**). These maps thus represent "images" of the local sources of monosynaptic input, arising from small clusters of approximately 100 neurons at each stimulus location, to individual CSMN. Labeled CSMN in brain slices were targeted for patch-clamp recording and synaptic mapping so that their excitatory and inhibitory connectivity maps can be generated.

Differences in connectivity maps obtained from the motor cortex of $hSOD1^{G93A}$ and WT mice could potentially be explained by differences in the photoexcitability of presynaptic neurons, rather than differences in synaptic connectivity. To investigate this possibility, we performed EPs—maps revealing the number and spatial distribution of photoexcitable sites across individual neurons—to quantitatively measure photoexcitability of presynaptic neurons directly as shown previously (Wood and Shepherd, 2010). In these calibration experiments, which were interleaved with synaptic input mapping from other neurons in the same slices, we recorded from L2/3 pyramidal neurons in loose seal mode for both WT and $hSOD1^{G93A}$ mice

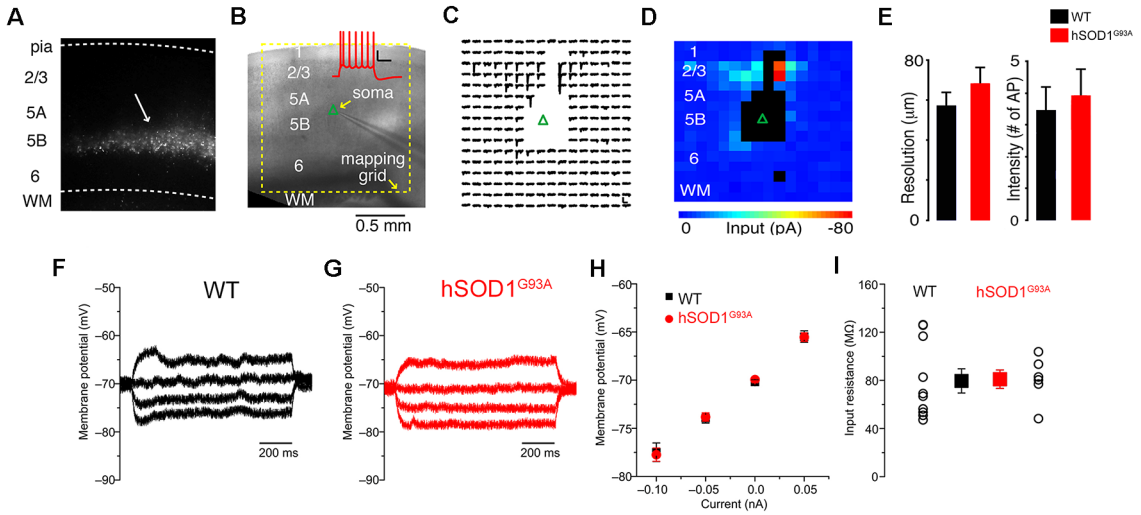

FIGURE 1 | Excitation profiles (EPs) and intrinsic properties of corticospinal motor neurons (CSMN) in the motor cortex of wild type (WT) and hSOD1^{G93A} mice at P30. **(A)** Retrograde bead labeling of CSMN in the motor cortex. **(B)** Bright-field image of mapping configuration for CSMN (inset); Corticospinal action potentials generated from 100 pA current injection. **(C)** Trace map (16 × 16,100 μm spacing) showing EPSCs following stimulation of local presynaptic areas. The blank area represents areas that resulted in the direct stimulation of the recorded neuron. **(D)** Color map representing local excitatory inputs in **(C)**. **(E)** *Left*: resolution of photostimulation (the mean distance of spike evoking sites from the soma), *right*: intensity of photostimulation (total number of spikes per map per cell); WT (black) and hSOD1^{G93A} (red). The intrinsic properties of neurons from hSOD^{G93A} and WT mice were largely identical. The input resistance was measured from the slope of a linear fit to the voltage response to hyper- and depolarizing steps: Representative recordings of a **(F)** WT and **(G)** hSOD1^{G93A} CSMN. **(H)** Average V-I plot of WT (black) and hSOD1^{G93A} (red). **(I)** Summary plot showing that the input resistance is very similar between the groups (WT: n = 10; hSOD1^{G93A}: n = 6).

while mapping their photoexitability using the same conditions as for synaptic input mapping (**Figure 1D**). We focused on L2/3 neurons as they are within the main presynaptic region of interest observed in synaptic input maps. The EP data sets were analyzed to determine: (1) the mean distance of spike evoking sites from the soma, an estimator of the resolution of photostimulation (**Figure 1E**, left); and (2) total number of spikes per map per cell, an estimator of the intensity of photostimulation (**Figure 1E**, right). These EP data suggested that photoexcitability between L2/3 neurons in hSOD1^{G93A} and WT littermates were comparable (**Figure 1E**).

Since intrinsic properties may also contribute to neuronal vulnerability, in a different set of experiments, we measured basic passive properties using a potassium-based intrapipette solution (**Figures 1F–I**). Resting membrane potential and input resistance were comparable between CSMN of WT and hSOD1^{G93A} mice (**Figures 1F–I**).

CSMN of hSOD1^{G93A} Mice Receive Strong Inhibitory Input

Our second set of experiments aimed to determine differences in local excitatory circuit strength of CSMN in hSOD1^{G93A} mice compared to WT littermates. Both WT (n = 25) and hSOD1^{G93A} CSMN (n = 27) in L5 received strong descending input from L2/3 (**Figure 2A**), as data obtained by averaging the maps and performing region-of-interest analyses revealed (**Figure 2B**). When the excitatory maps for each group were pooled, row analysis of inputs from a defined breadth of columns revealed similarities between two groups (**Figure 2C**). We next focused our analysis on a region of interest around the area of strongest L2/3 input (**Figure 2D**) and found no significant difference in excitatory circuit strength between CSMN of WT and hSOD1^{G93A} mice.

Unlike excitatory input maps, the inhibitory circuit mapping studies revealed a striking difference, especially at the site of L2/3 of the motor cortex. Using a cesium-based pipette (intracellular) solution and recording at a holding potential of ∼0 mV, close to the reversal potential for glutamatergic inputs, we found inhibitory responses following stimulation of L2/3 and L5 for both WT and hSOD1^{G93A} CSMN (**Figure 2E**). We recorded inhibitory input maps from CSMN of hSOD1^{G93A} (n = 16) and WT (n = 12) mice, and performed a region-of-interest analysis (**Figure 2F**). When the inhibitory maps for each group were pooled, row analysis of inputs (**Figure 2G**) showed significantly larger inhibitory responses following stimulation of L2/3 and L5B. Although perisomatic L5B inhibitory responses appeared larger for CSMN of hSOD1^{G93A} mice, it was not significant. However, focused analysis around the region of strongest L2/3 input showed that inhibitory input resulting from L2/3 was significantly larger in CSMN of hSOD1^{G93A} mice ($p < 0.05$; **Figure 2H**).

CPN Synaptic Input Confirms Cell-Type Specificity

To further investigate possible differences in photoexcitability, and to explore whether similar inhibitory and/or excitatory inputs are also observed in other projection neurons, we labeled CPNs at P30 by injecting fluorescent microspheres into the

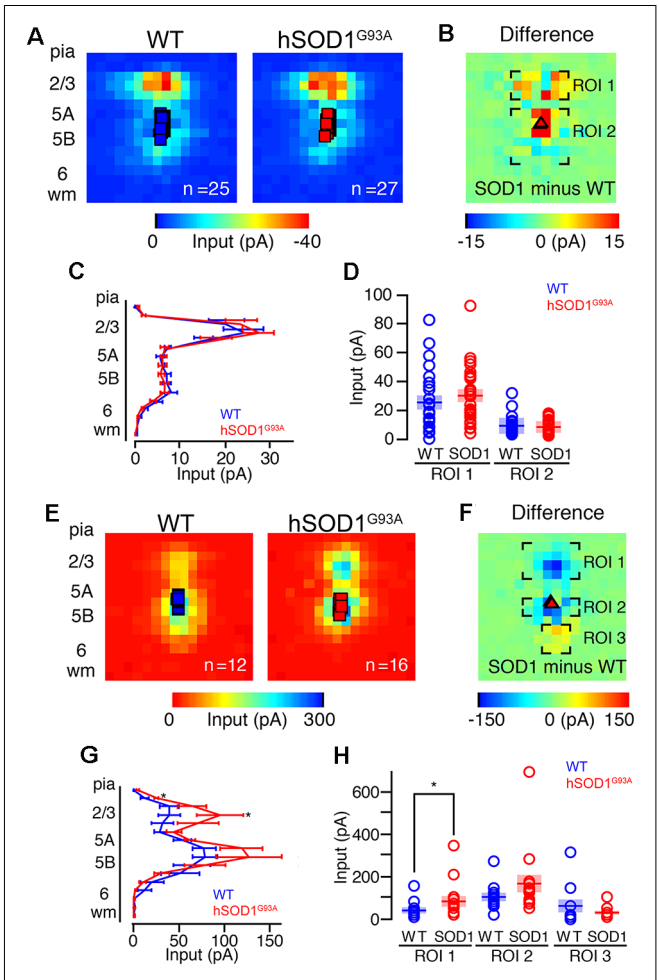

FIGURE 2 | Excitation and inhibitory profiles of CSMN in the motor cortex of WT and hSOD1^{G93A} mice at P30. **(A)** Examples of EPs for WT (left) and hSOD1^{G93A} (right) neurons with excitatory color maps. Voids represent areas of direct excitation on the recorded neuron. **(B)** Mapping grid (16 × 16) depicting areas of analysis; Region-of-interest = ROI. **(C)** Row average of excitatory inputs within the analysis region. **(D)** Comparison of presynaptic excitatory input region-of-interest for WT and hSOD1^{G93A} CSMN. **(E)** Example inhibitory input trace maps for WT (left) and hSOD1^{G93A} (right) CSMN. **(F)** Mapping grid (16 × 16) depicting areas of analysis. **(G)** Row average of inhibitory inputs within the analysis region. **(H)** Comparison of inhibitory input region-of-interest for WT and hSOD1^{G93A} CSMN. *$p < 0.05$, Kruskal–Wallis test.

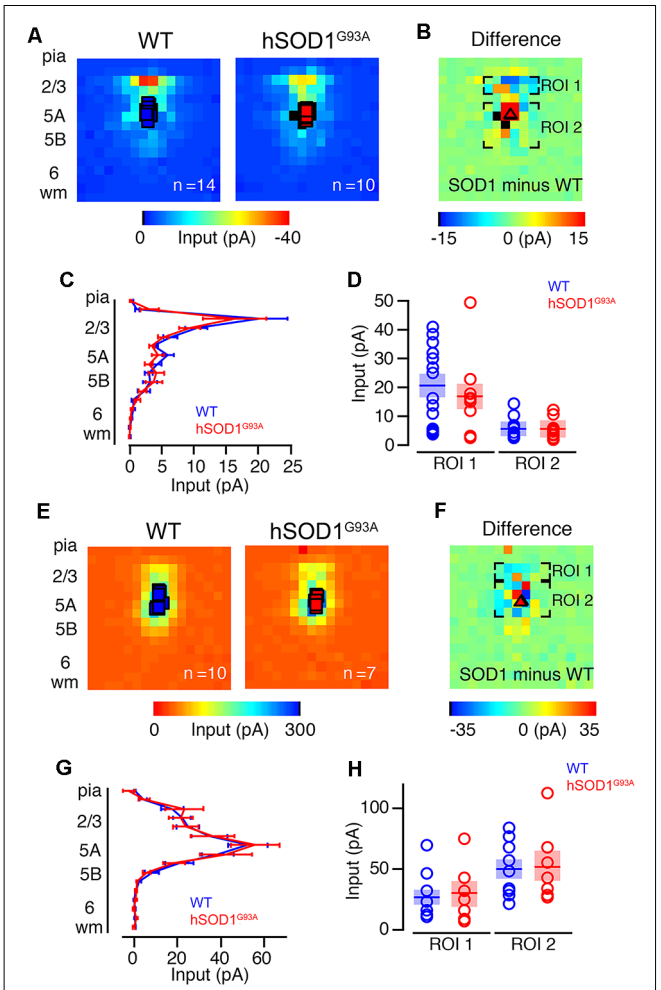

FIGURE 3 | Excitation and inhibitory profiles of callosal projection neuron (CPN) in the motor cortex of WT and hSOD1^{G93A} mice at P30. Excitatory input maps for CPN of P30 WT and hSOD1^{G93A} mice. **(A)** Average excitatory color maps for WT (left) and hSOD1^{G93A} (right) CPN neurons. Voids represent areas of direct excitation on the recorded neuron. **(B)** Mapping grid (16 × 16) depicting areas of analysis; Region-of-interest = ROI. **(C)** Row average of excitatory inputs within the analysis region. **(D)** Comparison of presynaptic excitatory input region-of-interest for WT and hSOD1^{G93A} CPN neurons. Inhibitory input maps for CPN of WT and hSOD1^{G93A} mice at P30. **(E)** Average inhibitory color maps for WT (left) and hSOD1^{G93A} (right) CPN. **(F)** Mapping grid (16 × 16) depicting areas of analysis. **(G)** Row average of inhibitory inputs within the analysis region. **(H)** Comparison of inhibitory input region-of-interest for WT and hSOD1^{G93A} CPN.

contralateral motor cortex at P21. We next mapped their excitatory and inhibitory inputs. CPN is located in lower layer 5A and receives strong input from layer 2/3 pyramidal neurons (Anderson et al., 2010), and therefore provides a relatively direct comparison to CSMN. Also, because CPN does not display early vulnerability in ALS, they serve as a good control to investigate whether observed effects are related to the disease state. CPN in WT and hSOD1^{G93A} mice in L5A showed strong excitatory inputs from L2/3 (**Figures 3A–C**). We recorded excitatory input maps from CPN of hSOD1^{G93A} (n = 10) and WT (n = 14) mice (**Figure 3A**), and mapping differences between WT and hSOD1^{G93A} (**Figure 3B**). These data showed no difference in L2/3 excitatory input for both row average (**Figure 3C**) and region-of-interest analysis (**Figure 3D**). As with CSMN, we found inhibitory responses following stimulation of L2/3 and L5 for CPN both in L5A of WT and hSOD1^{G93A} mice (**Figure 3E**). Analysis of inhibitory input maps recorded from CPN in hSOD1^{G93A} (n = 7) and WT (n = 10) mice (**Figure 3F**) also revealed comparable results between genotypes, further suggesting that the stronger inhibition observed in L2/3 of the motor cortex of hSOD1^{G93A} mice was specific to CSMN (**Figures 3G,H**).

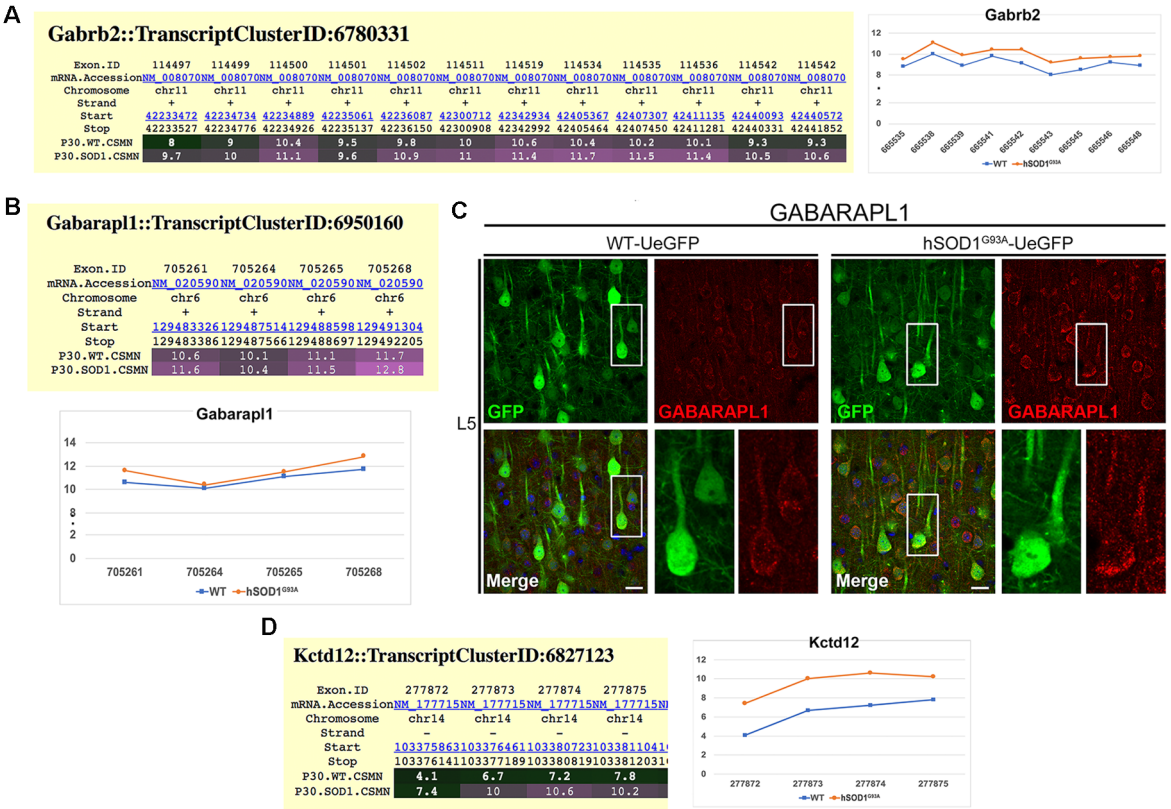

FIGURE 4 | Molecular evidence of altered inhibitory transmission in hSOD1^{G93A} CSMN. **(A)** Gene expression analysis of Gabarb2. Expression values for each exon are plotted to the right. **(B)** Gene expression analysis data for Gabarapl1. Expression values for each exon is plotted at the bottom. **(C)** Representative images of GABARAPL1 expression in L5 motor cortex of WT-UeGFP (left) and hSOD1^{G93A}-UeGFP (right). CSMN (green) and GABARAPL1 (red); insets are enlarged in the bottom right panels. Scale bar: 25 μm. **(D)** Gene expression analysis of Kctd12. Expression values for each exon are plotted to the right.

Inhibitory Transmission Is Altered in hSOD1^{G93A} CSMN

Since cortical connectivity studies suggested that CSMN receives increased inhibitory inputs especially at the site of L2/3, we next investigated whether the expression profile of inhibitory receptors was also altered in diseased CSMN. Exon microarray analysis performed using FACS-purified CSMN isolated from WT and hSOD1^{G93A} mice at P30, revealed that the expression profile of a distinct subset of $GABA_A$ subunits were altered. For example, the expression of *Gabra4* and *Gabrb1* genes, coding for the α4 and β1 subunits (**Supplementary Figure S1**), and *Garb2* gene, which codes for the β2 subunits of the GABA receptor (**Figure 4A**) displayed increased expression profile in CSMN of hSOD1^{G93A} mice. In addition to the receptor subunits, auxiliary proteins also play a role in modulating the GABA receptor function. Therefore, we investigated potential changes in the expression profiles of some key modulators. Interestingly, the expression of GABA type A receptor-associated protein-like 1 (GABARAPL1), which plays a key role in its modulation (Chen et al., 2000), was also evident by immunofluorescence in WT CSMN (1745.65 ± 24.84 a.u. n = 88 cells) and in hSOD1^{G93A} CSMN (2148.1 ± 142.27 a.u. n = 113 cells; p = 0.098; t-test, **Supplementary Figure S2**, **Figure 4B**). Interestingly, the location of GABARAPL1 was primarily in discrete domains within the somatic membrane (**Figure 4C**). Also, the expression of Kctd12 (K channel tetramerization domain-containing protein 12), an important modulator of GABA towards desensitization, was present mainly in CSMN of hSOD1^{G93A} mice (**Figure 4D**).

Intrinsic Electrical Properties of hSOD1^{G93A} CSMN and Their Molecular Background

The input resistance of hSOD1^{G93A} CSMN was not affected, as revealed by hyper- and hypo-polarization steps (**Figures 1F,G**). However, when injected with supra-threshold currents these neurons fired less because of a shallower current dependent increase in firing (the slope of a linear regression was 6.8 spikes/100 pA for WT CSMN (n = 9), and 5.4 spikes/100 pA for hSOD1^{G93A} CSMN (n = 13); $p \leq 0.05$; **Figure 5A**). The maximum frequency with a 700 pA current injection was also lower in hSOD1^{G93A} CSMN (43.9 ± 2.8 Hz) vs. WT CSMN (34.4 ± 3.2 Hz, $p \leq 0.05$; **Figures 5A,B**). This difference suggests the differential activity of a distinct voltage-

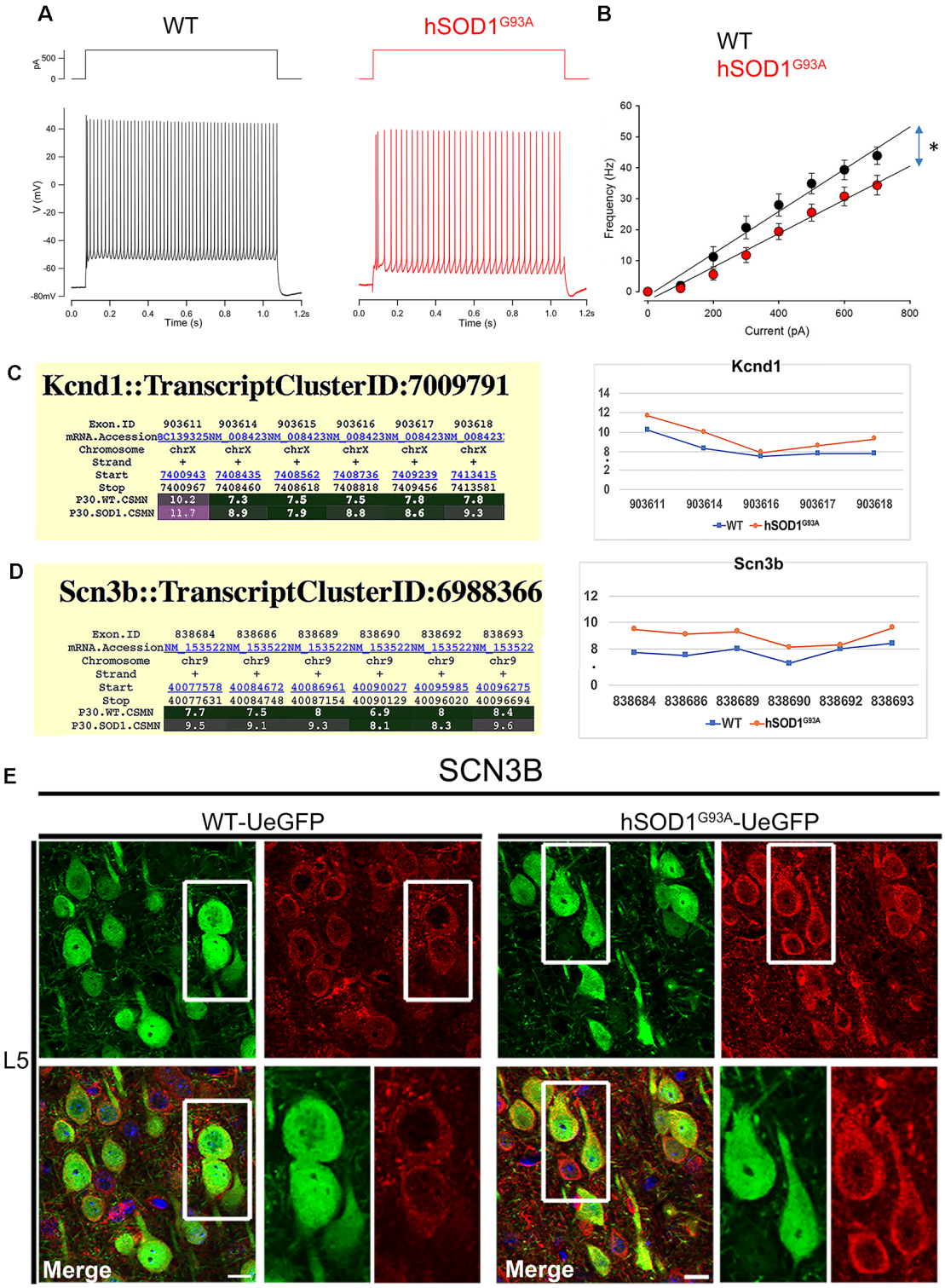

FIGURE 5 | The excitability of CSMN in hSOD1^{G93A} mice. The excitability was measured as the number of action potential fired in response to 1 s depolarizing current steps of increasing amplitudes (Δ 0.05 nA). **(A)** Representative responses of WT and hSOD1^{G93A} CSMN to a 0.4 nA current step. **(B)** Average f-I curve of CSMN in WT and hSOD1^{G93A} mice. WT (black; $n = 9$) and hSOD1^{G93A} (red; $n = 13$). **(C)** Gene expression analysis of Kcnd1. Expression values for each exon are plotted to the right. **(D)** Gene expression analysis of Scn3b. Expression values for each exon are plotted to the right. **(E)** Representative images of Scn3b expression in L5 motor cortex of WT-UeGFP (left) and hSOD1^{G93A}-UeGFP (right). CSMN (green) and Scn3b (red); insets are enlarged in the bottom right panels. Scale bar: 20 μm; *$p \leq 0.05$.

gated Na^+ and K^+ channels. Since CSMN of hSOD1^{G93A} mice fired less, we investigated the potential changes in the expression profile of voltage-gated K^+ and Na^+ channel subunits. Among all subunits, Kcnh5, Kcnq2 (**Supplementary Figure S1**), and Kcnd1 (**Figure 5C**) expression was prominent in diseased CSMN at P30. Among Na^+ subunits, we found that Scn2b (**Supplementary Figure S1**) and Scn3b (**Figure 5D**) were particularly increased in the CSMN of hSOD1^{G93A} mice at P30. Gene expression of Scn2b was also confirmed by immunocytochemical analysis (**Figure 5E**) and intensities of expression displayed an significant increase from WT CSMN (1,738.8 ± 33.9 a.u.; n = 73 cells) to hSOD1^{G93A} CSMN (2,463.5 ± 110.0 a.u.; n = 75 cells; p = 0.015; t-test, **Supplementary Figure S2**).

Interestingly, the properties of the first action potential generated by near-rheobase depolarizing current steps were comparable between WT and hSOD1^{G93A} CSMN (**Figure 6A**), including AP threshold (**Figures 6B,C**) and half duration [WT CSMN: 0.63 ± 0.017 ms (n = 9); hSOD1^{G93A} CSMN: 0.64 ± 0.04 ms (n = 13)], suggesting that the differences in spiking may depend on relatively slow K^+ channels that are not activated during individual APs. Our data may suggest that differential expression of the A-type potassium channel subunit Kcnd1 (**Figure 5C**) and outward rectifying channel subunit Kcnh5 (**Supplementary Figure S1**) may contribute to the observed slower firing. Interestingly, expression of Kcnv1, which slows inactivation of Kv2 channels and is a negative modulator of Kv3 (Salinas et al., 1997) and thus may contribute to slower firing was present less in WT than in hSOD1^{G93A} CSMN, as revealed by exon microarray (**Figure 7A**, **Supplementary Figure S2**) and immunocytochemical analysis (WT CSMN: 2044.5 ± 132.5 a.u.; n = 61 cells; hSOD1^{G93A} CSMN: 2445.4 ± 146.8 a.u.; n = 67 cells; p = 0.22; t-test; **Figure 7B**). The presence of Kcnv1 may also help explain why having Kcnc2 (Kv3.2; **Figure 6D**) does not appear to affect AP duration.

DISCUSSION

Understanding the factors that contribute to UMN vulnerability and progressive degeneration has been an important quest for building effective treatments for numerous neurodegenerative diseases, in which voluntary movement is impaired. Since the cortex is complex and heterogeneous, we believe that the underlying causes are also complex and multi-factorial. The UMNs may have intrinsic problems related to their genes and/or proteins, but the environment they are in can also contribute to their disease state.

The UMNs are located in L5 of the motor cortex and they have a very long apical dendrite that extends towards the top layers of the brain. These neurons are unique in their ability to be connected by many different neuron types so that they can be properly modulated to convey cortical input towards spinal cord targets. Building evidence reveals spine loss is an early event in ALS (Jara et al., 2015). Also, extensive apical dendrite

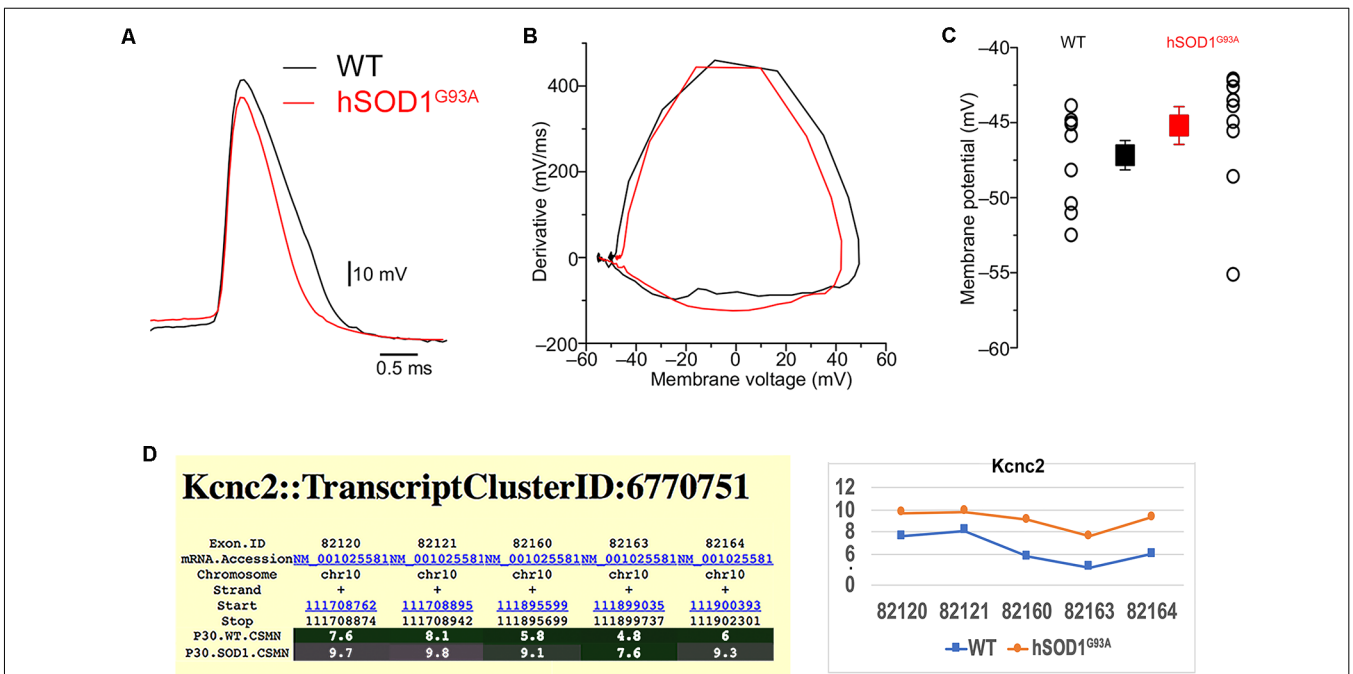

FIGURE 6 | The form of action potential and the threshold in hSOD1^{G93A} CSMN. **(A)** Representative traces of action potentials in WT (black) and hSOD1^{G93A} (red) CSMN. The action potential threshold was measured from the first action potential fired in response to depolarizing current steps at the point where the first derivative was 10 mV/ms. **(B)** First derivatives of the traces in **(A)**. **(C)** Summary plot showing the action potential threshold for WT and hSOD1^{G93A} CSMN (WT: −47.2 ± 0.9 mV, n = 9; hSOD1^{G93A}: −45.2 ± 1.3 mV, n = 13). **(D)** Gene expression analysis of Kcnc2. Expression values for each exon are plotted to the right.

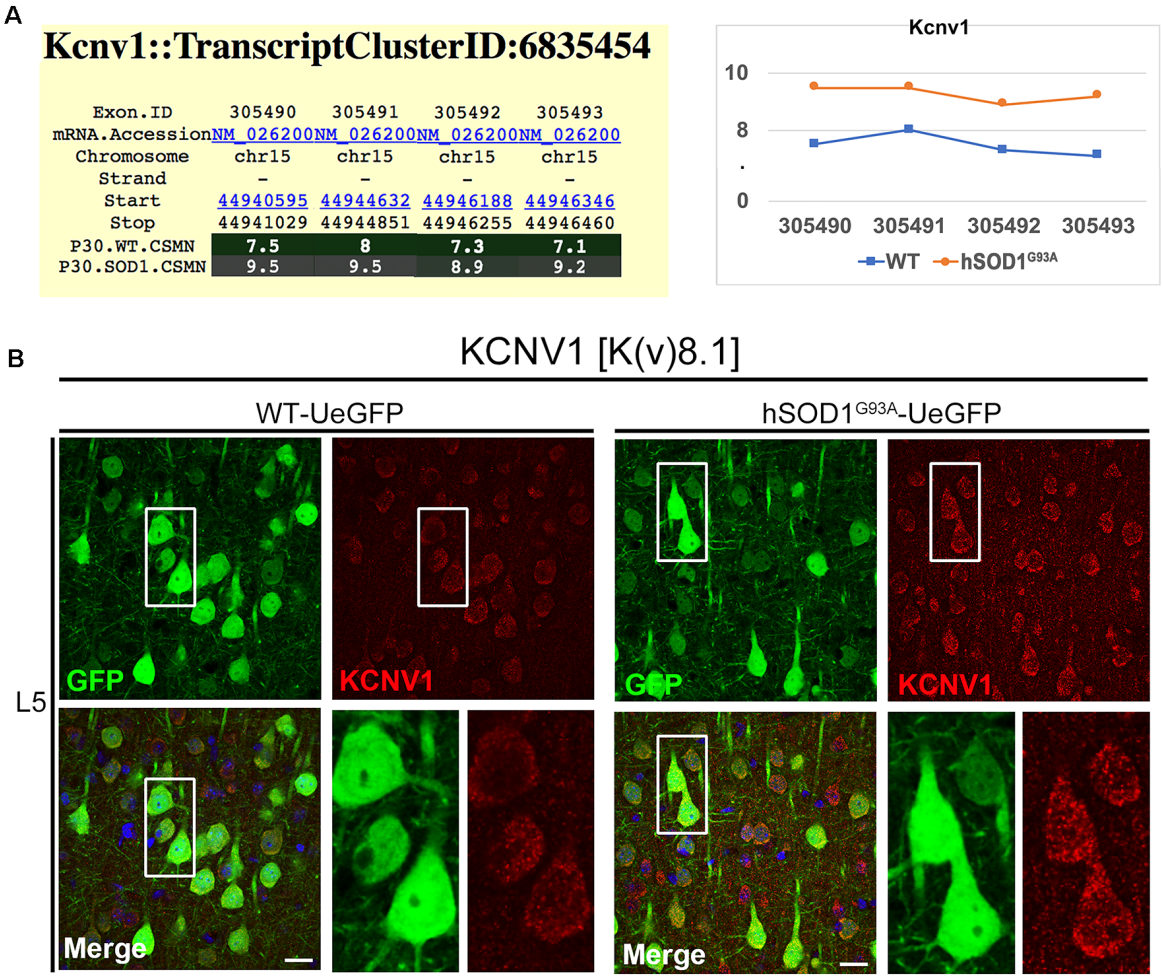

FIGURE 7 | KCNV1 expression levels are increased in diseased CSMN. **(A)** Gene expression analysis of Kcnv1. Expression values for each exon are plotted to the right. **(B)** Representative images of Kcnv1 expression in L5 motor cortex of WT-UeGFP (left) and hSOD1^{G93A}-UeGFP (right). CSMN (green) and Kcnv1 (red); insets are enlarged in the bottom right panels. Scale bar: 20 μm.

degeneration is observed in CSMN of many different mouse models of ALS (Ozdinler et al., 2011; Gautam et al., 2016, 2019; Genç et al., 2016) as well as Betz cells of a broad spectrum of ALS patients, including fALS, sALS and ALS/FTLD pathologies (Genç et al., 2017). Such architectural defects would impair proper modulation of UMNs, and would in part affect the motor neuron circuitry.

Previously, it was thought that the UMN loss is simply a byproduct of the ongoing spinal motor neuron degeneration. However, recent evidence revealed that cortical degeneration is an early event in ALS, so much so that cortical hyperexcitation occurs even before symptom onset in patients (Geevasinga et al., 2016). Hyperexcitation of neurons could be mediated by many different means. The neurons could be excited more by the excitatory neurons that converge unto them, the inhibitory neurons that inhibit them could be inhibited, or the neurons themselves may modulate expression profiles of key genes that code for the subunits of ion channels that help modulate their excitation and inhibition responses. Therefore, we expect that maintaining homeostasis is a dynamic state and perturbation of this state is the leading cause of neuronal vulnerability.

Studies in ALS patients (Caramia et al., 2000; Vucic et al., 2008; Van den Bos et al., 2018; Menon et al., 2019) demonstrate intracortical excitability, which can ultimately lead to spasticity and hyperreflexia, hallmarks of cortical pathology in ALS. ALS patients with C9orf72 expansions showed hyperexcitability as a feature of only symptomatic ALS patients (Geevasinga et al., 2015; Schanz et al., 2016), while other studies showed that cortical hyperexcitability appears early in the disease process in sALS patients (Eisen et al., 1993; Prout and Eisen, 1994; Mills and Nithi, 1997; Ziemann et al., 1997; Vucic and Kiernan, 2006), and precede the onset of the disease in fALS patients with SOD1 mutation (Vucic et al., 2008).

To understand the cortical abnormalities found in patients, several studies investigated the role of cortical neurons in the hSOD1^{G93A} ALS mouse model (Gurney et al., 1994).

Different studies in motor areas of the neocortex found evidence for an increase in inhibitory circuits (Minciacchi et al., 2009) but also an increase in glutamate in the region of the motor cortex of symptomatic ALS hSOD1^{G93A} mice at P80 (Choi et al., 2009). A more recent study demonstrated early changes in pyramidal neurons in the motor cortex of the hSOD1^{G93A} mice before symptoms arise at P21 (Fogarty et al., 2015). Pyramidal neurons showed apical dendritic regression and intrinsic electrophysiological properties such as an increase in EPSC. Although this study does not directly implicate CSMN, it supports previous reports showing CSMN apical dendrite defects and spine loss. Our previous studies suggest that apical vacuolation and loss of spines in the hSOD1^{G93A} mice might play a key role in the local and distal microcircuits and that it might lead to CSMN dysfunction and overactivity by lack of proper neuronal modulation (Jara et al., 2014).

To reveal the underlying causes of neuronal vulnerability, we focused our attention on P30, a critical time point in CSMN vulnerability in the hSOD1^{G93A} mice. At this age, CSMN numbers are not yet significantly reduced and the mice show no behavioral defects. Interestingly, a thorough analysis of CSMN connectivity and electrophysiological properties at different stages of development and disease also suggested this age to be a critical time of vulnerability, as the neurons manage to maintain homeostasis briefly at this stage (Kim et al., 2017). Therefore, understanding the events that occur within and outside CSMN at this particular age is of biomedical significance. We thus analyzed CSMN functional connectivity in cortical circuits using glutamate uncaging and LSPS (Anderson et al., 2010), and intrinsic properties of CSMN (Martina et al., 2007).

We performed the first application of LSPS and cortical circuit mapping to CSMN in hSOD1^{G93A} mice. Also, we investigated the changes in the gene expression of key components of ion channel subunits, to examine the potential intrinsic changes that occur in diseased CSMN. We find subtle and yet important differences, some reaching significance, some not, during this early stage. For example, there is an enhancement of local inhibitory input especially following excitation of L2/3 for CSMN, but the same phenomenon is not observed in CPN, suggesting that the observed defects are cell-type specific. Likewise, CSMN appears to respond to inhibitory input, but it also activates expression of some key genes that are important for modulating voltage-gated Na^+ and K^+ currents, and thus an excitable state.

Neurons can receive inhibitory and excitatory inputs at the same time and from thousands of different neurons simultaneously. This is an immense undertaking. Especially UMNs, which are extensively modulated by both long-distance excitatory neurons and local circuitry neurons that are both excitatory and inhibitory, the balance between excitation and inhibition is very challenging to maintain. However, healthy neurons achieve this task and they become vulnerable only when they fail to maintain homeostasis.

For this study, inhibitory inputs were recorded using glutamate uncaging while holding a patch-clamped neuron at the reversal potential for glutamatergic responses. Inhibitory neurons are also a complex group of neurons with many different subtypes and specific functions (Kawaguchi and Kubota, 1997; Kawaguchi and Kondo, 2002; Apicella et al., 2012). They are present throughout the motor column and numerous studies tried to reveal potential changes in their numbers concerning disease progression. Even though some results appear to contradict, overall analyses suggest that the distribution and the function of interneurons are an important component of UMN circuitry (Ziemann et al., 1997; Clark et al., 2018). The inhibitory input can be monosynaptic (direct) and disynaptic (*via* another neuron). Therefore, understanding the imminent impact of the inhibitory input is challenging. Recorded inputs thus represent both monosynaptic inhibitory inputs resulting from stimulation of interneurons and disynaptic inhibitory inputs resulting from stimulation of pyramidal neurons, which subsequently excite interneurons. Our analysis shows that inhibitory inputs following L2/3 stimulation were significantly different. In a recent study, the main L2/3 → L5 inhibitory pathway for CSMN was shown to result from descending disynaptic excitation of low-threshold spiking interneurons in L5 (Apicella et al., 2012). Since the inhibitory input was mainly increased in L2/3, and not L5, we speculate that the difference in inhibitory inputs following L2/3 stimulation is due to a strengthening of the L2/3 → L5 inhibitory pathway, and not due to changes in enhanced L5 inhibitory neuron excitation. This in part may suggest that, since inhibitory neurons located in L2/3, whose goal is to inhibit the inhibitory neurons in L5, are more activated, they may thus inhibit the inhibitory neurons in L5 more. Dual clamp experiments are required to investigate the accuracy of this phenomenon.

The electrical properties of CSMN at this early stage of P30 demonstrated conflicting excitatory and inhibitory factors. Similar to our findings, there are reports to support hyperexcitability (van Zundert et al., 2008; Vucic et al., 2009; Wainger et al., 2014; Fogarty, 2018), but on the other hand also on reduced excitability (Mills, 2003; Delestrée et al., 2014; Leroy et al., 2014; King et al., 2016; Clark et al., 2018). We believe that hyper and/or hypo excitability is a dynamic phenomenon, and it is a function of disease state.

Interestingly, hyperexcitability has been reported as early as P4 and P5 (van Zundert et al., 2008; Kim et al., 2017), and in the course of development and disease progression neurons adapt their functional properties to normalize cortical excitability at P26–40 (Kim et al., 2017). However, as the disease progresses without intervention at P90–129 hyperexcitability appears again (Kim et al., 2017). The question arises if the cause of this modulation of excitability is extrinsic or intrinsic. Although based on the LSPS experiments and cortical circuit mapping, the extrinsic local inhibitory circuitry could not be excluded, several intrinsic factors were pointing to the specificity of CSMN electrical changes in the ALS mouse model. Foremost, in line with the increase in the inhibitory maps in L2/3, the inhibitory synapses to L5 CSMNs are strengthened as indicated by overexpression of $GABA_A$ receptor subunits genes *Gabra4* *Gabrb1*, and *Gabrb2* (α4, β1 and

β2 subunits, respectively). Clustering of these receptors at the postsynaptic membrane may also contribute to synaptic strengthening, and in fact, it was found by gene analysis and immunocytochemistry that the GABARAPL1 was upregulated in CSMN. This protein is known to cause the clustering of $GABA_A$ receptors at the cell membrane (Chen et al., 2000), but it can also promote autophagy, particularly in neurons (Le Grand et al., 2013). The latter could be a housekeeping mechanism by which to regulate overinhibition of CSMN, which also serves as a compensatory mechanism. On the other hand, we have observed an abundant overexpression of the Kctd12 gene for the modulatory protein that acts on the kinetics of activation and desensitization of $GABA_B$ receptors and thus may counteract the rise of the inhibitory input by $GABA_A$ receptors (Li et al., 2017). This is rather significant because Kctd12 is one of the most potent modulators of GABA inhibition and has the demonstrated potential to reverse its effect. Only diseased CSMN express very high levels of Kctd12 and it could represent its effort to counteract the GABA inhibition.

On the other hand, the intrinsic basis of the perturbed balance of excitatory and inhibitory factors was evidenced by further gene expression analysis demonstrating overexpression of potassium voltage-gated channels Kcnc2, as well as Kcnd1 and Kcnh5, known to decrease neuronal firing (Bean, 2007; Martina et al., 2007; Brown and Passmore, 2009; Buskila et al., 2019). We also found that upon current injection, $hSOD1^{G93A}$ CSMN fire at a slower pace compared to CSMN of WT littermates. Gene expression analysis revealed a potential explanation for the molecular background of such behavior in an overexpression of sodium channel beta subunits, particularly beta 2 and 3 (Scn2b and Scn3b), which were also found to be overexpressed in $hSOD1^{G93A}$ mouse spinal cord MNs, albeit at later stages (Nutini et al., 2011, also see van Zundert et al., 2008; King et al., 2016; Sirabella et al., 2018). On the other hand, intense punctate staining was revealed on CSMN somata for the Kcnv1 (Kv8.1) potassium channel known to act as a negative modulator of Kv2 and Kv3 channels (Salinas et al., 1997), thus suggesting also an excitatory profile.

Our studies begin to reveal the complex nature of events that occur at the motor cortex as well as the response mechanism CSMN develops to maintain homeostasis at this critical time of neuronal vulnerability. Even though CSMN does not yet show signs of neuronal degeneration at P30, it is in a very active state with enhanced gene expression of key GABA receptor subunits, modulatory proteins as well as subunits of voltage-gated ion channels. Also, the activation of inhibitory neurons, especially in L2/3, deserves much more attention to gain a full understanding of the intrinsic and the extrinsic mechanisms responsible for UMN vulnerability. Here, we reveal the key players involved in CSMN excitation and inhibition at this critical hour of neuronal vulnerability. Our findings suggest key targets for direct modulation of UMN activity either towards inhibition or excitation states. This information is required for building effective and long-term treatment strategies by helping vulnerable neurons retain their homeostasis.

DATA AVAILABILITY STATEMENT

All datasets generated for this study are included in the **Supplementary Material**.

ETHICS STATEMENT

The animal study was reviewed and approved by Northwestern University Animal Care and Use Committee.

AUTHOR CONTRIBUTIONS

PS, JJ, and PO designed the photostimulation electrophysiology experiments. PS conducted and analyzed the LSPS electrophysiology data. MN, JJ, MM, and PO designed the electrophysiology experiments to evaluate CSMN intrinsic properties. JJ performed all exon microarray experiments. MN conducted and analyzed the electrophysiology data. CB, DH, MP, PO, and JJ performed and analyzed all immunocytochemistry data. JJ performed all surgical procedures. JJ, PS, MM, PA, and PO wrote the manuscript.

FUNDING

This work was funded by NIA-RO1AG061708 (to PO), Les Turner ALS Foundation (to PO), National Institutes of Health (NIH) grant NS066675 (to PS), Amyotrophic Lateral Sclerosis Association (ALSA) Milton Safenowitz Postdoctoral Fellowship (to JJ), and European Commission (EC) H2020 MSCA RISE grant 778405 (to PA and PO).

ACKNOWLEDGMENTS

We thank Dr. Gordon MG Shepherd for his help and guidance on the connectivity mapping studies, and Dr. Derya Ozyurt for converting exon microarray data into GEO compatible format.

SUPPLEMENTARY MATERIAL

The Supplementary Material for this article can be found online at: https://www.frontiersin.org/articles/10.3389/fnmol.2020.00073/full#supplementary-material.

FIGURE S1 | List of all genes investigated for their expression profile using exon microarray. CSMN isolated from WT and $hSOD1^{G93A}$ mice at P30 is used for these gene expression analyses. The table displays the average of three independent experiments, and the results are log 2 transformed and color-coded to reveal the difference in levels of expression.

FIGURE S2 | Bar graph representation for the average intensity of fluorescence for GABARAPL1, SCN3B, and KCNV1 expression in CSMN of WT (black box) and $hSOD1^{G93A}$ (white box) mice at P30. Data are shown as mean ± SEM of three independent experimental replicates. *T*-test is used to determine statistical significance, and $^*p < 0.05$ is considered significant.

REFERENCES

Anderson, C. T., Sheets, P. L., Kiritani, T., and Shepherd, G. M. (2010). Sublayer-specific microcircuits of corticospinal and corticostriatal neurons in motor cortex. *Nat. Neurosci.* 13, 739–744. doi: 10.1038/nn.2538

Apicella, A. J., Wickersham, I. R., Seung, H. S., and Shepherd, G. M. (2012). Laminarly orthogonal excitation of fast-spiking and low-threshold-spiking interneurons in mouse motor cortex. *J. Neurosci.* 32, 7021–7033. doi: 10.1523/JNEUROSCI.0011-12.2012

Bean, B. P. (2007). The action potential in mammalian central neurons. *Nat. Rev. Neurosci.* 8, 451–465. doi: 10.1038/nrn2148

Brown, D. A., and Passmore, G. M. (2009). Neural KCNQ (Kv7) channels. *Br. J. Pharmacol.* 156, 1185–1195. doi: 10.1111/j.1476-5381.2009.00111.x

Brown, R. H. Jr., and Robberecht, W. (2001). Amyotrophic lateral sclerosis: pathogenesis. *Semin. Neurol.* 21, 131–139. doi: 10.1055/s-2001-15260

Bruijn, L. I., Miller, T. M., and Cleveland, D. W. (2004). Unraveling the mechanisms involved in motor neuron degeneration in ALS. *Annu. Rev. Neurosci.* 27, 723–749. doi: 10.1146/annurev.neuro.27.070203.144244

Buskila, Y., Kékesi, O., Bellot-Saez, A., Seah, W., Berg, T., Trpceski, M., et al. (2019). Dynamic interplay between H-current and M-current controls motoneuron hyperexcitability in amyotrophic lateral sclerosis. *Cell Death Dis.* 10:310. doi: 10.1038/s41419-019-1538-9

Caramia, M. D., Palmieri, M. G., Desiato, M. T., Iani, C., Scalise, A., Telera, S., et al. (2000). Pharmacologic reversal of cortical hyperexcitability in patients with ALS. *Neurology* 54, 58–64. doi: 10.1212/wnl.54.1.58

Chen, L., Wang, H., Vicini, S., and Olsen, R. W. (2000). The gamma-aminobutyric acid type A ($GABA_A$) receptor-associated protein (GABARAP) promotes $GABA_A$ receptor clustering and modulates the channel kinetics. *Proc. Natl. Acad. Sci. U S A* 97, 11557–11562. doi: 10.1073/pnas.190133497

Choi, J. K., Küstermann, E., Dedeoglu, A., and Jenkins, B. G. (2009). Magnetic resonance spectroscopy of regional brain metabolite markers in FALS mice and the effects of dietary creatine supplementation. *Eur. J. Neurosci.* 30, 2143–2150. doi: 10.1111/j.1460-9568.2009.07015.x

Clark, R. M., Brizuela, M., Blizzard, C. A., and Dickson, T. C. (2018). Reduced excitability and increased neurite complexity of cortical interneurons in a familial mouse model of amyotrophic lateral sclerosis. *Front. Cell. Neurosci.* 12:328. doi: 10.3389/fncel.2018.00328

Delestrée, N., Manuel, M., Iglesias, C., Elbasiouny, S. M., Heckman, C. J., and Zytnicki, D. (2014). Adult spinal motoneurones are not hyperexcitable in a mouse model of inherited amyotrophic lateral sclerosis. *J. Physiol.* 592, 1687–1703. doi: 10.1113/jphysiol.2013.265843

Eisen, A., Pant, B., and Stewart, H. (1993). Cortical excitability in amyotrophic lateral sclerosis: a clue to pathogenesis. *Can. J. Neurol. Sci.* 20, 11–16. doi: 10.1017/s031716710004734x

Fil, D., DeLoach, A., Yadav, S., Alkam, D., MacNicol, M., Singh, A., et al. (2017). Mutant Profilin1 transgenic mice recapitulate cardinal features of motor neuron disease. *Hum. Mol. Genet.* 26, 686–701. doi: 10.1093/hmg/ddw429

Fogarty, M. J. (2018). Driven to decay: excitability and synaptic abnormalities in amyotrophic lateral sclerosis. *Brain Res. Bull.* 140, 318–333. doi: 10.1016/j.brainresbull.2018.05.023

Fogarty, M. J., Noakes, P. G., and Bellingham, M. C. (2015). Motor cortex layer V pyramidal neurons exhibit dendritic regression, spine loss and increased synaptic excitation in the presymptomatic hSOD1(G93A) mouse model of amyotrophic lateral sclerosis. *J. Neurosci.* 35, 643–647. doi: 10.1523/JNEUROSCI.3483-14.2015

Gautam, M., Jara, J. H., Kocak, N., Rylaarsdam, L. E., Kim, K. D., Bigio, E. H., et al. (2019). Mitochondria, ER, and nuclear membrane defects reveal early mechanisms for upper motor neuron vulnerability with respect to TDP-43 pathology. *Acta Neuropathol.* 137, 47–69. doi: 10.1007/s00401-018-1934-8

Gautam, M., Jara, J. H., Sekerkova, G., Yasvoina, M. V., Martina, M., and Özdinler, P. H. (2016). Absence of alsin function leads to corticospinal motor neuron vulnerability *via* novel disease mechanisms. *Hum. Mol. Genet.* 25, 1074–1087. doi: 10.1093/hmg/ddv631

Geevasinga, N., Menon, P., Nicholson, G. A., Ng, K., Howells, J., Kril, J. J., et al. (2015). Cortical function in asymptomatic carriers and patients with C9orf72 amyotrophic lateral sclerosis. *JAMA Neurol.* 72, 1268–1274. doi: 10.1001/jamaneurol.2015.1872

Geevasinga, N., Menon, P., Özdinler, P. H., Kiernan, M. C., and Vucic, S. (2016). Pathophysiological and diagnostic implications of cortical dysfunction in ALS. *Nat. Rev. Neurol.* 12, 651–661. doi: 10.1038/nrneurol.2016.140

Genç, B., Jara, J. H., Lagrimas, A. K., Pytel, P., Roos, R. P., Mesulam, M. M., et al. (2017). Apical dendrite degeneration, a novel cellular pathology for Betz cells in ALS. *Sci. Rep.* 7:41765. doi: 10.1038/srep41765

Genç, B., Jara, J. H., Schultz, M. C., Manuel, M., Stanford, M. J., Gautam, M., et al. (2016). Absence of UCHL 1 function leads to selective motor neuropathy. *Ann. Clin. Transl. Neurol.* 3, 331–345. doi: 10.1002/acn3.298

Gurney, M. E., Pu, H., Chiu, A. Y., Dal Canto, M. C., Polchow, C. Y., Alexander, D. D., et al. (1994). Motor neuron degeneration in mice that express a human Cu,Zn superoxide dismutase mutation. *Science* 264, 1772–1775. doi: 10.1126/science.8209258

Jara, J. H., Genç, B., Cox, G. A., Bohn, M. C., Roos, R. P., Macklis, J. D., et al. (2015). Corticospinal motor neurons are susceptible to increased ER stress and display profound degeneration in the absence of UCHL1 function. *Cereb. Cortex* 25, 4259–4272. doi: 10.1093/cercor/bhu318

Jara, J. H., Genç, B., Klessner, J. L., and Ozdinler, P. H. (2014). Retrograde labeling, transduction, and genetic targeting allow cellular analysis of corticospinal motor neurons: implications in health and disease. *Front. Neuroanat.* 8:16. doi: 10.3389/fnana.2014.00016

Jara, J. H., Genç, B., Stanford, M. J., Pytel, P., Roos, R. P., Weintraub, S., et al. (2017). Evidence for an early innate immune response in the motor cortex of ALS. *J. Neuroinflammation* 14:129. doi: 10.1186/s12974-017-0896-4

Jara, J. H., Villa, S. R., Khan, N. A., Bohn, M. C., and Ozdinler, P. H. (2012). AAV2 mediated retrograde transduction of corticospinal motor neurons reveals initial and selective apical dendrite degeneration in ALS. *Neurobiol. Dis.* 47, 174–183. doi: 10.1016/j.nbd.2012.03.036

Joyce, P. I., Mcgoldrick, P., Saccon, R. A., Weber, W., Fratta, P., West, S. J., et al. (2015). A novel SOD1-ALS mutation separates central and peripheral effects of mutant SOD1 toxicity. *Hum. Mol. Genet.* 24, 1883–1897. doi: 10.1093/hmg/ddu605

Kawaguchi, Y., and Kondo, S. (2002). Parvalbumin, somatostatin and cholecystokinin as chemical markers for specific GABAergic interneuron types in the rat frontal cortex. *J. Neurocytol.* 31, 277–287. doi: 10.1023/a:1024126110356

Kawaguchi, Y., and Kubota, Y. (1997). GABAergic cell subtypes and their synaptic connections in rat frontal cortex. *Cereb. Cortex* 7, 476–486. doi: 10.1093/cercor/7.6.476

Kim, J., Hughes, E. G., Shetty, A. S., Arlotta, P., Goff, L. A., Bergles, D. E., et al. (2017). Changes in the excitability of neocortical neurons in a mouse model of amyotrophic lateral sclerosis are not specific to corticospinal neurons and are modulated by advancing disease. *J. Neurosci.* 37, 9037–9053. doi: 10.1523/JNEUROSCI.0811-17.2017

King, A. E., Woodhouse, A., Kirkcaldie, M. T., and Vickers, J. C. (2016). Excitotoxicity in ALS: overstimulation, or overreaction? *Exp. Neurol.* 275, 162–171. doi: 10.1016/j.expneurol.2015.09.019

Le Grand, J. N., Bon, K., Fraichard, A., Zhang, J., Jouvenot, M., Risold, P. Y., et al. (2013). Specific distribution of the autophagic protein GABARAPL1/GEC1 in the developing and adult mouse brain and identification of neuronal populations expressing GABARAPL1/GEC1. *PLoS One* 8:e63133. doi: 10.1371/journal.pone.0063133

Lemon, R. N. (2008). Descending pathways in motor control. *Annu. Rev. Neurosci.* 31, 195–218. doi: 10.1146/annurev.neuro.31.060407.125547

Leroy, F., Lamotte d'Incamps, B., Imhoff-Manuel, R. D., and Zytnicki, D. (2014). Early intrinsic hyperexcitability does not contribute to motoneuron degeneration in amyotrophic lateral sclerosis. *Elife* 3:e04046. doi: 10.7554/eLife.04046

Li, M., Milligan, C. J., Wang, H., Walker, A., Churilov, L., Lawrence, A. J., et al. (2017). KCTD12 modulation of $GABA_B$ receptor function. *Pharmacol. Res. Perspect.* 5:e00319. doi: 10.1002/prp2.319

Martina, M., Metz, A. E., and Bean, B. P. (2007). Voltage-dependent potassium currents during fast spikes of rat cerebellar Purkinje neurons: inhibition by BDS-I toxin. *J. Neurophysiol.* 97, 563–571. doi: 10.1152/jn.00269.2006

Menon, P., Yiannikas, C., Kiernan, M. C., and Vucic, S. (2019). Regional motor cortex dysfunction in amyotrophic lateral sclerosis. *Ann. Clin. Transl. Neurol.* 6, 1373–1382. doi: 10.1002/acn3.50819

Mills, K. R. (2003). The natural history of central motor abnormalities in amyotrophic lateral sclerosis. *Brain* 126, 2558–2566. doi: 10.1093/brain/awg260

Mills, K. R., and Nithi, K. A. (1997). Corticomotor threshold is reduced in early sporadic amyotrophic lateral sclerosis. *Muscle Nerve* 20, 1137–1141. doi: 10.1002/(sici)1097-4598(199709)20:9<1137::aid-mus7>3.0.co;2-9

Minciacchi, D., Kassa, R. M., Del Tongo, C., Mariotti, R., and Bentivoglio, M. (2009). Voronoi-based spatial analysis reveals selective interneuron changes in the cortex of FALS mice. *Exp. Neurol.* 215, 77–86. doi: 10.1016/j.expneurol.2008.09.005

Nutini, M., Spalloni, A., Florenzano, F., Westenbroek, R. E., Marini, C., Catterall, W. A., et al. (2011). Increased expression of the beta3 subunit of voltage-gated Na^+ channels in the spinal cord of the SOD1G93A mouse. *Mol. Cell. Neurosci.* 47, 108–118. doi: 10.1016/j.mcn.2011.03.005

Ozdinler, P. H., Benn, S., Yamamoto, T. H., Güzel, M., Brown, R. H. Jr., and Macklis, J. D. (2011). Corticospinal motor neurons and related subcerebral projection neurons undergo early and specific neurodegeneration in $hSOD1^{G93A}$ transgenic ALS mice. *J. Neurosci.* 31, 4166–4177. doi: 10.1523/JNEUROSCI.4184-10.2011

Prout, A. J., and Eisen, A. A. (1994). The cortical silent period and amyotrophic lateral sclerosis. *Muscle Nerve* 17, 217–223. F doi: 10.1002/mus.880170213

Salinas, M., de Weille, J., Guillemare, E., Lazdunski, M., and Hugnot, J. P. (1997). Modes of regulation of *Shab* K^+ channel activity by the Kv8.1 subunit. *J. Biol. Chem.* 272, 8774–8780. doi: 10.1074/jbc.272.13.8774

Schanz, O., Bageac, D., Braun, L., Traynor, B. J., Lehky, T. J., and Floeter, M. K. (2016). Cortical hyperexcitability in patients with C9ORF72 mutations: relationship to phenotype. *Muscle Nerve* 54, 264–269. doi: 10.1002/mus.25047

Sirabella, R., Valsecchi, V., Anzilotti, S., Cuomo, O., Vinciguerra, A., Cepparulo, P., et al. (2018). Ionic homeostasis maintenance in ALS: focus on new therapeutic targets. *Front. Neurosci.* 12:510. doi: 10.3389/fnins.2018.00510

Suter, B. A., O'Connor, T., Iyer, V., Petreanu, L. T., Hooks, B. M., Kiritani, T., et al. (2010). Ephus: multipurpose data acquisition software for neuroscience experiments. *Front. Neural. Circuits* 4:100. doi: 10.3389/fncir.2010.00100

Van den Bos, M. A. J., Higashihara, M., Geevasinga, N., Menon, P., Kiernan, M. C., and Vucic, S. (2018). Imbalance of cortical facilitatory and inhibitory circuits underlies hyperexcitability in ALS. *Neurology* 91, e1669–e1676. doi: 10.1212/wnl.0000000000006438

van Zundert, B., Peuscher, M. H., Hynynen, M., Chen, A., Neve, R. L., Brown, R. H. Jr., et al. (2008). Neonatal neuronal circuitry shows hyperexcitable disturbance in a mouse model of the adult-onset neurodegenerative disease amyotrophic lateral sclerosis. *J. Neurosci.* 28, 10864–10874. doi: 10.1523/JNEUROSCI.1340-08.2008

Vucic, S., Cheah, B. C., and Kiernan, M. C. (2009). Defining the mechanisms that underlie cortical hyperexcitability in amyotrophic lateral sclerosis. *Exp. Neurol.* 220, 177–182. doi: 10.1016/j.expneurol.2009.08.017

Vucic, S., Nicholson, G. A., and Kiernan, M. C. (2008). Cortical hyperexcitability may precede the onset of familial amyotrophic lateral sclerosis. *Brain* 131, 1540–1550. doi: 10.1093/brain/awn071

Vucic, S., and Kiernan, M. C. (2006). Novel threshold tracking techniques suggest that cortical hyperexcitability is an early feature of motor neuron disease. *Brain* 129, 2436–2446. doi: 10.1093/brain/awl172

Wainger, B. J., Kiskinis, E., Mellin, C., Wiskow, O., Han, S. S., Sandoe, J., et al. (2014). Intrinsic membrane hyperexcitability of amyotrophic lateral sclerosis patient-derived motor neurons. *Cell Rep.* 7, 1–11. doi: 10.1016/j.celrep.2014.03.019

Weiler, N., Wood, L., Yu, J., Solla, S. A., and Shepherd, G. M. (2008). Top-down laminar organization of the excitatory network in motor cortex. *Nat. Neurosci.* 11, 360–366. doi: 10.1038/nn2049

Wood, L., and Shepherd, G. M. (2010). Synaptic circuit abnormalities of motor-frontal layer 2/3 pyramidal neurons in a mutant mouse model of Rett syndrome. *Neurobiol. Dis.* 38, 281–287. doi: 10.1016/j.nbd.2010.01.018

Yasvoina, M. V., Genç, B., Jara, J. H., Sheets, P. L., Quinlan, K. A., Milosevic, A., et al. (2013). eGFP expression under UCHL1 promoter genetically labels corticospinal motor neurons and a subpopulation of degeneration-resistant spinal motor neurons in an ALS mouse model. *J. Neurosci.* 33, 7890–7904. doi: 10.1523/JNEUROSCI.2787-12.2013

Ziemann, U., Winter, M., Reimers, C. D., Reimers, K., Tergau, F., and Paulus, W. (1997). Impaired motor cortex inhibition in patients with amyotrophic lateral sclerosis. Evidence from paired transcranial magnetic stimulation. *Neurology* 49, 1292–1298. doi: 10.1212/wnl.49.5.1292

Conflict of Interest: The authors declare that the research was conducted in the absence of any commercial or financial relationships that could be construed as a potential conflict of interest.

frontiers in Molecular Neuroscience

REVIEW
published: 25 May 2020
doi: 10.3389/fnmol.2020.00074

Motoneuronal Spinal Circuits in Degenerative Motoneuron Disease

*Mélanie Falgairolle and Michael J. O'Donovan**

Section on Developmental Neurobiology, National Institute of Neurological Disorders and Stroke, National Institutes of Health, Bethesda, MD, United States

The most evident phenotype of degenerative motoneuron disease is the loss of motor function which accompanies motoneuron death. In both amyotrophic lateral sclerosis (ALS) and spinal muscular atrophy (SMA), it is now clear that dysfunction is not restricted to motoneurons but is manifest in the spinal circuits in which motoneurons are embedded. As mounting evidence shows that motoneurons possess more elaborate and extensive connections within the spinal cord than previously realized, it is necessary to consider the role of this circuitry and its dysfunction in the disease process. In this review article, we ask if the selective vulnerability of the different motoneuron types and the relative disease resistance of distinct motoneuron groups can be understood in terms of their intraspinal connections.

Keywords: locomotion, spinal muscular atrophy, amyotrophic lateral sclerosis, central pattern generator, recurrent collaterals

OPEN ACCESS

Edited by:
George Mentis, Columbia University, United States

Reviewed by:
Francisco Javier Alvarez, Emory University, United States
Angel M. Pastor, University of Seville, Spain
Marco Beato, University College London, United Kingdom

****Correspondence:***
Michael J. O'Donovan
odonovm@ninds.nih.gov

Received: *21 February 2020*
Accepted: *15 April 2020*
Published: *25 May 2020*

Citation:
Falgairolle M and O'Donovan MJ (2020) Motoneuronal Spinal Circuits in Degenerative Motoneuron Disease. Front. Mol. Neurosci. 13:74. doi: 10.3389/fnmol.2020.00074

INTRODUCTION

Degenerative motoneuron diseases are devastating conditions whose underlying causes are poorly understood. Two of these diseases, amyotrophic lateral sclerosis (ALS) and spinal muscular atrophy (SMA), result in loss of motoneurons, leading to reduced motor function and ultimately death (Cleveland and Rothstein, 2001; Wee et al., 2010). Although both disorders have been considered autonomous motoneuron diseases, it is now clear that their pathology is not restricted to motoneurons and that dysfunction is more widespread, particularly within the brainstem and spinal circuits in which the motoneurons are embedded (Schütz, 2005; Ling et al., 2010; Mentis et al., 2011). Because of this, the primary, cell-autonomous pathologies caused by the conditions are compounded by secondary effects that result from disruptions in the spinal circuitry. The resulting motor deficits are, therefore, due to the interactions between the primary and secondary processes.

In this review article, we will first discuss the spinal circuit abnormalities in both SMA and ALS. We will then describe the sensitivity of the different motoneuron types to the diseases, and finally, we will consider these differences in susceptibility in light of recent discoveries showing that the intraspinal connections of motoneurons are more extensive than previously appreciated (Bhumbra and Beato, 2018; Chopek et al., 2018). These new connections create the likelihood of additional secondary effects that will further complicate interpretation of the disease process. We will conclude the review by considering these novel findings in relation to the motor dysfunction, and we will ask if the known susceptibility of different motoneuron types and different motoneuron pools to disease can be understood by considering differences in their intraspinal connectivity.

MOTONEURONAL CIRCUITS IN DEGENERATIVE MOTONEURON DISEASE

The SMNΔ7 mouse model of SMA lacks the SMN gene but expresses two copies of the human SMN2 gene (Le et al., 2005). These mice exhibit several motor defects, including weakness and an inability to right themselves, and they eventually die at 2 weeks of age. The proximal muscles are more affected than the distal muscles, with the epaxial and hypaxial muscles being the most severely weakened (Montes et al., 2009; Mentis et al., 2011). One of the first pathological changes in the disease is a decline in the strength of muscle spindle afferent synaptic input to motoneurons (Ling et al., 2010; Mentis et al., 2011; Fletcher and Mentis, 2017; Fletcher et al., 2017). This loss of muscle afferent input to motoneurons is due to a decrease in the amount of glutamate released from the afferents onto motoneurons (Fletcher et al., 2017). In addition to a loss of proprioceptive input to motoneurons, there is a reduction in the number of vesicular glutamate transporter (VGLUT)2^+ terminals on motoneurons in SMNΔ7 mice (Ling et al., 2010) that can be derived from local (Ling et al., 2010) or descending (Du Beau et al., 2012) glutamatergic interneurons. Loss of somatic vesicular gamma aminobutyric acid (GABA) transporter (VGAT) terminals was not observed, suggesting that the inhibitory inputs to motoneurons are less affected in the disease than excitatory inputs (Ling et al., 2010).

The decreased glutamate output from primary muscle spindle afferents triggers several changes in the properties of motoneurons, including an increase in input impedance and a downregulation of the Kv2.1 potassium channel (Fletcher et al., 2017). These responses are probably compensatory because they also occur in wild-type mice in which transmitter release from muscle afferents is abrogated by tetanus toxin (Fletcher et al., 2017). Proof of the secondary nature of the altered motoneuron electrical properties in SMA comes from experiments in which the SMN protein was selectively restored in afferents or motoneurons (Fletcher et al., 2017). Restoration of the protein in afferents, but not in motoneurons, normalized Kv2.1 expression and partially restored the firing of motoneurons to current injection (Fletcher et al., 2017). These findings illustrate that the pathology exhibited in SMA is a combination of cell-autonomous abnormalities, secondary changes due to the interaction of motoneurons with abnormally functioning afferents, and the compensatory responses of both motoneurons and afferents to their primary and secondary defects (Brownstone and Lancelin, 2018). Although secondary, the motoneuronal changes contribute significantly to the motor deficits in SMA.

If the reduced synaptic input from primary afferents to motoneurons reflected generalized afferent dysfunction and was independent of motoneuron pathology, then we would predict that afferent loss should also be observed on other intraspinal targets of primary afferents. This idea was tested by examining the number of VGLUT1 primary afferent terminals on Renshaw cells (RCs) in SMNΔ7 neonatal mice (Thirumalai et al., 2013). However, in contrast to the findings in motoneurons, the number of VGLUT1 terminals on RCs was increased rather than decreased. While this suggests that not all branches of proprioceptive afferents exhibit the same fate, it is not known if the proprioceptive synapses on RCs are functional. The cause of this increased afferent innervation is unknown, but one possibility is that primary afferents sprout in response to the loss of inputs to motoneurons. Interestingly, the number of cholinergic vesicular acetylcholine transporter (VAChT)$^+$ terminals was also increased onto RCs in the rostral lumbar segments at P13 even though there was a substantial loss of motoneurons in these segments. Again, the mechanisms responsible for this are unclear, but it may also represent sprouting because the remaining motoneurons will have lost a significant portion of their motoneuronal targets (Nishimaru et al., 2005; Bhumbra and Beato, 2018). The consequences of these changes in connectivity within motor circuits are not known. An increased innervation of RCs, if functional, could serve to inhibit motoneuron firing, thereby exacerbating the weakness exhibited by these animals.

There are several mouse models of ALS, but here we will concentrate on the superoxide dismutase (SOD)1 G93A model because most work has been done using this line (Rosen et al., 1993). Unlike the SMNΔ7 model of SMA, the natural history of the disease in the SOD1 G93A mouse is much more prolonged with animals living to 150 days. Furthermore, in contrast to the findings in SMA, inhibitory spinal circuits exhibit abnormalities early in the disease. Some of these changes can be detected even before birth. For example, in SOD-93 mice, the GABA equilibrium potential recorded in motoneurons is more depolarized than in wild-type animals, indicating an alteration in chloride homeostasis at E17.5 (Branchereau et al., 2019). At this early stage, there is also a deficiency of inhibitory synaptic terminals on motoneurons which persists into postnatal life (Martin and Chang, 2012; Branchereau et al., 2019). Studies of cultured motoneurons and interneurons showed that glycine currents are smaller in motoneurons from the mutant mice compared to their wild-type counterparts. The loss of glycinergic function appears to be specific for large motoneurons because it is not observed in presumed gamma and small, fatigue-resistant (S-type) motoneurons that innervate type I muscle fibers (Chang and Martin, 2011). The reduced inhibitory input could be due to loss of inhibitory interneurons or to weaker inputs from inhibitory neurons (Chang and Martin, 2009; Wootz et al., 2013). Consistent with the latter idea, Wootz et al. (2013) showed that the innervation of RCs by motoneurons was lost at early stages of the disease and was associated with a downregulation of VAChT in motoneurons. Eventually, a majority of the motoneuronal synapses on RCs are lost. It seems likely that the synaptic projections of motoneurons to other motoneurons and to V3 interneurons will also be lost at some stage in the disease.

Muscle spindle afferent inputs to motoneurons are also affected in the SOD1 mouse model of ALS. VGLUT1 immunoreactivity, presumed to originate from proprioceptive afferents, is reduced in the motor nucleus at day 110 and is almost absent at day 130, indicating loss of muscle spindle afferent input to motoneurons (Schütz, 2005).

This was confirmed by Vaughan et al. (2015) who showed that proprioceptive nerve endings initially degenerate in the periphery, and this is followed by loss of their central projections onto motoneurons. Electrophysiological studies of monosynaptic afferent connections in sacral motoneurons have shown that the evoked response recorded from the ventral roots declines with age, and although this was attributed to a loss of motoneurons (Jiang et al., 2009), it seems likely that it also reflects loss of proprioceptive input to motoneurons. Proprioceptive afferents in the mesencephalic nucleus of the SOD1 mouse exhibit reduced excitability at P11 due to reduced expression of Nav1.6-type Na^+ currents, which could lead to compensatory increases in the excitability of their target motoneurons (Seki et al., 2019).

MOTONEURON CLASSES AND THEIR SUSCEPTIBILITY TO THE DISEASE PROCESS

Degenerative diseases do not affect all motoneuron classes uniformly. For instance, in both SMA and ALS, the motoneurons innervating the extraocular muscles and the anal and bladder sphincters are spared (Comley et al., 2016; Nijssen et al., 2017). In this section, we consider the different motoneuron types and ask if their susceptibility to the disease differs and whether this is correlated with any features of their intraspinal circuitry.

In mammals, motoneurons innervating skeletal muscles comprise three classes (for a review, see Manuel and Zytnicki, 2011): α-motoneurons that innervate the extrafusal fibers, γ-motoneurons that innervate intrafusal muscle fibers (Kuffler et al., 1951), and β-motoneurons that innervate both (Bessou et al., 1963). α-Motoneurons can be further subdivided into fast-twitch fatigable (FF) motoneurons that control type IIb muscle fibers, fast-twitch fatigue-resistant (FR) motoneurons that control type IIa muscle fibers, and slow (S) motoneurons that control type I muscle fibers (Burke et al., 1971). There are two types of γ-motoneurons: static type that innervates the bag2 and chain fibers of the spindle, and dynamic type that innervates the bag1 fiber of the spindle (Matthews, 1963; Brown et al., 1965). Static β-motoneurons innervate type II extrafusal muscle fibers and the bag 2 and the chain fibers of the muscle spindle, whereas the dynamic β-motoneurons preferentially innervate type I skeletal muscle fibers and the muscle spindle bag1 fiber. β-Motoneurons innervate from 30% to 70% of the muscle spindles (McWilliam, 1975) and constitute from 11% to 30% of the axons supplying the extrafusal muscle fibers (Emonet-Dénand and Laporte, 1975; McWilliam, 1975). In both ALS and SMA, the largest motoneurons (FF) are the most vulnerable, followed by the FR, with the S motoneurons being the last to degenerate (for a review, see Kanning et al., 2010). While γ-motoneurons are resistant to ALS and SMA, β-motoneurons appear to be as vulnerable to the disease as α-motoneurons (Lalancette-Hebert et al., 2016; Powis and Gillingwater, 2016).

In addition, the external anal sphincter of the cat (innervated by motoneurons in Onuf's nucleus) is a slow twitch muscle (Bowen and Bradley, 1973) that is presumably innervated by type S motoneurons. This might explain some of the resistance of these motoneurons to disease. In contrast, the extraocular muscles comprise six different types of muscle fiber including slow- and fast-twitch fibers and multiply-innervated non-twitch fibers (Evinger et al., 1979; Yu et al., 2005; Nijssen et al., 2017), suggesting that the resistance of the motoneurons to disease is not explained by the types of muscle fiber they innervate, consistent with transplant studies between SOD1-G93A and wild-type mice (Carrasco et al., 2010).

Many explanations have been proposed to account for the differences in the susceptibility of motoneurons to disease pathology. Here, we focus on the synaptic inputs and outputs of motoneurons innervating the hind limb and ask if any aspect of this connectivity is correlated with the susceptibility of the different motoneuron types to disease.

SYNAPTIC INPUTS TO MOTONEURONS

One difficulty in drawing general conclusions is that the work on motoneuron connectivity has been done in different species at different ages and on a relatively limited set of motoneuron pools. Electron microscopy studies in cat have shown that α-motoneurons have four main types of boutons (McLaughlin, 1972b; Conradi et al., 1979a; Brännström, 1993): S-type boutons (small diameter with spherical synaptic vesicles), F-type boutons (small diameter with flattened synaptic vesicles), C-type boutons (large diameter with subsynaptic cisterns), and M-type boutons (large diameter that disappear after dorsal root section). The S-type boutons have been associated with excitatory synapses, the F-type with inhibitory synapses (Uchizono, 1965; Brännström, 1993), M-type with afferent inputs (McLaughlin, 1972a), and C-type with cholinergic inputs arising from V0c neurons expressing the pituitary homeobox (PITX)-2 transcription factor (Hellström et al., 2003; Zagoraiou et al., 2009). Ia afferent synapses are either S-type (Fyffe and Light, 1984) or the larger M-type that are apposed to P-type presynaptic boutons (Ornung et al., 1995).

The different motoneuron classes do not receive the same number or type of inputs. In particular, C-boutons are much more frequent on F-type motoneurons than on S-type motoneurons (Conradi et al., 1979b; Kellerth et al., 1979; Brännström, 1993; Hellström et al., 2003), and the number of Ia synaptic contacts is higher on FF motoneurons than on the S-type (Burke and Glenn, 1996). γ-Motoneurons appear to lack C-boutons and Ia contacts in cats and rodents and have less diversity in their synaptic inputs than α-motoneurons with only S- and F-type boutons on their proximal dendrites and their cell bodies lacking the M-, a C-type synapse found on α-motoneurons (Arvidsson et al., 1987; Simon et al., 1996; Ichiyama et al., 2006).

A review of literature reveals that the synaptic efficacy of the inputs to motoneurons, measured as the size of the excitatory postsynaptic potential (EPSP) or inhibitory postsynaptic potential (IPSP), is generally highest in the type S motoneurons followed by the type FR and then the type FF (**Figure 1**). This is true for the monosynaptic inputs from

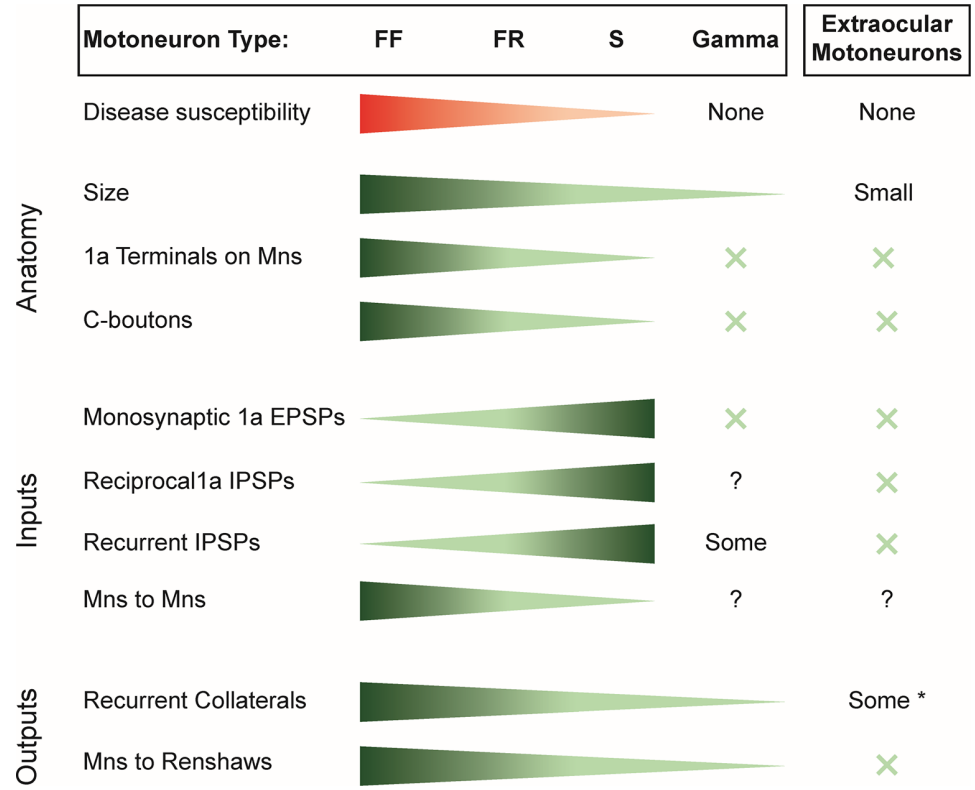

FIGURE 1 | Summary of the susceptibility of motor unit types to spinal muscle atrophy (SMA) and amyotrophic lateral sclerosis (ALS) and the distribution of inputs and outputs of the different motoneuron classes. X indicates the absence of the variable considered. *Note that only some extraocular motoneurons have recurrent collaterals; others have none. EPSP, excitatory postsynaptic potential; IPSP, inhibitory postsynaptic potential; FF, fast-twitch fatigable motoneuron; FR, fast-twitch fatigue-resistant motoneuron; S, slow motoneuron.

muscle spindle afferents (Burke and Rymer, 1976) even though the number of afferent synaptic contacts on motoneurons exhibits the reverse distribution (Burke and Glenn, 1996). The discrepancy between the distribution of synaptic efficacy and the number of afferent terminals reflects differences in the input impedance of the different motoneurons, with the highest in type S and the lowest in type F. The synaptic efficacy of inhibitory inputs, including disynaptic 1a inhibition (Burke and Rymer, 1976) and recurrent inhibition (Hultborn et al., 1988), is also highest in type S motoneurons and weakest in type FF motoneurons. In contrast, γ-motoneurons lack monosynaptic primary afferent inputs but do receive polysynaptic excitatory and inhibitory inputs from other afferents (Eccles et al., 1960; Appelberg et al., 1983a,b,c) as well as inhibition from RCs (Ellaway and Murphy, 1981; Appelberg et al., 1983d).

Thus, within the α-motoneuron population, there is an inverse relation between the strength of synaptic inputs and the susceptibility of the different motoneuron types to disease. Accordingly α-motoneurons have the largest inputs from muscle spindle afferents, 1a inhibitory interneurons, and recurrent inhibition. However, this correlation fails when the disease-resistant, γ-motoneurons and extraocular motoneurons are considered because they receive only weak or no input from these synaptic sources (**Figure 1**).

SYNAPTIC OUTPUTS OF MOTONEURONS AND THEIR EFFECTS ON SPINAL CIRCUITS

The best described output connection of motoneurons is to the inhibitory Renshaw cell population (Renshaw, 1946; Eccles et al., 1954, 1961). In the adult cat, it has been estimated that the largest inputs to RCs are from FF motoneurons with progressively fewer from FR and type S motoneurons (Hultborn et al., 1988). The distribution of inputs from motoneurons to RCs appears to reflect the number of collateral swellings, presumed to be presynaptic terminals, which is greatest on the type FF motoneurons followed by FR and S (Cullheim and Kellerth, 1978). In addition, γ-motoneurons have very few recurrent collaterals (Cullheim and Ulfhake, 1979; Westbury, 1982). It was also known from work in adult cats that α-motoneuron recurrent collaterals project to other α-motoneurons irrespective of their motor unit type (Cullheim et al., 1977, 1984). However, at least in the adult cat, it is not clear that these are functional because no reports have described excitatory synaptic connections between feline motoneurons.

Recently, new evidence has emerged, showing that motoneurons have more extensive intraspinal synaptic targets

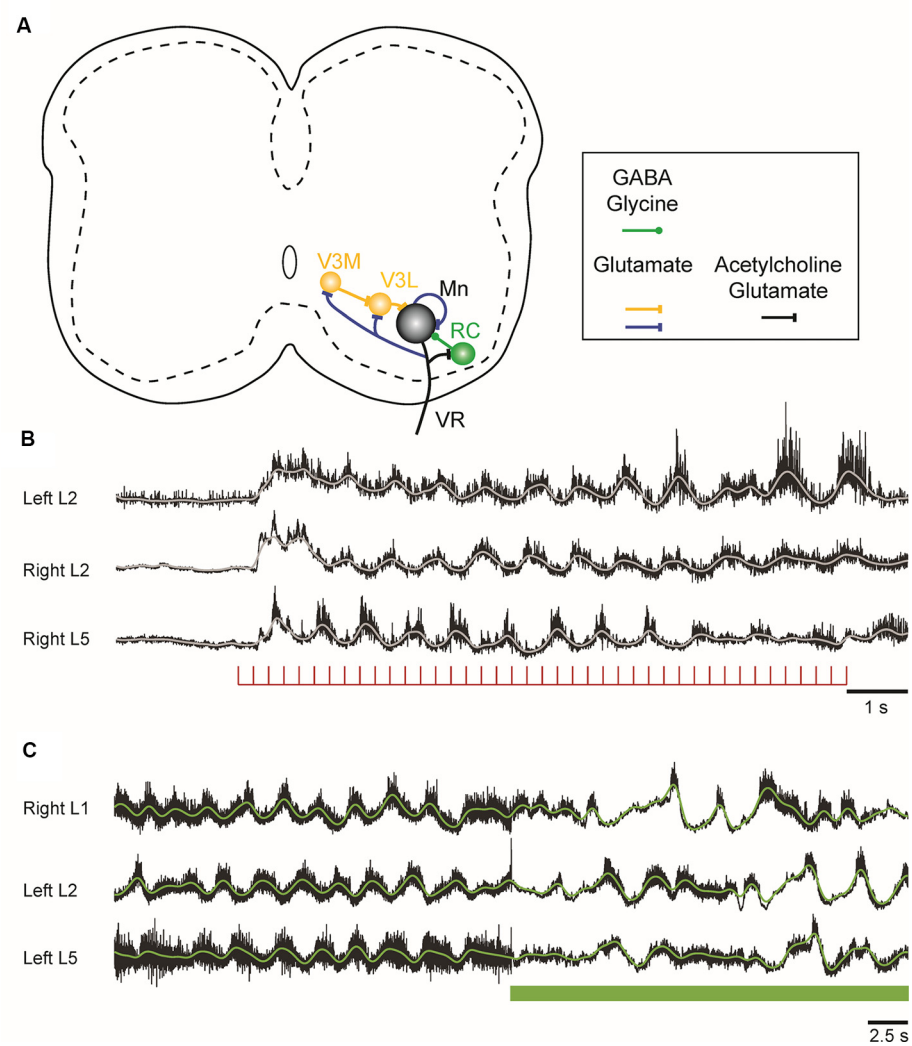

FIGURE 2 | (A) Schematic showing the connections of motoneurons within the lumbar spinal cord of the neonatal mouse. Motoneurons project to each other, to inhibitory Renshaw cells (RCs), and to a medial (V3M) and a lateral (V3L) population of V3 interneurons. The lateral V3 population and RCs project back to motoneurons. The neurotransmitters released at the different sites are indicated in the box under the schematic. **(B)** Locomotor-like activity can be evoked in the neonatal mouse cord by a train of stimuli applied to the ventral roots. The records are the neurograms recorded from the indicated ventral roots in response to a train of stimuli applied to the right L6 ventral root. The continuous traces are the integrated records of ventral root discharge. **(C)** Optogenetic reduction of motoneuron firing slows and disrupts the locomotor-like rhythm induced by drugs. Ventral root recordings of locomotor-like activity induced by bath application of serotonin and N-methyl-D-aspartate (NMDA) on a spinal cord expressing the inhibitory opsin archaerhodopsin in cholinergic neurons. On exposure to green light (green bar), the neurons expressing the opsin are hyperpolarized, leading to a slowing and disruption of the locomotor rhythm.

that were previously realized. In 2005, it was demonstrated that motoneurons release an excitatory amino acid—probably glutamate—in addition to acetylcholine at their central connections with RCs in the neonatal mouse spinal cord (Mentis et al., 2005; Nishimaru et al., 2005) and confirmed a few years later in both the neonate (Lamotte d'Incamps and Ascher, 2008) and the adult mouse (Lamotte d'Incamps et al., 2017). Subsequent work in neonatal and juvenile mice showed that motoneurons make powerful glutamatergic connections with each other, with the largest inputs to type F motoneurons (**Figure 2A**; Bhumbra and Beato, 2018). This surprising finding indicates that motoneurons release different transmitters at different axonal branches apparently contravening Dale's principle (Dale, 1935; Eccles et al., 1954). However, it is possible that both transmitters are present at the motoneuronal terminals on motoneurons because the failure to detect cholinergic responses could be due to the absence of postsynaptic acetylcholine receptors at the synapse. In addition, motoneurons in the neonatal mouse spinal cord also project exclusively glutamatergic synapses to a class of glutamatergic, commissural spinal interneurons called V3 interneurons (Chopek et al., 2018).

In the neonatal mouse cord, stimulation of motor axons can initiate locomotor-like activity (**Figure 2B**; Mentis et al., 2005; Pujala et al., 2016), and optogenetic manipulations of

motoneuron firing regulate the frequency of the locomotor rhythm during drug-induced locomotor-like activity (**Figure 2C**; Falgairolle et al., 2017). The mechanisms by which motoneurons influence the central pattern generator (CPG) are not fully understood (Falgairolle and O'Donovan, 2019a). Surprisingly, it occurs in the absence of cholinergic transmission and depends instead on glutamatergic transmission (Mentis et al., 2005; Falgairolle et al., 2017). It has been proposed that these excitatory effects of motoneuron stimulation on spinal circuitry are most simply explained by the presence of an excitatory interneuron interposed between the locomotor central pattern generator and motoneurons (Machacek and Hochman, 2006; Bonnot et al., 2009; Falgairolle et al., 2017). The glutamatergic V3 interneuronal population is clearly a candidate for such a neuron because it receives direct monosynaptic input from motoneurons. The V3 interneurons comprise a medial and a lateral group. The medial V3 neurons project to the lateral group which in turn projects back to motoneurons, thus forming a recurrent excitatory connection with motoneurons (**Figure 2A**; Chopek et al., 2018). The existence of this pathway probably explains earlier observations that revealed recurrent, disynaptic excitation of motoneurons in the neonatal rat (Schneider and Fyffe, 1992; Ichinose and Miyata, 1998). However, the effects of genetic silencing or elimination of V3 interneurons on the locomotor rhythm are not the same as optogenetic hyperpolarization of motoneurons. The silencing experiments show that V3 neurons are required to balance the excitatory locomotor drive to both sides of the cord (Zhang et al., 2008), whereas hyperpolarization of motoneurons slows the locomotor frequency (Falgairolle et al., 2017). Furthermore, optogenetic excitation of V3 interneurons expressing channelrhodopsin slows the locomotor-like rhythm (Danner et al., 2019), in contrast to the acceleration that occurs when motoneurons are optogenetically excited. This suggests that the V3 neurons do not mediate the excitatory effects of motoneurons on the locomotor CPG, raising the possibility that other—currently unidentified—classes of interneurons are targeted by motoneurons.

Furthermore, it is not clear if glutamate release from the VGLUT2 from motoneurons mediates the excitatory effects of motoneurons because selective elimination of VGLUT2 from cholinergic neurons—including motoneurons—has no effect on locomotor-like activity (Caldeira et al., 2017). However, because this was a chronic study, some type of compensation may have occurred to offset the absence of motoneuronal glutamatergic inputs. Alternatively, glutamate release from motoneurons may not be mediated exclusively by VGLUT2, although it is difficult to support this idea given that the glutamatergic component of the motoneuron–Renshaw synapse is abolished in the VGLUT2 knockout (Talpalar et al., 2011).

In the adult zebrafish, motoneurons have also been shown to modulate locomotion (Song et al., 2016). In this animal, motoneurons have reciprocal hybrid chemical/electrical synapses with a class of excitatory interneurons (V2a) that are believed to be important in generating the swimming rhythm (Eklöf-Ljunggren et al., 2012). Motoneuron membrane polarization can modulate transmitter release from the V2a interneurons by polarizing the V2a terminals on motoneurons. In addition, motoneuron membrane potential can directly modulate the firing of V2a interneurons and the swimming frequency. In the neonatal mouse spinal cord, this mechanism does not appear to be responsible for the effects of motoneuron activity on the rhythm because blockade of gap junctions with carbenoxolone does not attenuate the effect of motoneuron activity on the frequency of the rhythm (Falgairolle et al., 2017). Consistent with this idea, application of the α-amino-3-hydroxy-5-methyl-4-isoxazolepropionic acid (AMPA) receptor antagonist NBQX, blocked the effects of motoneuron activity on the rhythm, suggesting that motoneuronal connections to the CPG are mediated by an excitatory interneuron contacted by motoneurons (Machacek and Hochman, 2006; Bonnot et al., 2009; Falgairolle et al., 2017). Furthermore, it has also been shown that V2a interneurons do not receive synaptic or electrical inputs from motoneurons in the neonatal mouse (Bhumbra and Beato, 2018).

SYNAPTIC CONNECTIONS OF MOTONEURONS AND THEIR SUSCEPTIBILITY TO DISEASE

In the final section of this review, we ask if any of the input or output connections of the different motoneuron types, the extraocular motoneurons, and Onuf's nucleus (Comley et al., 2016; Nijssen et al., 2017) are correlated with their susceptibility to disease.

Several correlations are apparent in the data of **Figure 1**. For example, the most resistant motoneurons are the smallest, and they receive the fewest and the least diverse synaptic inputs. Thus, within the α-motoneuron population, the number of 1a terminals progressively decreases from type FF to S and are absent on γ-motoneurons, extraocular motoneurons (Keller and Robinson, 1971), and Onuf's nucleus (Lalancette-Hebert et al., 2016). Similarly, C-boutons are absent on extraocular motoneurons (Hellström et al., 2003; Rozani et al., 2019) and γ-motoneurons (Arvidsson et al., 1987), with a gradient of inputs from type S to type F α-motoneurons (Hellström et al., 2003). However, at least for primary afferents, their presence or absence does not seem to be associated with motoneuron cell death. For instance, although the number of VGLUT1$^+$ primary afferents on motoneurons decreases before motoneuron death, their restoration does not prevent motoneuron death (Fletcher et al., 2017). In ALS, by contrast, ablation of primary afferents exerts a protective effect on α-motoneurons (Lalancette-Hebert et al., 2016). Similarly, although the least susceptible motoneurons lack C-boutons in both diseases, during the progression of ALS, C-boutons become more numerous on vulnerable α-motoneurons, and the number of cholinergic interneurons in Lamina X (presumably the source of C-boutons) increases. Although both decrease toward the end of the disease, the initial changes may reflect compensatory adaptations to maintain motoneuron excitability (Milan et al., 2015). In SMA, the number of cholinergic interneurons does not change (Powis and Gillingwater, 2016), and furthermore,

when the C-boutons are restored in the ALS mouse model, they extend survival time (Lasiene et al., 2016), suggesting that the presence of C-boutons and their normal function may facilitate motoneuron survival. Collectively, these observations suggest that the distribution of primary muscle spindle afferents and C-boutons on motoneurons is probably not the factor that contributes to their vulnerability.

A more consistent association emerges when we consider the number of recurrent collaterals produced by the different motoneurons. Those with the greatest number of intraspinal collaterals (type F) are the most susceptible, and those with the fewest γ-motoneurons and extraocular motoneurons are the least (Evinger et al., 1979). About half the motoneurons in Onuf's nucleus have no recurrent collaterals (Sasaki, 1994). This relationship may also extend to the well-known difference in the sensitivity of proximal and distal muscles to the disease process in both SMA and ALS. In the adult cat, the most distal limb muscles, including many of the foot and forepaw muscles, lack recurrent collaterals (Hörner et al., 1991; McCurdy and Hamm, 1992; Illert and Kümmel, 1999), and recurrent inhibition is much more pronounced in motoneurons innervating the muscles of the elbow than of the wrist (Hahne et al., 1988). Furthermore, motoneurons innervating the intercostal muscles have been shown to have axon collaterals and receive recurrent inhibition (Kirkwood et al., 1981; Lipski and Martin-Body, 1987), and axial motoneurons receive recurrent inhibition (Jankowska and Odutola, 1980), suggesting that they have axon collaterals projecting to RCs as do α-motoneurons. Why would the number of motoneuron collaterals be associated with disease susceptibility? Before motoneurons die, their intraspinal connections to RCs are lost (Wootz et al., 2013) and any functions associated with these connections will also be lost. For example, loss of motoneuron input to the locomotor CPG could compromise locomotion, although this could be compensated by interneurons that also influence locomotor function (Gosgnach et al., 2006; Dougherty et al., 2013; Talpalar et al., 2013; Falgairolle and O'Donovan, 2019b).

It might seem paradoxical that an absence of recurrent collaterals, and presumably Renshaw inhibition, would be associated with a protection against the disease process. Enhanced motoneuron excitability, particularly at early stages of the disease, is often proposed as one of the mechanisms contributing to pathophysiology of motoneurons (Kuo et al., 2004, 2005; Jiang et al., 2017). The Renshaw pathway exerts a powerful inhibitory effect on motoneurons (Moore et al., 2015) and would therefore be expected to temper any increases in motoneuron excitability. However, motoneurons also receive monosynaptic glutamatergic input from other motoneurons and recurrent excitation from V3 glutamatergic interneurons. If motoneuronal inputs to inhibitory RCs are lost before those to motoneurons, this would result in powerful, recurrent glutamatergic excitation of motoneurons unbalanced by recurrent inhibition particularly in the type-F population which receives the strongest excitatory input from other motoneurons (Bhumbra and Beato, 2018). This could lead to glutamate toxicity and a compensatory reduction of motoneuron excitability. Consistent with this suggestion, a reduction of motoneuron excitability in type-F motoneurons is observed to precede denervation in the SOD1-G93A and FUS-P525L mouse models of ALS (Martinez-Silva et al., 2018).

As with their central connections, type FF motoneurons have the most intramuscular synaptic connections (Burke, 1978). Because synapses are energetically demanding (Harris et al., 2012), the FF motoneurons have the highest metabolic demands (Le Masson et al., 2014) which may increase their susceptibility to the disease given that mutant SOD1 can compromise mitochondrial function (Pasinelli et al., 2004).

An alternative and complementary interpretation for the relation between the number of recurrent collaterals and disease susceptibility derives from the idea that a neuron is dependent on *all* its synaptic targets for trophic support. It is well known that during development, motoneuron survival depends on its target muscle for survival, but as the animal matures, this dependence is reduced (de la Cruz et al., 1996). What is less clear is the extent to which the functions and properties of motoneurons also depend on trophic support from their synaptic targets within the central nervous system. The recent discoveries that spinal motoneurons have novel synaptic targets within the cord mean that trophic support from these neuronal populations has necessarily been underappreciated. According to this idea, as motoneurons disconnect from their synaptic targets within the spinal cord (Wootz et al., 2013), they lose the trophic support normally provided by these targets. The motoneurons lacking recurrent collaterals would thus be resistant to this process because they presumably derive their trophic needs from other sources including the motoneurons themselves and the muscles they innervate. Consistent with this hypothesis, the disease-resistant extraocular muscles express higher levels of neurotrophins than other brainstem neurons that are sensitive to disease (Hernández et al., 2017; Silva-Hucha et al., 2017). Extraocular muscles also contain high levels of insulin-like growth factor (IGF) compared to other cranial or spinal motoneurons (Allodi et al., 2016). Remarkably, IGF-2 delivered by viruses to spinal motoneurons preserves the motoneurons and induces nerve regeneration in ALS (Allodi et al., 2016). It is not known if the different types of α-motoneuron or γ-motoneurons differ in their expression of trophic factors. γ-Motoneurons uniquely express the glial cell-derived neurotrophic factor (GDNF) receptor and require GDNF derived from the muscle spindle for their survival (Shneider et al., 2009). Unfortunately, trials of neurotrophins in humans have not been successful, but this is complicated by difficulties in delivering the molecules to neurons and because the appropriate neurotrophins may not have been discovered (for a review, see Kanning et al., 2010).

One observation that appears to contradict this hypothesis is the finding that motoneuron cell death is associated with an increase in the number of $VAChT^{+}$ terminals on RCs in the SMNΔ7 model of SMA (Thirumalai et al., 2013). It is not known if these additional synapses originate exclusively from motoneurons. However, if they do, then this behavior differs from the loss of motoneuron terminals on RCs that precedes motoneuron cell death in the SOD1-G93A mouse model of ALS

(Wootz et al., 2013). This difference in behavior may reflect the different ages at which motoneurons die in the two diseases. In the SMNΔ7 mouse model, motoneuron cell death begins in the neonatal period when motoneurons are not fully mature and may have an enhanced sprouting ability. It is possible therefore that the sprouting of motoneuron axons, which presumably occurs in the remaining motoneurons, is a characteristic of their immaturity rather than a fundamental difference between the two diseases.

AUTHOR CONTRIBUTIONS

MO'D and MF wrote and approved the article.

FUNDING

This research was supported by the Intramural Research Program of the National Institute of Neurological Disorders and Stroke (NINDS), National Institutes of Health (NIH).

REFERENCES

Allodi, I., Comley, L., Nichterwitz, S., Nizzardo, M., Simone, C., Benitez, J. A., et al. (2016). Differential neuronal vulnerability identifies IGF-2 as a protective factor in ALS. *Sci. Rep.* 6:25960. doi: 10.1038/srep25960

Appelberg, B., Hulliger, M., Johansson, H., and Sojka, P. (1983a). Actions on gamma-motoneurones elicited by electrical stimulation of group I muscle afferent fibres in the hind limb of the cat. *J. Physiol.* 335, 237–253. doi: 10.1113/jphysiol.1983.sp014531

Appelberg, B., Hulliger, M., Johansson, H., and Sojka, P. (1983b). Actions on gamma-motoneurones elicited by electrical stimulation of group II muscle afferent fibres in the hind limb of the cat. *J. Physiol.* 335, 255–273. doi: 10.1113/jphysiol.1983.sp014532

Appelberg, B., Hulliger, M., Johansson, H., and Sojka, P. (1983c). Actions on gamma-motoneurones elicited by electrical stimulation of group III muscle afferent fibres in the hind limb of the cat. *J. Physiol.* 335, 275–292. doi: 10.1113/jphysiol.1983.sp014533

Appelberg, B., Hulliger, M., Johansson, H., and Sojka, P. (1983d). Recurrent actions on gamma-motoneurones mediated via large and small ventral root fibres in the cat. *J. Physiol.* 335, 293–305. doi: 10.1113/jphysiol.1983.sp014534

Arvidsson, U., Svedlund, J., Lagerbäck, P. A., and Cullheim, S. (1987). An ultrastructural study of the synaptology of gamma-motoneurones during the postnatal development in the cat. *Brain Res.* 465, 303–312. doi: 10.1016/0165-3806(87)90251-3

Bessou, P., Laporte, Y., and Emonetdenand, F. (1963). Occurrence of intrafusal muscle fibres innervation by branches of slow alpha motor fibres in cat. *Nature* 198, 594–595. doi: 10.1038/198594a0

Bhumbra, G. S., and Beato, M. (2018). Recurrent excitation between motoneurones propagates across segments and is purely glutamatergic. *PLoS Biol.* 16:e2003586. doi: 10.1371/journal.pbio.2003586

Bonnot, A., Chub, N., Pujala, A., and O'Donovan, M. J. (2009). Excitatory actions of ventral root stimulation during network activity generated by the disinhibited neonatal mouse spinal cord. *J. Neurophysiol.* 101, 2995–3011. doi: 10.1152/jn.90740.2008

Bowen, J. M., and Bradley, W. E. (1973). Some contractile and electrophysiological properties of external anal-sphincter muscle of cat. *Gastroenterology* 65, 919–928. doi: 10.1016/s0016-5085(19)32985-3

Branchereau, P., Martin, E., Allain, A. E., Cazenave, W., Supiot, L., Hodeib, F., et al. (2019). Relaxation of synaptic inhibitory events as a compensatory mechanism in fetal SOD spinal motor networks. *Elife* 8:e51402. doi: 10.7554/eLife.51402

Brännström, T. (1993). Quantitative synaptology of functionally different types of cat medial gastrocnemius alpha-motoneurons. *J. Comp. Neurol.* 330, 439–454. doi: 10.1002/cne.903300311

Brown, M. C., Crowe, A., and Matthews, P. B. (1965). Observations on the fusimotor fibres of the tibialis posterior muscle of the cat. *J. Physiol.* 177, 140–159. doi: 10.1113/jphysiol.1965.sp007582

Brownstone, R. M., and Lancelin, C. (2018). Escape from homeostasis: spinal microcircuits and progression of amyotrophic lateral sclerosis. *J. Neurophysiol.* 119, 1782–1794. doi: 10.1152/jn.00331.2017

Burke, R. E. (1978). Motor units—physiological-histochemical profiles, neural connectivity and functional specializations. *Am. Zool.* 18, 127–134. doi: 10.1093/icb/18.1.127

Burke, R. E., and Glenn, L. L. (1996). Horseradish peroxidase study of the spatial and electrotonic distribution of group Ia synapses on type-identified ankle extensor motoneurons in the cat. *J. Comp. Neurol.* 372, 465–485. doi: 10.1002/(sici)1096-9861(19960826)372:3<465::aid-cne9>3.0.co;2-0

Burke, R. E., Levine, D. N., and Zajac, F. E. III. (1971). Mammalian motor units: physiological-histochemical correlation in three types in cat gastrocnemius. *Science* 174, 709–712. doi: 10.1126/science.174.4010.709

Burke, R. E., and Rymer, W. Z. (1976). Relative strength of synaptic input from short-latency pathways to motor units of defined type in cat medial gastrocnemius. *J. Neurophysiol.* 39, 447–458. doi: 10.1152/jn.1976.39.3.447

Caldeira, V., Dougherty, K. J., Borgius, L., and Kiehn, O. (2017). Spinal Hb9::Cre-derived excitatory interneurons contribute to rhythm generation in the mouse. *Sci. Rep.* 7:41369. doi: 10.1038/srep41369

Carrasco, D. I., Bichler, E. K., Seburn, K. L., and Pinter, M. J. (2010). Nerve terminal degeneration is independent of muscle fiber genotype in SOD1(G93A) mice. *PLoS One* 5:e9802. doi: 10.1371/journal.pone.0009802

Chang, Q., and Martin, L. J. (2009). Glycinergic innervation of motoneurons is deficient in amyotrophic lateral sclerosis mice a quantitative confocal analysis. *Am. J. Pathol.* 174, 574–585. doi: 10.2353/ajpath.2009.080557

Chang, Q., and Martin, L. J. (2011). Motoneuron subtypes show specificity in glycine receptor channel abnormalities in a transgenic mouse model of amyotrophic lateral sclerosis. *Channels* 5, 299–303. doi: 10.4161/chan.5.4.16206

Chopek, J. W., Nascimento, F., Beato, M., Brownstone, R. M., and Zhang, Y. (2018). Sub-populations of spinal V3 interneurons form focal modules of layered pre-motor microcircuits. *Cell Rep.* 25, 146.e3–156.e3. doi: 10.1016/j.celrep.2018.08.095

Cleveland, D. W., and Rothstein, J. D. (2001). From Charcot to Lou Gehrig: deciphering selective motor neuron death in ALS. *Nat. Rev. Neurosci.* 2, 806–819. doi: 10.1038/35097565

Comley, L. H., Nijssen, J., Frost-Nylen, J., and Hedlund, E. (2016). Cross-disease comparison of amyotrophic lateral sclerosis and spinal muscular atrophy reveals conservation of selective vulnerability but differential neuromuscular junction pathology. *J. Comp. Neurol.* 524, 1424–1442. doi: 10.1002/cne.23917

Conradi, S., Kellerth, J. O., and Berthold, C. H. (1979a). Electron microscopic studies of serially sectioned cat spinal alpha-motoneurons: II. A method for the description of architecture and synaptology of the cell body and proximal dendritic segments. *J. Comp. Neurol.* 184, 741–754. doi: 10.1002/cne.901840407

Conradi, S., Kellerth, J. O., Berthold, C. H., and Hammarberg, C. (1979b). Electron microscopic studies of serially sectioned cat spinal alpha-motoneurons. IV. Motoneurons innervating slow-twitch (type S) units of the soleus muscle. *J. Comp. Neurol.* 184, 769–782. doi: 10.1002/cne.901840409

Cullheim, S., and Kellerth, J. O. (1978). A morphological study of the axons and recurrent axon collaterals of cat alpha-motoneurones supplying different functional types of muscle unit. *J. Physiol.* 281, 301–313. doi: 10.1113/jphysiol.1978.sp012423

Cullheim, S., Kellerth, J. O., and Conradi, S. (1977). Evidence for direct synaptic interconnections between cat spinal alpha-motoneurons via recurrent axon collaterals—morphological-study using intracellular injection of horseradish-peroxidase. *Brain Res.* 132, 1–10. doi: 10.1016/0006-8993(77)90702-8

Cullheim, S., Lipsenthal, L., and Burke, R. E. (1984). Direct monosynaptic contacts between type-identified alpha-motoneurons in the cat. *Brain Res.* 308, 196–199. doi: 10.1016/0006-8993(84)90937-5

Cullheim, S., and Ulfhake, B. (1979). Observations on the morphology of intracellularly stained gamma-motoneurons in relation to their axon conduction-velocity. *Neurosci. Lett.* 13, 47–50. doi: 10.1016/0304-3940(79)90073-9

Dale, H. (1935). Pharmacology and nerve-endings (walter ernest dixon memorial lecture): (section of therapeutics and pharmacology). *Proc. R. Soc. Med.* 28, 319–332.

Danner, S. M., Zhang, H., Shevtsova, N. A., Borowska-Fielding, J., Deska-Gauthier, D., Rybak, I. A., et al. (2019). Spinal V3 interneurons and left-right coordination in mammalian locomotion. *Front. Cell. Neurosci.* 13:516. doi: 10.3389/fncel.2019.00516

de la Cruz, R. R., Pastor, A. M., and Delgado-García, J. M. (1996). Influence of the postsynaptic target on the functional properties of neurons in the adult mammalian central nervous system. *Rev. Neurosci.* 7, 115–149. doi: 10.1515/revneuro.1996.7.2.115

Dougherty, K. J., Zagoraiou, L., Satoh, D., Rozani, I., Doobar, S., Arber, S., et al. (2013). Locomotor rhythm generation linked to the output of spinal shox2 excitatory interneurons. *Neuron* 80, 920–933. doi: 10.1016/j.neuron.2013.08.015

Du Beau, A., Shakya Shrestha, S., Bannatyne, B. A., Jalicy, S. M., Linnen, S., and Maxwell, D. J. (2012). Neurotransmitter phenotypes of descending systems in the rat lumbar spinal cord. *Neuroscience* 227, 67–79. doi: 10.1016/j.neuroscience.2012.09.037

Eccles, J. C., Eccles, R. M., Iggo, A., and Lundberg, A. (1960). Electrophysiological studies on gamma motoneurones. *Acta Physiol. Scand.* 50, 32–40. doi: 10.1111/j.1748-1716.1960.tb02070.x

Eccles, J. C., Eccles, R. M., Iggo, A., and Lundberg, A. (1961). Electrophysiological investigations on Renshaw cells. *J. Physiol.* 159, 461–478. doi: 10.1113/jphysiol.1961.sp006821

Eccles, J. C., Fatt, P., and Koketsu, K. (1954). Cholinergic and inhibitory synapses in a pathway from motor-axon collaterals to motoneurones. *J. Physiol.* 126, 524–562. doi: 10.1113/jphysiol.1954.sp005226

Eklöf-Ljunggren, E., Haupt, S., Ausborn, J., Dehnisch, I., Uhlén, P., Higashijima, S., et al. (2012). Origin of excitation underlying locomotion in the spinal circuit of zebrafish. *Proc. Natl. Acad. Sci. U S A* 109, 5511–5516. doi: 10.1073/pnas.1115377109

Ellaway, P. H., and Murphy, P. R. (1981). A comparison of the recurrent inhibition of alpha- and gamma-motoneurones in the cat. *J. Physiol.* 315, 43–58. doi: 10.1113/jphysiol.1981.sp013731

Emonet-Dénand, F., and Laporte, Y. (1975). Proportion of muscles spindles supplied by skeletofusimotor axons (beta-axons) in peroneus brevis muscle of the cat. *J. Neurophysiol.* 38, 1390–1394. doi: 10.1152/jn.1975.38.6.1390

Evinger, C., Baker, R., and McCrea, R. A. (1979). Axon collaterals of cat medial rectus motoneurons. *Brain Res.* 174, 153–160. doi: 10.1016/0006-8993(79)90810-2

Falgairolle, M., and O'Donovan, M. J. (2019a). Feedback regulation of locomotion by motoneurons in the vertebrate spinal cord. *Curr. Opin. Physiol.* 8, 50–55. doi: 10.1016/j.cophys.2018.12.009

Falgairolle, M., and O'Donovan, M. J. (2019b). V1 interneurons regulate the pattern and frequency of locomotor-like activity in the neonatal mouse spinal cord. *PLoS Biol.* 17:e3000447. doi: 10.1371/journal.pbio.3000447

Falgairolle, M., Puhl, J. G., Pujala, A., Liu, W., and O'Donovan, M. J. (2017). Motoneurons regulate the central pattern generator during drug-induced locomotor-like activity in the neonatal mouse. *Elife* 6:e26622. doi: 10.7554/eLife.26622

Fletcher, E. V., and Mentis, G. Z. (2017). "Motor circuit dysfunction in spinal muscular atrophy," in *Spinal Muscular Atrophy: Disease Mechanisms and Therapy*, eds C. J. Sumner, S. Paushkin and C. P. Ko (London: Elsevier), 153–165.

Fletcher, E. V., Simon, C. M., Pagiazitis, J. G., Chalif, J. I., Vukojicic, A., Drobac, E., et al. (2017). Reduced sensory synaptic excitation impairs motor neuron function via Kv2.1 in spinal muscular atrophy. *Nat. Neurosci.* 20, 905–916. doi: 10.1038/nn.4561

Fyffe, R. E., and Light, A. R. (1984). The ultrastructure of group Ia afferent fiber synapses in the lumbosacral spinal cord of the cat. *Brain Res.* 300, 201–209. doi: 10.1016/0006-8993(84)90831-x

Gosgnach, S., Lanuza, G. M., Butt, S. J., Saueressig, H., Zhang, Y., Velasquez, T., et al. (2006). V1 spinal neurons regulate the speed of vertebrate locomotor outputs. *Nature* 440, 215–219. doi: 10.1038/nature04545

Hahne, M., Illert, M., and Wietelmann, D. (1988). Recurrent inhibition in the cat distal forelimb. *Brain Res.* 456, 188–192. doi: 10.1016/0006-8993(88)90362-9

Harris, J. J., Jolivet, R., and Attwell, D. (2012). Synaptic energy use and supply. *Neuron* 75, 762–777. doi: 10.1016/j.neuron.2012.08.019

Hellström, J., Oliveira, A. L. R., Meister, B., and Cullheim, S. (2003). Large cholinergic nerve terminals on subsets of motoneurons and their relation to muscarinic receptor type 2. *J. Comp. Neurol.* 460, 476–486. doi: 10.1002/cne.10648

Hernández, R. G., Silva-Hucha, S., Morcuende, S., de la Cruz, R. R., Pastor, A. M., and Benitez-Temiño, B. (2017). Extraocular motor system exhibits a higher expression of neurotrophins when compared with other brainstem motor systems. *Front. Neurosci.* 11:399. doi: 10.3389/fnins.2017.00399

Hörner, M., Illert, M., and Kümmél, H. (1991). Absence of recurrent axon collaterals in motoneurones to the extrinsic digit extensor muscles of the cat forelimb. *Neurosci. Lett.* 122, 183–186. doi: 10.1016/0304-3940(91)90853-l

Hultborn, H., Katz, R., and Mackel, R. (1988). Distribution of recurrent inhibition within a motor nucleus. II. Amount of recurrent inhibition in motoneurones to fast and slow units. *Acta Physiol. Scand.* 134, 363–374. doi: 10.1111/j.1748-1716.1988.tb08503.x

Ichinose, T., and Miyata, Y. (1998). Recurrent excitation of motoneurons in the isolated spinal cord of newborn rats detected by whole-cell recording. *Neurosci. Res.* 31, 179–187. doi: 10.1016/s0168-0102(98)00043-1

Ichiyama, R. M., Brown, J., Edgerton, V. R., and Havton, L. A. (2006). Ultrastructural synaptic features differ between alpha- and gamma-motoneurons innervating the tibialis anterior muscle in the rat. *J. Comp. Neurol.* 499, 306–315. doi: 10.1002/cne.21110

Illert, M., and Kümmel, H. (1999). Reflex pathways from large muscle spindle afferents and recurrent axon collaterals to motoneurones of wrist and digit muscles: a comparison in cats, monkeys and humans. *Exp. Brain Res.* 128, 13–19. doi: 10.1007/s002210050812

Jankowska, E., and Odutola, A. (1980). Crossed and uncrossed synaptic actions on moto-neurons of back muscles in the cat. *Brain Res.* 194, 65–78. doi: 10.1016/0006-8993(80)91319-0

Jiang, M. C., Adimula, A., Birch, D., and Heckman, C. J. (2017). Hyperexcitability in synaptic and firing activities of spinal motoneurons in an adult mouse model of amyotrophic lateral sclerosis. *Neuroscience* 362, 33–46. doi: 10.1016/j.neuroscience.2017.08.041

Jiang, M., Schuster, J. E., Fu, R., Siddique, T., and Heckman, C. J. (2009). Progressive changes in synaptic inputs to motoneurons in adult sacral spinal cord of a mouse model of amyotrophic lateral sclerosis. *J. Neurosci.* 29, 15031–15038. doi: 10.1523/jneurosci.0574-09.2009

Kanning, K. C., Kaplan, A., and Henderson, C. E. (2010). Motor neuron diversity in development and disease. *Annu. Rev. Neurosci.* 33, 409–440. doi: 10.1146/annurev.neuro.051508.135722

Keller, E. L., and Robinson, D. A. (1971). Absence of a stretch reflex in extraocular muscles of the monkey. *J. Neurophysiol.* 34, 908–919. doi: 10.1152/jn.1971.34.5.908

Kellerth, J. O., Berthold, C. H., and Conradi, S. (1979). Electron microscopic studies of serially sectioned cat spinal alpha-motoneurons: III. Motoneurons innervating fast-twitch (type FR) units of the gastrocnemius muscle. *J. Comp. Neurol.* 184, 755–767. doi: 10.1002/cne.901840408

Kirkwood, P. A., Sears, T. A., and Westgaard, R. H. (1981). Recurrent inhibition of intercostal motoneurones in the cat. *J. Physiol.* 319, 111–130. doi: 10.1113/jphysiol.1981.sp013895

Kuffler, S. W., Hunt, C. C., and Quilliam, J. P. (1951). Function of medullated small-nerve fibers in mammalian ventral roots; efferent muscle spindle innervation. *J. Neurophysiol.* 14, 29–54. doi: 10.1152/jn.1951.14.1.29

Kuo, J. J., Schonewille, M., Siddique, T., Schults, A. N., Fu, R., Bär, P. R., et al. (2004). Hyperexcitability of cultured spinal motoneurons from presymptomatic ALS mice. *J. Neurophysiol.* 91, 571–575. doi: 10.1152/jn.00665.2003

Kuo, J. J., Siddique, T., Fu, R., and Heckman, C. J. (2005). Increased persistent Na^+ current and its effect on excitability in motoneurones cultured from mutant SOD1 mice. *J. Physiol.* 563, 843–854. doi: 10.1113/jphysiol.2004.074138

Lalancette-Hebert, M., Sharma, A., Lyashchenko, A. K., and Shneider, N. A. (2016). Gamma motor neurons survive and exacerbate alpha motor neuron degeneration in ALS. *Proc. Natl. Acad. Sci. U S A* 113, E8316–E8325. doi: 10.1073/pnas.1605210113

Lamotte d'Incamps, B., and Ascher, P. (2008). Four excitatory postsynaptic ionotropic receptors coactivated at the motoneuron-Renshaw cell synapse. *J. Neurosci.* 28, 14121–14131. doi: 10.1523/jneurosci.3311-08.2008

Lamotte d'Incamps, B., Bhumbra, G. S., Foster, J. D., Beato, M., and Ascher, P. (2017). Segregation of glutamatergic and cholinergic transmission at the mixed motoneuron Renshaw cell synapse. *Sci. Rep.* 7:4037. doi: 10.1038/s41598-017-04266-8

Lasiene, J., Komine, O., Fujimori-Tonou, N., Powers, B., Endo, F., Watanabe, S., et al. (2016). Neuregulin 1 confers neuroprotection in SOD1-linked amyotrophic lateral sclerosis mice via restoration of C-boutons of spinal motor neurons. *Acta Neuropathol. Commun.* 4:15. doi: 10.1186/s40478-016-0286-7

Le Masson, G., Przedborski, S., and Abbott, L. F. (2014). A computational model of motor neuron degeneration. *Neuron* 83, 975–988. doi: 10.1016/j.neuron.2014.07.001

Le, T. T., Pham, L. T., Butchbach, M. E. R., Zhang, H. L., Monani, U. R., Coovert, D. D., et al. (2005). SMN Delta 7, the major product of the centromeric survival motor neuron (SMN2) gene, extends survival in mice with spinal muscular atrophy and associates with full-length SMN. *Hum. Mol. Genet.* 14, 845–857. doi: 10.1093/hmg/ddi078

Ling, K. K., Lin, M. Y., Zingg, B., Feng, Z., and Ko, C. P. (2010). Synaptic defects in the spinal and neuromuscular circuitry in a mouse model of spinal muscular atrophy. *PLoS One* 5:e15457. doi: 10.1371/journal.pone.0015457

Lipski, J., and Martin-Body, R. L. (1987). Morphological properties of respiratory intercostal motoneurons in cats as revealed by intracellular injection of horseradish-peroxidase. *J. Comp. Neurol.* 260, 423–434. doi: 10.1002/cne.902600308

Machacek, D. W., and Hochman, S. (2006). Noradrenaline unmasks novel self-reinforcing motor circuits within the mammalian spinal cord. *J. Neurosci.* 26, 5920–5928. doi: 10.1523/jneurosci.4623-05.2006

Manuel, M., and Zytnicki, D. (2011). Alpha, beta and gamma motoneurons: functional diversity in the motor system's final pathway. *J. Integr. Neurosci.* 10, 243–276. doi: 10.1142/s0219635211002786

Martin, L. J., and Chang, Q. (2012). Inhibitory synaptic regulation of motoneurons: a new target of disease mechanisms in amyotrophic lateral sclerosis. *Mol. Neurobiol.* 45, 30–42. doi: 10.1007/s12035-011-8217-x

Martinez-Silva, M. D., Imhoff-Manuel, R. D., Sharma, A., Heckman, C. J., Shneider, N. A., Roselli, F., et al. (2018). Hypoexcitability precedes denervation in the large fast-contracting motor units in two unrelated mouse models of ALS. *Elife* 7:e30955. doi: 10.7554/elife.30955

Matthews, P. B. (1963). The response of de-efferented muscle spindle receptors to stretching at different velocities. *J. Physiol.* 168, 660–678. doi: 10.1113/jphysiol.1963.sp007214

McCurdy, M. L., and Hamm, T. M. (1992). Recurrent collaterals of motoneurons projecting to distal muscles in the cat hindlimb. *J. Neurophysiol.* 67, 1359–1366. doi: 10.1152/jn.1992.67.5.1359

McLaughlin, B. J. (1972a). Dorsal root projections to the motor nuclei in the cat spinal cord. *J. Comp. Neurol.* 144, 461–473. doi: 10.1002/cne.901440405

McLaughlin, B. J. (1972b). The fine structure of neurons and synapses in the motor nuclei of the cat spinal cord. *J. Comp. Neurol.* 144, 429–460. doi: 10.1002/cne.901440404

McWilliam, P. N. (1975). The incidence and properties of beta axons to muscle spindles in the cat hind limb. *Q. J. Exp. Physiol. Cogn. Med. Sci.* 60, 25–36. doi: 10.1113/expphysiol.1975.sp002287

Mentis, G. Z., Alvarez, F. J., Bonnot, A., Richards, D. S., Gonzalez-Forero, D., Zerda, R., et al. (2005). Noncholinergic excitatory actions of motoneurons in the neonatal mammalian spinal cord. *Proc. Natl. Acad. Sci. U S A* 102, 7344–7349. doi: 10.1073/pnas.0502788102

Mentis, G. Z., Blivis, D., Liu, W. F., Drobac, E., Crowder, M. E., Kong, L., et al. (2011). Early functional impairment of sensory-motor connectivity in a mouse model of spinal muscular atrophy. *Neuron* 69, 453–467. doi: 10.1016/j.neuron.2010.12.032

Milan, L., Courtand, G., Cardoit, L., Masmejean, F., Barriere, G., Cazalets, J. R., et al. (2015). Age-related changes in pre- and postsynaptic partners of the cholinergic c-boutons in wild-type and SOD1G93A lumbar motoneurons. *PLoS One* 10:e0135525. doi: 10.1371/journal.pone.0135525

Montes, J., Gordon, A. M., Pandya, S., De Vivo, D. C., and Kaufmann, P. (2009). Clinical outcome measures in spinal muscular atrophy. *J. Child Neurol.* 24, 968–978. doi: 10.1177/0883073809332702

Moore, N. J., Bhumbra, G. S., Foster, J. D., and Beato, M. (2015). Synaptic connectivity between renshaw cells and motoneurons in the recurrent inhibitory circuit of the spinal cord. *J. Neurosci.* 35, 13673–13686. doi: 10.1523/jneurosci.2541-15.2015

Nijssen, J., Comley, L. H., and Hedlund, E. (2017). Motor neuron vulnerability and resistance in amyotrophic lateral sclerosis. *Acta Neuropathol.* 133, 863–885. doi: 10.1007/s00401-017-1708-8

Nishimaru, H., Restrepo, C. E., Ryge, J., Yanagawa, Y., and Kiehn, O. (2005). Mammalian motor neurons corelease glutamate and acetylcholine at central synapses. *Proc. Natl. Acad. Sci. U S A* 102, 5245–5249. doi: 10.1073/pnas.0501331102

Ornung, G., Ragnarson, B., Grant, G., Ottersen, O. P., Storm-Mathisen, J., and Ulfhake, B. (1995). Ia boutons to CCN neurones and motoneurones are enriched with glutamate-like immunoreactivity. *Neuroreport* 6, 1975–1980. doi: 10.1097/00001756-199510010-00006

Pasinelli, P., Belford, M. E., Lennon, N., Bacskai, B. J., Hyman, B. T., Trotti, D., et al. (2004). Amyotrophic lateral sclerosis-associated SOD1 mutant proteins bind and aggregate with Bcl-2 in spinal cord mitochondria. *Neuron* 43, 19–30. doi: 10.1016/j.neuron.2004.06.021

Powis, R. A., and Gillingwater, T. H. (2016). Selective loss of alpha motor neurons with sparing of gamma motor neurons and spinal cord cholinergic neurons in a mouse model of spinal muscular atrophy. *J. Anat.* 228, 443–451. doi: 10.1111/joa.12419

Pujala, A., Blivis, D., and O'Donovan, M. J. (2016). Interactions between dorsal and ventral root stimulation on the generation of locomotor-like activity in the neonatal mouse spinal cord. *eNeuro* 3:ENEURO.0101-16.2016. doi: 10.1523/eneuro.0101-16.2016

Renshaw, B. (1946). Central effects of centripetal impulses in axons of spinal ventral roots. *J. Neurophysiol.* 9, 191–204. doi: 10.1152/jn.1946.9.3.191

Rosen, D. R., Siddique, T., Patterson, D., Figlewicz, D. A., Sapp, P., Hentati, A., et al. (1993). Mutations in Cu/Zn superoxide-dismutase gene are associated with familial amyotrophic-lateral-sclerosis. *Nature* 362, 59–62. doi: 10.1038/362059a0

Rozani, I., Tsapara, G., Witts, E. C., Deaville, S. J., Miles, G. B., and Zagoraiou, L. (2019). Pitx2 cholinergic interneurons are the source of C bouton synapses on brainstem motor neurons. *Sci. Rep.* 9:4936. doi: 10.1038/s41598-019-39996-4

Sasaki, M. (1994). Morphological analysis of external urethral and external anal sphincter motoneurones of cat. *J. Comp. Neurol.* 349, 269–287. doi: 10.1002/cne.903490209

Schneider, S. P., and Fyffe, R. E. (1992). Involvement of GABA and glycine in recurrent inhibition of spinal motoneurons. *J. Neurophysiol.* 68, 397–406. doi: 10.1152/jn.1992.68.2.397

Schütz, B. (2005). Imbalanced excitatory to inhibitory synaptic input precedes motor neuron degeneration in an animal model of amyotrophic lateral sclerosis. *Neurobiol. Dis.* 20, 131–140. doi: 10.1016/j.nbd.2005.02.006

Seki, S., Yamamoto, T., Quinn, K., Spigelman, I., Pantazis, A., Olcese, R., et al. (2019). Circuit-specific early impairment of proprioceptive sensory neurons in the SOD1(G93A) mouse model for ALS. *J. Neurosci.* 39, 8798–8815. doi: 10.1523/jneurosci.1214-19.2019

Shneider, N. A., Brown, M. N., Smith, C. A., Pickel, J., and Alvarez, F. J. (2009). Gamma motor neurons express distinct genetic markers at birth and require muscle spindle-derived GDNF for postnatal survival. *Neural Dev.* 4:42. doi: 10.1186/1749-8104-4-42

Silva-Hucha, S., Hernandez, R. G., Benitez-Temino, B., Pastor, A. M., De La Cruz, R. R., and Morcuende, S. (2017). Extraocular motoneurons of the adult rat show higher levels of vascular endothelial growth factor and its receptor Flk-1 than other cranial motoneurons. *PLoS One* 12:e0178616. doi: 10.1371/journal.pone.0178616

Simon, M., Destombes, J., Horchollebossavit, G., and Thiesson, D. (1996). Postnatal development of alpha- and gamma-peroneal motoneurons in kittens: An ultrastructural study. *Neurosci. Res.* 25, 77–89. doi: 10.1016/0168-0102(96)01030-9

Song, J., Ampatzis, K., Bjornfors, E. R., and El Manira, A. (2016). Motor neurons control locomotor circuit function retrogradely via gap junctions. *Nature* 529, 399–402. doi: 10.1038/nature16497

Talpalar, A. E., Bouvier, J., Borgius, L., Fortin, G., Pierani, A., and Kiehn, O. (2013). Dual-mode operation of neuronal networks involved in left-right alternation. *Nature* 500, 85–88. doi: 10.1038/nature12286

Talpalar, A. E., Endo, T., Low, P., Borgius, L., Hagglund, M., Dougherty, K. J., et al. (2011). Identification of minimal neuronal networks involved in flexor-extensor alternation in the mammalian spinal cord. *Neuron* 71, 1071–1084. doi: 10.1016/j.neuron.2011.07.011

Thirumalai, V., Behrend, R. M., Birineni, S., Liu, W., Blivis, D., and O'Donovan, M. J. (2013). Preservation of VGLUT1 synapses on ventral calbindin-immunoreactive interneurons and normal locomotor function in a mouse model of spinal muscular atrophy. *J. Neurophysiol.* 109, 702–710. doi: 10.1152/jn.00601.2012

Uchizono, K. (1965). Characteristics of excitatory and inhibitory synapses in the central nervous system of the cat. *Nature* 207, 642–643. doi: 10.1038/207642a0

Vaughan, S. K., Kemp, Z., Hatzipetros, T., Vieira, F., and Valdez, G. (2015). Degeneration of proprioceptive sensory nerve endings in mice harboring amyotrophic lateral sclerosis-causing mutations. *J. Comp. Neurol.* 523, 2477–2494. doi: 10.1002/cne.23848

Wee, C. D., Kong, L. L., and Sumner, C. J. (2010). The genetics of spinal muscular atrophies. *Curr. Opin. Neurol.* 23, 450–458. doi: 10.1097/WCO.0b013e32833e1765

Westbury, D. R. (1982). A comparison of the structures of alpha and gamma-spinal motoneurones of the cat. *J. Physiol.* 325, 79–91. doi: 10.1113/jphysiol.1982.sp014137

Wootz, H., Fitzsimons-Kantamneni, E., Larhammar, M., Rotterman, T. M., Enjin, A., Patra, K., et al. (2013). Alterations in the motor neuron-renshaw cell circuit in the Sod1(G93A) mouse model. *J. Comp. Neurol.* 521, 1449–1469. doi: 10.1002/cne.23266

Yu, C. Y., Man, W., Chinnery, P. F., and Griffiths, P. G. (2005). Extraocular muscles have fundamentally distinct properties that make them selectively vulnerable to certain disorders. *Neuromuscul. Disord.* 15, 17–23. doi: 10.1016/j.nmd.2004.10.002

Zagoraiou, L., Akay, T., Martin, J. F., Brownstone, R. M., Jessell, T. M., and Miles, G. B. (2009). A cluster of cholinergic premotor interneurons modulates mouse locomotor activity. *Neuron* 64, 645–662. doi: 10.1016/j.neuron.2009.10.017

Zhang, Y., Narayan, S., Geiman, E., Lanuza, G. M., Velasquez, T., Shanks, B., et al. (2008). V3 spinal neurons establish a robust and balanced locomotor rhythm during walking. *Neuron* 60, 84–96. doi: 10.1016/j.neuron.2008.09.027

Conflict of Interest: The authors declare that the research was conducted in the absence of any commercial or financial relationships that could be construed as a potential conflict of interest.

frontiers in Molecular Neuroscience

REVIEW
published: 02 September 2020
doi: 10.3389/fnmol.2020.00163

Epidural Electrical Stimulation: A Review of Plasticity Mechanisms That Are Hypothesized to Underlie Enhanced Recovery From Spinal Cord Injury With Stimulation

Jaclyn T. Eisdorfer[1], Rupert D. Smit[2], Kathleen M. Keefe[1], Michel A. Lemay[1], George M. Smith[2] and Andrew J. Spence[1]**

[1]Department of Bioengineering, College of Engineering, Temple University, Philadelphia, PA, United States, [2]Department of Neuroscience, Shriners Hospitals Pediatric Research Center, Lewis Katz School of Medicine, Temple University, Philadelphia, PA, United States

Spinal cord injury (SCI) often results in life-long sensorimotor impairment. Spontaneous recovery from SCI is limited, as supraspinal fibers cannot spontaneously regenerate to form functional networks below the level of injury. Despite this, animal models and humans exhibit many motor behaviors indicative of recovery when electrical stimulation is applied epidurally to the dorsal aspect of the lumbar spinal cord. In 1976, epidural stimulation was introduced to alleviate spasticity in Multiple Sclerosis. Since then, epidural electrical stimulation (EES) has been demonstrated to improve voluntary mobility across the knee and/or ankle in several SCI patients, highlighting its utility in enhancing motor activation. The mechanisms that EES induces to drive these improvements in sensorimotor function remain largely unknown. In this review, we discuss several sensorimotor plasticity mechanisms that we hypothesize may enable epidural stimulation to promote recovery, including changes in local lumbar circuitry, propriospinal interneurons, and the internal model. Finally, we discuss genetic tools for afferent modulation as an emerging method to facilitate the search for the mechanisms of action.

Keywords: plasticity, electrical epidural stimulation, propriospinal detours, monosynaptic connections, internal motor copy, efferent motor copy, designer receptor exclusively activated by designer drugs (DREADDs), afferent stimulation

OPEN ACCESS

Edited by:
John Martin, City College of New York (CUNY), United States

Reviewed by:
Lorenzo Cangiano, University of Pisa, Italy
Gerardo Rojas-Piloni, National Autonomous University of Mexico, Mexico

***Correspondence:**
George M. Smith
george.smith@temple.edu
Andrew J. Spence
aspence@temple.edu

Received: *31 January 2020*
Accepted: *07 August 2020*
Published: *02 September 2020*

Citation:
Eisdorfer JT, Smit RD, Keefe KM, Lemay MA, Smith GM and Spence AJ (2020) Epidural Electrical Stimulation: A Review of Plasticity Mechanisms That Are Hypothesized to Underlie Enhanced Recovery From Spinal Cord Injury With Stimulation. Front. Mol. Neurosci. 13:163. doi: 10.3389/fnmol.2020.00163

INTRODUCTION

Spinal cord injury (SCI) often results in life-long sensorimotor dysfunction. Although regeneration within the adult spinal cord is limited, some spontaneous or activity-dependent sensorimotor recovery still occurs, mostly mediated by localized sprouting and plasticity of axon terminals (Waters et al., 1996; Burns et al., 1997). Substantial recovery after trauma is challenging because of the poor ability of supraspinal axons to regenerate and form functional networks below the level of injury. The loss of these vital inputs reduces the generation, regulation, and patterning of motor outputs. Improvements in motor function can be achieved with locomotor training, rehabilitation, and/or increased neuronal activity.

These methods activate axonal growth pathways (e.g., GAP43; Storer and Houle, 2003) to enhance sprouting and plasticity to either establish circuits that bypass the lesion to relay motor commands and/or increase connections onto vital motor circuits. Over the years, direct electrical stimulation of cortical or supraspinal neurons demonstrated that activity plays an important role in mediating plasticity induced sensorimotor recovery (Martin, 2016). More recently, stimulation of spinal sensory axons with electrodes placed epidurally has shown benefits in promoting functional recovery. Indeed, epidurally placed electrodes can stimulate afferents in specific patterns to increase the excitability of networks to drive voluntary and autonomically controlled motor responses (Edgerton and Harkema, 2011). Although multiple mechanisms have been proposed, the neuroplastic changes that underlie these improvements are not yet well understood. A better understanding of these mechanisms or circuits would be beneficial in the development of combined therapies to augment sensorimotor improvements using epidural stimulation to further enhance the recovery of sensorimotor function in individuals with SCI.

The foundation of artificially modulating neurons with electrical stimulation was borne from the search for pain management. In the first century AD, Scribonius Largus, a Roman physician, reportedly advised patients to sit in pools of water electrified by torpedo fish to numb distal extremity pain (Moller, 1995). It was not until 1967, however, that epidural stimulation was first used and approved by the FDA for suppression of intractable pain (Shealy et al., 1967). Then, in 1976, epidural electrical stimulation (EES) was introduced to alleviate spasticity due to Multiple Sclerosis, and it was anecdotally noticed that patients improved in motor function (Cook, 1976). EES was also identified to reduce spasticity (Barolat et al., 1988) and allow for voluntary mobility across the knee or ankle in several SCI patients, further indicating its utility in supplementing motor activation (Dimitrijevic et al., 1986).

Activity-based training in conjunction with EES can bolster use-dependent plastic changes in sensorimotor circuits caudal to the injury site (Courtine et al., 2009). In a seminal paper by Harkema et al. (2011), it was demonstrated in humans that EES can enhance weight-bearing standing, stepping, and volitional movement of leg muscles when in a supine position. This work was followed up with similar demonstrations in individuals with motor complete paralysis for intentional control of movements of the lower limbs (Angeli et al., 2014; Grahn et al., 2017) as well as independent stepping during EES activation (Gill et al., 2018). Similarly, in clinical studies, central and peripheral electrical stimulation improved sensorimotor function (Guiraud et al., 2014; Possover, 2014), such as weight-bearing, standing (Crosbie et al., 2014), and walking (Herman et al., 2002; Hardin et al., 2007; Karimi et al., 2013; Possover, 2014). Emerging evidence suggests that closed-loop and/or phasic EES is more efficacious in promoting functional recovery in humans than tonic stimuli. Unlike closed-loop and phasic stimuli, continuous input increases the probability of antidromic collisions in proprioceptive afferents, thereby disrupting sensory information, especially in humans, as they have longer nerves. As such, stimulation protocols restricted to a range of frequencies and amplitudes appear to better facilitate recovery and locomotion (Formento et al., 2018).

In addition to enhanced sensorimotor recovery, EES can improve cardiovascular (Harkema et al., 2018; West et al., 2018), autonomic (Gad et al., 2014, 2018), and respiratory (Hachmann et al., 2017) functions as well as body weight composition (Terson de Paleville et al., 2019) in individuals with motor complete paralysis. Despite relatively small sample sizes, EES has shown remarkable therapeutic potential as an intervention for SCI. However, the mechanisms that underlie EES-induced long-term recovery remain elusive. It is widely believed that EES activates large and medium diameter afferents within the posterior roots in humans and animals (Murg et al., 2000; Rattay et al., 2000; Courtine et al., 2009; Capogrosso et al., 2013). Indeed, computational modeling studies corroborated with electrophysiological and pharmacological data of afferent populations indicate specifically that group Ia/Ib/II proprioceptive and low-threshold cutaneous afferents are all affected by electrical stimulation (Bouyer and Rossignol, 1998; Rossignol et al., 2006; Capogrosso et al., 2016). Recent data suggest that proprioceptive input has the greatest influence on circuit reorganization during recovery and that the ablation of proprioceptors permanently reverts sensorimotor improvements to the injured state (Capogrosso et al., 2013; Takeoka et al., 2014; Takeoka and Arber, 2019; Takeoka, 2020). Congruently, Formento et al. (2018) proposed that if the chosen EES stimuli block proprioceptive input, individuals with SCI are unable to show meaningful locomotor improvements.

Here we explore three endogenous mechanisms of sensorimotor plasticity by which EES may induce locomotor recovery through stimulation of peripheral proprioceptive afferents: direct strengthening of monosynaptic connections; dynamic reorganization of Propriospinal neurons (PNs) around and below the lesion site; and the influence of the internal models for error correction and learning proper patterning (*via* interneurons). These mechanisms would likely behave synergistically, integrating, and functioning in concert to promote recovery. In this review, we discuss these mechanisms and their putative roles in supporting sensorimotor improvements after SCI and consider how molecular tools for afferent modulation can accelerate uncovering the changes in circuitry that drive recovery.

PLASTICITY MECHANISMS THAT ARE HYPOTHESIZED TO ENABLE EES TO PROMOTE ENHANCED LOCOMOTOR RECOVERY AFTER SCI

Hypothesis 1: Strengthening of Monosynaptic Connections Between Proprioceptive Afferents and Motorneurons

Perhaps the most straightforward form of plasticity for enhancing motor output with EES after SCI is strengthened

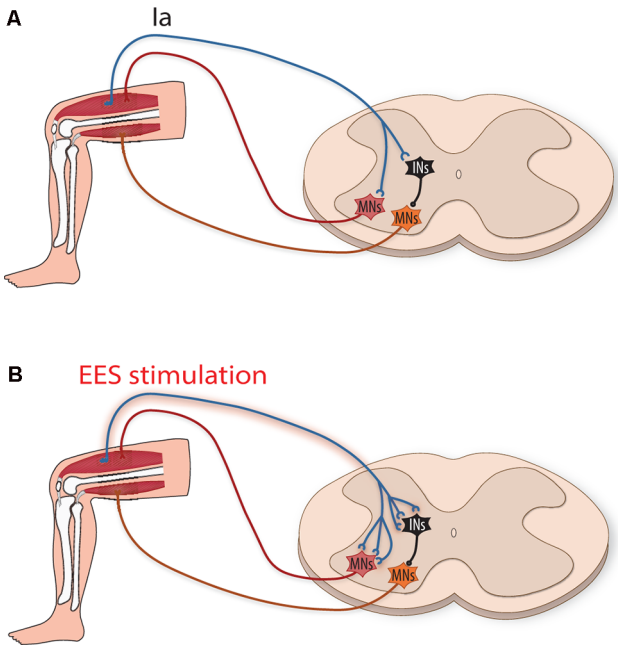

FIGURE 1 | Strengthening of monosynaptic connections by epidural electrical stimulation (EES) induced activation of group Ia afferents. **(A)** Schematic illustration depicting group Ia afferents directly activating motoneurons (MNs, red) to activate agonistic muscles and indirectly (orange MNs) to inhibit antagonistic muscles (*via* inhibitory interneurons, iINs, black). **(B)** After spinal cord injury (SCI), EES increases the activity of type Ia afferents, putatively strengthening their connections by inducing sprouting and new synapse formation onto MNs and iINs.

connections between stimulated afferents and motoneurons that reside in nearby lumbar spinal cord segments (**Figure 1**). Within sensory afferent populations, proprioceptive neurons provide information concerning muscle length, velocity, and force development that are thought to be used to estimate limb position and other aspects of movement dynamics. Within the spinal cord cutaneous and proprioceptive axons branch extensively, relaying limb positional information and force dynamics to multiple spinal cord levels, and supraspinal and somatosensory cortical regions. Of these sensory afferents, group Ia proprioceptive axons establish direct monosynaptic connections onto motoneurons that innervate agonist muscles as well as interneuronal circuits within motor pools. Both of these circuits involving proprioceptive afferents thought to be critical for locomotor recovery after SCI (for a recent review see Takeoka, 2020). Animal models lacking muscle spindle feedback (Takeoka et al., 2014) or after the loss of proprioceptive afferents (Takeoka and Arber, 2019) fail to regain control of affected hindlimbs and inappropriately reorganize descending circuitry (Takeoka, 2020). Proprioceptive ablation following recovery from SCI also permanently regresses sensorimotor improvements to the injured state (Takeoka and Arber, 2019). While EES can activate large and medium diameter afferents of the dorsal roots, proprioceptive afferents have been proposed to be the most influential in regaining volitional control of affected muscles.

During activity, EES is thought to work by boosting muscle recruitment *via* the activation of Ia muscle spindle afferents (Moraud et al., 2016). Although this procedure works well in animal models, the length of peripheral nerves in humans makes it less effective by increasing the probability of antidromic collisions, thereby reducing the propagation of naturally occurring proprioceptive action potentials (Retamal et al., 2018). Recent forms of EES that employ spatiotemporal modulation (Wenger et al., 2016; Wagner et al., 2018) show improvement in human locomotion because they activate appropriate muscles (*via* spatial localization within the cord—flexors vs. extensors, hip vs. ankle, etc.) in concordance to swing-stance rhythmicity without negatively effecting endogenous proprioceptive information.

Activity-dependent stimulation can strengthen connections between neurons by enhancing the efficacy of existing synapses (Davis et al., 1985), as well as by inducing growth-promoting factors that enhance axonal sprouting and result in the formation of new synapses (Retamal et al., 2018; Xu et al., 2019). Whether these mechanisms occur between group Ia afferents and motoneurons (**Figure 1**) is an open question (Wolpaw and Lee, 1989). If they do occur, it would enhance group Ia afferent drive of motoneurons and possibly the motoneuron drive (Heckman and Enoka, 2012). This, in turn, would enhance muscle activity by supplementing activity provided from partially denervated motor subsystems that, after SCI, contribute insufficient locomotor drive. Interestingly, although the majority of Ia connections onto motoneurons occur within the same muscle target, they also establish a lower number of connections onto functionally related muscles (Eccles et al., 1957). Thus, sprouting of group Ia afferents onto these muscle synergists could increase the activation of several muscles within a particular extensor or flexor group, thereby increasing the overall force generated.

Not only do proprioceptive group Ia afferents activate the agonist muscle (Mears and Frank, 1997), they also indirectly inhibit the antagonist muscles *via* inhibitory neurons (Hultborn et al., 1971; **Figure 1**). EES facilitation or sprouting of additional synapse formation of group Ia afferents onto inhibitory interneurons could help facilitate locomotion by supporting stronger inhibition of antagonist muscle activity at appropriate phases of movement. Whether local plastic changes in proprioceptors such as these can influence helpful rearrangement of descending pathways is unknown (Lamy et al., 2010), but mice with genetic ablation of these proprioceptors are unable to form these functional reorganizations (Takeoka et al., 2014; Takeoka, 2020).

Hypothesis 2: Reorganization of Propriospinal Circuitry Around the Lesion Site and Within the Lumbar Central Pattern Generator to Promote Rhythmic Activity and Hindlimb Coordination

PNs play a crucial role in locomotion by integrating sensory and motor information to coordinate multiple muscle groups. Functionally they may work to achieve tasks such as maintenance

of balance and may be part of the neural substrate that results in "motor synergies," acting to, e.g., adjust the dynamics of synergistic muscles after perturbation (Miller and Van der Burg, 1973; Levine et al., 2014). For this review, we use the definition of a PN as proposed by Flynn et al. (2011): a neuron whose soma is located within a spinal segment and whose axons project ipsilaterally and/or contralaterally to a different spinal segment and/or to supraspinal centers. Anatomically, PNs can be classified as "short" if their projections span less than seven spinal segments, including commissural interneurons and several genetically defined interneuronal types, and "long" if they span seven or more spinal segments (Conta and Stelzner, 2009; Flynn et al., 2011). PN circuits are modulated by descending input from supraspinal pathways (e.g., information containing motor commands) and/or sensory input from peripheral afferents (Cowley and Schmidt, 1997; Levine et al., 2014).

Modeling and experimental studies have demonstrated that PNs (short and long) may be an important CPG supraspinal target for the control of locomotion and fore-hind coordination (Ballion et al., 2001; Danner et al., 2017; Ausborn et al., 2019; Lin et al., 2019; for reviews see Flynn et al., 2011; Laliberte et al., 2019). In its traditional formulation, the vertebrate locomotor CPGs (one CPG each per hindlimb) are located within the spinal cord, and each consists of a "half-center" oscillator where flexors and extensors mutually inhibit each other (Brown, 1914). Current versions have the half-centers organized into two-levels—rhythm generator and pattern formation networks—which are both susceptible to supraspinal and peripheral afferent modulation during locomotion, but can also generate rhythmic behavior in the absence of these feedbacks (Brown, 1911; Rybak et al., 2006a,b). Interactions between these half-centers are coordinated by the activities of short (commissural, V01, etc.) and long PNs under the control of the supraspinal centers (Rybak et al., 2006a,b, 2015; Cowley et al., 2008, 2010; Zaporozhets et al., 2011).

Contained within the spinal cord, PNs are well-suited to relay information to motor pools below a lesion site (Han et al., 2019). Many receive inputs from supraspinal motor systems, and after unilateral lesion, corticospinal tract (CST) or reticulospinal (ReST) tract axons can sprout onto cervical PNs to relay these motor commands past the lesion site (Bareyre et al., 2004; Filli et al., 2014). After injury PNs upregulate GAP-43, neurotrophic factors, tubulins, and neurofilaments, all of which contribute to elongation and axonal sprouting (Fernandes et al., 1999; Siebert et al., 2010; Taccola et al., 2018; Wang et al., 2018). Indeed, 8 weeks after unilateral thoracic hemisection, long descending PNs bypassing the lesion undergo distal sprouting and show a doubling of connectivity onto lumbosacral motoneurons (Bareyre et al., 2004). Reorganization of PN networks is 2-fold: the circumnavigation of the injury site and plasticity below the level of injury. Delayed staggered hemisection studies demonstrated the ability of PNs to detour around the lesion to provide a surrogate flow of supraspinal locomotor commands to motor pools below the level of injury (Kato et al., 1984; Courtine et al., 2008; May et al., 2017). Propagation of these locomotor commands through PNs can elicit the rhythmic activity of motoneurons of the lumbar CPG (Cowley et al., 2008). Detouring lesions cannot occur in a complete SCI, however, animal models often exhibit some sensorimotor recovery. This is due to the plasticity of the PN network below the level of injury (Howland et al., 1995; Fenrich and Rose, 2009; Laliberte et al., 2019). Even after disrupting the flow of supraspinal motor commands, exogenously-augmented changes in PN circuitry can lead to the re-emergence of locomotion. In multiple animal models, PN networks induce locomotor-like activity in the absence of supraspinal input as shown in, for example, an *ex vivo* preparation of the spinal cord with drug administration (Zaporozhets et al., 2011) and after complete spinal cord transection with electrical stimulation (Yakovenko et al., 2007). Thus, these interneuronal networks can adapt to the loss of supraspinal input *via* dynamic reorganization, and can partially compensate for the loss of higher-level control if their activity is directly or indirectly bolstered by an exogenous source.

Although EES does not directly target PNs, evidence suggests EES can indirectly recruit and modulate these circuits, through the activation of peripheral sensory afferents, to facilitate hindlimb stepping (Capogrosso et al., 2013; Moraud et al., 2016; Formento et al., 2018). Notably, enhanced proprioceptive input provides critical guidance to organize the plasticity of PNs to circumvent a lesion site and relay information below the level of injury (Courtine et al., 2008; Takeoka and Arber, 2019). Also, Hebbian-like processes directed by electrically-enhanced sensory afferents and spared supraspinal projections could strengthen terminal contacts of PNs within motor pools in the lumbar CPG, which may be susceptible to Hebbian facilitation (Righetti et al., 2006). Even though spared supraspinal projections provide insufficient drive to activate locomotion, the additional drive provided by PN bypass relays could enhance supraspinal control to promote regain of function in animal models with severe SCI (Courtine et al., 2008). Spared PN circuitry, which can remain dormant after injury, may also play a vital role in this relay mechanism. Indeed, recovery of some volitional control in chronically paralyzed patients (Harkema et al., 2011; Angeli et al., 2014) may be a consequence of reactivating dormant spared PN circuitry indirectly *via* EES. Prolonged electrical stimulation may also promote propriospinal neuronal sprouting, which can strengthen newly formed and spared connections (**Figure 2**).

Several genetically identified PNs may play distinct roles in locomotor recovery in part by propagating locomotor commands to the lumbar CPGs (Laliberte et al., 2019). V1 PNs are inhibitory interneurons that project ipsilaterally onto motoneurons, as well as onto other V1 PNs and inhibitory interneurons. V1 PNs putatively inhibit motoneurons that innervate flexor muscles for the facilitation of coordination of flexor and extensor activity (Alvarez et al., 2005). Likewise, V2b PNs coordinate flexor and extensor activity, but possibly do so *via* inhibition of extensor muscles (Britz et al., 2015). V2a PNs, however, act as excitatory messengers to commissural interneurons for left-right coordination. For example, Dougherty and Kiehn (2010) proposed that a subpopulation of nonrhythmic V2a interneurons mediate sensory-evoked locomotor-like activity by being recruited at different speeds to help regulate right-left coordination and ipsilateral firing of motoneurons. V3 PNs are also excitatory interneurons, but function to stabilize ipsilateral

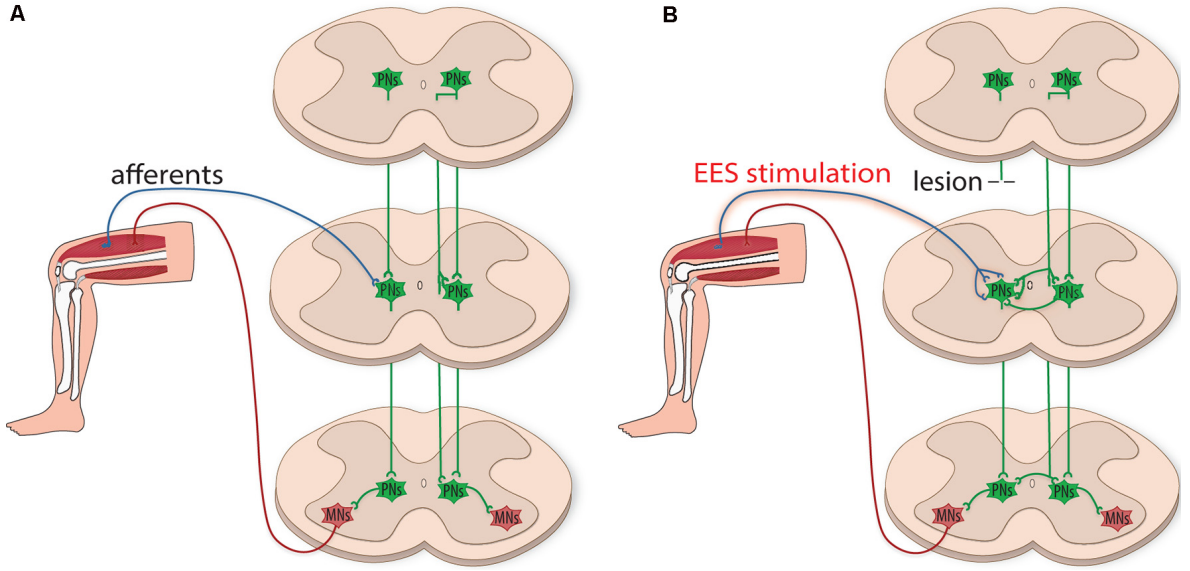

FIGURE 2 | Plasticity of propriospinal neuronal circuitry after injury. **(A)** Schematic illustration depicting the integration of sensory and motor information by propriospinal neurons (PNs, green). PNs project ipsilaterally and contralaterally onto motoneuron pools (MNs, red) and contribute to interlimb coordination by integrating information relayed from supraspinal centers and received from sensory input. **(B)** After the injury, PNs have the plastic potential for dynamic reorganization. EES can indirectly recruit and modulate propriospinal circuits, creating functional networks caudal to the lesion site. PNs can relay supraspinal input by circumventing the injury, providing a surrogate flow of supraspinal locomotor commands to MNs. PNs can also reorganize below the level of injury, sprouting contralaterally to facilitate communication across multiple spinal segments.

and contralateral patterns of locomotion. Further, during postmitotic development, V3 interneurons migrate dorsally or ventrally and develop distinct functions: dorsal V3 interneurons receive robust input from group Ia proprioceptive neurons and might be indirectly involved in adjusting right-left coordination, whereas ventral V3 interneurons were suggested to synchronize motor output amongst multiple motoneuron pools (Borowska et al., 2013; Lin et al., 2019). This work was followed with a computational model of the locomotor CPG demonstrating that as speed increases, sensory afferents relay limb speed onto V3 interneurons, with V3 interneurons assisting in the transition from alternating to synchronized gaits (Danner et al., 2017). dI3 PNs also receive sensory information from the periphery and directly activate motoneuron pools in the cervical and lumbar CPGs driving ipsilateral agonist muscles (Bui et al., 2013, 2016). Importantly, dI3 PNs have been identified to promote rhythmic locomotor recovery after SCI even in the absence of supraspinal input, suggesting an essential role of these PNs in the transmission of activity between adjacent spinal segments that contain lumbar CPG components (Bui et al., 2016). Together, plasticity among different types of PNs could influence locomotion by enhancing supraspinal drive through relays bypassing the lesion as well as supporting rhythm generation to increase stepping patterning.

As CPGs may be sensitive to Hebbian facilitation (Righetti et al., 2006), it is the convergence of activity (e.g., peripheral afferents with increased activity from EES, PN networks, and spared supraspinal projections) within lumbar motor pools that is likely responsible for driving locomotor recovery after SCI (Dimitrijevic et al., 1998; Guertin, 2013). Ultimately, it is the activation of the lumbar CPGs that may facilitate improvements in individuals with incomplete SCI (Herman et al., 2002) and generate stepping-like movements *via* tonic input in individuals with complete SCI (Minassian et al., 2004, 2007). Importantly, peripheral afferent activation from EES can modulate the lumbar CPGs to adapt to perturbations and entrain it appropriately to drive recovery (Young, 2015). However, studies with split-belt locomotion suggest that this phenomenon results from side-specific proprioceptive input and PNs are necessary to transfer information to contralateral sides of the spinal cord (Prokop et al., 1995). As such, PNs are not only recruited by EES, particularly those that are susceptible to afferent input (e.g., V3 and dI3 PNs) but perhaps are also required for the transmission of rhythmic activity throughout the lumbar CPGs to elicit hindlimb coordination.

Hypothesis 3: Spatiotemporal Integration of the Internal Model With Peripheral Afferent Input Within Interneuronal Networks to Aid Learning of Correct Motor Output

Motor activity requires precise timing to coordinate a series of individual muscle contractions in sequence so that the movement can proceed smoothly. Disruption of descending motor control pathways reduces vital input into spinal motor systems reducing coordination and inducing movement errors. Here, we discuss circuits known to influence the timing of muscle contraction,

error correction, motor learning, and movement patterning as possible mechanisms by which increased afferent activation could enhance recovery.

Error correction and motor memory have been studied extensively within cerebellar circuits. One such circuit is the internal forward dynamic model; derived from internally generated motor signals, this circuit is used to predict the motor and sensory consequences of an action (Wolpert et al., 1995; Wolpert and Ghahramani, 2000; Bui et al., 2013). These predictions are then compared with actual sensory data to either identify errors in the motor program or possible external perturbations of the limb. Prediction calculations are primarily performed in the cerebellum from planned motor commands driving a forward model of the limb. Simultaneously, proprioceptive and low-threshold cutaneous information is transmitted to the cerebellum (*via* the dorsal and ventral spinocerebellar tracts respectively), where comparative analysis of the incoming information is processed and directed back to the spinal cord through the ReST. Anatomically, the ventral spinocerebellar pathway is also responsible for carrying a spinal copy of motor commands of rhythmic activity (e.g., locomotion) back to the cerebellum (Brownstone et al., 2015). The reticulospinal tract extends from the caudal midbrain through the pons and medulla with its axons descending *via* the ventrolateral funiculus of the spinal cord, eventually forming glutamatergic synapses with spinal interneurons and primary motoneurons (Brownstone and Chopek, 2018). With the repetition of the task, discrepancies in the motor program are eliminated to generate a progressively more refined motor memory (Tuthill and Azim, 2018).

When discussing the internal model, which is composed of the inverse model, forward model, and efferent copy, it is important to define the pathways involved. The inverse model determines the motor commands necessary to achieve the desired movement, where the inputs are the desired state of a limb, and the outputs are the motor commands needed to achieve that state. The forward model simulates the forward dynamics of the limb given a set of motor commands and produces an estimate of the final state (motor and sensory) of the limb; the inputs are the commands issued by the central nervous system, and the outputs are the predicted limb outcomes (Wolpert and Miall, 1996; Kawato, 1999). The efference copy is a copy of the motor command delivered to the muscles and can be used as input to the forward model to predict expected motor output and sensory feedback (Kawato, 1999). For this review, we refer to the entirety of this endogenous system (including the ReST) as the descending supraspinal control, and we propose that it is a contributory mechanism involved in recovery from SCI both with and without spinal cord stimulation.

In the absence of pathology, the descending supraspinal control is hypothesized to be involved in three aspects of motor physiology: sensory prediction, real-time adjustments, and motor memory. For example, Straka et al. (2018) discuss how the efference copy, in conjunction with the forward model, predicts the sensory consequences of action so that the central nervous system can routinely ignore the self-generated sensory input produced during the behavior. Azim and Alstermark (2015) used the term internal motor copy to describe the efference copy that is conveyed to the cerebellum to generate predictions of motor actions. The forward model can predict the consequences of a motor command and adjust the output in real-time without having to rely on delayed proprioceptive feedback (Wolpert and Miall, 1996). However, the forward model can also respond to ongoing sensory feedback to refine the accuracy of the outputs (**Figure 3**).

Post-injury, the descending supraspinal control potentially assumes a principal role in the recovery of locomotion. Asboth et al. (2018) found that residual ReST fibers in a rat contusion study were fundamental to regaining locomotive function. The study involved severe thoracic spine contusions designed to abolish CST fibers, followed by the retraining of lumbar circuits using a strict neurorehabilitation program. Before the injury, the rats were randomly assigned to untrained and trained groups for neurorehabilitation. All the rats that received a rehabilitation program while simultaneously receiving electrochemical neuromodulation regained weight-bearing locomotion, whereas none of the untrained rats were able to produce locomotion (even in the presence of electrochemical neuromodulation). Additionally, the majority of the animals who did not receive any neuromodulation but did receive neurorehabilitation were able to recover locomotion, illustrating that the underlying process was organic in nature. Neuroanatomical tracing confirmed that the contusions interrupted all motor cortex projections to the lumbar segments and that only neurons in the ventral gigantocellular reticular nuclei (vGi), raphe, and the parapyramidal region retained connectivity across the lesion. They concluded that neurorehabilitation and neuromodulation synergistically promoted the reorganization of glutamatergic cortical projections to the vGi and the growth of ReST fibers across the injury, which relayed the cortical commands downstream. Importantly, with the application of Designer Receptors Exclusively Activated by Designer Drugs (DREADDs), they established that these ReST fibers are of little consequence in uninjured animals, and the extensive reorganization of cortico-reticulospinal circuits becomes critical in SCI.

The internal model may have a spinal component functioning independently of the cerebellum. Brownstone et al. (2015) refer to the spinal component in the context of motor learning. They infer that the alpha-motoneurons of the spinal cord may function similarly to the deep cerebellar nuclei by measuring motor command errors during motor learning. The alpha-motoneurons, which produce muscle contraction, receive excitatory sensory information from Ia afferents, inhibitory inputs from Renshaw cells, as well as provide the Renshaw cells with an efferent copy of the commands. They describe the alpha-motoneurons as comparators that assess the discrepancy between motor commands and motor outputs in essence arguing that the cerebellum is not the only CNS structure where forward models are expressed. Takeoka (2020) discusses how the proprioceptive feedback may contribute to intrinsic spinal cord circuitry, and how proprioception helps construct an internal motor command that executes outputs in the event of severed descending pathways. In fact, "movement-specific activation of

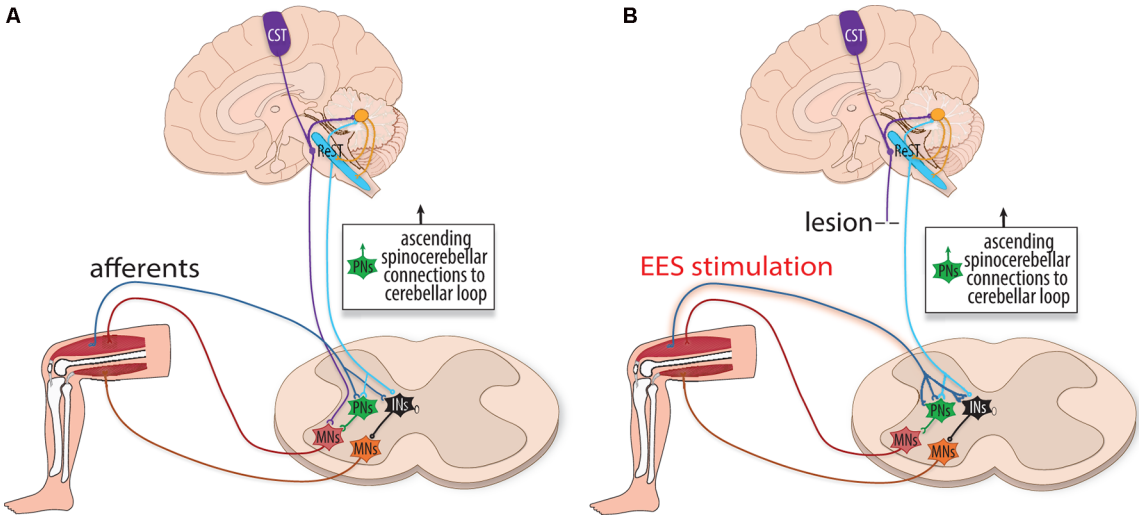

FIGURE 3 | The influence of internal motor copy circuitry during rehabilitation. **(A)** Schematic illustration depicting the internal motor copy, a cerebellar loop that makes a forward prediction of sensory input. It is thought to be primarily performed in the cerebellum and, to a lesser extent, within local spinal circuits. Predictions are compared (and respond) to incoming proprioceptive information to adjust motor actions in real-time before the completion of the movement. Supraspinal networks, including the cortical spinal tract (CST, purple), reticulospinal tract (ReST, blue), and rubrospinal tract (not shown) relay planned motor information to the cerebellum to generate the internal motor copy. Multiple internal motor copies are relayed to the cerebellar loop *via* the Lateral Reticular Nucleus. Simultaneously, sensory information from the periphery is relayed to the cerebellum *via* spinocerebellar tracts. Comparative analyses are performed within this cerebellar loop to communicate what the intended motor command accomplished. Supraspinal fibers converge onto interneurons (INs, black), including (PNs, green), to indirectly excite motoneurons. **(B)** With lesion, fibers from the reticulospinal tract (ReST, blue) may relay cortical commands, as the internal motor copy is unaffected by the lesion and spared and injured PNs can dynamically reorganize after SCI. With EES, input from the ReST spatiotemporally combines with increased activity of group Ia afferents to achieve supra-threshold activation of interneurons as well as indirectly activating motoneurons (MNs, red and orange).

spinal interneurons and motoneurons combined with intrinsic plasticity of the spinal cord network facilitates learning to walk with limited brain input" (Takeoka, 2020). For example, Forssberg (1979) noted that completely transected cats were able to adjust limb trajectory during the swing phase of locomotion upon encountering an obstacle, thus underlining the existence of an intrinsic spinal network independent of descending input. The conceptual framework of the forward model may thus be separated into two distinctive entities, one confined to the hindbrain and one located in the spinal cord, that are implicated in the recovery of locomotion.

Certain spinal interneurons may contribute to the spinal internal motor circuitry. Bui et al. (2016) demonstrated that dI3 interneurons receive afferent inputs and project onto intermediate and ventral regions of the spinal cord. "The dI3 interneurons are positioned between multimodal sensory input and spinal locomotor circuits, and have a bi-directional relationship with these locomotor circuits, receiving an efference copy of their activity." They surmised that this spinal microcircuitry is not necessary for normal locomotor activity, but is critical in driving locomotion following transection as it continues to integrate sensory input. In their rodent model, dI3 knockout mice with spinal transection displayed a significant reduction in generating locomotor activity when compared to spinalized control mice. They performed lower thoracic spinal cord transections on both dI3 knockout mice and control mice and then compared locomotor recovery. The performance was quantified using forelimb/hindlimb step ratios, with any forward excursions of the toes ("forward excursions") counted as steps, and qualitatively assessed using high-speed kinematic video recordings. During recovery, they found that the knockout mice had half the number of steps of the control mice. Furthermore, the knockout mice displayed linear kinematics not at all reflective of locomotion when compared to the control mice using horizontal movement, vertical movement, and joint angles as parameters. As such, dI3 interneurons and the associated circuits could promote sensory-mediated recovery of function in the absence of any descending motor commands, mirroring the automaticity of the proposed descending supraspinal control.

Rehabilitative training with or without EES could provide error correction by either rerouting cerebellar instructions past the injury or at local spinal cord circuit levels. For cerebellar modulation following SCI, descending supraspinal control could be responsive to EES. Lesion studies have found that severed ReST fibers sprout in an ipsilesional manner above the injury to form excitatory boutons, and while descending supraspinal fibers struggle to penetrate the hostile micro-environment of a lesion, they do converge onto interneurons (e.g., PNs) as intermediaries (Flynn et al., 2011; Filli et al., 2014). The reorganization and prioritization of glutamatergic ReST neurons with ancillary projections below the injury could, therefore, relay error adjusted commands following SCI (Fink and Cafferty, 2016; Kim et al., 2017; Asboth et al., 2018). The descending reticulospinal control may facilitate recovery through heterosynaptic plasticity in concordance with EES sensory afferents: the activity of the ReSTs spatiotemporally combines with group Ia afferents to

help overcome a threshold needed for interneuronal activation (**Figure 3**). Therapies utilizing spinal cord stimulation help promote recovery in part by fortifying the spatiotemporal consolidation of activity at the intersection between ReST fibers and group Ia afferents, which in turn stimulate motoneurons.

USING CHEMOGENETIC TECHNOLOGY TO UNCOVER EES-INDUCED MECHANISMS OF RECOVERY

Although remarkable progress has been made in identifying pathways that support enhanced recovery after SCI with EES, the daunting challenge of pinpointing new and enhanced connections at the cellular and synaptic levels, some of which were illustrated above, remains. Genetic tools may help in this task. Genetic tools enable: (1) targeted, reversible manipulation of specific pathways and neuronal subpopulations; (2) labeling of precisely which neurons have been modulated (not definitively known with electrical stimulation); and (3) identification and subsequent tracing of secondary circuits that have been influenced. Multiple genetically encoded tools for remote control of the nervous system now exist on timescales ranging from milliseconds (e.g., optogenetics) to hours (e.g., chemogenetics), as well as viral and transgenic methods to restrict their expression to defined neural groups or phenotypes (e.g., motor, proprioceptive, or nociceptive; Towne et al., 2013; Iyer et al., 2016).

Unlike optogenetics, chemogenetics provides the advantage of not requiring a tether, thus neuromodulation can be studied in freely behaving animals. Chemogenetic technology has the potential to achieve behaviorally relevant excitation or inhibition of neural phenotypes upon administration of an actuator molecule (either an injected drug or given food item). DREADDs are perhaps the most well established chemogenetic tool for neuromodulation and work by manipulating G-protein coupled pathways (**Figures 4A,C**; Armbruster et al., 2007; Roth, 2016). Relevant to neural dysfunction and repair, Jaiswal and English (2017) found that activation of motoneurons with excitatory DREADDs in a rat peripheral nerve injury model could improve functional recovery. In a rat contusion model of SCI, targeted DREADDs-silencing was used to identify glutamatergic neurons of the ventral gigantocellular reticular and vestibular nuclei as responsible for transmitting a cortical command to lumbar neurons for trunk stability and patterned movements (Asboth et al., 2018). In a mouse staggered bilateral hemisection model of SCI, DREADDs hyperpolarization of inhibitory interneurons identified these interneurons as the limiting factor preventing supraspinal commands from propagating into relay circuits (and putatively lumbar CPG centers) after injury (Chen et al., 2018). Although the mechanism of action of DREADDs agonist clozapine-*N*-oxide (CNO) has been questioned (Gomez et al., 2017; Mahler and Aston-Jones, 2018), experimental designs with between-subject controls can make CNO (3–5 mg/kg) a suitable DREADD agonist (Jendryka et al., 2019). Another chemogenetic tool, Pharmacologically Selective Actuator Modules and their Effector

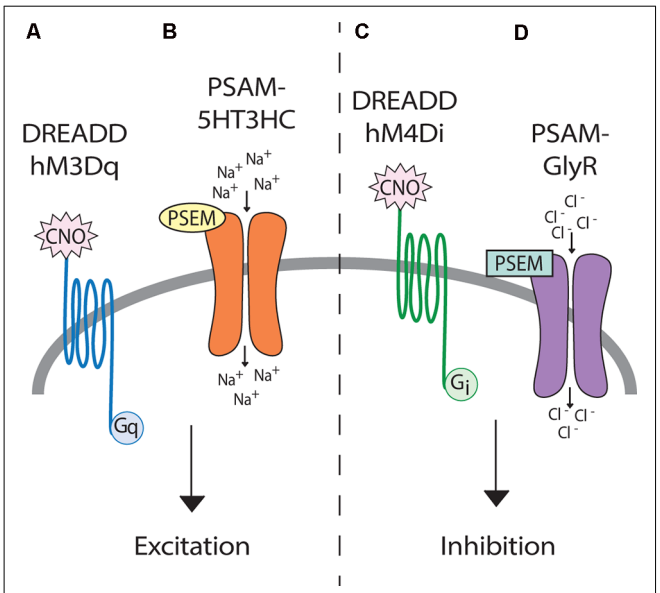

FIGURE 4 | Genetic tools for afferent modulation. (Left) Both DREADD hM3Dq **(A)** and PSAM-5HT3HC **(B)** can make neurons more excitable through depolarization. (Right) Both DREADD hM4Di **(C)** and PSAM-GlyR **(D)** can inhibit neuronal activity through hyperpolarization. Upon clozapine-*N*-oxide (CNO) binding, DREADDs activate G-protein coupled signaling cascades, which ultimately change cellular membrane potentials. In contrast, upon binding by PSEMs, PSAMs directly open ion channels allowing the influx of sodium (excitatory) or chloride (inhibitory).

Molecules (PSAMs/PSEMs), works *via* directly opening ion channels in neurons (**Figures 4B,D**) for robust neural excitation and silencing (Magnus et al., 2011). A recently developed PSAM, PSAM^4-GlyR, is an ultrapotent chemogenetic receptor for varenicline, an FDA-approved smoking cessation drug. PSAM^4-GlyR overcomes limitations from using traditional PSEMs, such as short clearance times (30–60 m) and low-micromolar potency, making it highly applicable for *in vivo* studies (Magnus et al., 2019). The control of specific neurons *via* administration of a drug, and subsequent neuronal tracing capability, make chemogenetics an important tool for modulating circuits to understand molecular mechanisms of plasticity.

Importantly, chemogenetic manipulation of *afferent* activity holds promise to uncovering molecular and circuit mechanisms of EES-induced recovery from SCI. For example, if chemogenetics was restricted to, and altered excitability of, afferents activated by EES (medium and large diameter afferents within the posterior roots) in SCI models, the neural circuit changes that were induced by these afferents could be quantified in postmortem histological analyses. In addition to tracing modulated pathways and definitive knowledge of which afferents were affected, it opens the door to combinatorial modulation of subsets of types of afferents (e.g., excite only proprioceptors without affecting exteroceptors, whilst inhibiting nociceptors). As with EES, locomotor changes from afferent excitation (or *inhibition* with chemogenetic tools) can be identified using assays such as high-speed kinematics. However, the main strength of chemogenetic tools lies in the unique advantage of

identification of plastic mechanisms that occur during recovery from SCI, a unique ability that EES cannot replicate.

CONCLUSION

EES is a potentially effective therapy to enhance sensorimotor recovery following SCI. However, the exact mechanisms underlying recovery remain elusive. This review identifies several plasticity mechanisms that may be evoked by EES through the activation of peripheral afferents. Resultant recovery is likely due to local lumbar, propriospinal, and internal models acting together synergistically. While the propriospinal network and the descending reticulospinal command are putatively most contributive to recovery from anatomically incomplete lesions, recovery from complete lesions is likely due to local lumbar circuit plasticity driven by afferent input. The identification of these mechanisms of plasticity will likely be accelerated by genetic tools for afferent modulation.

AUTHOR CONTRIBUTIONS

All authors contributed to the conceptualization and writing. JE led the writing process. KK led the artwork and figures. RS led the writing on the introduction, history, and internal motor copy. ML, GS, and AS contributed to the conceptualization, writing, and editing.

FUNDING

This work was supported by Shriners Hospitals for Children Grant #85115 to AS and grant SHC 86000 to GS. This work was further supported by Craig H. Neilsen Foundation Senior Research Grant #546798 to AS.

REFERENCES

Alvarez, F. J., Jonas, P. C., Sapir, T., Hartley, R., Berrocal, M. C., Geiman, E. J., et al. (2005). Postnatal phenotype and localization of spinal cord V1 derived interneurons. *J. Comp. Neurol.* 493, 177–192. doi: 10.1002/cne.20711

Angeli, C. A., Edgerton, V. R., Gerasimenko, Y. P., and Harkema, S. J. (2014). Altering spinal cord excitability enables voluntary movements after chronic complete paralysis in humans. *Brain* 137, 1394–1409. doi: 10.1093/brain/awu038

Armbruster, B. N., Li, X., Pausch, M. H., Herlitze, S., and Roth, B. L. (2007). Evolving the lock to fit the key to create a family of G protein-coupled receptors potently activated by an inert ligand. *Proc. Natl. Acad. Sci. U S A* 104, 5163–5168. doi: 10.1073/pnas.0700293104

Asboth, L., Friedli, L., Beauparlant, J., Martinez-Gonzalez, C., Anil, S., Rey, E., et al. (2018). Cortico-reticulo-spinal circuit reorganization enables functional recovery after severe spinal cord contusion. *Nat. Neurosci.* 21, 576–588. doi: 10.1038/s41593-018-0093-5

Ausborn, J., Shevtsova, N. A., Caggiano, V., Danner, S. M., and Rybak, I. A. (2019). Computational modeling of brainstem circuits controlling locomotor frequency and gait. *eLife* 8:e43587. doi: 10.7554/eLife.43587

Azim, E., and Alstermark, B. (2015). "Skilled forelimb movements and internal copy motor circuits," in *Current Opinion in Neurobiology*, eds O. Kiehn, and M. Churchland (London, UK: Elsevier Limited), 16–24.

Ballion, B., Morin, D., and Viala, D. (2001). Forelimb locomotor generators and quadrupedal locomotion in the neonatal rat. *Eur. J. Neurosci.* 14, 1727–1738. doi: 10.1046/j.0953-816X.2001.01794.x

Bareyre, F. M., Kerschensteiner, M., Raineteau, O., Mettenleiter, T. C., Weinmann, O., and Schwab, M. E. (2004). The injured spinal cord spontaneously forms a new intraspinal circuit in adult rats. *Nat. Neurosci.* 7, 269–277. doi: 10.1038/nn1195

Barolat, G., Myklebust, J. B., and Wenninger, W. (1988). Effects of spinal cord stimulation on spasticity and spasms secondary to myelopathy. *Appl. Neurophysiol.* 51, 29–44. doi: 10.1159/000099381

Borowska, J., Jones, C. T., Zhang, H., Blacklaws, J., Goulding, M., and Zhang, Y. (2013). Functional subpopulations of V3 interneurons in the mature mouse spinal cord. *J. Neurosci.* 33, 18553–18565. doi: 10.1523/JNEUROSCI.2005-13.2013

Bouyer, L. J. G., and Rossignol, S. (1998). The contribution of cutaneous inputs to locomotion in the intact and the spinal cat. *Ann. N Y Acad. Sci.* 860, 508–512. doi: 10.1111/j.1749-6632.1998.tb09090.x

Britz, O., Zhang, J., Grossmann, K. S., Dyck, J., Kim, J. C., Dymecki, S., et al. (2015). A genetically defined asymmetry underlies the inhibitory control of flexor-extensor locomotor movements. *eLife* 4:e13038. doi: 10.7554/eLife.13038

Brown, G. T. (1911). The intrinsic factors in the act of progression in the mammal. *Proc. Biol. Sci.* 84, 308–319. doi: 10.1098/rspb.1911.0077

Brown, G. T. (1914). On the nature of the fundamental activity of the nervous centres; together with an analysis of the conditioning of rhythmic activity in progression and a theory of the evolution of function in the nervous system. *J. Physiol.* 48, 18–46. doi: 10.1113/jphysiol.1914.sp001646

Brownstone, R. M., and Chopek, J. W. (2018). Reticulospinal systems for tuning motor commands. in *Front. Neural Circuits* 12, 1–10. doi: 10.3389/fncir.2018.00030

Brownstone, R. M., Bui, T. V., and Stifani, N. (2015). "Spinal circuits for motor learning," in *Current Opinion in Neurobiology*, eds O. Kiehn, and M. Churchland (London, UK: Elsevier Limited), 166–173.

Bui, T. V., Akay, T., Loubani, O., Hnasko, T. S., Jessell, T. M., and Brownstone, R. M. (2013). Circuits for grasping: spinal dI3 interneurons mediate cutaneous control of motor behavior. *Neuron* 78, 191–204. doi: 10.1016/j.neuron.2013.02.007

Bui, T. V., Stifani, N., Akay, T., and Brownstone, R. M. (2016). Spinal microcircuits comprising dI3 interneurons are necessary for motor functional recovery following spinal cord transection. *eLife* 5:e21715. doi: 10.7554/eLife.21715

Burns, S. P., Golding, D. G., Rolle, W. A., Graziani, V., and Ditunno, J. F. (1997). Recovery of ambulation in motor-incomplete tetraplegia. *Arch. Phys. Med. Rehabil.* 78, 1169–1172. doi: 10.1016/S0003-9993(97)90326-9

Capogrosso, M., Milekovic, T., Borton, D., Wagner, F., Moraud, E. M., Mignardot, J. B., et al. (2016). A brain-spine interface alleviating gait deficits after spinal cord injury in primates. *Nature* 539, 284–288. doi: 10.1038/nature20118

Capogrosso, M., Wenger, N., Raspopovic, S., Musienko, P., Beauparlant, J., Luciani, L. B., et al. (2013). A computational model for epidural electrical stimulation of spinal sensorimotor circuits. *J. Neurosci.* 33, 19326–19340. doi: 10.1523/JNEUROSCI.1688-13.2013

Chen, B., Li, Y., Yu, B., Zhang, Z., Brommer, B., Williams, P. R., et al. (2018). Reactivation of dormant relay pathways in injured spinal cord by KCC2 manipulations. *Cell* 174, 521.e13–535.e13. doi: 10.1016/j.cell.2018.06.005

Conta, A. C., and Stelzner, D. J. (2009). "Chapter 12-The propriospinal system," in *The Spinal Cord*, eds. C. Watson, G. Paxinos, and G. Kayalioglu (San Diego: Academic Press), 180–190.

Cook, A. W. (1976). Electrical stimulation in multiple sclerosis. *Hosp. Pract.* 11, 51–58. doi: 10.1080/21548331.1976.11706516

Courtine, G., Gerasimenko, Y., van den Brand, R., Yew, A., Musienko, P., Zhong, H., et al. (2009). Transformation of nonfunctional spinal circuits into functional states after the loss of brain input. *Nat. Neurosci.* 12, 1333–1342. doi: 10.1038/nn.2401

Courtine, G., Song, B., Roy, R. R., Zhong, H., Herrmann, J. E., Ao, Y., et al. (2008). Recovery of supraspinal control of stepping *via* indirect propriospinal relay connections after spinal cord injury. *Nat. Med.* 14, 69–74. doi: 10.1038/nm1682

Cowley, K. C., and Schmidt, B. J. (1997). Regional distribution of the locomotor pattern-generating network in the neonatal rat spinal cord. *J. Neurophysiol.* 77, 247–259. doi: 10.1152/jn.1997.77.1.247

Cowley, K. C., Zaporozhets, E., and Schmidt, B. J. (2008). Propriospinal neurons are sufficient for bulbospinal transmission of the locomotor command signal in the neonatal rat spinal cord. *J. Physiol.* 586, 1623–1635. doi: 10.1113/jphysiol.2007.148361

Cowley, K. C., Zaporozhets, E., and Schmidt, B. J. (2010). Propriospinal transmission of the locomotor command signal in the neonatal rat. *Ann. N Y Acad. Sci.* 1198, 42–53. doi: 10.1111/j.1749-6632.2009.05421.x

Crosbie, J., Tanhoffer, A. I. P., and Fornusek, C. (2014). FES assisted standing in people with incomplete spinal cord injury: a single case design series. *Spinal Cord* 52, 251–254. doi: 10.1038/sc.2013.158

Danner, S. M., Shevtsova, N. A., Frigon, A., and Rybak, I. A. (2017). Computational modeling of spinal circuits controlling limb coordination and gaits in quadrupeds. *eLife* 6:e31050. doi: 10.7554/eLife.31050

Davis, B. M., Collins, W. F., and Mendell, L. M. (1985). Potentiation of transmission at Ia-motoneuron connections induced by repeated short bursts of afferent activity. *J. Neurophysiol.* 54, 1541–1552. doi: 10.1152/jn.1985.54.6.1541

Dimitrijevic, M. R., Gerasimenko, Y., and Pinter, M. M. (1998). Evidence for a spinal central pattern generator in humans. *Ann. N Y Acad. Sci.* 860, 360–376. doi: 10.1111/j.1749-6632.1998.tb09062.x

Dimitrijevic, M. R., Illis, L. S., Nakajima, K., Sharkey, P. C., and Sherwood, A. M. (1986). Spinal cord stimulation for the control of spasticity in patients with chronic spinal cord injury: II. Neurophysiologic observations. *Cent. Nerv. Syst. Trauma* 3, 145–152. doi: 10.1089/cns.1986.3.145

Dougherty, K. J., and Kiehn, O. (2010). Firing and cellular properties of V2a interneurons in the rodent spinal cord. *J. Neurosci.* 30, 24–37. doi: 10.1523/JNEUROSCI.4821-09.2010

Eccles, J. C., Eccles, R. M., and Lundberg, A. (1957). The convergence of monosynaptic excitatory afferents on to many different species of alpha motoneurones. *J. Physiol.* 137, 22–50. doi: 10.1113/jphysiol.1957.sp005794

Edgerton, V. R., and Harkema, S. J. (2011). Epidural stimulation of the spinal cord in spinal cord injury: current status and future challenges. *Expert Rev. of Neurother.* 11, 1351–1353). doi: 10.1586/ern.11.129

Fenrich, K. K., and Rose, P. K. (2009). Spinal interneuron axons spontaneously regenerate after spinal cord injury in the adult feline. *J. Neurosci.* 29, 12145–12158. doi: 10.1523/JNEUROSCI.0897-09.2009

Fernandes, K. J., Fan, D. P., Tsui, B. J., Cassar, S. L., and Tetzlaff, W. (1999). Influence of the axotomy to cell body distance in rat rubrospinal and spinal motoneurons: differential regulation of GAP-43, tubulins and neurofilament-M. *J. Comp. Neurol.* 414, 495–510. doi: 10.1002/(sici)1096-9861(19991129)414:4<495::aid-cne6>3.0.co;2-s

Filli, L., Engmann, A. K., Zörner, B., Weinmann, O., Moraitis, T., Gullo, M., et al. (2014). Bridging the gap: a reticulo-propriospinal detour bypassing an incomplete spinal cord injury. *J. Neurosci.* 34, 13399–13410. doi: 10.1523/JNEUROSCI.0701-14.2014

Fink, K. L., and Cafferty, W. B. J. (2016). Reorganization of intact descending motor circuits to replace lost connections after injury. *Neurotherapeutics* 13, 370–381. doi: 10.1007/s13311-016-0422-x

Flynn, J. R., Graham, B. A., Galea, M. P., and Callister, R. J. (2011). The role of propriospinal interneurons in recovery from spinal cord injury. *Neuropharmacology* 60, 809–822. doi: 10.1016/j.neuropharm.2011.01.016

Formento, E., Minassian, K., Wagner, F., Mignardot, J. B., Le Goff-Mignardot, C. G., Rowald, A., et al. (2018). Electrical spinal cord stimulation must preserve proprioception to enable locomotion in humans with spinal cord injury. *Nat. Neurosci.* 21, 1728–1741. doi: 10.1038/s41593-018-0262-6

Forssberg, H. (1979). Stumbling corrective reaction: a phase-dependent compensatory reaction during locomotion. *J. Neurophysiol.* 42, 936–953. doi: 10.1152/jn.1979.42.4.936

Gad, P. N., Kreydin, E., Zhong, H., Latack, K., and Edgerton, V. R. (2018). Non-invasive neuromodulation of spinal cord restores lower urinary tract function after paralysis. *Front. Neurosci.* 12:432. doi: 10.3389/fnins.2018.00432

Gad, P. N., Roy, R. R., Zhong, H., Lu, D. C., Gerasimenko, Y. P., and Edgerton, V. R. (2014). Initiation of bladder voiding with epidural stimulation in paralyzed, step trained rats. *PLoS One* 9:e108184. doi: 10.1371/journal.pone.0108184

Gill, M. L., Grahn, P. J., Calvert, J. S., Linde, M. B., Lavrov, I. A., Strommen, J. A., et al. (2018). Neuromodulation of lumbosacral spinal networks enables independent stepping after complete paraplegia. *Nature Med.* 24, 1677–1682. doi: 10.1038/s41591-018-0175-7

Gomez, J. L., Bonaventura, J., Lesniak, W., Mathews, W. B., Sysa-Shah, P., Rodriguez, L. A., et al. (2017). Chemogenetics revealed: DREADD occupancy and activation *via* converted clozapine. *Science* 357, 503–507. doi: 10.1126/science.aan2475

Grahn, P. J., Lavrov, I. A., Sayenko, D. G., Van Straaten, M. G., Gill, M. L., Strommen, J. A., et al. (2017). Enabling task-specific volitional motor functions *via* spinal cord neuromodulation in a human with paraplegia. *Mayo. Clin. Proc.* 92, 544–554. doi: 10.1016/j.mayocp.2017.02.014

Guertin, P. A. (2013). Central pattern generator for locomotion: anatomical, physiological and pathophysiological considerations. *Front. Neurol.* 3:183. doi: 10.3389/fneur.2012.00183

Guiraud, D., Azevedo Coste, C., Benoussaad, M., and Fattal, C. (2014). Implanted functional electrical stimulation: case report of a paraplegic patient with complete SCI after 9 years. *J. Neuroeng. Rehabil.* 11:15. doi: 10.1186/1743-0003-11-15

Hachmann, J. T., Grahn, P. J., Calvert, J. S., Drubach, D. I., Lee, K. H., and Lavrov, I. A. (2017). Electrical neuromodulation of the respiratory system after spinal cord injury. *Mayo Clin. Proc.* 92, 1401–1414.

Han, Q., Ordaz, J. D., Liu, N. K., Richardson, Z., Wu, W., Xia, Y., et al. (2019). Descending motor circuitry required for NT-3 mediated locomotor recovery after spinal cord injury in mice. *Nat. Commun.* 10:5815. doi: 10.1038/s41467-019-13854-3

Hardin, E., Kobetic, R., Murray, L., Corado-Ahmed, M., Pinault, G., Sakai, J., et al. (2007). Walking after incomplete spinal cord injury using an implanted FES system: a case report. *J. Rehabil. Res. Dev.* 44, 333–346. doi: 10.1682/JRRD.2007.03.0333

Harkema, S. J., Gerasimenko, Y., Hodes, J., Burdick, J., Angeli, C., Chen, Y., et al. (2011). Effect of epidural stimulation of the lumbosacral spinal cord on voluntary movement, standing and assisted stepping after motor complete paraplegia: a case study. *Lancet* 377, 1938–1947. doi: 10.1016/S0140-6736(11)60547-3

Harkema, S. J., Wang, S., Angeli, C. A., Chen, Y., Boakye, M., Ugiliweneza, B., et al. (2018). Normalization of blood pressure with spinal cord epidural stimulation after severe spinal cord injury. *Front. Hum. Neurosci.* 12:83. doi: 10.3389/fnhum.2018.00083

Heckman, C. J., and Enoka, R. M. (2012). "Motor unit", in *Comprehensive Physiology*, ed. R. Terjung (Hoboken, NJ: John Wiley & Sons, Inc.), 2629–2682.

Herman, R., He, J., D'Luzansky, S., Willis, W., and Dilli, S. (2002). Spinal cord stimulation facilitates functional walking in a chronic, incomplete spinal cord injured. *Spinal Cord* 40, 65–68. doi: 10.1038/sj.sc.3101263

Howland, D. R., Bregman, B. S., Tessler, A., and Goldberger, M. E. (1995). Development of locomotor behavior in the spinal kitten. *Exp. Neurol.* 135, 108–122. doi: 10.1006/exnr.1995.1071

Hultborn, H., Jankowska, E., Lindström, S., and Roberts, W. (1971). Neuronal pathway of the recurrent facilitation of motoneurones. *J. Physiol.* 218, 495–514. doi: 10.1113/jphysiol.1971.sp009630

Iyer, S. M., Vesuna, S., Ramakrishnan, C., Huynh, K., Young, S., Berndt, A., et al. (2016). Optogenetic and chemogenetic strategies for sustained inhibition of pain. *Sci. Rep.* 6:30570. doi: 10.1038/srep30570

Jaiswal, P. B., and English, A. W. (2017). Chemogenetic enhancement of functional recovery after a sciatic nerve injury. *Eur. J. Neurosci.* 45, 1252–1257. doi: 10.1111/ejn.13550

Jendryka, M., Palchaudhuri, M., Ursu, D., van der Veen, B., Liss, B., Kätzel, D., et al. (2019). Pharmacokinetic and pharmacodynamic actions of clozapine-N-oxide, clozapine and compound 21 in DREADD-based chemogenetics in mice. *Sci. Rep.* 9:4522. doi: 10.1038/s41598-019-41088-2

Karimi, M. T., Amiri, P., Esrafilian, A., Sedigh, J., and Fatoye, F. (2013). Performance of spinal cord injury individuals while standing with the mohammad taghi karimi reciprocal gait orthosis (MTK-RGO). *Australas. Phys. Eng. Sci. Med.* 36, 35–42. doi: 10.1007/s13246-013-0183-3

Kato, M., Murakami, S., Yasuda, K., and Hirayama, H. (1984). Disruption of fore- and hindlimb coordination during overground locomotion in cats with bilateral serial hemisection of the spinal cord. *Neurosci. Res.* 2, 27–47. doi: 10.1016/0168-0102(84)90003-8

Kawato, M. (1999). Internal models for motor control and trajectory planning. *Curr. Opini. Neurobiol.* 9, 718–727. doi: 10.1016/s0959-4388(99)00028-8

Kim, L. H., Sharma, S., Sharples, S. A., Mayr, K. A., Kwok, C. H. T., and Whelan, P. J. (2017). "Integration of descending command systems for the generation of context-specific locomotor behaviors," in *Frontiers in Neuroscience*, ed. Brian R. Noga (Lausanne, Switzerland: Frontiers Media S.A).

Laliberte, A. M., Goltash, S., Lalonde, N. R., and Bui, T. V. (2019). Propriospinal neurons: essential elements of locomotor control in the intact and possibly the injured spinal cord. *Front. Cell. Neurosci.* 13:512. doi: 10.3389/fncel.2019.00512

Lamy, J. C., Russmann, H., Shamim, E. A., Meunier, S., and Hallett, M. (2010). Paired associative stimulation induces change in presynaptic inhibition of Ia terminals in wrist flexors in humans. *J. Neurophysiol.* 104, 755–764. doi: 10.1152/jn.00761.2009

Levine, A. J., Hinckley, C. A., Hilde, K. L., Driscoll, S. P., Poon, T. H., Montgomery, J. M., et al. (2014). Identification of a cellular node for motor control pathways. *Nat. Neurosci.* 17, 586–593. doi: 10.1038/nn.3675

Lin, S., Li, Y., Lucas-Osma, A. M., Hari, K., Stephens, M. J., Singla, R., et al. (2019). Locomotor-related V3 interneurons initiate and coordinate muscles spasms after spinal cord injury. *J. Neurophysiol.* 121, 1352–1367. doi: 10.1152/jn.00776.2018

Magnus, C. J., Lee, P. H., Atasoy, D., Su, H. H., Looger, L. L., and Sternson, S. M. (2011). Chemical and genetic engineering of selective ion channel-ligand interactions. *Science* 333, 1292–1296. doi: 10.1126/science.1206606

Magnus, C. J., Lee, P. H., Bonaventura, J., Zemla, R., Gomez, J. L., Ramirez, M. H., et al. (2019). Ultrapotent chemogenetics for research and potential clinical applications. *Science* 364:eaav5282. doi: 10.1126/science.aav5282

Mahler, S. V., and Aston-Jones, G. (2018). CNO Evil? Considerations for the use of DREADDs in behavioral neuroscience. *Neuropsychopharmacology* 43, 934–936. doi: 10.1038/npp.2017.299

Martin, J. H. (2016). Harnessing neural activity to promote repair of the damaged corticospinal system after spinal cord injury. *Neural Regen. Res.* 11, 1389–1391.

May, Z., Fenrich, K. K., Dahlby, J., Batty, N. J., Torres-Espín, A., and Fouad, K. (2017). Following spinal cord injury transected reticulospinal tract axons develop new collateral inputs to spinal interneurons in parallel with locomotor recovery. *Neural Plast.* 2017:1932875. doi: 10.1155/2017/1932875

Mears, S. C., and Frank, E. (1997). Formation of specific monosynaptic connections between muscle spindle afferents and motoneurons in the mouse. *J. Neurosci.* 17, 3128–3135. doi: 10.1523/JNEUROSCI.17-09-03128.1997

Miller, S., and Van der Burg, J. (1973). *The Function of Long Propriospinal Pathways in the Co-ordination of Quadrupedal Stepping in the Cat.* Boston, MA: Springer 561–577.

Minassian, K., Jilge, B., Rattay, F., Pinter, M. M., Binder, H., Gerstenbrand, F., et al. (2004). Stepping-like movements in humans with complete spinal cord injury induced by epidural stimulation of the lumbar cord: electromyographic study of compound muscle action potentials. *Spinal Cord* 42, 401–416. doi: 10.1038/sj.sc.3101615

Minassian, K., Persy, I., Rattay, F., Pinter, M. M., Kern, H., and Dimitrijevic, M. R. (2007). Human lumbar cord circuitries can be activated by extrinsic tonic input to generate locomotor-like activity. *Hum. Mov. Sci.* 26, 275–295. doi: 10.1016/j.humov.2007.01.005

Moller, P. (1995). *Electric Fishes: History and Behavior*. London, New York: Chapman & Hall.

Moraud, E. M., Capogrosso, M., Formento, E., Wenger, N., DiGiovanna, J., Courtine, G., et al. (2016). Mechanisms underlying the neuromodulation of spinal circuits for correcting gait and balance deficits after spinal cord injury. *Neuron* 89, 814–828. doi: 10.1016/j.neuron.2016.01.009

Murg, M., Binder, H., and Dimitrijevic, M. R. (2000). Epidural electric stimulation of posterior structures of the human lumbar spinal cord: 1. muscle twitches—a functional method to define the site of stimulation. *Spinal Cord* 38, 394–402. doi: 10.1038/sj.sc.3101038

Possover, M. (2014). Recovery of sensory and supraspinal control of leg movement in people with chronic paraplegia: a case series. *Arch. Phys. Med. Rehabil.* 95, 610–614. doi: 10.1016/j.apmr.2013.10.030

Prokop, T., Berger, W., Zijlstra, W., and Dietz, V. (1995). Adaptational and learning processes during human split-belt locomotion: interaction between central mechanisms and afferent input. *Exp. Brain Res.* 106, 449–456. doi: 10.1007/BF00231067

Rattay, F., Minassian, K., and Dimitrijevic, M. R. (2000). Epidural electrical stimulation of posterior structures of the human lumbosacral cord: 2. quantitative analysis by computer modeling. *Spinal Cord* 38, 473–489. doi: 10.1038/sj.sc.3101039

Retamal, J., Reyes, A., Ramirez, P., Bravo, D., Hernandez, A., Pelissier, T., et al. (2018). Burst-like subcutaneous electrical stimulation induces BDNF-mediated, cyclotraxin B-sensitive central sensitization in rat spinal cord. *Front. Pharmacol.* 9:1143. doi: 10.3389/fphar.2018.01143

Righetti, L., Buchli, J., and Jan Ijspeert, A. (2006). Dynamic hebbian learning in adaptive frequency oscillators. *Physica D.* 216, 269–281. doi: 10.1016/j.physd.2006.02.009

Rossignol, S., Dubuc, R., and Gossard, J. P. (2006). Dynamic sensorimotor interactions in locomotion. *Physiol. Rev.* 86, 89–154. doi: 10.1152/physrev.00028.2005

Roth, B. L. (2016). DREADDs for Neuroscientists. *Neuron* 89, 683–694. doi: 10.1016/j.neuron.2016.01.040

Rybak, I. A., Dougherty, K. J., and Shevtsova, N. A. (2015). "Organization of the mammalian locomotor CPG: review of computational model and circuit architectures based on genetically identified spinal interneurons (1,2,3)," in *eNeuro*, ed. Christophe Renard (New York, NY: Society for Neuroscience), 1–20.

Rybak, I. A., Shevtsova, N. A., Lafreniere-Roula, M., and McCrea, D. A. (2006a). Modelling spinal circuitry involved in locomotor pattern generation: Insights from deletions during fictive locomotion. *J. Physiol.* 577, 617–639. doi: 10.1113/jphysiol.2006.118703

Rybak, I. A., Stecina, K., Shevtsova, N. A., and McCrea, D. A. (2006b). Modelling spinal circuitry involved in locomotor pattern generation: insights from the effects of afferent stimulation. *J. Physiol.* 577, 641–658. doi: 10.1113/jphysiol.2006.118711

Shealy, C. N., Mortimer, J. T., and Reswick, J. B. (1967). Electrical inhibition of pain by stimulation of the dorsal columns: preliminary clinical report. *Anesth. Analg.* 46, 489–491.

Siebert, J. R., Middelton, F. A., and Stelzner, D. J. (2010). Intrinsic response of thoracic propriospinal neurons to axotomy. *BMC Neurosci.* 11:69. doi: 10.1186/1471-2202-11-69

Storer, P. D., and Houle, J. D. (2003). BetaII-tubulin and GAP 43 mRNA expression in chronically injured neurons of the red nucleus after a second spinal cord injury. *Exp. Neurol.* 183, 537–547. doi: 10.1016/s0014-4886(03)00181-x

Straka, H., Simmers, J., and Chagnaud, B. P. (2018). A new perspective on predictive motor signaling. *Curr. Biol.* 28, R232–R243. doi: 10.1016/j.cub.2018.01.033

Taccola, G., Sayenko, D., Gad, P., Gerasimenko, Y., and Edgerton, V. R. (2018). And yet it moves: recovery of volitional control after spinal cord injury. *Prog. Neurobiol.* 160, 64–81. doi: 10.1016/j.pneurobio.2017.10.004

Takeoka, A. (2020). Proprioception: bottom-up directive for motor recovery after spinal cord injury. *Neurosci. Res.* 154, 1–8. doi: 10.1016/j.neures.2019.07.005

Takeoka, A., and Arber, S. (2019). Functional local proprioceptive feedback circuits initiate and maintain locomotor recovery after spinal cord injury. *Cell Rep.* 27, 71.e3–85.e3. doi: 10.1016/j.celrep.2019.03.010

Takeoka, A., Vollenweider, I., Courtine, G., and Arber, S. (2014). Muscle spindle feedback directs locomotor recovery and circuit reorganization after spinal cord injury. *Cell* 159, 1626–1639. doi: 10.1016/j.cell.2014.11.019

Terson de Paleville, D. G. L., Harkema, S. J., and Angeli, C. A. (2019). Epidural stimulation with locomotor training improves body composition in individuals with cervical or upper thoracic motor complete spinal cord injury: a series of case studies. *J. Spinal Cord Med.* 42, 32–38. doi: 10.1080/10790268.2018.1449373

Towne, C., Montgomery, K. L., Iyer, S. M., Deisseroth, K., and Delp, S. L. (2013). Optogenetic control of targeted peripheral axons in freely moving animals. *PLoS One* 8:e72691. doi: 10.1371/journal.pone.0072691

Tuthill, J. C., and Azim, E. (2018). Proprioception. *Curr. Biol.* 28, R194–R203. doi: 10.1016/j.cub.2018.01.064

Wagner, F. B., Mignardot, J.-B., Le Goff-Mignardot, C. G., Demesmaeker, R., Komi, S., Capogrosso, M., et al. (2018). Targeted neurotechnology restores walking in humans with spinal cord injury. *Nature* 563, 65–71. doi: 10.1038/s41586-018-0649-2

Wang, Y., Wu, W., Wu, X., Sun, Y., Zhang, Y. P., Deng, L. X., et al. (2018). Remodeling of lumbar motor circuitry remote to a thoracic spinal cord injury promotes locomotor recovery. *eLife* 7:e39016. doi: 10.7554/eLife.39016

Waters, R. L., Adkins, R. H., Yakura, J. S., and Sie, I. (1996). Effect of surgery on motor recovery following traumatic spinal cord injury. *Spinal Cord* 34, 188–192. doi: 10.1038/sc.1996.37

Wenger, N., Moraud, E. M., Gandar, J., Musienko, P., Capogrosso, M., Baud, L., et al. (2016). Spatiotemporal neuromodulation therapies engaging muscle synergies improve motor control after spinal cord injury. *Nat. Med.* 22, 138–145. doi: 10.1038/nm.4025

West, C. R., Phillips, A. A., Squair, J. W., Williams, A. M., Walter, M., Lam, T., et al. (2018). Association of epidural stimulation with cardiovascular function in an individual with spinal cord injury. *JAMA Neurol.* 75, 630–632. doi: 10.1001/jamaneurol.2017.5055

Wolpaw, J. R., and Lee, C. L. (1989). Memory traces in primate spinal cord produced by operant conditioning of H-reflex. *J. Neurophysiol.* 61, 563–572. doi: 10.1152/jn.1989.61.3.563

Wolpert, D. M., and Ghahramani, Z. (2000). Computational principles of movement neuroscience. *Nat. Neurosci.* 3, 1212–1217. doi: 10.1038/81497

Wolpert, D. M., and Miall, R. C. (1996). Forward models for physiological motor control. *Neural Netw.* 9, 1265–1279. doi: 10.1016/s0893-6080(96)00035-4

Wolpert, D. M., Ghahramani, Z., and Jordan, M. I. (1995). An internal model for sensorimotor integration. *Science* 269, 1880–1882. doi: 10.1126/science.7569931

Xu, J., Wei, X., Gao, F., Zhong, X., Guo, R., Ji, Y., et al. (2019). NADPH oxidase 2 derived ROS contributes to LTP of C-fiber evoked field potentials in spinal dorsal horn and persistent mirror-image pain following high frequency stimulus of the sciatic nerve. *Pain*. doi: 10.1097/j.pain.0000000000001761

Yakovenko, S., Kowalczewski, J., and Prochazka, A. (2007). Intraspinal stimulation caudal to spinal cord transections in rats. testing the propriospinal hypothesis. *J. Neurophysiol.* 97, 2570–2574. doi: 10.1152/jn.00814.2006

Young, W. (2015). Electrical stimulation and motor recovery. *Cell Transplant.* 24, 429–446. doi: 10.3727/096368915X686904

Zaporozhets, E., Cowley, K. C., and Schmidt, B. J. (2011). Neurochemical excitation of propriospinal neurons facilitates locomotor command signal transmission in the lesioned spinal cord. *J. Neurophysiol.* 105, 2818–2829. doi: 10.1152/jn.00917.2010

Conflict of Interest: The authors declare that the research was conducted in the absence of any commercial or financial relationships that could be construed as a potential conflict of interest.

Advantages of publishing in Frontiers

OPEN ACCESS
Articles are free to read for greatest visibility and readership

FAST PUBLICATION
Around 90 days from submission to decision

HIGH QUALITY PEER-REVIEW
Rigorous, collaborative, and constructive peer-review

TRANSPARENT PEER-REVIEW
Editors and reviewers acknowledged by name on published articles

Frontiers
Avenue du Tribunal-Fédéral 34
1005 Lausanne | Switzerland

Visit us: www.frontiersin.org
Contact us: frontiersin.org/about/contact

REPRODUCIBILITY OF RESEARCH
Support open data and methods to enhance research reproducibility

DIGITAL PUBLISHING
Articles designed for optimal readership across devices

FOLLOW US
@frontiersin

IMPACT METRICS
Advanced article metrics track visibility across digital media

EXTENSIVE PROMOTION
Marketing and promotion of impactful research

LOOP RESEARCH NETWORK
Our network increases your article's readership